

**CROSSCUTTING TECHNOLOGY DEVELOPMENT AT THE CENTER  
FOR ADVANCED SEPARATION TECHNOLOGIES**

SEMI-ANNUAL TECHNICAL PROGRESS REPORT

Report Period  
October 1, 2005 to March 31, 2006

Compiled by  
Christopher E Hull

Issued May 15, 2006

DOE Award Number:  
DE-FC26-02NT41607

## **DISCLAIMER**

This report was prepared as an account of work sponsored by an agency of the United States Government. Neither the United States Government nor any agency thereof, nor any of their employees, makes any warranty, express or implied, or assumes any legal liability or responsibility for the accuracy, completeness, or usefulness of any information, apparatus, product, or process disclosed, or represents that its use would not infringe privately owned rights. Reference herein to any specific commercial product, process, or service by trade name, trademark, manufacture, or otherwise does not necessarily constitute or imply its endorsement, recommendation, or favoring by the United States Government or any agency thereof. The views and opinions of authors expressed herein do not necessarily state or reflect those of the United States Government or any agency thereof.

## **ABSTRACT**

This Technical Progress Report describes progress made on the twenty nine sub-projects awarded in the second year of Cooperative Agreement DE-FC26-02NT41607: Crosscutting Technology Development at the Center for Advanced Separation Technologies. This work is summarized in the body of the main report: the individual sub-project Technical Progress Reports are attached as Appendices.

Note: SI is an abbreviation for “Le Systeme International d’Unites.”

## TABLE OF CONTENTS

<b>DISCLAIMER.....</b>	<b>2</b>
<b>ABSTRACT .....</b>	<b>3</b>
<b>TABLE OF CONTENTS .....</b>	<b>4</b>
<b>INTRODUCTION .....</b>	<b>7</b>
<b>EXPERIMENTAL .....</b>	<b>34</b>
<b>RESULTS AND DISCUSSION .....</b>	<b>35</b>
<b>CONCLUSIONS.....</b>	<b>36</b>
<b>REFERENCES .....</b>	<b>57</b>
<b>APPENDIX 1: DEVELOPMENT OF NOVEL ULTRAFINE SIZING METHODS (KY001/VA008)</b>	
<b>APPENDIX 2: DISPERSION AND FLOTATION OF CLAYS FROM NEW MEXICO POTASH ORES (NM001)</b>	
<b>APPENDIX 3: FLOTATION PROCESSES/EXPERIMENTS AND ANALYSIS (VT009)</b>	
<b>APPENDIX 4: COLUMN FLOTATION OF RELATIVE COARSE AND FINE DOLOMITIC PHOSPHATE PEBBLES (WV007)</b>	
<b>APPENDIX 5: BENEFICIATION OF MIXED POTASH ORES FROM NEW MEXICO (NM004)</b>	
<b>APPENDIX 6: DEVELOPMENT OF A NEW REAGENT SCHEDULE FOR FLOTATION OF DOLOMITE FROM PHOSPHATE ORES (NV002)</b>	
<b>APPENDIX 7: HIGH FREQUENCY EDDY CURRENT SEPARATION OF METALLIC RESIDUE FROM SLAGS, SANDS, ELECTRONIC SCRAPS AND OTHER WASTES (UT004)</b>	
<b>APPENDIX 8: DRY PARTICLE SEPARATION IN A CFB RISER SYSTEM (WV009)</b>	
<b>APPENDIX 9: STUDIES OF FROTH STABILITY AND MODEL DEVELOPMENT (VA002)</b>	
<b>APPENDIX 10: DIRECT MEASUREMENT OF FORCES IN FLOTATION (VA004)</b>	
<b>APPENDIX 11: IMPROVING DENSIFICATION OF FINE COAL REFUSE SLURRIES TO ELIMINATE SLURRY PONDS (KY002)</b>	
<b>APPENDIX 12: DEVELOPMENT AND TESTING OF A HORIZONTAL PRESSURE BELT FILTER (VA010)</b>	
<b>APPENDIX 13: DEVELOPMENT OF A FINE PARTICLE CENTRIFUGE (VA006)</b>	
<b>APPENDIX 14: IMPROVEMENTS IN SCREEN-BOWL CENTRIFUGE PERFORMANCE (VA013)</b>	

**APPENDIX 15: THE DEVELOPMENT AND UTILIZATION OF ALKALINE SULFIDE LEACHING AND RECOVERY OF GOLD (MT001)**

**APPENDIX 16: HYDROMETALLURGICAL PROCESSING OF CHALCOPYRITE CONCENTRATES (NV001)**

**APPENDIX 17: SIMULTANEOUS ELECTROLYSIS OF COPPER AND FERROUS IONS TO PRODUCE COPPER CATHODE AND TO REGENERATE FERRIC SULFATE - THE LIXIVANT TO DISSOLVE COPPER SULFIDE MINERALS (MT002)**

**APPENDIX 18: ION EXCHANGE RECOVERY OF COBALT FROM COPPER LEACH SOLUTIONS (NM002)**

**APPENDIX 19: THE EFFECT OF DIPHENYL OXIDE SURFACTANTS ON NUCLEATION AND GROWTH OF POTASSIUM SULFATE CRYSTALS: DEVELOPMENT OF ENHANCED SURFACTANTS FOR THE POTASH INDUSTRY (NM003)**

**APPENDIX 20: OVERCOMING TECHNOLOGICAL BARRIERS TO MORE EFFICIENT RECOVERY OF COPPER FROM CHALCOPYRITE (UT005)**

**APPENDIX 21: DEVELOPMENT OF CHEMICAL AND BIOCHEMICAL TECHNIQUES FOR THE EXTRACTION OF MERCURY FROM FINE COAL PARTICLE SOLUTIONS (WV010)**

**APPENDIX 22: COAL DESULFURIZATION WITH HYPOCHLORITE (WV011)**

**APPENDIX 23: PHYTO-EXTRACTION / FABRICATION OF GOLD AND SILVER NANOPARTICLES (WV012)**

**APPENDIX 24: ONLINE MONITORING AND DIAGNOSING OF COAL FINES DURING SEPARATION PROCESS (WV008)**

**APPENDIX 25: DEVELOPMENT OF A NOVEL OPTICAL RADIATION DEPOLARIZATION TECHNIQUE FOR ON-LINE MEASUREMENTS OF PARTICLE AND BUBBLE SIZES (KY003)**

**APPENDIX 26: MINERAL LIBERATION ANALYSIS IN 3D BY X-RAY MICROCT FOR THE EVALUATION OF PARTICLE SEPARATION EFFICIENCY (UT006)**

**APPENDIX 27: A COMPREHENSIVE STUDY OF FROTH BEHAVIOR (VA011)**

**APPENDIX 28: PORTABLE SENSOR FOR DETECTING MERCURY AND OTHER HEAVY METALS ENCOUNTERED IN COAL PROCESSING AND UTILIZATION (WV013)**

**APPENDIX 29: DETERMINING THE EFFECTIVENESS OF GOLD FILTERS FOR REMOVING MERCURY FROM COAL FIRED POWER PLANTS (MT003)**

**APPENDIX 30: DEVELOPMENT OF METALLIC FILTERS TO CONTROL MERCURY FROM COAL FIRED POWER PLANT FLUE GAS (MT004)**

**APPENDIX 31: RECOVERY OF CHROMIUM AND ARSENIC FROM TOXIC WASTE STREAM BY REACTIVE POLYMER-COATED ABSORBENTS (WV013)**

**APPENDIX 32: ALTERNATIVE MATERIALS FOR DENSE MEDIUM SEPARATIONS (KY004)**

**APPENDIX 33: DETERMINATION OF FACTORS AFFECTING THE SEPARATION OF POTENTIALLY HAZARDOUS TRACE ELEMENTS AND THEIR BEHAVIOR IN COAL TAILINGS IMPOUNDMENTS (KY005)**

**APPENDIX 34: ENHANCED FLOTATION PERFORMANCE THROUGH COLUMN FROTH ENRICHMENT (KY006)**

**APPENDIX 35: RECOVERY OF GOLD FROM THIOSULFATE LEACH LIQUOR USING ACTIVATED CARBON (MT005)**

**APPENDIX 36: THE EFFECT OF ALKYL DIPHENYL OXIDE AND SULFONATED OLEIC ACID SURFACTANTS ON NUCLEATION AND GROWTH OF POTASSIUM SULFATE CRYSTALS: OPTIMIZATION OF SURFACTANTS FOR THE POTASH INDUSTRY (NM005)**

**APPENDIX 37: THIOSULFATE AS A REPLACEMENT FOR CYANIDE IN THE PRESENCE OF ACTIVATORS (NV003)**

**APPENDIX 38: DEVELOPMENT OF A 3D LATTICE-BOLTZMANN MODEL FOR FLUID FLOW SIMULATION UNDER PARTIALLY-SATURATED CONDITIONS IN PACKED PARTICLE BEDS (UT007)**

**APPENDIX 39: ENGINEERING DEVELOPMENT OF A FINE PARTICLE HEAVY MEDIUM SEPARATOR (VA012)**

**APPENDIX 40: IMPROVED DESTRUCTION AND CONTROL OF RESIDUAL FLOTATION FROTHS (VA014)**

**APPENDIX 41: DEVELOPMENT OF A TURBULENT FLOTATION MODEL AND A COMPUTER SIMULATOR (VA015)**

**APPENDIX 42: MEASUREMENT OF SURFACE FORCES BETWEEN HYDROPHOBIC SURFACES (VA016)**

**APPENDIX 43: NOVEL SURFACTANTS AS COLLECTORS FOR FROTH FLOTATION (VA017) .....**

**APPENDIX 44: MERCURY REDUCTION FROM COAL POWER PLANT EMISSION USING FUNCTIONALIZED ORDERED MESOPOROUS CARBONS (FOMCS) (WV015)**

**APPENDIX 45: PHYTOMINING FOR NICKEL AND SILVER NANOPARTICLES (WV016)**

**APPENDIX 46: REMOVAL OF METAL IONS FROM ACID MINE DRAINAGE USING A NOVEL LOW-COST, LOW TECHNOLOGY (WV017)**

## INTRODUCTION

The U.S. is the largest producer of mining products in the world. In 2003, U.S. mining operations produced \$57 billion worth of raw materials that contributed a total of \$564 billion to the nation's wealth. Despite these contributions, the mining industry has not been well supported with research and development funds as compared to mining industries in other countries. To overcome this problem, the Center for Advanced Separation Technologies (CAST) was established to develop technologies that can be used by the U.S. mining industry to create new products, reduce production costs, and meet environmental regulations. Originally set up by Virginia Tech and West Virginia University, this endeavor has been expanded into a seven-university consortium – Virginia Tech, West Virginia University, University of Kentucky, University of Utah, Montana Tech, New Mexico Tech and University of Nevada, Reno - that is supported through U.S. DOE Cooperative Agreement No. DE-FC26-02NT41607: Crosscutting Technology Development at the Center for Advanced Separation Technologies.

Much of the research to be conducted with Cooperative Agreement funds will be longer-term, high-risk, basic research and will be carried out in five broad areas:

- a) Solid-solid separation
- b) Solid-liquid separation
- c) Chemical/Biological Extraction
- d) Modeling and Control, and
- e) Environmental Control.

Distribution of funds is handled via competitive solicitation of research proposals through Site Coordinators at the seven member universities. The first of these solicitations, referred to as the CAST II-Round 1 RFP, was issued on October 28, 2002. Thirty-eight proposals were received by the December 10, 2002 deadline for this RFP - eleven (11) Solid-Solid Separation, seven (7) Solid-Liquid Separation, ten (10) Chemical/Biological Extraction, six (6) Modeling & Control and four (4) Environmental Control. These were first reviewed and ranked by a group of technical reviewers (selected primarily from industry). Based on these reviews, and an assessment of overall program requirements, the CAST Technical Committee made an initial selection/ranking of proposals and forwarded these to the DOE/NETL Project Officer for final review and approval. This process took some 7 months to complete but 17 projects (one joint) were in place at the constituent universities (three at Virginia Tech, two at West Virginia University, three at University of Kentucky, three at University of Utah, three at Montana Tech, three at New Mexico Tech, and one at the University of Nevada, Reno) by May 17, 2003. These projects are listed below by category, along with brief abstracts of their aims and objectives.

a) *Solid-Solid Separation*

**1. Development of Novel Ultrafine Sizing Methods (Joint UK/VT Project) (KY001/VA008)**

Principal Investigators: R.-H. Yoon and G.H. Luttrell, Virginia Tech

Principal Investigators: R.Q. Honaker and BK. Parekh, University of Kentucky

Period of Performance: May 1, 2003- October 31, 2006 (2-Year Project)

The conventional techniques employed for sizing ultrafine particles in the coal and mineral processing industries have inherent inefficiencies that negatively impact on separation performance and production costs. In light of this problem, a broad based R&D program is proposed to investigate several innovative techniques for fine particle sizing. The processes to be evaluated will include a wide array of mechanical, hydraulic, and novel approaches for fine particle sizing. For each process, detailed tests programs will be conducted to optimize operating parameters so that maximum efficiency and capacity can be achieved while maintaining particle size cuts in the 25-50  $\mu\text{m}$  size range. The resultant test data will be used to mathematically simulate different circuit arrangements for the most promising technologies. A detailed economic study will be performed for those circuits that have the greatest potential for commercialization and industrial implementation. Due to the large scope of this project, the proposed work will be conducted as a joint effort between researchers at the University of Kentucky and Virginia Tech.

**2. Dispersion and Flotation of Clays from New Mexico Potash Ores (NM001)**

Principal Investigators: I. Gundiler, S. Titkov, and M. Yekeler, New Mexico Tech

Period of Performance: May 1, 2003-October 31, 2006 (1-Year Project)

New Mexico is the largest potash producer in the United States, supplying 70% of the domestic consumption of agricultural fertilizers. Potash mining began in the Carlsbad potash district in the early 1940s and while there are still vast reserves of potash minerals, producers are now dealing with low grade ores contaminated with clays and water-soluble magnesium minerals, which adversely affect the flotation of sylvite (KCl). Sylvite is floated from saturated brines with cationic collectors. The clays present in these brines absorb flotation reagents (thus increasing reagent costs), decrease recoveries of sylvite, contaminate the product and increase energy consumption for dewatering and drying. These clays are dispersed during grinding and/or attrition scrubbing and are then removed by hydrocyclones ahead of flotation. However, significant amounts of clay are carried over into flotation, where they are further dispersed by the mechanical action of impellers, thus hindering flotation. Furthermore, elevated brine temperatures during the summer affect collector adsorption on clays, depressing sylvite flotation. The presence of high concentrations of magnesium ions in the brine, which is peculiar to this district, also affects recoveries.

These technological problems must be solved for the state potash industry to remain viable and competitive. This study will investigate means of improving clay dispersion using organic and inorganic dispersants to increase the efficiency of slimes removal in existing facilities, and will study the effects of elevated magnesium ion concentrations

and elevated temperatures on the flotation of sylvite. Clay flotation, which has been shown to be superior to hydroseparators for clay removal in foreign operations, will also be investigated.

### **3. Flotation Technology for the Trona Industry (UT001)**

Principal Investigator: Jan D. Miller, University of Utah

Period of Performance: May 1, 2003- October 31, 2006 (2-Year Project)

Soda ash ( $\text{Na}_2\text{CO}_3$ ) produced from the trona deposits of the Green River Basin in Wyoming by chemical treatment is valued at approximately \$800 million per annum. Existing process technologies for the production of soda ash from trona involve dissolution in hot brine, drying, sedimentation and filtration for the removal of impurities, and subsequent crystallization and calcination for the recovery of soda ash. In this regard, mining and operating costs, particularly energy costs, are higher than desired. A preferred processing strategy might be to remove gangue mineral contaminants from the plant feed prior to dissolution in hot brine. It is expected that in this way improved productivity can be achieved in addition to significant savings in energy. Such a preprocessing strategy at ambient temperature and pressure has been limited by the lack of satisfactory process technology. Now based on recent results from laboratory research at the University of Utah it seems that the run-of-mine trona ore can be treated at ambient temperature and pressure using a special flotation procedure to separate the gangue minerals and make a trona concentrate with a purity of almost 99% trona at a recovery of more than 97%. Development and utilization of this new technology will allow for energy conservation, improved resource utilization, increased productivity and the development of a new product for the marketplace. In this regard a two-year research program involving industrial participation is proposed to develop the technology and demonstrate its effectiveness at a plant site.

### **4. Flotation Processes/Experiments and Analysis (VA009)**

Principal Investigators: D. Telionis and P. Vlachos, Virginia Tech

Period of Performance: May 1, 2003- October 31, 2006 (2-Year Project)

Flotation processes involve complex, three-phase flow interactions between a liquid, air bubbles and solid particles. For decades, engineers and researchers based their calculations on algebraic formulas that model these interactions. These formulas were derived from simple models, experimental data and/or arbitrary assumptions. Considerable progress has been made but this approach is still far from providing a reliable tool for the design of flotation machines.

We will take a more rigorous approach to the analysis and modeling of the flotation process. The proposed effort will combine detailed theoretical analysis and modeling with state-of-the-art, global, multi-phase flow measurements to quantify the effects of the various hydrodynamic parameters on the flotation process. We will employ a Digital Particle Image Velocimeter (DPIV) that can record velocity vectors of all three phases. We will measure three-phase flow interactions of bubbles and model particles of different hydrophobicity with a turbulent flow field. We will deliver global, time-resolved velocity distributions and turbulence characteristics for each phase. Our modeling approach will

incorporate all physical parameters that affect the collision efficiency of coal particles and flotation bubbles and the probabilities of attachment and detachment. An advanced model for predicting and quantifying the efficiency of the flotation process will be the final deliverable of this two-year effort. Such a tool will improve the design of flotation equipment and/or enhance the performance of existing systems.

**5. Column Flotation of Relative Coarse and Fine Dolomitic Phosphate Pebbles (WV009)**

Principal Investigator: Felicia F. Peng, West Virginia University

Period of Performance: May 1, 2003- October 31, 2006 (2-Year Project)

Dolomite in phosphate flotation concentrates is troublesome for down-stream operations. High dolomite contents cause higher consumption of sulfuric acid, reduce filtration rates and lower  $P_2O_5$  content in the fertilizer manufacturing process. However, the separation of dolomite particles from phosphate minerals is difficult because the dolomite is finely disseminated throughout the phosphatic pebbles and both are oxide type minerals with the same cationic component. Thus, they show similar electrokinetic, adsorptive and desorptive behavior in physical separation process such as flotation. Various flotation processes have been developed in the past four decades, but none is satisfactory due to high MgO content and/or low overall  $P_2O_5$  recovery in the final phosphate concentrate. In this research project, dolomitic phosphate pebbles from Florida will be treated by column flotation. A liberation analysis of the dolomite-phosphate matrix will be conducted to determine optimum grinding conditions; new selective mixtures of fatty acid collectors and non-ionic surfactants will be evaluated on relatively coarse (minus 300 microns) and fine (minus 150 microns) dolomite particles; appropriate mixtures of phosphoric acid/sulfuric acid will be used to depress phosphate particles; and the effect of addition of non-ionic surfactants on the separation performance will be determined. The goal is to produce a phosphate concentrate containing 30%  $P_2O_5$  and less than 1.0% MgO contents at high  $P_2O_5$  recoveries from low grade phosphatic pebbles stockpiled at plant sites and from pebbles generated from mining lower grade reserves.

**6. Beneficiation of Mixed Potash Ores From New Mexico (NM004)**

Principal Investigator: Ibrahim Gundiler, Lynn Brandvold, Tanja Pietraß, Stanislav Titkov, New Mexico Tech

Period of Performance: May 1, 2004- October 31, 2006 (2-Year Project)

New Mexico is the largest potash producer in the United States, which supplies 70% of the domestic production for agricultural fertilizers. Potash mining began in the Carlsbad potash district, in the southeastern corner of the state, in early 1940s. Although, there are still vast reserves of potash minerals, clean, high-grade ores are depleted. Sylvite (KCL) and langbeinite are the major minerals mined in the district, and New Mexico is the only location in the world where langbeinite concentrates are produced. Langbeinite, a double salt of potassium and magnesium, is the preferred form of potassium fertilizers for plants, which can not tolerate chloride ions.

Sylvite flotation is carried out from saturated brines with cationic collectors. Clay minerals adsorb flotation reagents, thus increase reagent costs and reduce recovery of

sylvite. Therefore, clays are dispersed during grinding and in attrition scrubbers, and removed by hydrocyclones. Furthermore, elevated brine temperatures during the summer also affect collector adsorption on clays, depressing sylvite flotation. Presence of high concentrations of magnesium ions, which is peculiar to this district, also affects the recovery.

Langbeinite ores are concentrated by gravity separation in coarse sizes and further cleaned by leaching halite (NaCl) with water. Some impurity minerals, which have similar specific gravity and solubility in water, however, contaminate the product. The present concentration process is water-intensive and availability of fresh water in drought-stricken southwest is becoming increasingly sensitive issue. Furthermore, as the high grade ores are depleted, mixed sylvite-langbeinite ores and langbeinite- kieserite ores have to be mined and processed. Technology for efficient separation of these minerals is not available, and, usually, one or more of the potash minerals are lost to the tailings.

For the potash industry of the state to remain viable and competitive, these technological problems have to be solved. This study will address to improve sylvite flotation from mixed ores in brines containing high concentrations of magnesium ions, and develop new flotation method for separation of sylvite, halite, and kieserite from mixed langbeinite ores.

Finally, the effect of elevated magnesium ion concentrations and elevated temperatures on the flotation of sylvite will be investigated. Flotation studies will be augmented with fundamental studies to investigate the hydration of KCl surfaces in Mg-containing brines using the Nuclear Magnetic Resonance, proton relaxation techniques, and changes in morphology and surface composition will be investigated using Atomic Force Microscopy and Electron Microprobe techniques. This study is expected to produce tangible results to improve the efficiency of the existing plants and contribute to the understanding of sylvite flotation from magnesium bearing brines, and soluble salt flotation in general.

## **7. Development of New Reagents for the Flotation of Dolomite from Phosphate Ore (NV002)**

Principal Investigators: Maurice C. Fuerstenau, Manoranjan Misra and Thomas W. Bell, University of Nevada, Reno

Period of Performance: May 1, 2004- October 31, 2006 (2-Year Project)

The United States is the largest producer of phosphate rock in the world, which corresponds to 30% of the world production. Florida accounts for 80% of the U.S. phosphate production. During the past century, the Florida phosphate industry has produced high quality phosphate with low MgO (< 0.5%) content. As low dolomitic phosphate reserves become exhausted, the remaining deposits contain lower amounts of phosphate with significantly higher dolomite (MgO) content. It is generally difficult to obtain a phosphate concentrate from such materials containing less than the desired MgO content of 1% MgO. The objective of the research work is to evaluate the effectiveness of new synthesized collectors for the selective flotation of dolomite from phosphate rock.

The experimentation will include evaluating the applicability of the new collectors through adsorption, electrokinetic and microflotation studies, and the flotation of dolomitic phosphate ores from Florida, Utah and Idaho

**8. High Frequency Eddy Current Separation of Metallic Residue from Slags, Sands, Electronic Scrap and Other Wastes (UT004)**

Principal Investigators: Raj K. Rajamani, University of Utah

Period of Performance: May 1, 2004- October 31, 2006 (2-Year Project)

The proposed work is to separate metallic grains from sands, slags or electronic scrap by means of a novel device called High Frequency Eddy Current Separator. The dry mixture of foundry sands is passed through the gap between the poles of a magnet. The metallic granules are repelled from the falling stream of sand, and hence are separated. This device has many technical and commercial advantages over the existing technologies (i.e. lower cost, no use of water or chemicals, absence of polluting gases, etc.).

A high frequency magnetic field is generated in the gap when radio-frequency current is passed through windings on a ferrite core. As the electrically conducting particle enters the field, an electromotive force (emf) is generated on the particle itself. Due to the emf, an eddy current flows on the particle. These currents, in turn, induce their own magnetic field around the particle. Lenz rule of physics states that the induced magnetic field is directly opposed to the original or imposed oscillating field. Hence, the particle experiences a repelling force. The repelling force depends on the strength of the magnetic field, the frequency of oscillations, and the cross-sectional area and electrical conductivity of the particle.

The object of this program is to develop third prototype for testing. The prototype engineering is based on the first lab unit developed at the University of Utah and the second lab unit built by EMPS Corporation, Salt Lake City, Utah. These two units used a ferrite toroid and a bi-polar amplifier to generate the high frequency magnetic field in the gap of the toroid. Invariably the choice of ferrite core limited the gap dimensions to about 10X10 mm. The unit proposed here is a larger toroid with 125 X125 mm gap to be driven by a direct drive electronic circuitry. This unit would be capable of processing 100 lb./hr of solid stream and hence suitable for process optimization and operating parameter study.

Present eddy-current devices, have been confined to the recovery of large aluminum cans from municipal wastes. For example Eriez Magnetics has a line of eddy current separators, which uses permanent magnets of alternating polarity spinning at high speeds under a belt conveyor. Hence this unit can only produce about 1 kHz frequency. Low frequency devices can separate only larger pieces, of size ½ inch, of metal. The proposed high-frequency separator uses magnetic-field frequencies of 50 to 100 kHz that enhances its ability to separate much smaller grains of size larger than 0.2 mm.

In copper production, both a copper-sulfur matte and a blister copper are formed, which are covered by a slag layer. In the production of aluminum and magnesium, electrolytic cells are used to electrowin the liquid metal at the cathode. A slag layer is also present in this process. Typically, there is mixing at the liquid metal/slag interface, which results in

droplets or prills of metal suspended in the slag phase. Approximately 3.6 million metric tons each of copper and phosphorous slag are produced each year in the U.S. The annual production of nickel, lead and zinc slag is estimated at 0.45 to 0.9 million metric tons. Electric and electronic goods comprise a vast and diverse spectrum of items that are sent to the landfills each year. A 1991 study estimates that 150 million personal computers and workstations will have been sent to landfills by the year 2005. The recovery of metallic copper, gold, palladium and aluminum from scrap is in the best interest of environmental protection. These waste streams are typical application targets for the high frequency separator proposed here.

**9. Continuation of Project WV002 - Dry Particle Separation in a CFB Riser System (WV009)**

Principal Investigator: Eric Johnson and Bruce W. Kang, West Virginia University  
Period of Performance: May 1, 2004- October 31, 2006 (2-Year Project)

The proposed project is a continuation of the study to determine the potential for separating small dense particles from small light particles in a CFB riser system. This exploratory work led to many interesting and practical results. It is proposed to now refine and expand our test conditions and develop a more comprehensive analysis of the results. The experimental conditions planned for this continuation project are 1) more closely matched particle size distributions for the heavy and light particles in the mixture, 2) smaller density difference between the heavy and light particles, 3) separation of particles based only on size differences, and 4) developing and employing a larger diameter riser to study the scaling of the separation processes in a riser.

**10. Studies of Froth Stability and Model Development (VA002)  
(Continuation from CAST I)**

Principal Investigator: Roe-Hoan Yoon, Virginia Tech  
Period of Performance: May 1, 2004- October 31, 2006 (2-Year Project)

Froth plays an important role in flotation. It determines the final grade of the product and the maximum carrying capacity (or throughput) of a flotation machine. Also, many operators use stronger frothers to produce smaller air bubbles and, hence, higher recovery and throughput. Despite its importance, little is known of the fundamentals of foam and froth stability. It is, therefore, proposed to study the various factors affecting the stability of flotation froth. This will be accomplished by using the thin film balance (TFB) technique of Scheludko and Exerowa (1959) and by monitoring the stability of froth in a bubble column using a video camera. The results will be used for developing a froth model and also for developing effective defoamers.

**11. Direct Measurement of Forces in Flotation (VA004)  
(Continuation from CAST I)**

Principal Investigator: Roe-Hoan Yoon, Virginia Tech  
Period of Performance: May 1, 2004- October 31, 2006 (2-Year Project)

The objective of this project is to directly measure the interaction force between a particle and bubbles as a function of separation distance. This force controls the attachment and

detachment of particles to bubbles, which is an essential step in determining the efficiency of a flotation process. A specially designed device will be fabricated for these measurements. The device will use the force-detection method employed by an Atomic Force Microscope and the separation-detection method employed by a Surface Forces Apparatus. The key advances are to explicitly measure both the separation between the particle and the bubble and the shape of the bubble at all times. Without this separation and shape data, it would be difficult to relate the measured forces to flotation results. After fabrication of the device, measurements of the interaction forces acting on hydrophilic, hydrophobic, and charged particles in aqueous solutions of surfactant molecules will be obtained.

## **12. Enhanced Flotation Performance Through Column Froth Enrichment**

Principal Investigators: Rick Q. Honaker and Daniel Tao, University of Kentucky  
Period of Performance: June 1, 2005-May 31, 2005 (2-Year Project)

Froth flotation is a process that separates particles based on their differences in physical and surface chemistry properties. For fine feed material that is comprised of particles having wide degrees of floatability, selectivity is often optimized by maximizing the differences in the flotation rates between the particles targeted for recovery in the froth concentrate and those needed to report to the underflow stream. The benefits of differential flotation rates are realized in the collection zone of a flotation system where bubble-particle collision and attachment occurs. However, selectivity between particles of varying floatability can be significantly enhanced in the froth zone through a reflux mechanism that circulates detached particles back to the collection zone. Particle detachment in the froth zone occurs due to bubble coalescence, which leads to an insufficient amount of bubble surface area to carry all of the material recovered in the collection zone. Based on previous research, the detachment process is selective in that particles having a lower degree of floatability (or hydrophobicity) are preferentially released from the bubble surfaces. Selectivity through the detachment process can be improved by the addition of a more hydrophobic material into the froth zone and possibly by recycling a portion of the flotation concentrate, thereby enriching the flotation froth.

In a recent study, froth zone and overall flotation recovery values were quantified for particles in an anthracite coal that were characterized as having wide differences in floatability potential. The unique aspect of the coal was the presence of 'bone' material in the high density fractions which had a relatively high degree of floatability. As a result, the minimum product grade achieved by froth flotation was about 15% despite washability data indicating the potential for achieving a product containing nearly 3% ash. Highly floatable material was added directly into the froth zone while treating the anthracite coal and then removed from the product and tailing samples using density fractionation. The enriched froth phase reduced the product ash content of the anthracite product by 5 absolute percentage points while maintaining coal recovery at the same level. These results support the findings of previous fundamental research conducted on hematite flotation with the addition of hydrophobic silica directly into the froth phase.

The proposed two-year project will further investigate the fundamentals of the detachment process as well as develop unique methods of commercial application that may be more useful for sulfide and precious mineral industries. Plastic material that contains an amount of magnetite that makes the plastic easily recoverable by a low-intensity magnetic separator will be directly added in the flotation froth through the wash water distributor of a flotation column. By varying the formulations of the plastic, surface hydrophobicity and thus floatability can be controlled. Initial tests will involve the flotation of silica that will be methylated to achieve varying degrees of floatability. External refluxing of a portion of the flotation froth will also be investigated using the methylated silica. To evaluate the commercial benefits, the improved selectivity achieved by froth enrichment using external refluxing and the addition of the magnetic material will be accessed for the flotation of coal, sulfide minerals and phosphate.

### **13. Engineering Development of a Fine Particle Heavy Medium Separator (VA012)**

Principal Investigators: Gerald H. Luttrell, Virginia Tech and Robert Moorhead, Krebs Engineers, Inc

Period of Performance: June 1, 2005-October 31, 2006 (2-Year Project)

The objective of this project is to develop an innovative heavy medium separator that can reduce the cost and improve the efficiency of fine coal cleaning. The technology is designed to replace inefficient water-based separators such as spirals and water-only cyclones that are currently used by industry to upgrade 1 x 0.15 mm run-of-mine coal. The new heavy medium separator incorporates novel design features that allow it make sharp separations without the need for costly micronized magnetite. As a result, the new technology can share circulating medium from other circuits, thereby avoiding the expense of installing and maintaining an additional medium circuit. These advantages, together with the low headroom design of the module, make it possible to integrate this technology into an existing plant with minimal retrofit costs. The project tasks will include (i) design and construction, (ii) pilot-scale testing, (iii) field testing, and (iv) flowsheet development

### **14. Improved Destruction and Control of Residual Flotation Froths (VA014)**

Principal Investigators: Gerald H. Luttrell and Roe-Hoan Yoon, Virginia Tech

Period of Performance: June 1, 2005-October 31, 2006 (2-Year Project)

Flotation froths containing large amounts of ultrafine particles can become excessively stable and create serious handling problems for coal preparation plants. Steps taken by operators to combat these problems, such as lowering the frother dosage, have resulted in large reductions in fine coal recovery and plant profitability. The objective of this project is to develop and evaluate several improved methods for the control and destruction of residual flotation froths. The first phase of the proposed work will focus on a detailed laboratory study of the physical and chemical parameters that impact froth stability. These studies will be followed by in-plant sampling campaigns at several coal plants to establish how frothing agents partition within different circuits and to determine whether modifications to the layout or dilution practices can minimize handling problems. The data obtained from these investigations will be used to develop improved mechanical and

chemical methods for froth control/destruction at an industrial plant site

**15. Development of a Turbulent Flotation Model and a Computer Simulator (VA015)**

Principal Investigators: Roe-Hoan Yoon and Gerald H. Luttrell, Virginia Tech

Period of Performance: June 1, 2005-October 31, 2006 (2-Year Project)

Flotation is the most widely used method of separating fine particles in the mining industry. The method of using air bubbles was awarded a U.S. patent in 1905, exactly 100 years ago. Yet, there are no flotation models incorporating both surface chemistry (e.g., hydrophobicity,  $\zeta$ -potential, and surface tension) and hydrodynamic (e.g., bubble size, particle size, energy dissipation) parameters under turbulent flow conditions. It is, therefore, proposed to develop a comprehensive flotation model incorporating practically all of the process variables employed in flotation practice. The turbulent flotation model will be able to describe the events taking place in both the pulp and froth phases. Laboratory experiments will be carried out to verify the model, and model will be transformed into a compute simulator that can predict complicated flotation circuits incorporating rougher, scavenger and cleaner operations.

**16. Novel Surfactants as Collectors for Froth Flotation (VA015)**

Principal Investigators: Richard D. Gandour, Virginia Tech

Period of Performance: June 1, 2005-October 31, 2006 (2-Year Project)

Our goals are to synthesize and study novel, inexpensive amphiphiles that can perform as co-surfactant collectors in mineral flotation. These surfactants will selectively bind to particles and create a hydrophobic coating on a particle. These novel surfactants will bind more selectively and provide hydrophobic sites where cheaper, less-selective collectors can bind. These novel surfactants have very hydrophobic, long chains, yet are sufficiently water soluble for mineral processing and coal-fines processing. These amphiphiles, which we call 'hydra surfactants', will have two tails and three heads. These novel molecules will be useful for many different separations in mineral processing.

***b) Solid-Liquid Separation***

**1. Improving Densification of Fine Coal Refuse Slurries to Eliminate Slurry Ponds (KY002)**

Principal Investigators: B.K. Parekh and R.Q. Honaker, University of Kentucky

Period of Performance: May 1, 2003-May 31, 2005 (2-Year Project)

Increased mechanization in underground coal mining has increased the volume of refuse generated by coal preparation plants. The fine refuse slurry, composed of coal and mineral matter, is usually disposed of in a holding pond (impoundment), but incidents of impoundment breakthrough have forced the industry to look for alternative methods for fine refuse storage in the future. The main objective of the proposed program is to evaluate a new technique known as "Paste Thickening Technology," which utilizes a DORR-OLIVER EIMCO DEEP CONE Thickener to discharge the waste slurry as a

paste. The paste material should be stackable at low repose angles and would dry over a period of time, thus avoiding the storage of slurries in ponds. The proposed study will be conducted on coal waste slurries obtained from two different preparation plants. Laboratory studies will involve the characterization of the slurries, bench-scale flocculation studies and rheological analysis of the flocculated materials to identify yield stresses at various solid concentrations. This information will be used to establish optimum conditions for the production of a thickened paste product. A pilot-scale study will then be conducted at one of the coal preparation sites to obtain technical and economic data for a commercial installation and operation. It is anticipated that the outcome of the study will be an effective and economical process for the safe disposal of fine coal refuse.

## **2. Development and Testing of a Horizontal Pressure Belt Filter (VA010)**

Principal Investigators: R.-H. Yoon & G.H. Luttrell, Virginia Tech

Period of Performance: May 1, 2003- October 31, 2006 (2-Year Project)

A variety of mechanical processes are available for dewatering fine particles in the coal and mineral processing industries. Unfortunately, many of these processes suffer from major shortcomings such as poor dewatering performance, low throughput capacity, and high capital and operating costs. This project seeks to overcome these problems by developing a new type of dewatering process that combines the operational flexibility of a continuous belt filter with the dewatering efficiency of a batch pressure filter. The proposed project involves the design, construction, testing, and evaluation of a prototype unit and pilot-scale test circuit having a production capacity of approximately 100 lb/hr. Test data obtained from the project will be used to promote the engineering development of a full-scale commercial unit.

## **3. Development of a Fine Particle Centrifuge (VA006)**

(Continuation from CAST I)

Principal Investigators: G.H. Luttrell & R.-H. Yoon, Virginia Tech

Period of Performance: May 1, 2004- October 31, 2006 (2-Year Project)

The solid-solid separation processes employed by modern coal preparation plants require large amounts of process water. After cleaning, the unwanted water must be removed from the surfaces of the particles using mechanical dewatering equipment. Coarse particles can be readily dewatered using simple screening systems, while finer particles require more complicated unit operations such as centrifuges and filters. Unfortunately, the processes used to dewater fine particles are inherently inefficient and expensive to operate and maintain. To overcome these problems, a novel centrifugal filter has been developed by researchers at Virginia Tech. Preliminary test data suggest that this new technology can reduce the moisture content of fine coal products by approximately 30-50% compared to existing dewatering processes. The objective of this project will be to construct a continuous prototype unit and to conduct a detailed experimental investigation of this new technology.

#### **4. Improvements in Screen Bowl Centrifuge Performance (VA013)**

Principal Investigators: Robert C. Bratton & G.H. Luttrell, Virginia Tech  
Period of Performance: May 1, 2004- October 31, 2006 (2-Year Project)

Screen-bowl centrifuges are the most commonly used method for dewatering fine coal in the United States. Unfortunately, this process is the least efficient and most costly dewatering operation in the preparation plant. The work outlined in this proposal will seek to develop an improved understanding of the operating characteristics and technical capabilities of screen-bowl centrifuges. Plant operators will be able to use this fundamental knowledge to improve the performance of their dewatering circuits and improve plant profitability. In addition, several new screen-bowl centrifuge features will be developed and evaluated as part of the proposed work. The innovations will include the development and testing of internal injection ports for (i) adding flocculant to the low-solids pool and (ii) adding dewatering aids and surface tension modifiers to the dewater screen solids. These technological enhancements are expected to improve moisture reduction and increase fine coal recovery

#### **c) Chemical/Biological Extraction**

##### **1. Bio-Assisted Heap Leaching of Nickel Laterites for the Development of a Domestic Nickel Industry (UT002)**

Principal Investigator: S. Duyvesteyn, University of Utah  
Period of Performance: May 1, 2003- October 31, 2006 (2-Year Project)

The U.S. currently imports all of its nickel, which is a strategic material used in stainless steels and other corrosion-resistant materials. Existing U.S. resources are worth around \$10 billion at current metal prices, but occur mostly in low-grade laterite deposits, for which conventional hydrometallurgical processes are not economically feasible production routes. These processes typically utilize mineral acids that cannot be recycled economically and can cause significant environmental problems. The solubilization of metal ions from ores by organic acids produced by microorganisms has been demonstrated to be a viable alternative for metal production with reduced environmental and remediation issues, as organic acids are readily biodegradable. The fact that many of these organic acids and other metabolites form strong chelating complexes with the base metal ions also results in a reduction in the acid requirements to achieve complete solubilization.

This research proposal involves a biotechnological approach, called bio-assisted heap leaching (BAHL), for the production of nickel metal from low-grade ore synergistically with the co-production of citric acid. The BAHL process can be described as follows: laterite nickel ore is combined with an organic nutrient and put on heaps where fungi, such as *Aspergillus niger*, produce organic acids during their natural metabolic cycle. Recycle solution is sprayed over the heaps and its percolation through the heaps results in the dissolution of nickel. The resulting nickel-containing leach solution is collected and the nickel and citrate values are recovered.

## **2. The Development and Utilization of Alkaline Sulfide Leaching and Recovery of Gold (MT001)**

Principal Investigator: C. Anderson and L.G. Twidwell, Montana Tech  
Period of Performance: May 1, 2003- October 31, 2006 (2-Year Project)

Due to the increasing concerns over the emission of sulfur dioxide from roasting and smelting, there has been an increased interest in pressure oxidation as a means of treating gold bearing ores and concentrates. One of the problems with the partial oxidation of the sulfide host matrix to form elemental sulfur is that sulfur containing streams are difficult to treat using cyanidation. In the present study, the alkaline sulfide system will be studied as an alternative to cyanide for recovering gold from elemental sulfur. A complete thermodynamic model of the alkaline sulfide gold leaching system will be developed using Stab-Cal software and the leaching system and its kinetics will be optimized.

## **3. Hydrometallurgical Processing of Chalcopyrite Concentrates (NV001)**

Principal Investigator: M. Misra and M. Fuerstenau, University of Nevada, Reno  
Period of Performance: May 1, 2003- October 31, 2006 (2-Year Project)

Hydrometallurgical processing of chalcopyrite at moderate temperature and pressure has been a goal of the copper industry for decades. Research has shown that a protective sulfur layer forms on chalcopyrite when leached with ferric salts in acidic medium. This layer limits the transport of electrons from the mineral surface to the oxidant and precludes the use of this technology for chalcopyrite processing. Research at the University of Nevada, Reno has shown that the introduction of finely-divided silica improves the kinetics of leaching dramatically. Silica adsorbs on the surface of chalcopyrite, and since it is an n-type conductor, conduction of electrons from the mineral surface to the oxidant occurs by photocatalysis of the sulfur product layer. Dissolution amounts of as much as 80% have been achieved under the limited conditions examined, namely at atmospheric pressure and 50°C.

## **4. Simultaneous Electrolysis of Copper and Ferrous Ions to Produce Copper Cathode and to Regenerate Ferric Sulfate - The Lixiviant to Dissolve Copper Sulfide Minerals (MT002)**

Principal Investigator: C. Young, H.-H. Huang and C. Fabian, Montana Tech  
Period of Performance: May 1, 2003- October 31, 2006 (2-Year Project)

Copper leaching is primarily conducted on oxidized ore bodies at low pH by using sulfuric acid ( $\text{H}_2\text{SO}_4$ ). The sulfate acts as the lixiviant to solubilize the copper as copper sulfate ( $\text{CuSO}_4$ ). An oxidant is also needed to enhance reaction rates – typically this is dissolved oxygen ( $\text{O}_2$ ) and/or ferric ( $\text{Fe}^{3+}$ ) ion. The dissolved copper must then be extracted from the water to separate it from other dissolved constituents including iron. Traditional solvent extraction and electrowinning (SX/EW) procedures do this and ultimately yield quality copper cathode as product. After SX/EW, leach solution is recycled to the leaching process and replenished with oxidant as needed. For example, biological activity can regenerate ferric ions or mechanical agitation can produce dissolved oxygen (which in turn can regenerate ferric ions).

Ferric ions can also be regenerated electrolytically and simultaneously to copper cathode production. This is the basis of the proposed research. To accomplish this, a porous membrane will be used to keep the anode and cathode compartments separated and modern rotating cylinder electrodes will be used to stir solutions, obtain high current densities and ultimately produce superior grade copper cathode. Although it is possible to avoid the SX step, it will be used to produce two streams: raffinate, which will go to the anode compartment where ferric is regenerated, and pregnant or advance solution, which will go to the cathode compartment where copper metal is produced. Various chemicals and additives may have to be added to control copper cathode formation and thereby avoid, for example, dendritic growth. Preliminary cost analyses show that copper can be produced for approximately \$0.30/lb with this new, more energy efficient, technique.

**5. Ion Exchange Recovery of Cobalt from Copper Leach Solutions (NM002)**

Principal Investigator: I. Gundiler and M. Hatch, New Mexico Tech

Period of Performance: May 1, 2003- October 31, 2006 (2-Year Project)

Cobalt is a strategic and critical metal which is used in production of super alloys for use in jet engine turbines, wear and corrosion resistant alloys, cutting tools, magnets and various other alloys and chemicals. It is not mined or refined in the United States; therefore, 80% of the cobalt consumed in the U.S. is imported. The remaining balance is met with recycled alloys and supplies from stockpiles. Although there is historical production and known reserves, these are not economical to exploit at the present. However, there is a readily available source of cobalt in the leach solutions generated in large copper mining operations in the Southwestern U.S. If only a fraction of this cobalt could be recovered, New Mexico and Eastern Arizona copper leach operations could potentially supply 20% of U.S. imports. Currently, the technology to recover the metal from these solutions economically is not available.

Ion exchange processes could recover this cobalt. However, commercially available resins are either too expensive, or do not function in acidic solutions. Absorption kinetics of these resins are also fairly slow. Three new resins will be synthesized at New Mexico Tech for copper and cobalt recovery from acidic solutions. The resins will be characterized and tested in the laboratory using pure chemicals, as well as process solutions to be obtained from the Phelps Dodge Mining Company, New Mexico operations. The performance of the synthesized resins will also be compared with that of commercially available resins.

**6. The Effect of Diphenyl Oxide Surfactants on Nucleation and Growth of Potassium Sulfate Crystals: Development of Enhanced Surfactants for the Potash Industry (NM003)**

Principal Investigator: G. Bond and C. Hockensmith, New Mexico Tech

Period of Performance: May 1, 2003- October 31, 2006 (2-Year Project)

Surfactant-controlled crystallization leads to an increase in the efficiency of potassium sulfate production, particularly when alkyl diphenyl oxide-type (ADO) surfactants are employed in synthesis. Improved control of crystallization in both the initiation and termination phases can increase the ratio of granular particles to fines, decreasing costs associated with production and facilitating the utilization of lower-grade ores. Mother liquors in potash extraction contain high percentages of magnesium as well as other ions including chloride and impurities such as clay and silica. Potassium sulfate crystals will be produced in the presence of different ADO surfactants, and evaluated by SEM, TEM, XRD, FTIR and AFM. Crystallization processes, particularly those that affect crystal morphology, size, initiation and termination, will be studied in relation to the surfactant effect. This information will be used to improve control of potassium sulfate precipitation and develop the next generation of surfactants to facilitate extraction of granular potassium sulfate.

**7. Overcoming Technological Barriers to More Efficient Recovery of Copper from Chalcopyrite (UT005)**

Principal Investigator: Michael L. Free, University of Utah

Period of Performance: May 1, 2004- October 31, 2006 (2-Year Project)

Extraction and recovery of copper from chalcopyrite is one of the most important processes in the nonferrous metals industry. It is currently performed using smelting, converting, and electrorefining, yet it also necessitates by-product sulfuric acid production at a rate of three tons of acid per ton of copper. Efforts to convert this process to leaching, solvent extraction, and electrowinning, which is a lower cost alternative to the smelting, converting, and electrorefining process that is practiced for most other copper minerals, have been unsuccessful. However, new technologies, such as halide leaching and electrowinning offer significant economic and environmental advantages over the current industrial practices.

Halide leaching and electrowinning requires only 25% of the energy needed to electrowin copper using traditional sulfate-based solution technology. The halide-based technology, which is also compatible with precious-metal recovery from sulfide minerals, also eliminates acid misting and solvent extraction, and it results primarily in the production of by-product elemental sulfur rather than sulfuric acid.

The halide leaching and electrowinning process has not been adopted by industry due to large capital investment in current smelters, the risk of new technology that has not been proven on a large scale, and the incompatibility with existing electrowinning operations due to the morphology of the deposit, which is granular, rather than smooth using current technology. This project is designed to modify the morphology of the resulting copper deposit to make it compatible with existing electrowinning processes.

**8. Development of Chemical and Biochemical Techniques for the Extraction of Mercury from Fine Coal Particle Solutions. (WV010)**

Principal Investigator: Scott M. Hurst, Anthony G. Abatjoglou and Jay M. Weidemann, West Virginia University

Period of Performance: May 1, 2004- October 31, 2006 (2-Year Project)

The WVU Tech Project, “Development of Chemical and Biochemical Techniques for the Extraction of Mercury from Fine Coal Particle Solutions”, includes three objectives: development of a biochemical technique to facilitate the conversion of organically bound forms of mercury to water soluble mercury, development of a chemical technique using physically adsorbed ligands that selectively removes mercury from an aqueous solution that contains relatively large concentrations of other metals, and the development of a biochemical process for extracting liquid mercury from the ligands. The results of this work will be the bases for the development of a novel process for extracting mercury from coal solutions in a “zero waste” manner.

#### **9. Coal Desulfurization with Hypochlorite (WV011)**

Principal Investigator: Ray K. Yang & Eung Ha Cho, West Virginia University

Period of Performance: May 1, 2004- October 31, 2006 (2-Year Project)

The utilization of coal as a feedstock to produce carbon materials is very much hampered by the presence of its sulfur content particularly organic sulfur content. However, the organic sulfur is extremely difficult to remove because much of its sulfur atoms are “inserted” into the matrix of the coal structure. Thus, unless the coal structure is “destroyed”, the sulfur atoms can not be removed. Chlorine is one of a few chemicals known today that have capability to reduce organic sulfur in a practical sense. However, this chemical chlorinates the coal structure especially at its low pHs, which becomes a roadblock for commercialization of a process utilizing this chemical. We observed through preliminary experiments that hypochlorite has a capability to reduce pyritic sulfur and organic sulfur at high temperatures in a solution. Hypochlorite is the predominant chlorine derivative at high pHs.

This proposal is for continuation of a current project entitled “Coal Desulfurization Using Hypochlorite and Cupric ion As a Catalyst – Feasibility Study,” funded by CAST for 2003 – 2004. During the past 6 months, more than 30 experiments were conducted to explore the feasibility of desulfurization of Pittsburgh No. 8 coal with hypochlorite and cupric ammine. It was found that cupric ammine and hypochlorite could not be prepared in the same solution because ammonia used to solubilize cupric reacts with hypochlorite to hydrazine (N<sub>2</sub>H<sub>4</sub>). It was also found that cupric ammine used in a pretreatment of coal did not catalyze the desulfurization of coal with hypochlorite in the next step. The catalysis is the major theme of the current project.

Thus, a new leaching scheme was used, and a couple of experiments were conducted. The coal was leached with hypochlorite and then the leach coal was hydrolyzed in a sodium hydroxide solution at high temperatures without having a pretreatment step. It was found that this desulfurization method was better than the proposed method which had an additional pretreatment step. The results of an experiment with the new method showed that the total sulfur was reduced from 3% to 1.8% or 40% reduction at 0.68 molar hypochlorite and 0.2 molar sodium hydroxide at 90 °C. This reduction is translated into 80% reduction of pyritic sulfur and 20% reduction of organic sulfur. The chlorine content

of the hydrolyzed coal was 0.6% which is much lower than any other reported values in the literature for chlorine leaching. It is felt that the sulfur reduction could be improved if more rigorous conditions such as higher temperatures above 90 0C (but lower than 100 0C) and higher concentrations of sodium hydroxide above 0.2 molar in the hydrolysis step were applied.

It is proposed in the continuation project that the coal desulfurization process with hypochlorite leaching and then hydrolysis with sodium hydroxide be optimized in terms of particularly hypochlorite concentration and temperature. The optimization will be based on a compromise between maximum sulfur reduction and minimum hypochlorite consumption. High-sulfur coals such as Illinois No. 6 and Upper Freeport coal will be used particularly in the continuation project. The desulfurization behaviors of these coals will be compared to that of Pittsburgh No. 8 coal which will be characterized for the rest of the current desulfurization project.

#### **10. Phyto-Extraction / Fabrication of Gold and Silver Nanoparticles (WV012)**

Principal Investigator: Ray K. Yang & Eung Ha Cho, West Virginia University

Period of Performance: May 1, 2004- October 31, 2006 (2-Year Project)

In the traditional cyanidation process, cyanide solutions are used extensively to leach precious metals from crushed ores, concentrates, and enriched tailings. Being extremely poisonous, cyanide solutions are heavily regulated, if not outright banned, in many regions around the world. One of the mid- to long-term research priorities of the Center for Advanced Separation Technologies is to develop such an alternative for precious metal extraction. An emerging alternative with great potential is phytomining i.e., growing plants that hyper-accumulate high concentrations of a target metal. A phytomining operation would entail planting a hyperaccumulator crop over a low-grade ore body or mineralized soil, followed by harvesting and incineration of the biomass to ash to produce “bio-ore”. Phytomining has several advantages over conventional mining. It offers the possibility of utilizing ore bodies or mineralized soils that are otherwise uneconomical, and its effect on the environment is minimal; the area to be mined may be “ready-vegetated”; a “bio-ore” has a higher metal content than a conventional ore and needs far less space for storage. Being in its infancy, phytomining is not yet commercialized, and more research and development are still needed to make this technology cost effective. One way to make its commercialization a reality is to produce products, such as gold nanoparticles which are highly valuable in today’s marketplace and are expected to be in ever increasing demands in the future.

The long-term goal of our phytomining program is to bridge together future mining industry with nanoparticle market via phytomining. This is to be done by re-focusing phytomining at producing, not just gold ingots, but more importantly, gold nanoparticles (crystallite or primary particles measuring less than 100 nm in size) for the rapidly expanding nanoparticle market. This new and re-oriented phytomining, which may gradually start to take shape as a result of successfully conducting the proposed research, has the potential of becoming a promising method to mass produce gold and other metallic nanoparticles, making the nanoparticles produced by future mining industry

competitive in the rapidly expanding nano-product market.

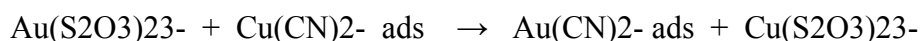
The proposed tasks of this proposal cover a broad front of experimentation in order to eventually achieve the long-term goal envisioned. The experimental studies, due to the exploratory nature of the proposed research, will focus on phyto-extraction/fabrication of gold nanoparticles from hyperaccumulator plants, bean sprouts, and plant cells grown in callus and suspension cultures. The research tasks aim at providing a better understanding of the gold nanoparticles produced by the various plants selected, the external factors that impact the forms and sizes of the nanoparticles produced in those plants, and the fundamental phyto-fabrication processes leading to their formations. One may term the proposed tasks as high risk exploratory research, but even if only one of tasks leads to a profound finding the pay-off could be reasonably high.

#### **11. Recovery of Gold from Thiosulfate Leach Liquor Using Activated Carbon (WV012)**

Principal Investigator: Courtney A. Young and Larry G. Twidwell, Montana Tech  
Period of Performance: June 1, 2005-October 31, 2006 (2-Year Project)

Gold is generally recovered from the ore by a cyanide leaching process. This procedure is used because of its simplicity and ability to work effectively at low concentrations. However, cyanide itself is highly toxic. Furthermore, it also leaches relatively non-specifically causing other metals to go into solution as well. These metal cyanide complexes can also be toxic. Resulting leach solutions have been accidentally released from various process facilities causing environmental damage. Consequently, particularly over the last decade, alternatives to cyanide leaching have been sought.

Particular attention has been given to thiosulfate; however, recovery of the gold from the thiosulfate leach presents a problem. Conventional carbon adsorption does not work so more expensive recovery processes have been investigated with resin adsorption being the most common. The research we propose to undertake investigates a novel use of activated carbon by pre-adsorbing cuprous cyanide at its surface and using it to exchange with gold in a metal-exchange, cementation-type reaction:



Resulting cuprous thiosulfate is recycled for further gold leaching with the copper serving as catalyst to the leaching process. Likewise, the adsorbed gold cyanide product can be eluted using a subsequent conventional gold recovery process common in traditional cyanide operations:



Consequently, the novel process is believed to be cost-effective and will ultimately allow thiosulfate leaching to be a viable alternative to cyanide. Because direct investigation of these adsorption reactions are masked by the location of the carbon adsorption sites in commercial activated carbons, we propose to study them in-situ using Raman spectroscopy.

We also propose to investigate using coal-based metathesis technologies to generate carbon alternatives to activated carbon. In this regard, carbon nanotubes, because of their graphite-like structure, is expected to have similar adsorption capacities and could therefore prove to be an extremely effective high surface-area alternative with high adsorptive capacity. Although nanotubes are currently expensive, their production from coal and other cheap carbon sources could be economically equivalent to coconut shell-based activated carbons.

**12. The Effect of Alkyl Diphenyl Oxide and Sulfonated Oleic Acid Surfactants on Nucleation and Growth of Potassium Sulfate Crystals: Optimization of Surfactants for the Potash Industry (NM005)**

Principal Investigator: Gillian Bond and Christa Hockensmith, New Mexico Tech  
Period of Performance: June 1, 2005-October 31, 2006 (2-Year Project)

We have shown that significant improvements occur in the crystal size distribution (CSD) of potassium sulfate crystallized from potassium sulfate/magnesium sulfate brine at 40°C in the presence of concentrations of Calfax 16L-35 {a linear, alkyl diphenyl oxide (ADO) disulfonate surfactant} well below the critical micelle concentration (CMC). The ratio of granular particles to fines is very greatly improved, with essentially all the crystals having sizes between 2 and 3mm. This size range is very desirable for potassium sulfate crystals that will be supplied for agricultural use as a spreadable fertilizer. However, the yield, at present, is too low for commercial application.

We now propose:

To optimize the yield obtainable with ADO disulfonate surfactants, while maintaining the desirable CSD.

To study the performance of sulfonated oleic acid surfactants with a view to improving CSD and yield.

The Carlsbad potash basin accounts for 85% of mined potash production in the United States and it is for the potash industry that this work's goals are set. A successful outcome to this work will benefit a critical industry in New Mexico, and help to ensure the viability of the new potassium sulfate production facility that is under construction near Carlsbad.

**13. Thiosulfate as a Replacement for Cyanide in the Presence of Activators**

Principal Investigator: Maurice C. Fuerstenau, University of Nevada, Reno  
Period of Performance: June 1, 2005-October 31, 2006 (2-Year Project)

The United States is the third largest producer of gold in the world, and Nevada is by far the largest gold-producing state in the country. In processing gold and other precious metals, cyanide is used universally as a lixiviant. It is effective and reasonably low cost and has been used for greater than a century commercially. It is an extremely toxic

reagent, however, and considerable care must be exercised to prevent personal injury and harm to the environment during and after metal processing. To obviate the downsides of the use of cyanide, considerable research has been conducted with other lixivants that are not as toxic as cyanide to establish if a replacement for cyanide can be found. These include the halides (chlorine, iodine and bromine), thiourea, thiosulfate and polysulfides. Of these reagents thiosulfate is the most promising. The problem with this reagent, however, is the stability of thiosulfate in solution. Oxidative conditions are essential for the dissolution of gold and under these conditions, some thiosulfate is oxidized to tetrathionate, and its effectiveness is greatly reduced. The development of reaction conditions is needed in which the kinetics of gold dissolution is increased, while the losses of thiosulfate by oxidation are minimized. In this investigation the use of activators in gold dissolution will be studied, and the interaction between the various parameters involved in thiosulfate leaching of gold will be carefully investigated.

#### **14. Phytomining for Nickel and Silver Nanoparticles (WV016)**

Principal Investigator: Ray K. Yang & Eung Ha Cho, West Virginia University  
Period of Performance: June 1, 2005- October 31, 2006 (2-Year Project)

Phytomining is the production of a metal by growing high-biomass plants that hyper-accumulate high concentrations of a target metal. A phytomining operation would entail planting a hyperaccumulator crop over a low-grade ore body or mineralized soil, followed by harvesting and incineration of the biomass to ash to produce “bio-ore”. Some plants are natural hyperaccumulators, while others require induction for hyperaccumulation. Phytomining has several advantages over conventional mining. It offers the possibility of utilizing ore bodies or mineralized soils that are otherwise uneconomical, and its effect on the environment is minimal; the area to be mined may be “ready-vegetated”; a “bio-ore” has a higher metal content than a conventional ore and needs far less space for storage.

The proposed research may eventually be able to bridge together future mining industry with nanoparticle market via phytomining using the nanobiotechnology techniques currently being developed at a fast pace. This may be done by re-focusing phytomining aiming to produce, not just metals, but more importantly, metallic nanoparticles for the rapidly expanding nanoparticle market. The nano-product market, on the other hand, may just as well find that the re-oriented phytomining has the potential of becoming a promising approach to mass produce nickel, silver and other metallic nanoparticles, with advantages similar to that of producing human and veterinary vaccines from plants.

The long-term goal of the proposed research is to tailor-make in large scale and at much reduced costs nickel and silver nanoparticles in the sizes and shapes suitable for use in a variety of industries with high demands for such nanoparticles. Exploratory research tasks, including investigations on nickel and silver nanoparticles in growing plants, as well as silver nanoparticles in bean sprouts and plant cells, will be conducted simultaneously through this two-year project using a scanning probe microscopy, aiming to achieve the following two objectives: (1) to show the existence of nickel and silver nanoparticles in a few carefully selected species of plants in various forms including their ashes, and (2) to study the sizes, shapes, surface characteristics, and other pertinent

features of the nickel and silver nanoparticles formed therein, and investigate the factors that influence their relevant properties.

*d) Modeling and Control*

**1. Online Monitoring and Diagnosing of Coal Fines During Separation Process (WVWV008)**

Principal Investigator: B.S. Kang and E.K. Johnson, West Virginia University  
Period of Performance: May 1, 2003- October 31, 2006 (2-Year Project)

The goal of this research program is to develop an on-line, non-contact, elemental analysis of coal fines during solid-solid separation process through the use of Laser-Induced Breakdown Spectroscopy (LIBS). Of particular interest is the detection and quantitative measurement of the amount of carbon, sulfur, mercury, and other trace elements in the separated coal fines. The proposed experimental technique will be applied to a circulating fluidized bed (CFB) riser system for determination of coal fines separation efficiency as well as optimization of the separation process variables using a fuzzy logic control approach.

**2. Development of a Novel Optical Radiation Depolarization Technique for On-Line Measurements of Particle and Bubble Sizes (KY003)**

Principal Investigators: D. Tao, M.P. Menguc and C. Crofcheck, University of Kentucky  
Period of Performance: May 1, 2003- October 31, 2006 (2-Year Project)

Grinding and froth flotation are the two most important processes for mineral beneficiation. The importance of grinding is well reflected in the fact that approximately 80% of beneficiation costs are for grinding, mainly due to high energy consumption. To reduce energy consumed by grinding, fines should be removed quickly from the grinding circuit. This requires a reliable on-line particle size analysis technique. Similarly, froth flotation is the most widely used solid-solid separation process for coal and minerals beneficiation and about 90% of mineral concentrates are produced by froth flotation. Air bubble size distribution plays an important role in flotation separation performance but optimization of bubble size distributions will only be possible if bubble size can be monitored on-line.

The proposed project is aimed at developing an optical radiation depolarization technique for on-line size measurement of particle sizes in grinding and bubble sizes in flotation. The technique is based on the analysis of angular and radial profiles of reflection and transmittance of an object subjected to a collimated, polarized light beam. A hybrid Monte Carlo/Ray Tracing method will be used to simulate the depolarization of radiation by particles or air bubbles and size distributions will be determined by best fitting experimentally determined vertical and horizontal polarization components of the radial and angular profiles of reflection and transmission. The proposed technique should also be able to determine water film thicknesses and bubble separation distance distributions in foams.

### **3. Mineral Liberation Analysis in 3D by X-Ray MicroCT for the Evaluation of Particle Separation Efficiency. (UT006)**

Principal Investigators: C. L. Lin, University of Utah

Period of Performance: May 1, 2004- October 31, 2006 (2-Year Project)

New processing technology for improved productivity and efficiency is the key to success in today's highly competitive market place. It has been well established that appropriate analytical control systems can provide for such improvements. This is especially true of the particle separation processes used in the coal and mineral industries. In general, the separation efficiency for multiphase particulate systems depends on the statistical characteristics of particle microstructures, such as composition distribution, surface exposure of mineral grains, etc. For continued technological progress in the field of multiphase particulate separation processes, the need for quantitative spatial analysis of multiphase particles in three-dimensions has increased significantly. Such quantitative information must be accurate enough so that the measured values can be used as parameters for simulation models, process design procedures, and control strategies. Cone-beam X-ray microtomography technology (XMT) offers a unique imaging capability that can produce high-resolution (a few micrometers) three-dimensional images of the internal structure of multiphase samples. We propose to adapt this new technology to the mining industry to provide for the advanced analysis of coal and ore samples; such analysis of on-line plant samples will allow continuous control of separation processes. In this regard, The primary objective of the proposed project is the development of x-ray microrotomography technology (XMT) for detailed 3D liberation/exposure analysis of coal and mineral samples. The secondary objective will be to evaluate the feasibility of the XMT technology for the control of separation processes. At present, results from traditional sink/float and polished-section analysis cannot be obtained in a reasonable amount of time to provide a satisfactory feedback mechanism for the control of various unit operations in coal preparation and mineral processing plants. This new XMT will combine the high-resolution 3-D XMT instrument and a classification algorithm in order to determine the sample composition and particle characteristics of plant samples. XMT will permit a fast, direct, and detailed 3-D analysis without sample preparation. Reconstruction of 3-D particle populations from XMT images will not only provide sufficient information to construct the true liberation spectrum for the coal and ore samples in question, but also provide information on the particle size distribution, grain size distribution, and exposed surface area of mineral matter grains contained in each particle of the population sample.

Results from the proposed research will improve the efficiency of valuable mineral recovery using direct measurement of liberation information in order to optimize the separation efficiency. The XMT technique will be of great utility for the liberation analysis of a wide variety of mineral resources, including coal, industrial minerals, and metallic ores. In this regard, the XMT technology for coal washability analysis will allow for blending control to maximize coal recovery from coal preparation plants at a specified product quality. The results from the proposed research can be easily incorporated into existing simulation and estimation software systems for convenient application in industrial practice, both in the coal industry and in the mineral industry. Development of

the XMT technology will allow for more rapid, detailed, and accurate analysis than previously thought possible.

**4. A Comprehensive Study of Froth Behaviour. (VT011)**

Principal Investigators: Roe-Hoan Yoon, Demetri Telionis and Pavlos Vlachos,  
Virginia Tech

Period of Performance: May 1, 2004- October 31, 2006 (2-Year Project)

Froth flotation is the most widely used and versatile method of separating one solid from another in the coal and minerals industries. In this process, air bubbles are used to selectively collect hydrophobic particles and rise to the surface of a flotation pulp, forming a froth phase. The stability of the froth plays an important role, as it determines the final grade, recovery and throughput. Despite its importance, little is known of the mechanisms involved in the stability of foam and, particularly, of flotation froth, as most of the information available in the literature is on dry foam without particles.

It is, therefore, proposed to conduct a comprehensive study on both dry and wet foams in the presence of particles. The proposed work will include determination of bubble size distribution, particle size distribution, liquid fraction (or air-hold-up), grade of hydrophobic particles along the heights of froth columns. The results will give information on the effects of both hydrodynamic and surface chemistry parameters on froth stability. The new information obtained in the present work will be used to develop a froth model. It will be combined with the model describing the bubble-particle interactions occurring in the pulp phase, so that a comprehensive flotation model will be developed. Since the combined model will be based on first principles, it will have predictive and diagnostic capabilities, and can be used for developing methods of improving flotation. The basic information obtained in the present work will be particularly useful for developing effective deformers, maximizing carrying capacity, and improving coarse particle flotation.

**5. Portable Sensor for Detecting Mercury and other Heavy Metals Encountered in Coal Processing and Utilization (WV013)**

Principal Investigators: A. Manivannan and Mohindar S. Seehra, West Virginia  
University

Period of Performance: May 1, 2004- October 31, 2006 (2-Year Project)

A two year research program is proposed to develop a portable and reliable sensor for on-site detection of mercury in solutions in the ppb range using boron-doped diamond (BDD) electrodes. This proposal is based on our demonstrated feasibility of detecting mercury in laboratory solutions in the ppb range using the BDD electrodes. Similar success has been accomplished for detecting Pb, Cd, and Cu in solutions. For mercury detection, the media used so far have been KCl, and KNO<sub>3</sub>. Proposed research include developing the necessary calibration curves for Hg in other media such as thiocyanate (KSCN), perchlorate, and EDTA, the use of a rotating disk electrode to improve sensitivity and reproducibility of results, and testing of the flue gas samples obtained from coal-fired plant at NETL (Pittsburgh). The tasks needed to develop a suitable

portable unit are appropriately addressed. Feasibility of similar portable system for detecting other heavy metal ions encountered in coal processing and utilization is described.

*e) Environmental Control*

**1. Electrolytic Solution Purification and Metal Recovery from Metal-Bearing Toxic Waste Streams (UT003)**

Principal Investigator: Michael L. Free, University of Utah

Period of Performance: May 1, 2003- October 31, 2006 (1-Year Project)

Industry creates numerous waste streams, many of which contain dissolved metal ions that must be removed to preserve the environment. Many of these waste streams can be created by natural processes that are accelerated by industry such as acid mine drainage, made as byproducts of chemical processing such as metal extraction, or as the result of manufacturing processes such as electronic component manufacturing. Often such wastes are complex and involve multiple metal ions. Regardless of the waste origin, toxic metal ions must be removed.

In the proposed project a novel method of removing multiple toxic metals from aqueous media by selective pulse-plating with high surface area electrodes will be evaluated and developed in a manner that will allow the metals to be recovered individually as purified metals in an environmentally sound way. The direct production of metal as a byproduct, rather than as a toxic waste, will contribute to better resource utilization as well as a reduction in toxic waste generation.

**2. Determining the Effectiveness of Gold Filters for Removing Mercury from Coal Fired Power Plants (MT003)**

Principal Investigator: K. Ganesan, Montana Tech

Period of Performance: May 1, 2003- October 31, 2006 (1-Year Project)

Because the US EPA is planning to regulate mercury emissions from power plants, there is a clear need to develop devices that can cost effectively remove mercury from power plant flue gases. Most current research has focused on transferring mercury from the air stream to fly ash or converting elemental mercury to divalent mercury to absorb it in wet scrubbers. However, when low chlorine content coal is combusted most of the mercury in the flue gas exists as elemental mercury, which is very hard to remove. Thus, to comply with the potential 90% mercury reduction proposed by EPA, one must oxidize the elemental mercury to either mercuric chloride or oxide as a way to collect particulates. In either case, mercury is merely converted to a form that is also difficult and expensive to recover. Therefore, it appears that directly removing mercury from the flue gas will be the most cost effective and environmentally friendly approach. This proposal is focused on removing elemental mercury from flue gas using gold filters. The main objective of this research is to evaluate the effectiveness of gold wire mesh in removing mercury vapor from flue gas. A wire mesh made of thin (<0.1 mm diameter) gold wires will be tested in the laboratory, initially with a synthetic gas stream containing

mercury vapor in the range of 1-300  $\mu\text{g}/\text{m}^3$ . Similar tests will be conducted in combustion gases by burning six types of western and eastern coals. The study will be conducted for six concentration levels of mercury; 5, 10, 25, 50, 100 and 300  $\mu\text{g}/\text{m}^3$ .

### **3. Development of Metallic Filters to Control Mercury From Coal Fired Power Plant Flue Gas (MT004)**

Principal Investigator: K. Ganesan, Montana Tech

Period of Performance: May 1, 2004- October 31, 2006 (1-Year Project)

The focus of this research is to develop metallic filters to remove vapor phase mercury from coal fired flue gas. Three types of metallic filters will be tested for its effectiveness in removing mercury vapor from gas streams. Based on the results, one of them will be tested for its performance in a flue gas stream of a coal fired power plant. The previous funding from CAST enabled the PI to investigate the potential of gold filters to remove mercury vapor from gas streams. The results indicate that the removal efficiency is over 90% with gold filters. In addition, preliminary tests with silver filters showed promising results. Therefore, this proposal is to test three metallic filters: copper wire with gold plating, copper wire with silver plating and copper wire mesh. These filters initially will be made in the laboratory and tests will be performed to compare their performance. Tests will be performed at concentration ranges of 1-100  $\mu\text{g}/\text{m}^3$  of vapor phase mercury. Tests also will be performed at elevated temperatures by heating the incoming air stream up to 250°F. Two bench scale systems will be designed based on the results of the laboratory and field study. These filters then will be tested in the field in a coal fired power plant flue gas stream. This field work will be conducted in collaboration with PPL Montana, in Colstrip where four coal fired power plants are in operation. The results of this field tests will provide valuable information of the performance of these filters in real world conditions. The data then will be used to design a pilot scale system for further testing.

### **4. Recovery of Chromium and Arsenic From Toxic Waste Streams by Reactive Polymer-Coated Absorbents (WV014)**

Principal Investigators: Dianchen Gang & Baolin Deng, West Virginia University

Period of Performance: May 1, 2004- October 31, 2006 (2-Year Project)

One of the major challenges facing coal and metal mining industries today is to address public concerns of environmental damage associated with the mining activities. Oxidation of pyrites and other metal sulfides in coal and metal mine tailings can generate high concentration of sulfuric acid, forming acid mine drainage (AMD) that may contain high concentrations of sulfate, iron, and many toxic elements such as arsenic (As) and chromium (Cr). The objective of this project is to develop a novel method of removing and recovering As and Cr from wastewater including AMD. Reactive polymers will be synthesized under defined conditions and their structure be optimized according to their capability for As and Cr removal and recovery. This study focuses on these anionic contaminants (i.e.,  $\text{AsO}_4^{3-}$ / $\text{AsO}_3^{3-}$  and  $\text{CrO}_4^{2-}$ ) because they are highly soluble and normally not removed by many of the treatment processes designed for divalent heavy metals such as lime neutralization and precipitation. The research objective is consistent

with the research roadmap developed by CAST on the chemical separations and environmental control issues. The development and successful testing of this material could potentially lead to a patent application.

**5. Determination of Factors Affecting the Separation of Potentially Hazardous Trace Elements and their Behavior in Coal Tailings Impoundments (KY005)**

Principal Investigators: Frank E. Huggins, Naresh Ahah, Gerald P. Huffman, University of Kentucky

Period of Performance: June 1, 2005- October 31, 2006 (2-Year Project)

A number of trace elements in coal are of significant environmental concern. Such potentially hazardous elements include As, Cr, Se, and Hg, and are regulated under either the 1990 Clean Air Act Amendments or the 1976 Resource Conservation and Recovery Act or both. Coal cleaning is performed principally to minimize the amount of pyrite and other mineral matter entering pulverized coal combustion. At the same time, hazardous trace elements associated with these minerals are also removed from coal combustion and hence their environmental impact during combustion is thereby reduced. However, such trace elements tend to be concentrated in the waste tailings from coal separation technologies, which normally are disposed of under water in coal waste impoundments. Here, trace elements may pose other environmental problems because both major and trace elements may be leached and mobilized. Consequently, the waters in such impoundments have to be isolated from the local groundwater in order to avoid possible contamination of local drinking water supplies. Despite concerns about solubilized trace elements in coal impoundments, relatively little is known about the concentrations and specific chemical forms of such trace elements that can be leached from coal minerals and mobilized in these waters. More data are clearly needed to assess the environmental hazard from mobilized ions in coal tailings impoundments.

The behavior of trace elements in both coal separation technologies and tailings disposal scenarios depends on their modes of occurrence and associations with major minerals or macerals in the coal or coal fractions. Such information is rarely determined, but is of vital importance to our understanding of trace elements in these processes. In this proposal, we intend to determine the mineral or chemical forms (mode of occurrence) and association of a number of critical trace elements (As, Cr, Se, Hg, etc.) in coals and coal fractions using a comprehensive array of conventional and advanced characterization methods. Our intention is to collaborate with other CAST-supported investigations of advanced coal separation technologies that can supply the clean coal and tailings fractions needed for this investigation. The information obtained will then be used (i) to determine the efficiency of various coal cleaning methods for specific trace element removal; (ii) to interpret the behavior of specific elemental forms and associations in coal tailings exposed to water in laboratory simulations of storage ponds; and (iii) to assess the actual environmental impact posed by specific trace elements in coal tailings impoundments.

**6. Mercury Reduction From Coal Power Plant Emission Using Functionalized Ordered Mesoporous Carbons (FOMCs) (WV015)**

Principal Investigators: Dianchen Gang & Baolin Deng, West Virginia University

Period of Performance: June 1, 2005- October 31, 2006 (2-Year Project)

One of the major challenges facing coal-fired power plants (CFPPs) today is to address the public concerns of mercury emissions. Mercury emitted from CFPPs exists in two valence states: elemental mercury (Hg<sup>0</sup>) and oxidized forms (Hg<sup>2+</sup>). Elemental mercury is normally dominant, accounting for 92% to 99% of the total mercury in the flue gas. The effectiveness of an individual control technology for Hg emission depends largely on its chemical speciation. For example, Hg<sup>0</sup> is highly volatile with low water solubility, therefore, it is not absorbed significantly by water-based scrubbing processes. The objective of this project is to develop and evaluate functionalized ordered mesoporous carbons (FOMCs) for the maximum Hg removal from flue gas emissions at high temperature (80 – 200°C). Highly ordered mesoporous carbons (OMCs) with uniform nanopore size will be synthesized under defined conditions and their structure optimized according to their capability toward Hg removal in the high particulate environment. OMCs will be functionalized by elemental sulfur and other chemicals to enhance Hg uptake. The research objective is consistent with the research roadmap developed by CAST on the chemical separations and environmental control issues. The development and successful testing of this material could potentially lead to a patent application.

**7. Removal of Metal Ions from Acid Mine Drainage using a Novel Low-Cost, Low Technology (WV017)**

Principal Investigators: Benjamin Dawson-Andoh, West Virginia University

Period of Performance: June 1, 2005- October 31, 2006 (2-Year Project)

Acid Mine Drainage (AMD) produced by active and dormant coal mines continues to pose a major threat to the environment. One of the goals of the National Energy Policy developed by President Bush in 2001 is “to ensure the steady supply of affordable energy in environmentally responsible and sustaining manner.” Current technologies employed to remove toxic environmental polluting metals from AMD are expensive and economically challenging to the Coal Mining Industry. The work proposed here seeks to evaluate a low-cost, low technology that employs renewable biomaterials: wood and fungal biomass, to remove toxic metals that occur in AMD. Additionally, the proposed work also seeks to determine the recovery potential of toxic metals from the biomaterials and the regeneration and re-use of the biomaterials. West Virginia is one of the premier hardwood States in the US and tremendous amount of wood biomass is available as residue. The proposed study if successful will provide an avenue for the use of the tremendous wood biomass generated by both the primary and secondary forestry operations in West Virginia.

## **EXPERIMENTAL**

The CAST initiative is comprised of a diverse group of subprojects, most of which are multistage, task-oriented developmental projects that cannot be conveniently categorized by the traditional reporting criteria required by the DOE Uniform Reporting Requirements. For example, several of the projects have required the construction of unique test equipment, others the generation of simulation models, etc., as preliminary tasks in the overall execution of the project. As such, they are more appropriately described and discussed as “Project Tasks” within the context of the individual Technical Progress Reports. These reports are attached to this document as Appendices and should be referred to for this information.

## **RESULTS AND DISCUSSION**

The CAST initiative is comprised of a diverse group of subprojects, most of which are multistage, task-oriented developmental projects that cannot be conveniently categorized by the traditional reporting criteria required by the DOE Uniform Reporting Requirements. For example, several of the projects have required the construction of unique test equipment, others the generation of simulation models, etc., as preliminary tasks in the overall execution of the project. As such, the presentation of results is more appropriately described and discussed within the context of the individual Technical Progress Reports. These reports are attached to this document as Appendices and should be referred to for this information.

## CONCLUSIONS

There are currently forty six (46) sub-projects being funded of which three (3) are completed and final reports will be issued.. A six-month Progress Report (covering the period October, 2005 1-March 31 30, 2006) for the active projects was generated for each of these sub-projects and has been attached to this document as an Appendix. A brief summary of progress during thereportin period, along with plans for the future on each of the sub-projects is given below.

### *a) Solid-Solid Separation*

#### **1. Development of Novel Ultrafine Sizing Methods. (Joint UK/VT Project) (KY001/VA008)**

Principal Investigators: R.-H. Yoon and G.H. Luttrell, Virginia Tech

Principal Investigators: R.Q. Honaker and BK. Parekh, University of Kentucky

Period of Performance: May 1, 2003-October 31, 2006 (2-Year Project)

Project work was continued during the past reporting period to investigate a variety of techniques for high efficiency sizing of ultrafine particles. Much of the work conducted to date focused on improving the performance of classifying cyclone system with a new water injection apex. This effort included (i) installation of automatic sampling system and testing of a new water injection system, (ii) preprocessor work for Computational Fluid Dynamics (CFD) analysis using GAMBIT v 2.0 software (i.e. geometry construction and meshing generation). The test work conducted to date indicates that a new water injection apex substantially reduces the amount of ultrafine solids that are bypassed to the coarse fraction without increasing the particle cutsize.

Work will continue to evaluate the classification performance of the hydrocyclone equipped with the water injection apex. Furthermore, a wide variety of theoretical studies will be continued in an attempt to develop a better understanding of the problems associated with ultrafine particle sizing. These studies will include computational fluid dynamics (CFD) application to predict classifier performance.

#### **2. Dispersion and Flotation of Clays from New Mexico Potash Ores. (NM001)**

Principal Investigators: I. Gundiler, S. Titkov, and M. Yekeler, New Mexico Tech

Period of Performance: May 1, 2003- October 31, 2006 (1-Year Project)

The beneficial effects of dispersants on desliming of medium ores and on subsequent KCl flotation recoveries have been demonstrated, and feasibility of flotation desliming following the first stage coarse ore mechanical desliming has been presented. Beneficiation of very high-clay ores (11% IR) by two stage mechanical desliming followed by slime flotation has also been achieved. Those results will be presented in the next report.

**3. Flotation Technology for the Trona Industry. (UT001)**

Principal Investigator: Jan D. Miller, University of Utah

Period of Performance: May 1, 2003- October 31, 2006 (2-Year Project)

The project is complete and a final report is to be issued.

**4. Flotation Processes/Experiments and Analysis. (VT009)**

Principal Investigators: D. Telionis and P. Vlachos, Virginia Tech

Period of Performance: May 1, 2003- October 31, 2006 (2-Year Project)

In many industrial applications, like in mineral flotation, interactions of solid particles and/or bubbles and particles depend on the characteristics of turbulent flow. In many analytical models, the rate of collision is a function of turbulence dissipation. It has been known that dissipation is larger in the neighborhood of the agitating mechanism, in our case the Rushton impeller. This is somewhat anti-intuitive, because energy is dissipated at the smallest eddy scales, and the immediate vicinity of the impeller contains large vortical structures and provides little space or time for such structures to break down. In this paper we provide further evidence that larger dissipation values in the vicinity of the impeller is consistent with the dynamic motion generated by the blade passage. The flow in the impeller stream of a Rushton impeller can be best summarized as a radial jet with a pair of tip vortices. The maximum and mean normalized dissipation in the impeller stream showed decreasing trends with the Reynolds number. Other normalized turbulence quantities, namely  $U_{rms}$ ,  $V_{rms}$  and vorticity magnitude scaled as constant values with the Reynolds number. Estimates of turbulence characteristics and in particular distributions of turbulent energy dissipation determined in this study will be used in estimating rates of collisions of bubbles and particles in flotation cells.

This project has been essentially completed. We are further analyzing the data obtained and preparing the final report.

**5. Column Flotation of Relative Coarse and Fine Dolomitic Phosphate Pebbles. (WV007)**

Principal Investigator: Felicia F. Peng, West Virginia University

Period of Performance: May 1, 2003- October 31, 2006 (2-Year Project)

Additional dolomitic phosphate sample was received from Mosaic Co. (IMC Global, Inc.), FL recently. We have scheduled to run the tests on the next relative coarser size level of the sample, by applying FAS-40A dolomite collector with some frothing agent supplied by ARR-MAZ, FL. The material will be characterized and dolomite flotation will be tested in a stirred tank cell for determination of the range of reagent requirements and improvement of flotation conditionings. Based on the stirred tank cell flotation results, the column cell flotation will be conducted.

**6. Beneficiation of Mixed Potash Ores From New Mexico. (NM004)**

Principal Investigator: Ibrahim Gundiler, Lynn Brandvold, Tanja Pietraß, Stanislav

Titkov, New Mexico Tech

Period of Performance: May 1, 2004- October 31, 2006 (2-Year Project)

Investigations on improving the efficiency of sylvite (KCl) recovery from mixed ores in order to prepare feedstock for langbeinite flotation continued during this phase. One-stage slime flotation from dry ground ores conducted to eliminate rod mill grinding and desliming steps which are time consuming and lead to higher solubility losses during tests. Effect of excess guar on flotation of KCl was investigated along with the concentrations of oil and frother in the amine emulsions. Reverse flotation, i.e., flotation of halite from langbeinite fines were initiated to upgrade high-grade fines and eliminate water leaching of halite. Tests on direct flotation of langbeinite from halite and sylvite brines are currently underway. The results will be reported in the next progress report.

Investigations on the recovery of langbeinite from sylvite tailings in mixed ores, flotation and separation of langbeinite and kieserite from low-grade langbeinite ores will be pursued using a variety of collector families and flotation schemes. At the same time fundamental studies for better understanding of soluble salts flotation will be initiated. These studies will include brine chemistry and temperature, zeta potential measurements, AFM and NMR studies.

#### **7. Development of New Reagents for the Flotation of Dolomite from Phosphate Ore. (NV002)**

Principal Investigators: Maurice C. Fuerstenau, Manoranjan Misra and Thomas W. Bell, University of Nevada, Reno

Period of Performance: May 1, 2004- October 31, 2006 (2-Year Project)

Flotation collectors, hexadecyl citric acid ester and lauryl sarcosine were tested as flotation collectors. Results indicate that selectivity of dolomite from apatite may be possible with hexadecyl citric acid ester as collector at about pH 6. Flotation was not achieved from an ore with lauryl sarcosine. Analogs of this reagent with longer hydrocarbon chains are being synthesized for testing as flotation collectors for selective separation of dolomite from phosphate rock.

Additional collectors are being synthesized and are to be tested for selectivity in the flotation separation of dolomite over apatite and phosphate rock..

#### **8. High Frequency Eddy Current Separation of Metallic Residue from Slags, Sands, Electronic Scrap and Other Wastes. (UT004)**

Principal Investigators: Raj K. Rajamani, University of Utah

Period of Performance: May 1, October 31, 2006 (2-Year Project)

From the above experiments it was concluded that shape changing and circuit optimization were heading in the right direction. A very high force was experienced by the particles in the magnetic field. The average deflection for copper was found to be much higher than the aluminum particles. This suggests that change in particle size could also affect the deflections

Further optimization of the circuit will be carried out to about 1-5 KHz frequency. More particle drop and pendulum tests will be carried out at these frequencies to understand the effect of lower frequency magnetic field on the particles. Small separation experiments will be carried out at this scale. A bigger core has been under investigation and will be ordered very soon. Proper pilot scale separation will be carried out with this bigger core and finally the setup will be tested for industrial scale separations

**9. Dry Particle Separation in a CFB Riser System. (WV009)  
(Continuation from CAST 1)**

Principal Investigator: Eric Johnson and Bruce W. Kang, West Virginia University

Period of Performance: May 1, 2004- October 31, 2006 (2-Year Project)

To date, we have successfully completed Tasks 1 and 2. The results of these tasks show that particles may be effectively separated by either density or size difference. For Task 3, the initial tests with waste coal have been disappointing. The basic reason for the ineffective separation are: 1) the size of the coal particles are so small that the desired lateral forces are not developed, and 2) the waste coal possess a combined continuous size distribution and a continuous variation in density. The particles employed in Tasks 1 and 2 were larger and possessed a fixed density. However, these initial tests have provided an insight into how to improve the separation process for the waste coal. The riser systems are now being modified and a new set of operating conditions have been selected.

In order to complete Task 3, the riser system modifications will be completed by mid-June, 2006. A new set of operating parameters will be employed in the next set of tests. These tests should be completed by early September, 2006. The final analysis of the data will then be completed. This analysis will investigate the conditions necessary to scale the experimental systems to industrial size systems. It is now anticipated that the final results from this effort will be completed and presented in the final report, due in December 2006.

**10. Studies of Froth Stability and Model Development. (VA002)**

(Continuation from CAST I)

Principal Investigator: Roe-Hoan Yoon, Virginia Tech

Period of Performance: May 1, 2004-May 31, 2006 (2-Year Project)

The film thinning kinetics of PPG has been studied using the thin film pressure balance technique (TFPB). It is found that the hydrophobic force in the thin films decreases systematically with increasing PPG concentration. As compared to MIBC, PPG is more capable of reducing the hydrophobicity of air bubbles and, therefore, a more powerful frother.

Future work will investigate the surface forces in foam films in the presence of polymers.

**11. Direct Measurement of Forces in Flotation. (VA004)**  
**(Continuation from CAST I)**

Principal Investigator: Roe-Hoan Yoon, Virginia Tech

Period of Performance: May 1, 2004- October 31, 2006 (2-Year Project)

The equilibrium film thicknesses of a wetting film in different NaCl solutions on oxidized hydrophilic silicon wafer surface were measured. The experimental results show that equilibrium film thickness decreases with salt concentration increasing. The experimental data are a little larger than those from calculation of classical DLVO theory. The experimental equilibrium film thicknesses at different salt concentrations are generally a little larger than those obtained from theoretical calculation. It may originate from the underestimate of the capillary diameter, which accordingly decreases the theoretical equilibrium film thickness. In another possibility, the surface charge density on oxidized silicon wafer may be higher than the one used in theoretical calculation, of which the value is for silica.

Experimental techniques are to be improved to decrease the experiment error hydrophilic substrates. Systemic measurements of equilibrium film thickness for wetting film in electrolyte solutions at different salt concentrations are to be done on hydrophobic substrates with different hydrophobicity. The results attained on hydrophobic surfaces will help detect the existence and range of the “hydrophobic force”.

**12. Enhanced Flotation Performance Through Column Froth Enrichment**

Principal Investigators: Rick Q. Honaker and Daniel Tao, University of Kentucky

Period of Performance: June 1, 2005-May 31, 2005 (2-Year Project)

A graduate research assistant joined the research team with the responsibility of performing the tests required in this investigation under the direction of the principal investigator. A significant portion of the reporting period was devoted to flotation operation training and optimization. At the present time, research findings regarding selective detachment as a means of enhancing flotation performance have not developed from the current investigation. However, tests are being performed to optimize the conditions in the collection and froth zones of a flotation column.

The coal sample that will be used in this investigation was obtained from a Consol preparation plant located in Pennsylvania. The plant treats coal from the Pittsburgh No. 8 seam. The sample was obtained from the run-of-mine feed stream to the preparation plant. Upon arriving at the UK laboratory, the sample was crushed and ground to a particle size needed for the flotation experiments.

First priority will be finish with the optimum setting of flotation column by doing some test that guarantee correct performance, comparing their results with release analysis results obtain for the same sample used in flotation column. The step will be to prepare enough samples (crushing and screening process) to first program test and finally run some program schedule test.

**13. Engineering Development of a Fine Particle Heavy Medium Separator (VA012)**

Principal Investigators: Gerald H. Luttrell, Virginia Tech and Robert Moorhead, Krebs Engineers, Inc  
Period of Performance: June 1, 2005-October 31, 2006 (2-Year Project)

Initial work has begun to design, fabricate and construct a prototype heavy medium cyclone specifically designed for treating fine coal. The work completed to date includes shipping of the necessary components from Krebs Engineers to the Virginia Tech test facility, assembly of these parts with components fabricated at Virginia Tech, and the initial setup of the associated pilot-scale circuitry necessary to evaluate the new technology. A preliminary test plan has also been developed for future testing of the prototype separator.

Future work will focus on the completion of construction activities and initiation of preliminary shakedown tests for the prototype heavy medium cyclone.

**14. Improved Destruction and Control of Residual Flotation Froths (VA014)**

Principal Investigators: Gerald H. Luttrell and Roe-Hoan Yoon, Virginia Tech  
Period of Performance: June 1, 2005-October 31, 2006 (2-Year Project)

During this reporting period, frother partitioning studies and froth evaluation tests were conducted at an industrial plant site. The frother partitioning studies indicate that the samples must be taken in the field to avoid frother decomposition and/or adsorption on coal particles that interfere with the measurements. Preliminary results from the froth evacuation tests indicate that direct evacuation is not by itself capable of deaerating coal flotation froths. Modifications have been made to the test apparatus in an attempt to improve this technique.

During the next reporting period, plant water will be analyzed with the new approach described above for its frother content (surface tension measurements), size distribution, combustibles and ash content and, chemical composition. Froth stability tests will also be carried out to develop a better understanding of the effects of particles size and frother content on froth stability. A modified froth evacuation system will also be examined in more detail.

**15. Development of a Turbulent Flotation Model and a Computer Simulator (VA015)**

Principal Investigators: Roe-Hoan Yoon and Gerald H. Luttrell, Virginia Tech  
Period of Performance: June 1, 2005-October 31, 2006 (2-Year Project)

CAST has developed a new flotation model using energy barriers and kinetic energies for bubble-particle interactions in turbulent flow. This model could predict flotation from both surface chemistry and hydrodynamic parameters. The model developed in the present work is by no means complete, as flotation is a complex three-phase phenomenon and much is still unknown. The most difficult part of modeling flotation under turbulent flow conditions is to accurately determine the kinetic energies involved in the subprocesses of bubble-particle attachment and detachment, which in turn are related to the energy dissipation. In the present work, a flotation cell was subdivided into two compartments, i.e., high and low energy dissipation zones. The model simulations showed good agreement with experimental data from the literature.

Better understandings and modeling may be made from the studies of local energy dissipations via CFD (Computational Fluid Dynamics). The model can also be implemented by taking into account the bubble size changes due to energy input. In addition, a more analytical, not the empirical, model of froth recovery is another key factor for advanced model.

**16. Novel Surfactants as Collectors for Froth Flotation (VA015)**

Principal Investigators: Richard D. Gandour, Virginia Tech  
Period of Performance: June 1, 2005-October 31, 2006 (2-Year Project)

The following was accomplished:

Accomplished fabrication of micromanipulator which is used to glue small spherical particles to cantilever.

Gold spheres were produced by melting the gold micro powder in a high temperature furnace.

A Hamaker constant of  $1.2 \times 10^{-20}$  J was derived from surface force measurement on bare gold surface.

Attractive hydrophobic force was observed on the thiol treated gold surface, while no step was found in the force measurement.

The following future work is planned:

Conduct force measurement on gold which will be treated with a thiol solution at different electrochemical potentials.

Conduct force measurement using spheres and plates of zinc sulfide.

Conduct force measurement using spheres and plates of silver.

## ***b) Solid-Liquid Separation***

### **1. Improving Densification of Fine Coal Refuse Slurries to Eliminate Slurry Ponds. (KY002)**

Principal Investigators: B.K. Parekh and R.Q. Honaker, University of Kentucky

Period of Performance: May 1, 2003- October 31, 2006 (2-Year Project)

The laboratory scale continuous Deep Cone Thickener tests confirmed that it is possible to reproduce the results achieved in a semi-continuous T- Flocc apparatus on a continuous basis. An underflow percent solids of about 52% could be obtained from a slurry containing 10% solids on a continuous basis. The effect of cationic flocculant is evident at higher bed depths, which helps to release the water from the flocs.

We are in the process of preparing a final report on the project.

### **2. Development and Testing of a Horizontal Pressure Belt Filter. (VA010)**

Principal Investigators: R.-H. Yoon & G.H. Luttrell, Virginia Tech

Period of Performance: May 1, 2003- October 31, 2006 (2-Year Project)

During the latest project period, construction and assembly of the major components of the pressure belt filter were completed. The pressure vessel was shipped to a fabrication and welding shop to have two sight glasses installed, to check all of the welds for safety reasons, and to manufacture two end plates for the vessel. Also, the fabrication shop performed a hydrostatic test on the completed vessel and determined that vessel is structurally sound. All of the electrical and pressure vessel safety checks have been completed. Shakedown testing is now underway (i) to complete the performance testing

all of the major components, (ii) to test their operational effectiveness of the unit, and (iii) to remedy any design weaknesses that may be identified.

Work during the next reporting period will continue to include some fabrication and assembly activities as required based on the results obtained from the shakedown tests. This work will be followed by a detailed test program and economic evaluation. The detailed test program will include a study of key operating variables including feed flow rate, feed solids content, feed size distribution, filter belt speed, filter cloth mesh size, and applied pressure.

### **3. Development of a Fine Particle Centrifuge. (VA006)**

(Continuation from CAST I)

Principal Investigators: G.H. Luttrell & R.-H. Yoon, Virginia Tech

Period of Performance: May 1, 2004- October 31, 2006 (2-Year Project)

During this reporting period, construction of a continuous unit was continued and the problem in the mechanical water seal was eliminated. Several series of shakedown tests were carried out in batch mode. The data indicate that the moisture reduction is significantly better at higher rotation speeds and with the injection of air. However, the capabilities of the prototype cannot be fully established until additional tests are completed with the unit operating in continuous mode. This mode of operation required the integration of a thickening unit into the test circuitry. This modification makes it possible to improve fines recovery by circulating fines previously lost through the screen back to the circuit feed.

Future work will involve any improvements necessary to achieve a stable process. Once proven, detailed tests will be run to fully evaluate the capabilities of the unit for a variety of coal samples and over a wide range of operating conditions.

### **4. Improvements in Screen Bowl Centrifuge Performance. (VA013)**

Principal Investigators: Robert C. Bratton & G.H. Luttrell, Virginia Tech

Period of Performance: May 1, 2004- October 31, 2006 (2-Year Project)

Field tests conducted in the present work again demonstrate that flocculant injection can be used to effectively reduce the solids content of main effluent that is discarded by a screen-bowl centrifuge. The in-plant tests indicate that both reagent dosage and type is important in obtaining the best overall results. The test data also suggest that the moisture content of the screen-bowl product may increase slightly due to the recovery of fine particles displaced from the main effluent. For the tests conducted to date, the data suggest that the increase in moisture is only about 2 percentage points.

During the next reporting period, test work will again focus on the characterization of full-scale screen-bowl centrifuge performance at an industrial site. The tests are to be performed as a function of key operating variables (i.e., feed slurry flow rate and solids content).

c) *Chemical/Biological Extraction*

**1. Bio-Assisted Heap Leaching of Nickel Laterites for the Development of a Domestic Nickel Industry. (UT002)**

Principal Investigator: S. Duyvesteyn, University of Utah

Period of Performance: May 1, 2003- October 31, 2006 (2-Year Project)

This project is completed and a final report is to be issued.

**2. The Development and Utilization of Alkaline Sulfide Leaching and Recovery of Gold. (MT001)**

Principal Investigator: C. Anderson and L.G. Twidwell, Montana Tech

Period of Performance: May 1, 2003- October 31, 2006 (2-Year Project)

Notable progresses have been achieved in proving activated carbon as the optimal substrate to remove gold from ASGLS solution. Also, a tremendous step forward has been achieved in the development of waste solution treatment of the system. It has been proven that NaOH can be regenerated using the electrodialysis process and can effectively be recirculated to the leaching stage of the system. Additional leaching of real industrial concentrates, in which cyanide has been traditionally been less effective, proved that the ASGLS is a highly effective and selective system. Finally, a simple bench-scale batch simulation was developed to test the cohesiveness of the three unit processes developed for the ASGLS (leaching, recovery, and waste treatment). Plenty of precious data regarding the stability and parameters of the solution before and after each unit processes were able to be collected; thus simulating, as close as possible, a real working circuit by only using lab-scale equipments.

Future work will be focused in the following three areas:

Optimization of the proposed treatment methods of the produced H<sub>2</sub>SO<sub>4</sub> solution from the electrodialysis process: ammonium sulfate and gypsum production.

A bench-scale batch simulation with PDGS pyrite concentrate as feed material to test for system consistency and monitoring of important parameters of the system.

A method for stripping gold from activated carbon.

**3. Hydrometallurgical Processing of Chalcopyrite Concentrates. (NV001)**

Principal Investigator: M. Misra and M. Fuerstenau, University of Nevada, Reno

Period of Performance: May 1, 2003- October 31, 2006 (2-Year Project)

The project has been completed and a final report will be issued.

**4. Simultaneous Electrolysis of Copper and Ferrous Ions to Produce Copper Cathode and to Regenerate Ferric Sulfate - The Lixiviant to Dissolve Copper Sulfide Minerals. (MT002)**

Principal Investigator: C. Young, H.-H. Huang and C. Fabian, Montana Tech

Period of Performance: May 1, 2003- October 31, 2006 (2-Year Project)

Various tests were conducted over a three-year period to investigate the feasibility of electrowinning copper (Cu<sup>0</sup>) from cupric (Cu<sup>2+</sup>) while simultaneously oxidizing ferrous (Fe<sup>2+</sup>) to ferric (Fe<sup>3+</sup>) using a membrane cell. Results indicated that several variables were important to consider to minimize the applied voltage while keeping current density at a maximum. These variables included electrolyte concentrations (Cu<sup>2+</sup> and Fe<sup>2+</sup>), agitation/flow-rate, applied voltage, and temperature. Other variables were also tested: cathode type, anode type, membrane type, and cell design; however, certain ones showed superior behavior and included carbon-cloth as the anode, microporous ceramic (used in car batteries) as the membrane, and the THC-design as the electrowinning cell. Although 304 Stainless Steel was selected for the cathode, copper starter sheet performed equally as well and could have been selected. Ensuing factorial-design experiments were therefore conducted with these 4 variables fixed in order to investigate the effects of the other variables. For simplicity and to minimize the number of experiments, the temperature was held constant at 200C (room temperature). Concentrations of Cu<sup>2+</sup> and Fe<sup>2+</sup> were varied between 10 and 50 g/L, flowrates were varied between 0 and 540 mL/min, and the applied voltage was varied between 0.8-2.5 Volts. Results were then statistically analyzed using StatEase software and yielded the following model:

$$\begin{aligned} \text{Log}_{10} (\text{Current Density}) = & 0.97876 + 3.56 \cdot 10^{-3} \cdot [\text{Cu}^{2+}] - 3.95 \cdot 10^{-4} \cdot [\text{Fe}^{2+}] + \\ & 0.51 \cdot \text{Volts} \\ & + 8.13 \cdot \text{Flowrate} - 3.1 \cdot 10^{-4} \cdot \text{Volt} \cdot \text{Flowrate} \end{aligned}$$

From the model, it was concluded that the current density and therefore copper production would be increased by increasing the cupric concentration, applied voltage, and/or flowrate; however, a small binary effect between flowrate and applied voltage was observed that had a negative effect on the system. Furthermore, a negative effect on current density was also realized by increasing the ferrous concentration. Applied voltage and flowrate are the most significant variables due to the large values of their respective coefficients. Optimization of the model indicates that the voltage can be decreased from an industrial standard of approximately 2.0 Volts to between 1.5-1.7 Volts which equates to energy savings of 15-25%. Furthermore, the model concurs with fundamental understanding of electrowinning principles including equations for solution capacitance, Butler-Volmer, Fick's and Tafel.

Various tests were also conducted in collaboration with Montana Resources, a local Montana mining company in Butte, to see if ferric leaching could be used on their Central Zone Ore (CZO) and implemented along with the membrane electrowinning technology. It was noted that CZO does not respond as well as to their flotation operations as the traditional East and West Zone Ores do. Recoveries run low between 85-90% but should be in excess of 90% whereas grades run between 15-20% copper but should be in excess of 28%. This poor metallurgical performance is attributed to the different mineralization. Instead of the major copper mineral being chalcopyrite (CuFeS<sub>2</sub>), it is a coating of covellite (CuS), digenite (Cu<sub>1.8</sub>S) and chalcocite (Cu<sub>2</sub>S) on pyrite (FeS<sub>2</sub>). In order to recover these secondary copper minerals, the pyrite must be floated which, of course,

dilutes the concentrate grade. Furthermore, because the copper minerals are present as coatings, comminution likely causes their fines and thus leads to a low recovery as well.

On the other hand, the mineralogy is perfect for ferric leaching. In this regard, preliminary test helped establish important variables for leaching and included particle size of the ore, percent solids by weight, temperature of the system, and duration of the leach. Factorial design experiments were therefore conducted to develop a model that would lead to optimal leaching conditions. Unfortunately, results indicated that no more than approximately 60% extraction could be achieved. Diagnostic leach tests indicated that primary copper sulfide minerals must be present (i.e., chalcopyrite) in CZO because they do not leach well with ferric. A literature search of the geology and mineralization concurred and thereby concluded that ferric leaching is not a method to consider for copper extraction. However, as a result of this study, Montana Resources is exploring options for recovering the copper by leaching. It is recommended that they do so by processing the CZO through their current facilities and using an agitation leach on the resulting flotation concentrate to minimize the amount of material being contacted. This would also prevent problems from the clay content which is present in the CZO but would be mostly removed by the flotation process.

This is the final report for this project. It is likely that MR and the PI's will team up again to write a follow-up proposal in the next CAST cycle pending everyone's availability. In this regard, future work is planned. Overall, the project met with many successes as noted by the Publications and Presentations list in the second to next section. It is particularly worthy to note that the project supported 3 graduate students instead of the 1 that was originally proposed. Mr. Dave Douglas graduated in May of 2005 but, due to unfortunate circumstances, had to go non-thesis. This, together with the unfortunate loss of Eric Dahlgren as the postdoc, forced the project to be extended. Mr. Francis Dakubo graduated in May of 2006 with a thesis on the electrowinning work. Mr. Thom McIntyre also graduated in May of 2006 with a thesis on the ferric leaching work. Both were more than happy to be engaged in a fully funded project thanks to CAST.

## **5. Ion Exchange Recovery of Cobalt from Copper Leach Solutions. (NM002)**

Principal Investigator: I. Gundiler and M. Hatch, New Mexico Tech

Period of Performance: May 1, 2003- October 31, 2006 (2-Year Project)

valuation tests on two of our new chelating resins, a highly picolylated diethylene triamine resin (CHEL-38), and a less picolylated diethylene triamine resin (CHEL-40), were described in the last report. Absorption capacity tests for Cu, Co, Ni, Al and Fe cations were made at varied pH and metal concentrations in comparison with the commercially available resins. The present report describes tests and results for small column operating tests on actual copper mining raffinate solutions. Comparison tests were made with the commercially available hydroxypropyl picolyamine resin (HPPR, Dow XFS-43084) and dipicolyamine resin (DPAR, Dow XFS-43578) ground to similar particle sizes. Our new picolylated polyamine resin (CHEL-40) showed the best

comparative capacity for cobalt, copper and nickel, and desirably, the least Fe<sup>3+</sup> capacity in the column absorption tests at fast flow rates. Both our new resins performed better than the commercially available resins, especially for cobalt absorption capacity from the pH 2.1 mining raffinate. When 200 bed volumes of the raffinate solution was passed at high flow rates on a small bed of the best performing new resin (CHEL-40), significant amounts of cobalt and nickel were absorbed on the resin along with only a minor amounts of iron from the raffinate. The absorbed cobalt (along with nickel, iron and zinc) could be eluted easily from the resins by using water and 0.1M H<sub>2</sub>SO<sub>4</sub>. The absorbed copper required 1M H<sub>2</sub>SO<sub>4</sub> solutions for effective elution.

Further laboratory development work will include (1) the improvement and scale up of our syntheses of picolyated diethylenetriamine resins and (2) further column work on the performance with mining solutions of these and other new resins.

**6. The Effect of Diphenyl Oxide Surfactants on Nucleation and Growth of Potassium Sulfate Crystals: Development of Enhanced Surfactants for the Potash Industry. (NM003)**

Principal Investigator: G. Bond and C. Hockensmith, New Mexico Tech

Period of Performance: May 1, 2003- October 31, 2006 (2-Year Project)

Although the total crystal yield (including unusable fines) is reduced by additions of Calfax surfactants, appropriate amounts of surfactant result in very substantial increases in the yields of crystals in a desirable, marketable size range. Both Calfax 16L-35 and Calfax DB-45 have shown promising results in limiting nucleation, increasing crystal size, and narrowing the CSD's.

Future work will include the analysis of the influence of Calfax 16L-35 and DB-45 additions is being completed. Tests will then be extended to other surfactants. Candidates currently under consideration are other Calfax surfactants provided by Pilot Chemical Company (Santa Fe Springs, CA), and oleic acid surfactants, to determine whether the combination of marketable crystal yield and CSD can be further enhanced.

**7. Overcoming Technological Barriers to More Efficient Recovery of Copper from Chalcopyrite. (UT005)**

Principal Investigator: Michael L. Free, University of Utah

Period of Performance: May 1, 2004- October 31, 2006 (2-Year Project)

Copper electrodeposit morphology is controlled to a significant extent by mass transport. Improvement in the mass transport resulted in smoother deposits. It was also shown that pulsing also reduced surface roughness. Gelatin gave more uniform for longer deposition times deposits compared to those obtained without any additives. The surface roughness in solution containing gelatin slightly increased with increase in *i/i<sub>L</sub>* ratio.

Further work will be conducted to investigate the effect of waveforms on nucleation and growth process of electrodeposited copper, develop the understanding of why the

gelatin works better than other organic additives and study the effect of inorganic additives on the surface roughness.

## **8. Development of Chemical and Biochemical Techniques for the Extraction of Mercury from Fine Coal Particle Solutions. (WV010)**

Principal Investigator: Scott M. Hurst, Anthony G. Abatjoglou and Jay M. Weidemann, West Virginia University

Period of Performance: May 1, 2004- October 31, 2006 (2-Year Project)

We have isolated and definitively identified bacteria from a coal wastewater containment pond and cultured them in the presence of 1.5 mM Hg<sup>2+</sup>. These bacteria were genetically characterized with respect to the Mer genes. We have isolated plasmids for one strain of Hg<sup>2+</sup>-resistant bacteria. Subsequently we have transferred non-resistant bacteria with that plasmid. Preliminary results indicate this plasmid confers resistance to mercury compounds. A new class of adsorbents that are very effective in removing low concentrations of mercury and other metals from water has been discovered. These novel adsorbents, unlike prior art adsorbents, are easy to prepare and regenerate at low cost. A patent application on these adsorbents has been written and will be submitted to the US patent office in February. A large number of mercury organic ligands have been surveyed searching for mercury-selective binding ligands. We have extensively studied a class of bio-organic ligands (proteins) called “metallothioneins” which are used to regulate metal ions in living organisms. The ongoing goal is to understand the nature of the coordination chemistry of the binding sites of these large molecules and extend their specificity for mercury binding to common ligands for use in this process. If successful, the basis has been found for the development of a novel process for extracting mercury from coal solutions in a “zero waste” manner.

The next step in the biochemical study is to genetically characterize the bacteria with respect to the Mer genes. Because these genes have been shown, in general, to be highly diverse, we are likely to encounter different versions of these genes in each of the bacteria we have identified. We will thus isolate plasmid and chromosomal DNA separately in order to discover where the Mer genes are located in each species. PCR assays using primer pairs designed to amplify conserved regions of known Mer genes will allow us to ascertain which Mer genes, if any, our bacteria carry. Conjugation experiments with non mercury-resistant E. coli will also be employed in order to demonstrate the presence of the Mer genes on plasmids. Assuming Mer genes are detected in our plasmid preparations, we will attempt to transform non-resistant E. coli with those plasmids.

More purification steps are required to isolate MerA from the crude bacterial extract. Hydrophobic chromatography or molecular weight chromatography techniques are being developed to better purify MerA. The MerA activity assessment will be followed by the volatilization of metallic mercury from the assay mixture by an atomic absorption spectrometer. The former experiment for the partial purification of MerA will be repeated and the volatilization of metallic mercury from the assay mixture will be monitored. Finally, we will directly analyze the rates of mercury metabolism by our

various bacterial species using atomic absorption spectrometry. This aspect of the project is in its initial stages now.

The next step in the modeling and process definition consists of identifying locations in the processing of coal and/or its burning where we can effectively use the Mer group of proteins. The simplest process is to bind Mer P to a substrate in a column and use it like an ion exchange column. The rate of Mer P binding mercury is very fast; the formation constant is very large, but only for mercury. When the column is “exhausted” (all of the active sites become bound), denaturant is added, Mer P loses its binding conformation and the bound mercury is released in a concentrated stream directed to a biological treatment pond and converted to its elemental form and recovered.

#### **9. Coal Desulfurization with Hypochlorite. (WV011)**

Principal Investigator: Ray K. Yang & Eung Ha Cho, West Virginia University

Period of Performance: May 1, 2004-May 31, 2006 (2-Year Project)

The results show that the effects of temperature and sodium hydroxide concentration on sulfur reduction are minimal. It was observed that the pyritic sulfur reduction was by 65% in maximum and the organic sulfur reduction was by only 9% in maximum. The leaching behavior of the Kingwood coal was similar to that of Pittsburgh No. 8 coal, and concluded that these coals are not particularly amenable to hypochlorite leaching. It was also found that the ammonia pretreatment was not needed in leaching of Illinois No. 6 coal.

Future experimental work will be conducted to study the leaching of Illinois No. 6 coal at higher solid concentrations.

#### **10. Phyto-Extraction / Fabrication of Gold and Silver Nanoparticles. (WV012)**

Principal Investigator: Ray K. Yang & Eung Ha Cho, West Virginia University

Period of Performance: May 1, 2004-May 31, 2006 (2-Year Project)

During this reporting period, our investigation on gold nanoparticles in mung bean and alfalfa sprouts indicates that (based on data presented in Table 1 and Figures 1-4), overall, as the concentration of gold in the potassium tetrachloroaurate solution used in the sprouters increases from 10, 40, 80 to 160 ppm, the gold content in the bio-ore (ash) from sprouts also increases. In addition, overall, alfalfa sprouts appear to extract and retain higher concentrations of gold than mung bean sprouts. But, most importantly, all the gold concentrations in the bio-ores obtained from sprouts, expressed as milligram gold per gram of un-burnt dry biomass, are much higher than that of the threshold concentration in hyperaccumulator plants for gold.

Callus and suspension cultures of “carrot light”, “carrot dark”, and periwinkle were successfully initiated, established, and maintained continuously during this reporting period. Shown in Table 1 (bottom three rows) and Figure 5 are gold contents of cells of periwinkle, “carrot light” and “carrot dark” after exposing the cells to 20 ppm of gold in the suspension cultures for one week. As expected, compared to sprouts much higher

percents of gold were transported to cells, which lead to higher contents of gold in plant cells cultivated in suspension culture. This encouraging result, though preliminary so far, points to the potential of using suspension culture of plant cells for large scale production of gold nanoparticles as originally envisioned in the proposal.

We found from our test runs on growing hyperaccumulator plants (mustard, carrot, and beet) that the seeds of these plants germinated equally well directly from pure silica sand and auriferous sand in ordinary plant-growing pots. This eliminates the time and effort for transplanting the seedlings from seed-germinating units to pots, and avoids mixing of sands with potting soils in pots. But more importantly, the plants grow better, as transplanting of carrot and beet usually lead to crooked or otherwise poorly shaped roots. This finding was applied to our 10-week 120-pot large scale greenhouse experiment involving two cultivars of carrot, beet, and mustard that started on September 9, 2005.

Future work will comprise investigation of gold nanoparticles in hyperaccumulator plants, gold nanoparticles in sprouts and gold nanoparticles in plant cells.

**11. Recovery of Gold from Thiosulfate Leach Liquor Using Activated Carbon (WV012)**

Principal Investigator: Courtney A. Young and Larry G. Twidwell, Montana Tech  
Period of Performance: June 1, 2005-October 31, 2006 (2-Year Project)

No report submitted

**12. The Effect of Alkyl Diphenyl Oxide and Sulfonated Oleic Acid Surfactants on Nucleation and Growth of Potassium Sulfate Crystals: Optimization of Surfactants for the Potash Industry (NM005)**

Principal Investigator: Gillian Bond and Christa Hockensmith, New Mexico Tech  
Period of Performance: June 1, 2005-October 31, 2006 (2-Year Project)

No report submitted

**13. Thiosulfate as a Replacement for Cyanide in the Presence of Activators (NV003)**

Principal Investigator: Maurice C. Fuerstenau, University of Nevada, Reno  
Period of Performance: June 1, 2005-October 31, 2006 (2-Year Project)

The concentrations of cupric ion, ammonia and thiosulfate are all important in gold leaching. Cupric being the oxidant in this system oxidizes both gold and thiosulfate. Higher cupric concentrations increase the rate of gold dissolution; the extent of thiosulfate oxidation will have to be established. Ammonia is necessary because it maintains the cupric and cuprous ions as ammonia complexes. Dissolution as a function of rotational velocity of the stirrer shows that the reaction is mass transfer controlled through the boundary layer.

Future work will involve establishing the optimum levels of cupric ion, ammonia and ammonium thiosulfate addition for maximal gold dissolution and minimal thiosulfate oxidation.

## **15. Phytomining for Nickel and Silver Nanoparticles (WV016)**

Principal Investigator: Ray K. Yang & Eung Ha Cho, West Virginia University

Period of Performance: June 1, 2005- October 31, 2006 (2-Year Project)

Preliminary results indicate that two cultivars of geranium, “Rober’s Lemon Rose” and “Rose”, may be used for biosynthesis of silver nanoparticles.

We expect all tasks of the project will move in full speed during the summer months of 2006 starting May; a research assistant will join the project at that time, and the PIs, with no teaching during the summer, will be able to focus their academic efforts fully on the project. No qualified research assistant, who can devote fully to the project, was available for the Spring semester 2006, causing a slow start on this project

Future experimental work to be conducted include: (1) To continue our investigation on the formation of silver nanoparticles by geranium and the factors affecting their formation; (2) To grow nickel-hyperaccumulator plants, *Alyssum murale* Waldst & Kit (or *Alyssum murale*), *Alyssum corsicum* Duby (or *Alyssum corsicum*), and *Alyssum bertolonii*, and study the nickel nanoparticles formed in those plants; (3) To initiate and develop suspension cultures from the callus cultures developed so far, and to study the silver nanoparticles produced from these suspension cultures; and (4) To investigate silver nanoparticles produced in the sprouts of mung bean and alfalfa.

### ***d) Modeling and Control***

#### **1. Online Monitoring and Diagnosing of Coal Fines During Separation Process. (WV008)**

Principal Investigator: B.S. Kang and E.K. Johnson, West Virginia University

Period of Performance: May 1, 2003- October 31, 2006 (2-Year Project)

A LIBS system has been developed to detect C, Fe, and Hg in coal. Significant information has been obtained in analyzing the signals. The ability to detect C, Fe, S, and Hg by this system has produced mixed results. Upon obtaining data, the strength of the modified intensity signal from the collected light was plotted with respect to known concentration in the specimen. The graph of relative intensity with respect to concentration resulted in a strong correlation within the carbon and mercury emission lines. Carbon, which ranged from 61 – 81% mass within the synthetic coal mixture, resulted in strong correlations between line intensities and signal strength. Since there were some discrepancies of the identity of the two emission lines, pure carbon was tested and added to Figures 4, 5, and 6. The test showed that the line intensities from pure carbon were stronger than the intensities from the test samples, proving that carbon could be identified qualitatively as well as quantitatively within the 431-452nm wavelength range.

Use of the 436nm emission line as a means of detecting mercury was accurate to 800ppm. A plot between the signal strength and the concentration yielded a strong correlation, with only one discrepancy point, possibly due to a mixing error. The 800ppm limitation was due to the system hardware. A more sensitive detection instrument is required to attain lower detection limits.

Sulfur could not be detected using this experimental apparatus. This may be due the air quenching effect reported earlier [7]. Since the most sensitive emission lines in the sulfur spectrum are below 200nm, a combination of special optics and a vacuum environment are required to optimize the detection of sulfur.

Iron emission lines showed poor correlation between signal strength and concentration. This could be due to the mixing of pure iron in powder form within the synthetic mixtures as opposed to iron oxide. It is hypothesized that during the grinding and mixing process, the iron was drawn together instead of dispersed evenly, creating pockets of highly concentrated iron within the samples.

Based on qualitative and semi-quantitative analysis, dynamic LIBS testing provides basic information on the lifetime and temporal characteristics for individual emission lines. Mercury seems to have a more sudden decay, while carbon and iron show a slight delay before actual decay occurs. The data upon observation of emission lines of one specie compared to another suggests that emission lines possess differing temporal characteristics.

## **2. Development of a Novel Optical Radiation Depolarization Technique for On-Line Measurements of Particle and Bubble Sizes. (KY003)**

Principal Investigators: D. Tao, M.P. Menguc and C. Crofcheck, University of Kentucky  
Period of Performance: May 1, 2003- October 31, 2006 (2-Year Project)

An elliptically polarized light scattering (EPLS) approach was investigated as a technique for monitoring the mean bubble size and total gas hold-up of GL mixtures. A series of experiments were conducted which showed that the profiles of scattering matrix elements are sensitive to the bubble size and gas-holdup. This sensitivity suggests that the measurement of these parameters at a limited number of back-scattering angles can provide a robust approach for monitoring mean bubble size, flow rate, and gas hold-up. M11, M33, and M44 values at  $\theta = 120^\circ$  yield promising performance for monitoring of GL systems at a low-to-medium flow rates and surfactant concentrations. On the other hand, M22 values at  $\theta = 120^\circ$  can be used to monitor gas-hold-up at high flow rates and surfactant concentrations. There are two disadvantages associated with the M12-based monitoring 1) it decreases at low surfactant concentration with increasing gas hold-up, but it increases when surfactant concentration medium-high and 2) because of multiple scattering affect, its value can be very small and may not show any a trend for different gas flow rates at medium-high flow rates and surfactant concentrations.

For the next two quarters, research efforts will be focused on the characterization of particle size based on light scattering. Particular attention will be directed toward optical

thickness of the slurry, bimodal polydisperse characteristics of size distribution, and different optical properties of mineral and coal particles.

**3. Mineral Liberation Analysis in 3D by X-Ray MicroCT for the Evaluation of Particle Separation Efficiency. (UT006)**

Principal Investigators: C. L. Lin, University of Utah

Period of Performance: May 1, 2004- October 31, 2006 (2-Year Project)

Two major components, namely, the segmentation of individual particles from packed particle bed and compositional classification of each particle, are need to be developed for detailed 3D liberation/exposure analysis of coal and mineral samples using XMT. In this regard, 3D watershed segmentation process was developed which allow us to identify individual particles in packed particle beds. Further, the density and attenuation coefficient relation associated to the use of Finite Mixture Distributions allow us to discriminate between different materials. These two components are used to show practical applications in mineral processing studies. The washability curve of coal samples from Illinois No. 5 seam calculated with the XMT data follows very well the experimental sink-float data.

During the period of 2006, evaluate the performance of the XMT under plant conditions will be evaluated based on plant samples and the data will be used to assess the accuracy for monitoring effectiveness of particle separation processes.

**4. A Comprehensive Study of Froth Behaviour. (VT011)**

Principal Investigators: Roe-Hoan Yoon, Demetri Telionis and Pavlos Vlachos,  
Virginia Tech

Period of Performance: May 1, 2004- October 31, 2006 (2-Year Project)

**5. Portable Sensor for Detecting Mercury and other Heavy Metals Encountered in Coal Processing and Utilization. (WV013)**

Principal Investigators: Mohindar S. Seehra, West Virginia University

Period of Performance: May 1, 2004- October 31, 2006 (2-Year Project)

During this reporting period, we focused theoretically on the remaining issue of reproducibility of calibration curves and interpretation of the shift of the peaks with concentration. A decision to use “internal standard method” for the quantification of Hg was made in order to overcome the problem of reproducibility of the calibration curves. A new set of BDD electrodes has been acquired and experiments to solve the reproducibility issue are now in progress.

As noted above, our focus in the coming months will be to use the “internal standard method” in experiments to quantify mercury. The goal is to develop a method so that a single reading (or step) may be sufficient for mercury quantification, preferably with the

use of the same electrode for several analyses. Experiments to test this concept will be carried out.

**6. Development of a 3D Lattice-Boltzmann Model for Fluid Flow Simulation under Partially-Saturated Conditions in Packed Particle Beds**

Principal Investigators: A. Manivannan and Mohindar S. Seehra, West Virginia University  
Period of Performance: May 1, 2004- October 31, 2006 (2-Year Project)

Up to this moment the corner-stone of a 3D LBM has been developed. Comparison of the results with analytical solutions for a Poiseuille flow under Stokes fluid flow conditions shows good agreement. In fact, we are able to predict the range of the Reynolds numbers resulting from the simulation and we have shown independency of the results to the size of the image. Verification of the results with real 3D porous samples acquired with a XMT is in initial stage but the software platform for analysis and display of results has been successfully developed.

In general we will follow the approach explained before in the Objective and Approach section. In days to come we have to finish the verification of the simple one component fluid flow with real samples to increase our confidence and the reliability of the model. Issues such as the computer requirements, procedure and boundary effects will be evaluated in order to come up with a standard methodology to measured saturated permeability.

For the next report we expect to have the second stage of the model development. The incorporation of solid-liquid interaction and verification of the model with real problems will be addressed. Also, a preliminary evaluation of two liquid phases interaction is expected to be done.

*e) Environmental Control*

**1. Electrolytic Solution Purification and Metal Recovery from Metal-Bearing Toxic Waste Streams. (UT003)**

Principal Investigator: Michael L. Free, University of Utah  
Period of Performance: May 1, 2003- October 31, 2006 (1-Year Project)

The project is complete and a final report is to be issued.

**2. Determining the Effectiveness of Gold Filters for Removing Mercury from Coal Fired Power Plants. (MT003)**

Principal Investigator: K. Ganesan, Montana Tech  
Period of Performance: May 1, 2003- October 31, 2006 (1-Year Project)

This project is complete and a final report is to be issued

**3. Development of Metallic Filters to Control Mercury From Coal Fired Power Plant Flue Gas. (MT004)**

Principal Investigator: K. Ganesan, Montana Tech

Period of Performance: May 1, 2004- October 31, 2006 (1-Year Project)

In summary during this reporting period a laboratory scale thermal de-sorption system was fabricated. And an in-house plating setup has been built to plate the base filters. Further a newer sponge with higher surface area was successfully plated.

Future work includes thermal desorption of used filters using the new de-sorption system and to test the efficiency of the new sponge. The plating will be done in-house instead of a vendor if it proves to be equally effective.

**4. Recovery of Chromium and Arsenic From Toxic Waste Streams by Reactive Polymer-Coated Absorbents. (WV014)**

Principal Investigators: Dianchen Gang & Baolin Deng, West Virginia University

Period of Performance: May 1, 2004-May 31, 2006 (2-Year Project)

In the past six months, Task 3 was finished. Chromium desorption and regeneration were conducted. The maximum desorption efficiency by NaOH was 80%, and by NH<sub>4</sub>OH was 55%. The desorption study confirmed that the desorption rate was fast, due to the larger surface area of the adsorbent. The regenerated adsorbent was used in the isotherm experiments. Adsorption capacities were decreased by 35%-45%. The column study results showed that the breakthrough point was at 600 empty bed volumes (EBV) when the flow rate was 4 ml/hr and 760 bed volumes when flow rate is 0.85 ml/hr. Comparing the column operation with the batch adsorption process, column operation has higher removal capacity. In addition, iron-chitosan beads were prepared for arsenic removal. SEM micrograph of the iron-chitosan demonstrated that the beads are porous in structure. Iron-chitosan could effectively remove arsenic from water and pH had no obvious effect on As (V) removal from DI water at pH 5.8-7.3. The removal efficiency was always higher than 88% under the experimental conditions

In the next reporting period, tasks 2 and 3 for arsenic removal will be finished. The efforts will include: (1) Further characterization of iron-chitosan using X-ray photoelectron spectroscopy (XPS); (2) Determination the adsorption capacity of the adsorbent by studying the equilibrium isotherm; (3) Effects of competing anions on As absorption, and (4) Evaluation the As adsorption kinetics using a pseudo-second-order reaction model.

**5. Determination of Factors Affecting the Separation of Potentially Hazardous Trace Elements and their Behavior in Coal Tailings Impoundments (KY005)**

Principal Investigators: Frank E. Huggins, Naresh Ahah, Gerald P. Huffman, University of Kentucky

Period of Performance: June 1, 2005- October 31, 2006 (2-Year Project)

Work on the project has been initiated by the sampling, preparation, and division of four streams of the Illinois #6 coal from the Peabody Preparation plant, Coulterville, IL, into various fractions for the many coal, mineralogical, and forms-of-occurrence analyses that will constitute the basic data needed for detailed understanding of trace element partitioning in coal cleaning processes and their behavior in coal impoundment simulations. Preliminary analyses relating to iron and arsenic indicate a strong association of these elements with pyrite and virtually no oxidation or weathering of the coal.

Over the next six months, we should be able to gather most, if not all, of the data needed for the evaluation of trace element partitioning in gravity separation procedures employed at the Peabody Preparation Plant, Coulterville, IL. In addition, we will immediately begin the leaching testing of the tailings fractions.

**6. Mercury Reduction From Coal Power Plant Emission Using Functionalized Ordered Mesoporous Carbons (FOMCs) (WV015)**

Principal Investigators: Dianchen Gang & Baolin Deng, West Virginia University

Period of Performance: June 1, 2005- October 31, 2006 (2-Year Project)

In the first project time period, we have set up main experimental apparatus and instrumentation for the project, refined the procedure for OMC preparation, and prepared significant amount of OMC for further testing. Sample characterization and assessment for mercury removal is underway.

Because significant amount of ordered mesoporous carbons have already been synthesized, the next step of the research will focus on functionalizing the OMCs with sulfur, iodine, and chlorine to enhance Hg uptake; and optimizing conditions for mercury removal. Task 1 will be finished, and tasks 2 and 3 will be initiated in the second project time period

**7. Removal of Metal Ions from Acid Mine Drainage using a Novel Low-Cost, Low Technology (WV017)**

Principal Investigators: Benjamin Dawson-Andoh, West Virginia University

Period of Performance: June 1, 2005- October 31, 2006 (2-Year Project)

Initial studies have commenced and some results will be ready be next report period.ORK

Future studies will focus on the effect of fungal hyphae oo removal of metal ions and the kinetics of metal adsorption by wood.

## **REFERENCES**

References utilized by the individual sub-projects are reported in the relevant Technical Progress Report in the attached Appendices.

**Appendix 1: Development of Novel Ultrafine Sizing Methods**

**(KY001/VA008)**

## TECHNICAL PROGRESS REPORT

Contract Title and Number:

Establishment of the Center for Advanced Separation  
Technologies (DE-FC26-01NT41091)

Period of Performance:

Starting Date: 10/1/2002  
Ending Date: 10/31/2006

Sub-Recipient Project Title:

Development Of Novel Ultrafine Sizing Methods

Report Information:

Type: Semi-Annual  
Number: 6  
Period: 10/1/05-3/31/06  
Date: 4/30/06  
Code: VA008

Principal Investigators:

Roe-Hoan Yoon and Gerald H. Luttrell

Contact Address:

146 Holden Hall  
Virginia Tech, Blacksburg, VA 24061

Contact Information:

Phone: (540) 231-4508  
Fax: (540) 231-3948  
E-Mail: cast@vt.edu

Subcontractor Address:

No subcontracts issued.

Subcontractor Information:

Phone:  
Fax:  
E-Mail:

### ABSTRACT

The objective of this project is to develop a broad base of new equipment and improved methods for fine particle sizing. The processes evaluated in this work include a wide variety of mechanical, hydraulic, and novel approaches. For each process, experimental test programs have been undertaken to optimize operating parameters so that maximum efficiency and throughput capacity can be achieved while maintaining particle size cuts in the 25-50  $\mu\text{m}$  size range. The resultant test data has been used to mathematically simulate different circuit arrangements for the most promising technologies. Due to the large scope of this project, the proposed work has been carried out as a joint effort between researchers at the University of Kentucky and Virginia Tech. During this reporting period, an automatic proportional sampling system was constructed for the hydrocyclone test circuit used to evaluate a novel water injection system. The goal of this work is to simultaneously reduce particle size cut point ( $D_{50}$ ) and bypass using the new water injection apex. Also, geometry construction and mesh generation associated with Computational Fluid Dynamics (CFD) were also carried out during this period for the water injection apex.

## **INTRODUCTION**

### Background

Most mineral and coal processing plants are forced to size their particulate streams in order to maximize the efficiency of their unit operations. These sizing techniques commonly include various types of screens and classifiers. Screens exploit differences in the physical dimensions of particles by allowing fines to pass through a perforated plate or open mesh while coarser solids are retained. Unfortunately, screening systems are generally limited to particle size separations coarser than approximately 250 $\mu\text{m}$  due to limitations associated with capacity and blinding. Hydraulic classifiers are generally employed for finer size separations, including both static and centrifugal devices. Hydraulic classifiers exploit differences in the settling rates of particles and are influenced by factors such as particle shape and density as well as particle size. Classifiers are generally considered to be more practical than screens for fine sizing, but the separation efficiency decreases dramatically for particles smaller than approximately 150 $\mu\text{m}$  (Heiskanen, 1993). In addition, classifiers commonly suffer from bypass, which occurs when a portion of the ultrafine particles (slimes) are misplaced by hydraulic carryover into the oversize product. The unwanted misplacement can have a large adverse impact on downstream separation processes.

### Objective and Approach

The development of efficient techniques for fine particle sizing is widely considered to be a high research priority by both the mineral processing and coal preparation industries. In particular, the development of new screening and classification technologies, or improvements on existing technologies, is needed to overcome the current shortcoming of existing processes for fine particle sizing. Therefore, the primary objective of this project is to develop a broad base of new sizing equipment or techniques that can be used to efficiently size ultrafine particles. Processes to be evaluated in the proposed work will include a wide array of mechanical, hydraulic, and novel approaches for fine particle sizing. Because of the inherent difficulties and large scope of work associated with this problem, the research program is being carried out as a joint research program between researchers at Virginia Tech and the University of Kentucky. During this reporting period, much of the project work focused on the evaluation of techniques for improving the performance of classifying cyclone circuits. This effort included (i) installation of automatic sampling system and testing of a new water injection system, (ii) preprocessor work for Computational Fluid Dynamics (CFD) analysis using GAMBIT v 2.0 software, i.e. geometry construction and meshing generation.

## **PROJECT TASKS**

### Task 1 - Development of Mechanical Sizing Methods

No additional test work was conducted under this particular task during the past reporting period.

## Task 2 – Development of Hydraulic Sizing Methods

No additional test work was conducted under this particular task during the past reporting period.

## Task 3 – Development of Novel Sizing Methods

No additional test work was conducted under this particular task during the past reporting period.

## Task 4 – Circuit Development and Evaluation

Work under this task has focused on reducing bypass through the application of a novel water injection apex system. Existing water injection systems tend to substantially increase the particle cut size, which makes it unacceptable for ultrafine sizing applications. In addition, existing systems typically require large amounts of clarified injection water that may not be readily available in industrial plants. In light of these problems, technical personnel from Krebs Engineers have worked with the project team to develop a new type of water injected cyclone. The new system is specifically designed to overcome some of the inherent limitations associated with existing apex washing systems. To evaluate this new technology, a proprietary prototype was provided to the project team for initial testing. The experimental test program required the construction of a complete closed-loop test circuit. The circuit, which is designed to be extremely flexible, incorporates a 6-inch diameter classifying cyclone with interchangeable components, an electronically controlled variable speed circulation pump, and an integrated linear-pass proportional sample cutter. During this reporting period, the sample cutter was modified with an automatic pneumatic sampling system to accurately control the amount of samples collected (see Figure 1).

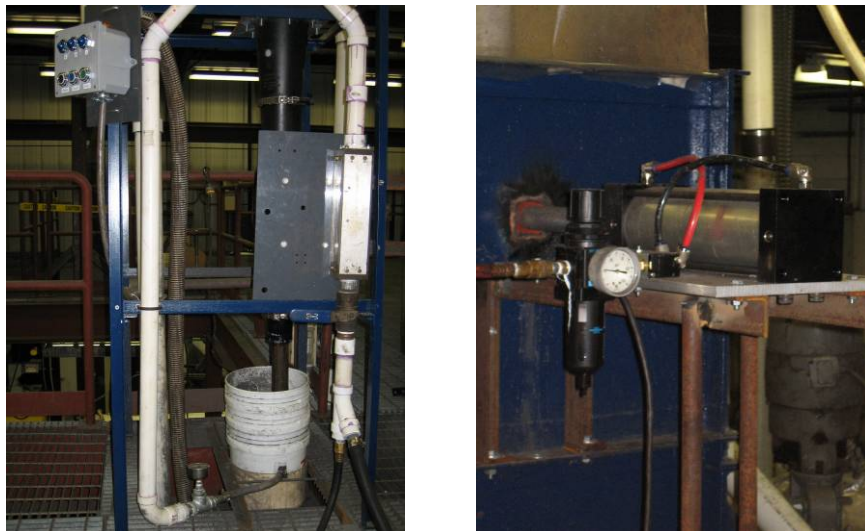


Figure 1. Water injection system and automatic pneumatic sampling system.

Several test runs were conducted during this reporting period to evaluate the effects of water injection pressure and volumetric flow rate. Experiments were carried out using water and minus 100 mesh coal slurry having a solids content of approximately 6.7% solids. The pressure drop across a cyclone was measured by taking the difference between the feed pressure and the overflow pressure. The test data given in Figure 1 show that the new apex washing system provides a higher volumetric throughput and a finer particle cut size at a lower pressure drop, independent of the size of the vortex finder. In fact, a larger vortex finder results in a lower pressure drop for the same volume flow or a greater capacity for the same pressure drop. Conversely, a smaller diameter vortex finder results in a larger pressure drop for the same volume flow. An increase in cyclone pressure usually leads to a higher volumetric throughput and a finer particle cut size (L. Svarovsky, 1984). Several tests for new water injection apex, compared with other apexes, was conducted to demonstrate the improved performance of the water injection apex on particle size cut point ( $D_{50}$ ) and bypass using a 1.5 inch vortex finder and 120 gpm volumetric flow rate. The data plotted in Figure 2 shows that the new water injection apex has the lowest bypass and particle size cut ( $D_{50}$ ).

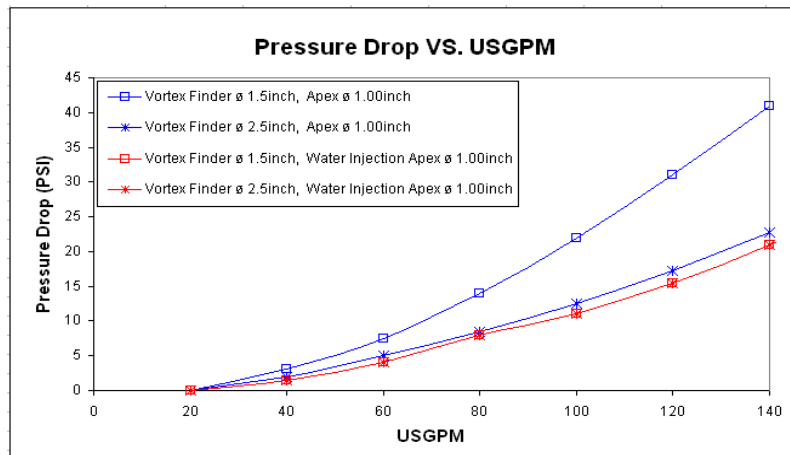


Figure 1. Effect of water injection apex on pressure drop and volumetric flow rate.

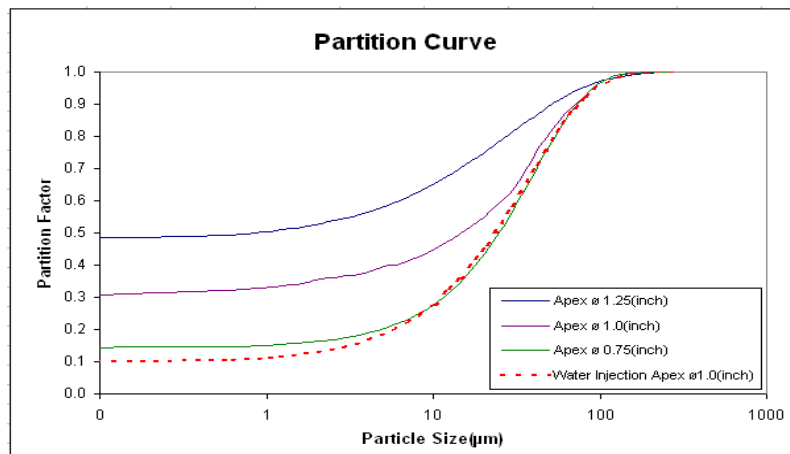


Figure 2. Effect of water injection apex on particle size cut point ( $D_{50}$ ) and bypass.

Theoretical studies of the new water injection apex were also undertaken during this reporting period using Computational Fluid Dynamics (CFD). This work was performed to investigate the phenomenon which occurs inside the hydrocyclone (i.e., prediction of air core locations, particle trajectory and velocity contours, etc.). During this reporting period, geometry construction and meshing for an actual 6-inch diameter cyclone was generated using the GAMBIT Ver. 2.0 software, which is a single integrated preprocessor for CFD analysis. Figure 3 shows a meshed cyclone equipped with the water injection apex. The mesh consists of 5773 nodes, 2902 mixed wall faces, 12,172 mixed interior faces and 4,763 mixed cells. Several simulations for investigating phenomenon of cyclone with water injection system are expected to be performed during the next reporting period.

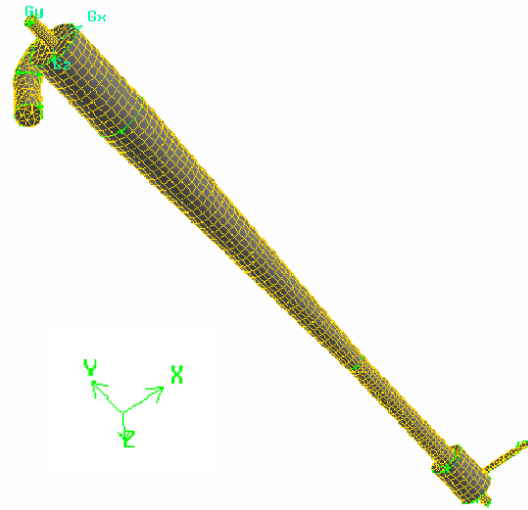


Figure 3. Geometry construction and mesh generation for a hydrocyclone equipped with a water injection apex.

## SUMMARY

Project work was continued during the past reporting period to investigate a variety of techniques for high efficiency sizing of ultrafine particles. Much of the work conducted to date focused on improving the performance of classifying cyclone system with a new water injection apex. This effort included (i) installation of automatic sampling system and testing of a new water injection system, (ii) preprocessor work for Computational Fluid Dynamics (CFD) analysis using GAMBIT v 2.0 software (i.e. geometry construction and meshing generation). The test work conducted to date indicates that a new water injection apex substantially reduces the amount of ultrafine solids that are bypassed to the coarse fraction without increasing the particle cutsize.

## FUTURE WORK

Work will continue to evaluate the classification performance of the hydrocyclone equipped with the water injection apex. Furthermore, a wide variety of theoretical studies will be continued in an attempt to develop a better understanding of the problems associated with ultrafine particle sizing. These studies will include computational fluid dynamics (CFD) application to predict classifier performance.

## REFERENCES

1. Heiskanen K, Particle Classification, Chapman & Hall, 1993.
2. Gambit v2.0 manual, Fluent Inc. 2002

**PUBLICATIONS/PRESENTATIONS**

None for the current reporting period.

**Appendix 2: Dispersion and Flotation of Clays from New Mexico**

**Potash Ores (NM001)**

# TECHNICAL PROGRESS REPORT

Contract Title and Number:

Crosscutting Technology Development at the Center for  
Advanced Separation Technologies  
(DE-FC26-02NT41607)

Period of Performance:

Starting Date: 10/1/2002  
Ending Date: 10/31/2006

Sub-Recipient Project Title:

Dispersion and Flotation of Clays from New Mexico  
Potash Ores

Report Information:

Type: Semi-Annual  
Number: 5  
Period: 10/1/05-3/31/06  
Date: 4/18/06  
Code: NM001-R05

Principal Investigators:

Gundiler, Titkov, Yekeler

Contact Address:

New Mexico Tech  
Socorro NM 87801

Contact Information:

Phone: (505) 835-5730  
Fax: (505) 835-6333  
E-Mail: gundiler@gis.nmt.edu

Subcontractor Address:

“No subcontracts issued.”

Subcontractor Information:

Phone:  
Fax:  
E-Mail:

## ABSTRACT

Effect of inorganic and organic dispersants, namely, sodium and calcium lignin sulfonates, and aluminum sulfate on flotation of sylvite from medium to high-clay potash ores have been investigated. All three substances have increased the overall IR recovery into the slimes fraction, decreased K<sub>2</sub>O losses into slimes, and decreased IR in desliming tailings (flotation feed). At the same level of flotation reagents consumption, K<sub>2</sub>O recovery increased and the concentrate quality improved

## INTRODUCTION

### Background

New Mexico is the largest potash producer in the United States, supplying the majority of the domestic production. Flotation is the main beneficiation method for sylvinitic (KCl-NaCl) ores for the recovery of sylvite (KCl). The flotation process is carried out from saturated brines with cationic collectors (long chain primary amines). Clay minerals present in the ore also absorb flotation reagents, thus increasing reagent costs, decrease recovery of sylvite, contaminate the product, and increase energy consumption for dewatering and

drying. Clays are dispersed during grinding and in attrition scrubbers; slimes are then removed by hydrocyclones and hydroseparators from sylvite flotation feed. Elevated brine temperatures during the summer months also affect collector adsorption on clays, depressing sylvite flotation.

Inorganic compounds, such as sodium silicate and poly-phosphates, have been utilized as dispersants for clay minerals in a number of flotation systems. However, in high ionic strength brines the surface charge on clay minerals is practically nil due to double layer compression. Inorganic clay dispersants added in the grinding circuit not only augment slime dispersion but also increase the selectivity of liberation of sylvite-halite mixed grains. Dispersant action of inorganic polyvalent salts, such as aluminum sulfate ( $\text{Al}_2(\text{SO}_4)_3$ ), have been postulated to be due to recharging of the clay particle surfaces in the presence of polyvalent ions.

Results of desliming and flotation tests conducted on low-clay ores (<2.5% IR) were reported previously (NM001-R04). Beneficial effects of dispersants, especially combination of organic and inorganic dispersants have been established in terms of improved  $\text{K}_2\text{O}$  recovery into potash concentrates (5 -7 %), decreased  $\text{K}_2\text{O}$  losses into slimes fractions, and decreased I.R. recovery in potash concentrates (25-30%). It has also been demonstrated that dispersants help as grinding aids and increase grinding efficiency.

### Objectives and Approach

This study was initiated to investigate possible means of improving sylvite recovery from Carlsbad potash ores by improving the mechanical desliming processes in the existing plants, and explore more efficient means of slime removal by the use of slime dispersants and/or flotation of slimes ahead of sylvite flotation. Studies on medium -clay ores are reported here.

## **PROJECT TASKS**

### Task 1 – Materials and Methods

In this phase of the study, aluminum sulfate and calcium lignin sulfonates have been used either individually or in combination in different proportions. Medium clay (~3 %) and high clay (~11%) ore samples were collected from Carlsbad potash operations. Minus 8 mm ore samples were scrubbed with or without the addition of dispersant for 5 minutes at 50%, solids for 5 minutes at 600 rpm agitation speed. Coarse ore was then diluted to 16% solids and deslimed by siphon decantation (stage-1), ground in a laboratory rod mill to minus 14 mesh (1.18 mm), diluted and again deslimed (stage-2). High-clay ores were deslimed 3 or 4 times as needed. Slimes were filtered, dried, and analyzed for insoluble residue (I.R.) and  $\text{K}_2\text{O}$  content, sands were placed in a flotation cell, conditioned with flotation reagents and sylvite was floated. Concentrates and tailings were also filtered, dried, and analyzed for I.R. and  $\text{K}_2\text{O}$  content.

## Task 2 – Desliming and Potash Flotation Tests

### Medium-Clay Sylvite Ores

Majority of the experimental effort was directed towards the medium clay ore during this period. In order to better ascertain the effects of dispersants on flotation behavior of these ores, tests were conducted on material ground for 3 minutes (- 8 mesh, 2.36 mm) and 5 minutes (- 14 mesh, 1.18 mm) as reported previously (NM001-R04). Desliming tests with or without dispersants, and subsequent flotation tests are summarized in the following figures.

Figures-1 and 2 show the overall effects of dispersants, aluminum sulfate, calcium lignin sulfonates, or combination of both, on the stage-wise IR recovery into slimes fractions and K<sub>2</sub>O loses in 3 minute (7 tests) and 5 minute (9) grinding tests. On the average the 1st stage (coarse) desliming removes 30% of IR without dispersants and 37% with dispersants. K<sub>2</sub>O loses to 1st stage slimes lightly increases in coarse ore desliming due to increased volume of slimes, however, decreases in 2nd stage during ground ores desliming in the presence of dispersants.

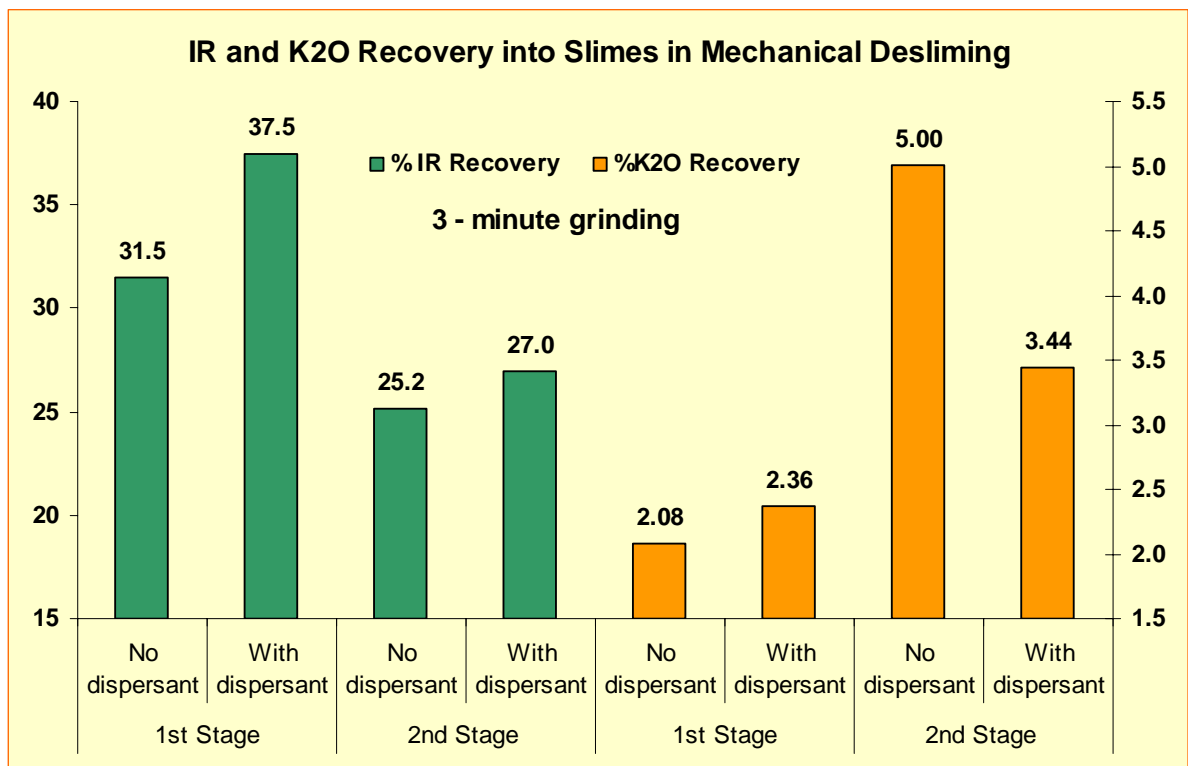


Figure-1 Overall effect of dispersants on IR and K<sub>2</sub>O recovery into slimes fractions after 3-minute grinding of medium clay ores.

Similar increase of IR recovery into slimes is observed in the first stage desliming however, the IR and K<sub>2</sub>O recoveries are very similar in 5-minute fine-ground samples (Figure-2). The differences in the IR and K<sub>2</sub>O recoveries in the first stage (coarse ore)

desliming in Figures 1 and 2 are due to slight variations of batches ore used in those tests. Further data on different dispersants are presented in Figure-3.

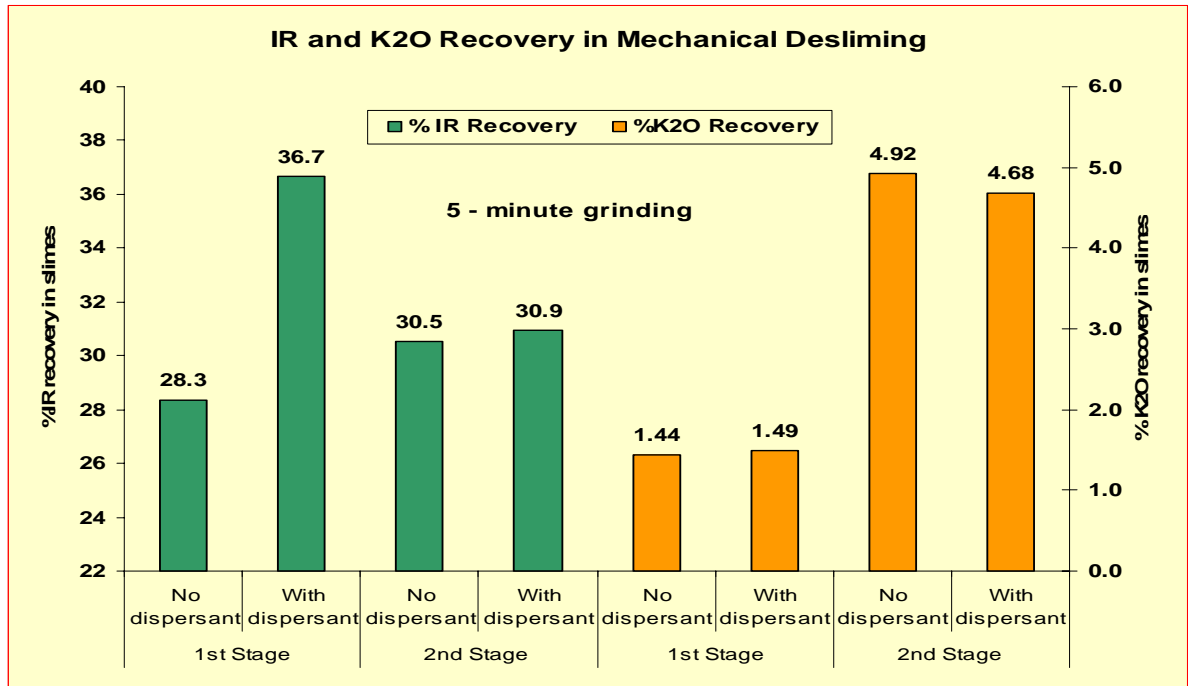


Figure-2 Overall effects of dispersants on IR and K2O recovery into slimes fractions after 5-minute grinding of medium clay ores.

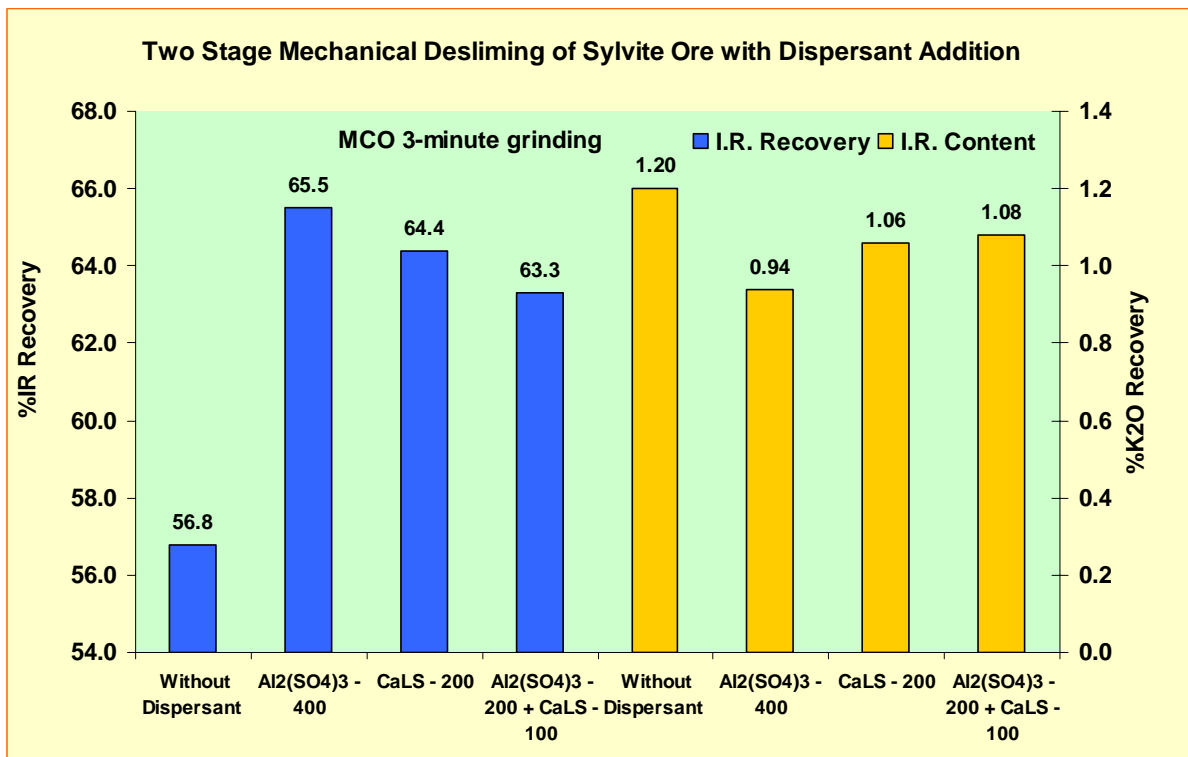


Figure-3 Influence of dispersants on 2-stage mechanical desliming of coarse-ground ore.

The influence of dispersants on desliming potash flotation recoveries from deslimed ores are given in Figures 4 and 5, for finer (5-minutes) ground ores respectively.

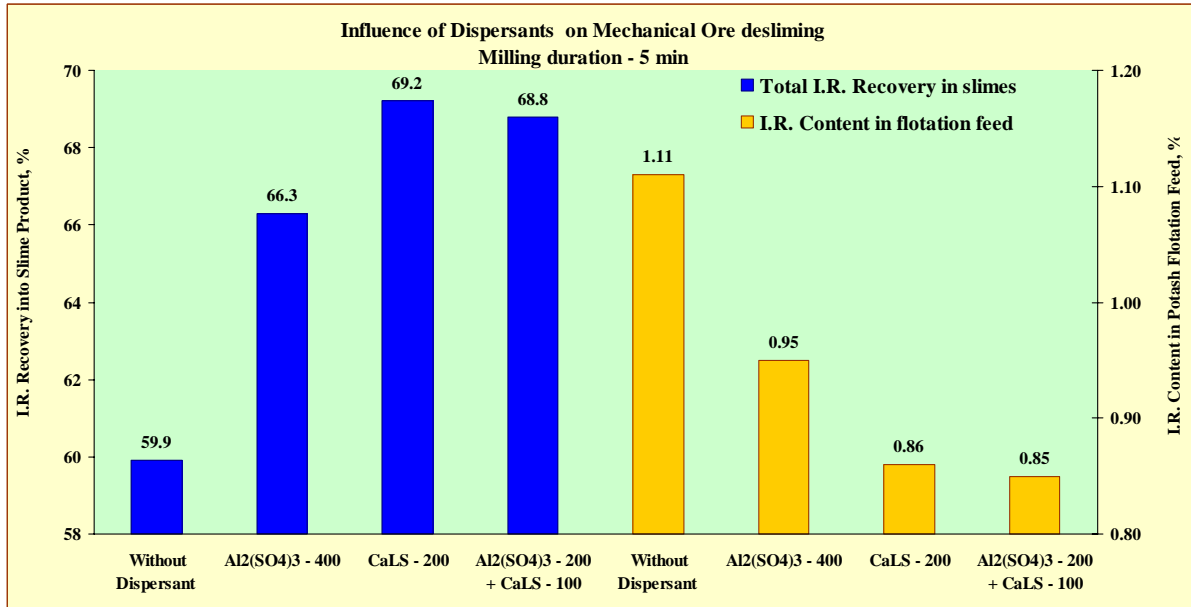


Figure-4 The influence of different dispersants on mechanical desliming of fine-ground ores.

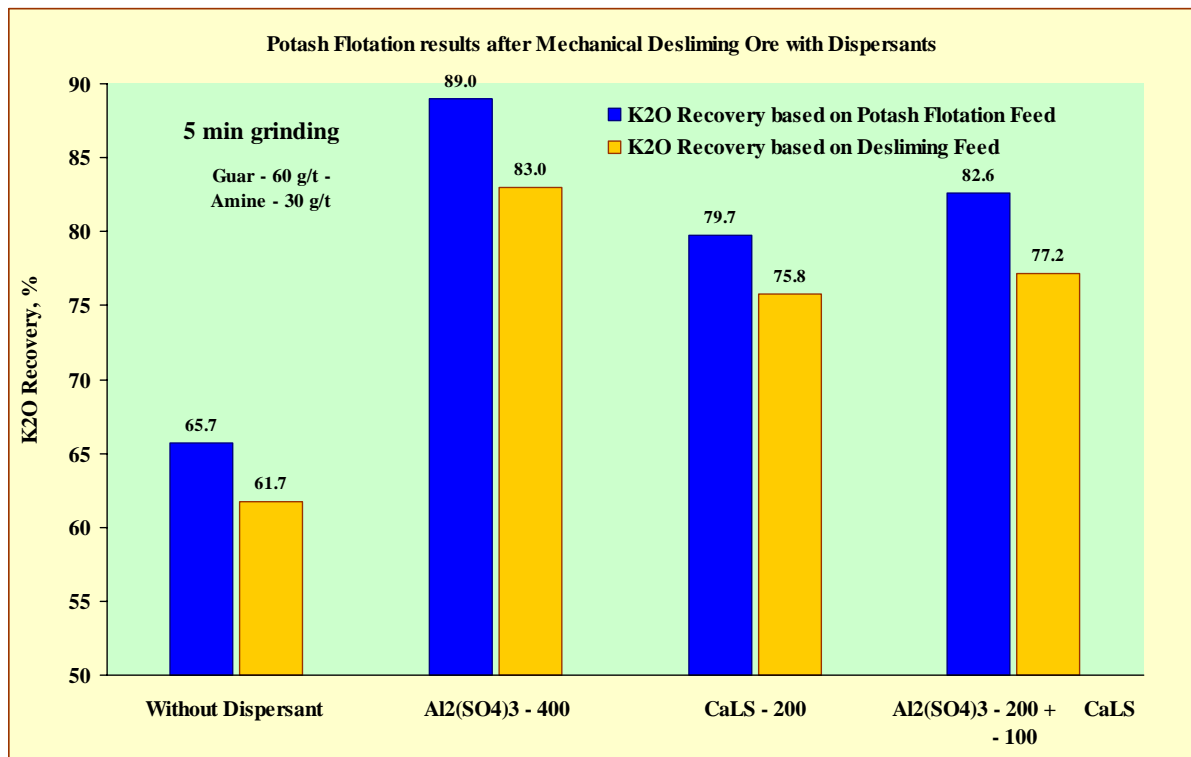


Figure-5 The influence of dispersants on potash flotation recovery from deslimed ores.

Comparison of the effects of dispersants on desliming and flotation results indicates although calcium lignin sulfonates (CaLS) yield highest IR rejection into slimes, hence lowest IR content in the flotation feed, the flotation recoveries are not the best. It has been shown that excess of negatively charged sulfonate ions can interact with the positively charged amine molecules, thus hindering potash (KCl) flotation (Titkov, et. al., XXI IMPC). In plant practice lignin sulfonates are also known to promote frothing in slime thickeners.

Flotation desliming of medium clay ores and comparison of potash flotation results with ores deslimed with or without dispersants are shown in Figure-6. It has been shown that coarse ore mechanical desliming followed by 1-stage flotation desliming using oxyethylated fatty acid or fatty amine collectors are equally effective in processing medium clay ores. The significance of flotation-desliming was highlighted in processing high-clay (>5% I.R.) ores which, so far, could not be treated economically. Results of high-clay ore desliming and potash flotation tests will be provided in the final report.

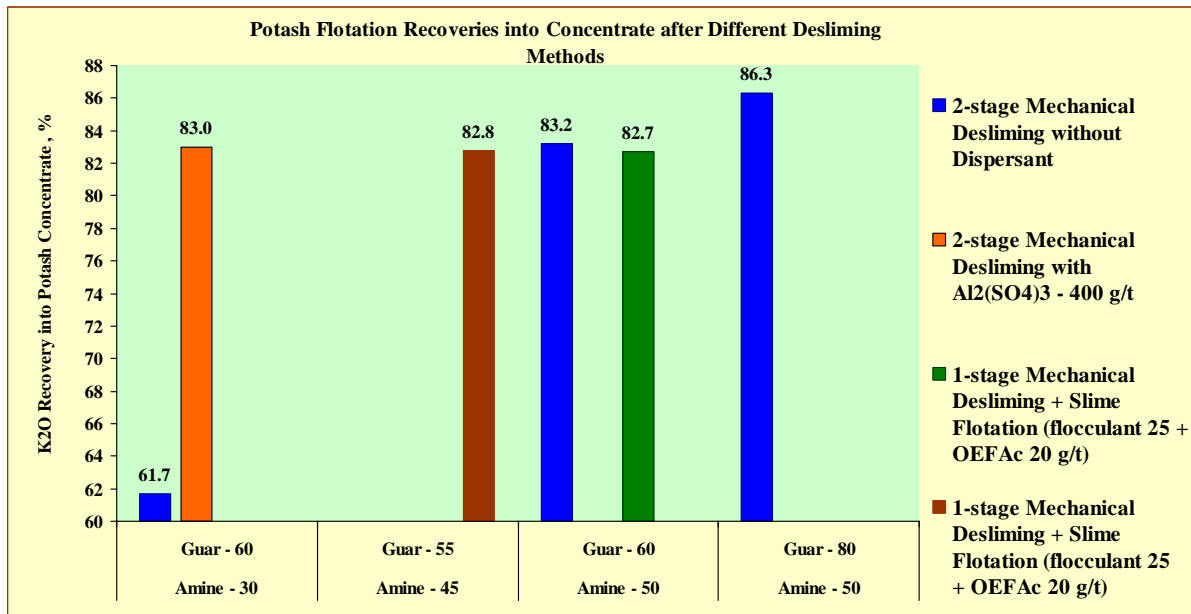


Figure-6 Comparison of potash flotation results following flotation or mechanical desliming of medium clay ores with or without dispersants.

## SUMMARY

The beneficial effects of dispersants on desliming of medium ores and on subsequent KCl flotation recoveries have been demonstrated, and feasibility of flotation desliming following the first stage coarse ore mechanical desliming has been presented. Beneficiation of very high-clay ores (11% IR) by two stage mechanical desliming followed by slime flotation has also been achieved. Those results will be presented in the next report.

### **Appendix 3: Flotation Processes/Experiments and Analysis (VT009)**

## TECHNICAL PROGRESS REPORT

<u>Contract Title and Number:</u> Crosscutting Technology Development at the Center for Advanced Separation Technologies (DE-FC26-02NT41607)	<u>Period of Performance:</u> Starting Date: 4/1/03 Ending Date: 10/31/06
--	---

<u>Sub-Recipient Project Title:</u> Flotation Processes/ Experiments and Analysis	<u>Report Information:</u> Type: Semi-Annual Number: 6 Period: 10/1/05 to 3/31/06 Date: 9/30/05 Code: VA 009-R06
<u>Principal Investigators:</u> Demetri P. Telionis and Pavlos P. Vlachos	
<u>Contact Address:</u> Virginia Tech Engineering Science and Mechanics Dept. 219 Norris Hall Blacksburg, VA, 24061	<u>Contact Information:</u> Phone: 540-231-7492 Fax: 540-231-3867 E-Mail: <a href="mailto:Telionis@vt.edu">Telionis@vt.edu</a>
<u>Subcontractor Address:</u> No subcontracts issued.	<u>Subcontractor Information:</u> Phone: Fax: E-Mail:

### ABSTRACT

Flotation processes involve complex, three-phase flow interactions between a liquid, bubbles and solid particles. For decades engineers and researchers based their calculations on algebraic formulas that model these interactions. These formulas were derived from simple models, from experimental data or just from arbitrary assumptions. Considerable progress has been made so far but this approach is far from providing a reliable tool for the design of flotation machines.

Most of the experimental data were obtained decades ago with literally primitive methods. Modern experimental tools are employed in this effort to measure with great accuracy the basic features of the motion of all three phases in homogenous isotropic turbulent flow and in a model flotation cell. So far we carried out measurements in a water tunnel with controlled grid turbulent fluid motions. In the previous reporting period we described a model stirring tank and presented some preliminary results obtained in this tank. In the present report we discuss more data obtained in this tank.

We employ a unique in the US Digital Particle Image Velocimeter (DPIV) that can record with great accuracy and kHz temporal resolution velocity vectors of all three phases, namely the fluid, the solid particles and the air bubbles. In this report we describe our work in estimating experimentally the turbulence dissipation.

### Nomenclature

Subscript p	particle
Subscript b	bubble
Subscript l	liquid
Superscript *	nondimensional quantity
$\langle \rangle$	time average
$C_{12}$	collision frequency coefficient [ $m^3 \cdot s^{-1}$ ]
$d_i$	diameter of i [m]
$d_{12}$	sum of diameters of particle and bubble
$N_i$	number density of i [ $m^{-3}$ ]
$R_{12}$	radius of collision [m] = $(d_1 + d_2)/2 = R_1 + R_2$
$u_i$	$i^{\text{th}}$ component of fluctuating velocity
$\sqrt{\overline{U_i^2}}$	root-mean-squared velocity of i with respect to flow [ $m \cdot s^{-1}$ ]
$\overline{U_i^2}$	variance of i with respect to flow [ $m^2 \cdot s^{-2}$ ]
$U^2$	variance of flow velocity
$Z_{12}$	collision frequency between particle and bubble [ $m^{-3} \cdot s^{-1}$ ]
$\varepsilon$	Kinetic Energy Dissipation rate [ $m^2 \cdot s^{-3}$ ]
$\nu$	kinematic viscosity [ $m^2 \cdot s^{-1}$ ]
$\rho_i$	density of i [ $kg \cdot m^{-3}$ ]
$\tau_i$	relaxation time of i [s]
L	Characteristic length
$U_0$	Free stream velocity
Re	Reynolds number
T	flow time scale

## **INTRODUCTION**

### Background

In our previous progress report we discussed our experimental efforts to monitor three phases, namely water, particles and bubbles in grid turbulence. This was homogeneous, isotropic turbulent flow, which may be realistic in some regions of a flotation cell. Such flows were generated in a water tunnel downstream of a grid. In this report we describe our initial steps in the design, construction and testing of a stirred tank.

There is a wealth of experimental and numerical results of the turbulent characteristics of the flow in stirred tanks. These are cylindrical tanks in which a stirring

device generates turbulence. A typical stirrer is the Rushton turbine, which is essentially a set of flat plates with their plane positioned in the radial direction and parallel to the axis of symmetry of the device. In the tests reported here, we use an impeller type of a stirrer. The aim has always been to measure the basic parameters that characterize turbulence. Recall that each of the models discussed in our previous report, relies on the accurate determination of the kinetic energy dissipation rate. Our measurement technique to determine the dissipation rate is now discussed.

Researchers used a variety of methods to record velocity fluctuations in stirred tanks, as for example hot wire velocimetry, (Rao and Brodkey 1972), laser-Doppler velocimetry (Costes and Couderc 1988, Wu et al. 1989, Okamoto et al. 1981, Wu and Patterson 1989) and more recently particle-image velocimetry (Saarenrinne and Piirto 2000). Wu et al. (1989) performed an energy balance on measured turbulent kinetic energy over a control volume to obtain local values of turbulent dissipation. Rao and Brodkey (1972) and Okamoto et al. (1981) applied power spectrum methods, while others (Rao and Brodkey 1972, Wu and Patterson 1989 and Kresta and Wood 1993) estimated the integral scale by integration of the auto-correlation function.

A well-documented approach of the performance of flotation cells is based on analytical or numerical determination of the rate constant (Moon, et al. (2002). An accepted estimate of the collision rate is given by the Abrahamson (1975) equation, which requires the root-mean square of the velocities of phase 1 and 2, here the coal particles and the bubbles relative to the fluid, respectively. Abrahamson's analysis is valid only if the phase density is much larger than the fluid density. This is the case for coal particles but not for bubbles.

Schubert (1999) proposes instead

$$\overline{U_i^2} = 0.33 \frac{\varepsilon^{4/9} d_i}{\nu^{1/3}} \left( \frac{\rho_i - \rho_f}{\rho_f} \right)^{2/3}$$

This formulation is an empirical, curve-fitting procedure carried out by Liepe and Moeckel (1976), based on experimental data collected by many authors. All these data were obtained decades ago, with almost primitive tools. Levins and Glastonbury (1972) for example record visual data in a flotation machine, along two planes and then proceed to measure manually thousands of particle-path segments. From such data they then generate the RMS of flow and particle velocity fluctuations.

### Objective and Approach

We are investigating three-phase flow, namely particle-bubble-turbulence interaction via time-resolved digital particle image velocimetry (DPIV). This study is conducted downstream of a grid that generates turbulence. This design provides an approximate but controlled simulation of the motion in a flotation machine, where next to the impeller we find large vortical structures, which again break down, populating the field with smaller vortices and ultimately lead to fully-developed turbulence. We are measuring the spatial and temporal evolution of turbulence properties like length scales,

time scales, Reynolds stresses and finally turbulent dissipation, which appears in both the Schubert and the Abrahamson formulations. Our aim here is to compare the performance of different models in isotropic turbulence and extend the work to nonisotropic turbulence.

## **PROJECT TASKS**

Work on this project has been progressing for a little more than one year. The following tasks have been defined at the beginning of this project.

### ➤ **Task 1: Phase velocities**

We employ DPIV to study experimentally the direct interaction of bubbles and particles. The streams are seeded with two types of particles. The first type are particle sizes the order of  $100\ \mu$  and simulate coal particles. Different levels of hydrophobicity will be tested. The second type of particles are sized down to the order of  $1\ \mu$  and their purpose is to allow accurate measurements of the instantaneous velocity field around the bubbles. We will document the individual velocities and turbulence fluctuations of each individual phase.

### ➤ **Task 2: Particle/bubble interaction**

We measured the trajectories and velocities of solid particles traveling around bubbles in homogenous isotropic turbulence. These trajectories were compared with trajectories computed by BBO equation. From the experimental results are computing the energy dissipation rate, which we will be incorporated into Schubert's formulation for the efficiency estimation of flotation processes. We will be extending these measurements to nonisotropic turbulence. These data were obtained in grid turbulence. Work is now extended to obtain similar data in a stirring tank.

### ➤ **Task 3: Measurement of collision rates**

By varying parameters like sizes of particles and bubbles, as well as the density and hydrophobicity of particles, we will generate statistical distributions for the probabilities of attachment and detachment. We will thus be able to evaluate the effect of different parameters on flotation efficiency. We found that this task is more difficult than we had anticipated. We are not sure what progress we will be able to make on this task in this project.

### ➤ **Task 4: Tests in a model flotation machine**

We are continuing our experimental measurements in a model flotation machine. This machine is described in this progress report. We also present data obtained in this machine.

## PROGRESS

### 1 INTRODUCTION

There is a wealth of experimental and numerical results of the turbulent characteristics of the flow in stirring tanks. These are cylindrical tanks in which a stirring device generates turbulence. Stirring tanks are widely used in a large number of applications in industries to promote blending, chemical reaction, micro mixing etc. Industry needs suitably designed stirring vessels to increase production, product quality and reduce maintenance costs. Mixing processes are very important elements in many industrial devices, but at the same time they involve complex phenomena, since in most cases, the flow is turbulent over the entire volume and strongly inhomogeneous and anisotropic.

The flow in mixing vessels is typically generated with rotors or impellers. The impeller agitates the flow and creates shear characteristics in accordance with the requirements of the mixing process. Bladed impellers can cause strong gradients in the flow, which lead to turbulence and higher shear rates. As the rotor agitates the flow, recirculation regions form. Lamberto et al.<sup>[1]</sup> showed that the flow field in the tank generated by flat-bladed turbines is divided in half, and creates two distinct toroidal regions above and below the impeller. They also noted that the two regions act as a barrier to mixing by increasing the blend time. Therefore, revealing the flow field and the characteristic quantities of turbulence (vorticity, kinetic energy, and turbulent kinetic energy etc) is of great significance.

Researchers used a variety of methods to record velocity fluctuations in stirring tanks, as for example hot wire velocimetry, (Rao and Brodkey<sup>[2]</sup>1972), laser-Doppler velocimetry (Costes and Couderc<sup>[3]</sup> Okamoto et al.<sup>[4]</sup>, Wu and Patterson<sup>[5]</sup>) and more recently particle-image velocimetry (Piiro and Saarenrinne<sup>[6]</sup>). Wu and Patterson<sup>[5]</sup> performed an energy balance on measured turbulent kinetic energy over a control volume to obtain local values of turbulent dissipation. Rao and Brodkey<sup>[2]</sup> and Okamoto et al.<sup>[4]</sup> applied power spectrum methods, while others (Rao and Brodkey<sup>[1]</sup>, Wu and Patterson<sup>[5]</sup> and Kresta and Wood<sup>[7]</sup>) estimated the integral scale by integration of the auto-correlation function.

Mununga et al.<sup>[9]</sup> simulated the laminar flow in an unbaffled mixing vessel stirred by a solid disk rotor and a 4-blade impeller using the CFD package FLUENT. Although mixing in stirring tanks has been extensively studied in the past years computationally<sup>[10-13]</sup> and experimentally<sup>[1-5], [14], [15]</sup> our understanding of the underlying physics of mass, inertia and energy transport and turbulent mixing is not yet complete. The main objective of the present study is to record the flow field with great temporal and spatial resolution to provide better understanding of the nature of mixing in a stirring vessel in which inhomogeneous anisotropic turbulence is present.

Although previous efforts provided valuable insight of the mixing process in Rushton tanks, no experimental effort has been directed at resolving the global character of the flow with sufficient temporal resolution. The present effort addresses this issue by

employing state-of-the-art, non-invasive flow diagnostics, allowing spatially resolved measurements with kHz sampling frequency. Thus both the spatial and temporal dynamics of the mixing process are revealed.

## 2 FACILITIES AND INSTRUMENTATION

The experimental apparatus used in this study consisted of a small-scale cylindrical, baffled stirring vessel known as a Rushton tank, made of Plexiglas with diameter  $D_T=0.1504\text{m}$  (shown in Figure 1). Four equally-spaced axial baffles with width ( $w_b$ ) one tenth of the tank diameter were mounted along the wall. A Rushton impeller with six blades was located at a height  $0.0762\text{m}$  from the bottom. The ratio between the vessel and the impeller diameter was  $D_{imp}/D_T=1/3$ . The ratio of blade width ( $w_i$ ) to the impeller diameter ( $D_{imp}$ ) was  $0.25$ . The tank was open at the top, and was filled with deionized water as the working fluid.

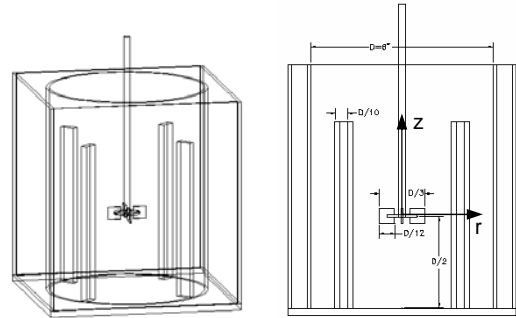


Figure 1. Dimensions of the stirring tank used for the PIV experiment

The height of the water was maintained at  $0.1504\text{ m}$ , which is equal to the tank diameter. The cylindrical tank was housed in an outer rectangular tank filled with water to eliminate the optical distortion of light beams passing through a curved boundary of media with different indices of refraction. The flow was seeded with  $8\text{ }\mu\text{m}$  diameter spherical, hollow glass flow tracers made with a specific gravity of  $1.05$ . The Reynolds number  $Re = N \cdot D_{imp}^2 / \nu$  was based on the impeller diameter. Furthermore, the Kolmogorov length scale  $\eta = D_{imp} \cdot (Re)^{-3/4}$  was estimated to be on the order of  $15.2\text{ }\mu\text{m}$  for the highest  $Re$  number of  $Re=50,000$ . The experiments were performed with a dual pulsing laser-camera system at a Magnification of  $32\text{ }\mu\text{m}/\text{pixel}$ . Previous experiments have shown that the majority of the turbulence takes place in the vicinity of the impeller. The relatively high pixel displacements necessitated use of the double pulsing capability of our PIV system. Two closely spaced laser pulses separated between  $28$  and  $100\text{ }\mu\text{s}$ , depending on the Reynolds number, were used to record the image pairs. Each image pair was cross-correlated to give a single velocity field. The sampling frequency of each pair of images was  $250\text{Hz}$ .

The region most interesting in a Rushton Tank is the region immediately adjacent to the impeller. We chose this region because of the extreme increase in velocities and turbulent statistics from the rest of the tank. The interrogation area encompassed the rectangular region  $0.2 < r/D_{imp} < 1$  and  $-0.2 < z/D_{imp} < 0.2$ . The laser sheet was focused on a plane of about  $1\text{mm}$  thickness, parallel to the impeller shaft. Measurements were performed at 7 Reynolds numbers ( $Re$ ) in the range  $20000-50000$  –shown in Table 1– corresponding to impeller rotational speeds of  $529-1323\text{ rpm}$  and blade tip-velocities  $u_{tip}=1.4-3.52\text{ m/sec}$ . All distances are normalized with the impeller Diameter  $D_{imp}$  and the velocities are normalized with the blade tip velocity,  $u_{tip}$ . The reference coordinate system is fixed at the center of the impeller. Each case contained 2000 images. Five hundred (500) images were used for the time-averaged results.

Although Digital Particle Image Velocimetry (DPIV) is currently the most widely used experimental fluids tool that delivers non-invasive velocity measurements, time resolved measurements are not easily attainable. Conventional DPIV systems provide a limited temporal resolution ( $\sim 30\text{Hz}$ ), which is insufficient for resolving the fluctuations present in a turbulent flow field. For moderate Reynolds numbers ( $10^3$ - $10^5$ ) and small length

Case	1	2	3	4	5	6	7
$10^3$ Re	20	25	30	35	40	45	50

Table 1. Test Matrix

scales, which are common in a laboratory environment, the sampling frequency necessary to resolve adequately the turbulent characteristics of the flow is in the order of  $10^3$  Hz. In the present study we use an in-house developed time-resolved DPIV system capable of delivering sampling frequencies on the order of 30 kHz.

The system is comprised of an IDT X-Stream camera. The camera is synchronized with a Lee-Lasers Nd-Yag pulsing laser with an emission wavelength of 532 nm. The pulse duration was in the order of 100 nsec, which is sufficient for performing measurements at low and moderate speeds. The laser was passed through a series of optics forming a 1mm light sheet that illuminated the area of interrogation. The camera magnification was adjusted such that the particles registered an image of approximately 3x3 pixels. FFT-based cross-correlation PIV methodology with an iterative multi-pass scheme with second-order discrete window offset was used. The first pass interrogation window size was 32x32 pixels satisfying the  $\frac{1}{4}$  rule for the maximum resolvable displacement.

### 3 RESULTS AND DISCUSSION

Figure 2 (a)-(f) shows instantaneous vorticity contours superimposed with streamtraces over one complete blade cycle for  $Re=20000$ . The time elapsed between frames is  $1/250$  sec, corresponding to an angular displacement of a blade equal to 10.0 degrees. This corresponds to about 36 frames per impeller revolution for the smallest Reynolds number. In these figures the passage of the blade is evident in terms of the large velocity magnitudes that persist for the entire sequence. Figure 2 (a) is the start of the cycles when one of the impeller blades is parallel to the laser sheet. The general flow pattern is a radial jet with a pair of tip vortices. In Figure 2 (f), a new set of tip vortices are generated, and the old pair that was generated in Figure 2 (a) is still convecting outward. Apparently the flow is sustained for a certain period after the blade has cut through the plane of interrogation. The 2-D vortices shown are actually a vortex ring extending outward, most likely with a strong out of plane velocity component.

Turbulence is also evident in the distribution of the time-averaged results shown in Figures 3 and 4 for the extreme two Reynolds numbers, 20000 and 50000 . The results were averaged over 500 velocity fields, or 1000 frames. The vorticity distribution in Figures 3 (a) and 4 (a) clearly shows the dominant role the tip vortices have as they convect all the way out, until the end of the interrogation region. The distribution of the diagonal component of the Reynolds stresses, and the  $u_r$  RMS clearly show unsteady fluctuations in the velocity.

Figures 5 through 8 describe the power spectrum of the  $u_z$  velocity for two Reynolds numbers, 20000 and 40000. Figure 5 shows a line at  $r/D_{imp}=0.56$  and three points. A series of power spectra were calculated along this line and are shown as contour plots in Figures 6 and 7. A total of 153 power spectra were performed to generate each of the two plots. The normalized Power Spectral Density is shown as a function of  $z$  in the impeller stream and the normalized (with the blade passing) frequency. The relative maxima at a normalized frequency of 1 in both contour plots indicate a very sharp spectrum. Also, notice Figures 6 and 7 contain two relative maxima in the impeller stream, precisely where the tip vortices pass by. The center of the impeller stream, which corresponds to the  $z/D_{imp} = 0$ , does not contain high power at the blade frequency. Three of the 153 power spectra are taken out of Figure 6 and displayed as line plots in Figure 8 (a)-(c). These are located at the three points shown in Figure 5.

Figures 9-13 show how some selected turbulence statistics scale with the Reynolds number. We show dissipation contours in the impeller stream for  $Re=30000$  in Figure 9, and a corresponding rectangular region where a maximum and a mean value were determined. Turbulent dissipation rate is a very important quantity directly connected with turbulent mixing. A variety of methods are available for the calculation of turbulent dissipation rate. We chose a direct method from the strain rate tensor, based on the assumption of isotropy.

$$\varepsilon = 15\nu \left( \overline{\left( \frac{\partial u_r}{\partial x_r} \right)^2} \right) \quad (1) \quad \text{Figures 10 and 11 show how}$$

maximum and mean dissipation in the impeller stream scale with Reynolds number. The dissipation is normalized with  $N^3 D^2$ , which is consistent with previous publications. A general decreasing trend is observed for the normalized dissipation with increasing Reynolds number. Excellent agreement with a previous study was obtained (Baldi and Yianneskis<sup>[17]</sup>). Other quantities, namely vorticity magnitude,  $U_{rms}$  and  $V_{rms}$  appear to follow constant trends in the range of Reynolds numbers investigated here.

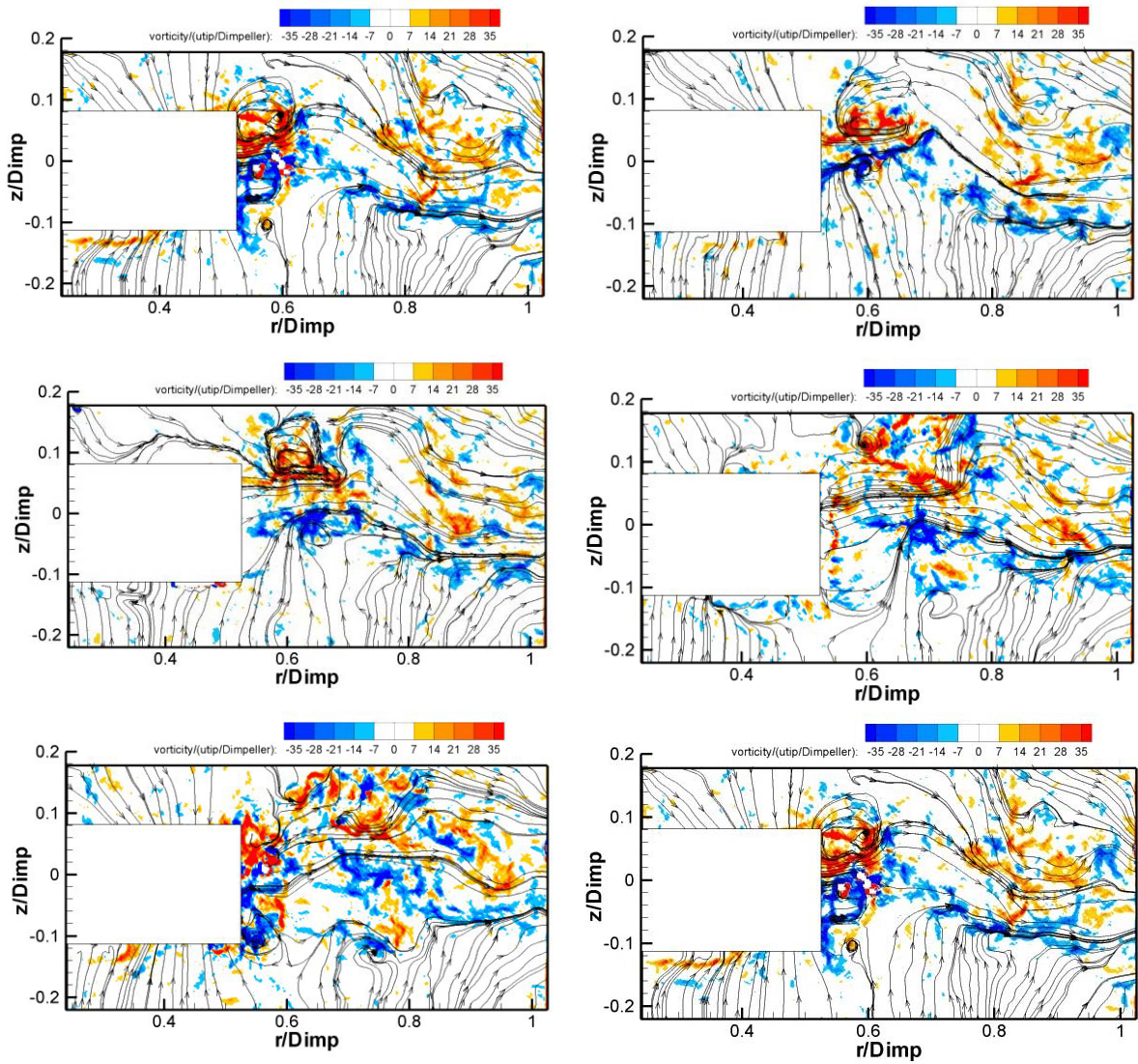


Figure 2(a)-(f) left to right, top to bottom. Instantaneous vorticity contours with streamtraces over one blade cycle.  $\Delta t=1/250$  sec

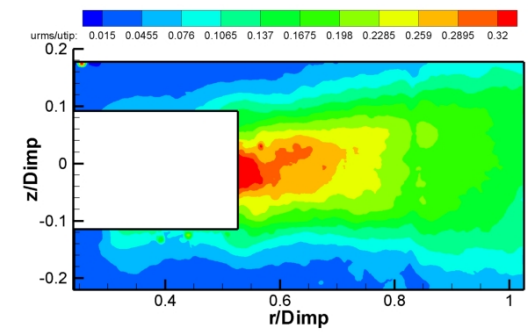
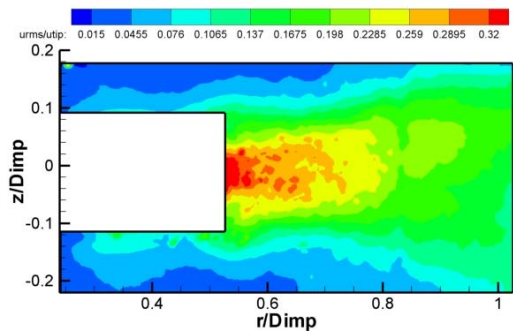
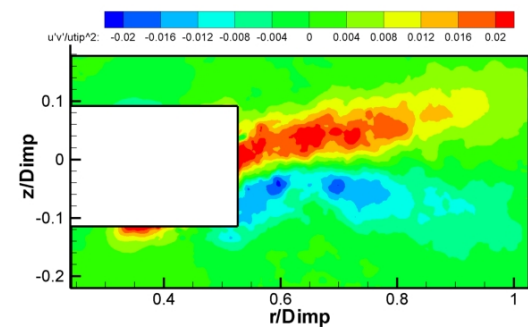
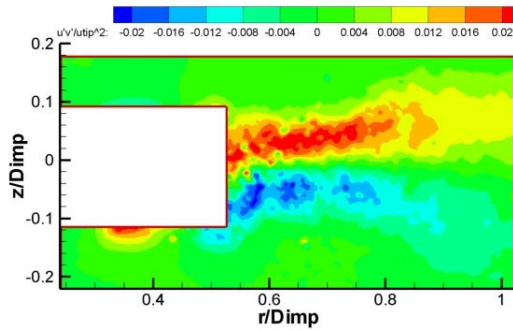
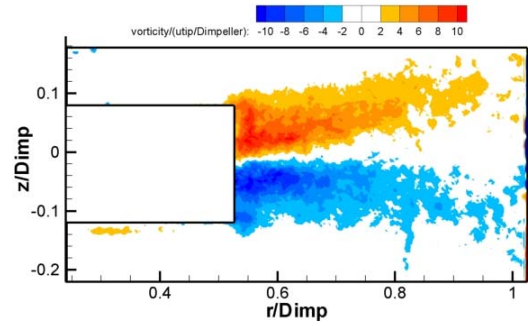
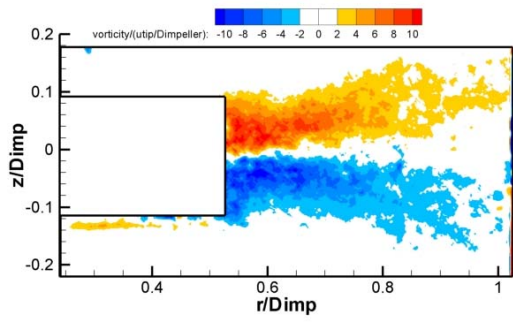


Figure 3 (a), (b), (c).  $Re=20000$ , time average. top to bottom: vorticity,  $u_r'u_z'$  Reynolds stress and  $u_r$  RMS. all normalized with  $u_{tip}$  and Dimpeller

Figure 4 (a), (b), (c).  $Re=50000$ , time average. top to bottom: vorticity,  $u_r'u_z'$  Reynolds stress and  $u_r$  RMS. all normalized with  $u_{tip}$  and Dimpeller

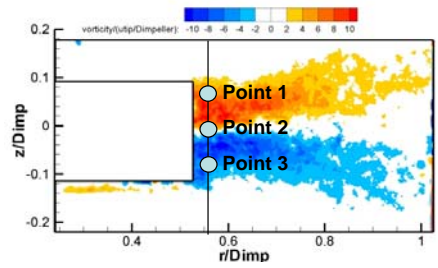


Figure 5. Schematic showing locations where Power Spectrums were taken. Line located at  $r/D_{imp}=0.56$

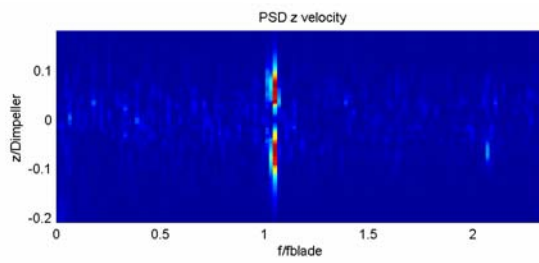


Figure 6. Contours of Power Spectrum of  $u_z$ ,  $Re=20,000$ . frequency normalized with blade frequency

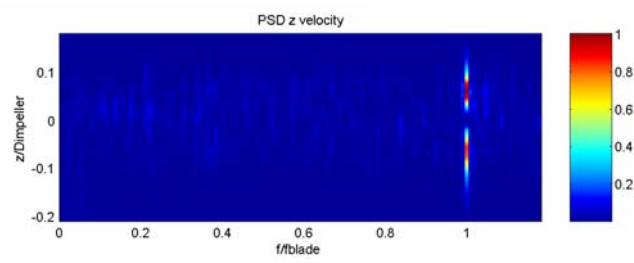


Figure 7. Contours of Power Spectrum of  $u_z$ ,  $Re=40,000$ . frequency normalized with blade frequency

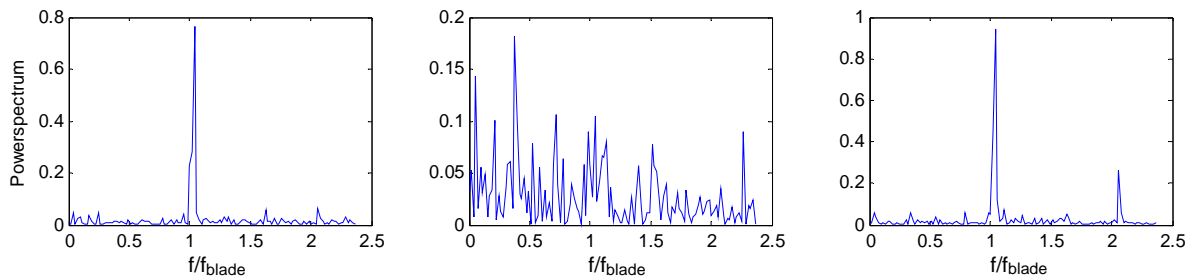


Figure 8 (a), (b), (c) left to right. Power Spectrum of  $u_z$ , for  $Re=20,000$ . (a) corresponds to point 1 in Figure 25, (b) to point 2, and (c) to point 3

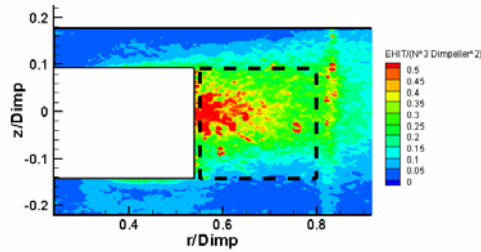


Figure 9. Dissipation contours in the impeller stream for  $Re=30000$ .

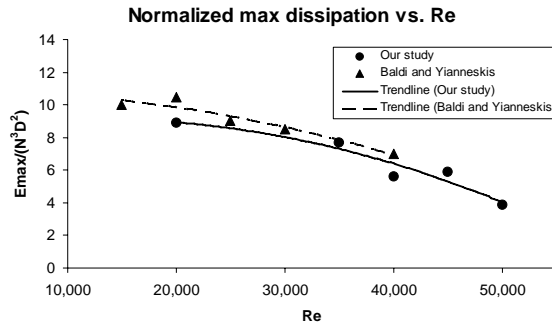


Figure 10 Normalized max dissipation vs. Re in dashed region of Figure 28

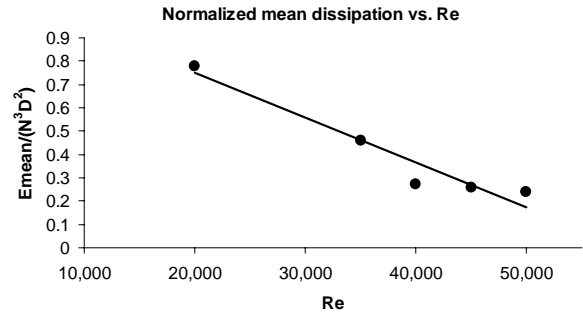


Figure 11. Normalized mean dissipation vs. Re in dashed region of figure 28

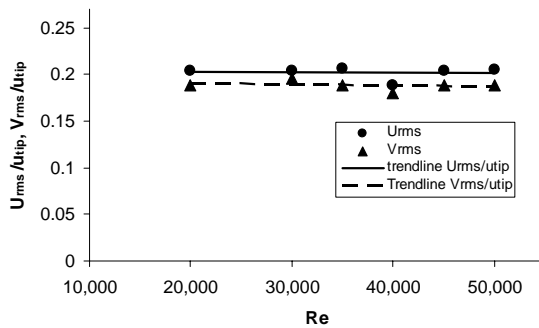


Figure 12 Normalized mean  $U_{rms}$  and  $V_{rms}$  vs. Re in dashed region of Figure 28

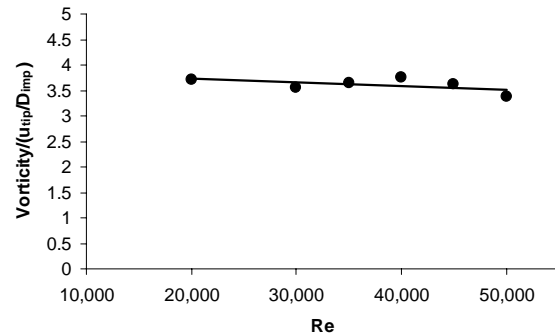


Figure 13 Normalized mean Vorticity magnitude vs. Re in dashed region of Figure 28

## 4. CONCLUSIONS

In many industrial applications, like in mineral flotation, interactions of solid particles and/or bubbles and particles depend on the characteristics of turbulent flow. In many analytical models, the rate of collision is a function of turbulence dissipation. It has been known that dissipation is larger in the neighborhood of the agitating mechanism, in our case the Rushton impeller. This is somewhat anti-intuitive, because energy is dissipated at the smallest eddy scales, and the immediate vicinity of the impeller contains large vortical structures and provides little space or time for such structures to break down. In this paper we provide further evidence that larger dissipation values in the vicinity of the impeller is consistent with the dynamic motion generated by the blade passage. The flow in the impeller stream of a Rushton impeller can be best summarized

as a radial jet with a pair of tip vortices. The maximum and mean normalized dissipation in the impeller stream showed decreasing trends with the Reynolds number. Other normalized turbulence quantities, namely  $U_{rms}$ ,  $V_{rms}$  and vorticity magnitude scaled as constant values with the Reynolds number. Estimates of turbulence characteristics and in particular distributions of turbulent energy dissipation determined in this study will be used in estimating rates of collisions of bubbles and particles in flotation cells.

## FUTURE WORK

This project has been essentially completed. We are further analyzing the data obtained and preparing the final report.

## REFERENCES

- [1] Lamberto, D.J., Muzzio, F.J., Swanson, P.D. and Tonkovich, A.L., (1996) "Using Time-Dependent RPM to Enhance Mixing in Stirred Vessels", *Chem. Engng. Sci.*, **51**, 1996, 733-741.
- [2] Rao, M A and Brodkey, R S, (1972). Continuous flow stirred tank turbulence parameters in the impeller stream, *Chemical Engineering Science*, 27:137-156.
- [3] Costes, J and Couderc, J P, (1988). Study by laser doppler anemometry of the turbulent flow induced by a rushton turbine in a stirred tank: influence of the size of the units-1. Mean flow and turbulence, *Chemical Engineering Science*, 43:2751-2764.
- [4] Okamoto, Y, Nishikawa, N and Hashimoto, K, (1981). Energy dissipation rate distribution in mixing vessels and its effects on liquid-liquid dispersion and solid-liquid mass transfer, *International Chemical Engineering*, 21:88-94.
- [5] Wu, H and Patterson, G K, (1989). Laser-doppler measurements of turbulent-flow parameters in a stirred mixer, *Chemical Engineering Science*, 44:2207-2221.
- [6] Piiro M., Saarenrinne P., Eloranta H., Karvinen R. (2003) Measuring Turbulence Energy with PIV in a Backward-facing Step Flow. *Experiments in Fluids*, 35, pp. 219-236.
- [7] Kresta, A M and Wood, P E, (1993). The flow field produced by a pitched blade turbine: characterization of the turbulence and estimation of the dissipation rate, *Chemical Engineering Science*, 48:1761-1774.
- [8] Vlachos, P. (2000) "A spatio-temporal analysis of separated flows over bluff bodies using quantitative flow visualization". PhD. Dept. of Eng. Science and Mechanics, Virginia Tech.
- [9] Mununga L., Hourigan K. and Thompson M. (2001) "Comparative study of flow in a mixing vessel stirred by

- a solid disk and a four bladed impeller” *14th Australasian Fluid Mechanics Conference Adelaide University, Adelaide, Australia 10-14 December 2001*
- [10] Yoon H.S., Sharp K.V., Hill D. F., Adrian R. J., Balachandrar S, Haa M. Y., Kard K. (2001) “Integrated experimental and computational approach to simulation of flow in a stirred tank” *Chemical Engineering Science* 56 pp.6635–6649
- [11] Sheng J., Meng H., Fox R. O.(2000) “A large eddy PIV method for turbulence dissipation rate estimation” *Chemical Engineering Science* 55 (2000) pp.4423-4434
- [12] Jenne M., Reuss M (1999). “A critical assessment on the use of *k*-*e* turbulence models for simulation of the turbulent liquid flow induced by a Rushton-turbine in baffled stirred-tank reactors”, *Chemical Engineering Science* 54 (1999) pp.3921-3941
- [13] Montante G., Leeb K. C., Brucato A., Yianneskis M.(2001), “Numerical simulations of the dependency of flow pattern on impeller clearance in stirred vessels” *Chemical Engineering Science* 56 (2001) pp.3751–3770
- [14] La Fontaine, R. F., Shepherd I. C.,(1996) “Particle Image Velocimetry Applied to a Stirred Vessel ”, *Experimental Thermal and Fluid Science* (1996) 12, pp. 256-264
- [15] Fan J., Rao Qi., Wang Y., Fei W.(2004) “Spatio-Temporal analysis of macro-instability in a stirred vessel via digital particle image velocimetry (DPIV) *Chemical Engineering Science* 59 (2004) pp.1863-1873
- [16] Vlachos, P. (2000) “A spatio-temporal analysis of separated flows over bluff bodies using quantitative flow visualization”. PhD. Dept. of Eng. Science and Mechanics, Virginia Tech.
- [17] Baldi, S. and Yianneskis, M. (2004) “On the quantification of energy dissipation in the impeller stream of a stirred vessel from fluctuating velocity gradient measurements” *Chem. Eng. Sci.*, 59, pp. 2659-2671.

These are the references to the general part of the progress report.

Abiven, C, Vlachos, P P, 2002. Comparative study of established DPIV algorithms for planar velocity measurements ASME IMECE, IMECE2002-33170.

Abrahamson, J, 1975. Collision rates of small particles in a vigorously turbulent fluid, *Chemical Engineering Science*, 30, 1371-1379.

Adrian, R J, 1991: Particle-imaging techniques for experimental fluid mechanics. *ARFM*, 23, 261-304.

Adrian, R J, 1997: Dynamic ranges of velocity and spatial resolution of particle image velocimetry, *Measurement Science and Technology*, 8 1393-1398.

Adrian, R J, Yao, C-S, 1985: Pulsed laser technique application to liquid and gaseous flows and the scattering power of seed materials, *App Optics*, 24, 44-52.

Boedec, T, Simoens, S, 2001: Instantaneous and simultaneous planar velocity field measurements of two phases for turbulent mixing of high pressure sprays. *Experiments in Fluids*, 31, 506-518.

Costes, J and Couderc, J P, 1988. Study by laser doppler anemometry of the turbulent flow induced by a rushton turbine in a stirred tank: influence of the size of the units-1. Mean flow and turbulence, *Chemical Engineering Science*, 43:2751-2764.

Cowen, B and Monismith, S, 1997: A hybrid digital particle tracking velocimetry technique. *Experiments in Fluids*, 22, 199-211.

Guezennec, Y G and Kiritsis, N, 1990. Statistical investigation of errors in particle image velocimetry. *Experiments in Fluids*, 10, 138-146

Hinze, J O, 1994. **Turbulence**. New York: McGraw-Hill, Inc.

Höfken, M, Schäfer, M and Durst, F, 1996. Detaillierte Untersuchung des Strömungsfeldes innerhalb eines Sechs-Blatt-Scheibenrührers, *Chemie Ingenieur Technik*, 68:803-809.

Huang, H T and Gharib, M, 1997: Processing error in digital particle image velocimetry, *FEDSM97*-3068.

Huang, H T, Dabiri, D and Gharib, M 1997: On Errors of digital particle image velocimetry, *Meas. Science and Technology*, .8, 1427-1440.

Khalitov, D A, Longmire, E K, 2002: Simultaneous two-phase PIV by two-parameter phase discrimination, *Experiments in Fluids*, 32, 252-268.

Kresta, A M and Wood, P E, 1993. The flow field produced by a pitched blade turbine: characterization of the turbulence and estimation of the dissipation rate, *Chemical Engineering Science*, 48:1761-1774.

Laufhütte, H D and Mersmann, A, 1985. *Proceedings of 5<sup>th</sup> European Conference on Mixing*, 331 (BHRA Fluid Eng., Cranfield, England).

Lecordier, B and Trinite, M, 1999: Time resolved PIV measurements for high speed flows,

Third International Workshop on Particle Image Velocimetry. (Santa Barbara, 16-18 Sept 1999).

Lee, C A and Erickson, L E. Bubble breakup and coalescence in turbulent gas-liquid dispersions, *Chemical eng. comm.* 59(1-6), 65-84.

Levins, B E and Glastonbury, J R, 1972. *Trans. Instn. Chem. Engrs.*, 50, 32, 132.

Levins, D M, Glastonbury, J R, 1972. Particle-liquid hydrodynamics and mass transfer in a stirred vessel, Part I-particle-liquid vessel, *Trans. Instn. Chem. Engrs.*, 40:32-41.

Liepe, F-M, Hans, O, 1976. Untersuchungen zum Stoffvereinigen in Flüssiger Phase, *Chem. Techn.*, 28, Jg., Heft 4.

Okamoto, Y, Nishikawa, N and Hashimoto, K, 1981. Energy dissipation rate distribution in mixing vessels and its effects on liquid-liquid dispersion and solid-liquid mass transfer, *International Chemical Engineering*, 21:88-94.

Piirto M., Saarenrinne P., Eloranta H., Karvinen R. 2003 Measuring Turbulence Energy with PIV in a Backward-facing Step Flow. *Experiments in Fluids*, 35, pp. 219-236.

Rao, M A and Brodkey, R S, 1972. Continuous flow stirred tank turbulence parameters in the impeller stream, *Chemical Engineering Science*, 27:137-156.

Saarenrinne P., Piirto M. 2000. Turbulent Kinetic Energy Dissipation Rate Estimation from PIV Velocity Vector Fields. *Experiments in Fluids*, [Suppl.], pp. S300-307.

Saffman, PG, Turner, J S, 1956. On the collision of drops in turbulent clouds. *Journal of Fluid Mechanics*, 1, 16-30

Sheng J., Meng H., Fox R.O. 2000 A Large Eddy PIV Method for Turbulence Dissipation Rate Estimation. *Chemical Engineering Science*, 55, pp. 4423-4434.

Scarano, F and Rieuthmuller, M L, 1999: Iterative multigrid approach in PIV image processing with discrete window offset, *Experiments in Fluids*, 26, 513-523.

Schubert, H, 1999. On the Turbulence-Controlled Microprocesses in Flotation Machines. *Int. J. Mier. Process.*, 56, 257-276.

Sheng, J, Meng, H and Fox, R O, 2000. A large eddy PIV method for turbulence dissipation rate estimation, *Chemical Engineering Science*, 55:4423-4434.

Upatnieks, A, Laberteaux, K, Ceccio, S L, 2002: A kilohertz frame rate cinematographic PIV system for laboratory-scale turbulent and unsteady flows, *Experiments in Fluids*, 32, 87-98.

Vlachos, P, 2000: A spatio-temporal analysis of separated flows over bluff bodies using quantitative flow visualization. PhD. Dissertation, Department of Engineering Science and Mechanics, Virginia Polytechnic Institute and State University, Blacksburg, VA

Wereley, S T, Meinhart, C D, 2001: Second-order accurate particle image velocimetry. *Experiments in Fluids*, 31, 258-268.

Westerweel, J, 1993a. **Digital Particle Image Velocimetry, Theory and Application**, Delft University Press, Delft, The Netherlands.

Westerweel, J, 1993b. Analysis of PIV interrogation with low pixel resolution. In Optical diagnostics in fluid and thermal flow, (ed) Trolinger J. D., Proc SPIE Vol. 2005, pp. 624-635. (San Diego July 1993).

Wu, H and Patterson, G K, 1989. Laser-doppler measurements of turbulent-flow parameters in a stirred mixer, *Chemical Engineering Science*, 44:2207-2221.

## **PUBLICATIONS/PRESENTATIONS**

1. "Turbulent Particle Bubble Interactions Measured by Particle Image Velocimetry". By Mike Brady, Demetri Telionis, Pavlos Vlachos, Ian Sherrell and Roe-Hoan Yoon. Presented at the SME Conference. Denver Colorado, February 2004.

2. "Velocities of Particles and Bubbles in Grid Turbulence Measured by Particle Image Velocimetry". By Mike Brady, Demetri Telionis, Pavlos Vlachos and Roe-Hoan Yoon. Presented at the Centenary of Flotation 2005 Symposium, Australia, June 2005, also submitted for publication to the International Journal of Mineral Processing.

3. "Stirring Tank Estimates of Turbulent Energy Dissipation". By Mike Brady, Demetri Telionis, Pavlos Vlachos and Roe-Hoan Yoon. Presented at the First IC-EpsMso (First International Conference on Experiments/Process/System Modeling/Simulation/Optimization) Athens in July 2005.

**Appendix 4: Column Flotation of Relative Coarse and Fine Dolomitic  
Phosphate Pebbles (WV007)**

## TECHNICAL PROGRESS REPORT

Contract Title and Number:

Crosscutting Technology Development at the Center for  
Advanced Separation Technologies  
(DE-FC26-02NT41607)

Period of Performance:

Starting Date: 10/1/2002  
Ending Date: 10/31/2006

Sub-Recipient Project Title:

Column Flotation of Relatively Coarse and Fine  
Dolomite Phosphate Pebbles

Report Information:

Type: Semi-Annual  
Number: 6  
Period: 10/1/05-3/31/06  
Date: 3/31/06  
Code: WV007-R06

Principal Investigators:

Peng

Contact Address:

West Virginia University  
359F Mineral Resources Building  
Morgantown WV 26506

Contact Information:

Phone: (304) 293-7680 x3308  
Fax: (304) 293-5708  
E-Mail: ffpeng@mail.wvu.edu

Subcontractor Address:

No subcontracts issued.

Subcontractor Information:

Phone:  
Fax:  
E-Mail:

### ABSTRACT

In this period the additional dolomitic phosphate pebble sample was received from Mosaic Co., FL, and was in the process of preparation for material characterization. In this period we were focus on the investigation of pH effect on the "natural" dolomitic phosphate flotation to separate dolomite from francolite. From literature study, the work published for understanding of pH effect on the dolomite and francolite flotation performance was based on the study of the "pure" and mixture of "pure" dolomite and francolite samples. The flotation performance data obtained from the literatures using pure minerals showed very different than the founding obtained from this study using "natural" Florida dolomitic phosphate ore. The explanations of the difference between the founding in this study and published are given.

### INTRODUCTION

#### Background

In Florida, the phosphate ore processing operations due to the lack of the economic technology in rejection of high dolomite from the phosphate ore, a large quantity of the high dolomite content phosphate ores is stockpiled at the phosphate processing plants. These

discards are known as dolomitic phosphate pebbles. If the phosphate flotation in the plant produces relatively low dolomite content, the pebble discards will be used to blend with the low dolomite content of flotation product and produce the final marketable product. As the phosphate mining moves toward the southeast of Florida, the reserve quality becomes lower and has higher content of dolomite. In order to maintain the steady supply to the fertilizer industry for the nation, the development of the phosphate separation technology to remove dolomite is urgently needed. Although some fine dolomite phosphate ore flotation technologies have been developed to meet this need, the separation processes can be treated at the relatively coarser particle size range is desirable to conserve the energy consumption during the phosphate liberation steps.

### Objective and Approach

The objectives of this proposed research project is to develop the relatively coarse and fine dolomitic phosphate flotation technology to produce a phosphate concentration at the level of marketable final products with less than 1% MgO content, from low grade dolomitic phosphate pebbles stockpiled at the phosphate plant sites. Various fatty acid collectors and other reagents required to achieve the goal, will be selected for relatively coarse and fine size dolomitic phosphate flotation. The optimal operation conditions for the flotation techniques used will also be determined to achieve the maximum dolomite rejection and phosphate recovery.

### **PROJECT TASKS**

Task II - Batch flotation cells and Denver automatic flotation machine is used in study of fatty collector for dolomite and phosphoric acid/sulfuric acid depressants additions. Task III and IV - Equipment Set-up: Flotation column has been set-up and in the processing of modifications by addition of fluidizing water supply and water flow rate adjustment to prepare for coarse size flotation column tests.

### **SUMMARY**

Xiao and Somasundaran (1987) reported their investigation on the flotation behavior of dolomite and francolite at different oleate concentrations and pH. In their study, individual pure dolomite and francolite mineral samples were used. Potassium oleate was selected as collector, KOH and HNO<sub>3</sub> as pH modifiers. The microflotation results showed that the floatability of individual dolomite and francolite is quite similar and very sensitive to the collector concentration. The flotation recovery of both dolomite and francolite as a function of pH at potassium oleate concentration of  $1.7 \times 10^{-4}$  M is shown in Fig. 1. The figure shows that selective flotation of francolite is possible above pH 9.0 and dolomite below pH 5.0. The float% curves for dolomite and francolite are crossed at pH 7.5. In their additional experiments with the mixture of pure dolomite and francolite samples using the same microflotation conditions, they found that the selective separation could not be achieved at all at the pH range they studied. These authors explained that the loss of selectivity of separation of dolomite from francolite minerals could be due to the alteration of the surface properties of both minerals by the dissolved mineral species such as Ca<sup>2+</sup> and Mg<sup>2+</sup>.

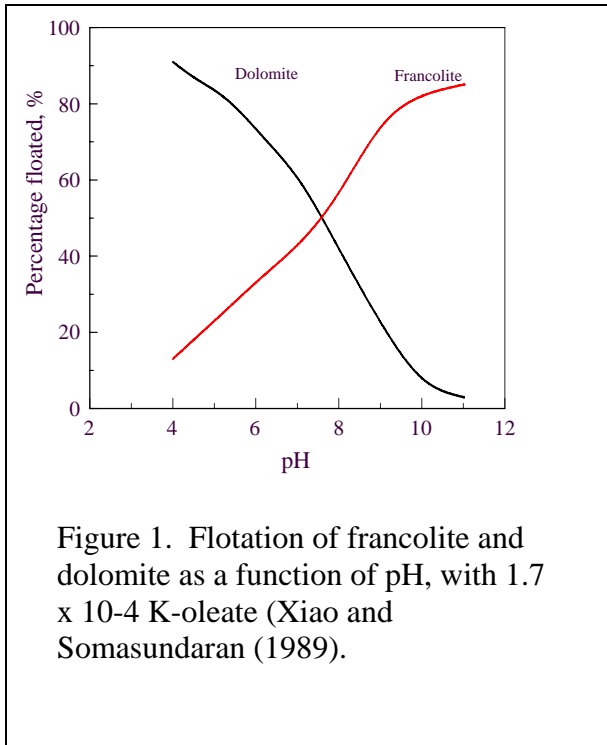


Figure 1. Flotation of francolite and dolomite as a function of pH, with  $1.7 \times 10^{-4}$  K-oleate (Xiao and Somasundaran (1989)).

Although some researches (Smani et al., 1975; Mougil and Chanchani, 1985; Xiao and Somasundaran, 1989; Moudgil and Ince, 1991) have been conducted to understand the flotation behaviors of both dolomite and phosphate using pure mineral samples for years, little work has been published on natural dolomitic phosphate samples due to the extreme complexity of the components in its flotation system.

In this study, natural high dolomitic phosphate sample (Sample B) are obtained from IMC Global, Inc., mine site in FL, is used to evaluate the effect of pH on the flotation performance of separating dolomite from phosphate. Fatty acid type collector, FAS-40A was used as collector,

phosphoric acid and sodium hydroxide as pH modifier (no depressant is used for this study). The collector dosage used for the flotation is 2.5 kg/t of feed. Phosphoric

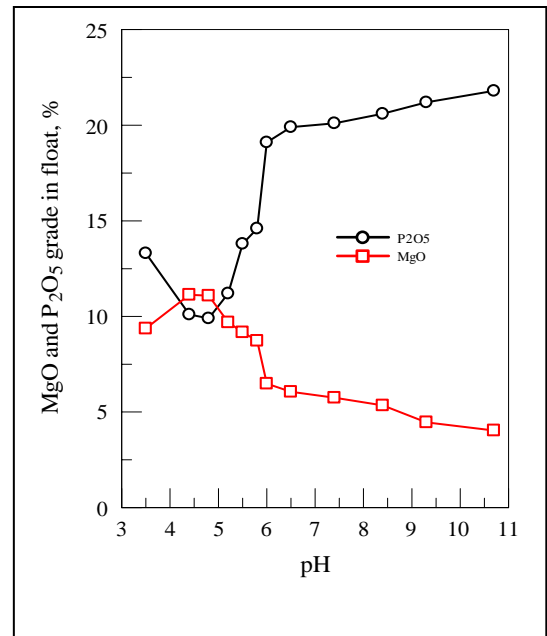
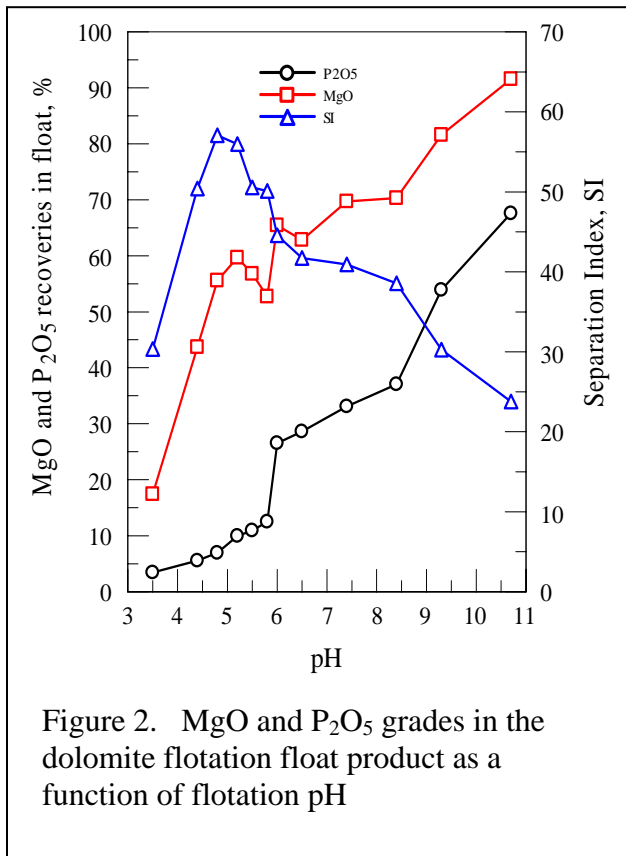
acid is applied to adjust acidic pH and sodium hydroxide to adjust alkaline pH. The MgO and  $P_2O_5$  grade in the float of dolomite flotation as a function of pH is given in Fig. 2. It is observed that, to some extent, one curve mirrors another one, suggesting higher MgO corresponding lower  $P_2O_5$  and higher  $P_2O_5$  corresponding lower MgO at the pivot point of pH 4.7. Below pH 4.7, MgO grade starts to increase and  $P_2O_5$  decrease with the increase the values of pH. Between pH 4.7 and pH 6, there is a sharp increase in  $P_2O_5$  and decrease in MgO grades. As the pH value become beyond pH 6, the changes in both MgO and  $P_2O_5$  grade are much slower. Higher  $P_2O_5$  and lower MgO grade in the float product means the poor selectivity for the separation. At low pH, bubbles are brittle and easily coalescent. The froth layer is not thick enough to allow a secondary concentration or cleaning process, which causes more phosphate particles to float and entered into froth. In order to raise the pH, only sodium hydroxide is used, and there is no depressant applied to inhibit the phosphate flotation. At higher pH (>6), it can be considered as phosphate flotation rather than dolomite flotation, and dolomite is entrapped into the froth. Therefore, the MgO grade is much lower than  $P_2O_5$  grade in the float product.

Fig. 3 presents the MgO and  $P_2O_5$  recoveries in the float product and Separation Index, SI<sub>p</sub>, of dolomite phosphate flotation process at different pH values. The published data using pure dolomite and francolite mineral for the flotation did not exhibit the monotonous decreasing in the recoveries of MgO and  $P_2O_5$  within the whole pH range. In the present study using natural dolomitic phosphate sample, the flotation recoveries of both dolomite and phosphate in the float, increase with the increase of pH value, with the MgO recovery higher than  $P_2O_5$  recovery. At pH 3.5, both dolomite and phosphate particles are depressed and their recoveries are quite low. From pH 3.5 to 5.4, the MgO recovery increases very sharply and reaches it peak around pH 5.4, while there is only slow increase in  $P_2O_5$  recovery. Above pH 5.4, the MgO recovery decreases. At about pH 6, there is a sharp increase in both MgO and

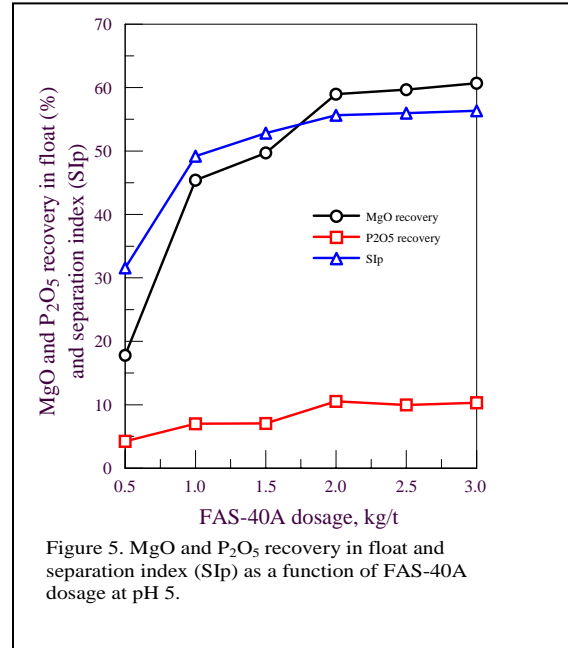
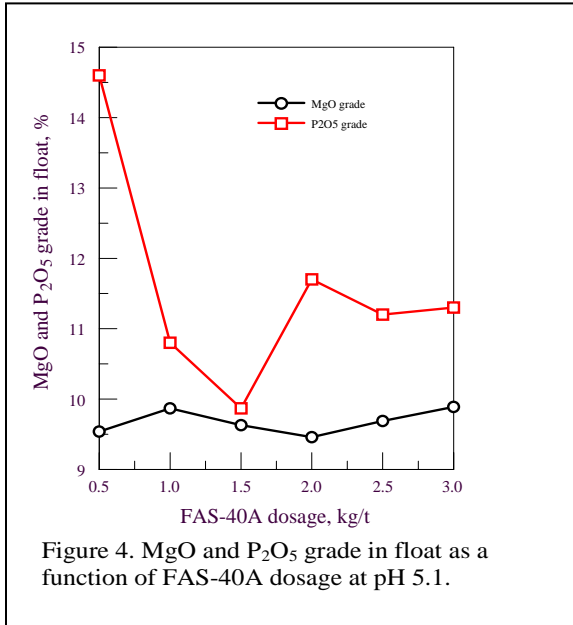
P<sub>2</sub>O<sub>5</sub>. This is because there is no phosphoric acid being used to obtain the neutral and alkaline pH above pH 6.

As described in the previous section, the phosphoric acid functions as both pH modifier and phosphate depressant in dolomite phosphate flotation. Without the presence of the depressant, much more phosphate particles are floated and dolomite particles also float with phosphate particles. This continues from neutral pH to whole range of alkaline pH. The objective of dolomite flotation process is to prevent as much as dolomite particles in the float while to recover as much as phosphate particles in the sink. The larger the difference between MgO and P<sub>2</sub>O<sub>5</sub> recoveries indicates the better selective separation.

In Fig. 3, it can be observed that the maximum recoveries in the float occurs at pH range of 4.5 to 5.8. Separation Index curve in Fig. 3 shows there is an optimum pH exists. The best separation can be achieved at about pH 5.0 with all the major factors such as grade and quantities of MgO and P O considered.



Figs. 4 and 5 show the grades and recoveries of dolomite and phosphate particles in the floats as the function of the collector dosage of FAS-40A used at pH 5. The separation index, SI<sub>p</sub> as the function of collector dosage is also included in Fig. 5. From the observation of the flotation results, the best amount of the collector dosage is at 1.5-2.0 kg/ton dolomitic phosphate. From the observations in this study, compared to the published data, the flotation behaviors of “natural” dolomite particles and phosphate particles in the dolomite flotation, exhibit quite different in that of individual “pure” dolomite particles and “pure” phosphate, or mixture of “pure” particles.



## FUTURE WORK

Additional dolomitic phosphate sample was received from Mosaic Co. (IMC Global, Inc.), FL recently. We have scheduled to run the tests on the next relative coarser size level of the sample, by applying FAS-40A dolomite collector with some frothing agent supplied by ARR-MAZ, FL. The material will be characterized and dolomite flotation will be tested in a stirred tank cell for determination of the range of reagent requirements and improvement of flotation conditionings. Based on the stirred tank cell flotation results, the column cell flotation will be conducted.

## REFERENCES

- Moudgil, B. M., and Chanchani, R., 1985, "Flotation of Apatite and Dolomite Using Sodium Oleate as the Collector," *Minerals and Metallurgical Processing*, Vol. 6, No. 2, pp. 13-19.
- Moudgil, B. M., and Ince, D., 1991, "Effect of sodium chloride on flotation of dolomite from apatite," *Minerals and Metallurgical Processing*, Vol. 6, No. 2, pp. 139-143.
- Smani, M. S., Blazy, P., and Cases, J. M., 1975, "Beneficiation of Sedimentary Moroccan Phosphate Ores – Part 3 Selective Flotation and Recovery," *SME/AIME Transaction*, Vol. 258, pp. 258-180.
- Xiao, I., and Somasundaran, P., 1989, "Interactions between oleate collector and alizarin modifier in dolomite/francolite flotation system," *Minerals and Metallurgical Processing*, Vol. 6, No. 2, pp. 100-103.

**PUBLICATIONS/PRESENTATIONS:** No.  
**(APPENDICES (IF ABSOLUTELY NECESSARY):** No.

**Appendix 5: Beneficiation of Mixed Potash Ores From New Mexico**

**(NM004)**

## TECHNICAL PROGRESS REPORT

Contract Title and Number:

Crosscutting Technology Development at the Center for  
Advanced Separation Technologies  
(DE-FC26-02NT41607)

Period of Performance:

Starting Date: 6/1/2004  
Ending Date: 10/31/2006

Sub-Recipient Project Title:

Beneficiation of Mixed Potash Ores from New Mexico

Report Information:

Type: Semi-Annual  
Number: 2  
Period: 10/1/05-3/31/06  
Date: 04/30/06  
Code: NM004-R02

Principal Investigators:

Gundiler, Brandvold, Pietrab

Contact Address:

New Mexico Tech  
Socorro NM 87801

Contact Information:

Phone: (505) 835-5730  
Fax: (505) 835-6333  
E-Mail: [gundiler@gis.nmt.edu](mailto:gundiler@gis.nmt.edu)

Subcontractor Address:

No subcontracts issued.

Subcontractor Information:

Phone:  
Fax:  
E-Mail:

### ABSTRACT

Investigations for improving the sylvite recovery from mixed ores before attempting the recovery of sulfate minerals were continued. In order to simplify the experimental procedures, desliming and potash flotation from dry ground low-clay ores was studied by mechanical and flotation desliming methods. Effects of excess slimes depressor guar on sylvite flotation, as well as emulsion composition were also investigated. Halite flotation from high-grade langbeinite ore fines using alkylmorpholine collectors was also studied. Halite did not float from saturated halite brines, yet floated readily from double-saturated sylvite brines, although reagent consumption was much higher than in conventional flotation systems. Flotation tests from sylvite tailings and from low-grade langbeinite ores were conducted with fatty acids and fatty acid sulfonates; analytical results are not yet available.

### INTRODUCTION

#### Background

Potassium is an essential element vital for plant and animal life. Potash is the common term that denotes the element potassium in a water-soluble form in a variety of

chemical combinations. Over 90% of the potash produced is used as agricultural fertilizer. The potassium content in potash ores and fertilizer products is reported as %K<sub>2</sub>O as a means to compare different potash minerals.

The most abundant potash ore, sylvinite, is a mechanical mixture of sylvite (KCl) and halite (NaCl), including minor amounts of clays, silica, anhydrite (CaSO<sub>4</sub>), and potassium complexes as carnallite, polyhalite, kainite, langbeinite and leonite. The chemical composition of principal potash minerals is given in Table 1. Sylvinite and langbeinite are the only major ore minerals mined in New Mexico.

Table 1. Common potash minerals

Mineral	Formula	Specific gravity	% K <sub>2</sub> O
Sylvite	KCl	1.99	63.17
Carnallite	KCl.MgCl <sub>2</sub> .6H <sub>2</sub> O	1.60	16.95
Kainite	KCl.MgSO <sub>4</sub> .3H <sub>2</sub> O	2.13	18.92
Langbeinite	K <sub>2</sub> SO <sub>4</sub> .2MgSO <sub>4</sub>	2.83	22.70
Leonite	K <sub>2</sub> SO <sub>4</sub> .MgSO <sub>4</sub> .4H <sub>2</sub> O	2.25	25.69
Schoenite	K <sub>2</sub> SO <sub>4</sub> .MgSO <sub>4</sub> .6H <sub>2</sub> O	2.15	23.39
Polyhalite	K <sub>2</sub> SO <sub>4</sub> .MgSO <sub>4</sub> .2CaSO <sub>4</sub> .2H <sub>2</sub> O	2.78	15.62

Langbeinite is mined only in New Mexico. Low chloride content and lower solubility of the potassium sulfate products make them desirable for certain crops, such as tobacco, potato, and citrus crops, and soil conditions. Langbeinite has lower solubility than halite and high-grade ores are simply leached with water to produce 22% K<sub>2</sub>O concentrates. Polyhalite and kieserite, however, have solubility similar to langbeinite. They remain with the concentrate and lower the product grade. The water leaching method to produce a marketable form of langbeinite, however, requires high water consumption that has a significant impact on the region.

Mixed langbeinite-sylvite ores are treated in heavy media cyclones; langbeinite is separated, leached with water, dried and screened to produce market grades. In the past, sylvite product was obtained by flotation from heavy media tailings. Langbeinite in mixed sylvite - langbeinite ores, which could range as high as 15% by weight, and other double (K-Mg) sulfate minerals, can not be recovered at present, and are lost to the sylvite tailings. There are also large reserves of langbeinite ore that are not exploited due to high concentrations of kieserite contamination. An efficient method to separate fine halite and kieserite from langbeinite does not exist.

### Objective and Approach

The primary objectives of this work is then summarized as i) improving the efficiency of desliming and sylvite flotation, ii) recovery of langbeinite and kieserite form sylvite tailings, iii) flotation separation of langbeinite and kieserite from mixed concentrates, and iv) flotation separation of halite from langbeinite ores to produce high-grade langbeinite concentrates. Secondary objectives are to investigate the effects of magnesium ion concentration, brine temperature, and amine composition one sylvite flotation.

## **PROJECT TASKS**

### Task 1 - Materials and Methods

Several tons of sylvite ore samples with low (~2%), medium (2.5-4.5%), and high clay (>8%) content were collected from operating plants and underground workings, and brought back to our laboratories. Most of the low-clay ores were ground to minus 2 mm and used to prepare brines for desliming and sylvite flotation experiments. In addition, several hundred pounds each of mixed sylvite-langbeinite, high-grade langbeinite, high-kieserite langbeinite ore samples, sylvite and langbeinite concentrates, and several drums of plant brines were also collected.

### Task 2 - Chemical Analyses

Analysis of potassium in high concentrations requires traditional techniques that are highly specialized and time consuming. To date over 1,700 samples were analyzed for K<sub>2</sub>O and IR involving slimes, flotation concentrates and tailings on experiments with sylvite ores. Mixed-ores, however, require for each sample to be analyzed for Na, K, Ca, Mg, Cl, and sulfate ions as well as water of hydration at 110, 330, and 440 C to be able to make a mass balance on mineralogical composition of the initial ore samples (Table-1) and final products using the Fuchsman method. Chemical and mineralogical composition of all mixed-ore samples have been successfully completed and verified by duplicate assays at the potash plant laboratories.

### Task 3 – Experimental Results and Discussions

#### Slime Flotation

Before attempting the separation of mixed ores, synthetic mixtures were prepared by adding a known amount of langbeinite concentrate to low-clay sylvite ores. Previously, the coarse ore (8-9.5 mm) was deslimed by siphon decantation (1st stage), ground in a rod-mill, deslimed (2nd stage), and sylvite was floated with amine-oil-frother emulsion as described previously (NM 004 – R01). In order to simplify the procedure and shorten the duration of experiments, the coarse ore was dry ground to -14 mesh (1.18 mm) deslimed in one stage either by mechanical decantation (with or without dispersants) or with one-stage slime flotation.

Figure -1 summarizes the results of one-stage desliming either with mechanical (siphon) decantation, or with slime flotation with oxyethylated fatty amines (OEFAM) or fatty acids (OEFAC). Slime flotation, with either amine or acid type collectors, reduces the IR content of the deslimed ore lower than the mechanical flotation. At higher concentrations of OEFAC the IR content of the flotation feed is the lowest, however, the K<sub>2</sub>O loss to the slimes fraction also increases. Figure-2 shows a comparison of flotation recoveries after desliming. Much higher amine and guar concentrations are required after mechanical desliming the ore for comparable potash recoveries to (slime) flotation desliming.

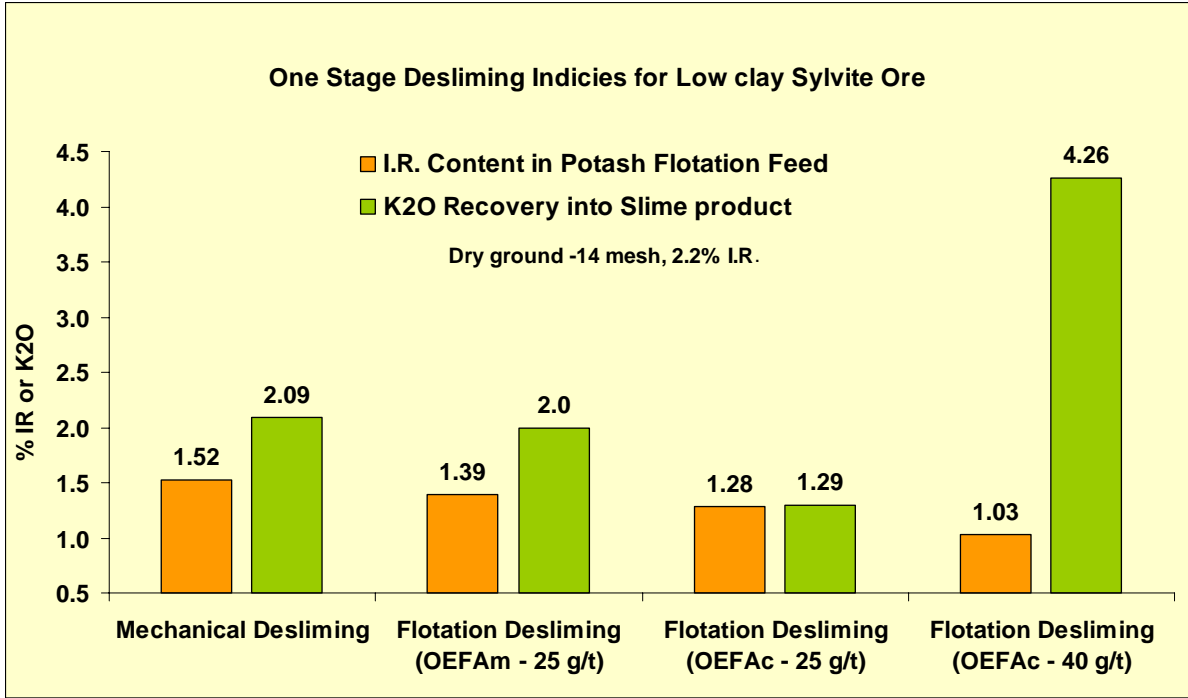


Figure 1 – IR and K<sub>2</sub>O recovery into flotation feed and slime product, respectively.

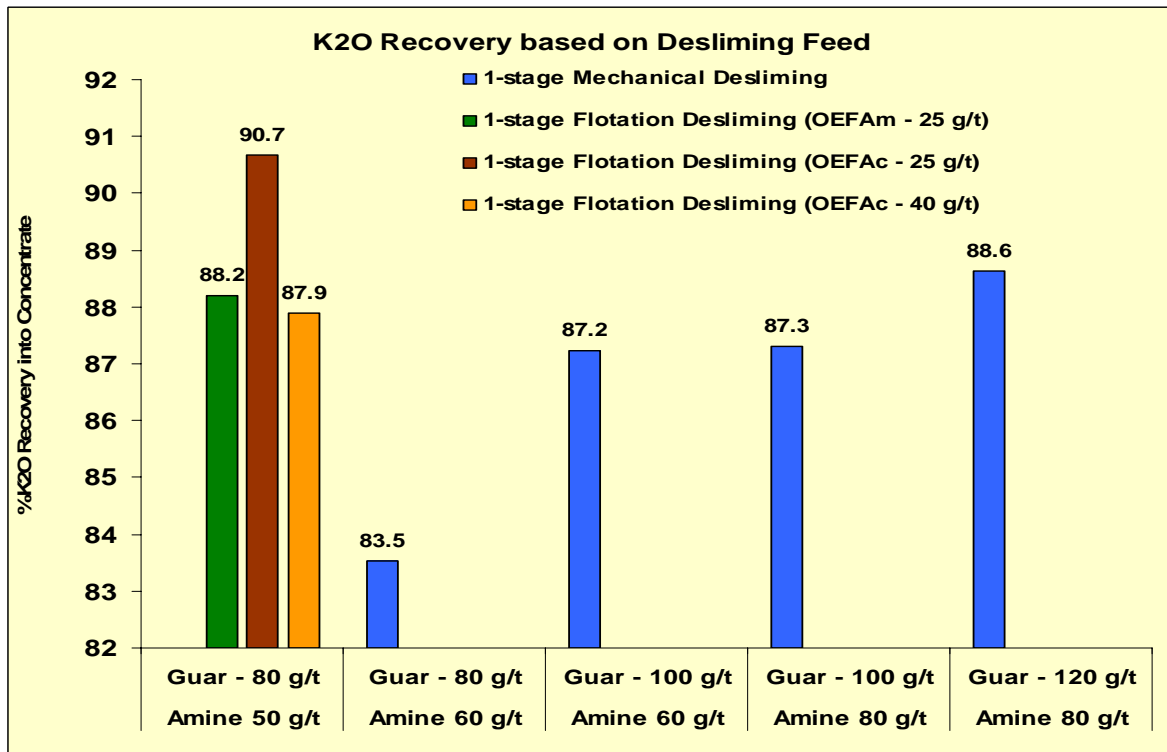


Figure – 2 Comparison of overall K<sub>2</sub>O recovery into the potash flotation concentrate.  
*Frothers Emulsions and Depressants*

Generally, oil-frother-amine emulsions were prepared keeping oil and frother concentrations in the emulsion 30% of the amine concentration for all flotation tests reported here. A 2-level 3-factorial experimental design was attempted to delineate the optimum oil-frother ratios in the amine emulsion and the possible interaction of clay depressant guar on flotation recoveries of potash from deslimed ore samples. Changing oil or frother ratio to 20% and 40% of the amine for low and high levels oil and frother concentrations did not yield discernible results. It was also observed that dispersion of the organic melt in aqueous HCl solution was more difficult and time consuming when 20% frother was used. This was more pronounced with glycol esters than when alcohols were used.

The effect of excess guar concentrations was studied independently using industrial grade white KCl obtained from the hot-brine leach-crystallization plant at Carlsbad, NM. Very little effect was observed (Figure - 3) until guar concentration in brine reaches to 100 mg/L (670g guar / ton KCl). Whereas Titkov et al. (1999) showed that when lignin sulfonate was used at concentrations higher than 20 mg/L potash flotation recovery is drastically reduced.

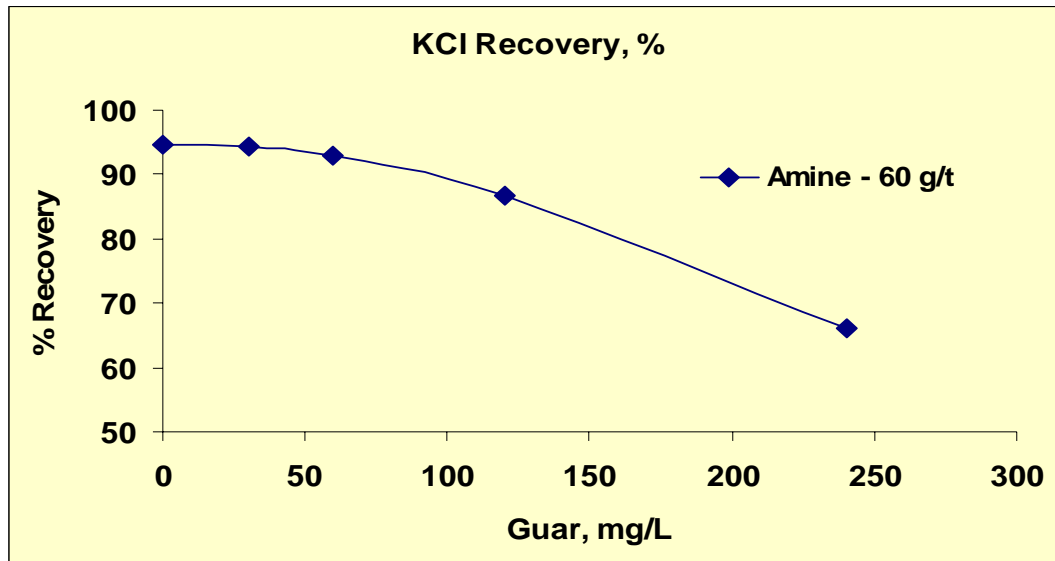


Figure-3 Effect of excess guar concentration on KCl flotation.

Therefore, further experiments using 2-level 2-factorial design were conducted using 30 and 60% levels for oil and an alcohol type frother. It is expected that at higher levels of oil flotation of coarser particles (>1mm) should improve, however analytical results are not yet available. Preliminary experiments conducted in this phase also showed that 1% amine emulsions yielded better recoveries than the 2% amine emulsions, presumably due to better reagent dispersion and interaction with the ore minerals.

### Halite Flotation

Halite flotation was considered as an alternative to water leaching to upgrade the fine (<10 mesh) fraction of high-grade langbeinite ores using alkyl morpholine reagents (Titkov et al., 2003). Halite flotation was not possible from saturated halite brines. Further investigations,

however, showed that halite floats readily from double saturated (NaCl-KCl-H<sub>2</sub>O) brines (Figure - 4). Halite flotation from in sylvinite brines has not yet been investigated. However, preliminary experiments for langbeinite flotation with fatty acids and sulfonates have been conducted. Analytical results are not yet available.

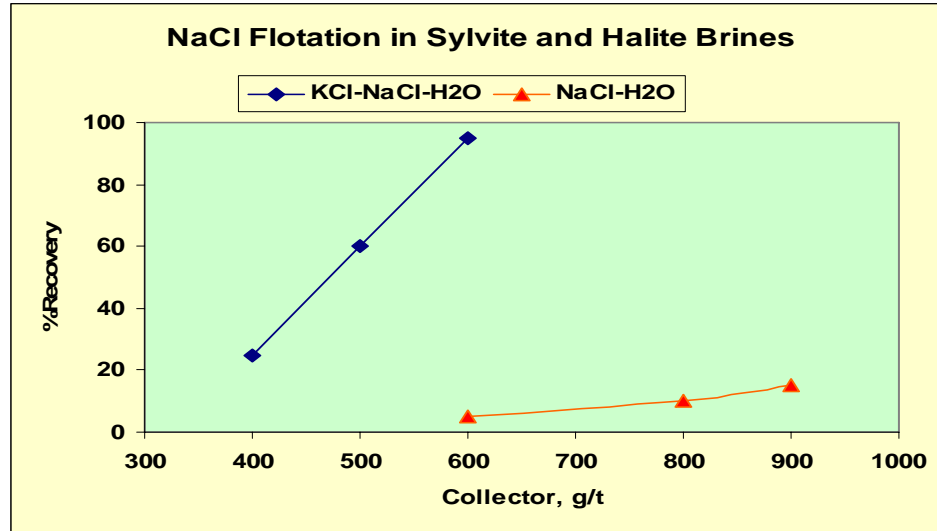


Figure-4 Halite flotation from saturated halite and sylvite brines

## SUMMARY

Investigations on improving the efficiency of sylvite (KCl) recovery from mixed ores in order to prepare feedstock for langbeinite flotation continued during this phase. One-stage slime flotation from dry ground ores conducted to eliminate rod mill grinding and desliming steps which are time consuming and lead to higher solubility losses during tests. Effect of excess guar on flotation of KCl was investigated along with the concentrations of oil and frother in the amine emulsions. Reverse flotation, i.e., flotation of halite from langbeinite fines were initiated to upgrade high-grade fines and eliminate water leaching of halite. Tests on direct flotation of langbeinite from halite and sylvite brines are currently underway. The results will be reported in the next progress report.

## FUTURE WORK

Investigations on the recovery of langbeinite from sylvite tailings in mixed ores, flotation and separation of langbeinite and kieserite from low-grade langbeinite ores will be pursued using a variety of collector families and flotation schemes. At the same time fundamental studies for better understanding of soluble salts flotation will be initiated. These studies will include brine chemistry and temperature, zeta potential measurements, AFM and NMR studies.

## REFERENCES

Titkov, S., Sabirov, R., and Panteleeva, N., "Investigations of Alkalmorpholines", Minerals Engineering, (2003) v. 16, pp. 1161-1166.

**Appendix 6: Development of a New Reagent Schedule for Flotation of  
Dolomite from Phosphate Ores (NV002)**

## TECHNICAL PROGRESS REPORT

Contract Title and Number:

Crosscutting Technology Development at the Center for  
Advanced Separation Technologies  
(DE-FC26-02NT41607)

Period of Performance:

Starting Date: 6/1/2004  
Ending Date: 10/31/2006

Sub-Recipient Project Title:

Development of New Reagents for the Flotation of  
Dolomite from Phosphate Ore

Report Information:

Type: Semi-Annual  
Number: 3  
Period: 10/1/05-3/31/06  
Date: 3/27/06  
Code: NV002-R03

Principal Investigators:

Fuerstenau, Misra, Bell

Contact Address:

168 Macay School of Mines  
University of Nevada Reno  
Reno NV 89557

Contact Information:

Phone: (775) 784-4310  
Fax: (775) 784-4764  
E-Mail: mcf@unr.edu

Subcontractor Address:

University of Nevada, Reno  
Reno, NV 89557

Subcontractor Information:

Phone: (775) 784-4312  
Fax: (775) 784-6680  
E-Mail: Jerry\_best@vpaf.unr.edu

### ABSTRACT

Reagents, hexadecyl citric acid ester and lauryl sarcosine, were tested as flotation collectors. Results indicate that selectivity of dolomite from apatite may be possible with hexadecyl citric acid ester as collector at about pH 6. Flotation of phosphate ore will be conducted to test this observation. Flotation was not achieved from an ore with lauryl sarcosine as collector. Analogs of this reagent with longer hydrocarbon chains are being synthesized.

### INTRODUCTION

The United States is the largest phosphate rock producer in the world. About 30 % of the total world production in 1990 was produced by the United States (1). Florida accounts for approximately 80 % of the U.S. phosphate production (2). During the past 100 years, the Florida phosphate industry has produced high quality products having a MgO content of less than 0.5 %. Phosphate reserves and resources in Florida have the potential to continue production at a rate of about 40-55 million metric tons/year for hundreds of years (3).

Resources with relatively-low MgO (dolomite) content are being depleted, and future production is going to have to utilize those resources containing significant dolomitic carbonate.

The processing of these reserves will require special beneficiation techniques to produce concentrates containing less than the practical limit of about 1 % MgO.

Over the past several years, five flotation processes have been developed to separate dolomite from phosphate or phosphate from dolomite (4). They are the TVA (Tennessee Valley Authority) phosphonic acid process, the UF (University of Florida) two-stage conditioning process, the University of Alabama process, the USBM (United States Bureau of Mines) process, and the IMC (International Minerals and Chemical Corporation) cationic process.

None of these processes has been commercialized for a variety of reasons. In order to further exploit Florida dolomitic phosphate pebbles and to improve phosphate beneficiation, the development of effective collectors for dolomite appears to be essential.

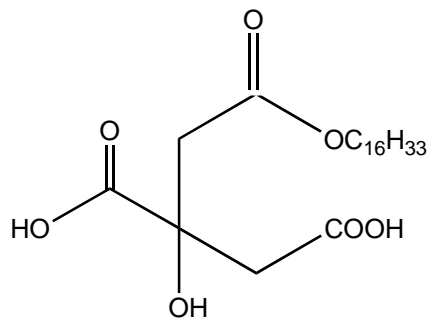
### Objective and Approach

The objective of this investigation is to synthesize collectors that have specificity for magnesium and, hence, dolomite. Flotation characteristics of apatite, dolomite and phosphate rock will be determined with those collectors to establish whether physical separation of dolomite from phosphate rock can be obtained.

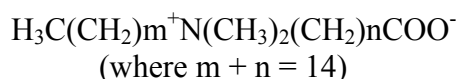
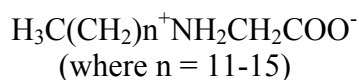
## **PROJECT TASKS**

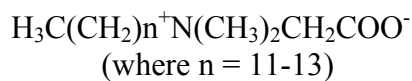
### Flotation Collector Synthesis

The synthesis of malonate-based surfactants and a series of monoesters of citric acid were described earlier. Another collector, monohexadecyl citric acid ester, has been synthesized.



Analogs of a new target molecule, sarcosine, are being designed. N-lauryl sarcosine has been tested; no flotation from phosphate ore was achieved. It is felt that the hydrocarbon chain length is too short for this reagent to function as a collector. In this view longer-chain analogs are being synthesized. These are:





### Flotation Experiments

Flotation experiments were conducted with monohexadecyl citric acid ester as collector for apatite and dolomite using a Hallimond tube. One gram of mineral, 150 x 106 μm, was added to 150 ml of solution. Conditioning was conducted for three minutes at the desired collector concentration and pH. Each sample was floated for one minute with nitrogen bubbled through the Hallimond tube at 0.060 SLPM. Collector concentration and pH were varied to determine the effects of each upon flotation. Flotation responses are shown in Figures 1 – 4.

Flotation recovery of dolomite as a function of monohexadecyl citric acid ester concentration is shown in Figure 1. Collector concentrations greater than  $1 \times 10^{-4}$  M were not used due to solubility limitation of this reagent. As can be noted, about 70 percent flotation recovery was obtained with  $1 \times 10^{-4}$  M.

Flotation recovery of dolomite as a function of pH with  $1 \times 10^{-4}$  M collector shows two mechanisms in flotation response (Figure 2). Flotation at about pH 6 can be attributed to physical adsorption of hexadecyl citric acid ester on the positively-charged dolomite surface. Flotation observed in basic medium can be attributed to chemisorption or surface reaction/precipitation of metal collector.

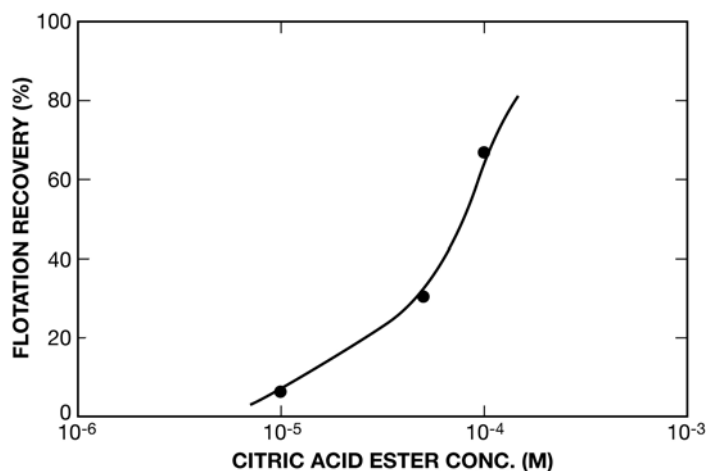


Figure 1. Flotation recovery of dolomite as a function hexadecyl citric acid ester concentraton at pH 9.2.

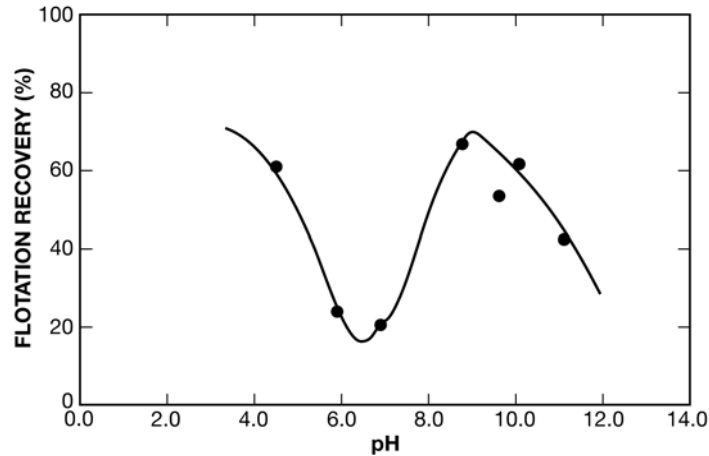


Figure 2. Flotation recovery of dolomite as a function of pH with  $1 \times 10^{-4}$  M hexadecyl citric acid ester.

The response of apatite to flotation with hexadecyl citric acid ester at constant pH is shown in Figure 3. The much stronger affinity of this collector for the apatite surface is obvious. Essentially complete flotation was obtained with  $1 \times 10^{-4}$  M, while about 50 percent recovery was obtained with  $1 \times 10^{-5}$  M.

The high adsorption potential of this collector for apatite is also shown in Figure 4. Essentially complete flotation was obtained from about pH 6 to 11 with  $1 \times 10^{-4}$  M hexadecyl citric acid ester.

Selectivity in flotation between the two minerals is indicated at about pH 6. Flotation of phosphate ore will be tested to determine whether such a separation is possible under those conditions.

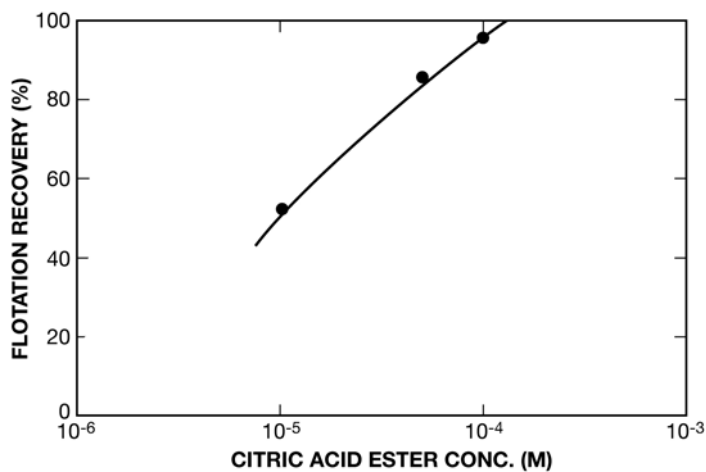


Figure 3. Flotation recovery of apatite as a function of hexadecyl citric acid concentration at constant pH 6.4.

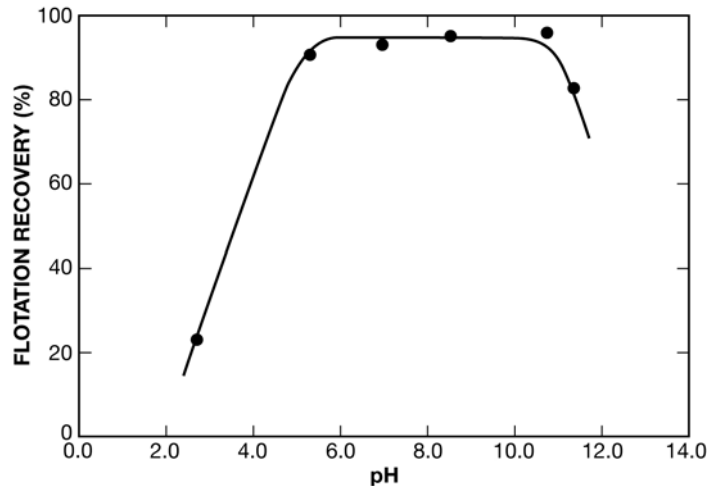


Figure 4. Flotation recovery of apatite as a function of  $1 \times 10^{-4}$  M hexadecyl citric acid ester.

## SUMMARY

Flotation collectors, hexadecyl citric acid ester and lauryl sarcosine were tested as flotation collectors. Results indicate that selectivity of dolomite from apatite may be possible with hexadecyl citric acid ester as collector at about pH 6. Flotation was not achieved from an ore with lauryl sarcosine. Analogs of this reagent with longer hydrocarbon chains are being synthesized for testing as flotation collectors for selective separation of dolomite from phosphate rock.

## FUTURE WORK

Additional collectors are being synthesized and are to be tested for selectivity in the flotation separation of dolomite over apatite and phosphate rock.

## REFERENCES

1. Bartels, J. J., and Gurr, T. M. 1994. "Phosphate Rock." Industrial Minerals and Rocks. 6<sup>th</sup> Edition. D. D. Carr. Ed. Society for Mining, Metallurgy and Exploration, Littleton, CO. pp 751-764.
2. Harben, P. 1991. "Where is Florida's Phosphate Industry Going?" Industrial Minerals, No. 148. pp. 48-55.
3. Sandvik, P. O. 1979. "U. S. Phosphate-Abundant Resources Will Last for Hundreds of Years." Eng. & Min. J., 180:99-101.
4. El Shall, H. 1994. "Evaluation of Dolomite Separation Techniques. FIPR Contract No. 93-02-994, Final Report.

**Appendix 7: High Frequency Eddy Current Separation of Metallic Residue  
from Slags, Sands, Electronic Scraps and Other Wastes (UT004)**

## TECHNICAL PROGRESS REPORT

### Contract Title and Number:

Crosscutting Technology Development at the Center for  
Advanced Separation Technologies  
(DE-FC26-02NT41607)

### Period of Performance:

Starting Date: 6/1/2004  
Ending Date: 10/31/2006

### Sub-Recipient Project Title:

High Frequency Eddy Current Separation of  
Metallic Residue from Slags, Sands, Electronic  
Scrap and Other Wastes

### Principal Investigators:

Raj K. Rajamani

### Report Information:

Type: Semi-Annual  
Number: 3  
Period: 10/1/05-3/31/06  
Date: 3/30/06  
Code: UT004-R03

### Contact Address:

University of Utah  
135 South 1460 E. Room 412  
Salt Lake City UT 84112

### Contact Information:

Phone: (801) 581-3107  
Fax: (801) 581-8119  
E-Mail: rajamani@mines.utah.edu

### Subcontractor Address:

University of Utah  
135 South 1460 E. Room 412  
Salt Lake City UT 84112

### Subcontractor Information:

Phone: (801) 581-3107  
Fax: (801) 581-4937  
E-Mail: Raj.rajamani@mines.utah.edu

## ABSTRACT

The separation of materials was carried out based on the applied magnetic field in a toroidal core. The objectives were to: 1) study the magnetic field intensity at various points between the opening of the core gap, 2) design a new optimally shaped core and, 3) test the newly shaped core with sample particles. The effect of the field on the particle was studied with the help of a pendulum, which was placed at various points in the magnetic field. The circuit was optimized by trying out all possible combinations of resistance, inductance and capacitance. The circuit so designed showed very high magnetic flux and separation was possible between copper and aluminum particles which lead to the conclusion that increasing the number of turns or/and increasing the size of the core would lead to greater separation capacity.

## INTRODUCTION

### Background

To increase the capacity of separation the main concept was to increase the flow rate of the feed through the dipole. This increased flow rate could be achieved by increasing the flow

area through the dipole through which the feed could pass. To increase the area, the gap in the dipole had to be increased. This increase in gap would decrease the effective magnetic field in the region. To counter this effect the electromagnetic field between the ends of the dipole had to be increased. This was made possible by increasing the stored potential of the LCR-circuit (This was achieved by increasing the amplification factor of the amplifier).

### Objective and Approach

The main objective of this phase's research was to optimize the eddy current circuit, check the deflection of the particles at various points of the core gap, separate the particles using the old shape and increase the separation efficiency by conducting experiments with newly shaped cores, to move further to pilot scale separation experiments.

## **PROJECT TASKS**

### **Equipments used**

Ferrite core: OW 48613 TC  
Oscilloscope: HP 54645D  
Function generator: HP 33120A  
Power supply: HP E3631A  
Multimeter: HP 34401

### **TASK-I: System setup characterization**

The first task was to study the magnetic field intensity at various points between the opening of the core gap. The main objective was to determine the field strength at various positions which would determine the correct position of the feed to be fed from the top. It would also help in determining the proper shape of the core opening. Experiments were also conducted to study and optimize the new electrical circuit by changing the capacitance and feedback resistance along with the effect of magnetic field on particle separation.

### **Setup**

1. System was set up to give about 5400 V at 11.349 kHz. In order to study the magnetic field, copper (6 mm diameter approx.) and aluminum (3.5mm diameter approx.) particles were suspended by weightless strings. The strings were moved from various positions and the field strength was studied.
2. Voltage across the core was 2300 V at frequency of 10.215 kHz. Vertical height from which the particles were dropped was 13 cm.

### **Observations with setup-1**

- (a) **Aluminum particle:** When aluminum particle was suspended, it was found that its interaction with the magnetic field destabilized the field. In order to verify this, the

copper particle was suspended next. The aluminum particle weighed 0.0601 gm. Its diameter was 3.5 mm.

**(b) Copper particle:** Similar result was observed for copper particle. Hence, it was concluded that the voltage across the core had to be reduced in order to sustain the magnetic field. The copper particle weighed 1.3396 gm. Its diameter was 6 mm.

Based on the earlier conclusion the voltage was reduced to 4000 V and similar experiments were reconducted. It was found that at a voltage of 4000 V or lower across the core, the system was stable. Figure 1 shows the direction of deflection of copper particle as was observed during the experiment:

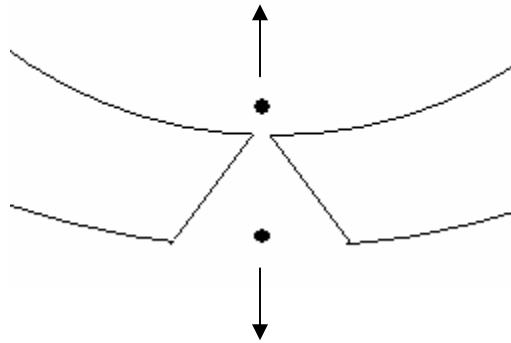


Figure 1: Deflections observed at different locations of the core opening

It was found that aluminum particles experienced little or no deflection when suspended at any point. The copper particle showed maximum deflection at the inner edge than at the outer edge. From the above, it was concluded that the magnetic field intensity at the inner edge was much stronger than at the outer edge. Hence a new design of the core opening was proposed. The design looks as shown in the Figure 2 below.

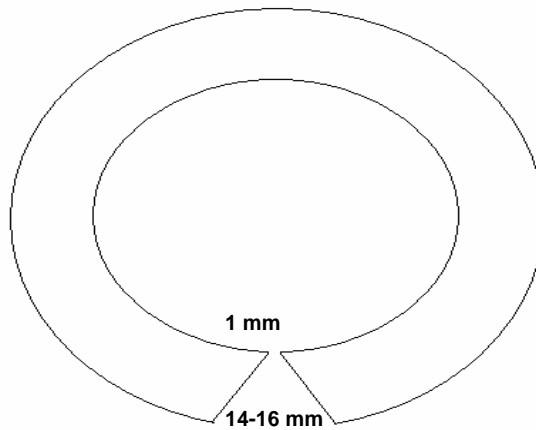


Figure 2: Proposed shape of the core openings

## Observations with setup-2

The effect on the particles was studied on the newly designed core. The experiments were conducted to study the new optimized circuit by changing the capacitance and feedback resistance along with the effect of magnetic field on the particle. Experiments were also conducted to study the deflections of copper and aluminum particles on the generated magnetic field. At first a copper particle of spherical shape (7 mm diameter) was taken and dropped in to the magnetic field generated by the new core. The particles were made to fall up from a height of 13 cm where it touched a horizontal surface. The horizontal distance up to which the particle traveled was recorded by using a scale. Seven similar experiments were conducted for one particle size and results were noted down. Similar seven experiments were conducted for 5mm and 3 mm particles and the results were recorded. Results are shown for the circuit optimization, which was done to get maximum and stable field within the core.

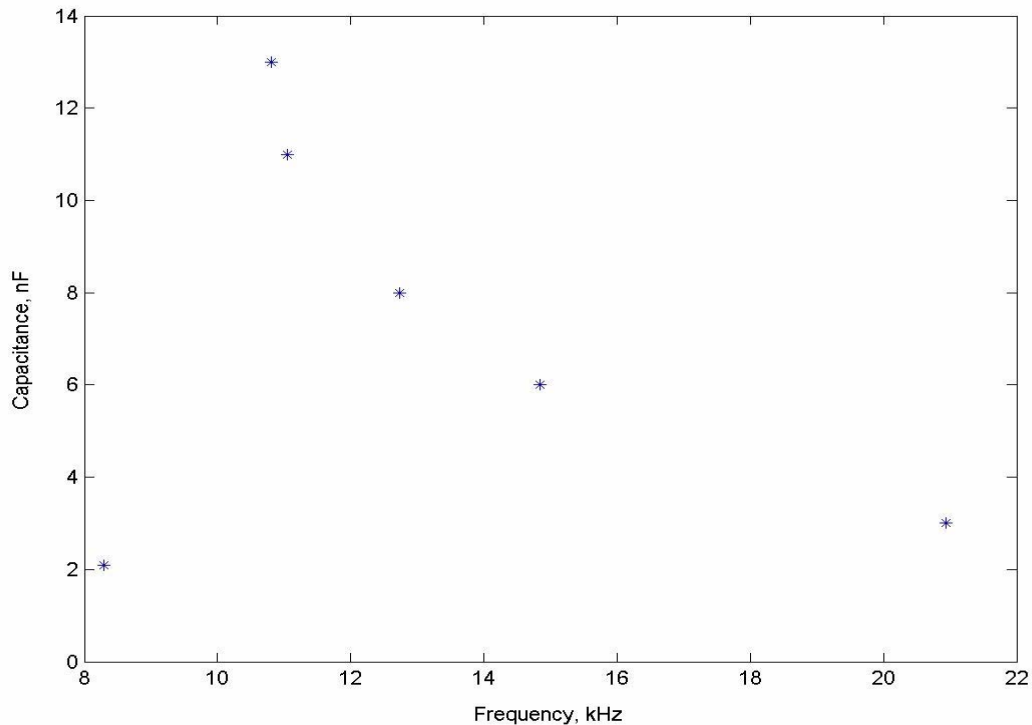


Figure 3: Capacitance (nF) versus frequency (kHz)

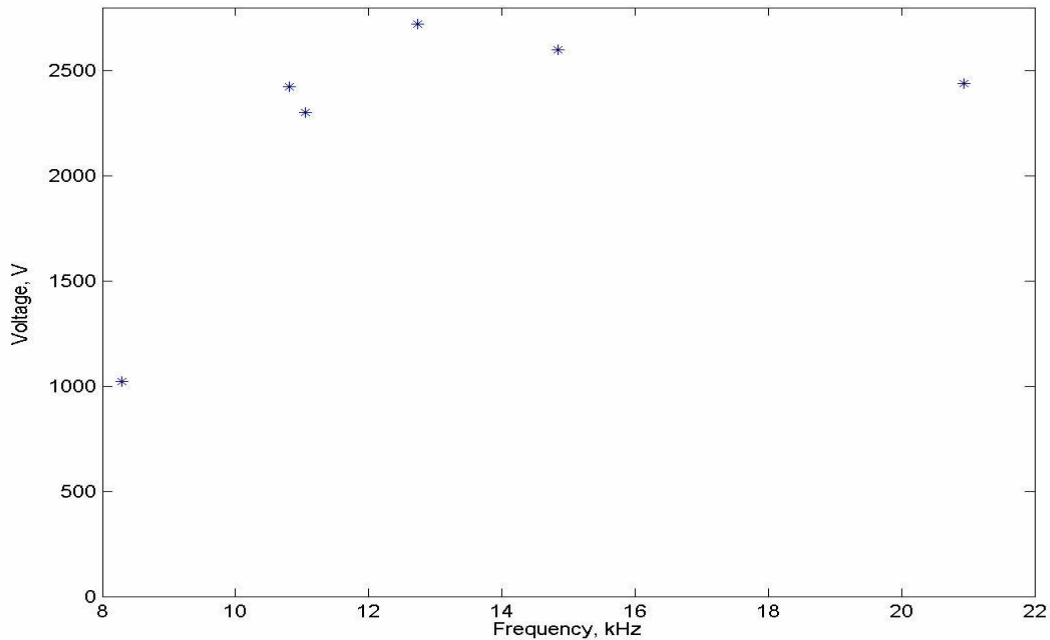


Figure 4: Frequency (kHz) versus output voltage (volts)

From figure 3, it was found that as capacitance increased, the frequency, at which maximum output was obtained, dropped except for the very first reading, which can be neglected because the output voltage was only around 1000 volts. When interpolated, it was presumed that for 20 nF capacitance, we should get about 4 kHz. From Figure 4, it was found that the output voltage almost stabilized and did not change much with increase in capacitance or decrease in frequency. The feedback resistance was set as 100 kilo Ohms as it was found to be near optimum for the entire range of capacitance.

Following readings were recorded when particles were dropped from 13 cm height:

Table 1: Horizontal distance covered by copper particles of different diameters

Diameter	7mm	5 mm	3 mm
Copper	<b>Horizontal distance covered (cm)</b>		
	6	6.5	5
	6	7.5	6
	4	7	5
	4.5	7.5	5
	6	6.5	6
	4.5	7	5
	6	7	5.5
<b>Average</b>	<b>5.3</b>	<b>7</b>	<b>5.3</b>

## **SUMMARY**

From the above experiments it was concluded that shape changing and circuit optimization were heading in the right direction. A very high force was experienced by the particles in the magnetic field. The average deflection for copper was found to be much higher than the aluminum particles. This suggests that change in particle size could also affect the deflections.

## **FUTURE WORK**

Further optimization of the circuit will be carried out to about 1-5 KHz frequency. More particle drop and pendulum tests will be carried out at these frequencies to understand the effect of lower frequency magnetic field on the particles. Small separation experiments will be carried out at this scale. A bigger core has been under investigation and will be ordered very soon. Proper pilot scale separation will be carried out with this bigger core and finally the setup will be tested for industrial scale separations.

**APPENDIX**  
**(List of figures and tables)**

Figure 1 - Deflections observed at different locations of the core opening

Figure 2 - Proposed shape of the core openings

Figure 3 - Capacitance (nF) versus frequency (kHz)

Figure 4 – Frequency (kHz) versus output voltage (Volts)

Table 1 - Horizontal distance covered by copper particles of different diameters

## **Appendix 8: Dry Particle Separation in a CFB Riser System (WV009)**

## TECHNICAL PROGRESS REPORT

Contract Title and Number:

Crosscutting Technology Development at the Center  
for Advanced Separation Technologies  
(DE-FC26-02NT41607)

Period of Performance:

Starting Date: 6/1/2004  
Ending Date: 10/31/2006

Sub-Recipient Project Title:

Continuation of Project-Dry Particle Separation in a  
CFB Rise System

Report Information:

Type: Semi-Annual  
Number: 3  
Period: 10/1/05-3/31/06  
Date: 3/30/06  
Code: WV009-R03

Principal Investigators:

Johnson, Kang

Contact Address:

West Virginia University  
337 Engineering Science Building  
Morgantown WV 26506

Contact Information:

Phone: (304) 293-3111 x2309  
Fax: (304) 293-6689  
E-Mail: johnson@cemr.wvu.edu

Subcontractor Address:

No subcontracts issued

Subcontractor Information:

Phone:  
Fax:  
E-Mail:

### ABSTRACT

During this reporting period, work was done on two of the three tasks. The investigation of the separation of steel shot and sand with the same size distribution was completed in the previous reporting period. The separation of sand by size has been completely reformulated and the results are now being evaluated. The first attempts to remove pyrite containing coal from relatively clean coal had produced inconclusive results. A second set of tests to separate the dirty (containing pyrite) coal from the clean coal is now being formulated.

### INRODUCTION

This project is a continuation of the study to determine the potential for separating small dense particles from small light particles in a CFB riser system. The early exploratory work led to many interesting and practical results. This continuation project focuses on the refinement and expansion of our test conditions and the development of more comprehensive analysis of the results. The experimental conditions planned for this project are 1) separation according to size, 2) separation of particles due only to density differences, and 3) separation of pyrite from coal. Progress in completing Task 2 and 3 has been slowed due to equipment problems. In these initial tests, the mass closure was

not acceptable. Basically, there were more of the larger particles after each test than before the test. A new procedure for determining the size distribution was instituted and the mass closure problems have been solved. During this time period, the riser system was modified to eliminate most of the places where particles could be trapped. These problems were generic to both of the remaining two tasks.

## PROJECT TASKS

Task 1 The approach to achieve the goal of Task 1 has been reformulated as a result of the experiences encountered during the initial tests. Initially, a binomial size distribution for sand was to be produced. This mixture was then to be separated into large size particles and small size particles. Problems appeared, as described in the Introduction section of this report. However, good separation of the particles by size was observed. The new approach developed to achieve the goal was to use an as-delivered sample of sand. The size distribution of the as-delivered sand was then determined. A superficial gas velocity was then selected, which corresponds to a separation diameter, denoted as  $d_p^*$ . A sample of the sand was then run through the riser system and the mass and size distribution of the particles reporting to the product bin and the dense bin were determined. Six tests have been completed and the results shown in Table 1. The performance parameters employed are based on the material in the product hopper:

$$\text{Product Bin Quality} \quad \omega_p(d_p^*) = \frac{\text{mass of particles} < d_p^* \text{ collected}}{\text{mass of mixture in product bin}}$$

$$\text{Capture Efficiency} \quad \eta_p(d_p^*) = \frac{\text{mass of particles} < d_p^* \text{ collected}}{\text{mass of particles} < d_p^* \text{ in initial mixture}}$$

$$\text{Mineral recovery} \quad \varepsilon_p(d_p^*) = \frac{\text{mass of particles} < d_p^* \text{ collected}}{\text{mass of initial mixture}}$$

These tests were conducted with as-delivered construction sand. Each test consisted of a single pass of material through the riser.

At present, attempts to produce a product consisting of a rather narrow range of particle sizes, is underway. This involves passing the sand through the riser several times, each at a different superficial gas velocity. Preliminary tests have shown excellent results, and these results are now going through final analysis. A paper on this effort is now under preparation. Task 1 has now been essentially completed.

Task 2. Completed, see reference 1.

Task 3. Waste coal from a CONSOL coal preparation plant has continued to be the material used in the separation tests. The tests, to date, with the small separation system

using waste coal with a diameter less than 150 $\mu$ m, have not been successful. The experience gained from these initial tests has led to a redesign of the small system and an indication at what test conditions we should use in the future. The redesign consisted of selecting instrumentation for lower flow rates and eliminating sections where the particles could be trapped.

The tests in the original riser system, using waste coal with a diameter larger than 200 $\mu$ m, produced mixed results. A float-sink test of the coal in the product hopper had a lower specific gravity than the sample of the initial coal. However, the chemical analysis of the coal in the product hopper showed essentially the same sulfur content as in the initial coal. The problem appears to be that the chemical analysis involves three samples of coal in the milligram range. These small quantities produced a rather large variation in sulfur readings so that the average for the three samples produced a large degree of uncertainty. A new approach to determine the sulfur content of the coal sample is now being investigated. In addition, the riser system is being modified to produce a more accommodating flow field for separation of the smaller particles.

## **SUMMARY**

To date, we have successfully completed Tasks 1 and 2. The results of these tasks show that particles may be effectively separated by either density or size difference. For Task 3, the initial tests with waste coal have been disappointing. The basic reason for the ineffective separation are: 1) the size of the coal particles are so small that the desired lateral forces are not developed, and 2) the waste coal possess a combined continuous size distribution and a continuous variation in density. The particles employed in Tasks 1 and 2 were larger and possessed a fixed density. However, these initial tests have provided an insight into how to improve the separation process for the waste coal. The riser systems are now being modified and a new set of operating conditions have been selected.

## **FUTURE WORK**

In order to complete Task 3, the riser system modifications will be completed by mid-June, 2006. A new set of operating parameters will be employed in the next set of tests. These tests should be completed by early September, 2006. The final analysis of the data will then be completed. This analysis will investigate the conditions necessary to scale the experimental systems to industrial size systems. It is now anticipated that the final results from this effort will be completed and presented in the final report, due in December 2006.

## **REFERENCE**

1. Johnson, E. and Kang, B. "Dry Particle Separation in a CFB Riser System", CAST Semi-Annual Technical Progress Report, no.3, October 2005.

## PUBLICATION/PRESENTATIONS

Johnson, E. and Kang, B. (2005), “Dry Particle Separation System Based on Density Difference”, Poster Presentation, Particulate Processes in the Pharmaceutical Industry Conference, Montreal, Canada, June 26-30.

Johnson, E. and Kang, B. (2005) “Separation of Small Particles Due to Density Difference in a CFB Riser System” Poster Presentation, CAST 2005 Annual Workshop, Blacksburg VA, July 26-28.

Johnson, E., Regester, J., and Kang, B. ”Fluidized Bed Riser as a Dry Particle Separation System”, Mineral & Metallurgical Processes, vol.22, no.3, August 2005

TABLE 1

		Test 1	Test 2	Test 3	Test 4	Test 5	Test 6
Superficial Velocity	$u_0 \frac{m}{s}$	2.4			2.0		
Mass Flux	$G \frac{kg}{m^2s}$	1.24	1.48	1.90	1.22	1.45	1.71
Separation Diameter	$d_p^* \mu m$	460			400		
Product Bin Quality	$\omega_p(d_p^*)$	99.95%	99.82%	99.67%	93.82%	94.71%	94.53%
Capture Efficiency	$\eta_p(d_p^*)$	56.21%	68.76%	69.93%	60.89%	55.36%	59.96%
Mineral Recovery	$\varepsilon_p(d_p^*)$	55.61%	68.02%	69.17%	38.42%	34.93%	37.83%

## **Appendix 9: Studies of Froth Stability and Model Development (VA002)**

## TECHNICAL PROGRESS REPORT

Contract Title and Number:

Establishment of the Center for Advanced Separation  
Technologies (DE-FC26-01NT41607)

Period of Performance:

Starting Date: 9/17/01  
Ending Date: 5/30/05

Sub-Recipient Project Title:

Studies of Froth Stability and Model Development

Report Information:

Type: Semi-Annual  
Number: 7  
Period: 10/1/05-3/30/06  
Date:  
Code: VA002

Principal Investigators:

Roe-Hoan Yoon

Contact Address:

146 Holden Hall  
Virginia Polytechnic Institute & State University  
Blacksburg, VA 24061

Contact Information:

Phone: (540)231-4508  
Fax: (540)231-3948  
E-Mail: cast@vt.edu

Subcontractor Address:

No subcontracts issued.

Subcontractor Information:

Phone:  
Fax:  
E-Mail:

### ABSTRACT

This report describes the hydrophobic interactions between air bubbles stabilized by a common frother, polypropylene glycol (PPG) with a molecular weight of 400 in aqueous solutions. It is found that the hydrophobic force in the thin films decreases systematically with increasing PPG concentration. As compared to methyl isobutyl carbinol (MIBC), PPG appears to be more capable of reducing the hydrophobicity of air bubbles.

### INTRODUCTION

#### Background

The stability of froth (three-phase foam) is closely related to the stability of bubbles and foams (two-phase foams). In flotation, the concentrations of surfactants are very low, so that the surfactant adsorption renders the bubbles partially hydrophilic. It has been shown that surface tension changes very little and the changes in film elasticities are small at MIBC concentrations employed in flotation practice (Wang and Yoon, 2006). They found, on the other hand, that the low levels of frother additions cause significant changes in the attractive hydrophobic force, which may be the major destabilizing force for foam films. It was

suggested, therefore, that dampening hydrophobic force may be an important role of frother in flotation.

### Objective and Approach

The lifetime of a foam film is controlled by drainage and rupture. For a horizontal foam film, the driving force for the drainage process is the capillary pressure, which is determined by the curvature at the Plateau boarder and the surface tension. The initial process of film thinning is controlled by capillary pressure, while the subsequent process is controlled by surface forces. The thinning kinetics of small films can be described by the Reynolds equation (Scheludko and Platikanov, 1961; Scheludko, 1967, Angarska *et al.*, 2004, Ivanov *et al.*, 2005):

$$-\frac{dH}{dt} = \frac{2H^3 \Delta P}{3\mu R_f^2} \quad [1]$$

where  $t$  is drainage time,  $\mu$  dynamic viscosity,  $R_f$  film radius, and  $\Delta P$  is the driving force for film thinning. In view of the discussions above, the driving force may be represented by the following relation:

$$\Delta P = P_c - \Pi \quad [2]$$

where  $P_c$  is the capillary pressure represented by Eq. [5], and  $\Pi$  is the disjoining pressure represented by

$$\Pi = \Pi_{el} + \Pi_{vw} + \Pi_{hb} \quad [3]$$

where  $\Pi_{el}$  represents the electrostatic double-layer repulsion,  $\Pi_{vw}$  represents the van der Waals force, and  $\Pi_{hb}$  represents the hydrophobic force.

The accuracy of determining the magnitudes of hydrophobic force depends critically on the double-layer potentials (Wang and Yoon, 2004, 2005). Therefore, 0.1 M NaCl was used to form the films so that the kinetics of film thinning were studied under conditions of  $\Pi_{el} \approx 0$ , in which case the extended DLVO theory (Eq. [3]) is reduced to:

$$\Pi = \Pi_{vw} + \Pi_{hb} \quad [4]$$

By substituting this into Eq. [2] and then to Eq. [1], one can predict the kinetics of film thinning using the Reynolds equation.

## **PROJECT TASKS**

### Task 1 — Foam/Froth Studies

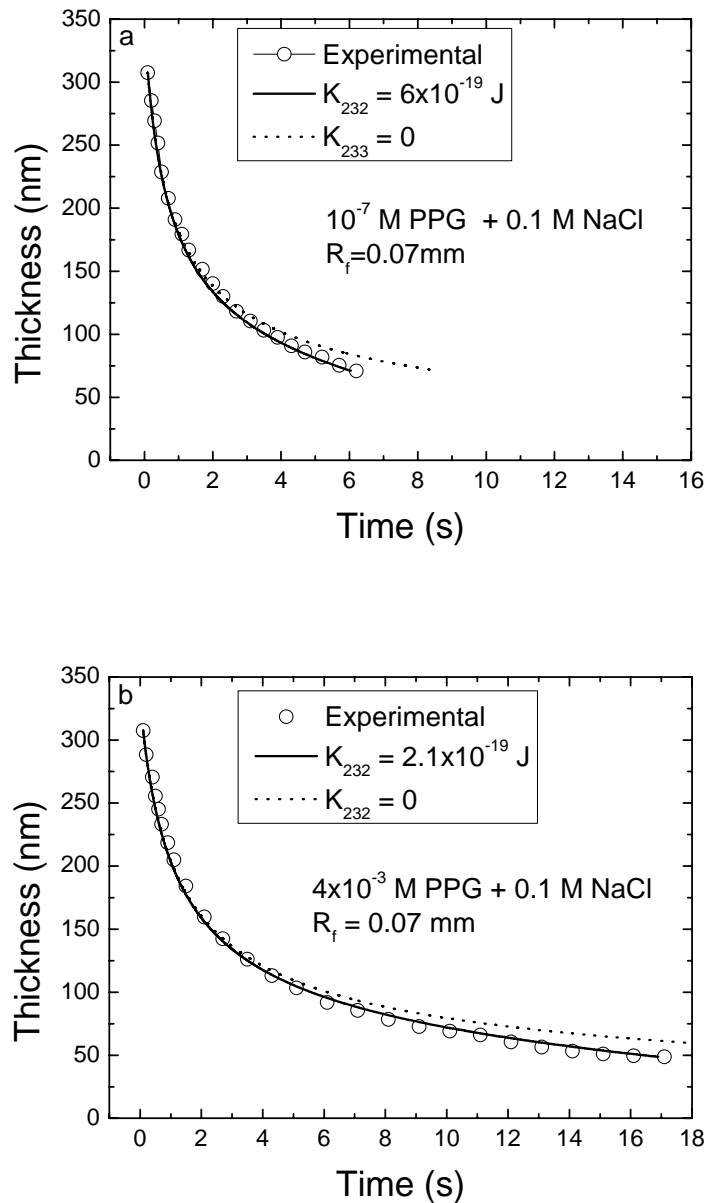


Figure 1. Kinetics of film thinning at a)  $10^{-7}$  M PPG and 0.1 M NaCl; b)  $4 \times 10^{-3}$  M PPG and 0.1 M NaCl. The solid line represents the Reynolds equation (Eq.[1]) with considering hydrophobic force, while the dotted line represents the Reynolds equation with the DLVO theory in the absence of hydrophobic force (Wang and Yoon, 2005).

Figure 1 shows the results of the film thinning kinetics measurements conducted on two horizontal foam films stabilized at two different concentrations of PPG in the presence of 0.1 M NaCl. In both cases, the initial film thinning is fast and can be described by the Reynolds equation with its driving force ( $\Delta P$ ) represented by Eq. [2] with  $\Pi = 0$ , that is, the

process is controlled solely by capillary force. As the film thickness ( $H$ ) is reduced to below approximately 200 nm, however, surface forces begin to influence the film thinning process. The film thinning kinetics curve obtained at a relatively low PPG ( $10^{-7}$  M) concentration and in the absence of NaCl cannot be described by the Reynolds equation without considering the contribution from the hydrophobic force to  $\Delta P$ . At  $10^{-7}$  M PPG and 0.1 M NaCl, the kinetics of film thinning is considerably faster than predicted (dotted line) without considering the hydrophobic force, *i.e.*,  $K_{232} = 0$ . The experimental data can be fitted to the Reynolds equation (solid line) with  $K_{232} = 6.0 \times 10^{-19}$  J, and with the  $A_{232}$  values determined by considering the retardation effects. The detailed information on how to calculate  $A_{232}$  can be found in Wang and Yoon (2006). The film is shown to rupture at 71.0 nm in 6.2 s. At  $4 \times 10^{-3}$  M PPG and 0.1 M NaCl, the film becomes less unstable and ruptures at 48.7 nm in 17.1 s, and the kinetics curve can be fitted to the Reynolds equation with  $K_{232} = 2.1 \times 10^{-19}$  J.

The kinetics of film thinning was also studied at other PPG concentrations in the presence of 0.1 M NaCl, and the  $K_{232}$  values determined in the manner described in the foregoing paragraph have been plotted as a function of PPG concentration in Figure 2. At  $10^{-7}$  M PPG,  $K_{232}$  is  $6.0 \times 10^{-19}$  J, which is about 15 larger than the non-retarded Hamaker constant ( $3.7 \times 10^{-20}$  J). At  $4 \times 10^{-3}$  M PPG,  $K_{232}$  is  $2.1 \times 10^{-19}$  J, which is about 6 times larger than the Hamaker constant. As shown, the hydrophobic force systematically decreases with increasing PPG concentration.

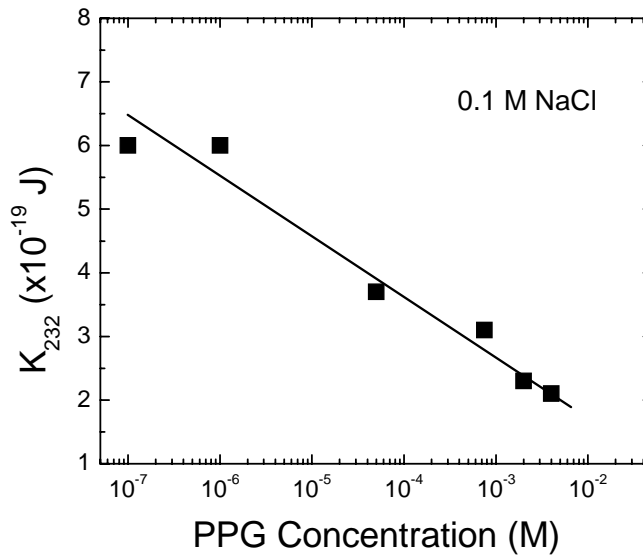


Figure 2. Effect of PPG concentration on  $K_{232}$  at 0.1 M NaCl.

It would be of interest to compare the film thinning kinetics of PPG-400 to that of MIBC. Figure 3 shows that PPG-400 gave slightly lower  $K_{232}$  values than MIBC. This finding is not surprising as the hydrophile-lipophile balance (HLB) number of PPG is 9.8, which is larger than the HLB number of MIBC (*i.e.*, 6.1). It suggests that the former can

render the bubble surface hydrophilic more readily than the latter. In other words, the hydrophobic interactions between MIBC-laden bubbles appear to be larger than those between PPG-laden bubbles. This also explains at least partially why PPG is often referred to as a more powerful frother than MIBC.

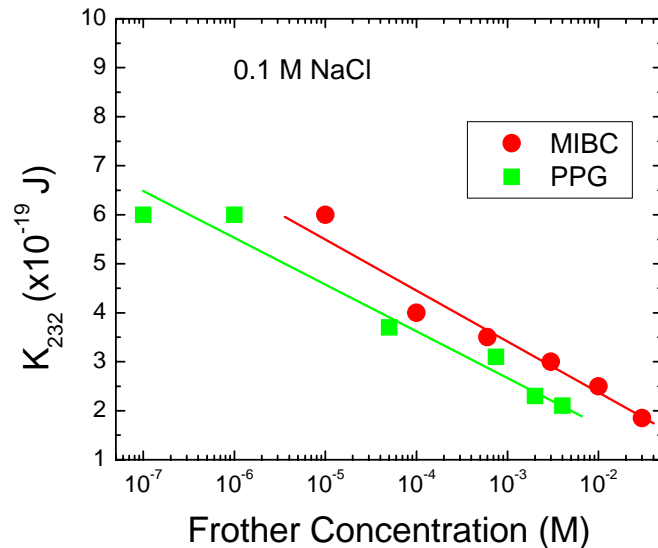


Figure 3. Comparison of  $K_{232}$  values between PPG and MIBC.

## SUMMARY

The film thinning kinetics of PPG has been studied using the thin film pressure balance technique (TFPB). It is found that the hydrophobic force in the thin films decreases systematically with increasing PPG concentration. As compared to MIBC, PPG is more capable of reducing the hydrophobicity of air bubbles and, therefore, a more powerful frother.

## FUTURE WORK

Further investigate on the surface forces in foam films in the presence of polymers will be carried out.

## REFERENCES

- J.K. Angarska, B.S. Dimitrova, K.D. Danov, P.A. Kralchevsky, K.P. Ananthapadmanabhan, A. Lips, *Langmuir* 20 (2004) 1799.
- I.B. Ivanov, *Adv. Colloid Interf. Sci.* 114– 115 (2005) 61.

A. Scheludko, *Adv. Colloid and Interface Sci.* 1 (1967) 391.

A. Scheludko, D. Platikanov, *Kolloid Z.* 175 (1961) 150.

L. Wang and R.-H. Yoon, *Langmuir*, 20 (2004) 11457.

L. Wang and R.-H. Yoon, *Colloids and Surfaces A*. 263 (2005) 267.

L. Wang and R.-H. Yoon, *Colloids and Surfaces A*, in press (2006).

#### **PUBLICATIONS/PRESENTATIONS**

Liguang Wang and Roe-Hoan Yoon, Hydrophobic Forces in Foam Films Stabilized by Sodium Dodecyl Sulfate: Effect of Electrolyte, *Langmuir*, 20 (2004) 11457.

Liguang Wang and Roe-Hoan Yoon, Hydrophobic Forces in Thin Aqueous Films and Their Role in Film Thinning, *Colloids and Surfaces A: Physicochemical and Engineering Aspects*, 263 (2005) 267.

Liguang Wang and Roe-Hoan Yoon, Role of Hydrophobic Force in The Thinning of Foam Films Containing a Nonionic Surfactant, *Colloids and Surfaces A: Physicochemical and Engineering Aspects*, in press (Available online 15 December 2005).

Liguang Wang, and Roe-Hoan Yoon, Effects of Surface Forces and Film Elasticity on Froth Stability, *SME Annual Meeting*, St. Louis, Missouri, March 26-29, 2006, preprint 06-007.

#### **APPENDICES (IF ABSOLUTELY NECESSARY)**

## **Appendix 10: Direct Measurement of Forces in Flotation (VA004)**

## TECHNICAL PROGRESS REPORT

Contract Title and Number:

Crosscutting Technology Development at the Center  
for Advanced Separation Technologies  
(DE-FC26-02NT41607)

Period of Performance:

Starting Date: 6/1/2004  
Ending Date: 10/31/2006

Sub-Recipient Project Title:

Direct Measurement of Forces in Flotation

Report Information:

Type: Semi-Annual  
Number: 8  
Period: 10/1/05-3/31/06  
Date:  
Code: VA004-R08

Principal Investigators:

Yoon

Contact Address:

Contact Information:

Phone: 540-231-7056  
Fax:  
E-Mail: ryoon@vt.edu

Subcontractor Address:

“No subcontracts issued.”

Subcontractor Information:

Phone:  
Fax:  
E-Mail:

### ABSTRACT

The objective of this project is to directly measure the interaction,  $F$ , between a particle and bubbles as a function of separation distance,  $H$ . This force is important for bubble/particle attachment and detachment; thus it is vital for the study of kinetics and efficiency of in flotation practice. We specifically designed and fabricated the wetting film apparatus to directly measure the interaction between a solid and a air bubble. It is found that wetting films were stable on oxidized hydrophilic silicon wafer in nano-pure water and electrolyte solutions of different NaCl concentrations. The stability of wetting film is due to a repulsive total disjoining pressure as a result of electrostatic, van der waals and capillary pressure components. The equilibrium film thickness in different NaCl solution on hydrophilic surface has been obtained using the technique described in previous investigation and the results are compared to the classical DLVO theory. The wetting film on hydrophobic solid surface is not stable instead. Systemic film thickness measurements were to be done in different electrolyte solutions for hydrophobic substrates.

## **INTRODUCTION**

### Background

Froth flotation is the most important solid-solid separation process for upgrading run-of-the-mine (ROM) ores and coal (Leja, 1982). In froth flotation, a stream of small air bubbles is introduced to the bottom of a tank (or flotation cell) in which a finely ground ore is suspended in water. The air bubbles rise to the top of the tank under a buoyancy force, and in doing so, they collide with suspended particles. Purification of the ore is based on differences in the attachment and/or detachment of particles to the bubbles. It is believed that the attachment of particles to a bubble surface is caused by a “hydrophobic” interaction. Several investigators have attempted to directly measure the forces between air bubbles and particles, but the results are not consistent with experience from flotation practice. The main difficulty lies in the fact that bubbles deform during the interaction. This deformation leads to confusion as to the real separation between a particle and a bubble. Knowledge of the separation is vital to elucidate the range of the force, and thus the mechanism of the interaction. The range of the force is a required input for calculation of the kinetics of flotation.

### Objective and Approach

The overall objective of this project is to perform direct measurements of the interaction between solid particles of different surface hydrophobicity and a air bubble. The obtained information will be utilized to analyze the effect of surface hydrophobicity of solid on the solid/bubble interaction. Results are also to be compared to classical DLVO theory. Thus it is possible to determine the relative importance of long-range and short-range forces in flotation and to examine the role of collectors (surfactants) in controlling these forces. In particular, the data make it possible to develop a better understanding of the nature of the “hydrophobic” interaction (Zhang et al. 2005) that is thought to be responsible for the capture of particles by bubbles.

## **PROJECT TASKS**

### Task 1 – Design and Fabrication

The Wetting Film Balance has been fabricated and used for film thickness measurement. The film thickness was obtained through the mechanism shown as follows (Fig. 1). In practice, the instrument is able to not only measure the equilibrium film thickness, but also the kinetic thinning of the wetting films. The problem of gas leaking has been greatly improved, however, for hydrophobic surfaces, because of the relative short life time of wetting film, an exact gastight system is to be done to increase the accuracy and repeatability of the experiments.

### Task 2 – Experimental Measurements

The thickness of wetting film at different NaCl solution has been carried out on oxidized hydrophilic Silicon wafer. Also, the kinetics of film thinning in certain salt solution

was studied. However, due to the existence of the “dimple” at the time of film forming, the kinetics of film thinning is not compared to the theoretical calculation based on the Reynold equation. The equilibrium film thickness was obtained and the value was compared to that calculated from classical DLVO theory.

The theoretical disjoining pressure at different salt concentrations can be calculated using the following equations (Schulze, 2001) from Eq. (1) to Eq. (5) and plotted as Fig. 2. The theoretical equilibrium film thickness can be obtained by picking up the point at which the disjoining pressure is 194 Pi, which equals the capillary pressure,  $P_c$  in present wetting film system, on the disjoining pressure-distance curves for each salt concentration; thus the obtained distance,  $H$  gives the equilibrium film thickness,  $H_e$  from the DLVO theory.

$$\Pi = \Pi_{el} + \Pi_{vdw} \quad (1)$$

$$\Pi - P_c = 0 \quad (2)$$

$$P_c = \frac{2\gamma}{R_c} \quad (3)$$

$$\Pi_{vdw} = -\frac{A_{slv}}{6\pi h^3} \quad (4)$$

$$\Pi_{el} = -\frac{1}{2} \left[ \kappa \left( \frac{\sigma_2^2}{\varepsilon_0 \varepsilon \kappa} - \varepsilon_0 \varepsilon \kappa \Psi_1^2 \right) \frac{1}{\cosh^2(\kappa h)} - 2\kappa \Psi_1 \sigma_2 \frac{\sinh(\kappa h)}{\cosh^2(\kappa h)} \right] \quad (5)$$

in which,

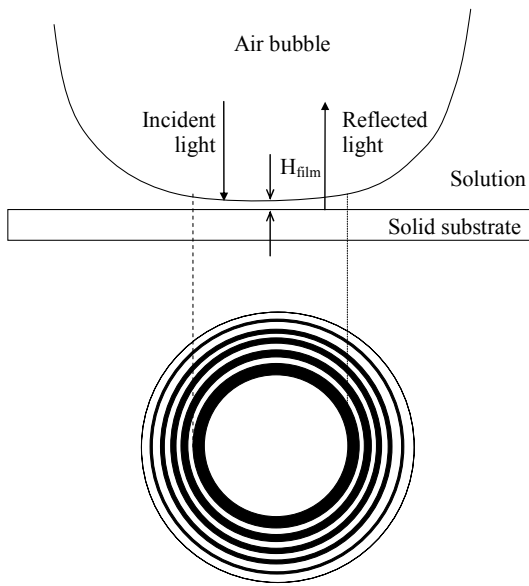
- $\kappa$  : Debye-Huckel Parameter;
- $\varepsilon_0$  : absolute dielectric constant;
- $\varepsilon$  : relative dielectric constant;
- $\sigma_2$  : charge density of silica surface;
- $\Psi_1$  : surface potential of gas bubble;
- $h$  : film thickness;
- $\gamma$  : surface tension of liquid.
- $R_c$  : radius of capillary tube;
- $A_{slv}$  : Hamaker constant for wetting film (silica/water/air system),  $\sim 1 \times 10^{-20}$  J.

For example, the equilibrium film thickness,  $H_e$ , in  $1 \times 10^{-3}$  M NaCl solutions should be 39 nm at a capillary pressure of 194 pi from Figure 2 and the film thickness is 22 nm accordingly in  $5 \times 10^{-3}$  M solutions.

Figure 3 shows the kinetic thinning of wetting film on an oxidized silicon wafer in  $1 \times 10^{-3}$  M NaCl solutions. The initial film thickness was set at 102 nm, after which film keeps on thinning until the strong repulsive disjoining pressure makes the two interfaces apart. After nearly 15 seconds, an equilibrium film thickness is obtained and the film thickness is calculated using the equation of film thickness calculation shown in Figure 2. Due to the formation of dimple at the time of film forming, the experiment results show some variations. It is shown in the figure that the equilibrium film thickness varies from 45 nm to 55 nm. This experiment error is much higher than that obtained in foam film thickness measurement.

The experimental equilibrium film thicknesses measured in NaCl solutions at different salt concentrations are listed in Figure 4. In addition, the theoretical values of film thicknesses are shown in Figure 4 for comparison. The figure shows that, both from theoretical and experimental data, the equilibrium film thickness decreases with salt concentration increasing. This is due to the compression of repulsive double layer disjoining pressure with ionic strength increasing in solution, while the van der Waals force doesn't change much at large surface separation.

The experimental equilibrium film thicknesses at different salt concentrations are generally a little larger than those obtained from theoretical calculation. It may originate from the underestimate of the capillary diameter, which accordingly decreases the theoretical equilibrium film thickness. In another possibility, the surface charge density on oxidized silicon wafer may be higher than the one used in theoretical calculation, of which the value is for silica. The difference between experimental and theoretical data is to be clarified in next investigation. In addition, experimental techniques are to be improved to decrease the experiment error.



$$H_{film} = \frac{\lambda}{2n} \left( \frac{1}{2} - \frac{1}{\pi} \arcsin \sqrt{\frac{I_t - I_{min}}{I_{max} - I_{min}}} \right)$$

**Figure 1. Film Thickness Measured Using a Micro-interference Technique**

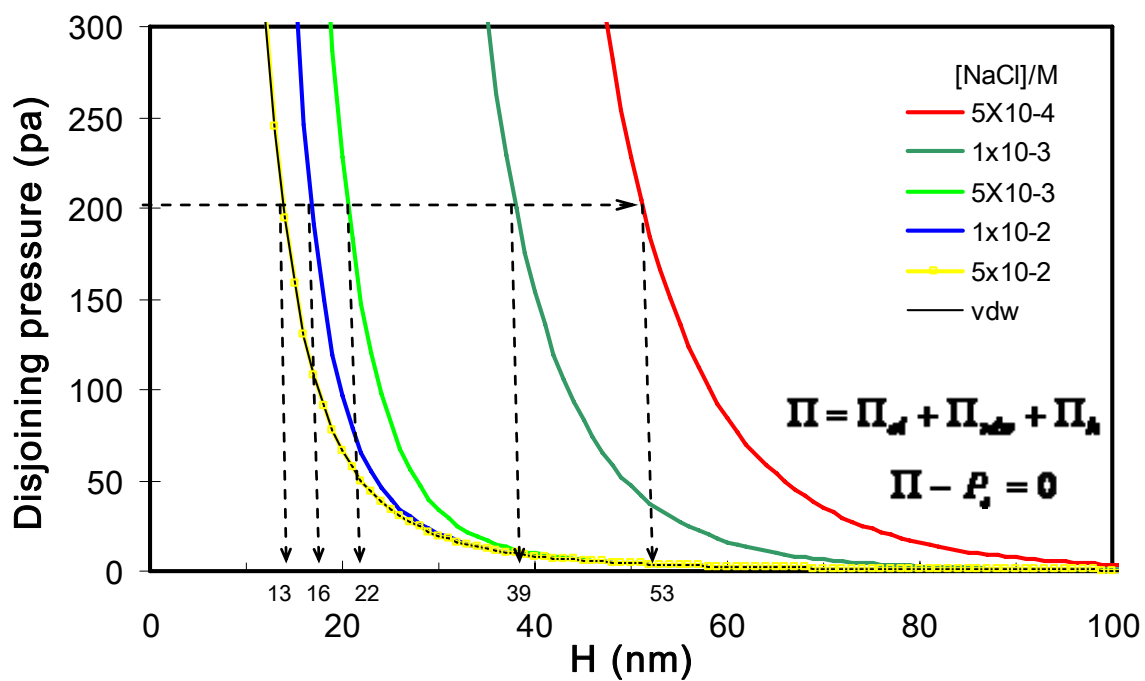


Figure 2. Theoretical Equilibrium Film Thickness at Different Salt Concentrations

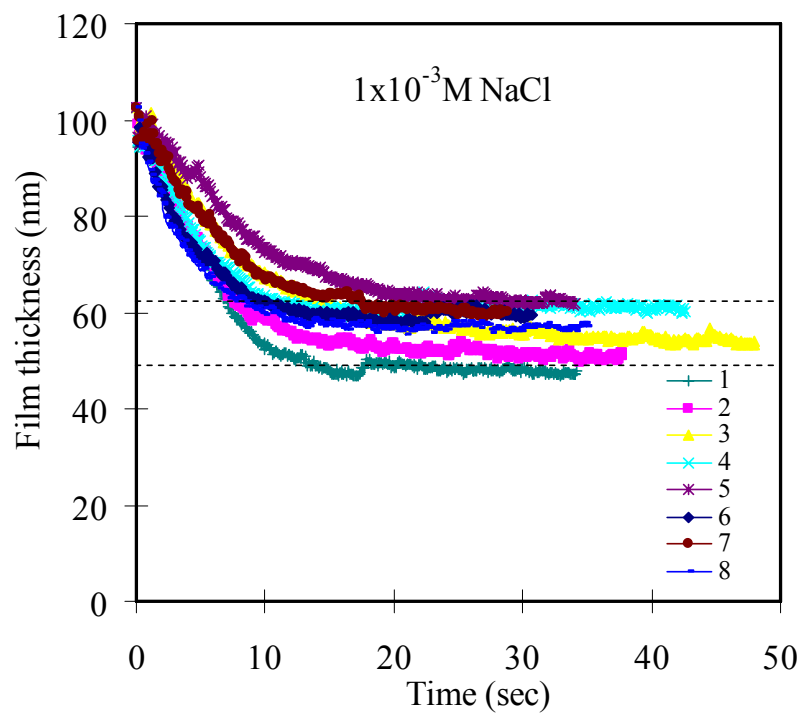
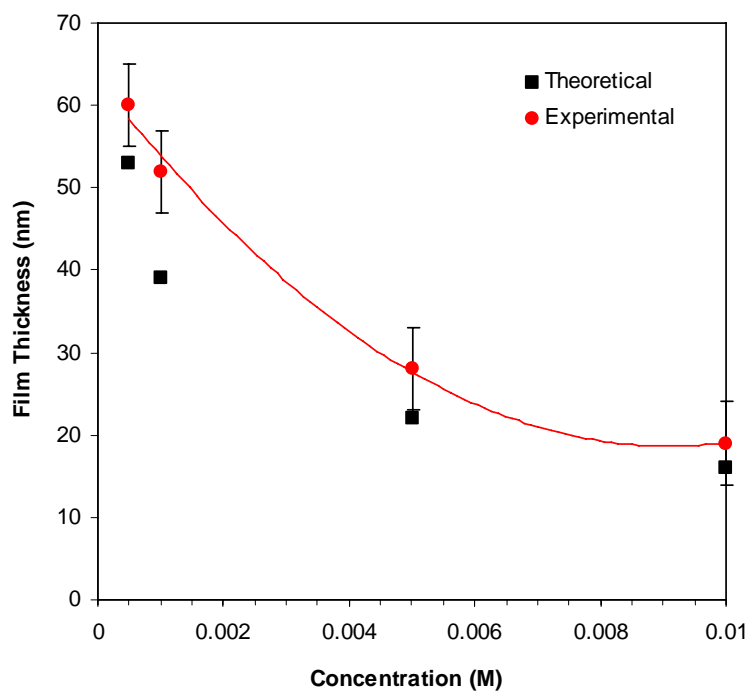


Figure 3. Experimental Equilibrium Film Thickness at 1x10<sup>-3</sup> M NaCl Concentration

**Table 1. Experimental and Theoretical Equilibrium Film Thickness at different NaCl Concentration.**

Concentration (M)	Equilibrium Film Thickness Theoretical (nm)	Equilibrium Film Thickness Experimental(nm)
0.0005	53	60
0.001	39	52
0.005	22	28
0.01	16	20



**Figure 4. Experimental and Theoretical Equilibrium Film Thickness at different NaCl Concentration.**

## **SUMMARY**

The equilibrium film thicknesses of a wetting film in different NaCl solutions on oxidized hydrophilic silicon wafer surface were measured. The experimental results show that equilibrium film thickness decreases with salt concentration increasing. The experimental data are a little larger than those from calculation of classical DLVO theory. The experimental equilibrium film thicknesses at different salt concentrations are generally a little larger than those obtained from theoretical calculation. It may origin from the underestimate of the capillary diameter, which accordingly decreases the theoretical equilibrium film thickness. In another possibility, the surface charge density on oxidized silicon wafer may be higher than the one used in theoretical calculation, of which the value is for silica.

## **FUTURE WORK**

Experimental techniques are to be improved to decrease the experiment error hydrophilic substrates. Systemic measurements of equilibrium film thickness for wetting film in electrolyte solutions at different salt concentrations are to be done on hydrophobic substrates with different hydrophobicity. The results attained on hydrophobic surfaces will help detect the existence and range of the “hydrophobic force”.

## **REFERENCES**

- Leja, J., 1982. Surface Chemistry of Froth Flotation, Plenum Press, New York, N.Y.
- H.J. Schulze, K.W. Stockelhuber and A. Wenger, The influence of acting forces on the rupture mechanism of wetting films — nucleation or capillary waves, Colloids and Surfaces A: Physicochemical and Engineering Aspects 192 (2001) 61–7.
- Zhang Jinhong, Yoon Roe-Hoan, Mao Min, and Ducker, William A. 2005 Effects of Degassing and Ionic Strength on AFM Force Measurements in Octadecyltrimethylammonium Chloride Solutions, Langmuir. 21, 5831-5841.

## **PUBLICATIONS/PRESENTATIONS**

- Zhang Jinhong, Yoon Roe-Hoan, Mao Min, and Ducker, William A. 2005 Effects of Degassing and Ionic Strength on AFM Force Measurements in Octadecyltrimethylammonium Chloride Solutions, Langmuir. 21, 5831-5841.
- Jinhong Zhang, Roe-Hoan Yoon, Min Mao and William A. Ducker, “*Effect of Dissolved Gas on the Force between Silica and Glass in Aqueous Octadecyltrimethylammonium Chloride Solutions*”, Centenary of Flotation, Brisbane Australia, June 5-9 2005.
- Min Mao, Jinhong Zhang, Roe-Hoan Yoon, and William A. Ducker; “*Is There a Thin Film of Air at the Interface between Water and Smooth Hydrophobic Solids?*”, Langmuir 2004, 20, 1843-1849.

## **APPENDICES**

No appendices are included in this report.

**Appendix 11: Improving Densification of Fine Coal Refuse Slurries to  
Eliminate Slurry Ponds (KY002)**

## TECHNICAL PROGRESS REPORT

Contract Title and Number:

Crosscutting Technology Development at the Center for  
Advanced Separation Technologies  
(DE-FC26-02NT41607)

Period of Performance:

Starting Date: 10/1/2002  
Ending Date: 10/31/2006

Sub-Recipient Project Title:

Densification of Fine Coal Refuse Slurries to Eliminate  
Slurry Ponds

Principal Investigators:

Parekh, Honaker

Contact Address:

University of Kentucky  
201 Kinkhead Hall  
Lexington KY 40506

Subcontractor Address:

"No subcontracts issued.

Report Information:

Type: Semi-Annual  
Number: 6  
Period: 10/1/05-3/31/06  
Date: 03/31/2006  
Code: KY002-R06

Contact Information:

Phone: (859) 257-0239  
Fax: (858) 323-1962  
E-Mail: parekh@caer.uky.edu

Subcontractor Information:

Phone:  
Fax:  
E-Mail:

## **ABSTRACT**

During this reporting period, tests were conducted using a continuous operating lab scale Deep Cone Thickener using the thickener underflow obtained from the Arch Coal Inc. A statistical design of experiments was conducted to identify the optimum operating conditions. The study found that the model developed with the factorial design gave results close to the actual values. The percent solids in the thickened paste was about 52 weight percent. Effect of a higher amount of cationic flocculant usage provided better dewatering at higher bed depth of the paste. A final report on the project is being prepared

## **INTRODUCTION**

### Background

Increased mechanization in the underground coal mining industry has decreased selectivity and increased the volume of refuse. Coal preparation separates non-combustibles material from coal. Depending on the source, 20 to 50 percent of the run-of-mine material ends up in reject streams. A recent study conducted by the National Research Council defined the impoundment problem in detail and provided several recommendations to avoid the slurry spillage. One of the recommendations referred to utilizing advanced dewatering technology, which would reduce or eliminate discharge of slurry.

An advanced thickening technique known as “Paste Thickening Technology” marketed by Dorr-Oliver EIMCO has been successfully applied in the alumina processing industry, for dewatering ‘red mud’. The thickened material could be stacked at a low angle of repose rather than stored in a pond. Thus, the fine refuse slurry ponds could be completely eliminated. The project addresses the need to develop a process alternative to conventional ponding of the waste slurry. This semi-annual report summarizes laboratory data on the Arch Coal of W.Va’s refuse slurry.

### Objective and Approach

The main objective of the proposed program is to evaluate the application of DEEP CONE technology for the disposal of fine coal refuse. The program includes study of the basic rheological properties of the flocculated fine refuse solids for producing highly-thickened solids capable of disposal as a paste.

## **PROJECT TASKS**

### Task 1. Acquisition and Characterization of Samples:

Characterizations of tailings from three coal preparation plants have been completed.

### Task 2. Laboratory Studies:

Based on the results of the semi-continuous laboratory experiments using T\_Floc apparatus, a 6 inch diameter deep cone thickener was fabricated (Figure 1) and tests were conducted

with the Arch Coal thickener underflow sample after diluting the percent solids from 29% to 10%. A factorial experimental design was used to evaluate the three important variables; residence time, slurry bed height and cationic dosage.

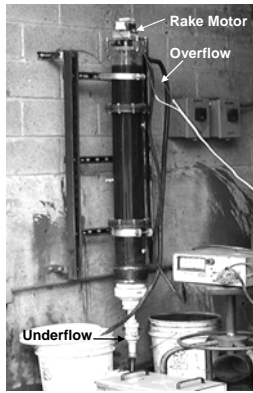


Figure 1: Photograph of continuous laboratory scale deep cone thickener

Nine experiments were performed using the factorial design. The underflow sample was collected from each experiment after the required residence time and solids weight percent was determined. The experimental conditions and responses are provided in Table 1

Table 1: Factorial design parameters with responses

Run No.	Bed Height (A) (cm)	Residence Time (B) (hr)	Cationic Floc (C) (g/t)	U/F solids (%)
1	100	4	100	49.85
2	100	4	0.00	46.89
3	40	4	0.00	42.35
4	100	8	0.00	48.81
5	100	8	100	54.46
6	70	6	50	53.45
7	40	8	100	45.42
8	40	4	100	43.21
9	40	8	0.00	44.62

The model equations relating the parameters and their interactions for response underflow percent solids can be written as;

$$\text{Under flow \% solids} = 46.95 + 3.05 \times A + 1.38 \times B + 1.28 \times C + 0.87 \times A \times C$$

Table 2 shows that all three parameters (slurry bed height, residence time and cationic floc dosage) have significant effects on the underflow percent solids as indicated by their Prob > F values. The effects of all three parameters on underflow percent solids are summarized in Figure 2. It is clear from Figure 2 that the underflow percent solids increases with increases in parameter values, with bed height being more predominant than the other two parameters.

Table 2: Analysis of variance (various?) data for the response underflow percent solids

Source	Sum of Squares	DF	Mean Square	F Value	Proc>F
Model	108.66	4	27.21	34.96	0.0075
A-Bed height	74.48	1	74.48	95.68	0.0023
B-Res Time	15.15	1	15.15	19.47	0.0216
C-Cat. Floc. Dos.	13.18	1	13.18	16.94	0.0260
AC	6.04	1	6.04	7.76	0.0687
Residual	2.34	3	0.78	----	--
Total	148.73	8			--

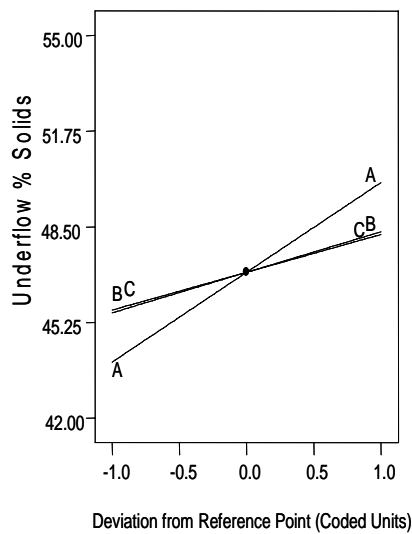


Figure 2: Perturbation plot showing the effect of parameters on underflow percent solids.

The parameter interaction between bed height and cationic flocculant dosage is shown in Figure 3. It is evident from Figure 3 that at lower bed height there is no interaction between the parameters. However, as the bed height and cationic flocculant dosage increase, the underflow percent solids increases. This indicates that the cationic flocculant modifies the floc structure, which helps to release the water from the floc and is a function of bed height.

#### *Parameter Optimization*

The goal of the optimization process was to maximize the underflow slurry density while varying the parameters within their experimental ranges. The optimized conditions generated from the model were used to conduct further tests with continuous laboratory scale Deep Cone Thickener. Tests were also conducted to reduce residence time, to examine the possibility of maintaining a reasonable underflow density (Table 3).

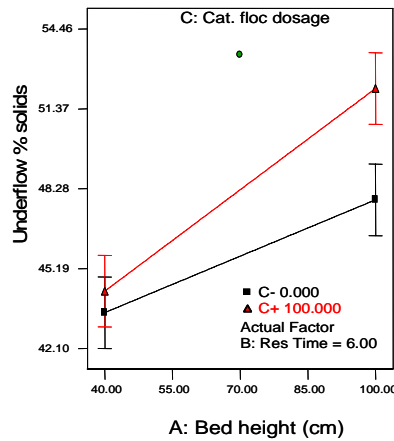


Figure 3: Graphical representation of interaction of parameters; bed height and cationic flocculent dosage

Table 3: Optimized test conditions for the underflow percent solids of the laboratory scale Deep Cone Thickener.

Run No.	Experimental Conditions			Underflow Solids (%)	
	Bed ht. (cm)	Res. Time (hr)	Cat. Floc. g/t	Predicted	Actual
1	100	8	99.81	53.52	53.02
2	100	4	100	50.77	49.23
3	100	6	100	51.28	52.15

### Task 3: Pilot-Scale Testing and Process Optimization Studies:

Pilot-scale testing of the Deep Cone Thickener at three coal preparation plants has been completed.

### SUMMARY

- The laboratory scale continuous Deep Cone Thickener tests confirmed that it is possible to reproduce the results achieved in a semi-continuous T- Floc apparatus on a continuous basis. An underflow percent solids of about 52% could be obtained from a slurry containing 10% solids on a continuous basis.
- The effect of cationic flocculant is evident at higher bed depths, which helps to release the water from the flocs.

### FUTURE WORK

We are in the process of preparing a final report on the project.

### PUBLICATIONS/PRESENTATIONS:

“Densification of Fine Coal Refuse Slurries to Eliminate Slurry Ponds” Clearwater Coal Conference, Clearwater, FL, May.22-24,2006.

## **Appendix 12: Development and Testing of a Horizontal Pressure Belt**

### **Filter (VA010)**

## PROGRESS REPORT

Contract Title and Number:

Crosscutting Technology Development at the Center for  
Advanced Separation Technologies (DE-FC26-02NT41607)

Period of Performance:

Starting Date: 10/1/2002  
Ending Date: 10/31/2006

Sub-Recipient Project Title:

Development and Testing of a Horizontal Pressure Belt  
Filter

Principal Investigators:

Gerald H. Luttrell and Roe-Hoan Yoon

Contact Address:

146 Holden Hall  
Virginia Tech, Blacksburg, VA 24061

Subcontractor Address:

No subcontracts issued.

Report Information:

Type: Semi-Annual  
Number: 6  
Period: 10/1/05-3/31/06  
Date: 4/30/06  
Code: VA010

Contact Information:

Phone: (540) 231-4508  
Fax: (540) 231-3948  
E-Mail: cast@vt.edu

Subcontractor Information:

Phone:  
Fax:  
E-Mail:

### ABSTRACT

A variety of mechanical processes are available for dewatering fine particles in the coal and mineral processing industries. Unfortunately, many of these processes suffer from major shortcomings such as poor dewatering performance, low throughput capacity, and high capital and operating costs. This project seeks to overcome these problems by developing a new type of dewatering process that combines the operational flexibility of a continuous belt filter with the dewatering efficiency of a batch pressure filter. The proposed project involves the design, construction, testing, and evaluation of a prototype unit and pilot-scale test circuit having a production capacity of approximately 100 lb/hr. Test data obtained from the project will be used to promote the engineering development of a full-scale commercial unit. During the past reporting period, most of the work conducted under this project has focused on the continued construction and shakedown testing of the prototype test unit.

## INTRODUCTION

### Background

Filtration processes are commonly used in the coal and minerals processing industry to remove excess moisture from the surfaces of fine particles. However, in order to overcome difficulties associated with the poor performance, extensive maintenance requirements, and high capital/operating costs of existing filter designs, a tremendous incentive exists to develop a filtration system. Ideally, the new filtration system needs to (i) make use of a high differential pressure, (ii) operate in a continuous mode, (iii) minimize filter cloth blinding while avoiding blow back of moisture, and (iv) offer operational flexibility in terms of independent control of cake thickness and drying cycle time. A process that is capable of meeting all of these criteria is a *horizontal belt pressure filter*. This new technology is very similar in design to that of a conventional horizontal belt vacuum filter, except the filtering mechanism is enclosed inside a pressurized chamber. During operation, feed is injected into the pressured chamber at the head of the filter belt. The high pressure drives the water through the filter cloth/belt where it is discharged into an effluent collection chamber maintained at atmospheric conditions. The filter cake is dropped into an air lock that sequentially opens and closes to continuously discharge the dried solids. Because of the high pressure differential, the filter cake produced by the new filter would be significantly drier than that obtained using disc or belt vacuum filters that are limited to a practical maximum differential pressure of approximately 0.8 atm. The elimination of the blow back of moisture during cake removal ensures that the driest possible cake is produced. Also, the capital cost of the compressor or staged blower can be less than 20% of the cost of a vacuum pump with an equivalent volumetric capacity. This difference would significantly reduce the cost of the proposed belt filtration system in comparison to vacuum based filters.

### Objective and Approach

The primary objective of this project is to develop and test a *horizontal belt pressure filter* that is capable of efficiently dewatering fine coal in a cost effective manner. The new filter combines the operational benefits of a continuous belt filter with the dewatering efficiency of a batch pressure filter. The proposed project activities include project planning, equipment design/construction, shakedown testing, and detailed testing. In addition, a complete technical and economic evaluation of the new technology will be performed after the proposed experimental work has been completed.

## PROJECT TASKS

### Task 1 – Equipment Design/Construction

The mechanical construction of the prototype horizontal belt pressure filter was continued during this reporting period. Much of the work focused on the final assembly of the fabricated parts and the procurement of end caps for the pressure chamber. Figures 1 through 3 provide photographs of the key components of the assembled prototype.

## Task 2 – Shakedown Testing and Modification

During the past reporting period, several series of shakedown runs were conducted at the Virginia Tech pilot-plant facility. The shakedown testing were necessary (i) to resolve deficiencies that were overlooked in the initial engineering design and construction of the prototype unit and (ii) to confirm that pumping capacities, pipe sizes, electrical supplies, control systems, etc., are adequate. Several technical issues that were resolved during this reporting period are discussed below.

- A new spring-loaded idler assembly was fabricated to control the tension in the filter cloth. This component was found to be necessary to ensure proper tension, alignment and tracking of the filter cloth which rides on the carrier belt (see Figure 5).
- The disc-shaped end plates that allowed access through each end of the pressure vessel were found to be inadequate to withstand the pressure force generated by the unit. As a result, the entire pressure vessel was shipped to an off-site contractor where the Plexiglas end plates were replaced by thicker (1-inch) steel end plates (see Figure 5). For safety reasons, the vessel was also pressure tested at 120 PSI using water to ensure that the unit could function at the maximum expected pressure of 60 PSI.
- Preliminary shakedown testing indicated that the aperture of the original filter cloth may not be suitable for all of the different types of coal slurries to be examined in the proposed experimental test program. Therefore, a second type of filter cloth with a larger aperture was purchased for the prototype unit.
- The peristaltic feed pump used to feed coal slurry into the pressure vessel was found to be inadequate to achieve the desired production rate when operated under pressure. A ball-and-seat diaphragm pump was also found to be unsuitable for the same reasons. Therefore, a progressive cavity pump was procured and successfully placed into service for feeding the fine coal slurry into the pressure vessel.
- The preliminary shakedown tests indicated that the reciprocal valves used for the cake discharge system did not seal adequately. This problem made it impossible to increase the air pressure in the test unit to the target values. This issue was resolved by returning the originally purchased valves to the manufacturer and replacing them with sealed-seat valves.
- The shakedown tests indicated that the Teflon-strip sealing system under the carrier belt needed to be improved to reduce gas consumption. Several modifications are currently underway to minimize this problem. These modifications include the addition of multiple bands of plastic “weather” stripping underneath the longitudinal length of the carrier belt and the installation of flexible rubber seals under each end of the belt.

## **SUMMARY**

During the latest project period, construction and assembly of the major components of the pressure belt filter were completed. The pressure vessel was shipped to a fabrication and welding shop to have two sight glasses installed, to check all of the welds for safety reasons, and to manufacture two end plates for the vessel. Also, the fabrication shop performed a hydrostatic test on the completed vessel and determined that vessel is structurally sound. All of the electrical and pressure vessel safety checks have been completed. Shakedown testing is now underway (i) to complete the performance testing all of the major components, (ii) to test their operational effectiveness of the unit, and (iii) to remedy any design weaknesses that may be identified..

## **FUTURE WORK**

Work during the next reporting period will continue to include some fabrication and assembly activities as required based on the results obtained from the shakedown tests. This work will be followed by a detailed test program and economic evaluation. The detailed test program will include a study of key operating variables including feed flow rate, feed solids content, feed size distribution, filter belt speed, filter cloth mesh size, and applied pressure.

## **REFERENCES**

1. "Advances in Solid-Liquid Separation," (H. Muralidhara, Ed.), Distributed by the Royal Society of Chemistry, Burlington House, London, England, Battelle Press Publishing, Columbus, Richmond, England, 1986, 485 pp.
2. "SME Mineral Processing Handbook," (N. Weiss, Ed.), American Institute of Mining, Metallurgical, and Petroleum Engineers, Inc., Kingsport Press Publishers, Kingsport, Tennessee, 1985, pp. 9-14 – 9-26.

## **PUBLICATIONS/PRESENTATIONS**

No publications or presentations have been given during the current reporting period.

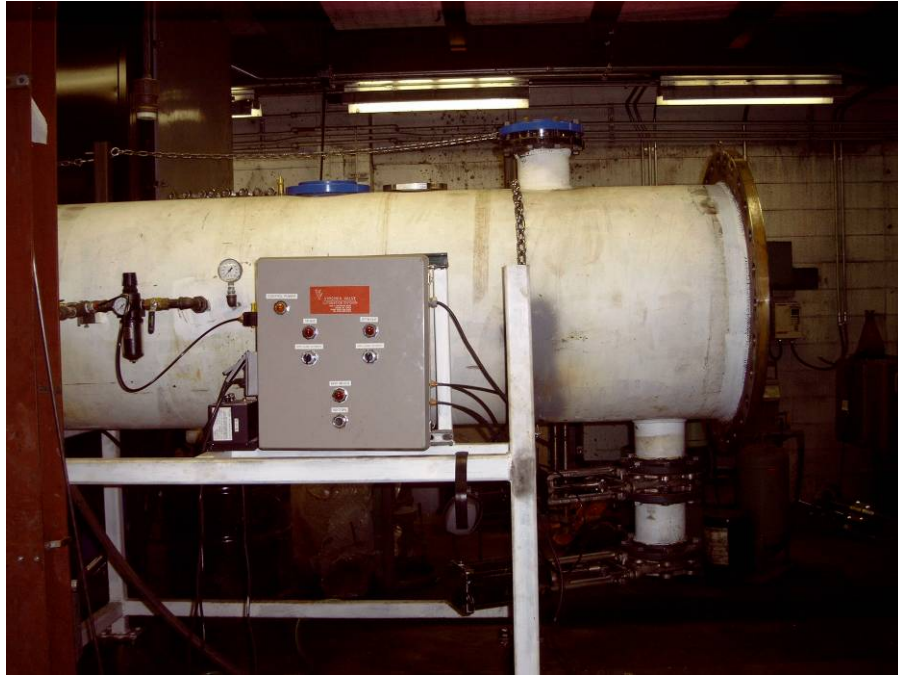


Figure 1. Photograph of the assembled prototype horizontal belt pressure filter.



Figure 2. Side view of the pressure vessel with the belt assembly removed.



Figure 3. Side view of the horizontal belt filter assembly.

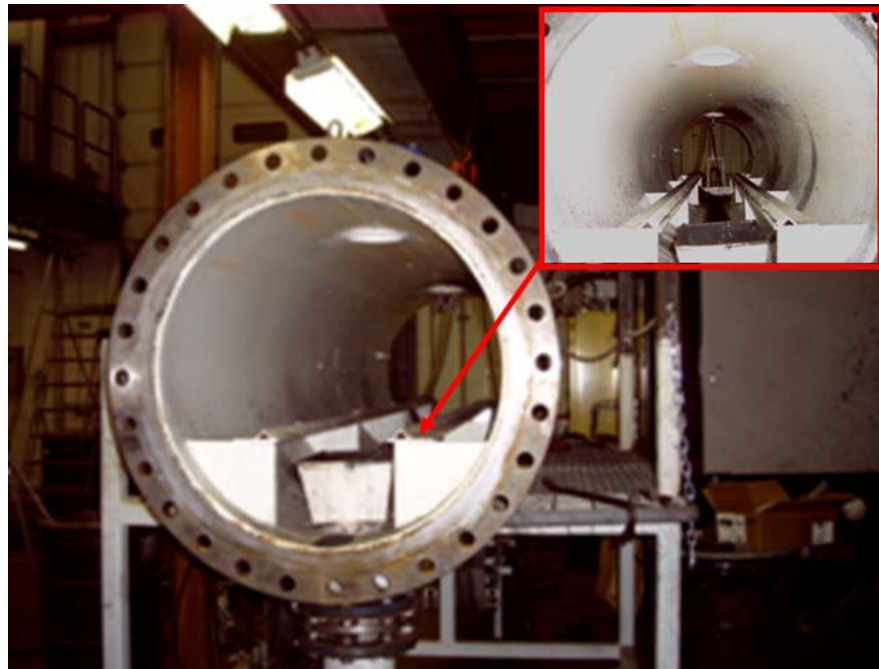


Figure 4. Track assembly inside the pressure vessel.

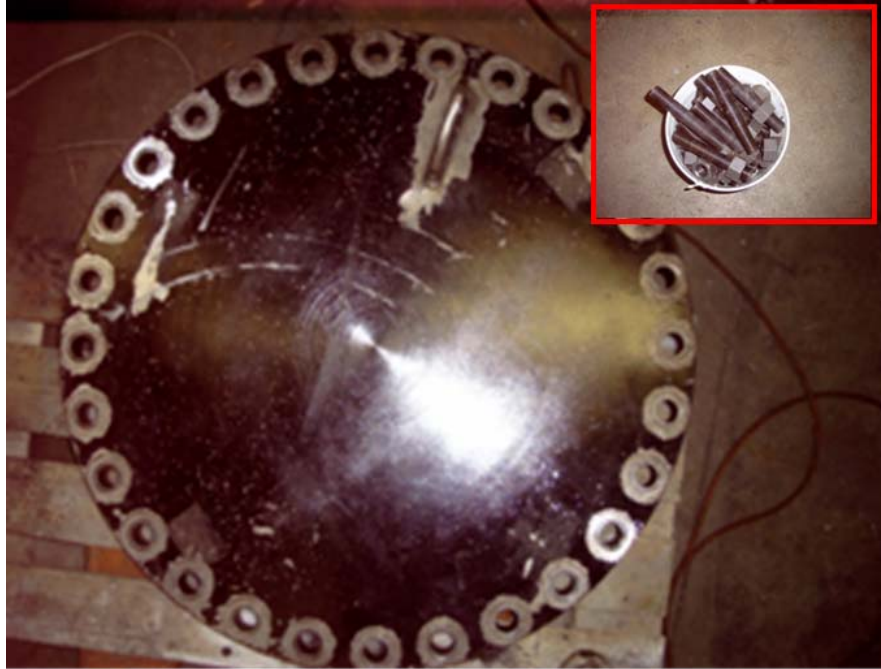


Figure 5. New end plate for the pressure vessel with 1-1/4 inch fastening bolts-nuts.

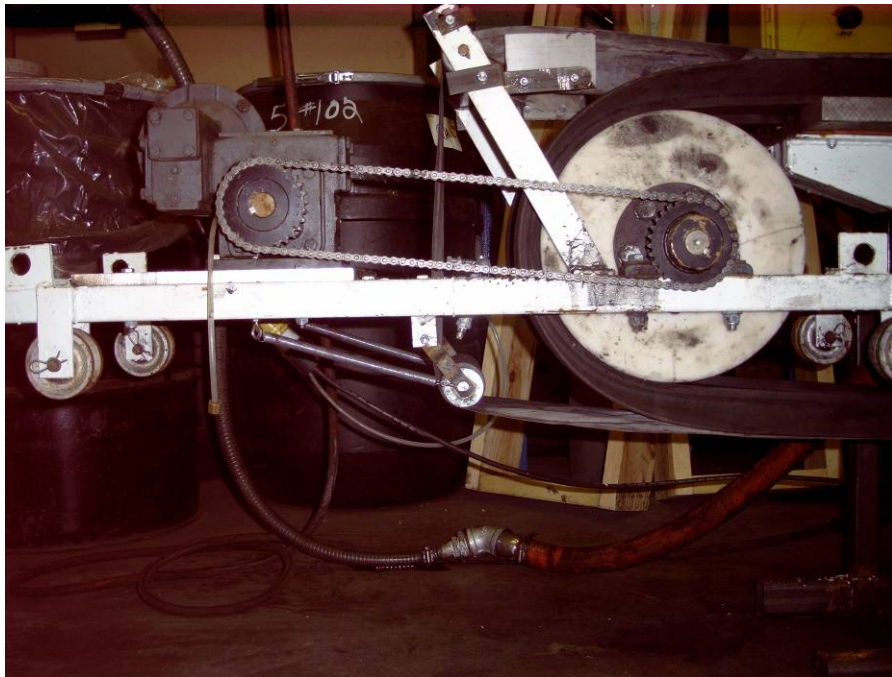


Figure 6. Spring tensioning idler used to tension the filter cloth belt.

## **Appendix 13: Development of a Fine Particle Centrifuge (VA006)**

## PROGRESS REPORT

Contract Title and Number:

Crosscutting Technology Development at the Center for  
Advanced Separation Technologies  
(DE-FC26-02NT41607)

Period of Performance:

Starting Date: 6/1/04  
Ending Date: 10/31/06

Sub-Recipient Project Title:

Development of a Fine Particle Centrifuge

Report Information:

Type: Semi-Annual  
Number: 4  
Period: 10/1/05-3/31/06  
Date: 4/30/06  
Code: VA006

Principal Investigators:

Roe-Hoan Yoon and Gerald H. Luttrell

Contact Address:

146 Holden Hall  
Virginia Polytechnic Institute & State University  
Blacksburg, VA 24061

Contact Information:

Phone: (540) 231-4508  
Fax: (540) 231-3948  
E-Mail: luttrell@vt.edu

Subcontractor Address:

No subcontracts issued.

Subcontractor Information:

Phone:  
Fax:  
E-Mail:

### ABSTRACT

The solid-solid separation processes employed by modern coal preparation plants require large amounts of process water. After cleaning, the unwanted water must be removed from the surfaces of the particles using mechanical dewatering equipment. Unfortunately, the processes used to dewater fine particles are inherently inefficient and costly to operate and maintain. To overcome this problem, a novel hyperbaric centrifugal filter has been developed by researchers at Virginia Tech. Preliminary test data obtained using a batch unit suggest that this new technology can reduce the moisture content of fine coal products by approximately 30-50% as compared to existing dewatering processes. The objective of this project is to construct a continuous prototype unit and to conduct a detailed experimental study of this new technology. During the current reporting period, three sets of shakedown tests were performed in batch mode to identify and resolve any additional operating problems. The preliminary test data show that moisture reduction is significantly improved with the injection of air, particularly at higher rotation speeds. In addition, circuit modifications have been made to allow the unit to operate in continuous mode to improve the capture of fines. These mechanical modifications have been completed and the continuous tests are underway.

## **INTRODUCTION**

### Background

One of the most difficult and costly steps in coal preparation is the removal of moisture from the surfaces of fine coal particles. Although thermal dryers can effectively reduce moisture, these units require large capital expenditures and stringent air quality standards make it impossible to obtain new operating permits. As a result, coal producers resort to mechanical systems for fine coal dewatering. Unfortunately, the performance of mechanical dewatering equipment diminishes sharply for particles finer than 0.1 mm. The unacceptably high moisture content associated with this fraction forces the majority of coal producers to discard their coal fines to waste impoundments. In the U.S. alone, approximately 2 billion tons of fine coal has been discarded in abandoned ponds and 500 to 800 million tons in active ponds. On a yearly basis, U.S. coal producers discard approximately 30 to 40 million tons of fresh coal fines into ponds. This represents a loss of valuable natural resources, loss of profit for coal producers, and creation of significant environmental concerns.

### Objective and Approach

The availability of a low-cost mechanical dewatering device that can efficiently remove moisture from fine coal will greatly benefit the U.S. coal industry. In light of this need, researchers at Virginia Tech have developed a novel hyperbaric filter centrifuge that can reduce the moisture contents of fine coal by 30-50% as compared to currently available dewatering methods (Yoon and Asmatulu, 2000). The new technology employs both gas pressure and centrifugal force to increase the driving force for removing water from the fine capillaries present in a filter cake. The specific objectives of this project are (i) to construct a small-scale continuous prototype unit for testing, (ii) to evaluate the effects of key operating and design variables, and (iii) to demonstrate the capabilities of the new technology using fine coals from different coal preparation plants.

## **PROJECT TASKS**

### Task 1 – Filter Centrifuge Design/Construction

Most of the work done during this reporting period focused on the construction of the new drum seal and the fabrication of the parts needed to run the unit in continuous mode. The problem which allowed water to drip inadvertently into the cake collection chute was eliminated by the new seal design. The design of the feeding mechanism was also upgraded to allow the unit to run as a continuous unit. The batch unit mainly consisted of a pressurized rotating filter basket and a feed tank which is kept mixed all the time. The loss of ultrafine coal particles through the screen section of the rotating drum was the biggest issue with the batch unit. Preliminary tests indicated that up to 50% of the solids were reporting to the effluent for some fine feed coal samples.

To overcome the loss of fines, a thickener has been installed as a feed tank when the unit is operated in continuous mode. In this configuration, the thickener underflow is fed to the centrifuge while the effluent is fed back to the thickener (see Figure 1). This layout makes it possible to control cake moisture using the centrifuge and to control solids recovery using the thickener. Since maintaining a constant bed level in the thickener is critical for having a stable process, a fresh feed must be fed to the thickener when the bed level drops below a

certain predefined point. Another well mixed feed tank is used to supply fresh coal to the thickener tank. An electronic optical system has been installed and is being evaluated to automatically control the bed level in the thickener feed tank.

### Task 2 – Filter Centrifuge Testing

During this period of reporting, several series of shakedown tests were conducted in batch mode with the newly fabricated drum seal. The coal samples used in these tests were obtained from screen-bowl centrifuge feeds at existing coal preparation plants. The first set of tests were conducted at a constant fill time of 15 sec and air injection times of 0 (no air), 15 and 120 sec. The rotation speed was held constant at 1,100 rpm. A baseline moisture content of 15.6% was obtained when no air was injected. This value was reduced to 10.3% by injecting air for 15 sec and further reduced to 6.7% after 120 sec of pressurized air injection.

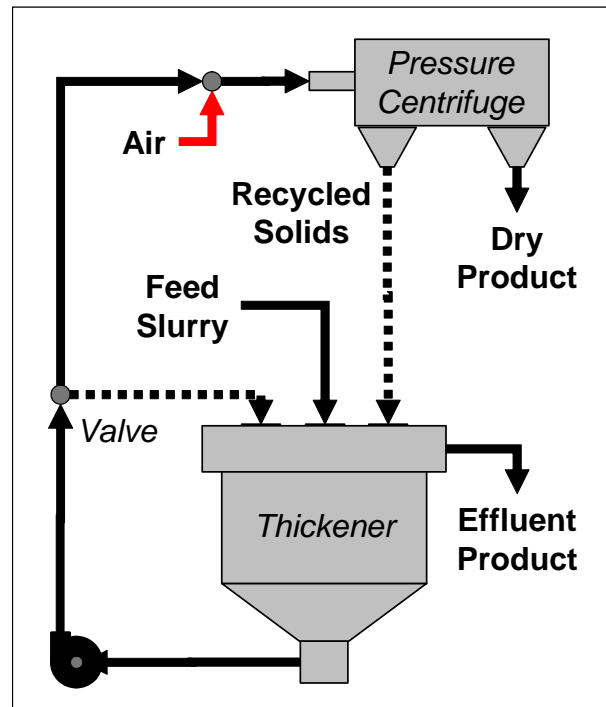


Figure 1. Hyperbaric filter centrifuge circuit.

Based on these promising results from the initial shakedown tests, a second set of test runs were conducted using a fresh coal sample from the same industrial plant site. The tests were conducted using a 15 sec fill time and air injection times of 5, 10, 30, 60 and 120 sec. Three sets of tests were performed at rotation speeds of 1000, 1250 and 1500 rpm. The test results, which are summarized in Table 1, show that the moisture dropped from just over 20% at the lowest air injection time and rotation speed to below 11% at the largest air injection time and rotation speed. The data are plotted in Figure 1 for comparison. This plot shows that an increase in air injection time from 5 to 120 sec incrementally improved the moisture removal by about 5 percentage points for the lowest rotation speed of 1000 rpm. The incremental improvement was somewhat (i.e., about 3 percentage points) for the higher rotation speeds of 1250 and 1500 rpm. Unfortunately, a baseline test (with no air injection) was not run due to plugging of the feed line that occurred when no air was introduced.

One problem with the previous set of tests is that the total time of centrifugation increased as the air injection time increased. Therefore, it was not possible to distinguish whether the reduction in moisture observed in Figure 1 was due to a longer period of air injection or a longer period of centrifugation. To overcome this problem, a third set of shakedown tests was conducted in which the machine was rotated for the same total duration with and without the addition of air. A freshly acquired coal sample from the same preparation plant site was again used in these experiments. The test runs were conducted at the highest rotation speed (1500 rpm – 390 g's) centrifugation times of 5, 10, 30, 60 and 120 sec. The tests were repeated with and without injecting air for each of centrifugation time. In addition, the feed time was increased from 15 to 30 sec in this particular series of tests to increase the amount of solids retained within the unit. The results of these tests are summarized in Table 2. A comparison of the data is also provided in Figure 2.

Table 1. Batch test results obtained using the hyperbaric filter centrifuge (15 sec fill time).

Air Time (sec)	Rotation Speed (rpm)	Rotation Force (g's)	Moisture Content (%)	Cake Weight (gms)
5	1000	142	20.1	16.5
10	1000	142	20.2	18.51
30	1000	142	14.7	22.79
60	1000	142	18.3	31.5
120	1000	142	15.0	33.95
5	1250	222	13.3	7.18
10	1250	222	14.5	14.43
30	1250	222	14.2	18.31
60	1250	222	13.9	20.71
120	1250	222	13.9	25.62
5	1500	319	13.3	14.89
10	1500	319	13.9	12.66
30	1500	319	13.3	15.09
60	1500	319	13.2	14.69
120	1500	319	10.9	17.87

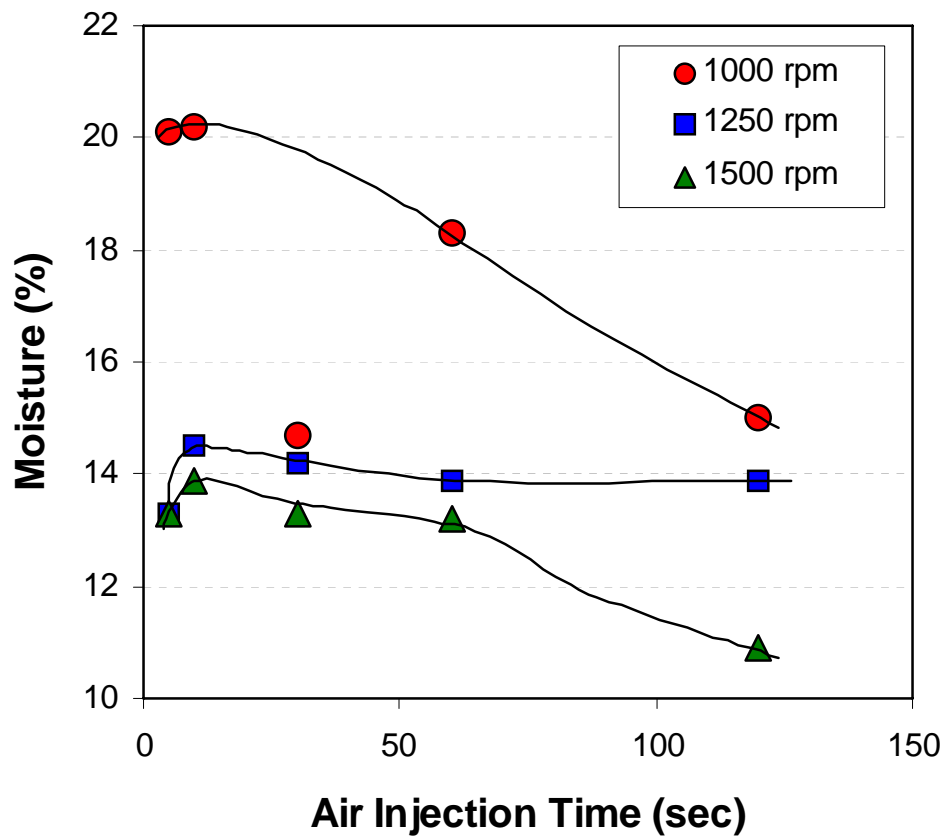


Figure 1. Batch test results obtained using the hyperbaric filter centrifuge (15 sec fill time).

Table 2. Batch test results obtained using the hyperbaric filter centrifuge (30 sec fill time, 1500 rpm rotation speed – 390 g's).

Air Injection Used?	Rotation Time (sec)	Moisture Content (%)	Cake Weight (gms)
No	5	12.6	77.15
No	10	11.2	94.37
No	30	10.8	95.73
No	60	10.2	104.6
No	120	9.6	96.89
Yes	5	10.6	116.62
Yes	10	10.3	86.91
Yes	30	9.6	130.96
Yes	60	8.3	72.4
Yes	120	9.7	109.83

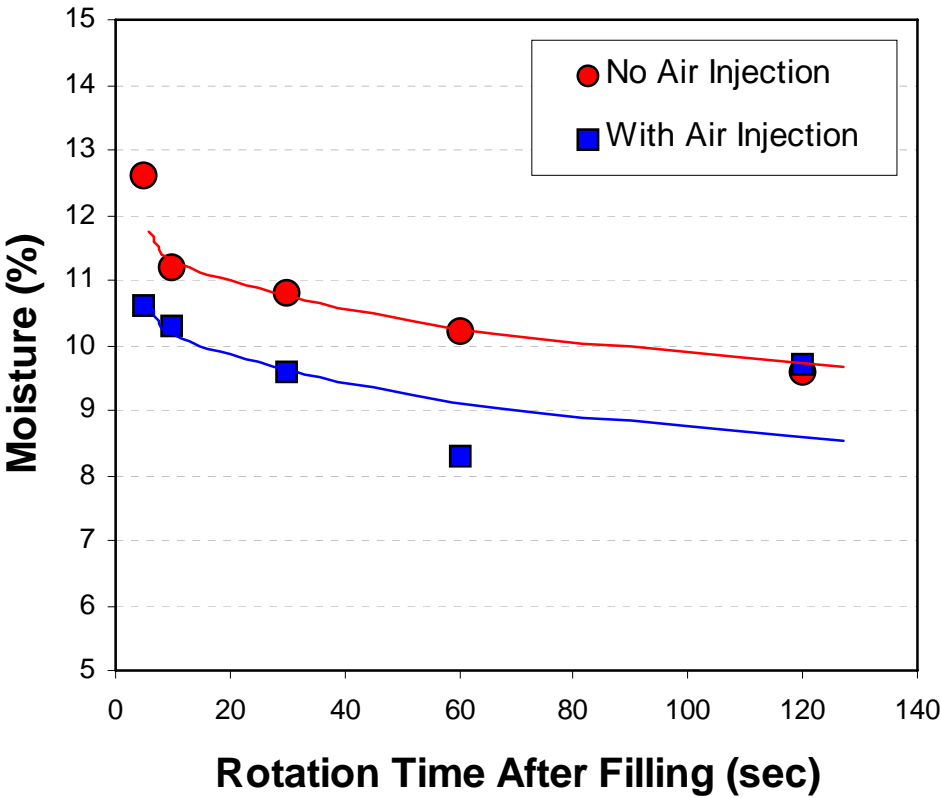


Figure 2. Batch test results obtained using the hyperbaric filter centrifuge (30 sec fill time, 1500 rpm rotation speed – 390 g's).

The test data indicate that the injection of air provided an incremental reduction in moisture removal of only about 1 percentage point. However, all of the moisture values obtained in this series of tests is already very low (around 12% total moisture or less). In fact, the values obtained with air injection at centrifugation drying times of 30 sec or greater are all single-digit values. These results suggest that either (i) the coal sample used in these tests contains very little fines or (ii) a large amount of the fines were lost through the screen section in the batch tests. Previous laboratory tests indicate that the differences in moisture obtained with and without air injection are much greater for cakes containing larger amounts of fine particles. Therefore, a much larger difference in moisture is expected once the continuous circuitry (i.e., integrated thickener) is operating and a proper circulating load of fines is maintained within the prototype. Continuous mode tests will be performed using the prototype during the next reporting period in order to verify this hypothesis.

### Task 3 – Engineering Design

To date, no projective activities have been carried out under this particular task pending the completion of the construction and testing of the prototype unit.

### **SUMMARY**

During this reporting period, construction of a continuous unit was continued and the problem in the mechanical water seal was eliminated. Several series of shakedown tests were carried out in batch mode. The data indicate that the moisture reduction is significantly better at higher rotation speeds and with the injection of air. However, the capabilities of the prototype cannot be fully established until additional tests are completed with the unit operating in continuous mode. This mode of operation required the integration of a thickening unit into the test circuitry. This modification makes it possible to improve fines recovery by circulating fines previously lost through the screen back to the circuit feed.

### **FUTURE WORK**

Future work will involve any improvements necessary to achieve a stable process. Once proven, detailed tests will be run to fully evaluate the capabilities of the unit for a variety of coal samples and over a wide range of operating conditions.

### **REFERENCES**

Yoon, R.-H. and R. Asmatulu, "Methods of Improving Centrifugal Filtration," U.S. Patent Application Serial No. 09/531,373, filed March 21, 2000.

Yoon R.-H. and R. Asmatulu, PCT Patent Application Serial No. PCT/US02/11318, filed April 12, 2002.

### **PUBLICATIONS/PRESENTATIONS**

To date, no major publications have resulted from this project.

**Appendix 14: Improvements in Screen-Bowl Centrifuge  
Performance (VA013)**

## TECHNICAL PROGRESS REPORT

<u>Contract Title and Number:</u> Establishment of the Center for Advanced Separation Technologies (DE-FC26-01NT41091)	<u>Period of Performance:</u> Starting Date: 6/1/04 Ending Date: 10/31/06
--	---

<u>Sub-Recipient Project Title:</u> Improvements in Screen-Bowl Centrifuge Performance	<u>Report Information:</u> Type: Semi-Annual Number: 3 Period: 10/1/05-3/31/06
<u>Principal Investigators:</u> Gerald H. Luttrell and Roe-Hoan Yoon	Date: 4/30/06 Code: VA013

<u>Contact Address:</u> 146 Holden Hall Virginia Polytechnic Institute & State University Blacksburg, VA 24061	<u>Contact Information:</u> Phone: (540) 231-4508 Fax: (540) 231-3948 E-Mail: cast@vt.edu
---	--

<u>Subcontractor Address:</u> No subcontracts issued.	<u>Subcontractor Information:</u> Phone: Fax: E-Mail:
--	--

### ABSTRACT

Screen-bowl centrifuges are the most commonly used method for dewatering fine coal in the United States. Unfortunately, this process is the least efficient and most costly dewatering operation in the preparation plant. In light of these difficulties, a broad-based research project has been undertaken to develop technological enhancements that improve moisture reduction and increase fine coal recovery for screen-bowl centrifuges. The first part of this work involves a detailed in-plant test program to experimentally define the baseline operating capabilities of screen-bowl centrifuges. This fundamental information is needed so that plant operators can optimize the performance of their existing dewatering circuits. The second part of this work will involve the testing of internal injection ports for (i) adding flocculant to the low-solids pool and (ii) adding dewatering aids and surface tension modifiers to the dewater screen solids. During the past reporting period, several series of field tests were performed to further assess the performance of the flocculant injection system at an additional industrial plant site. These tests showed that the flocculant type and dosage is very important in maintaining low effluent solids. Work was also performed to complete the collection and analysis of samples needed to characterize the in-plant performance a a full-scale industrial screen-bowl centrifuge. Unfortunately, the test results obtained to date were inconclusive due to the large degree of scatter in the experimental test data.

## **INTRODUCTION**

### Background

The solid-solid separation processes employed by modern coal preparation plants require large amounts of process water. After cleaning, the unwanted water must be removed from the surfaces of the particles using mechanical dewatering equipment. Coarse particles can be readily dewatered using simple screening systems, while finer particles require more complicated unit operations such as centrifuges and filters for effective dewatering. In select cases, thermal drying may even be required to remove additional moisture so that the final product can meet customer specifications. Moisture that is not removed by these processes reduces the heating value of the final coal product and increases the transportation costs for the solid fuel. In addition, excess moisture can create significant handling problems for both the coal producer and downstream consumers by plugging chutes, bins, rail cars, etc. The problem can be particularly severe during winter months because of freezing.

Most of the preparation plants in the U.S. use screen-bowl centrifuges to dewater their fine products. Despite this popularity, there is surprisingly little fundamental information available that can be used to optimize centrifuge performance. Most existing guidelines for centrifuge selection and operation are based on empirical relationships or rule-of-thumb recommendations. For example, product moisture is typically estimated from the percentage of minus 325 mesh material present in the feed slurry. This relationship was originally developed in the early 1970s (Orphanos, 1974) and is often applied incorrectly. The actual correlation was developed using the percentage of minus 325 mesh material in the dewatered product and not the percentage present in the feed slurry. As a result, product moistures are often higher in actual practice than predicted by this relationship. Likewise, coal recovery is generally estimated by assuming that all the material coarser than 325 mesh will be recovered along with 50% of the minus 325 mesh. Obviously, neither of these relationships accurately account for site-specific differences in other characteristics of the feed slurry (e.g., particle size distribution, coal wettability, feed solids content, etc.) or variations in machine design and operating variables (e.g., feed rate, weir settings, scroll speed differential, bowl volume, screen length, etc.).

### Objective and Approach

An improved understanding of the operating characteristics and technical capabilities of screen-bowl centrifuges would make it possible for plant operators to improve the performance of their dewatering circuits. Therefore, the objectives of this project are (i) to formulate detailed engineering criteria for optimizing the performance of industrial screen-bowl centrifuges and (ii) to develop and evaluate technological enhancements in screen-bowl centrifuge design that will improve moisture reduction and/or increase fine coal recovery.

## PROJECT TASKS

### Task 1 - Field Evaluation

This task involves the detailed evaluation of an industrial screen-bowl centrifuge at an industrial preparation plant site. The ultimate objectives of this work are (i) to derive engineering expressions that can be used to predict the moisture content and solids recovery attainable as a function of the various operating and design variables and (ii) to provide data that can be used to calculate the incremental moisture of the material that is discharged as the operation of the centrifuge is adjusted. During this reporting period, a mass-balance routine was developed to analyze the test data obtained from samples collected around an industrial-scale screen-bowl centrifuge. A typical set of size-by-size performance data is provided in Table 1. The individual groups of samples generally mass balanced well and, as such, were believed to be reliable. However, comparison of the results from tests conducted under different conditions indicated that there was considerable random variation in the samples (i.e., no clear trend could be observed between solids content or moisture as a function of feed flow rate or percent solids). As indicated in the last technical report, the large variation is believed to be due to large fluctuations in plant conditions created by variations in coal types, size distributions, etc. A second test site which is subject to less variability is currently being sought for conducting a second round of in-plant tests.

Table 1. Typical set of size-by-size mass balance data for a screen-bowl centrifuge.

	Experimental Data				Balanced Data			
	Feed	Product	Drain	Effluent	Feed	Product	Drain	Effluent
Total Mass (% stream):								
Plus 100 M	63.62	<b>69.81</b>	<b>53.48</b>	<b>0.16</b>	63.33	70.38	53.31	0.16
100 x 325 M	13.82	<b>14.71</b>	<b>23.69</b>	<b>0.05</b>	12.99	14.44	24.04	0.05
325 M x 0	22.57	<b>15.48</b>	<b>22.83</b>	<b>99.78</b>	23.68	15.18	22.65	99.79
Overall	100.01	100.00	100.00	99.99	100.00	100.00	100.00	100.00
Total Mass (tph):								
Plus 100 M	63.62	62.92	3.21	0.02	63.33	63.31	7.78	0.02
100 x 325 M	13.82	13.26	1.42	0.00	12.99	12.99	3.51	0.01
325 M x 0	22.57	13.95	1.37	9.84	23.68	13.65	3.31	10.03
Overall	<b>100.00</b>	90.13	6.00	9.87	100.00	89.95	14.60	10.05
Ash (% stream):								
Plus 100 M	4.44	<b>5.87</b>	<b>5.35</b>	<b>59.84</b>	5.01	5.00	5.30	59.82
100 x 325 M	10.97	<b>7.48</b>	<b>15.40</b>	<b>26.11</b>	8.08	8.07	16.03	26.11
325 M x 0	16.65	<b>12.71</b>	<b>19.69</b>	<b>23.85</b>	17.13	12.53	19.59	23.39
Overall	8.09	7.17	11.00	23.91	8.28	6.58	11.12	23.45
Total Ash (tph):								
Plus 100 M	282.24	369.36	17.17	0.94	317.23	316.26	41.26	0.96
100 x 325 M	151.57	99.18	21.89	0.13	104.99	104.86	56.27	0.13
325 M x 0	375.61	177.34	26.97	234.79	405.76	171.10	64.79	234.66
Overall	809.34	645.87	66.03	235.88	827.97	592.22	162.31	235.75
Slurry Data:								
Solids (%)	24.51	<b>83.37</b>	<b>29.57</b>	<b>3.29</b>	24.18	83.36	29.57	3.29
Rate (tph)	407.99	108.11	20.29	299.88	413.49	107.90	49.36	305.59

## Task 2 – Flocculant Addition

Several series of field tests were performed at an additional plant site to verify that the injection of polymer flocculant into the dilute pool section of a screen-bowl centrifuge would improve solids recovery. In this particular series of tests, a specially formulated polymer (SR polymer) prepared by Nalco chemical was compared with traditional cationic and anionic flocculants. The results obtained these in-plant tests are summarized in Table 1. In each experimental run, the as-received reagents (polymer or flocculant) were diluted with fresh water down to a 1% solution before being injected into the screen-bowl. The test data from the first series of tests (day 1) show that the solids content in the main effluent was reduced as the polymer dosage was increased up to 4.5 GPM. The highest dosage rate of 4.5 GPM reduced the solids content from about 3.9% to 0.6% (2.30 to 0.36 TPH). Poorer solids contents of about 2.7% were obtained at lower dosages of 1.25 and 2.50 GPM of polymer. In addition, test results obtained from a second series of tests (day 2) conducted at a fixed reagent dosage of 4.5 GPM showed that the polymer was superior to traditional anionic flocculant. The cationic flocculant also appeared to work well in the injection tube and reduced the solids content from 4.2% down to just over 1%. The moisture and ash contents of the dewatered products from these tests increased slightly when adding polymer due to the capture of ultrafine particles.

Table 1. Summary of screen-bowl centrifuge injection tests.

Test Description	Reagent Addition (GPM)	Dewatered Product			Effluent Discard		
		Ash (%)	Moist. (%)	Rate (TPH)	Ash (%)	Solids (%)	Rate (TPH)
No Reagent	--	8.70	12.84	25.72	9.58	3.94	2.30
SR Polymer	1.25	8.63	12.26	26.45	9.44	2.69	1.57
SR Polymer	2.50	8.48	15.77	26.47	8.61	2.66	1.55
SR Polymer	4.50	8.97	16.54	27.66	8.32	0.62	0.36
No Reagent	--	8.94	11.44	25.69	9.10	3.99	2.33
No Reagent		8.17	11.62	25.57	11.99	4.19	2.45
SR Polymer	4.50	9.23	16.96	27.41	9.74	1.84	1.07
Cationic Floc	4.50	8.65	15.31	25.93	10.07	1.05	0.61
Anionic Floc	4.50	8.74	11.66	25.36	9.68	3.58	2.09

## Task 3 – Surfactant Addition

No additional experimental test work or analyses were performed under this task during this reporting period.

## **SUMMARY**

Field tests conducted in the present work again demonstrate that flocculant injection can be used to effectively reduce the solids content of main effluent that is discarded by a screen-bowl centrifuge. The in-plant tests indicate that both reagent dosage and type is important in obtaining the best overall results. The test data also suggest that the moisture content of the screen-bowl product may increase slightly due to the recovery of fine particles displaced from the main effluent. For the tests conducted to date, the data suggest that the increase in moisture is only about 2 percentage points.

## **FUTURE WORK**

During the next reporting period, test work will again focus on the characterization of full-scale screen-bowl centrifuge performance at an industrial site. The tests are to be performed as a function of key operating variables (i.e., feed slurry flow rate and solids content).

## **REFERENCES**

1. Orphanos, J.S., 1974. "Experience with the Screen-Bowl and Solid-Bowl Centrifugals," Presentation Handout, Minerals Engineering Society, North and South Midlands Sections Meeting, Rockingham Social Welfare Hall, Rockingham, England, March 14, 1974.

## **PUBLICATIONS/PRESENTATIONS**

R.T. Burchett, K.M. McGough and G.H. Luttrell, 2005. "Improved Screen-Bowl Centrifuge Recovery Using Polymer Injection Technology," *22th Annual International Coal Preparation Exhibition and Conference*, Lexington, Kentucky, 10 pp.

G.H. Luttrell, R.T. Burchett, K. McGough and F. Stanley, 2006., "Improving Screen-Bowl Centrifuge Performance," *SME Annual Meeting*, St. Louis, Missouri, March 26-29, 2006, 5 pp.

**Appendix 15: The Development and Utilization of Alkaline Sulfide  
Leaching and Recovery of Gold (MT001)**

## TECHNICAL PROGRESS REPORT

Contract Title and Number:

Establishment of the Center for Advanced Separation  
Technologies (DE-FC26-01NT41091)

Period of Performance:

Starting Date: Apr. 1, 2003  
Ending Date: Sept. 1, 2006

Sub-Recipient Project Title:

Development of alkaline sulfide leaching and recovery  
of gold

Principal Investigators:

Corby G. Anderson  
Larry G. Twidwell

Contact Address:

Room 221, ELC Building  
1300 West Park Street  
Butte, MT 59701-8997

Subcontractor Address:

“No subcontracts issued.”

Report Information:

Type: Semi-Annual  
Number: 4  
Period: Sept. 30 – Mar. 31  
Date: Mar. 31, 2006  
Code: MT001

Contact Information:

Phone: (406) 496-4794  
Fax: (406) 496-4512  
E-Mail: canderson@mtech.edu

Subcontractor Information:

Phone: ---  
Fax: ---  
E-Mail: ---

### ABSTRACT

New progress has been achieved in the last year of research. Tremendous achievement in proving the ease of waste solution treatment of the alkaline sulfide system has been done using the autoclave oxidation and electro dialysis. Evenmore, a solution of regenerated NaOH from electro dialysis was able to be recirculated to the leaching stage of the alkaline sulfide process. As well ammonium sulfate was produced from the waste solutions. Additionally, industrial sulfide concentrates of pyrite and galena-sphalerite have been obtained and tested for leaching and has shown promising results with approximately 79.0% and 85.0% leaching of gold. Also, recovery of gold from pregnant alkaline sulfide solution has been proven to be effective on both high and low gold concentration in solution. All of these developed unit processes of the system have been tested cohesively in the developed bench-scale batch simulation. This simulation provided the opportunity to prove the consistency and reliability of the leaching system. More importantly, parameters of interest were able to be monitored before and after each unit processes; thus better understanding of the whole system was achieved.

## **INTRODUCTION**

### Background

An alternative, non-cyanide gold leaching process based on the use of environmentally benign sulfur compounds as both the oxidant and lixiviant components of the leach solution is currently under development. The use of non-cyanide reagents has become particularly relevant in light of recent public concerns and regulations involving the use of cyanide for gold production. Furthermore, the development of an alkaline sulfide based leaching processes is particularly well suited for treatment of sulfide gold ores pretreated with low temperature pressure oxidation whereby the majority of gold tends to accumulate in the elemental sulfur produced. Additional potential advantages of this process include the production of value added byproducts and improved public perception of gold mining through the use of an environmentally benign leaching process.

The technological issues that are currently hindering the use of alkaline sulfide leaching are a lack of basic understanding of the leaching chemistry and thermodynamics associated with the process. Thus, this study was undertaken to develop an understanding of the basic reaction chemistry of the alkaline sulfide leaching process and to establish a thermodynamic model in order to predict optimum leaching conditions under various conditions.

### Objectives and Approach

The objectives of this project:

#### *Phase I/Year 1*

- Task 1 - Develop a thermodynamic model of the alkaline sulfide leaching system;
- Task 2 - Optimize the chemistry of the alkaline sulfide gold leaching process; and,
- Task 3 - Study the optimized leaching system kinetics.

#### *Phase II/Year 2*

- Task 1 - Recovery of gold from an alkaline sulfide solution;
- Task 2 - Production of sodium sulfate as a treatment method for alkaline sulfide solutions; and,
- Task 3 - Application of the alkaline sulfide leaching system to refractory gold ores and concentrates.

## **PROJECT TASKS**

### Task 1 (Phase II)

Gold was successfully removed from solution with a carbon substrate. (See Table I.) A view ion-exchange membranes were also tested as a collaboration with PSI Inc. of The University of Montana. Inquiries have indicated the possibility of using silica based ion-exchange resins with different active ingredients to strip gold out of the alkaline sulfide solution. However, concerns related to the stability of the silica resins in the high pH system of the alkaline sulfide solution did exist. Thus, styrene based ion-exchange resins with equivalent active ingredients were tested. All tests were done in an alkaline sulfide solution of 80gr/L total sulfur concentration, 50gr/L NaOH concentration, and 18.77ppm gold.

TABLE I. Description of Substrate Used in the 1<sup>st</sup> Recovery Experimental Campaign

Test	Substrate	Active Ingredient	Base Material
RT1-T1	PSI WP2	Quartenary Amine	Silica
RT1-T2	Amberlite IRC748	Iminodiacetic Acid	Styrene-divinylbenzene
RT1-T3	Purolite S930	Iminodiacetic Acid	Styrene-divinylbenzene
RT1-T4	Sybron Lewatit® TP207	Iminodiacetic Acid	Styrene-divinylbenzene
RT1-T5	IRA400	Quartenary Amine	Styrene-divinylbenzene
RT1-T6	IRA68	Quartenary Amine	Styrene-divinylbenzene
RT1-T7	Activated Carbon	--	--

TABLE II. Results of 1<sup>st</sup> Recovery Experimental Campaign

Test	Substrate	Weight Post-Rec. (initially 20gr.)	% Rec Fire-Assay
1	PSI's WP2	N/A	N/A
2	IRC748	9.34	3.02
3	S930	11.22	1.67
4	TP207	10.46	0.16
5	IRA400	21.08	53.43
6	IRA68	10.34	0.16
7	Act. Carbon	20.83	70.06

Results shown in Table II shows the instability of PSI's WP2 ion-exchange membrane in the high pH of the alkaline sulfide solution. Only after 4-5hours of shaking, all of the silica-based resins were dissolved in the solution. Additionally, activated carbon was also proven to be the most effective substrate for gold recovery from the alkaline sulfide solution.

Additional experimental campaign was conducted to test the effectiveness of activated carbon and IRA400 ion exchange resin, two of the best performing substrate from previous campaign, in a lower concentration of gold in alkaline sulfide solution. An alkaline sulfide with 80gr/L total sulfur concentration, 50gr/L NaOH, and 0.4502ppm gold was used. (See Table III.) It can be concluded that activated carbon is the most effective substrate to remove gold from low concentration alkaline sulfide solution.

TABLE III. Result of 2<sup>nd</sup> Recovery Experimental Campaign

Test	Substrate	Weight Post-Rec. (initially 20gr.)	% Rec Fire-Assay
1	IRA400	19.3	63.79
2	Carbon	20.14	91.62
3	Carbon	21.32	90.17

### Task 2 (Phase II)

A method for sodium sulfate production has been successfully completed on a laboratory scale by oxidizing dissolved sulfides and polysulfides. The method is carried out in a laboratory scale autoclave. Alkaline sulfide solution is poured into the autoclave and the autoclave is heated. Pressurized oxygen is supplied to the autoclave so that the solution has sufficient oxidizer. The method was found to be highly dependent upon the agitation in the autoclave; very poor results were obtained at low agitations rates while 100% sulfide oxidation to sulfate was obtained with high agitation rates. Also, better oxidation was obtained when the system temperature was lowered from 170 to 150°C.

Detailed experiments have been conducted to better understand the kinetics of the sodium sulfate production using laboratory scale autoclave/pressure vessel. On a standard solution of 50gr/L total sulfur concentration, an experimental design was made using StatEase<sup>®</sup> design program with variables of:

1. Temperature: 75-150°C;
2. Oxygen overpressure: 20-80psi;
3. Time: 2-5 hours;
4. Initial NaOH concentration: 18-24 g/L; and
5. Total sulfur content: 24-50 gr/L.

Agitation is set to the maximum of 700psi to provide maximum oxygen and solution mixing. It was suspected that temperature, oxygen overpressure, and time would have a significant effect on kinetics; so, these variables are varied. The less obvious variable of initial NaOH was also investigated to ensure a good understanding of the process. Shown in Figure 1 is a model generated using StatEase regarding the SO<sub>4</sub><sup>2-</sup> production.

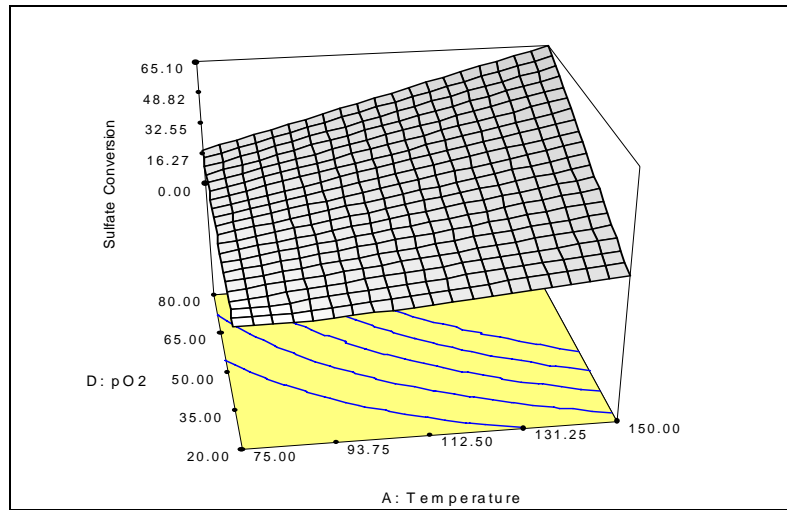


Figure 1. Sulfide/Polysulfide to Sulfate Conversion Model

As seen in Figure 1, oxygen overpressure and temperature are significant variables in this oxidation process; and no significant effects were observed from the initial NaOH concentration. As overpressure and temperature were increased, reaction kinetic was also increased. However, it also can be seen that after five hours, only a maximum conversion of approximately 65% was achieved. It can be derived that not enough time was allowed, in these pressure and temperature, to achieve 100% conversion. Consequently, a second set of experiment was done at higher time and temperature range to investigate the minimal time required.

With a temperature range of 150-170°C and time of 4-7 hours, it was found that 100% conversion could be achieved at 150°C, 7 hours, and 80psi. Initial experiment within these parameters produced sulfur solids due to the lack of NaOH concentration; this problem was solved with the increase of NaOH concentration. The optimal NaOH concentration was found to be 65gr/L. A set of experiments done to a higher concentration total sulfur of 80gr/L was also conducted, resulting in a total NaOH concentration of 100gr/L to achieve 100% conversion of sulfide/polysulfide to sulfate at 170° and 80psi, in 10hrs.

Additionally, waste treatment experiments were done using the Electrodialysis unit (EDU). In principle, the EDU uses ion-exchange membranes, bipolar membranes, and the application of electrical potential to achieve a cation-anion transfer. Experimental campaigns using the EDU were successfully done to split 1.5M Na<sub>2</sub>SO<sub>4</sub> feed solution into concentrated NaOH and H<sub>2</sub>SO<sub>4</sub> streams. Seen in Figure 2 are some experimental results achieved on the splitting of synthetic Na<sub>2</sub>SO<sub>4</sub> solution prepared from reagent standard chemicals.

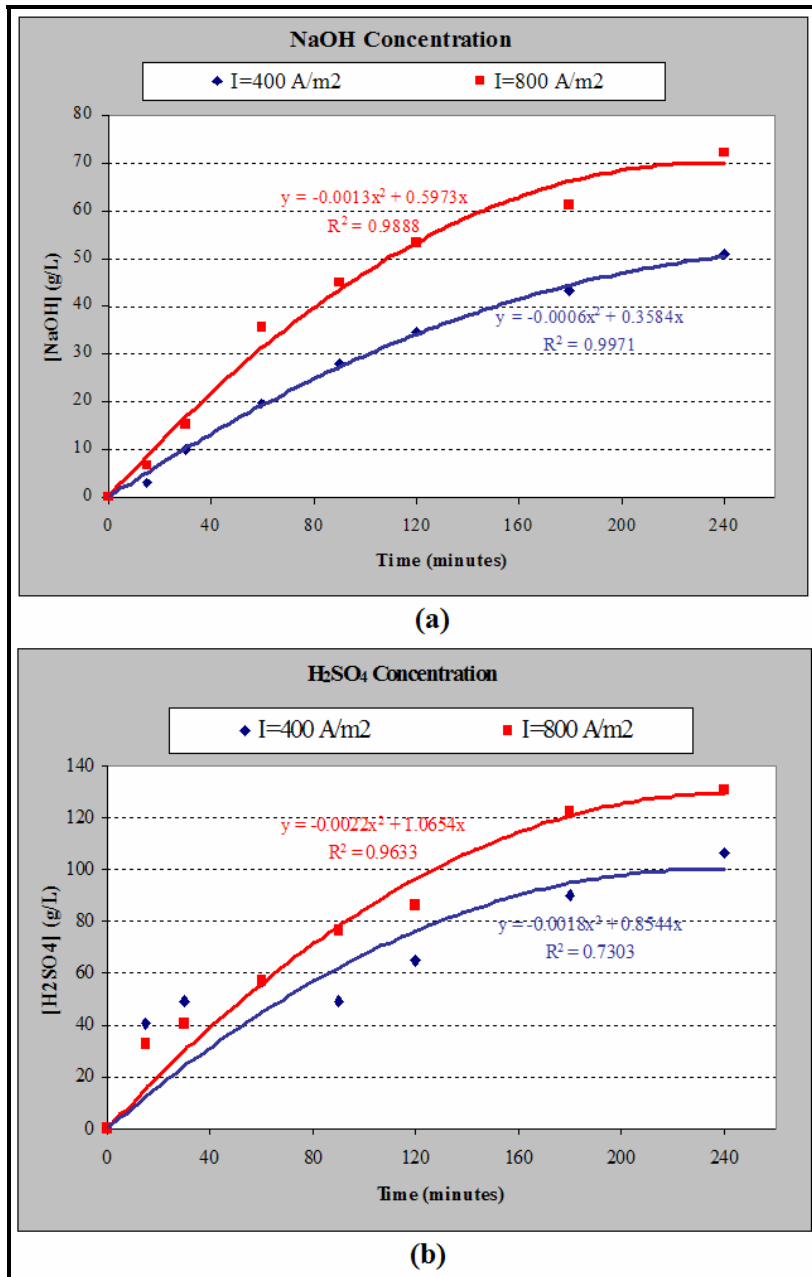


Figure 2. Results of EDU Experiments

As can be seen in Figure 2, NaOH and H<sub>2</sub>SO<sub>4</sub> concentration measured using titration methods were plotted versus time. After 240 minutes, it was found that a plateau was reached and approximate maximum concentrations of NaOH of 80gr/L and H<sub>2</sub>SO<sub>4</sub> of 130gr/L were achieved at a current density of 800A/m<sup>2</sup>. Plateau reached after 240 minutes was caused by the decrease in concentration differential of the base and acid solution in the system.

Additional experiments using real spent Na<sub>2</sub>SO<sub>4</sub> solution made through the autoclave were also conducted. Spent alkaline sulfide solution after leaching of Greens Creek Sulfide Concentrate were oxidized to 100% sulfate conversion and ran straight through the EDU. Similar results of 70gr/L NaOH and 100gr/L H<sub>2</sub>SO<sub>4</sub> were achieved without any significant indication of membrane fouling.

Preliminary work has already been commenced in investigating the treatment of H<sub>2</sub>SO<sub>4</sub> solution produced by the EDU. Proposed methods are the addition of hydrated lime [Ca(OH)<sub>2</sub>] and ammonium hydroxide [NH<sub>4</sub>OH] to respectively produce gypsum [CaSO<sub>4</sub>.2H<sub>2</sub>O] and ammonium sulfate [(NH<sub>4</sub>)<sub>2</sub>SO<sub>4</sub>]. Both products have minimal environmental risk considerations and potentially can be sold as by-products. Unfortunately, no quantitative data can be presented yet. However, it has been confirmed that the formation of (NH<sub>4</sub>)<sub>2</sub>SO<sub>4</sub> can be achieved just by adding NH<sub>4</sub>OH solution into the produced H<sub>2</sub>SO<sub>4</sub> in room temperature.

### Task 3 (Phase II)

Previous thesis project had successfully investigated the performance of the alkaline sulfide system to several industrial ores:

1. Gravity concentrate of Kennecott Greens Creek Mine (KGCMC);
2. Roaster calcine of Newmont Mining Company; and
3. Elkhorn sulfide concentrate.

These industrial samples were chosen to demonstrate the specific gold leaching capabilities. Leaching tests at elevated temperature (50-60°C) and high concentrations of total sulfur (2-3.14M) have achieved leaching performances of 93.5%, 84.0%, and 55.59% for the respective samples. Additionally, the high concentrations of sulfide and cyanides in KGCMC (Pb, Zn, and Cu) and Elkhorn (Cu) samples show the performance of ASGLS in feed materials where cyanide has traditionally been proven to be less effective.

Current research has focused on two additional feed materials: KGCMC Sulfide Composite Concentrate and Barrick's Golden Sunlight Mine (BGSM) Pyrite Concentrate. Through extensive analytical procedures, both of these sample materials have been mineralogically specified. KGCMC sulfide composite concentrate is a combination of galena (PbS) and sphalerite (ZnS) concentrate produced from a flotation circuit and contains 0.690opt gold and 89.8opt silver. These KGCMC concentrates are currently being sold straight to a smelter with gold credit less than 100%. In the other hand, PDGS concentrate is a pyrite (FeS<sub>2</sub>) concentrate produced by spiral gravity concentration, which currently being treated by concentrated cyanide solutions to leach the contained 0.104opt of gold.

Shown in Table IV are experimental results of leaching tests investigating the effects of total sulfur and hydroxide concentrations to the KGCMC composite concentrate. It was proven that a higher concentration of total sulfur and hydroxide improved the leaching performance of ASGLS on the composite concentrate. Leaching performances up to 79.0% were achieved.

TABLE IV. KGCMC Composite Concentrate Leaching Experiment Results

Test #	Na <sub>2</sub> S (gr/L)	S (gr/L)	NaOH (gr/L)	Temperature (°C)	Au TLS (opt)	Ag TLS (opt)	Au Leached (%)	Ag Leached (%)
LGC1-T1	40	10	24	50	0.524	79.5	19.0%	11.5%
LGC1-T2	80	20	24	50	0.503	77.9	22.3%	13.3%
LGC1-T3	160	40	24	50	0.496	78.8	23.3%	12.2%
LGC2-T1	160	40	50	50	0.235	78.5	63.7%	12.6%
LGC2-T2	160	40	50	50	0.218	82.1	66.3%	8.6%
LGC2-T3	160	40	50	50	0.136	74.5	79.0%	17.0%

Shown in Table V are results of leaching tests conducted to the BGSM pyrite concentrate. Similar to the KGCMC composite concentrate results, higher total sulfur concentration was proven to be more effective in extracting gold. It should also be noted that feed samples of tests LGS2-T1 and LGS2-T2 were roasted at 300°C and 400°C, respectively, for 12 hours prior to leaching. It can be noticed that, similar to the cyanide system, oxidation of sulfide system to sulfur will improve leaching performance.

TABLE V. BGSM Pyrite Concentrate Leaching Experiment Results

Test #	Na <sub>2</sub> S (gr/L)	S (gr/L)	NaOH (gr/L)	Temperature (°C)	Au Tails (opt)	Ag Tails (opt)	Au Leached (%)	Ag Leached (%)
LGS1-T1	80	20	25	50	0.042	0.4	59.6%	55.6%
LGS1-T2	160	40	50	50	0.024	0.4	76.9%	55.6%
LGS1-T3	160	40	50	50	0.029	0.4	72.1%	55.6%
LGS2-T1	160	40	50	50	0.016	0.4	84.6%	55.6%
LGS2-T2	160	40	50	50	0.024	0.3	76.9%	66.7%

Finally, a bench-scale batch simulation procedure and schedule have been developed to further test these developed unit processes together (leaching, recovery, and waste treatment). The objective of such simulation is to ultimately test the consistency of the system itself. Additionally, various parameters were monitored before and after each unit processes (Eh, pH, sulfide concentration, polysulfide concentration, etc), which couldn't be measured before. The effect of solution recirculation, and how much reagent addition in each recirculation needed, could also be investigated.

A bench-scale batch simulation has been conducted with KGCMC composite concentrate as feed and has shown an encouraging data where leaching performance was consistent. Additionally, a successful recirculation of NaOH solution produced using the EDU was achieved, producing a fresh alkaline sulfide solution to be added to the leaching stage. A bench-scale batch simulation of the BGSM pyrite concentrate will be commenced immediately to also test for leaching consistency and parameter control of the ASGLS.

## SUMMARY

Notable progresses have been achieved in proving activated carbon as the optimal substrate to remove gold from ASGLS solution. Also, a tremendous step forward has been achieved in the development of waste solution treatment of the system. It has been proven that NaOH can be regenerated using the electro dialysis process and can effectively be recirculated to the leaching stage of the system. Additional leaching of real industrial concentrates, in which cyanide has been traditionally been less effective, proved that the ASGLS is a highly effective and selective system. Finally, a simple bench-scale batch simulation was developed to test the cohesiveness of the three unit processes developed for the ASGLS (leaching, recovery, and waste treatment). Plenty of precious data regarding the stability and parameters of the solution before and after each unit processes were able to be collected; thus simulating, as close as possible, a real working circuit by only using lab-scale equipments.

## **FUTURE WORK**

Future work will be focused in the following three areas:

1. Optimization of the proposed treatment methods of the produced H<sub>2</sub>SO<sub>4</sub> solution from the electro dialysis process: ammonium sulfate and gypsum production.
2. A bench-scale batch simulation with PDGS pyrite concentrate as feed material to test for system consistency and monitoring of important parameters of the system.
3. A method for stripping gold from activated carbon.

## **PUBLICATIONS/PRESENTATIONS**

A presentation in the next IPMI conference in Las Vegas is currently being planned and prepared for.

## **Appendix 16: Hydrometallurgical Processing of Chalcopyrite Concentrates**

**(NV001)**

The PI has notified CAST that work is complete and a Final Report will be issued.

**Appendix 17: Simultaneous Electrolysis of Copper and Ferrous Ions to  
Produce Copper Cathode and to Regenerate Ferric Sulfate - The Lixiviant  
to Dissolve Copper Sulfide Minerals (MT002)**

## TECHNICAL PROGRESS REPORT

<u>Contract Title and Number:</u> Crosscutting Technology Development at the Center for Advanced Separation Technologies (DE-FC26-02NT41607)	<u>Period of Performance:</u> Starting Date: 10/1/2002 Ending Date: 10/31/2006
<u>Sub-Recipient Project Title:</u> Simultaneous Copper Cathode Production and Ferric Sulfate Regeneration	<u>Report Information:</u> Type: Semi-Annual Number: 6 Period: 10/1/05-3/31/06 Date: 05/02/2006 Code: MT002-R06
<u>Principal Investigators:</u> Courtney Young Hsin-Hsuing Huang	<u>Contact Information:</u> Phone: (406) 496-4158 Fax: (406) 496-4664 E-Mail: CYoung@mtech.edu
<u>Contact Address:</u> Metallurgical and Materials Engineering Montana Tech Butte MT 59701	<u>Subcontractor Information:</u> Phone: NA Fax: NA E-Mail: <a href="mailto:Cesimiro.Fabian@jcu.edu.au">Cesimiro.Fabian@jcu.edu.au</a>
<u>Subcontractor Address:</u> Ces Fabian Chemical Engineering and Industrial Chemistry James Cook University Townsend Queensland Australia	

### ABSTRACT

Various tests were conducted over a three-year period to investigate the feasibility of electrowinning copper ( $\text{Cu}^0$ ) from cupric ( $\text{Cu}^{2+}$ ) while simultaneously oxidizing ferrous ( $\text{Fe}^{2+}$ ) to ferric ( $\text{Fe}^{3+}$ ) using a membrane cell. Results indicated that several variables would be important to consider to minimize the applied voltage while keeping current density at a maximum. These variables included electrolyte concentrations ( $\text{Cu}^{2+}$  and  $\text{Fe}^{2+}$ ), agitation/flow-rate, applied voltage, and temperature. Other variables were also tested: cathode type, anode type, membrane type, and cell design; however, certain ones showed superior behavior. Ensuing factorial-design experiments were therefore conducted with these 4 variables fixed in order to investigate the effects of the other variables. For simplicity and to minimize the number of experiments, the temperature was held constant at  $20^\circ\text{C}$  (room temperature). Results were then statistically analyzed using StatEase software and yielded the following model:

$$\text{Log}_{10}(\text{Current Density}) = 0.97876 + 3.56 \cdot 10^{-3} \cdot [\text{Cu}^{2+}] - 3.95 \cdot 10^{-4} \cdot [\text{Fe}^{2+}] + 0.51 \cdot \text{Volts} \\ + 8.13 \cdot \text{Flowrate} - 3.1 \cdot 10^{-4} \cdot \text{Volt} \cdot \text{Flowrate}$$

From the model, it can be concluded that the current density and therefore copper production will be increased by increasing the cupric concentration (g/L), applied voltage

(V), and/or flowrate (ml/min); however, there was a small but noticeable binary effect between flowrate and applied voltage that had a negative effect on the system. Furthermore, a negative effect on current density would also be realized by increasing the ferrous concentration. It appears that the applied voltage and the flowrate are the most significant variables due to the large values of their respective coefficients. Optimization of the model indicates that the voltage can be decreased from an industrial standard of approximately 2.0 Volts to between 1.5-1.7 Volts which equates to energy savings of 15-25%. Furthermore, the model concurs with fundamental understanding of electrowinning principles.

Various tests were also conducted in collaboration with Montana Resources, a local Montana mining company in Butte, to see if ferric leaching could be used on their Central Zone Ore (CZO) and implemented along with the membrane electrowinning technology. CZO does not respond as well as the traditional East and West Zone Ores in their flotation operation: recoveries run low between 85-90% and should be in excess of 90% whereas grades run between 15-20% copper and should be in excess of 28%. The poor metallurgical performance is attributed to the different mineralization. Instead of the major copper mineral being chalcopyrite ( $\text{CuFeS}_2$ ), it is a coating of covellite ( $\text{CuS}$ ), digenite ( $\text{Cu}_{1.8}\text{S}$ ) and chalcocite ( $\text{Cu}_2\text{S}$ ) on pyrite ( $\text{FeS}_2$ ). In order to recover these secondary copper minerals, the pyrite must be floated which, of course, dilutes the concentrate grade. Furthermore, because the copper minerals are present as coatings, comminution likely causes their fines and thus leads to a low recovery as well. On the other hand, the mineralogy is perfect for ferric leaching. In this regard, preliminary tests were run to help establish important variables for leaching: particle size of the ore, percent solids by weight, temperature of the system, and duration of the leach. Factorial design experiments were therefore conducted to develop a model that would lead to optimal leaching conditions. Unfortunately, results indicate that no more than approximately 60% extraction can be achieved. Diagnostic leach tests indicate that primary copper sulfide minerals must be present (i.e., chalcopyrite) in CZO because they are known not to leach well with ferric. An exhaustive literature search of the geology and mineralization concurs thereby concluding that ferric leaching is not a method to consider for copper extraction. However, as a result of this study, Montana Resources is exploring options for recovering the copper by leaching. It is recommended that they do so by processing the CZO through their current facilities and using an agitation leach on the resulting flotation concentrate to minimize the amount of material being contacted. This would also prevent problems from the clay content which is present in the CZO but is mostly removed from the flotation process.

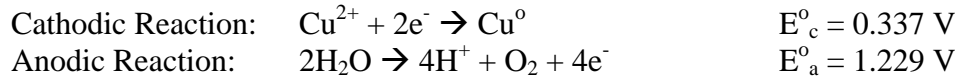
## **INTRODUCTION**

### Background

An integrated closed-circuit process for treating copper sulfide minerals based on acidic ferric leaching and the subsequent electrolytic recovery of copper was proposed as an alternative low cost method for copper production (Young et al., 2002; Fabian et al., 2001). The process was based on the simultaneous recovery of copper and regeneration

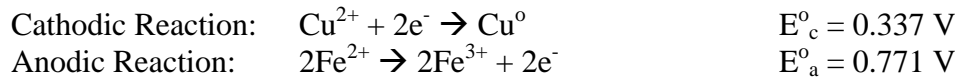
of ferric ions using a membrane-separated electrolytic cell divided into anolyte and catholyte compartments.

In conventional copper electrowinning, the cathodic reaction is the electrodeposition of copper on a stainless steel or copper starting sheet and the anodic reaction is the dissociation of water into hydrogen ions and oxygen resulting in the production of acid mist as described by the following electrochemical half-cell reactions:

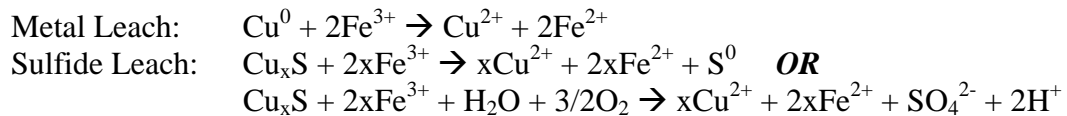


From the half-cell reactions (Bard et al., 1985), an overall theoretical cell voltage of 0.892V is calculated. However, this voltage is enough to barely get the reactions to occur and, as a result, applied voltages on an industrial scale are approximately 2 Volts. This is equivalent to an over-voltage of 1.1 Volts.

Alternatively, the electrochemical reactions occurring in the proposed electrolytic cell would result in the deposition of copper from cupric ions and the oxidation of ferrous ions to ferric ions:



In this case, the difference in voltage for the half-cell reactions yields a theoretical cell voltage of 0.434V. Because the over-voltage of 1.1 Volts is expected to be the same, an overall applied voltage of approximately 1.5 Volts is estimated for this system. Thus, the proposed cell would offer a net reduction from 2 Volts to 1.5 Volts and thereby reduce energy consumption by approximately 0.5 Volts and save as much as 25% on electrical costs. Resulting ferric ions ( $\text{Fe}^{3+}$ ) from the process would be recycled back to leaching:



where, for example,  $x=1$  (covellite),  $x=2$  (chalcocite) and  $x=1.8$  (digenite). The Mount Gordon process in Australia is based on this leaching technology and requires the solutions to be acidic ( $< \text{pH } 2$ ) to prevent iron precipitation (Baxter et al., 1999). Resulting cupric ions ( $\text{Cu}^{2+}$ ) and ferrous ions ( $\text{Fe}^{2+}$ ) can be electrowon directly (Marsden et al., 2005) but leads to poor quality of copper cathode or can be separated by conventional solvent extraction/electrowinning (SX/EW) technology (Twidwell et al., 1974) but can lead to high energy consumption as described earlier.

In this regard, a process was envisioned in which conventional SX is used to produce a pregnant solution of  $\text{Cu}^{2+}$  and a raffinate solution of  $\text{Fe}^{2+}$ . These solutions are fed into the proposed membrane-separated electrolytic cell as catholyte and anolyte respectively such that the simultaneous electrowinning of copper and regeneration of ferric ions can be

accomplished thereby reducing the energy consumption. Resulting copper is expected to be high-grade and resulting ferric ions would be recycled to leaching. Because oxygen evolution is eliminated, problems associated with acid-misting during electrowinning would also be prevented.

### Objective and Approach

Project objectives were four-fold and included (1) developing an electrolytic cell with two compartments separated by a membrane to allow for the simultaneous regeneration of ferric ions and electrowinning of copper, (2) optimizing the electrowinning process to minimize electrical consumption with maximum current density, (3) developing a ferric leaching process for implementation in an industrial setting, and (4) optimizing the leaching process for implementing, along with the electrowinning process, in an industrial setting. To do this, a systematic approach was taken for both the electrowinning and leaching studies.

For the electrowinning study, several cell designs were drafted and, if accepted for experimentation, were constructed and tested. All designs were based on conventional cell geometry but many were eliminated based on the difficulty of including the membrane in the construction. Three designs were eventually tested and, from these, one was selected based on performance as measured by maximum current density. Preliminary tests on this design were run in order to determine ranges for a number of variables including flowrate, concentration, temperature, membrane type, and applied voltage. With variable ranges established, factorial-design experiments were conducted and evaluated using statistical modeling with StatEase software (Anderson and Whitcomb, 2005). The resulting model was then optimized with constraints of minimum voltage and maximum current density. Mr. Francis Dakubo (2006) did this thesis work.

For the leaching study, an ore from a local company (Montana Resources) was determined to be appropriate for examination based on discussions with them (Czehura, 2004). Because mineralogical analyses showed that the ore contained significant amounts of clay, heap leaching methods were ignored and preliminary tests were conducted using two-liter kettles and mixers for agitation leaching. Solution and solid analyses for copper content were performed by the company using proprietary techniques. Results were used to determine % Cu extraction. Several variables were tested to establish their ranges as well: particle size, solids content, leach duration, and temperature. With variable ranges established, factorial design experiments were conducted and evaluated using StatEase software in hopes of developing a model for maximizing copper leaching. Mr. Thomas McIntyre (2006) did this thesis work.

## **PROJECT TASKS**

### Task 1 – Cell Design and Selection

Three electrolytic cells were constructed and tested. These designs included and named (1) Suspended Cathode Compartment (SCC), (2) Slotted Design (SD), and (3) Two-Half

Cell (THC) and are shown in Figures 1-3, respectively. Each design consisted of the following parts a membrane (M), Cathode(C), Cathode Compartment (CC), Anode (A), Anode Compartment (AC), Overflow Weir (OW), and Feed Port (FP) and are appropriately labeled. Obviously, the membrane (M) separates the cathode compartment (CC) from the anode compartment (AC). In order to provide continuous flow, feed ports (FP) were needed to distribute each electrolyte and overflow weirs (OW) were needed to collect each after they passed through. Typically, the cells were set-up so that the overflow recirculated back to the feed reservoir via peristaltic pumps.

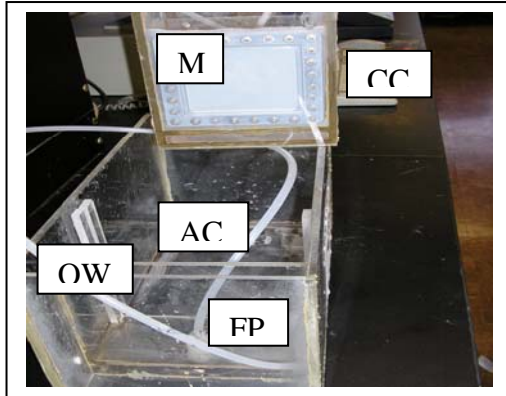


**Figure 1.** SCC electrolytic cell.

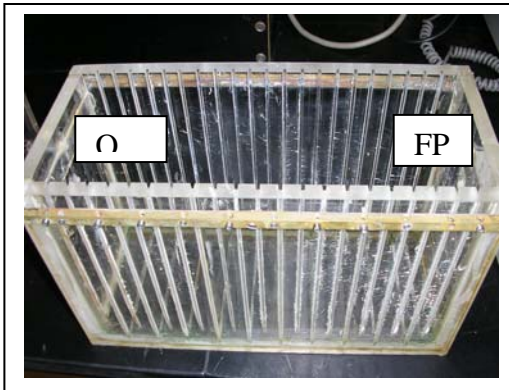


**Figure 2.** SD electrolytic cell.

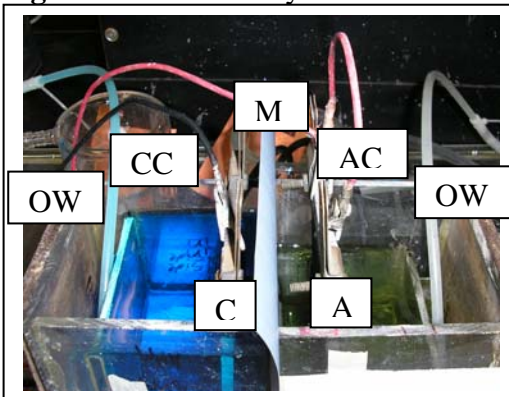


**Figure 3.** THC electrolytic cell.

Suspended Cathode Compartment (SCC). Figure 1 shows the SCC electrolytic cell. After the membrane is attached to the cathode compartment (CC), the compartment is lowered into the anode compartment but can be easily raised if the membrane ever needed to be replaced. Consequently, the design was also referred to as “cell-within-a-cell” design but proved to be too cumbersome to attach the membrane.

Slotted Design (SD). Figure 2 shows a photograph of the slotted electrolytic cell. The slots are equally spaced and are used to hold a membrane and any number of anodes and cathodes in alternate order which is in keeping with conventional cell designs. Electrolytes are introduced near the membrane and overflow a weir on the ends.

Two-Half Cell (THC). In this design, the anode and cathode compartments are mirror images of each other and are sandwiched together with the membrane in between and two gaskets on each side of the membrane (see Figure 3). Each half-cell is fed through the base via an up-flow distributor to help move the electrolytes through. The half-cells are pressed together with a vice which allowed for easy assembly (and disassembly) of the membrane. In this illustration, a microporous ceramic membrane used in car batteries is shown.

Each design was tested with fixed conditions: 30 g/L  $\text{Cu}^{2+}$ , 10 g/L  $\text{Fe}^{2+}$ , 150 g/L  $\text{H}_2\text{SO}_4$  for both solutions, 100 ml/min flowrate for both solutions, 304 Stainless Steel as cathode with 10-cm length and width dimensions yielding a surface area of 100  $\text{cm}^2$ , Pb plate as anode with the same dimensions placed approximately 8 cm from cathode, a microporous ceramic membrane equidistant from the anode and cathode, room temperature, and an applied voltage of 2 V. The THC design yielded the highest current density at 270  $\text{amps/m}^2$  compared to the SCC design at 220  $\text{amps/m}^2$  and the SD design at 100  $\text{amps/m}^2$ . In fact, each time other parameters were tested, the THC design was always found to be best and was attributed mostly to the improved flow through the compartments due to the up-flow distributor.

## Task 2 – Cell Optimization

In order to optimize the operating conditions of the THC design, preliminary experiments were conducted to help determine what materials would be best as an anode, cathode and membrane and what range of conditions would be useful for factorial design testing. Using conditions similar to those noted above, it was determined that (1) either Copper or 304 Stainless Steel could be used as the cathode, (2) Carbon-cloth performed better as an anode material than Graphite-rods, Pb-plate and Pb-wool, and (3) microporous ceramic worked well and appeared to last indefinitely as compared to both cation and anion exchange membranes which decomposed under the conditions examined.

Using Stainless-Steel cathodes, Carbon-cloth anodes and microporous ceramic membranes, single-variable tests were performed in which all variables were held constant except one. This helped to establish operating ranges for some variables and determine which did not have a significant effect on current density. Some results are shown in Figures 4-7. As can be seen from each figure, the current densities start at some maximum value and eventually decay to a much lower value which occurs when all of the ferrous has been converted to ferric. When this happens, oxygen evolution begins and the electro-winning reaction slows considerably.

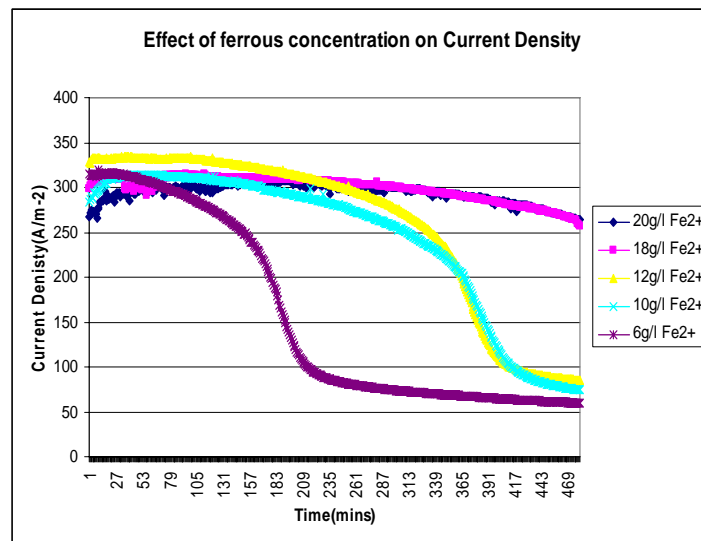


**Figure 4.** Effect of  $Fe^{2+}$  Concentration.

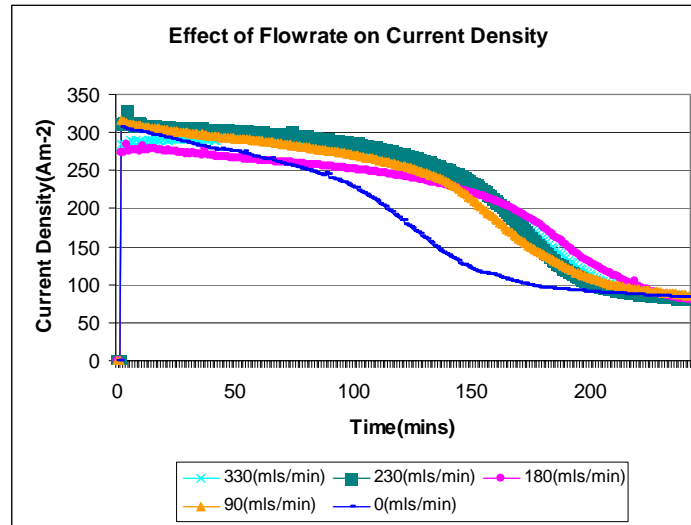


**Figure 5.** Effect of Flowrate

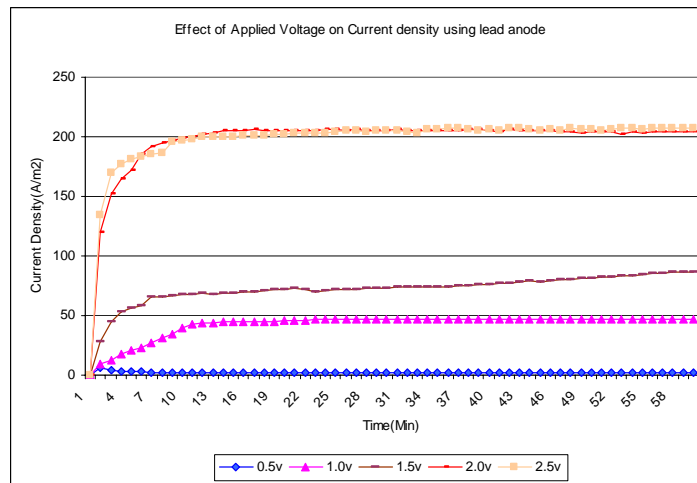


**Figure 6.** Effect of Applied Voltage

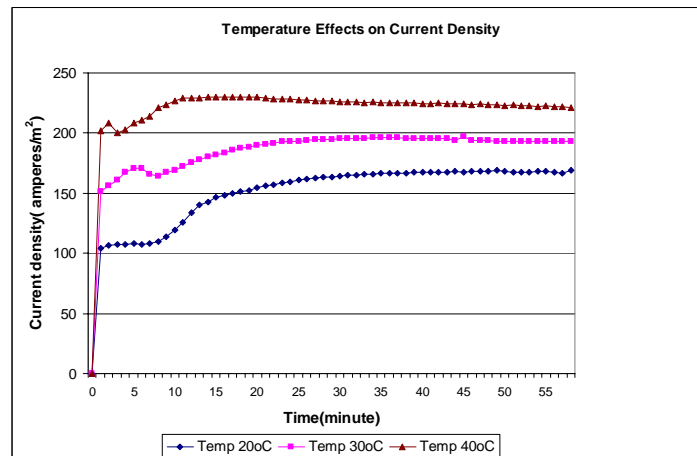


### Figure 7. Effect of Temperature

Because the solutions are being recirculated, higher ferrous concentrations simply allow the current density to be maintained longer as shown in Figure 4. In a real situation, this will depend on the residence time of the solution in the cell before it overflows and gets recycled to the leaching circuit. The same thing is observed in Figure 5 when flowrates are increased but is only apparent above stagnant. In this case, flow is needed to not only supply ferrous and cupric ions to their respective electrodes but also to remove ferric once it is produced. The slow step in these processes is envisioned to be supply ferrous to the anode because both are of the same charge. This explains why the high surface area electrodes were being considered and eventually the Carbon-cloth was selected. In regards to applied voltage, it is clear from Figure 6 that a voltage between 1.5-2 Volts is needed which is in agreement with expectations. Because an applied voltage of 2.5 Volts did not improve the results, it is evident that the system reached limiting current density. Furthermore, an examination of the copper cathode being produced showed that undesirable dendrites were beginning to form and would account for the low current efficiency of 90% as well as the noisy appearance of the plot. On the other hand, when voltages below 1.5 Volts were applied, current densities were too low to produce copper at an appreciable rate but yielded current efficiencies of 99.5%. In comparison, the current efficiency at 2 Volts was 98%. Finally, Figure 7 shows that current densities can be moderately increased by increasing temperatures from room temperature of 20 to 30 and 40°C.

Based on these results, factorial-design experiments were conducted with the THC design using Stainless-Steel cathodes, Carbon-cloth anodes and microporous ceramic membranes as well as fixed conditions for temperature (ambient temperature near room temperature of 20°C) and acidity (100 g/L H<sub>2</sub>SO<sub>4</sub>). It is worth noting that the acidity was never tested because it was decided to insure that iron precipitation as ferrihydrite would be avoided; furthermore, it was understood from the literature that such concentrations were common in leaching and SX circuits. Consequently, four variables were examined: cupric ion concentration from 10-50 g/L, ferric ion concentration from 10-50 g/L, applied voltage from 0.8-2.5 Volts, and solution flowrates from 0-540 mL/min.

In order to obtain the best results from a statistical study, a full factorial-design was completed in which mid-point values were also tested along with the end-points of the variable ranges. Because four variables were being tested (i.e, n=4), the study required 2<sup>n</sup> or 16 experiments be conducted along with 5 duplicate mid-point experiments for a total of 21. The conditions for each experiment are shown in the Appendix in Table A1 along with the results as measured by current density for each test (see Table A2). The ANOVA Table is shown in Table A3 and indicates that the four variables are significant because the values for “Prob>F” are less than 0.05 which is equivalent to being greater than 95% confidence thereby indicating there is excellent agreement between “R<sup>2</sup>” and the “Adjusted R<sup>2</sup>” values. In this case, the significant variables are cupric ion concentration, applied voltage, and flowrate along with a binary involving both applied voltage and flowrate. Although the ANOVA Table shows that the ferrous concentration is not significant, it was decided that it should still be considered due to the fact that current densities drop substantially at long duration times. In this regard, it is important

to note that the responses in Table A2 were determined after 30 minutes. In this regard, the following model was determined:

$$\text{Log}_{10}(\text{Current Density}) = 0.97876 + 3.56 \cdot 10^{-3} \cdot [\text{Cu}^{2+}] - 3.95 \cdot 10^{-4} \cdot [\text{Fe}^{2+}] + 0.51 \cdot \text{Volts} + 8.13 \cdot \text{Flowrate} - 3.1 \cdot 10^{-4} \cdot \text{Volt} \cdot \text{Flowrate}$$

This model predicts that the current density and therefore copper production will be increased by increasing the cupric concentration (g/L), applied voltage (V), and/or flowrate (ml/min). However, there is a small but noticeable binary effect between flowrate and applied voltage that has a negative effect on the system. Furthermore, a negative effect on current density is also realized by increasing the ferrous concentration. Applied voltage and flowrate are the most significant variables due to the large values of their respective coefficients.

Because the ANOVA Table also shows that the “model F-value” is of 37.06, it implies the model is also significant and suggests that there is only 0.01% chance that results are due to noise. This is illustrated in Figure 8 which shows a scatter plot between actual and predicted values has good linear agreement and additionally illustrates why the “Predicted R<sup>2</sup>” value of 0.84 is in reasonable agreement with the “Adjusted R<sup>2</sup>” value of 0.90. Likewise, the “Curvature F-value” of 24.71 implies there is significant curvature (as measured by difference between the average of the center points and the average of the factorial points) in the model and that there is only a 0.02% chance that results are due to noise. Similarly, because the “Adequate Precision” of 16.02 is greater than 4, the signal-to-noise ratio is adequate. Clearly, confidence in the results and significance of the the model are high. In this regard, the model can be used to adequately predict results and therefore can be used “to navigate the design space.” Doing so suggests that optimum conditions can be obtained with an applied voltage near 1.60 Volts and electrolyte concentrations of 30 g/L.

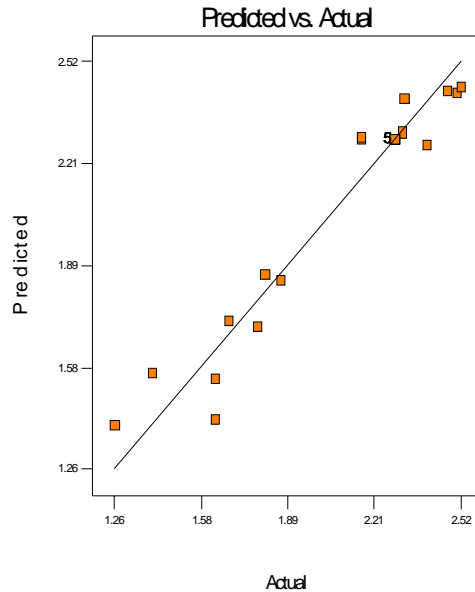


**Figure 8.** Scatter plot of predicted and actual electrowinning data.

Finally, a critical analysis of the model shows that the results are also in agreement with phenomenological equations involving electrochemical and transport fundamentals (Maron and Prutton, 1974; Bard and Faulkner, 1980). For example, when two plates in an electrolytic cell are separated by a distance  $d$ , the current carried by the ions between the plates is represented by the equation,  $I = \frac{nvze}{d}$ , where  $n$  represents the concentration of ions,  $v$  is the velocity of the ions,  $z$  the valence of each ion and  $e$  represent the charge on an electron which clearly shows that current, and thus current density, are influenced by concentration and flowrate. Likewise, according to the Butler-Volmer and Fick Equations, current is related to both the voltage and temperature. Similarly, the Tafel equation and resulting Tafel plots illustrate that increasing cupric concentrations and mass flowrates will increase the limiting current density and simultaneously reduce the voltage that needs to be applied; however, they also illustrate that increasing ferrous concentrations will have the reverse effect. These items are illustrated by both the positive and negative influences predicted by the model.

### Task 3 – Ferric Leaching Application

Montana Resources (MR), a copper mine and mill located in Butte, was contacted in 2004 to see if they had an interest in collaborating on this portion of the project. Ensuing discussions indicated they had a genuine interest in developing a leaching technology for their Central Zone Orebody (CZO) which contained mostly secondary copper sulfides (Czehura, 2004) such as covellite ( $\text{CuS}$ ), digenite ( $\text{Cu}_{1.8}\text{S}$ ) and chalcocite ( $\text{Cu}_2\text{S}$ ) and consequently should therefore be amenable to ferric leaching (Baxter et al., 1999). Furthermore, when MR processes CZO through their mill, recoveries run between 85-90% and grades run between 15-20% copper. This low metallurgical performance is attributed to secondary copper minerals being present as coatings on pyrite ( $\text{FeS}_2$ ) which, when ground, can produce copper fines that are difficult to recover; however, even when liberated, the pyrite ends up being recovered anyways which dilutes the concentrate. Poor recoveries and grades result. MR agrees that the only way that the CZO will be mined and processed is if a leaching technology can be employed on either the ore or a concentrate produced from the ore (Czehura, 2004). Furthermore, MR acknowledges that they would benefit greatly if they were to produce their own copper as opposed to selling their concentrate overseas to custom smelters. Currently, by comparison, MR processes their East and West Zone Ores and produces a chalcopyrite ( $\text{CuFeS}_2$ ) concentrate with greater than 90% recovery and grades in excess of 28% copper. By processing their CZO, their mine life would be extended by at least 25 years.

To begin this portion of the study, MR delivered four ore samples in 55-gallon drums to Montana Tech. The samples were crushed and homogenized. Sample splits were then taken analyzed. Assays were determined to be 0.18, 0.30, 1.0 and 1.5% Cu. The samples showed that the clay content was montmorillonite ( $\text{H}_2\text{Al}_2\text{Si}_4\text{O}_{12} \cdot n\text{H}_2\text{O}$ ) and was noted to generally increase with increasing copper concentration. Scoping tests were performed on each of samples to determine how effective ferric leaching was and thereby help identify conditions that would help optimize leaching performance. Variables included particle size, solids content, ferric ion concentration, sulfuric acid concentration, leach duration, and temperature. Because sulfuric acid concentrations between 50 and 150 g/L

did not effect the results, ensuing factorial-design experiments were fixed at the lower concentration of 50 g/L. On the other hand, because tests showed that increasing the ferric concentration from 5 to 30 g/L also had relatively no effect on leaching, the high iron concentration of 30g/L was selected to follow the optimal results obtained by Dakubo (2006). As expected, smaller particles sizes improved leaching as did lower percent solids and, in general, increased leaching times. However, surprisingly, increasing temperature was often found to be decrease leaching performance. Depending on the ore, extraction efficiencies from these preliminary scoping tests ranged from 25-65%.

These results suggested that optimal conditions in excess of 90% might be determined via factorial design experiments. For these studies, as just noted, the acid concentration was fixed at 50 g/L and the ferric concentration was fixed at 30 g/L. Particle sizes were varied from 38 to 74 microns (with a midpoint of 56 microns), solids content from 10 to 30% solids by weight (with a midpoint of 20%), leaching time from 1 to 4 hours (with a midpoint of 2.5 hours), and temperature from 25 to 90<sup>0</sup>C (with a midpoint of 60<sup>0</sup>C). In this case, only a half-factorial design study was desired; thus, only 8 experiments were needed along with 2 midpoint experiments for a total of 10. Table A4 in the Appendix shows the experimental matrix. Results are presented in Figure 9 as well as Table A5 and include numbers not only for overall extraction but also for extraction of acid-soluble (AS) copper based on head and tail assays. AS-copper refers to the carbonates of malachite (CuCO<sub>3</sub>Cu(OH)<sub>2</sub>) and azurite (2CuCO<sub>3</sub>Cu(OH)<sub>2</sub>); oxides of cuprite (Cu<sub>2</sub>O) and tenorite (CuO); and silicates of chrysocolla (CuSiO<sub>3</sub>\*2H<sub>2</sub>O). Non-AS soluble minerals would include the secondary sulfides such as covellite (CuS), digenite (Cu<sub>1.8</sub>S) and chalcocite (Cu<sub>2</sub>S) as well as the primary sulfides such as chalcopyrite (CuFeS<sub>2</sub>) and bornite (Cu<sub>5</sub>FeS<sub>4</sub>).

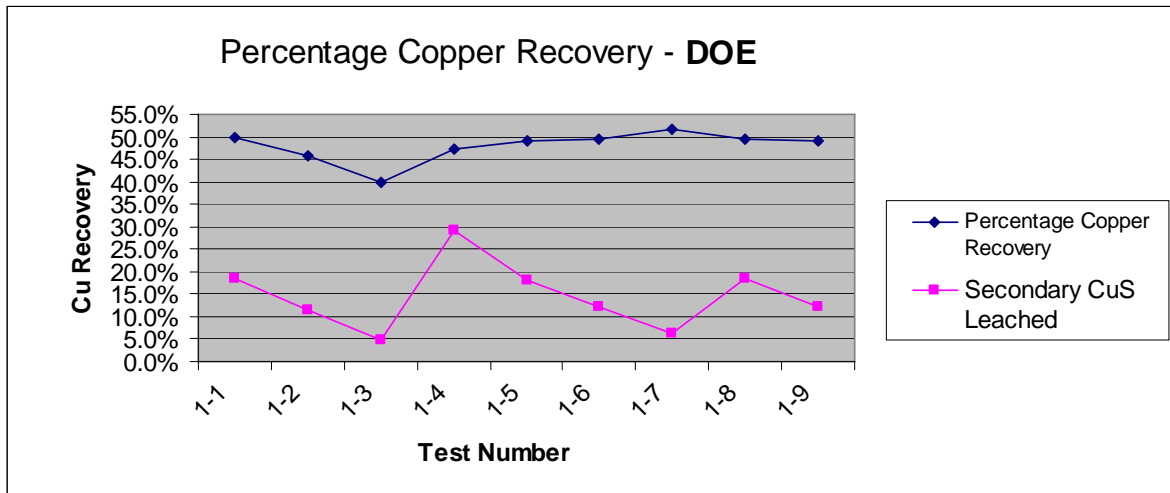


**Figure 9.** Total and secondary copper recovery as a function of test number.

As can be seen from the table and figure, the total copper recovery was near 50%. The majority of the copper recovered was from AS-content of the ore with practically 85% (average of all tests) coming from that fraction. The copper that was leached from secondary copper sulfides is estimated to be only about 15% of the total copper. Clearly, ferric leaching is not performing as expected even though the results of the statistical analysis from StatEase were termed significant such that there was excellent correlation between the adjusted  $R^2$  value and the predicted  $R^2$  value. In this regard, the ANOVA Table for the model is shown in Table A6. The correlation is graphically shown in Figure 10 and indicates that only one data point fell any significant distance from the predicted line. Nevertheless, the “predicted R-squared” value of 0.9585 is in excellent agreement with the “adjusted R-squared” value of 0.9658. Furthermore, because the “adequate precision” of 17.439 is greater than 4, the signal to noise ratio is good. In addition, the “F-values” are all much less than 0.1 which suggests that the coefficients determined for the model are significant. Consequently, the resulting model is acceptable.

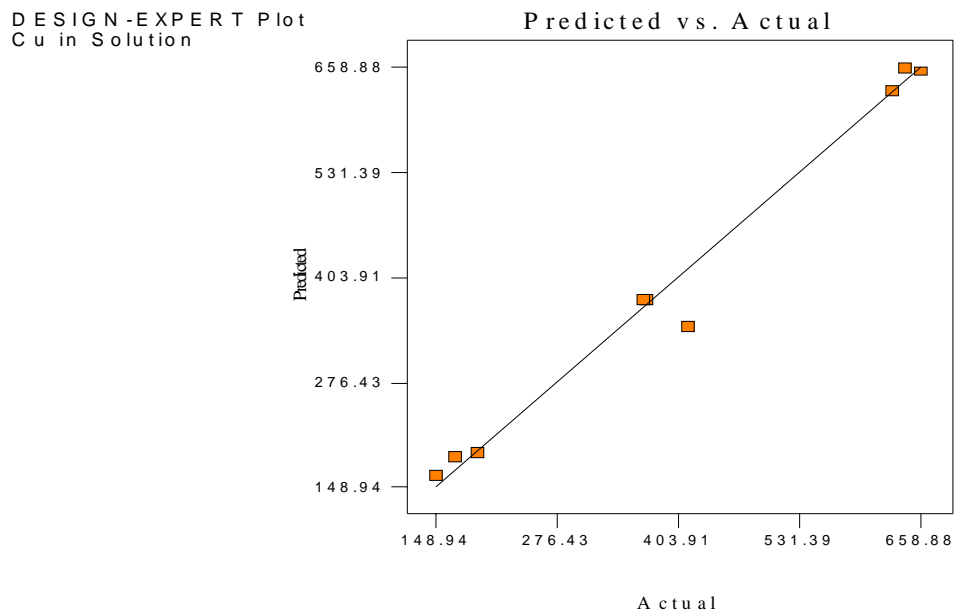


**Figure 10.** Scatter plot of predicted and actual leaching data.

Unfortunately, the model is not hierarchical and its equation cannot be shown but it still can be used to confidently navigate the design space. Examples are presented in Figures 11 and 12. The 3-dimensional plot in Figure 11 clearly shows that, at a fixed % solids of 30% and temperature of 25<sup>0</sup>C, large particles and short durations do not leach significant amounts of copper but, as the particles become smaller, duration becomes less significant and more copper is leached. Similarly, Figure 12 shows that increasing the % solids increases the amount of copper leached at a fixed temperature of 25<sup>0</sup>C and a long duration time of 4 hours but is relatively independent of particle size. Similar conclusions would be reached for other plots but, as already stated, can show that temperature has a negative impact on the system at 4 hours but not at 1 hour. This

phenomenon can be attributed to the preg-robbing behavior of the clay and therefore its ability to adsorb copper as it is being leached.

DESIGN-EXPERT Plot

Cu in Solution  
 X = A: Size  
 Y = C: Time

Actual Factors  
 B: Solids = 30.00  
 D: Temperature = 25.00

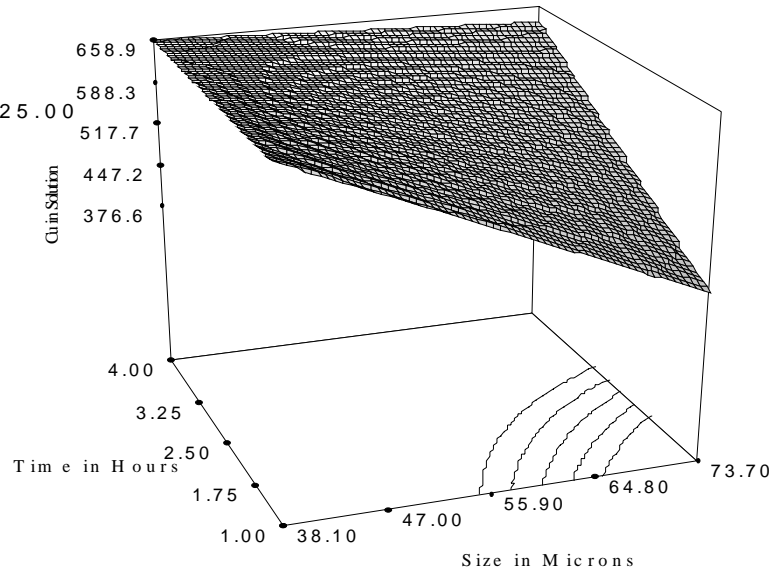


**Figure 11.** Concentration of Copper in Solution as a function of time and size at a fixed % solids of 30% and temperature of 25<sup>0</sup>C.

DESIGN-EXPERT Plot

Cu in Solution  
 ● Design Points

X = A: Size  
 Y = B: Solids

Actual Factors  
 C: Time = 4.00  
 D: Temperature = 25.00

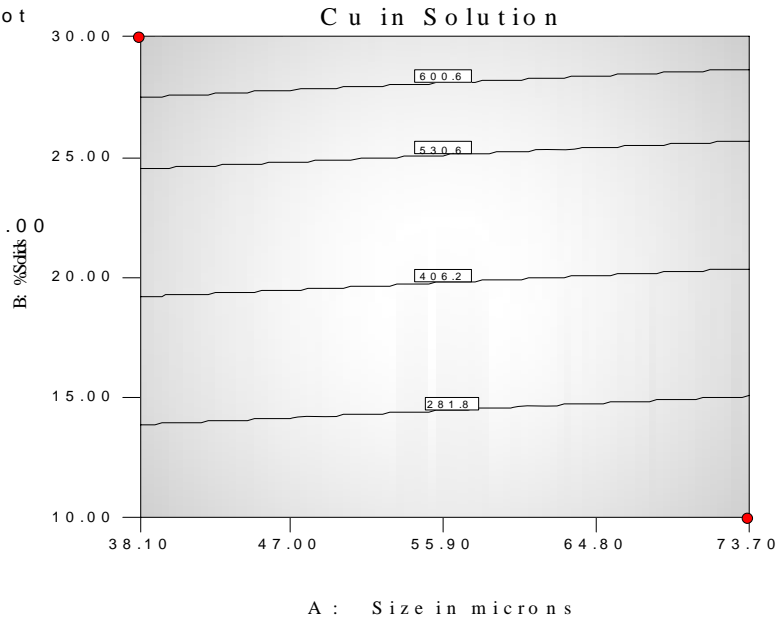


**Figure 12.** Concentration of copper in solution as a function of % solids and size at fixed temperature of 25<sup>0</sup>C and a long duration time of 4 hours.

#### Task 4 – Ferric Leaching Optimization

Because the ore samples gave similar scoping results, half-factorial design experiments were not conducted for the other ore samples. Furthermore, because only 15% of the secondary copper sulfide minerals were extracted, there also was no need to optimize the results. In this regard, Task 4 was not implemented due to the failure of Task 3 to yield total extraction efficiencies greater than 90% let alone for secondary minerals; however, Task 5 was created in order to explain the results.

#### Task 5 – Diagnostic Leach

In diagnostic leaching, samples are treated with increasing strengths of acid as well as oxidants to “quantitatively” determine the mineralogy that is present (Anderson, 1990). The 5-stage process determines the presence of (1) copper carbonate by an acetic acid leach, (2) copper oxides and silicates by a sulfuric acid/ sodium sulfite leach, (3) secondary copper sulfides by cyanide leach, (4) native copper by silver nitrate titration, and (5) primary copper sulfide by difference from total copper. Following each stage, the resulting solution is analyzed by AA or ICP and mass balances are conducted to determine the amount of each miner type present. Results are presented in Figure 13 with sample 1 being the high grade ore (1.5% Cu) and decreasing to sample 4 which is the low grade ore (0.2% Cu). As can be seen, AS-copper minerals account for 40-50% of the copper but is dependent on the sample. Likewise, the amount of secondary copper sulfides is has about the same range and are also sample-dependent. Nevertheless, the samples should have leached well with the exception of the two samples that unexpectedly showed significant significant amounts of primary copper minerals ranging between 5-15%. Even in the case of sample 1, an 85% copper extraction should have been observed. It is critical to note that these numbers are similar to those determined microscopically by Guilbert and Zeihen (1964).

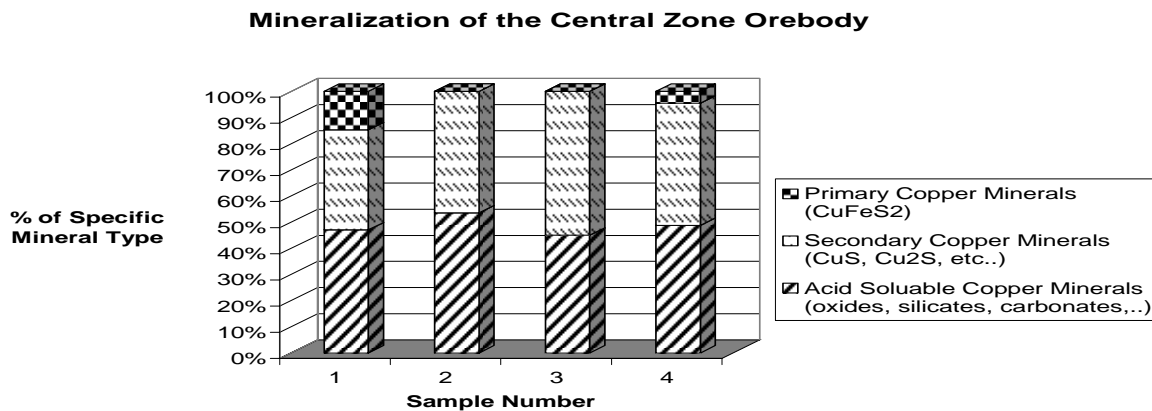


**Figure 13.** Mineralization of the CZO as determined by diagnostic leaching.

It is therefore summarized that the ore samples were difficult to leach due to the presence of significant amounts of pyrite. As leaching occurs, the ferric concentration decreases and, of course, ferrous concentration increases. When this happens appreciably in the presence of significant amounts of pyrite ( $\text{FeS}_2$ ), the solution potential can move from control by the  $\text{Fe}^{3+}/\text{Fe}^{2+}$  redox couple at 0.77 Volts to control by the  $\text{Fe}_2\text{O}_3/\text{FeS}_2$  redox couple near 0.35 Volts. These potentials are plotted on the  $E_{\text{H}}$ -pH diagram in Figure 14 and clearly indicate that, if control shifts to the lower potential, copper dissolution will be prevented. Furthermore, dissolved  $\text{Cu}^{2+}$  may precipitate out on the pyrite reminiscent of an activation process. This phenomenon is likely how the covellite/chalcocite coating formed geologically on the pyrite in the CZO and would also explain the decrease in copper concentration at longer leaching times.

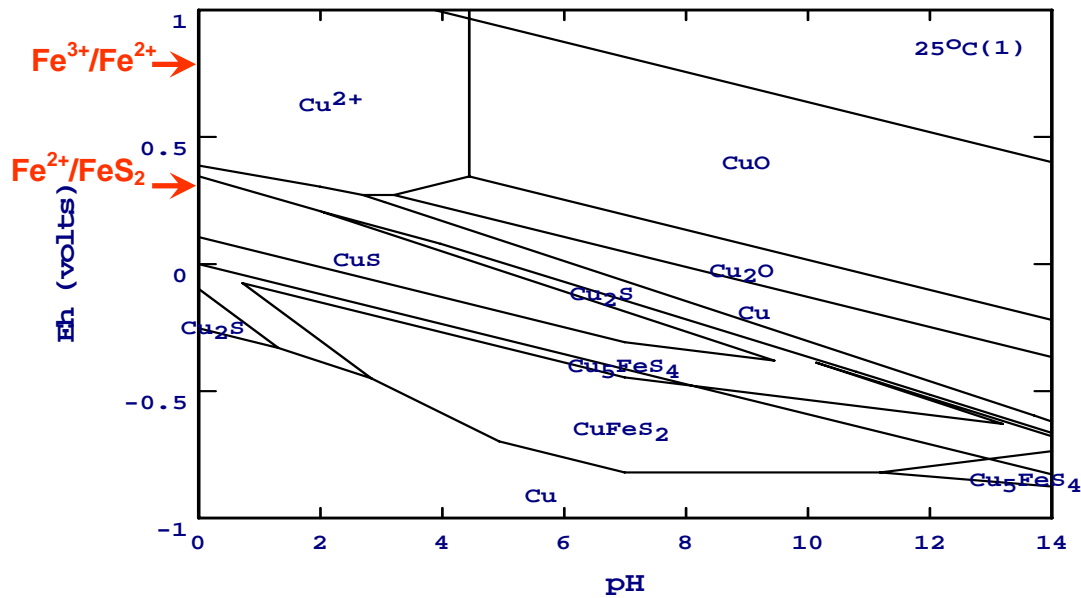


**Figure 14.**  $E_{\text{H}}$ -pH Diagram for Cu-species in Cu-Fe-S- $\text{H}_2\text{O}$  system with consideration of sulfur oxidation to sulfate ( $\text{SO}_4^{2-}$ ).

## SUMMARY

Various tests were conducted over a three-year period to investigate the feasibility of electrowinning copper ( $\text{Cu}^0$ ) from cupric ( $\text{Cu}^{2+}$ ) while simultaneously oxidizing ferrous ( $\text{Fe}^{2+}$ ) to ferric ( $\text{Fe}^{3+}$ ) using a membrane cell. Results indicated that several variables were important to consider to minimize the applied voltage while keeping current density at a maximum. These variables included electrolyte concentrations ( $\text{Cu}^{2+}$  and  $\text{Fe}^{2+}$ ), agitation/flow-rate, applied voltage, and temperature. Other variables were also tested: cathode type, anode type, membrane type, and cell design; however, certain ones showed superior behavior and included carbon-cloth as the anode, microporous ceramic (used in car batteries) as the membrane, and the THC-design as the electrowinning cell. Although 304 Stainless Steel was selected for the cathode, copper starter sheet performed equally as well and could have been selected. Ensuing factorial-design experiments were therefore conducted with these 4 variables fixed in order to investigate the effects of the

other variables. For simplicity and to minimize the number of experiments, the temperature was held constant at 20<sup>0</sup>C (room temperature). Concentrations of Cu<sup>2+</sup> and Fe<sup>2+</sup> were varied between 10 and 50 g/L, flowrates were varied between 0 and 540 mL/min, and the applied voltage was varied between 0.8-2.5 Volts. Results were then statistically analyzed using StatEase software and yielded the following model:

$$\text{Log}_{10} (\text{Current Density}) = 0.97876 + 3.56 \cdot 10^{-3} \cdot [\text{Cu}^{2+}] - 3.95 \cdot 10^{-4} \cdot [\text{Fe}^{2+}] + 0.51 \cdot \text{Volts} \\ + 8.13 \cdot \text{Flowrate} - 3.1 \cdot 10^{-4} \cdot \text{Volt} \cdot \text{Flowrate}$$

From the model, it was concluded that the current density and therefore copper production would be increased by increasing the cupric concentration, applied voltage, and/or flowrate; however, a small binary effect between flowrate and applied voltage was observed that had a negative effect on the system. Furthermore, a negative effect on current density was also realized by increasing the ferrous concentration. Applied voltage and flowrate are the most significant variables due to the large values of their respective coefficients. Optimization of the model indicates that the voltage can be decreased from an industrial standard of approximately 2.0 Volts to between 1.5-1.7 Volts which equates to energy savings of 15-25%. Furthermore, the model concurs with fundamental understanding of electrowinning principles including equations for solution capacitance, Butler-Volmer, Fick's and Tafel.

Various tests were also conducted in collaboration with Montana Resources, a local Montana mining company in Butte, to see if ferric leaching could be used on their Central Zone Ore (CZO) and implemented along with the membrane electrowinning technology. It was noted that CZO does not respond as well as to their flotation operations as the traditional East and West Zone Ores do. Recoveries run low between 85-90% but should be in excess of 90% whereas grades run between 15-20% copper but should be in excess of 28%. This poor metallurgical performance is attributed to the different mineralization. Instead of the major copper mineral being chalcopyrite (CuFeS<sub>2</sub>), it is a coating of covellite (CuS), digenite (Cu<sub>1.8</sub>S) and chalcocite (Cu<sub>2</sub>S) on pyrite (FeS<sub>2</sub>). In order to recover these secondary copper minerals, the pyrite must be floated which, of course, dilutes the concentrate grade. Furthermore, because the copper minerals are present as coatings, comminution likely causes their fines and thus leads to a low recovery as well.

On the other hand, the mineralogy is perfect for ferric leaching. In this regard, preliminary test helped establish important variables for leaching and included particle size of the ore, percent solids by weight, temperature of the system, and duration of the leach. Factorial design experiments were therefore conducted to develop a model that would lead to optimal leaching conditions. Unfortunately, results indicated that no more than approximately 60% extraction could be achieved. Diagnostic leach tests indicated that primary copper sulfide minerals must be present (i.e., chalcopyrite) in CZO because they do not leach well with ferric. A literature search of the geology and mineralization concurred and thereby concluded that ferric leaching is not a method to consider for copper extraction. However, as a result of this study, Montana Resources is exploring options for recovering the copper by leaching. It is recommended that they do so by processing the CZO through their current facilities and using an agitation leach on the

resulting flotation concentrate to minimize the amount of material being contacted. This would also prevent problems from the clay content which is present in the CZO but would be mostly removed by the flotation process.

## **FUTURE WORK**

This is the final report for this project. It is likely that MR and the PI's will team up again to write a follow-up proposal in the next CAST cycle pending everyone's availability. In this regard, future work is planned. Overall, the project met with many successes as noted by the Publications and Presentations list in the second to next section. It is particularly worthy to note that the project supported 3 graduate students instead of the 1 that was originally proposed. Mr. Dave Douglas graduated in May of 2005 but, due to unfortunate circumstances, had to go non-thesis. This, together with the unfortunate loss of Eric Dahlgren as the postdoc, forced the project to be extended. Mr. Francis Dakubo graduated in May of 2006 with a thesis on the electrowinning work. Mr. Thom McIntyre also graduated in May of 2006 with a thesis on the ferric leaching work. Both were more than happy to be engaged in a fully funded project thanks to CAST.

## **REFERENCES**

1. Young, C.A., Huang, H.H. and Fabian, C., "Simultaneous Electrolysis of Copper and Ferrous Ions to Produce Copper Cathode and Regenerate Ferric Sulfate," CAST Proposal, Montana Tech, Butte, MT (2002).
2. Fabian, C., Huang, H.H. and Young, C.A., "Copper Sulfide Hydrometallurgy: Plant Practice and Future Improvements," Preprint No. 02-202, SME, Littleton, CO (2001).
3. Bard, A.J., Parsons, R. and Jordan, J., Standard Potentials in Aqueous Solutions, Marcel Dekker, Inc., New York, NY (1985).
4. Baxter, K., Kaiser, C. and Richmond, G. "Design of Mt. Gordon Chalcocite Project," in: Proceedings of Alta Copper 1999 Sulfide Symposium, Sept. 5-10, pp. 1-21 (1999).
5. Marsden et al., "System for Direct Electrowinning of Copper," U.S. Patent No. 6,972,107 (2005).
6. Twidwell, L.G., Huang, H.H. and Miller, J.D., "Unit Operations in Extractive Metallurgy: Hydrometallurgy," Montana Tech, Butte, MT (1974).
7. Anderson, M.J. and Whitcomb, P.J., StateEase, V. 5.0, Minneapolis, MN (2004).
8. Dakubo, F. "Simultaneous Electrowinning of Copper and Oxidation of Ferrous to Ferric Using Membrane Technology", MS Thesis, Montana Tech, Butte, MT (2006).
9. Czehura, S., Personal Communications, Montana Resources, Butte, MT (2004).
10. McIntyre, T.F., "Ferric Leaching of Low Grade Secondary Copper Minerals", MS Thesis, Montana Tech, Butte, MT (2006).
11. Maron, S., Lando, J.B. and Prutton, C.F., Fundamentals of Physical Chemistry, Macmillan Publishing, New York, NY (1974).
12. Bard, A.J. and Faulkner, L.R., Electrochemical Methods, John Wiley & Sons, Inc., New York NY (1980).
13. Anderson C. G., "The Application of Diagnostic Leaching to Copper and Gold Ores," CAMP, Montana Tech, Butte, MT (1990).
14. Guilbert J.M. and Zeihen L.G., "The mineralogy of the Butte District – Montana,"

presented at NWMA, Spokane, WA (1964).

**PUBLICATIONS/PRESENTATIONS**

1. Young, C.A. et al., “Simultaneous Electrolysis of Copper and Ferrous Ions,” Poster Presentation, CAST 2003 Annual Workshop, Charleston, WV, Nov. 19-21 (2003).
2. Young, C.A., McIntyre, T.F., and Dakubo, F. “Application of Statistical Software for Hydrometallurgical Processing, Part I: Ferric Leaching,” Poster Presentation, CAST 2005 Annual Workshop, Blacksburg, VA, July 28-30 (2005)
3. Young, C.A., McIntyre, T.F., and Dakubo, F. “Application of Statistical Software for Hydrometallurgical Processing, Part II: Electrowinning,” CAST 2005 Annual Workshop, Blacksburg, VA, July 28-30 (2005)
4. Dakubo, F. “Simultaneous Electrowinning of Copper and Oxidation of Ferrous to Ferric Using Membrane Technology”, MS Thesis, Montana Tech, Butte, MT (2006).
5. McIntyre, T.F., “Ferric Leaching of Low Grade Secondary Copper Minerals”, MS Thesis, Montana Tech, Butte, MT (2006).
6. Dakubo, F. Huang, H.H., Fabian, C. and Young, C.A., “Optimization of a Membranic Copper-Electrowinning Technique,” accepted for presentation at SME Annual Meeting, Denver, CO (2007).

**APPENDICES (IF ABSOLUTELY NECESSARY)**

**Table A1.** Conditions for Full-Factorial Design Electrowinning Study.

Std	Run	A: [Cu <sup>2+</sup> ], g/L	B: [Fe <sup>2+</sup> ], g/L	C: Voltage, V	D: Flowrate, mL/min
10	1	50	10	0.8	540
6	2	50	10	2.5	0
17	3	30	30	1.65	270
12	4	50	50	0.8	540
19	5	30	30	1.65	270
9	6	10	10	0.8	540
14	7	50	10	2.5	540
11	8	10	50	0.8	540
7	9	10	50	2.5	0
5	10	10	10	2.5	0
15	11	10	50	2.5	540
2	12	50	10	0.8	0
20	13	30	30	1.65	270
3	14	10	50	0.8	0
8	15	50	50	2.5	0
4	16	50	50	0.8	0
18	17	30	30	1.65	270
21	18	30	30	1.65	270
16	19	50	50	2.5	540
13	20	10	10	2.5	540
1	21	10	10	0.8	0

**Table A2.** Response Table for Electrowinning Study.

Std	Run	Current, Amps	Current Density, Amps/m <sup>2</sup>
10	1	0.604	64.7
6	2	2.279	322.6
17	3	1.846	191.5
12	4	0.709	73.6
19	5	1.846	191.5
9	6	0.473	48
14	7	2.641	332.5
11	8	0.563	61
7	9	2.425	250.5
5	10	1.368	144.6
15	11	1.368	144.6
2	12	0.252	25.2
20	13	1.846	191.5
3	14	0.203	18.4
8	15	2.72	207.6
4	16	0.457	42.7
18	17	1.846	191.5
21	18	1.846	191.5
16	19	2.981	296.5
13	20	2.109	204.5
1	21	0.408	42.4

**Table A3.** ANOVA Table for Electrowinning Study.

Source	Sum of Squares	DF	Mean Squares	F Value	Prob>F	
Model	2.36	5	0.47	37.06	<0.0001	Significant
A	0.081	1	0.081	6.39	0.0241	
B	1.001x10 <sup>-0.003</sup>	1	1.001x10 <sup>-0.003</sup>	0.079	0.7832	
C	2.09	1	2.09	164.13	<0.0001	
D	0.11	1	0.11	8.30	0.0121	
CD	0.081	1	0.081	6.39	0.241	
Curvature	0.31	1	0.31	24.71	0.0002	Significant
Residual	0.18	14	0.013			
Lack of fit	0.18	10	0.018			
Pure Error	0.000	4	0.000			
Cor Total	2.85	20				

Std Dev.	0.11		R-squared	0.9298		
Mean	2.06		Adj.R-squared	0.9047		
C.v.	5.47		Pred.R-squared	0.8400		
PRESS	0.46		Adeq. Precision	16.022		

**Table A4. Conditions for Half-Factorial Design Leaching Study.**

RUN	A: Size, Microns	B: % Solids by Weight	C: Duration, Hours	D: Temperature, °C
1	73.7	30	4	25
2	73.7	10	1	25
3	38.1	30	1	25
4	38.1	30	4	90
5	55.9	20	2.5	60
6	38.1	10	4	25
7	38.1	10	1	90
8	73.7	10	4	90
9	73.7	30	1	90
10	55.9	20	2.5	60

**Table A5. Response Table for Leaching Study.**

Summary Table of Results									
DOE									
% Cu <sub>total</sub> Recovery = [(Wt. Cu <sub>heads</sub> - Wt. Cu <sub>tails</sub> ) / Wt. Cu <sub>heads</sub> ] * 100									
Test No.	Wt. Cu <sub>heads</sub>	Wt Cu <sub>tails</sub>	Total Wt % Cu Recovery	Wt of Copper Recovered	%AS Cu Recovered	Wt of AS Cu Recovered	Wt of Sulfide Cu Recovered	Wt of available Sulfide Cu	WT % Sulfide Cu Leached
1-1	1.465	0.736	49.8%	0.730	80.0%	0.584	0.146	0.794	18.4%
1-2	0.374	0.202	45.9%	0.172	86.7%	0.149	0.023	0.203	11.3%
1-3	1.443	0.868	39.8%	0.575	93.3%	0.537	0.038	0.782	4.9%
1-4	1.424	0.749	47.4%	0.674	66.7%	0.450	0.225	0.772	29.1%
1-5	0.844	0.429	49.2%	0.415	80.0%	0.332	0.083	0.458	18.1%
1-6	0.378	0.191	49.4%	0.187	86.7%	0.162	0.025	0.205	12.2%
1-7	0.374	0.182	51.5%	0.193	93.3%	0.180	0.013	0.203	6.3%
1-8	1.454	0.733	49.6%	0.721	80.0%	0.577	0.144	0.788	18.3%
1-9	1.443	0.735	49.0%	0.708	86.7%	0.613	0.094	0.782	12.1%
1-10	0.803	#VALUE!	#VALUE!	#VALUE!	80.0%	#VALUE!	#VALUE!	0.435	#VALUE!

**Table A6.** ANOVA Table for Leaching Study.

<b>SOURCE</b>	<b>SUM OF SQUARES</b>	<b>DEGREES FREEDOM</b>	<b>SQUARE</b>	<b>MEAN VALUE</b>	<b>F PROBABILITY &gt;F</b>
<b>Model</b>	3.346E+5	4	83641.53	57.56	<b>0.0009</b>
<b>B</b>	3.315E+5	1	3.315E+5	228.14	0.0001
<b>AC</b>	29037.8	1	29037.8	19.98	0.0111
<b>AD</b>	43230.02	1	43230.02	29.75	0.0055
<b>CD</b>	30895.18	1	30895.18	21.26	0.0099
<b>Residual</b>	5812.33	4	1453.08		
Std. Dev.	38.12	<b>R<sup>2</sup></b>	<b>0.9829</b>		
Mean	398.37	<b>Adjusted R<sup>2</sup></b>	<b>0.9658</b>		
C.V.	9.57	<b>Predicted R<sup>2</sup></b>	<b>0.9585</b>		
PRESS	14116.03	<b>Adeq. Precision</b>	<b>17.439</b>		

**Appendix 18: Ion Exchange Recovery of Cobalt from Copper Leach  
Solutions (NM002)**

# TECHNICAL PROGRESS REPORT

Contract Title and Number:

Establishment of the Center for Advanced Separation  
Technologies (DE-FC26-01NT41091)

Period of Performance:

Starting Date: 04/10/03  
Ending Date: 05/30/05

Sub-Recipient Project Title:

Ion Exchange Recovery of Cobalt  
From Copper Leach Solutions

Report Information:

Type: Semi-Annual  
Number: 006  
Period: 09/30/05-03/31/06  
Date: 04/20/06  
Code: NM002-R06

Principal Investigators:

I. Gundiler and M.J. Hatch

Contact Address:

New Mexico Tech  
Bureau of Geology & Min. Res.  
801 Leroy Place  
Socorro, NM 87801

Contact Information:

Phone: (505) 835-5730  
Fax: (505) 835-6333  
E-Mail: gundiler@gis.nmt.edu

Subcontractor Address:

"No subcontracts issued."

Subcontractor Information:

Phone:  
Fax:  
E-Mail:

## ABSTRACT

Two small particle size picolyated diethylenetriamine chelating ion exchange resins which we have synthesized were tested in small columns at fairly fast (CHEL-73) and quite slow (CHEL-40) flow rates for absorption of cobalt and copper from a pH 2.1 copper raffinate mining solution. With appropriate raffinate feed volumes and flow rates, both resins had a much higher absorption capacity for  $\text{Co}^{2+}$  than the commercially available resins. Elution of the loaded resins with 0.5-2M  $\text{H}_2\text{SO}_4$  was achieved readily. Most of the cobalt eluted was at over 10 times, and the copper over 50 times the concentrations in the feed solution.

## INTRODUCTION

### Background

Cobalt is a strategic and critical metal which is used in production of super alloys, and various other alloys and chemicals. It is not mined nor refined in the United States. The nation's needs are met with imported supplies and recycled alloys.

Leach solutions in large hydrometallurgical copper extraction operations in the Southwest generally contain 0.02-0.10  $\text{Kg/m}^3$  of cobalt. If cobalt can economically be recovered from the leach solutions, it could potentially supply a significant portion of the

U.S. imports. Currently, the technology to recover the metal from these solutions economically is not available.

Ion exchange processes could recover cobalt present at low concentrations in copper raffinate solutions but commercially available resins are either too expensive, or may not function in acidic solutions. Chelating ion exchange resins may also be considered as potential substitutes for the organic liquid extractants used for copper extraction to eliminate fire hazards and potential for ground water pollution.

### Objectives and Approach

This project was initiated to synthesize and test new chelating resins which could operate at low pH solutions and have higher capacity for copper and cobalt than available resin, and explore the possibility of recovering cobalt from the copper raffinate solutions.

In the earlier phase of this research we have studied the column operating performance of small shallow beds of our new chelating resins of fine particle size for absorbing  $\text{Co}^{2+}$ ,  $\text{Cu}^{2+}$  and other transition metal cations from a copper mining raffinate solution. The  $\text{Co}^{2+}$  and  $\text{Cu}^{2+}$  concentrations were only 18 and 42 ppm (parts per million). At high flow rates over ~20 bed volumes (BV) per hour and with ~ 200 BV of raffinate feed, our new picolyated diethylenetriamine resin (CHEL-40) gave the best  $\text{Co}^{2+}$  capacity. Similar fast flow step gradient elution of the loaded resin with  $\text{H}_2\text{O}$ , 0.1, 0.5, 1.0 and 2.0 M  $\text{H}_2\text{SO}_4$  was performed. The results indicated that even under these extremely unfavorable chromatography conditions, considerable improvement in the amount of  $\text{Co}^{2+}$  relative to most other metals, particularly  $\text{Fe}^{3+}$ ,  $\text{Zn}^{2+}$  and  $\text{Cu}^{2+}$ , could be obtained in the earliest eluate fraction. However, the concentration of  $\text{Co}^{2+}$  was relatively small, as might be expected.

Presently, there are two specific objectives for this project; 1) To evaluate the CHEL-40 resin further for the potential recovery of  $\text{Co}^{2+}$  by loading the resin bed with a limited amount of raffinate at a slow flow rate followed by a slow flow step-gradient elution with small volumes various concentrations of 0.5 to 2M  $\text{H}_2\text{SO}_4$ , 2) To evaluate the new resin CHEL-73, which was prepared by steps similar to the CHEL-40 resin as described in an earlier report. The only difference was that slightly less picolyl chloride was used in the picolylation step.

## **PROJECT TASKS**

### Task 1- Equipment

Small narrow neck glass tubes with glass wool filter bottoms and gravity-feed reservoirs attached to the tops of the columns were used as chromatography columns. Test tubes served as effluent receivers. Collected effluent fractions were analyzed by an atomic absorption spectrometer (AAS).

### Task 2-Experimental

### CHEL-40 Resin

Slow flow loading and elution studies were conducted on CHEL-40 resin with a raffinate solution low in cobalt and copper content (16ppm  $\text{Co}^{2+}$ , 40ppm  $\text{Cu}^{2+}$  due to some precipitate formation). About 300 bed volumes (BV) of raffinate at a flow rate of 2BV/hour were applied to the small CHEL-40 column (0.20  $\pm$  0.02 ml, bed depth 0.60 $\pm$  0.04 cm). Effluent fractions were collected and analyzed by AAS for  $\text{Co}^{2+}$  and  $\text{Cu}^{2+}$  content. The cumulative amounts absorbed on the resin (Figures-1 and 2) were calculated by the difference from the amounts in the feed. After the resin was stripped with acid and washed with water, it was then loaded with approximately 225 bed volumes of raffinate at 2BV/hr and eluted stepwise with 1BV  $\text{H}_2\text{O}$ , 2BV of 0.5M  $\text{H}_2\text{SO}_4$  at 1BV/hr. Collected eluate fractions were analyzed for  $\text{Co}^{2+}$  and  $\text{Cu}^{2+}$  concentrations as before.

### CHEL-73 Resin

A total of 300 BV copper leach raffinate solution (now ~10ppm  $\text{Co}^{2+}$ , 25 ppm  $\text{Cu}^{2+}$  due to co-precipitate formation in the aged raffinate solution) was applied at moderate flow rate of ~8BV/hr to a small column of CHEL-73 (bed volume 0.62  $\pm$  0.02ml, bed depth 1.80 $\pm$  0.04ml). The effluent fractions were analyzed as above for  $\text{Co}^{2+}$  and  $\text{Cu}^{2+}$  content and the amounts absorbed on the resin were calculated (Figure-3 and 4). Elution of the loaded bed with 4 BV of  $\text{H}_2\text{O}$  at 2BV/hr was followed by a total of 11.2 BV of 2M  $\text{H}_2\text{SO}_4$ . The collected fractions were analyzed as before for  $\text{Co}^{2+}$  and  $\text{Cu}^{2+}$ .

### Task-3 Data Analysis and Discussion

In the present work, we now have tested the CHEL-40 resin further. The raffinate solution was loaded at a slow flow rate, ~ 2BV/hr. Presumably as a result of more favorable kinetic factors for  $\text{Co}^{2+}$  absorption and lesser displacement by the advancing  $\text{Cu}^{2+}$  front, the maximum capacity for  $\text{Co}^{2+}$  retention on the column increased by about 80% (from ~0.5 to ~0.9 mg/ml of resin). Figure-1 shows these results for  $\text{Co}^{2+}$  and Figure-2 for  $\text{Cu}^{2+}$ . The capacity for  $\text{Cu}^{2+}$  was about the same as was determined previously for fast flow, since the stronger  $\text{Cu}^{2+}$  selectivity of the resin for  $\text{Cu}^{2+}$  increases the rate of  $\text{Cu}^{2+}$  absorption over that of less strongly absorbed  $\text{Co}^{2+}$ . The regenerated resin was loaded with ~225 BV of raffinate at the slow flow rate of 2BV/ml. Slow-flow step-gradient-elution with  $\text{H}_2\text{O}$ , 0.5, 1 and 2M  $\text{H}_2\text{SO}_4$  results for both  $\text{Co}^{2+}$  and  $\text{Cu}^{2+}$  were fairly similar, elution being completed essentially within 6BV, as shown in Figures-5 and 7. Most of the  $\text{Co}^{2+}$  was eluted at a concentration of about 200 ppm, over 12 times the concentration (16 ppm) in the feed solution; and most of the  $\text{Cu}^{2+}$  was eluted at an eluate concentration of about 3500 ppm, over 80 times the concentration (40 ppm) in the feed solution.

We also made and tested a new picolyated diethylenetriamine resin CHEL-73 which was fairly equivalent in its preparation to that of the CHEL-40 resin. Raffinate solution was applied (300 BV total, at flow rate of ~8BV/hr) to a small column bed of CHEL-73 which was about 3 times as deep as the CHEL-40 column. The amount of  $\text{Co}^{2+}$  absorbed on the resin was ~0.9 mg/ml of resin, and the amount of  $\text{Cu}^{2+}$  about 5 mg/ml, as shown in Figure-3 and 4.

The decreased capacity of the resin for  $\text{Cu}^{2+}$  compared to that of CHEL-40 is explained by its smaller concentration in the raffinate feed (25ppm vs. the earlier 40). The equivalent  $\text{Co}^{2+}$  capacity is explained by the idea that the lesser amount of  $\text{Cu}^{2+}$  absorbed on the bed reduced the displacement of the  $\text{Co}^{2+}$  on the lower part of the bed. Slow flow (2BV/hr) elution of the loaded bed with  $\text{H}_2\text{O}$ , 2M  $\text{H}_2\text{SO}_4$  eluted both  $\text{Co}^{2+}$  and  $\text{Cu}^{2+}$  quite similarly. Essentially all the  $\text{Co}^{2+}$  and  $\text{Cu}^{2+}$  were eluted within 11BV. Most of the  $\text{Co}^{2+}$  was eluted by the 2M  $\text{H}_2\text{SO}_4$  at a concentration of ~150ppm, well over 10 times the concentration in the feed solution. Most of the  $\text{Cu}^{2+}$  was eluted at a concentration of ~1500 ppm, about 60 times the feed concentration (Figures-5 and 6). That increase in  $\text{Cu}^{2+}$  concentration is less than attained with the CHEL-40 (slow flow) is explained by the lesser loading of  $\text{Cu}^{2+}$  on the CHEL-73 resin (~5g/ml vs. ~8g/ml).

## **SUMMARY**

Two small particle size picolyated diethylenetriamine ion exchange resins were tested in small columns at slow (CHEL-40) and moderately fast (CHEL-73) flow rates for absorption of cobalt and copper at very low concentrations (10, 16ppm  $\text{Co}^{2+}$ ; 25, 40ppm  $\text{Cu}^{2+}$ ) in a pH 2.1 copper raffinate solution. Tests at slow flow rates on the CHEL-40 resin showed that capacity for absorbing cobalt increased over that found in our earlier fast flow tests. However, the slow flow rates had little or no effect on the capacity for absorbing copper. Our new synthesized picolyated diethylenetriamine resin CHEL-73 (which was slightly less picolyated than the CHEL-40 resin) absorbed cobalt at moderately high flow rates as well as did a lesser volume of CHEL-40 at a slow flow rate. Both resins had a much higher absorption capacity for cobalt than the commercially available chelating resin showed in our previous tests. Elution with 0.5- 2M  $\text{H}_2\text{SO}_4$  of both the CHEL-40 and CHEL-73 resins which were loaded with appropriate volumes of raffinate feed gave main eluate fractions whose cobalt concentration was over 10 times, and the copper concentration over 50 times those present in the raffinate feed solutions.

## **REFERENCES**

1. Jeffers, T.H. and Harvey, M.R., Cobalt Recovery from Copper Leach Solutions, U.S. Bureau of Mines, Report of Investigations 8927, 1985, 12p
2. Jeffers, T.H., Separation and Recovery of Cobalt from Copper Leach Solutions, Journal of Metals, Jan. 1985, pp. 47-50
3. Bennet, P.G. and Jeffers, T.H., Recovery of Cobalt from Spent Copper Leach Solutions-Improved Elution and Impurity Removal Techniques, Revised Process Economics, U.S. Bureau of Mines, Report of Investigation 9190, 1988, 9p.
4. Grinstead, R.R., Copper-Selective Ion-Exchange Resin with Improved Iron Rejection, Journal of Metals, March 1979, pp 13-16.

## **PUBLICATION**

M.Sc. Thesis, Premchendar Nandhikonda (Nov. 2005), "Preparation, Characterization, and Performance of Several New Chelating Resins for Recovery of Cobalt and Copper from Acidic Mining Solutions", New Mexico Institute of Mining and Technology, Chemistry Dept Socorro, New Mexico, 87801 USA

## Cobalt and Copper Absorption Graphs

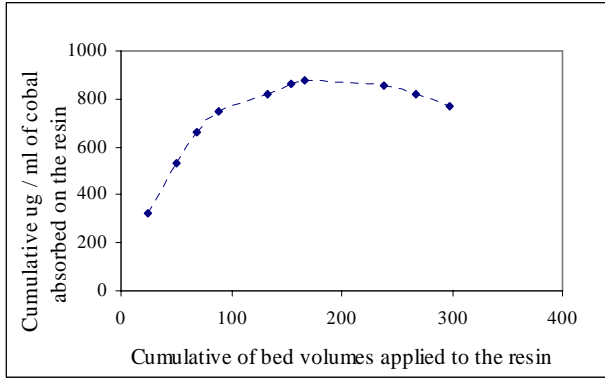


Figure 1. Cobalt absorption on CHEL-40 resin from mining raffinate at slow flow rate

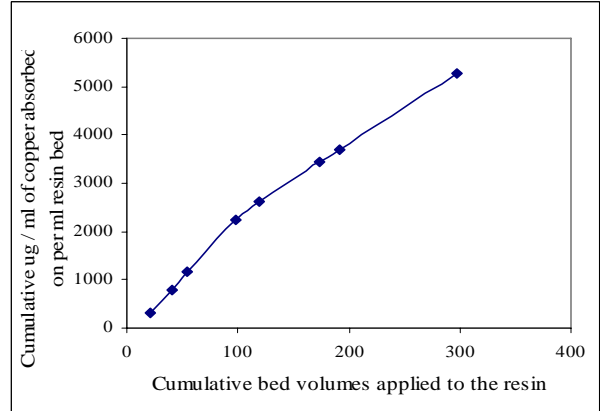


Figure 2. Copper absorption on CHEL-40 resin from mining raffinate at slow flow rate

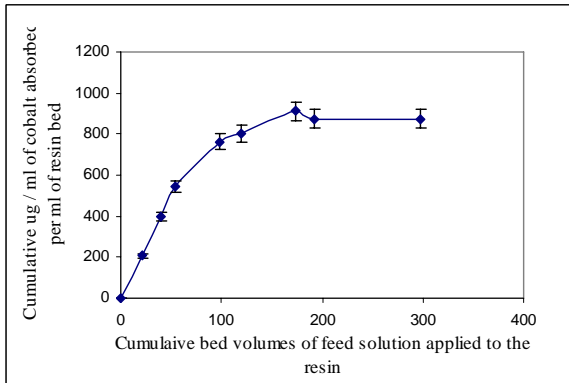


Figure 3. Cobalt absorption on CHEL-73 resin from mining raffinate at intermediate flow rate

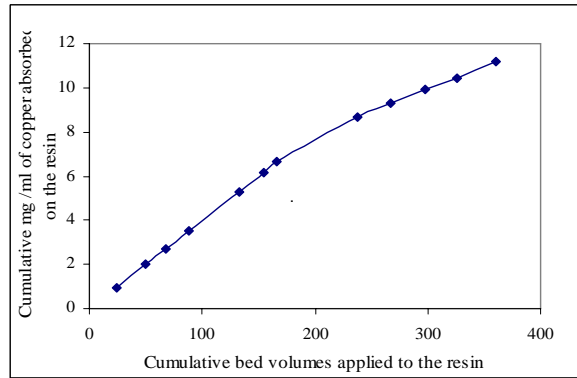


Figure 4. Copper absorption on CHEL-73 resin from mining raffinate at intermediate flow rate

## Cobalt and Copper Elution Graphs

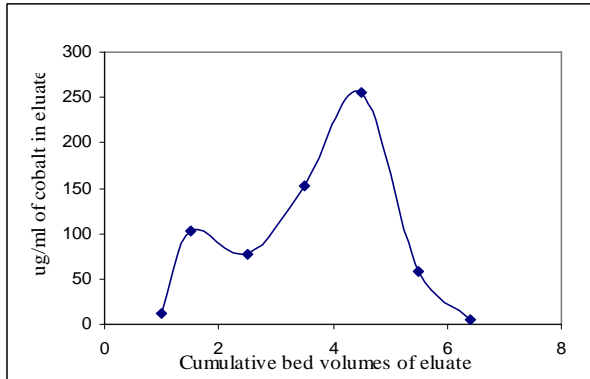


Figure-5. Cobalt elution from CHEL-40 resin

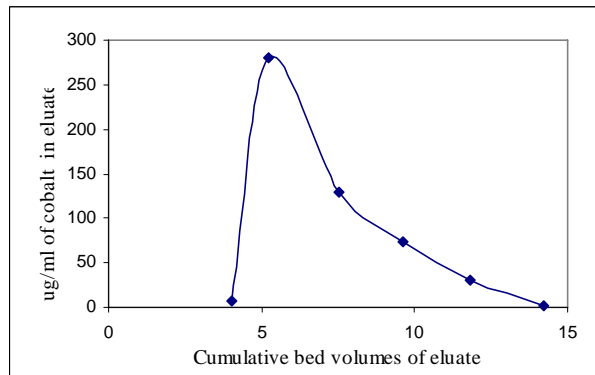


Figure-6. Cobalt elution from CHEL-73 resin

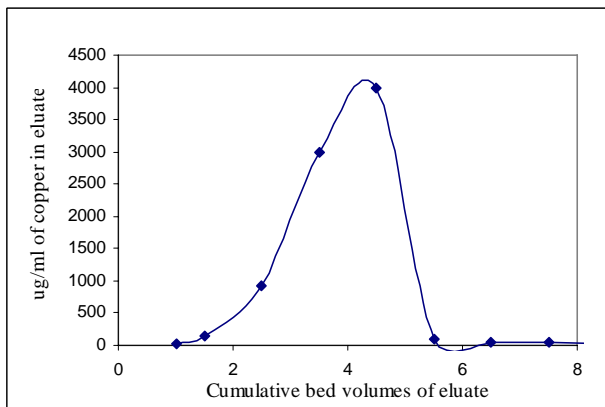


Figure-7. Copper elution from CHEL-40 resin

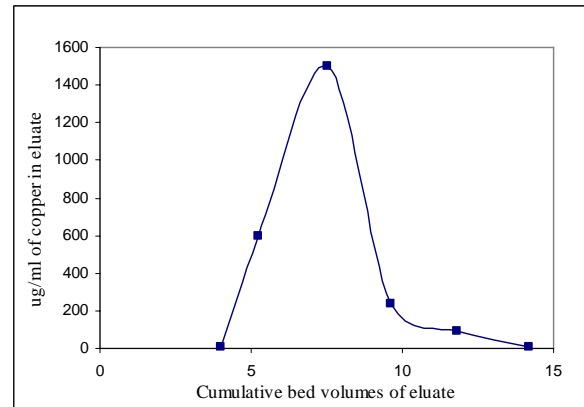


Figure-8. Copper elution from CHEL-73 resin

**Appendix 19: The Effect of Diphenyl Oxide Surfactants on Nucleation and  
Growth of Potassium Sulfate Crystals: Development of Enhanced  
Surfactants for the Potash Industry (NM003)**

**Appendix 20: Overcoming Technological Barriers to More Efficient  
Recovery of Copper from Chalcopyrite (UT005)**

## TECHNICAL REPORT

Contract Title and Number:

Crosscutting Technology Development at the Center for  
Advanced Separation Technologies  
(DE-FC26-02NT41607)

Period of Performance:

Starting Date: 06/01/2004  
Ending Date: 10/31/2006

Sub-Recipient Project Title:

Overcoming technological barriers to more efficient  
recovery of copper from chalcopyrite

Principal Investigators:

Michael L. Free

Contact Address:

Michael L. Free  
135 S. 1460 E. Room 412  
Salt Lake City, UT 84112

Subcontractor Address:

No subcontracts issued.

Report Information:

Type: Semi-Annual Report  
Number: 3  
Period: 10/01/05 – 03/31/06  
Date: Mar. 30, 2006  
Code: UT005-R03

Contact Information:

Phone: 801-585-9798  
Fax: 801-581-4937  
E-Mail: mfree@mines.utah.edu

Subcontractor Information:

Phone:  
Fax:  
E-Mail:

### ABSTRACT

One of the important technological barriers affecting the efficient recovery of copper from chalcopyrite is the morphology of the copper electrodeposits. This study identifies the effect of combination of different organic additives on the surface roughness of copper electrodeposits. A model predicting the surface roughness of the electrodeposits is evaluated for addition of organic additives. The roughness values for different organic additives were predicted reasonably well by the proposed model. The effect of different inorganic additives on the surface roughness of copper electrodeposits was also studied for constant current conditions. The roughness values of electrodeposits with zinc ion additions were substantially less than electrodeposits without any inorganic additives.

### INTRODUCTION

Background

In industrial practice the solution used for copper electrowinning contains some typical inorganic impurities. The major ones being tin, zinc, nickel and iron. For this reason

the effect of these additives on the surface roughness of copper electrodeposits obtained from chloride media is being investigated. Moreover metals like lithium, magnesium, calcium and aluminum can be present in copper electrowinning. These elements may reduce or enhance the surface roughness of electrodeposits and are therefore being investigated. The conventional electrowinning utilizes different types of additives either as separate compounds or as a combination of different additives. Hence, the effect of combination different organic additives on the surface roughness was studied.

### Objectives

- 1) Overcoming technological barriers to more efficient recovery of copper from chalcopyrite
  - a) To evaluate roughness model for different organic additives
  - b) To improve deposit morphology by investigating the influence of inorganic additives on surface roughness of electrodeposited copper from the solution containing chloride media.

## **PROJECT TASKS**

### Experimental procedures

Electrochemical tests were performed using an EG&G 273 potentiostat (operated using PowerSuite software made by Princeton Applied Research) and an AFASR rotator from Pine Instruments for potentiostatic and galvanostatic current transients. A three component cell with a platinum counter electrode and a saturated calomel electrode (SCE), against which are potentials are reported, were used. The working electrode was a copper disc (99.9998% pure) mounted in a Teflon holder with an area of 0.203 cm<sup>2</sup> exposed to the electrolyte. It was polished with a 600-grit polishing paper to remove the deposition products from the previous tests and then rinsed with pure water. This electrode was further polished with Micropolish alumina powder (0.5 $\mu$ ) to get a smooth clean, defect free surface. Finally the electrode is cleaned in an ultrasonic water bath to remove any polishing particles from the surface. All solutions were prepared using reagent grade chemicals and ASTM Type I water. Surface roughness was characterized by a CCD Iris camera made by SONY with the help of LEAD CAPTURE and LEAD CONVERT software (by LEAD technologies) along with Microimage software (University of Utah). Surface roughness calculations were performed by MATLAB (Mathworks Ltd.).

### Task 1: Additive Evaluations

#### Effect of combined organic additives on RMS roughness

The reduction of the surface irregularities in the plating processes can be accomplished by the addition of organic additives. The effects of combination of organic additives such as glycine, thiourea, PEG (Mn~200) on surface roughness were analyzed as

shown in Figure 1. The combination of glycine, PEG, and thiourea reduces the surface roughness by a factor of two compared to baseline test with no organic additive.

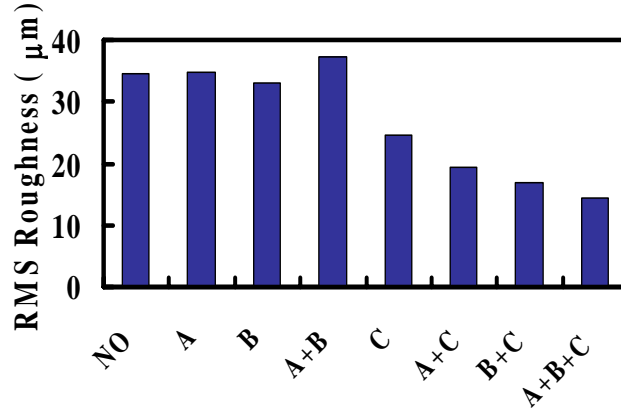


**Figure 1. Effect of 2.5 ppm glycine (A), 2.5 ppm thiourea (B), 7,500 ppm PEG (Mn~200) (C), and their combinations on the surface roughness of copper electrodeposits obtained from an electrolyte containing 0.1 mol/L CuCl, 4 mol/L NaCl and 0.01 mol/L HCl (base solution) at cathodic current density of 25 mA/cm<sup>2</sup> for 3 hours at 1000 rpm.**

#### RMS roughness model fitting

Electrodeposition morphology is a function of steady state nucleation and growth. Consequently, if the nuclei are assumed to be hemispheres, the associated root-mean-squared roughness for adjacent nuclei of uniform radius is equal to the average nucleus radius divided by the square root of three. Therefore, substitution for the average radius in terms of RMS roughness will lead to:

$$RMS_{roughness} = \frac{2ki}{\sqrt{3\pi}N_{\infty}} \exp\left(\frac{-\chi}{T\eta_s^2}\right)$$

Dividing by current density and taking the logarithm of both sides leads to<sup>1</sup>:

$$\ln\left(\frac{RMS_{roughness}}{i}\right) = \ln\left(\frac{2k}{\sqrt{3\pi}N_{\infty}}\right) - \frac{\chi}{T\eta_s^2}$$

where  $k$  is a proportionality constant,  $i$  is the current density,  $N_{\infty}$  is the baseline rate of nuclei formation,  $\chi$  is a constant ( $\chi$  and  $N_{\infty}$  are functions of valence, geometry, surface energy, and frequency of attachment and detachment),  $T$  is temperature and  $\eta_s$  is the surface overpotential. The data in Figures 2 show that this proposed model provides a reasonable description of the effect of additives on electrodeposit roughness.

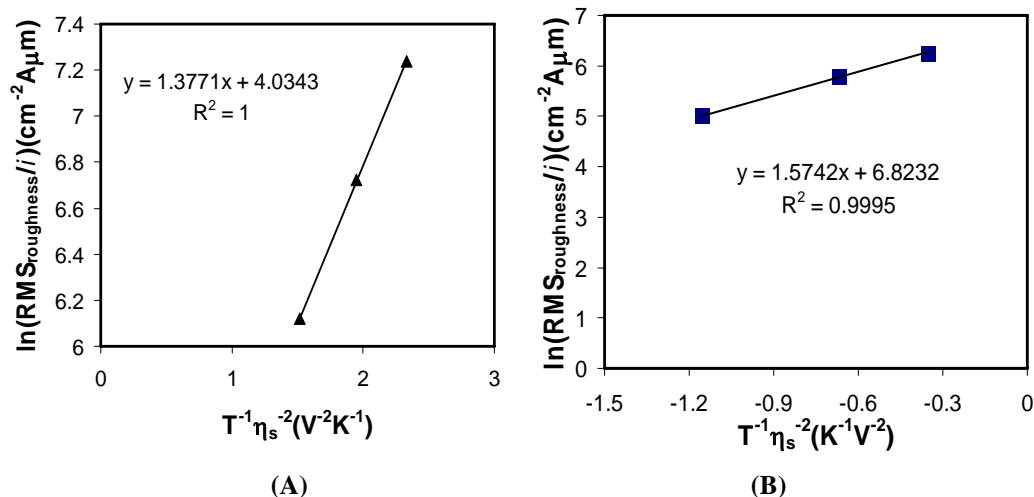


**Figure 2.** Comparison of the natural logarithm of the ratio of RMS roughness to current density versus the inverse temperature multiplied by the inverse surface overpotential squared. (A) Data based on galvanostatic copper electrodeposition from 0.1 M CuCl, 4 M KCl solution (1000 RPM, 25°C, 108 Coulombs/cm<sup>2</sup>, and -5, -10, and -25 mA/cm<sup>2</sup>). (B) Data based on galvanostatic copper electrodeposition from 0.1 M CuCl, 4 M KCl solution containing 0.1 vol % gelatin (1000 RPM, 25°C, 108 Coulombs/cm<sup>2</sup>, and -5, -10, and -25 mA/cm<sup>2</sup>).

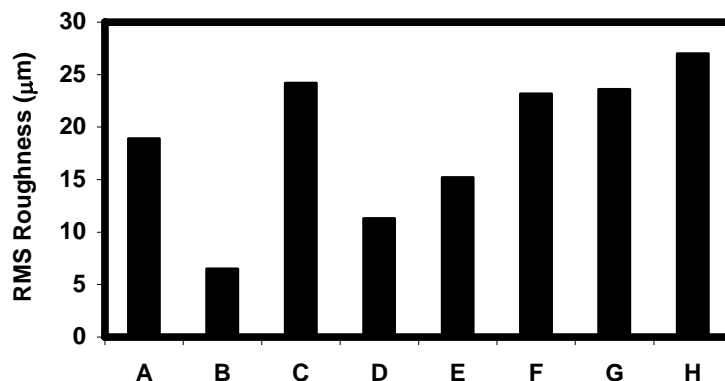


**Figure 3.** Effect of different cationic additives (A = no additive, B = 100ppm Zn<sup>+2</sup>, C=100ppm Li<sup>+2</sup>, D = 100ppm Mg<sup>+2</sup>, E = 100ppm Ni<sup>+2</sup>, F = 100ppm Ca<sup>+2</sup>, G= 100ppm Sn<sup>+2</sup>, and H = 100ppm Al<sup>+3</sup>) on surface roughness of copper electrodeposits obtained from an electrolyte containing 0.1 mol/L CuCl, 4 mol/L NaCl and 0.01 mol/L HCl at a cathodic current density of 25 mA/cm<sup>2</sup> for 2 hours at 1000 rpm.

#### Effect of inorganic additives on RMS roughness

As seen in figure 3, it was observed that an addition of 100 ppm zinc to the solution resulted in the highest improvement in smoothness of copper electrodeposits. This might be

due to the change in the electrochemical properties of the system due to the addition of zinc ions. Further investigation is required in order to establish the same.

## **SUMMARY**

The addition of inorganic additives like  $Zn^{2+}$  and organic compounds result in copper electrodeposits with lower surface roughness. Thus, electrodeposition limitations to implementing the energy efficient halide technology can be overcome to a significant extent through the use of additives.

## **FUTURE WORK**

- Develop the understanding of why the gelatin works better than other organic additives.
- Study the effect of temperature on the surface roughness of copper electrodeposits.
- Investigate the long term deposition characteristics of copper electrodeposits.

## **REFERENCE**

1. M. L. Free, R. Bhide, A. Rodchanarowan, N. Phadke, "Evaluation of the effects of additives, pulsing, and temperature on morphology of copper electrodeposited from halide media, accepted for publication in ECS Transactions, May 2006.

## **PUBLICATIONS/PRESENTATIONS**

1. M. L. Free, R. Bhide and A. Rodchanarowan, "Improving the morphology of copper electrodeposits from halide media using additives and mass transport control", accepted for publication in ECS Transactions: Green Electrodeposition, 2006.
2. A. Rodchanarowan, R. Bhide, M. Free, "The Effect of Additives on Morphology of Copper Electrodeposits from Halide Media," submitted to TMS Letters, 2006.
3. R. Bhide, A. Rodchanarowan, M. Free, "The Effect of Mass Transport on Morphology of Copper Electrodeposits from Halide Media," submitted to TMS Letters, 2006.
4. M. L. Free, R. Bhide, A. Rodchanarowan, N. Phadke, "Electrochemical Modeling of Electrowinning Performance," submitted for publication in Sohn International Symposium on Advanced Processing of Metals and Materials Edited by Florian Kongoli, TMS, 2006.
5. M. L. Free, "Improving the morphology of copper electrodeposits from halide media using additives and mass transport control," Presented at Electrochemical Society Annual Meeting, Los Angeles, Oct 20, 2005.
6. M. Free, A. Rodchanarowan, R. Bhide, "The Effect of Additives on Morphology of Copper Electrodeposits from Halide Media," Presented at TMS Annual Meeting, San Antonio, March 14, 2006.
7. M. Free, R. Bhide, A. Rodchanarowan, "The Effect of Mass Transport on Morphology of Copper Electrodeposits from Halide Media," presented at TMS Annual Meeting, San Antonio, March 14, 2006.

**Appendix 21: Development of Chemical and Biochemical Techniques for  
the Extraction of Mercury from Fine Coal Particle Solutions (WV010)**

## TECHNICAL PROGRESS REPORT

Contract Title and Number:

Crosscutting Technology Development at the Center for  
Advanced Separation Technologies  
(DE-FC26-02NT41607)

Period of Performance:

Starting Date: 6/1/2004  
Ending Date: 10/31/2006

Sub-Recipient Project Title:

Development of Chemical and Biochemical  
Techniques for the Extraction of Mercury from Fine  
Coal Particle Solutions

Principal Investigators:

Hurst, Abatjoglou, Wiedemann

Report Information:

Type: Semi-Annual  
Number: 3  
Period: 10/1/05-3/31/06  
Date: 3/31/06  
Code: WV010-R03

Contact Address:

West Virginia University  
405 Fayette Pike, Orndorff Hal  
Montgomery WV 25136

Contact Information:

Phone: (304) 442-3246  
Fax: (304) 442-1046  
E-Mail: Scott.Hurst@mail.wvu.edu

Subcontractor Address:

Insert address of subcontractor. If none awarded,  
insert "No subcontracts issued."

Subcontractor Information:

Phone:  
Fax:  
E-Mail:

### ABSTRACT

There are three main thrusts in the development of techniques for the extraction of mercury from fine coal particle solutions. In the chemical phase, adsorbents made by depositing ligands on macroporous polystyrene and activated carbon, were shown to be effective for removing low concentrations of mercury from water streams in batch and continuous extraction experiments. The demonstrated practical utility and novelty of these adsorbents has allowed us to submit a patent application.

In the biochemical phase, we are making progress on identifying and genetically characterizing mercury-resistant bacteria native to West Virginia in order to incorporate these native bacteria, genetically engineered versions of these bacteria, and/or biochemical components of these bacteria into mercury bioremediation schemes. Four species of bacteria have been isolated and definitively identified.

In the molecular modeling phase, a free-standing molecular model has been thoroughly studied, enabling to clearly identify the various substructures – alpha helices, beta-pleated sheets, and the random coils associated with the active mercury binding site and the conformational changes that occur when mercury is bound and unbound.

## INTRODUCTION

### Background

This research project, is comprised of three thrusts and consists of three collaborating subgroups. An additional effort will be undertaken to look at the possible engineering of any processes that are forthcoming from the work.

Work related to the biochemical processes consists of the production of partially purified bacterial metal-oxidation enzymes (oxidases) that convert organic-bound mercury and mercury (I) to mercury (II); the production of partially purified bacterial metal-reduction enzymes (reductases) and proteins that convert mercury (II) to mercury (0); and the isolation of specific genes so the relevant proteins may be over-expressed to produce the needed proteins in quantity at a low cost.

The chemical laboratory work on adsorbents/ligands involves the evaluation of extraction efficiency and other practical properties of novel mercury-scavenging adsorbents, and the assessment of synthetic pathways to develop novel mercury-scavenging adsorbents.

The computational and analytical support of the project comprises the analysis of adsorbent properties reported in the literature to assess correlations between commonly measured properties and the selective properties sought; the evaluation of structural and electronic properties best associated with selectivity through molecular modeling; and the establishment of kinetics and mechanism of bonding and release of mercury by a selected protein, Mer P.

## PROJECT TASKS

### The Biochemical Work

Our efforts focus on the biological aspects of mercury (Hg) removal from coal. Specifically, we are studying the application of bacteria inherently resistant to mercury to the bioremediation of mercury-contaminated coal waste. As shown by others over the past decade or so, some bacteria are capable of thriving in the presence of mercury levels that are otherwise toxic. These bacteria achieve this by metabolizing mercury in the surrounding environment, transporting  $\text{Hg}^{2+}$  into the cell and subsequently reducing it to  $\text{Hg}^0$ , a less toxic, volatile form which diffuses out of the cell. Such mercury-resistant bacteria bear a set of genes (the “*mer*” genes) which encode the highly-specific protein transporters and reductase enzymes involved in this metabolic pathway.

Our immediate goal is to identify and genetically characterize mercury-resistant bacteria native to West Virginia in order to incorporate these native bacteria, genetically engineered versions of these bacteria, and/or biochemical components of these bacteria into mercury bioremediation schemes. Toward this end, we have so far isolated and definitively identified 4 species of bacteria: 1 species (*Citrobacter freundii*) from a control sample (the Kanawha River), 1 species (*Enterobacter asburiae*) from a coal wastewater containment pond, and 2

species (*Enterobacter asburiae* and *Klebsiella pneumoniae*) from coal wastewater cultured in the presence of 1.5 mM Hg<sup>2+</sup>.

### The Molecular Modeling Work

A free-standing molecular model has been thoroughly studied, enabling us to clearly identify the various substructures – alpha helices, beta-pleated sheets, and the random coils associated with the active mercury binding site and the conformational changes that occur when mercury is bound and unbound. Matching the computational work with literature data enabled clear identification of the structural changes associated with the exclusive mercury binding site. There are numerous hydrogen bonds in the Mer P structure with only 6 or 7 of these likely to participate directly in Mer P binding mercury. These bonds and other structural features enable only mercury to bind and the binding is divalent and linear. On adding denaturants, all of the Mer P hydrogen bonds can be broken. The structure becomes somewhat random and releases any bound mercury. When removing the denaturants, the protein reassembles itself into its active conformation.

The complete denaturing is not the biologically active process. Work continues on the identification of the explicit mechanism for the binding and release of mercury (II) by the merP protein. By viewing crystal structures for mercury-bound and unbound structures for the mer P protein and attempting to compare the various changes to the model, we found it very difficult as there are many atoms that move in the process. We therefore considered it appropriate to construct an automated (computer) method of comparing atom movements from bound to unbound protein. The purpose would be to isolate those segments of the protein that remained essentially stationary from those that had the largest movement. Then, we could focus on modeling the segments with movement to try and estimate the associated energies, and subsequently devise a mechanism for the complexation of mercury. This more complete understanding of the selectivity and strength of the mer P protein might then suggest how to devise effective alternative agents to complex mercury in various solutions.

### The Chemical Work: Continuous Mercury Removal from Water Using Ligand-Modified Adsorbents.

The adsorbent used in this experiment was prepared as follows. A solution containing 1.144 grams (4 mmoles) octadecanethiol was dissolved in 3 ml toluene, was added to 4 grams of activated carbon spheres (Aldrich®, activated carbon, Darco®, 20-40 mesh, granular) held in a 100 ml round-bottom flask under vacuum. The solvent was then evaporated slowly on a rotary evaporator, and the dry sorbent was used of mercury extraction experiments, performed as follows. About 6.38 grams of the sorbent prepared as described above was slurry packed with the help of water into a 1 cm diameter glass chromatography column. A 5 ppm solution of mercury II nitrate in water was eluted through the column at a flow rate of 1 ml/min. Samples of the eluent from the column were collected as a function of time, and were analyzed for mercury concentration using flameless atomic absorption spectroscopy. The concentrations of Hg<sup>2+</sup> in the effluent fractions from the column are given in the Table 1.

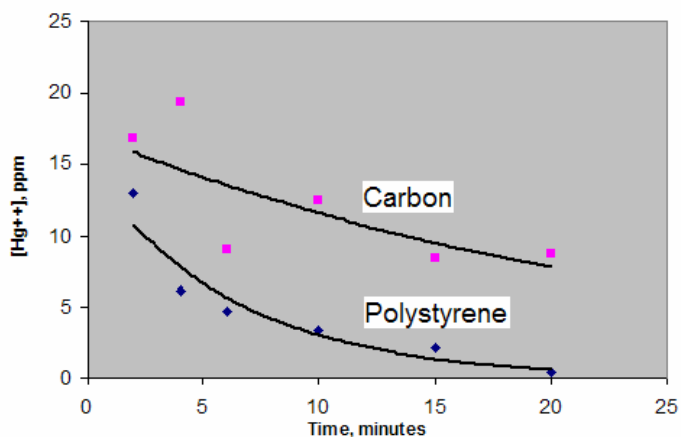
Table 1: Continuous mercury removal from water using a modified carbon adsorbent.

Volume of Eluted water (ml)	Mercury concentration in eluted water (in parts per billion)*
30	41.6
60	16.2
90	24.3
120	59.2
150	8.9

\* Mercury concentrations measured by Flameless Atomic Absorption Spectroscopy.

The adsorbents used in this study were prepared as detailed above using macroreticular poly(styrene-co-divinylbenzene) 300-800 microm beads, or Darco®, 20-40 mesh activated carbon. The experimental results of mercury extraction as a function of time were obtained as follows. A clean polypropylene bottle was charged with 50 ml of a synthetic 20 ppm mercury solution in water, and with 0.3 grams of polystyrene beads (or activated carbon beads) surface-loaded with 1 mmole/gram octadecanethiol as the mercury complexing agent. The bottle was capped and agitated using a mechanical agitator. Small size samples (0.8 ml) were withdrawn at 2, 4, 6, 10, 15 and 20 minutes. The samples were filtered through 0.2 microm Teflon filter-disks, and the filtrate was used for analysis of its mercury concentration by flameless Atomic Absorption spectroscopy. The experimental results are shown in Fig 1.

Figure 1. Kinetics of mercury extraction using modified polystyrene and activated carbon adsorbents.



## SUMMARY

In the biochemical studies our goal is to isolate plasmid DNA from *Citrobacter freundii*, *Enterobacter asburiae*, and *Klebsiella pneumoniae*. Towards this end we isolated plasmid DNA from *Klebsiella pneumoniae* and are in the process of analyzing the DNA for the mer genes.

The first phase of the modeling studies was to build a model program to monitor movement in the “backbone” of the 72 amino acids in the protein. This has been completed and we now have three main areas of movement: as expected, the active site is one of these areas as well as the nearby random coil portion of the backbone. Surprisingly these appear to move in

concert with the breaking of only a few hydrogen bonds. A speculative mechanism that appeared in the recent literature consisted of breaking of a number of hydrogen bonds; it does not appear viable in light of our recent work. The third site that shows movement germane to the complexation has us puzzled as to its function.

In the initial phases of the chemical studies we have been able to prepare novel adsorbents for the removal of low concentrations of mercury and other metals from water. We have also demonstrated the effectiveness of such adsorbents for batch and continuous extraction of mercury from water, and we have preliminary results on adsorbent regeneration and mercury recovery. The demonstrated practical utility and novelty of these adsorbents has allowed us to submit a patent application to the US patent office in February 2006. The ease of preparation of these adsorbents and the variety of ligands that can be employed with them make them suitable for use in the simultaneous removal of different metals in the form of cations, anions as well as neutral atoms.

## **FUTURE WORK**

The status of the current modeling research leads us to believe that soon we can propose a mechanism for the complexation of mercury by mer P. This will enable us to better design a commercial process for mer P as well as suggest additional ligands for mercury complexation trials.

Our discovery of “non-chemical binding of ligands on adsorbents for extraction of mercury from water” will be extended to ligands which may provide high selectivity of extraction relative to other metals. The structural features of these ligands will be gleaned from the theoretical calculations part of this study and from literature sources. In addition to selectivity studies work will be directed towards simple processes for mercury recovery and adsorbent regeneration recycle. The approach will be extended to adsorbents that are practical for the extraction of metal oxoanions (such as for example, chromate, arsenate, selenate) anions. Initial results for the extraction of chromate anion from water are very promising. The work will also be extended to suitable adsorbents for use in the vapor phase like it is detail in the patent application.

## **PUBLICATIONS/PRESENTATIONS**

1. Broschinski, A. E., Robinson, C. L., Wiedemann, J. M., and R. Squire, “Biochemical Approach for Removing Mercury from Coal Impoundment Ponds”, Undergraduate Research Day at the Capitol, Feb. 2006.
2. Abatjoglou, A. G.; “Non-chemical Binding of Ligands on Sorbents for Trace Extraction of Heavy Metals from Water”, Patent application submitted Feb. 2006. The initial results of work related to this invention were presented as a poster paper in the June 2005 DOE/NSF EPSCoR Conference in Morgantown, WV; and at the Undergraduate Research Day at the Capitol in February 2006.
3. J.E. Craft, C.L. Robinson, D.M. Bailey, M.J. Luce and J.M. Wiedemann, “A Biochemical Approach for Extracting Mercury from Coal”, Undergraduate Research Day at the Capitol, Feb. 2006.

**Appendix 22: Coal Desulfurization with Hypochlorite (WV011)**

## TECHNICAL PROGRESS REPORT

Contract Title and Number:

Crosscutting Technology Development at the Center  
for Advanced Separation Technologies  
(DE-FC26-02NT41607)

Period of Performance:

Starting Date: 6/1/2004  
Ending Date: 10/31/2006

Sub-Recipient Project Title:

Coal Desulfurization with Hypochlorite

Report Information:

Type: Semi-Annual  
Number: 3  
Period: 10/1/05-3/31/06  
Date: 3/24/06  
Code: WV011-R03

Principal Investigators:

Cho, Yang

Contact Address:

Department of Chemical Engineering  
West Virginia University  
Morgantown WV 26506

Contact Information:

Phone: (304) 293 2111x2433  
Fax:  
E-Mail: eung.cho@mail.wvu.edu

Subcontractor Address:

No subcontracts issued.

Subcontractor Information:

Phone:  
Fax:  
E-Mail:

### ABSTRACT

In this period, an Illinois No. 6 coal, IBC 112 (65 x 150 mesh) was used in leaching experiments. The coal was leached with one stage under various temperatures, hypochlorite and sodium hydroxide concentrations.

It was found that the leaching conversion of total sulfur increases slightly as temperature increases from 35 to 70°C. Also, it was found that the optimum leaching conditions were 0.6 molar hypochlorite, 0.4 molar sodium hydroxide and 70°C. Under these conditions, the total sulfur was reduced from 2.15% to 1.72 or by 20% reduction.

### INTRODUCTION

Background

It is known that aqueous chlorine can leach most of the coal pyrite and a significant fraction of organic sulfur.<sup>(1,2)</sup> However, the most serious problem with the method is that aqueous chlorine chlorinates the coal matrix at a level of 20-30 wt %. It has been reported that hypochlorite, a chlorine derivative which is stable at high pHs can leach a significant fraction of organic sulfur with only a mild chlorination of the coal matrix.<sup>(3)</sup> The present

research project deals with the optimization of operating conditions with a compromise by maximizing the sulfur reduction and minimizing the chlorination of coal.

### Objective

The major objective of this project is to optimize the conditions of the coal desulfurization using hypochlorite.

## **PROJECT TASKS**

### Task 1 – Sample Preparation

Illinois No. 6 coal, IBC 112 sample was crushed and screened to produce a size fraction of 65 x 150 mesh which was used for experiments. This size fraction was analyzed for sulfur forms and chlorine content according to ASTM methods. The analytical results were 2.15% total sulfur, 0.45% pyritic sulfur, 1.69% organic sulfur, 0.01% sulfate sulfur and 0.26% chlorine.

### Task 2 – Leaching Experiments

Leaching experiments were conducted with IBC 112 coal sample in a one-liter reactor immersed in a constant-temperature bath. The leaching experiments were conducted with one stage. Each experiment was conducted in a 500-ml hypochlorite solution for two hours at a stirring speed of 500 rpm. After leaching, the coal slurry was filtered, dried, and analyzed for sulfur forms and chlorine content.

Leaching was conducted with one stage under various conditions of temperature (25 – 70°C), hypochlorite concentration (0.4 – 0.8 molar) and sodium hydroxide concentration (0 – 0.8 molar). It was found that the optimum conditions were 0.6 molar hypochlorite, 0.4 molar sodium hydroxide and 70°C. Under these conditions, the total sulfur reduction was 20%; however, a significant weight loss of coal was found to be 23%.

### **Summary**

The results show that the effects of temperature and sodium hydroxide concentration on total sulfur reduction are minimal. It was observed that the total sulfur reduction was only 20% under the optimum conditions with one-stage leaching. The optimum conditions were 0.6 molar hypochlorite, 0.4 molar sodium hydroxide and 70°C. Under these conditions, the coal weight loss was found to be 23%. These results are not satisfactory; thus, other options will be taken to increase the leaching conversion of total sulfur while reducing the coal weight loss.

## **FUTURE WORK**

Future experimental work will be conducted to leach IBC 112 coal with two-stages; that is, the first stage at room temperature with hypochlorite and the second stage to hydrolyze the leach coal with sodium hydroxide at 80°C. Also, iodide will be tried in the first stage particularly to increase the total sulfur reduction.

## **REFERENCES**

- (1) G. C. Hsu et al., "Coal Desulfurization by Low-Temperature Chlorinolysis," Coal Desulfurization, T. D. Wheelock, ed., ACS Symp. Series 64, 1977, pp. 207-217.
- (2) E. H. Cho, "Coal Desulfurization with Aqueous Chlorine," Met. Trans. B, vol. 20B, Oct. 1989, pp. 567-571.
- (3) I. B. Brubarker and T. Stoicos, "Precombustion Coal Desulfurization with Sodium Hypochlorite," Proceedings of the First International Conference on Processing and Utilization of High Sulfur Coal, Oct. 13-17, 1985, Columbus, Ohio, edited by Y. A. Attia. pp. 311-326.

## **PUBLICATIONS/PRESENTATIONS**

No paper was presented or published.

**Appendix 23: Phyto-Extraction / Fabrication of Gold and Silver  
Nanoparticles (WV012)**

## TECHNICAL PROGRESS REPORT

Contract Title and Number:

Crosscutting Technology Development at the Center for  
Advanced Separation Technologies  
(DE-FC26-02NT41607)

Period of Performance:

Starting Date: 6/1/2004  
Ending Date: 10/31/2006

Sub-Recipient Project Title:

Phyto-Extraction / Fabrication of Gold Nanoparticles –  
Feasibility Study

Report Information:

Type: Semi-Annual  
Number: 3  
Period: 10/1/05-3/31/06  
Date: 3/31/06  
Code: WV012-R03

Principal Investigators:

Ray Y. K. Yang, Eung Ha Cho

Contact Address:

Ray Y. K. Yang  
Chemical Engineering Department  
West Virginia University  
Morgantown WV 26506-6102

Contact Information:

Phone: (304) 293 2111x2419  
Fax:  
E-Mail: ryang@mail.wvu.edu

Subcontractor Address:

No subcontracts issued

Subcontractor Information:

Phone:  
Fax:  
E-Mail:

### ABSTRACT

The contents of gold in the cells of carrot and periwinkle in suspension cultures and in the sprouts of mung bean and alfalfa are noticeably enhanced overall as the gold concentrations in contact with the plant cells or the sprouts increase, confirming the extraction and transportation of gold ions into the cells of the plants tested. All the gold concentrations in the bio-ores obtained from the plant cells and the sprouts are much higher than that of the threshold concentration in hyperaccumulator plants for gold, with the plant-cell data being several-fold higher compared to that of the sprouts. This indicates the potential of using suspension culture of plant cells for large scale production of gold nanoparticles

### INTRODUCTION

Background

Phytomining is the production of a metal by growing high-biomass plants that hyperaccumulate high concentrations of a target metal. A conventional phytomining operation would consist of planting a hyperaccumulator crop over a low-grade ore body or mineralized soil, followed by harvesting and incineration of the biomass to ash to produce “bio-ore”. In

this project, we have expanded conventional phytomining to include other forms of plants, notably sprouts and plant cells.

Some plants are natural hyperaccumulators, while others require induction for hyperaccumulation. For most metals the threshold concentration for hyperaccumulation is 1 mg/g dry biomass, except for gold, which is 1 µg/g dry biomass [1-4]. Red beet (*Beta vulgaris*), carrot (*Daucus carota*), and mustard (*Brassica juncea*) have been shown [2, 5] to be the plants with the best potential for phytomining for gold, if chemically induced by adding ammonium thiocyanate to the auriferous substrate to solubilize gold. The existence of gold nanoparticles in live alfalfa grown on agar-agar was observed using X-ray absorption spectroscopy and transmission electron microscopy by Gardea-Torresdey et al. [6].

### Objective and Approach

Three separate tasks are conducted simultaneously in this project to determine the capability of whole plants and plant cells to extract and transport gold, as well as to show the existence of gold nanoparticles. The objective is to provide a better understanding of gold nanoparticles phyto-extracted and phyto-fabricated by hyperaccumulator plants, sprouts, and plant cells grown in suspension cultures, aiming eventually to develop feasible processes for large scale phyto-production of gold nanoparticles.

## **PROJECT TASKS**

### Task 1 – Investigation of gold nanoparticles in hyperaccumulator plants

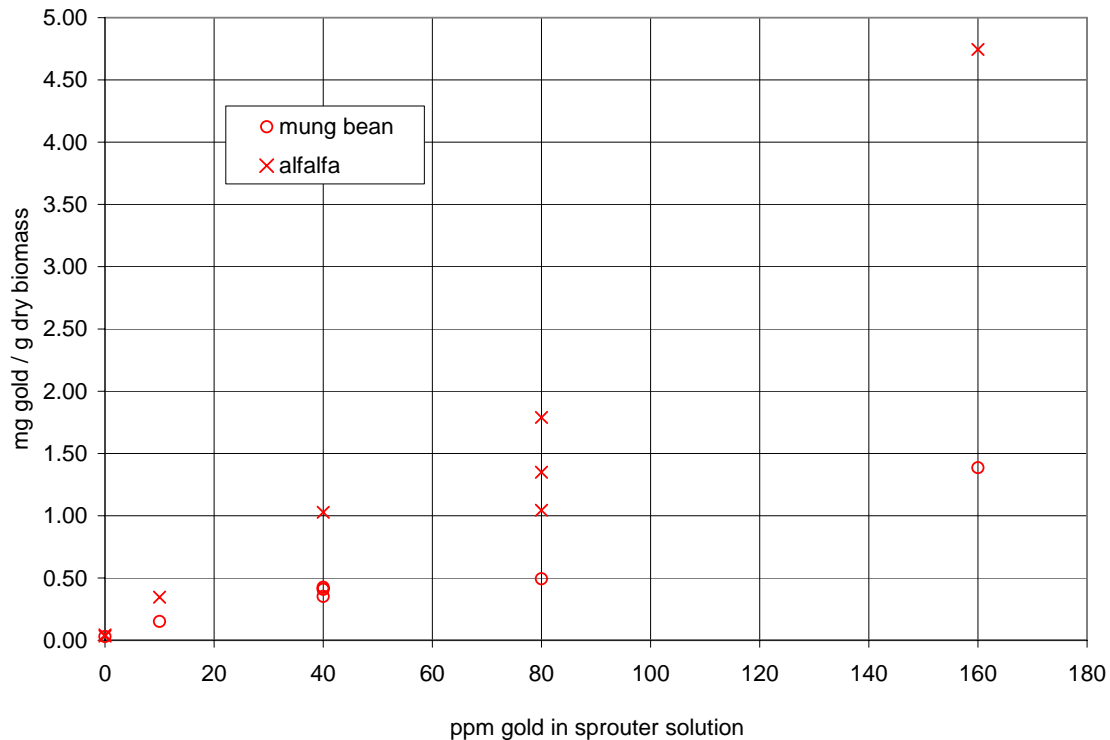
The plants grown in the 10-week large scale greenhouse experiment that involved six cultivars of hyperaccumulator plants (two different cultivars each for carrot, beet, and mustard) were treated with ammonium thiocyanate and, ten days later, harvested during the Thanksgiving Week of 2005. Each of the plants grown in the 120 pots (half of them in auriferous sand and the other half in pure sand) was carefully washed to remove the sands from all parts of the plant, including root, without losing any biomass, and left to dry on clean plastic surface for several weeks. Each completely dry plant is now stored in a separate clean new paper bag, and the “bio-ore” (ash) from each plant is currently being produced for analysis by an atomic absorbance spectrophotometer (AAS).

### Task 2 – Investigation of gold nanoparticles in sprouts

During this period, more mung bean (*Vigna radiata*) and alfalfa (*Mesa* variety) were grown from seeds on two different types of sprouter, A and S, using potassium tetrachloroaurate solution of different concentrations than that used in the previous reporting period. Difference in these two types of sprouters, as well as the procedures for production of soot-free ash (bio-ore) from the sprouts and for determination of gold contained therein using an AAS, were described in Progress Report No. 2 of this project. The results obtained so far for A-sprouter are presented in Figures 1 below. As expected, the sprout data indicate that, overall, as the concentrations of gold in the potassium tetrachloroaurate solutions used in the sprouters increase from 10, 40, 80 to 160 ppm, the gold contents in the bio-ores also increase.

In addition, overall, alfalfa sprouts appear to extract and retain higher concentrations of gold than mung bean sprouts. But, most importantly, all the gold concentrations in the bio-ores obtained from sprouts, expressed as milligram gold per gram of un-burnt dry biomass, are much higher than that of the threshold concentration in hyperaccumulator plants for gold.

**Figure 1. Dependence of gold concentrations in mung bean and alfalfa sprouts on gold concentration in sprouter solutions for type A sprouter**

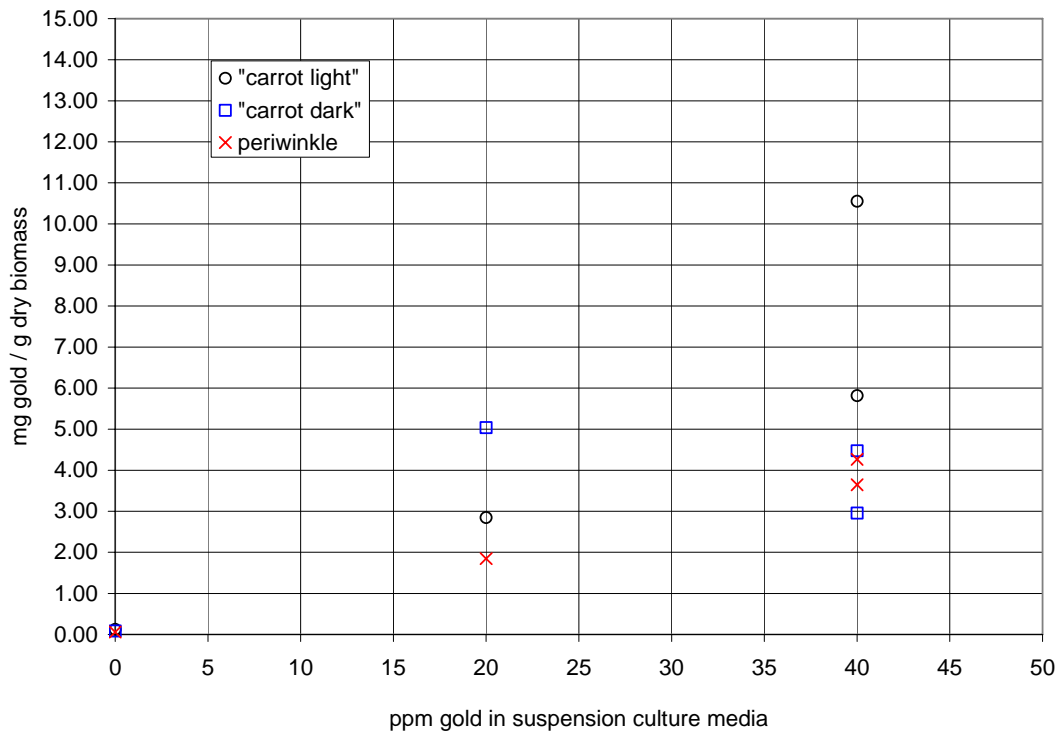


### Task 3 – Investigation of gold nanoparticles in plant cells

Callus cultures for both carrot (*Daucus carota*) and periwinkle (*Catharanthus roseus*) in Murashige and Skoog (MS) solid medium were successfully established in the PI's Bioreaction Engineering Laboratory from explants during the first reporting period. For carrot, two types of callus culture have since been established; one that has been kept in the dark all the time (designated as "carrot dark") and another in 12-hour light/dark (designated as "carrot light"). During this reporting period, these three callus cultures have continuously been maintained by subculturing every four weeks. In addition, callus culture of red beet (*Beta vulgaris*) on solid agar Gamborg's B5 medium has also been established now; it will be maintained by sub-culturing approximately every four weeks. The suspension cultures of "carrot light", "carrot dark" and periwinkle, that were successfully initiated and established from their corresponding callus cultures in the last reporting period, have been maintained in shakers located in two separate incubators in 12-hour light/dark (for periwinkle and "carrot light") or 24-hour dark (for "carrot dark") during this reporting period by subculturing every two weeks.

Shown in Figure 2 are the gold contents of cells of periwinkle, “carrot light” and “carrot dark” after exposing the cells to 20 ppm and 40 ppm of gold in the suspension cultures for one week. Similar to treatment for sprouts, the plant cells, after filtering out from their media, were washed repeatedly with distilled de-ioned (DD) water and then dried in an oven before burning in a muffle furnace to produce a soot-free ash, i.e., “bio-ore”. Each batch of bio-ore was dissolved in concentrated *aqua regia* and then analyzed for gold using an AAS. Details of the experimental procedures were described in Progress Report No. 2 of this project.

**Figure 2. Gold concentrations in carrot and periwinkle cells versus gold concentrations in suspension culture media**



The data in Figure 2 indicate that the gold contents in the “carrot light” cells are in general higher than that in the periwinkle cells. This is not surprising, as carrot is a hyperaccumulator for gold, while periwinkle is not. More importantly, as expected, comparing the data in Figures 1 and 2, one can observe that, in general, contents of gold in plant cells cultivated in suspension cultures are several-fold higher compared to that in sprouts. This preliminary result appears to indicate the potential of using suspension culture of plant cells for large scale production of gold nanoparticles.

## SUMMARY

The gold contents of “bio-ores” from sprouts of mung bean and alfalfa are noticeably enhanced as the gold concentrations in the solutions in contact with the sprouts increase from 10, 40, 80 to 160 ppm; alfalfa sprouts appear to extract and retain higher concentrations of gold than mung bean sprouts. All the gold concentrations in the bio-ores obtained from all

sprouts, expressed as milligram gold per gram of un-burnt dry biomass, are much higher than that of the threshold concentration in hyperaccumulator plants for gold. The plant-cell data obtained so far indicate that, in general, contents of gold in plant cells cultivated in suspension cultures are several-fold higher compared to that in the sprouts. This preliminary result appears to indicate the potential of using suspension culture of plant cells for large scale production of gold nanoparticles.

## **FUTURE WORK**

The progress of the project during the second half of this reporting period suffered greatly due to the unexpected departure of the project's sole graduate research assistant in early January 2006 to take up a position that he considered "I should not pass up as it meets my current and future goals perfectly" (a direct quote from his letter announcing his decision not to attend West Virginia University). A chemical engineering graduate student with a M.S. in Chemistry, but having no prior background and experience with the tasks of the project, joined the project in late January. The student, through almost two months of training, has now become familiar with the major tasks of the project. We expect very significant progress of this project during the next reporting period.

For the Task on Plant Cells, more atomic absorbance (AA) data for carrot, periwinkle, as well as red beet, will be obtained for different concentrations of potassium tetrachloroaurate solutions adding to the suspension cultures. Similarly, for the Task on Sprouts, more AA data will be added for both alfalfa and mung bean. For the Task on Hyperaccumulator Plants, AA data for the bio-ores from the large scale greenhouse experiment will be obtained as well. All the AA data from all tasks will be analyzed and compared. In addition, tissue samples of whole plants and plant cells, as well as their corresponding bio-ores collected, will be imaged using the scanning probe microscope (SPM) in the PI's Bioreaction Engineering Laboratory to confirm the existence of gold nanoparticles and to study their sizes, shapes and surface characteristics.

## **REFERENCES**

1. Brooks R. R. *et al.*, *Trends in Plant Science*, 3, 359 (1998).
2. Anderson, C. W. N. *et al.*, *Nature*, 395, 553 (1998).
3. Anderson, C. W. N. *et al.*, *J. Geochemical Exploration*, 67, 407 (1999).
4. Anderson, C. W. N. *et al.*, *Gold Bulletin*, 32, 48 (1999).
5. Msuya, F. A., *et al.*, *Gold Bulletin*, 33, 134 (2000).
6. Gardea-Torresdey, J. L. *et al.*, *Langmuir*, 19, 1357 (2003).

## **PUBLICATIONS/PRESENTATIONS**

A paper entitled "Phyto-Manufacturing of Gold Nanoparticles" by Yang, R. Y. K., Manint, J, and Cho, E. was presented by Ray Yang at the PACIFICHEM 2005 (International Chemical Congress of Pacific Basin Societies) in Honolulu, HI, December 15-20, 2005. (PACIFICHEM is a well established international conference jointly sponsored by the American Chemical Society and 17 other chemical societies around the Pacific Basin.)

**Appendix 24: Online Monitoring and Diagnosing of Coal Fines During  
Separation Process (WV008)**

## TECHNICAL PROGRESS REPORT

Contract Title/Number:

Crosscutting Technology Development at the Center for Advanced Separation Technologies  
(DE-FC26-02NT41607)

Period of Performance:

Starting Date: 5/15/03  
Ending Date: 10/31/06

Sub-Recipient Project Title:

On Line monitoring and diagnosing of coal fines during separation process using LIBS.

Principal Investigators:

Dr. Bruce Kang, WVU  
Dr. Eric Johnson, WVU

Contact Address:

Dr. Bruce Kang  
353 Engineering Science Building  
Evansdale Campus, WVU  
Morgantown, WV 26506

Subcontractor Address:

No subcontracts issued

Report Information:

Type: Semi-Annual  
Number: 6  
Report Period: 10/1/05-3/31/06  
Date: 3/31/06  
Code: WV008-R06

Contact Phone/e-mail:

Phone: (304)-293-3111 x2316  
Fax:  
Email: [Bruce.Kang@mail.wvu.edu](mailto:Bruce.Kang@mail.wvu.edu)

Subcontractor Information:

Phone:  
Fax:  
E-Mail:

### ABSTRACT

This research project investigates a fundamental study of applying Laser Induced Breakdown Spectroscopy (LIBS) to coal samples and coal fines. Apparatus and methodology were developed to quantify the content of carbon, sulfur, iron and mercury in coal. A list of the most sensitive emission lines for the elements of carbon, iron, mercury and sulfur were composed. The spectrograph was tuned and LIBS tests were done on each respective element. It was observed carbon and mercury could be quantified using LIBS.

### INTRODUCTION

Laser Induced Breakdown Spectroscopy (LIBS) is a technique that uses a powerful laser to ablate a sample of a desired material. This ablation causes a plasma formation in which the material is broken down into excited ionic and atomic states. The atoms then emit characteristic optical radiation known as an emission spectrum. Collection of the emitted light can be used to provide information on the elemental composition of the material.

The goal of this research project is to develop an on-line, non-contact, elemental analysis of coal samples and coal fines during solid-solid separation process through the use of LIBS. Of particular interest is the detection and quantitative measurement of the amount of carbon, sulfur, mercury, and other trace elements in the separated coal fines.

## PROJECT TASKS

### 1. Experimental Apparatus

In the process of LIBS testing, there are two separate experimental apparatus. The first apparatus is the sample preparation laboratory. In here, samples with known concentrations are prepared. In the second apparatus, the samples are subject to LIBS testing. The sample preparation apparatus consisted of a scale for massing chemicals, a grinding mill for homogenization of the mixtures, and a pellet press and die for making pellets out of the synthetic coal mixtures. Chemicals used in making the mixtures were all in solid powder form and included graphite powder, coal powder (NIST sample 1635), iron powder and mercuric oxide. Powders were used because they could be homogenized by a grinding mill and pressed into solids.

Figure 1 shows schematics of the LIBS system. The experimental LIBS apparatus allows optimum signal collection as well as temporal characteristics of the LIBS spark of coal. A Quanta Ray DCR 11 Q-switched Nd: YAG laser is fired, focused through a focusing lens and induces a plasma from a pellet of compressed material, which is held in place by a translatable sample holder by an air-tight sample chamber.

Once the laser spark occurs, the light is collected and collimated by a modular collimator system (designed in-house with parts purchased from ThorLabs). The modular collimator consists of a collection lens, a focusing lens, a pinhole, and a collimation lens. The collimated light travels to the polygonal scanning mirror (Lincoln Laser Company). The collimated light is reflected off one of the scanning mirror facets and goes a set of periscope mirrors, which reflects the light into a focusing lens. The lens focuses the collimated light down onto the entrance slit to the spectrograph (Horiba Jobin-Yvon HR640). Depending on whether the scanning mirror is enabled or disabled there is either a line or a focused spot on the entrance slit of the spectrometer.

When the scanning mirror is turned off, the LIBS spark is taken with no internal gating. Also, because of a lack of a shutter on the CCD camera, the CCD camera is fully exposed until the data is completely read out, which takes about 2.6 seconds. The image formed by the spark creates a spot on the entrance slit. This spot encompasses the entire lifetime of the laser-induced plasma, from the black body radiation in the beginning to the emission lines resulting from the recombination of atoms and molecules. This process was deemed “static LIBS”. Figures 2 and 3 shows a typical example of raw signal and processed Static LIBS test of a synthetic mixtures of coal sample.

When the scanning mirror is enabled, the image of the spark is spread out across the entrance slit because of the mirror’s motion. This creates a line on the entrance slit. Each point in the line represents a different time within the lifetime of the spark. This information provides us with an approximate lifetime of each emission line. This process was named “dynamic LIBS”.

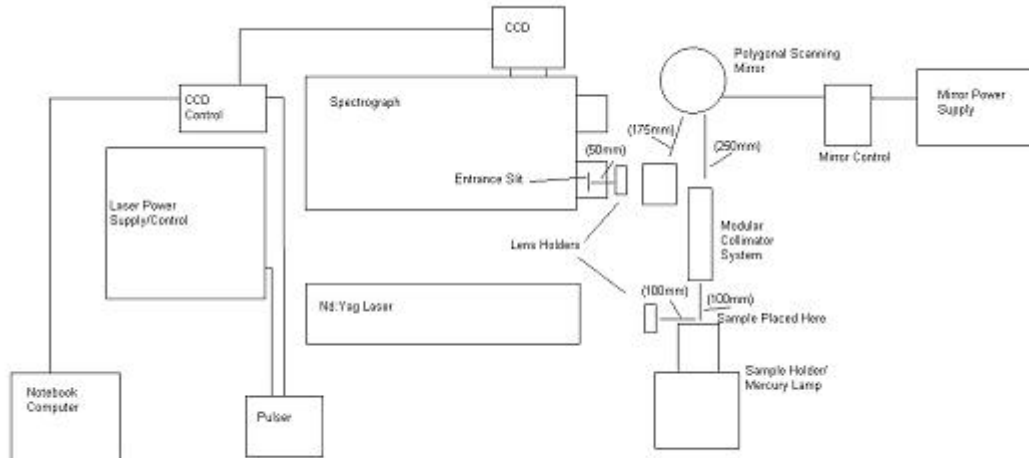


Figure 1 - Schematic of Experimental LIBS Apparatus

## **2. Experimental And Operating Data**

### **Initial LIBS Testing**

Because LIBS observes emission lines, initial testing for signal acquisition and optimization began with steel. This choice was made because iron has over 4000 emission lines, and can be observed throughout the spectral regions of interest, making it an optimal candidate for spectrograph calibration. Both static and dynamic LIBS testing were applied to steel.

The first studies were observed in the wavelength range of 530-545nm. This wavelength range was chosen because it had an abundance of iron lines, and included at least one emission line from each of the elements of interest according to the MIT Wavelength Tables (3 sulfur lines, 1 carbon line and 1 mercury line). Static LIBS was applied to pyrite, sulfur powder, coal powder and graphite powder. No signals from carbon or sulfur were observed in this wavelength region. Pyrite testing only revealed iron emission lines. Mercury was not tested in this region.

The spectrograph was tuned to mercury's most sensitive line, 254nm. In this range, the spectrograph would encompass the 254 nm line from mercury as well as the 248nm line in carbon. When LIBS testing was done on the coal sample from NIST, the expected carbon line was not observed in this range.

A list of the most sensitive emission lines for the elements of carbon, iron, mercury and sulfur was composed. The spectrograph was tuned to each one and LIBS testing was done on each respective element. In an attempt to find sulfur, the spectrograph was tuned to the most sensitive sulfur lines in the spectrum, and static LIBS testing was applied to a sulfur pellet. Sulfur showed no emission lines anywhere in the visible or infrared spectrum. It is

hypothesized that this could be due to effects of an air environment that seem to quench sulfur emission lines.

Upon further examination of the wavelength tables, another decision was made to select the wavelength range of 431-452nm. The spectrograph was calibrated by a combination of the ceiling light containing mercury and a LIBS spark from iron. After calibration, static LIBS testing was done on coal powder, coal pellets, graphite powder, graphite flakes, a carbon rod, sulfur powder, sulfur pellets, and a mercury-copper amalgam. Upon testing the powders, no lines were observed in graphite or sulfur. Static LIBS testing applied to coal powder revealed emission lines at approximately 445 nm and 447 nm, which were tested against a carbon rod and matched. The wavelengths were verified when LIBS was applied to pure carbon powder. The 436nm mercury emission line was observed in the testing, as well as several emission lines from the copper spectrum. After a consistent signal acquisition was obtained, the mercury-copper amalgam was subject to dynamic LIBS testing. An iron pellet and a small pyrite pebble were also subject to dynamic LIBS testing. Only iron emission lines appeared in the LIBS testing of the pyrite sample, no sulfur emission lines were observed. Since all carbon, iron and mercury were present within this wavelength range, this wavelength range was chosen.

### LIBS Testing of Synthetic Mixtures

Eleven synthetic mixtures of coal were made in order to test the LIBS process. Each mixture contained a homogenized blend of graphite powder, NIST 1635 (sub bituminous coal), iron powder, and mercuric oxide for elevating mercury levels in the mixtures. The concentration of each element varied with each mixture, creating various concentrations of C, Fe, and Hg for each pellet. Each chemical was massed on a weighing dish, and transferred into a grinding capsule. After the desired chemicals were massed and added into the capsule, the capsule was labeled, and ground together through a ball miller portable grinding unit. After grinding took place, the mixture was then placed in a pellet die and pressed to form a pellet.

	Mix1	Mix2	Mix3	Mix4	Mix5	Mix6	Mix7	Mix8	Mix9	Mix10	Mix11
Graphite	0.0770	0.3344	0 g	0.0082	0.0936	0	0.1519	0.2259	0.1757	0	0
NIST1635	0.0704	0	0.7575	0.3113	0.2985	0.2967	0.2415	0.2121	0.2715	0.7141	0.6357
Iron Powder	0.0138	0.0060	0.0998	0.0199	0.0213	0.0091	0	0.0017	0.0072	0.4141	0.0027
Mercuric Oxide	0.0108	0.0026	0.0111	0.0019	0.0003	0.0084	0.0132	0.1497	0.0138	0	0

Table 1 – Mix Compositions in grams

	Mix1	Mix2	Mix3	Mix4	Mix5	Mix6	Mix7	Mix8	Mix9	Mix10	Mix11
Carbon, %	73.42	97.49	61.06	66.24	73.12	67.75	81.20	81.21	78.11	65.93	69.73
Iron, %	8.12	1.75	11.70	6.05	5.32	3.18	0.15	0.46	1.68	6.04	0.62
Mercury, %	5.81	0.70	1.18	0.52	0.08	0.25	0.31	2.77	2.74	0	0

Table 2 – Elemental Concentration of Synthetic Mixtures

After the completion of sample preparation, the samples were subject to LIBS testing. Although the components to the synthetic mixtures were ground together, the final specimen was not a homogeneous pellet. To compensate for the lack of uniformity, 100 “static” LIBS shots were taken for each synthetic mixture. Standard deviation values of the shot intensities of each sample indicate that the mixtures were not thorough. After static testing of a specimen, the spinning mirror was then turned on for dynamic testing. Dynamic shots were collected from each sample, except for sample #2, which was destroyed during static testing. Static LIBS

### Qualitative Analysis

Qualitative analysis of the LIBS signals can be done with the data of the static LIBS shots. No processing of the data is necessary. Spectral lines are identified according to their wavelengths.

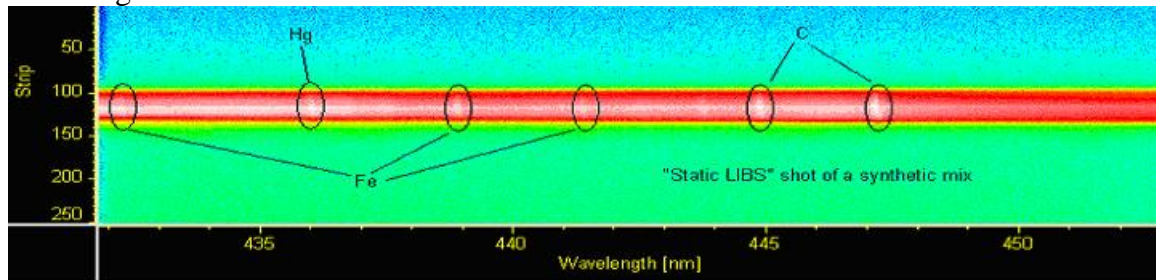


Figure 1 – Static LIBS Raw Data, mix#1, shot 59

### Quantitative Analysis

Quantitative analysis of the LIBS signal requires the data from the LIBS testing to be processed and converted into a spreadsheet. Each of the raw data files of the synthetic mixtures was converted and placed into Microsoft Excel. The data was then averaged, and analyzed for quantitative analysis. In this procedure, spectral signals were subtracted from the background (which included electronic response of the detector and the continuum radiation from the initial plasma formation). The intensity values were plotted and are expected to show a linear relationship with the concentration of the specified element.

$$I_{\text{relative}} = I_{\text{peak}} - I_{\text{baseline}}$$

Where  $I_{\text{peak}}$  is the intensity at the peak of the emission line, and  $I_{\text{baseline}}$  is the intensity at the baseline of the emission line. Because of the initial radiation resulting in a broad emission that interferes with the atomic and ionic emission signals, the baseline intensities to the left and right of the emission lines were averaged before subtracting the baseline value from the

peak intensity. The intensity of the emission lines resulting from LIBS are expected to be linear with respect to the elemental concentration of the specie within the sample.

### 100 Shot Average - Mix 1

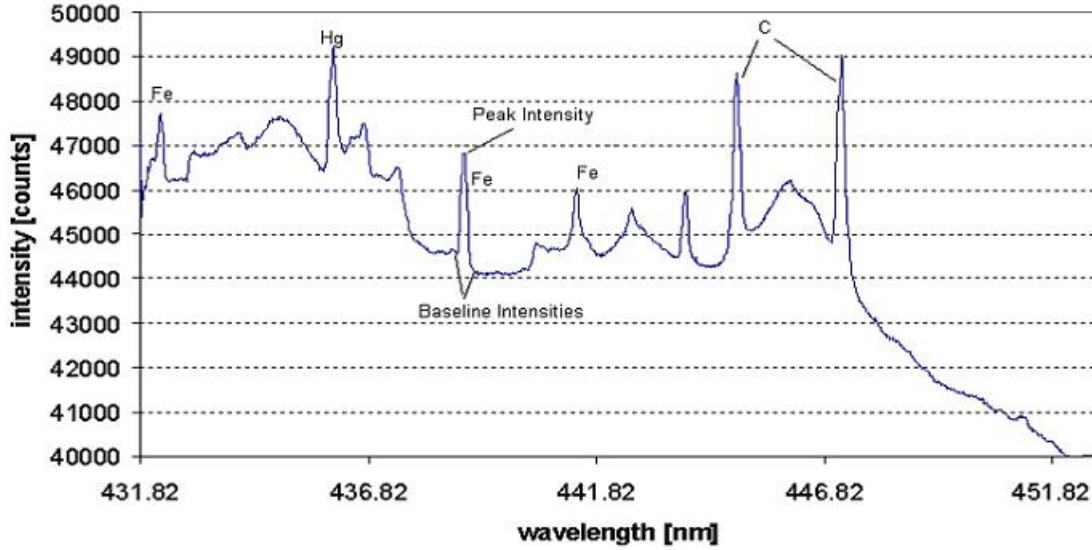


Figure 2 – 100 Shot Average of Mix 1 for qualitative and quantitative analyses

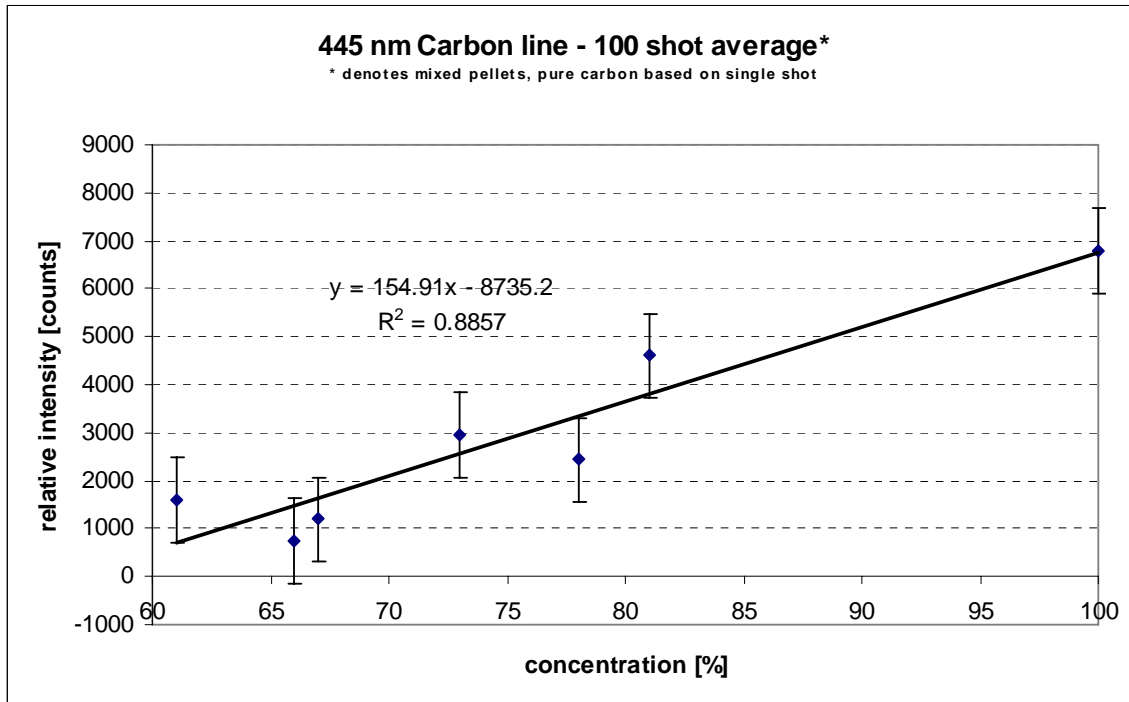


Figure 3 – Correlation of the 445nm Carbon - related line

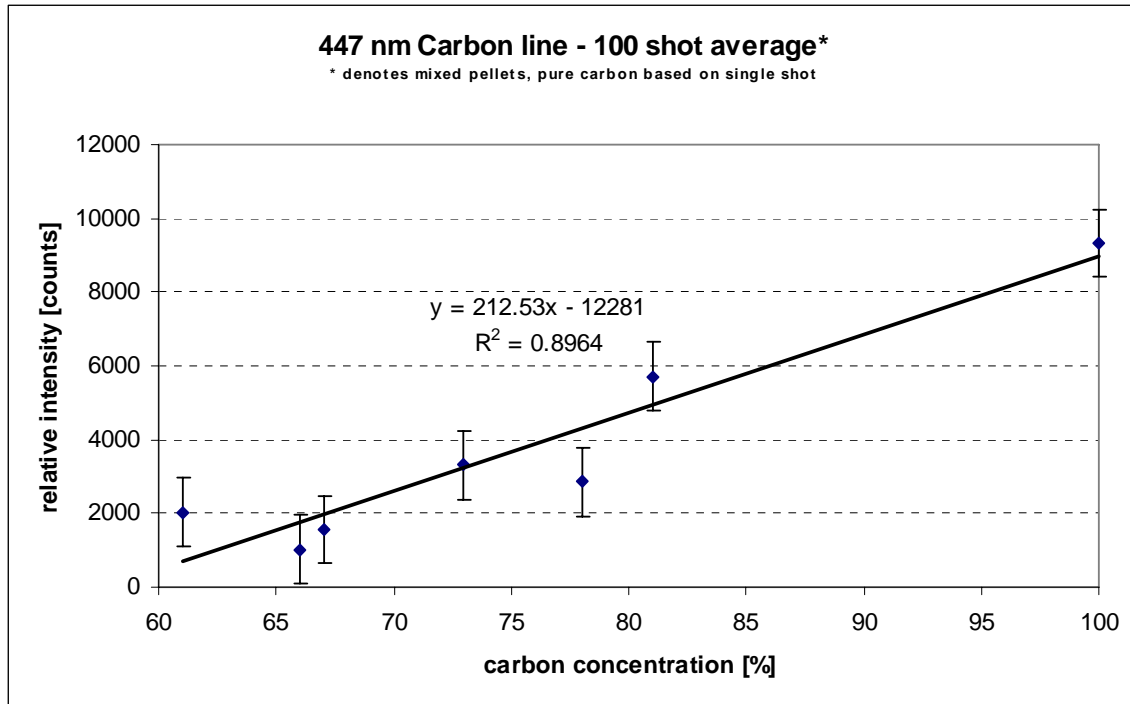


Figure 4 – Correlation of the 447 nm Carbon - related line

The linear fit observed in the 445 and 447 nm carbon-related lines showed a good correlation between elemental concentration and line intensity. Although these emission lines are not recorded in the MIT wavelength tables, they can be used as carbon-related lines to determine elemental concentration based on their intensity.

Mercury concentration ranged between 800 parts per million to 6 percent. While the strongest and most observed line is 253.6 [3-5], the 436nm emission line was chosen because of its close proximity to the carbon-related and iron emission lines. The 436 nm emission line proved to have a linear relation between line intensity and elemental concentration. There was one discrepancy point within the data set, which is hypothesized to be a measurement error that occurred during the pellet formation process.

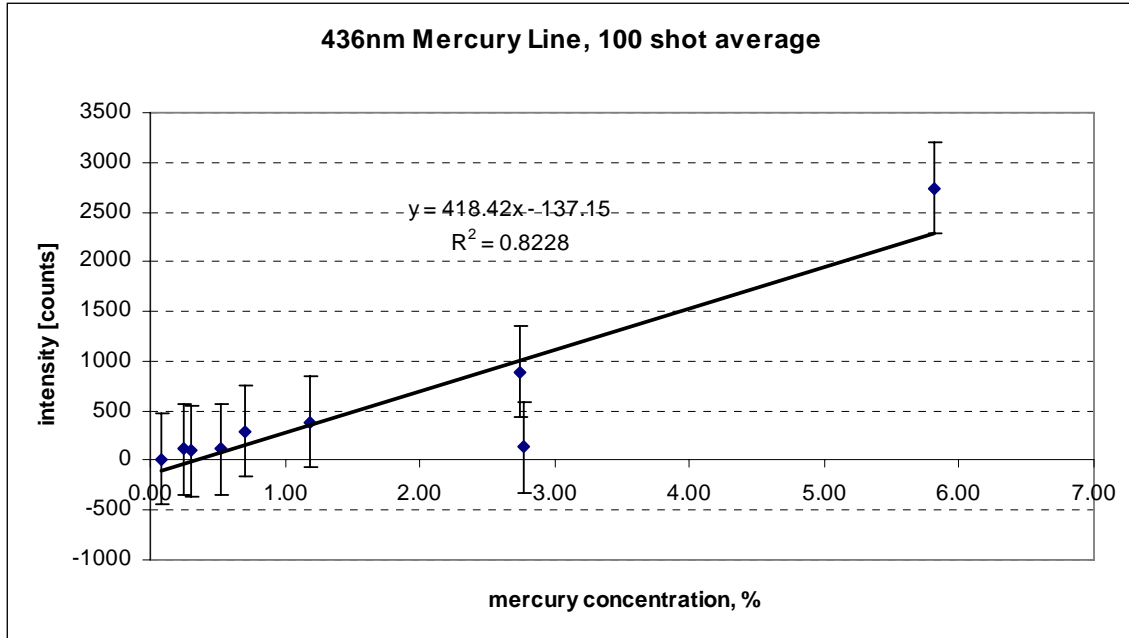


Figure 5 – Correlation of the 436nm Mercury Emission Line

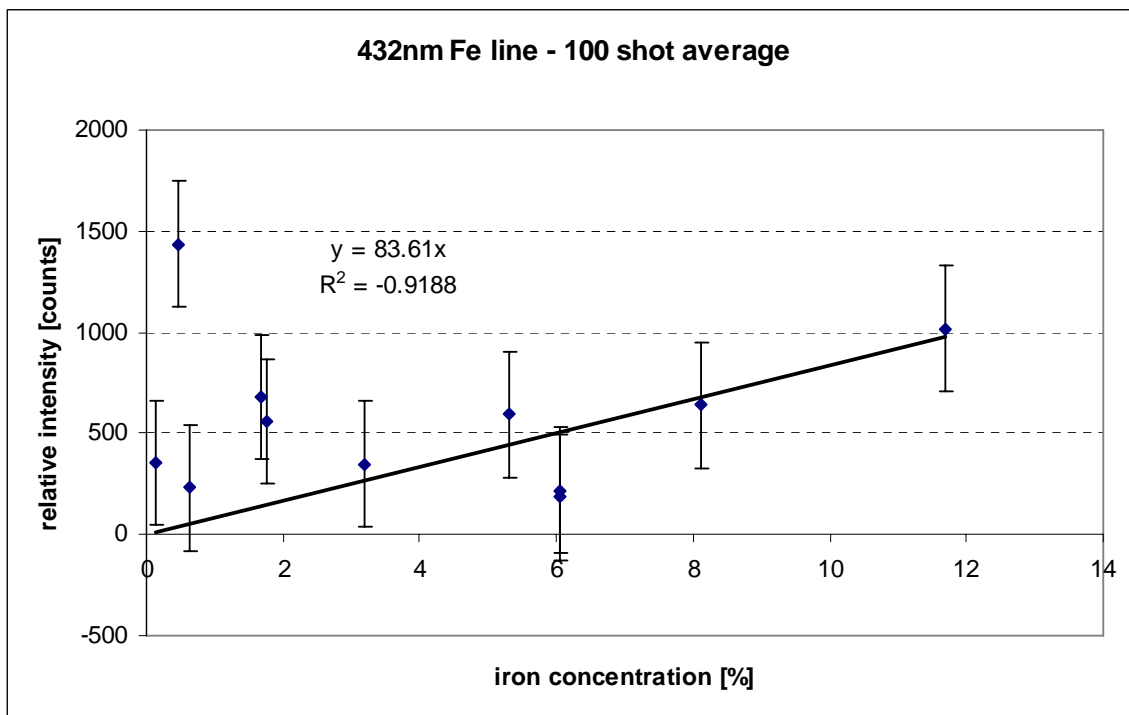


Figure 6 – Correlation of the 432nm Iron Emission Line

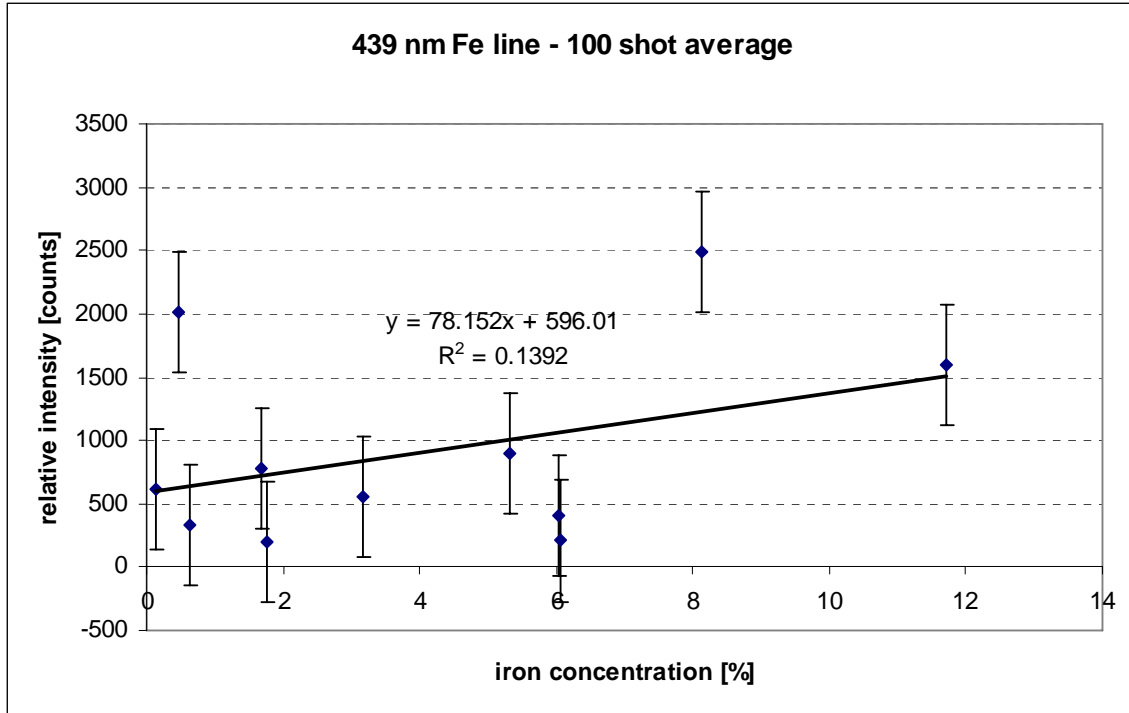


Figure 7 – Correlation of the 439nm Iron Emission Line

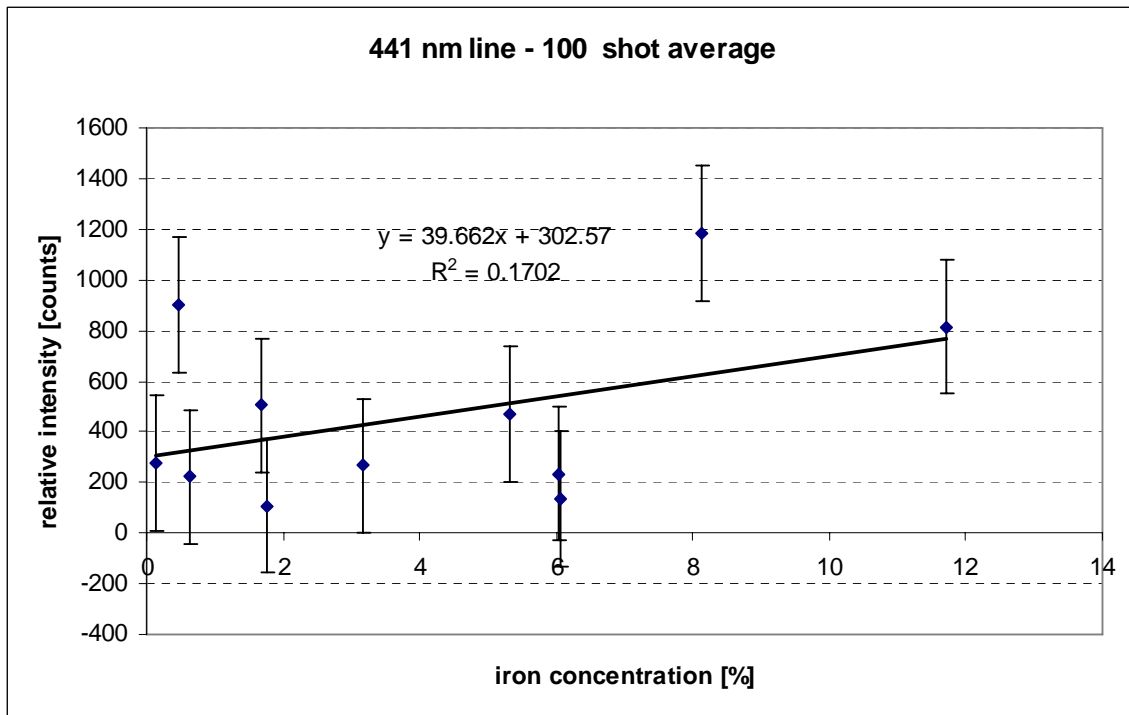


Figure 8 – Correlation of the 441nm Iron Emission Line

The iron lines showed a poor correlation between emission line intensity and elemental concentration. The iron found in coal is mostly mineral forms of iron, such as iron oxide [4]. The iron used to make the synthetic mixtures was pure iron powder. It is hypothesized that the iron powder formed together when subject to the grinding unit instead of being dispersed.

## **Dynamic LIBS**

### **Theory of Dynamic LIBS**

Since the LIBS spark is brief, it is necessary to have a time frame in which the characteristic line spectra can be observed. In their review, “Quantitative micro-analysis by laser-induced breakdown spectroscopy: a review of the experimental approaches”, Tognoni states that early stages of the laser-induced plasma will contain black body continuum radiation [6]. The continuum correlates to a physical process of plasma formation and cannot be reduced through averaging, though it can be normalized through use of Wien’s Law. The best way to compensate for the continuum emission is to activate the spectral acquisition with a proper delay after the laser-induced plasma has been produced. So far, LIBS experiments have been temporally resolved by the use of an Intensified CCD (or ICCD). The ICCD allows the option of temporal gating. This means that the end user of the equipment can set a delay time after the black body continuum has been reduced and during an optimal time for observing the characteristic line spectrum of the element in question.

The dynamic LIBS method was developed to observe temporal behaviors of multiple emission lines in a single LIBS spectrum. This system incorporated the use of a polygonal scanning mirror to achieve temporal differentiation within the emission spectrum. To current knowledge, this was the first time a polygonal scanning mirror was applied to a LIBS experiment for time-resolved studies. The polygonal scanning mirror reflected light off of one of its facets, creating a line image instead of a focused image of the LIBS spark. Each segment of the line will correspond to a different time. The scan line fell on the entrance slit of the spectrograph. The light fell on the CCD array in an area that correlated to a temporal profile, creating a temporally resolved, as well as a spatially resolved LIBS signal.

### **Calculation of the Dynamic LIBS Time Frame**

The mirror used was a disk-shaped mirror with 30 facets around the circumference of the disk. When the mirror was turned on for dynamic LIBS testing, it spun at 12,000 rpm. The spinning of the scanning mirror allowed for a time-dependent signal to be observed. The dimensions for each facet were 9.8mm high by 6.0 mm wide. The incident light on the facet was in the form of a circle with a diameter 8.9 mm. The light filled up the spinning facet, which reflected a line on the entrance slit to the spectrograph. Each different position in the “line” corresponded to a different time of the spark life. The line was not made up of discrete spots, but rather an overlapping of the spots, which resulted in a convoluted signal, though time-dependent characteristics could still be observed.

The number of facets and the rotation speed in the scanning mirror determined the time frame in which the laser spark was observed. The scanning mirror had 30 facets around

the circumference of a disk, which resulted in a 12 degree scan angle for each facet. The rotation speed of the scanning mirror was set at 200 revolutions per second. The value in revolutions per second was converted into degrees per second by multiplying by 360. The scanning mirror had a rotation speed of 72,000 degrees per second. The full 12 degree scan of an individual mirror facet would take 167 microseconds. To encompass the 167 microsecond in a single scan, the full 12 degrees of the scan had to be used. The focusing lens did not include the full scan of the mirror facets. The optical path from the scanning mirror to the focusing lens was 330 mm. For the full scan of a facet to be encompassed, the lens diameter would have to be 62.6mm. The diameter of the focusing lens was 25.4mm, resulting in a reduced scan angle, and therefore, a reduced time frame of observation.

To calculate the window of observation, the beam was modeled in OSLO. From the OSLO modeling, the length of the line incident on the entrance slit of the spectrometer was calculated to be 2 millimeters. The operational scan angle was calculated to be 2 degrees.

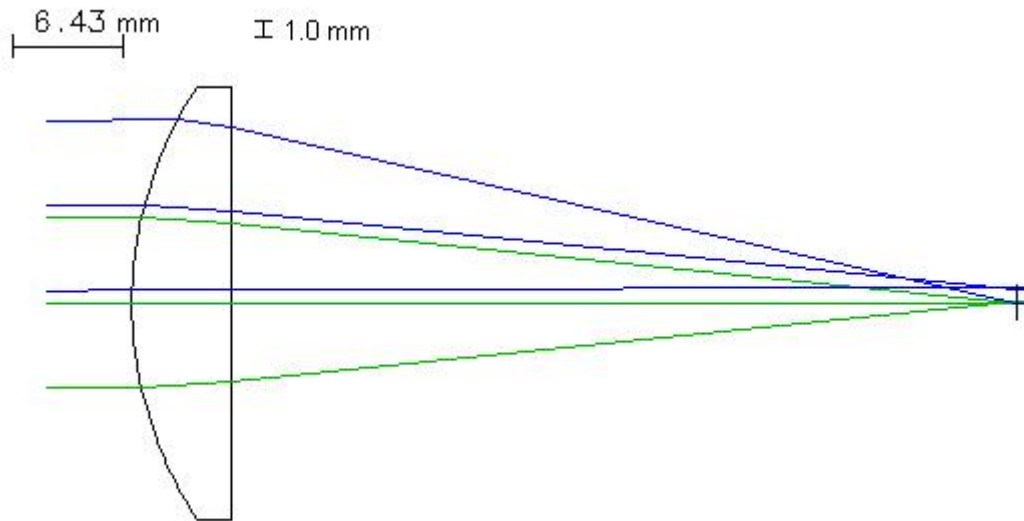


Figure 9 - Modeling in OSLO

From the rotation speed of the scanning mirror and the number of degrees per incident scan, the observation window was calculated at 27.8 microseconds. The size of the incident line (2mm) was used to calculate the region of the CCD used. The CCD has 256 pixels and is 6mm high. The incident line from the laser spark was 2mm high. Of the 256 pixels on the CCD, 86 pixels were actively collecting light from the laser spark. The time scale for the dynamic LIBS experiments was calculated to be 0.32 microseconds per pixel.

### Signal Processing and Analysis

The final focusing lens of the experimental set up eclipsed the dynamic LIBS signal. The signals of the true time-dependent characteristics of the emission lines were convoluted by the effects of the eclipsing. To recover this data, a function had to be formulated to deconvolute the effects of the eclipsing. The eclipsing of the beam and the lens was modeled in AUTOCAD. The modeling process calculated the areas of the incident beam of the laser spark as it moved off of the final focusing lens.

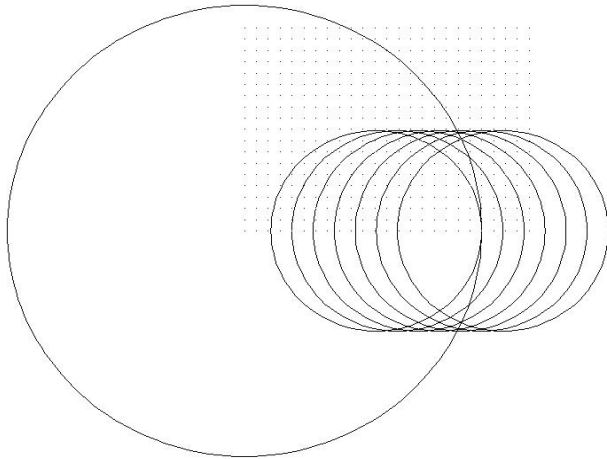


Figure 11- Traveling beam incident on the lens

The calculated areas were plotted with respect to center to center distance of the two circles. The larger circle modeled the clear aperture of the lens and the smaller circle modeled the incident light from the laser spark. A polynomial fit of the areas of the eclipsed smaller circle with respect to center to center distance was used to normalize the dynamic LIBS data. This equation best fit the trend in which the area of the eclipsed smaller beam decreased as the center to center distance of the two circles increased. The signal,  $S(x)$ , from the dynamic LIBS test can be described as the time dependent behavior, which convoluted with the eclipsing function, as shown in Figure 12.

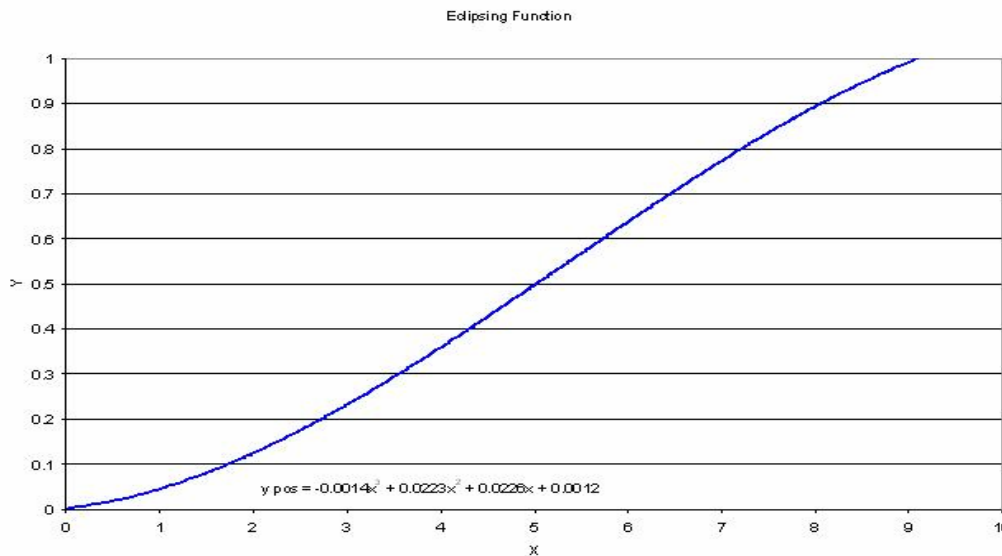


Figure 10 - Eclipsing Function

Dynamic LIBS shows time-dependent characteristics of multiple emission lines within a single laser spark. Complications arise in signal analysis due to experimental conditions. The scanning mirror was not synchronized with the rest of the experimental set up. This results in a “brute force” testing method and random time intervals. Another

complication was eclipsing, which was resolved by application of a normalizing function. The original dynamic LIBS signal was refined by background reduction and normalization before any trends in the data were observed.

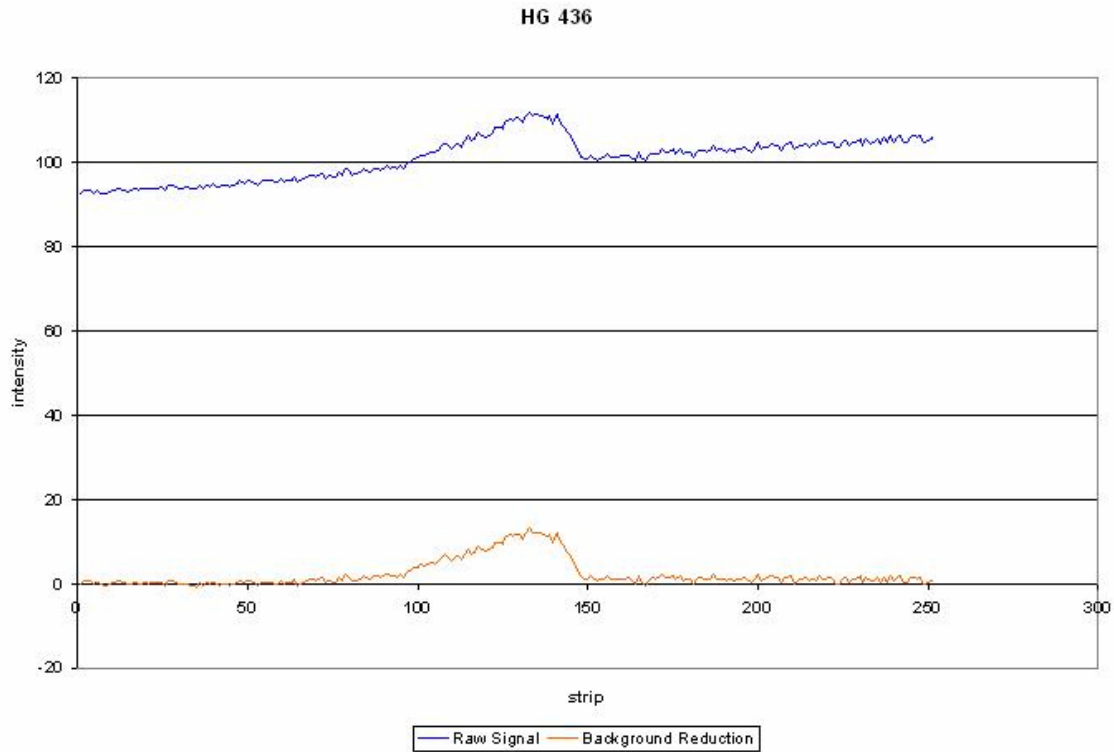


Figure 11 - Original and Background Corrected Signals

The application of a time scale and de-convolution of the eclipsing effect followed the initial background correction. Emission lines were plotted together to observe their temporal behavior simultaneously. Figure 14 shows processed data before the eclipsing effect was normalized. The solid line at  $x = 0$  is approximately where the laser spark begins. A fast rise time is indicative of plasma formation. Decay times for the emissions of iron and mercury follow shortly after the plasma formation, while carbon decay seems to either be delayed or have a much slower decay rate, as indicated by the plateau shape following the plasma formation in the carbon related lines.

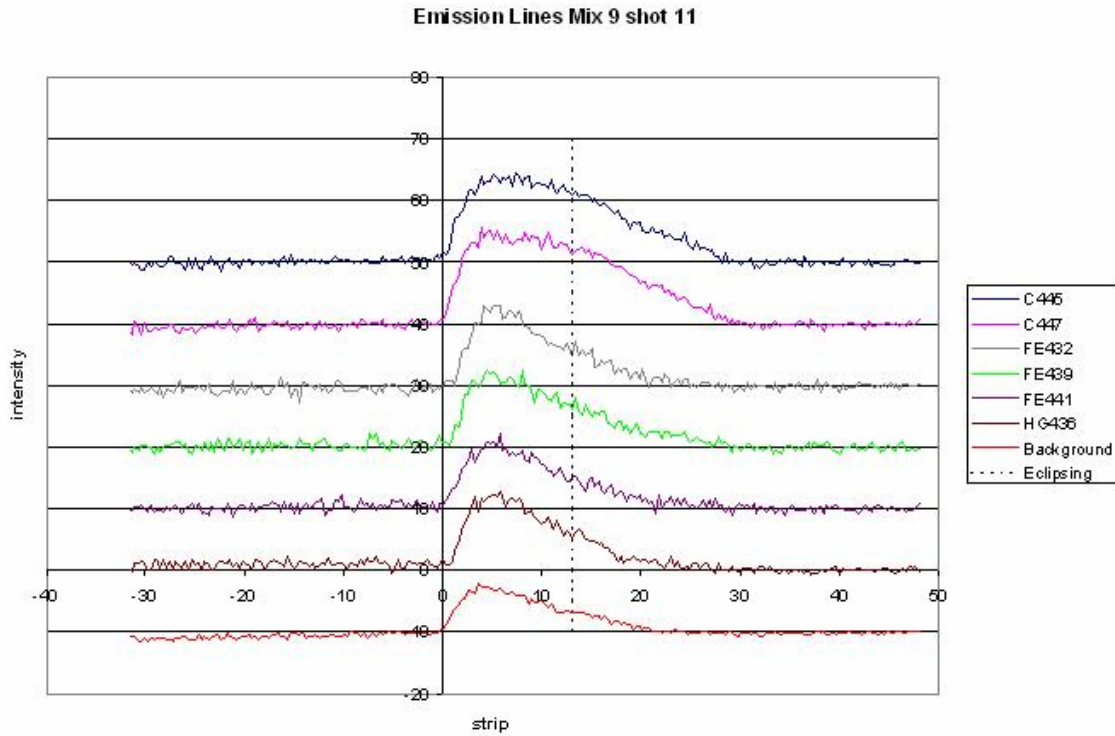


Figure 12 – Background Corrected, Time Scaled Dynamic LIBS Signal

The eclipsing effect, which takes place around ten to fifteen microseconds after spark formation, makes the remaining signal look linear. Normalization of the eclipsing effect revealed exponential decay in the emission lines. It was observed that the 436nm mercury line showed the most immediate and fastest decay rate. Iron lines seemed to have immediate decay, but a slower decay time than the mercury decay. All emission lines seem to show at least a 4 microsecond delay time before the decay begins. Carbon decay was the most difficult to observe. In some cases, carbon was observed to have a longer delay time before decay occurred. In other cases, carbon was shown to have a more gradual decay than iron or mercury. In either case, the carbon related emission lines showed drastically different characteristics than those of iron and mercury.

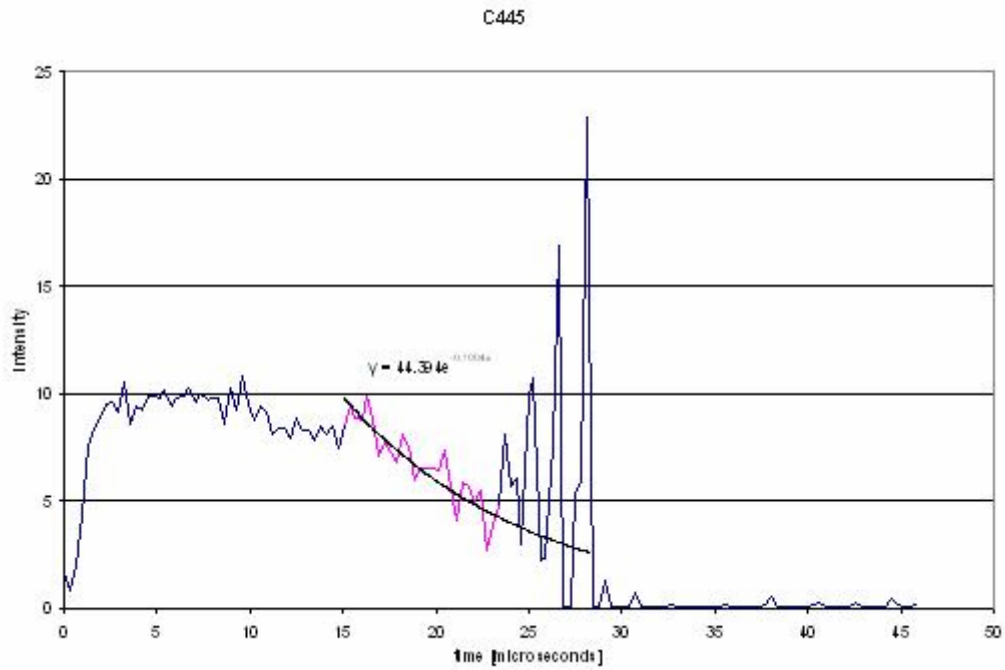


Figure 13 - C 445nm temporal behavior

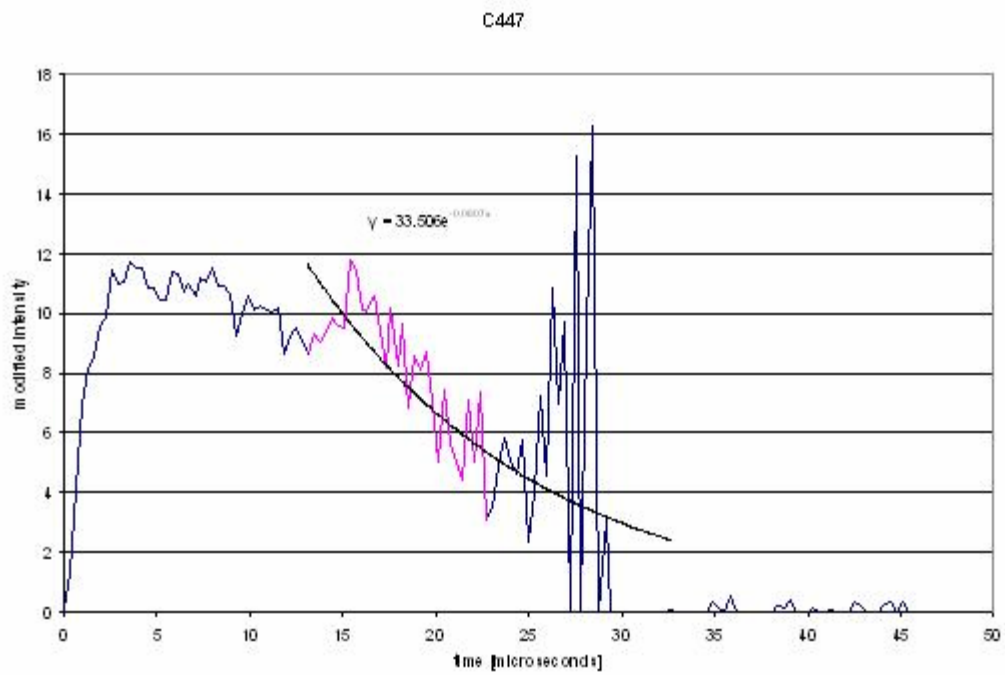


Figure 14 - C447nm temporal behavior

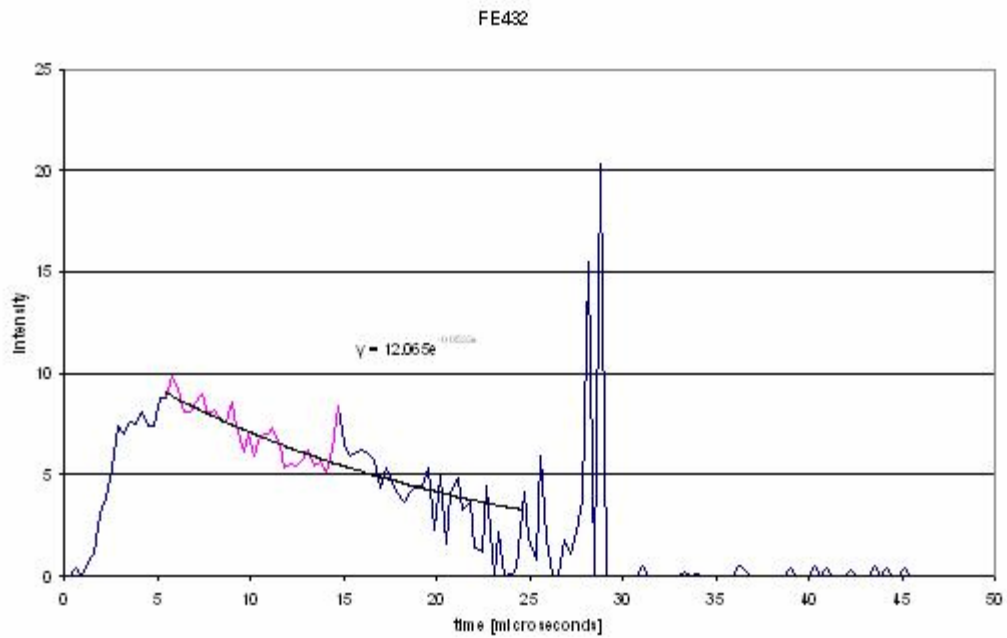


Figure 15 - FE 432 nm temporal behavior

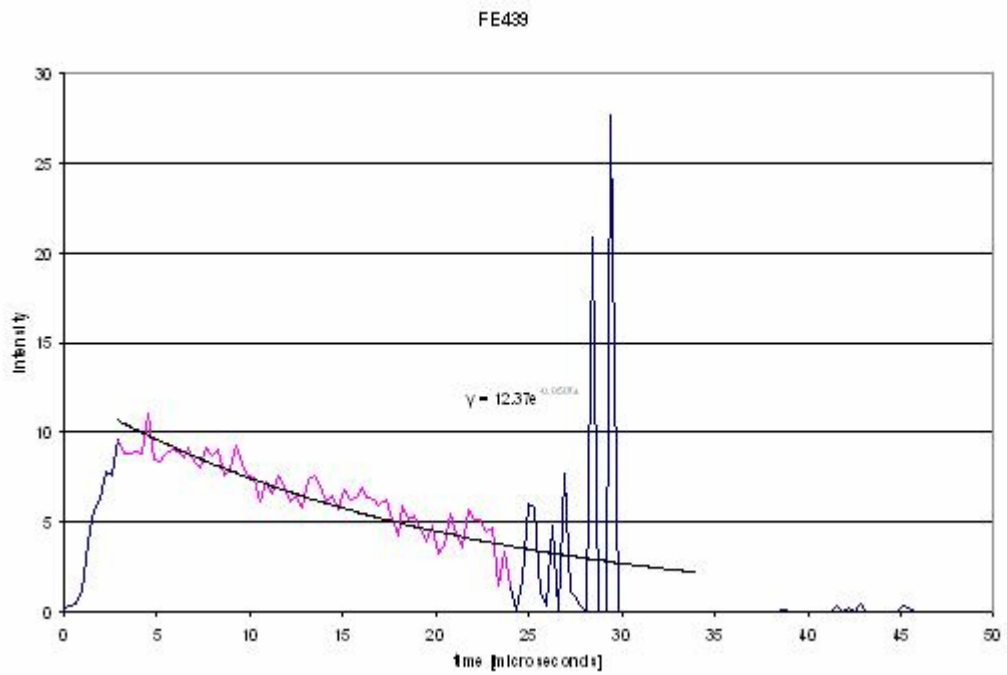


Figure 16 - FE 439 nm temporal behavior

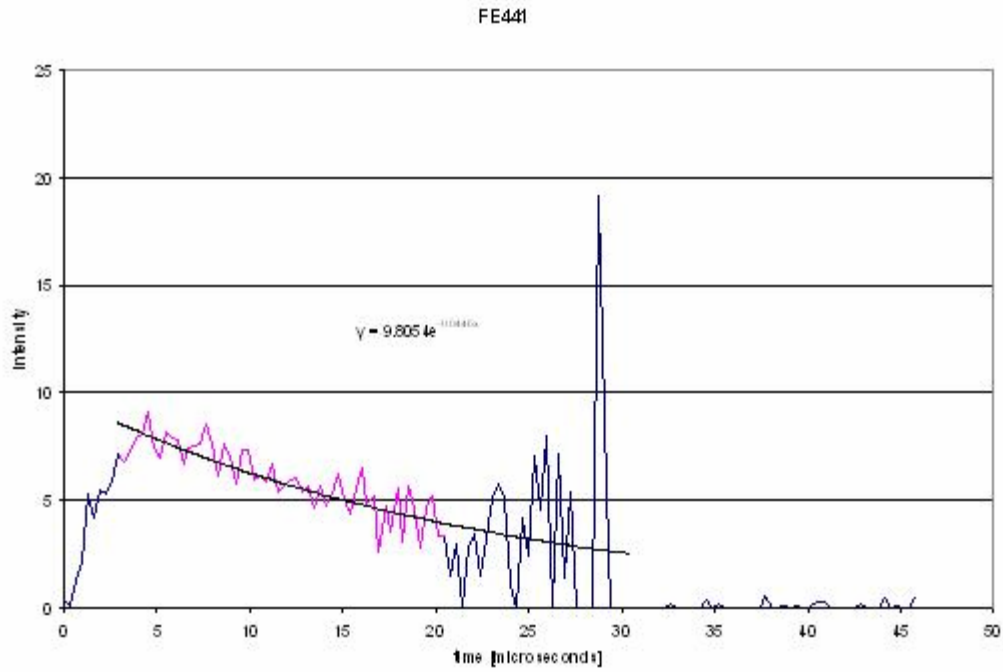


Figure 17 - FE 441 nm temporal behavior

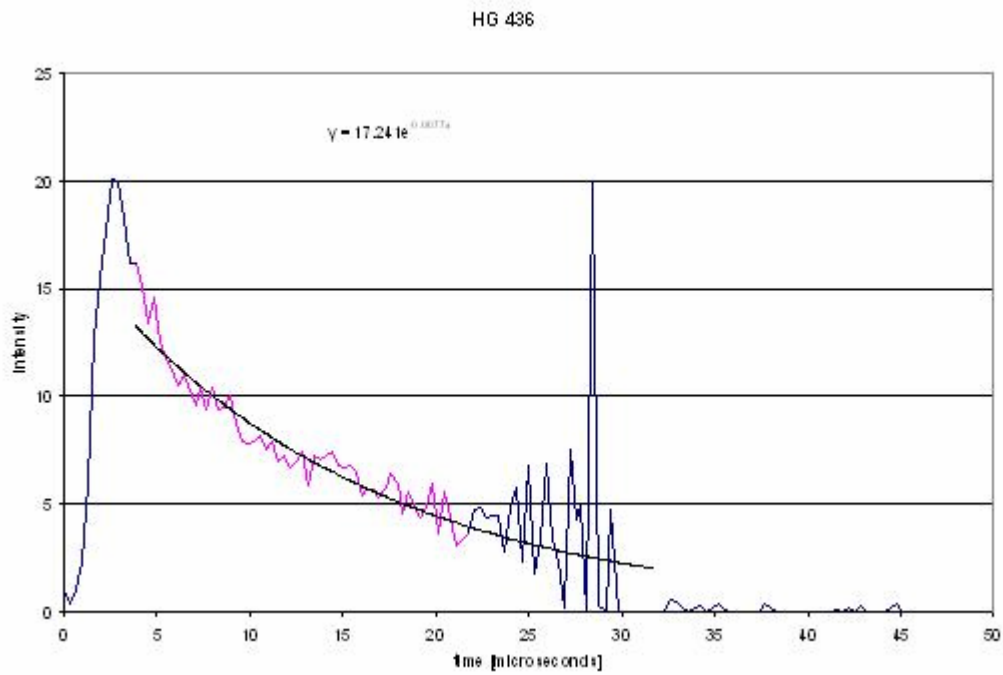


Figure 18 - HG 436 nm temporal behavior

## CONCLUSIONS

A LIBS system has been developed to detect C, Fe, and Hg in coal. Significant information has been obtained in analyzing the signals. The ability to detect C, Fe, S, and Hg by this system has produced mixed results. Upon obtaining data, the strength of the modified intensity signal from the collected light was plotted with respect to known concentration in the specimen. The graph of relative intensity with respect to concentration resulted in a strong correlation within the carbon and mercury emission lines. Carbon, which ranged from 61 – 81% mass within the synthetic coal mixture, resulted in strong correlations between line intensities and signal strength. Since there were some discrepancies of the identity of the two emission lines, pure carbon was tested and added to Figures 4, 5, and 6. The test showed that the line intensities from pure carbon were stronger than the intensities from the test samples, proving that carbon could be identified qualitatively as well as quantitatively within the 431-452nm wavelength range.

Use of the 436nm emission line as a means of detecting mercury was accurate to 800ppm. A plot between the signal strength and the concentration yielded a strong correlation, with only one discrepancy point, possibly due to a mixing error. The 800ppm limitation was due to the system hardware. A more sensitive detection instrument is required to attain lower detection limits.

Sulfur could not be detected using this experimental apparatus. This may be due the air quenching effect reported earlier [7]. Since the most sensitive emission lines in the sulfur spectrum are below 200nm, a combination of special optics and a vacuum environment are required to optimize the detection of sulfur.

Iron emission lines showed poor correlation between signal strength and concentration. This could be due to the mixing of pure iron in powder form within the synthetic mixtures as opposed to iron oxide. It is hypothesized that during the grinding and mixing process, the iron was drawn together instead of dispersed evenly, creating pockets of highly concentrated iron within the samples.

Based on qualitative and semi-quantitative analysis, dynamic LIBS testing provides basic information on the lifetime and temporal characteristics for individual emission lines. Mercury seems to have a more sudden decay, while carbon and iron show a slight delay before actual decay occurs. The data upon observation of emission lines of one specie compared to another suggests that emission lines possess differing temporal characteristics.

## FUTURE WORK

### System Improvements

The sensitivity and accuracy of the LIBS method developed within the scope of this research can be improved upon. This research has shown that all of the elements of interest have the possibility of being quantitatively analyzed much faster than the traditional ASTM methods. Because of the limited detection of mercury and sulfur within the synthetic coal

mixtures, future work should be focused on the development of the sensitivity limits and the synchronization of the current LIBS system.

Because of the effects of oxygen quenching mercury and sulfur emission lines, a vacuum environment or an inert gas environment could be created to enhance LIBS signals. To further enhance the signal, the CCD detector could be replaced by an Intensified CCD (ICCD) camera. An ICCD camera with time gating capabilities can be up to one thousand times more sensitive than a regular CCD camera. If the ICCD camera is used as a detector, and the samples are placed in a vacuum environment, the current LIBS apparatus could attain sensitivity in the part per billion range.

To improve upon the correlation of the iron signal, coal can be mixed with iron salts instead of pure iron. The iron salts should not be clumped together during grinding, and should produce a better distribution throughout the mixture. This would result in a better homogenization of iron throughout the synthetic mixtures, giving a more accurate representation of the iron concentration within the coal sample. Improvements within the pellet making procedure in this experiment can result in more accurate measurements and a better mixture for calibration of the LIBS system.

Dynamic LIBS testing gives us qualitative data of how different emission lines behave. The analysis of the dynamic LIBS signals allowed for observations of time-dependent characteristics of different emission lines. Because the system was not synchronized, a “brute force” method was relied upon to obtain usable dynamic LIBS signals. Synchronization of the spinning mirror in conjunction with the laser and the CCD camera would be necessary for commercialization of this apparatus. Anomalies in the dynamic LIBS data were observed. A further study of these anomalies will allow for a better understanding of the temporal behavior of the emission lines and the laser-induced plasma.

### **The Ideal LIBS Apparatus**

With all the recommended system improvements being implemented into one system, a significantly improved LIBS system can become a reality. The apparatus and procedure of this ideal apparatus is very similar to this experimental work. Differences between the ideal and current system would be the vacuum chamber in which LIBS testing can be done. Though the implementation of a vacuum chamber will result in the loss of instrument mobility and on-line measurements, ambient air that quenches sulfur and mercury emissions will be removed, resulting in a detectable sulfur signal and greater sensitivity to mercury. The ideal LIBS apparatus would have a high resolution spectrograph that interfaces with a specialized UV sensitive ICCD to select and tune the wavelength range, a vacuum chamber with specialized optics to tune in on the ultraviolet sulfur emission lines, synchronization between the laser and the spinning mirror. With these significant improvements to the system, an ideal LIBS apparatus can be built that can improve upon the existing results obtained in this research.

## REFERENCES

- [1] Kurihara, Ikeda, Izawa, Deguchi, Tarui; "Optimal boiler control through real-time monitoring of unburned carbon in fly ash by laser-induced breakdown spectroscopy", *Applied Optics* (2003), 42(30) 6159-6165
- [2] Ottesen, Baxter; "Laser Spark Emission Spectroscopy for in Situ, Real-Time Monitoring of Pulverized Coal Particle Composition", *Energy & Fuels* (1991) 304-312
- [3] Wiesburg, De Saro, Craparo; "Real Time, In-Situ Laser Sensor for Feedstock Monitoring in Gasifiers", *Proceedings of the International Technical Conference on Coal Utilization & Fuel Systems* (2004), 29th(Vol. 1) 445-456
- [4] Harrison; Massachusetts Institute of Technology Wavelength Tables, 1969 M.I.T Press, Cambridge MA
- [5] Lazzari, De Rosa, Rastelli, Ciucci, Palleschi, Salvetti; "Detection of mercury in air by time-resolved laser-induced breakdown spectroscopy technique", *Laser and Particle Beams* (1994), 12(3), 525-530
- [6] Tognoni, Palleschi, Corsi, Cristoforetti; "Quantitative micro-analysis by laser-induced breakdown spectroscopy: a review of the experimental approaches", *Spectrochimica Acta Part B* (2002), 57, 1115-1130
- [7] Sturm, Noll; "Laser-induced breakdown spectroscopy of gas mixtures of air, CO<sub>2</sub>, N<sub>2</sub>, and C<sub>3</sub>H<sub>8</sub> for simultaneous C, H, O and N measurement", *Applied Optics* (2003), 42(30) 6221-6225

**Appendix 25: Development of a Novel Optical Radiation Depolarization  
Technique for On-Line Measurements of Particle and Bubble Sizes  
(KY003)**

## TECHNICAL PROGRESS REPORT

Contract Title and Number:

Crosscutting Technology Development at the Center for  
Advanced Separation Technologies  
(DE-FC26-02NT41607)

Period of Performance:

Starting Date: 10/1/2002  
Ending Date: 10/31/2006

Sub-Recipient Project Title:

Development of a Novel Optical Radiation  
Depolarization Technique for ON-Line Measurements  
of Particle and Bubble Sizes

Principal Investigators:

Tao, Menguc, Crofcheck

Report Information:

Type: Semi-Annual  
Number: 6  
Period: 10/1/05-3/31/06  
Date: 4/1/2006  
Code: KY003-R06

Contact Address:

University of Kentucky  
234 MMRB  
Lexington KY 40506

Contact Information:

Phone: (859) 257-2953  
Fax: (859) 323-1962  
E-Mail: dtao@engr.uky.edu

Subcontractor Address:

No subcontracts issued.

Subcontractor Information:

Phone:  
Fax:  
E-Mail:

### ABSTRACT

The feasibility of using elliptically polarized light scattering (EPLS) method to monitor both bubble size and gas hold-up in a bubble laden medium was further studied. It has been shown that with the use of EPLS, normalized scattering matrix elements ( $M_{ij}$ 's) at different side and back scattering angles can be obtained, and then correlated as a function of required physical parameters. In the experiments, first, gas flow rate was related with bubble size for nitrogen-water (GL) flow and gas hold-up at different surfactant concentrations (10, 20, 100, 200 ppm) using a video and image processing system. Based on these images, bubbles were assumed to be spherical, and their normalized scattering matrix elements were calculated using the Lorenz-Mie theory. After the experiments were conducted, scattering matrix elements were determined using the intensity values measured for different polarization settings. It is observed that the change in bubble size yields significant changes in  $M_{11}$ ,  $M_{33}$ ,  $M_{44}$ , and  $M_{34}$  profiles for gas velocity range of 0.04 to 0.35 cm/s ( $ID = 4.5$  cm). Based on these results it is shown that both the bubble size and velocity can be monitored using scattering measurements at a single angle ( $\theta$ )  $120^\circ$ . The optimum angle to take light scattering measurements depends on frit pore size, column diameter, gas pressure and surfactant concentration.

## INTRODUCTION

### Background

Grinding and froth flotation are the two most important processes for mineral beneficiation. The importance of grinding is well reflected in the fact that approximately 80% of beneficiation costs are for grinding, mainly due to high energy consumption. To reduce energy consumed by grinding, fines should be removed quickly from the grinding circuit. This requires a reliable on-line particle size analysis technique. Froth flotation is the most widely used solid-solid separation process for coal and minerals beneficiation and about 90% of mineral concentrates are produced from froth flotation. It is now recognized that air bubble size distribution plays an important role in flotation separation performance [1]. Optimization of bubble size distribution is possible only if bubble size can be monitored on-line. Obviously, an on-line analysis technique for particle and bubble size is critical for enhanced grinding and flotation process efficiency.

Light scattering is one of the most effective concepts for characterization of particles and bubbles. When either vertically or horizontally polarized light is incident on the medium, it goes through a number of scattering events. Bubbles are considered much larger than the wavelength of the incident light, which is a reasonable approximation even for bubble diameters as small as 5  $\mu\text{m}$ .

### Objective and Approach

The overall objective of the proposed research program is to develop a concept based on optical radiation depolarization measurement technique for on-line real-time size analysis of grinding and flotation processes to minimize energy consumption during grinding and maximize flotation efficiency. The technique is based on use of angular and radial profiles of reflection and transmission of an object subjected to a collimated, polarized light beam.

## PROJECT TASKS

Even though most light scattering particles that are optically more dense than the surrounding medium ( $n' < 1$ ), relative refractive index for gas bubbles in the liquid is smaller than one ( $n' = 0.751$ : nitrogen bubbles in water). Therefore total reflection plays an important role on scattering and critical scattering angle creates two regions along scattering angle. Range of region-one where normal scattering occurs is from  $\theta = 0^\circ$  to  $\theta_c$  and region two from  $\theta = \theta_c$  to  $180^\circ$ . Definition of the critical scattering angle:  $\theta_c = 2 \cos^{-1}(n')$ .  $\theta_c = 82.8^\circ$  nitrogen gas bubbles in water. Scattering measurements taken in the region two indicate there is no total reflection effect between  $\theta = 90^\circ$  to  $160^\circ$  (side to back scattering). Another reason to choose back scattering angles to take scattering measurements is that the medium (bubbles in water) become optically thick when gas velocity and surfactant concentrations are increased. After converting intensity values to scattering matrix elements,  $M_{ij}$  values were plotted as a versus scattering angle for each flow rate (mean bubble size) as shown in Figure 1 for a surfactant concentration of 100 ppm.

Solid curves in the Figure 1 show ray tracing results for a 0.5 mm-diameter bubble in water. Details of the Ray-Tracing/Monte Carlo method are given in the literature [2]. In the model calculations, the influence of possible nonsphericity of bubbles, light absorption and multiple light scattering effects are neglected. Refractive index of nitrogen is assumed to be 1.000297 at  $\lambda = 632$  nm for model calculations. Depending on surfactant concentration and gas velocity, bubble shape changes from sphere to disk with a maximum aspect-ratio of 1.46 (for large bubbles at high flow rates) was observed from the digital bubble pictures. Therefore modeling results for two extreme shape cases (sphere and disk with aspect ration 1.46) are shown in Figure 1. Modeling results show shape effect on scattering radiation patterns are small because cross-section of bubbles in the plane where measurements taken are close to circular.

With the change mean bubble diameter,  $M_{11}$  curves change as well, as expected. However, in back scattering angles, for example around  $\theta = 145^\circ$ , the  $M_{11}$  values are relatively less sensitive to bubble diameter. On the other hand, the profile of  $M_{22}$  can reveal both the deviation of the bubble from presumed spherical shape and the demarcation zone between the single- and the multiple-scattering zones. When the flow rate increases, we observe from digital images that bubble size changes from sphere to oblate spheroid (Figure 1). The theoretical degree of linear polarization ( $DLP = -M_{12}$ ) that represents single scattering gives an upper border for light scattering measurements taken for a medium with many bubbles.  $DLP$  ( $-M_{12}$ ) does not show any trend to relate with gas velocity and  $DLP$  is small for all gas velocities. Especially when gas velocity is high,  $M_{12}$  information is disturbed by multiple scattering effects. The degree of circular polarization ( $DCP = M_{33}$  or  $M_{44}$ ) increases when mean bubble size increases. The  $M_{44}$  curve at lowest flow rate is close to curve from ray-tracing. Overall,  $M_{33}$  and  $M_{44}$  seem to be reasonable reliable parameters to monitor gas velocity between scattering angles 110 and  $150^\circ$ .

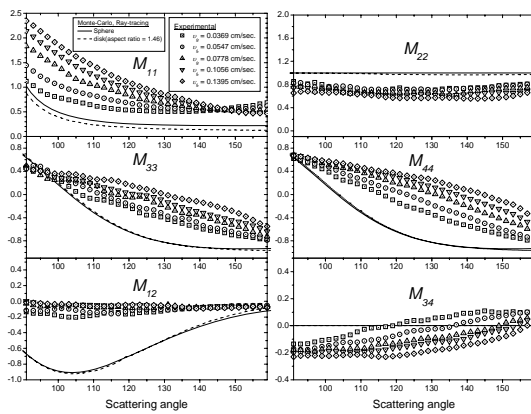


Figure 1. Scattering matrix elements ( $M_{ij}$ ) calculated from experimental intensity measurements between  $90^\circ$  and  $160^\circ$  at different superficial gas velocities and a surfactant concentration of 100 ppm.

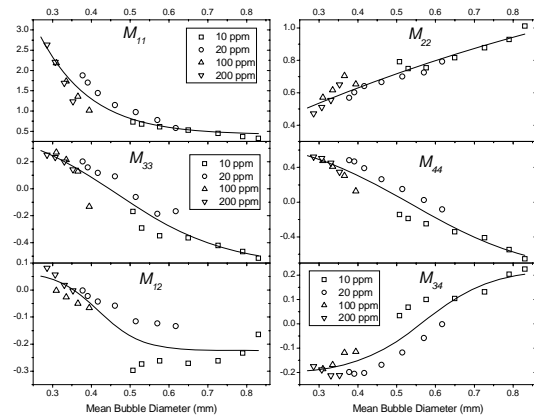


Figure 2. Scattering matrix elements ( $M_{ij}$ ) at  $120^\circ$  as a function of mean bubble diameter (mm). The solid lines indicate curve-fittings.

$M_{34}$  represents how much of linearly polarized light is converted to circularly polarized light by bubbles. The ray-tracing curve for  $M_{34}$  is always zero between  $\theta=90^\circ-160^\circ$ , because the bubbles can not transform linearly polarized light to circularly polarized light by scattering, if the scattering angle is greater than the critical angle ( $\theta > \theta_c = 82.8^\circ$ ) [3]. However, experimentally measured  $M_{34}$  values are not zero because increased gas velocity generates more bubbles, contributing to multiple scattering. The dynamic range of the experimentally measured  $M_{34}$  is large enough to be used to monitor gas velocity.

In order to understand relationship between gas velocity and  $M_{ij}$ , single angle scattered measurements were conducted at  $\theta=120^\circ$  where separation gas velocity curves with most of scattering matrix elements is possible. Gas velocities were converted to mean bubble diameter and gas hold-up and plotted against the measured  $M_{ij}$  values, as shown in Figure 2.

Figure 2 shows that it is possible to predict bubble diameter based on scattering measurements:  $M_{11}$ ,  $M_{22}$ ,  $M_{33}$ ,  $M_{44}$ , and  $M_{34}$  are sensitive to bubble diameter at low gas velocities with medium-low surfactant concentrations. At high superficial gas velocities ( $v_g > 0.2$  cm/s), there are little to no changes in the size of the bubbles as the flow rate increases, which illicit small changes in the matrix elements.

Figure 2 also shows how the amount of the gas in the water affects the scattering at a scattering angle of  $120^\circ$ . Even though the gas hold-up increases linearly with increasing gas velocity, effect of gas hold-up on  $M_{ij}$  depends on surfactant concentration. For a low-medium surfactant concentration,  $M_{11}$ ,  $M_{33}$ , and  $M_{44}$  increase as gas hold-up increases.  $M_{12}$  decreases rapidly and  $M_{34}$  increases when bubble size increases with increasing flow rate and surfactant concentration.  $M_{22}$  changes drastically at higher surfactant concentrations, unlike other scattering matrix elements, because the shape factor of bubbles is decreasing with increasing gas velocity and the number of bubbles increases (multiple scattering regime).  $M_{34}$  decreases at single scattering region but it decreases in the multiple scattering zone. Monitoring gas hold-up based on  $M_{ij}$  measurements is possible at some gas velocities for known surfactant concentrations.

## SUMMARY

An elliptically polarized light scattering (EPLS) approach was investigated as a technique for monitoring the mean bubble size and total gas hold-up of GL mixtures. A series of experiments were conducted which showed that the profiles of scattering matrix elements are sensitive to the bubble size and gas-holdup. This sensitivity suggests that the measurement of these parameters at a limited number of back-scattering angles can provide a robust approach for monitoring mean bubble size, flow rate, and gas hold-up.  $M_{11}$ ,  $M_{33}$ , and  $M_{44}$  values at  $\theta = 120^\circ$  yield promising performance for monitoring of GL systems at a low-to-medium flow rates and surfactant concentrations. On the other hand,  $M_{22}$  values at  $\theta = 120^\circ$  can be used to monitor gas-hold-up at high flow rates and surfactant concentrations. There are two disadvantages associated with the  $M_{12}$ -based monitoring 1) it decreases at low surfactant concentration with increasing gas hold-up, but it increases when surfactant concentration medium-high and 2) because of multiple scattering affect, its value can be very

small and may not show any a trend for different gas flow rates at medium-high flow rates and surfactant concentrations.

## **FUTURE WORK**

For the next two quarters, research efforts will be focused on the characterization of particle size based on light scattering. Particular attention will be directed toward optical thickness of the slurry, bimodal polydisperse characteristics of size distribution, and different optical properties of mineral and coal particles.

## **REFERENCES**

1. Tao D, Role of bubble size in flotation of coarse and fine particles - A review, *Separation Science and Technology* 2004; 39: 741-760.
2. Macke A. Monte Carlo calculations of light scattering by large particles with multiple internal inclusions. Chapter 10 in *Light Scattering by Nonspherical Particles*. Ed. Mishchenko MI, Hovenier JW, and Travis LD. New York: Academic Press, 2000.
3. Kokhanovsky AA. Optical properties of bubbles. *Journal of Optics-A* 2003; 5: 47-52.

**Appendix 26: Mineral Liberation Analysis in 3D by X-Ray MicroCT for  
the Evaluation of Particle Separation Efficiency (UT006)**

## TECHNICAL PROGRESS REPORT

Contract Title and Number:

Crosscutting Technology Development at the Center for  
Advanced Separation Technologies  
(DE-FC26-02NT41607)

Period of Performance:

Starting Date: 6/1/2004  
Ending Date: 10/31/2006

Sub-Recipient Project Title:

Mineral Liberation Analysis in 3D by X-Ray MicroCT  
for the Evaluation of Particle Separation Efficiency

Report Information:

Type: Semi-Annual  
Number: 3  
Period: 10/1/05-3/31/06  
Date: 04/30/06  
Code: UT006-R03

Principal Investigators:

Lin

Contact Information:

Phone: (801) 581-5309  
Fax: (801) 581-8119  
E-Mail: cllin@mines.utah.edu

Contact Address:

University of Utah  
135 South 1460 E. Room 412  
Salt Lake City UT 84112

Subcontractor Address:

No subcontracts issues.

Subcontractor Information:

Phone:  
Fax:  
E-Mail:

### ABSTRACT

For continued technological progress in the field of multiphase particulate separation processes, the need for quantitative spatial analysis of multiphase particles in three-dimensions has increased significantly. Such quantitative information must be accurate enough so that the measured values can be used as parameters for simulation models, process design procedures, and control strategies. Cone-beam X-ray microtomography technology (XMT) offers a unique imaging capability that can produce high-resolution (a few micrometers) three-dimensional images of the internal structure of multiphase samples. We propose to adapt this new technology to the mining industry to provide for the advanced analysis of coal and ore samples; such analysis of on-line plant samples will allow continuous control of separation processes. In this regard, The primary objective of the proposed project is the development of x-ray microrotomography technology (XMT) for detailed 3D liberation/exposure analysis of coal and mineral samples. The secondary objective will be to evaluate the feasibility of the XMT technology for the control of separation processes. This new XMT will combine the high-resolution 3-D XMT instrument and a classification algorithm in order to determine the sample composition and particle characteristics of plant samples. XMT will permit a fast, direct, and detailed 3-D analysis without sample preparation. Reconstruction of 3-D particle populations from XMT images

will not only provide sufficient information to construct the true liberation spectrum for the coal and ore samples in question, but also provide information on the particle size distribution, grain size distribution, and exposed surface area of mineral matter grains contained in each particle of the population sample.

Results from the proposed research will improve the efficiency of valuable mineral recovery using direct measurement of liberation information in order to optimize the separation efficiency. The XMT technique will be of great utility for the liberation analysis of a wide variety of mineral resources, including coal, industrial minerals, and metallic ores. In this regard, the XMT technology for coal washability analysis will allow for blending control to maximize coal recovery from coal preparation plants at a specified product quality. The results from the proposed research can be easily incorporated into existing simulation and estimation software systems for convenient application in industrial practice, both in the coal industry and in the mineral industry. Development of the XMT technology will allow for more rapid, detailed, and accurate analysis than previously thought possible.

## Background

New processing technology for improved productivity and efficiency is the key to success in today's highly competitive market place. It has been well established that appropriate analytical control systems can provide for such improvements. This is especially true of the particle separation processes used in the coal and mineral industries. Generally particulate materials are sampled from input and output streams and analyzed to evaluate the performance of the processing operations. In this regard, characterization and analysis of multiphase particles are of great technological importance. Most present methods to characterize and to analyze multiphase particles rely on heavy liquid fractionation<sup>(1)</sup> or on microscopic observation of a series of thin or polished sections<sup>(2,3)</sup> of the particulate sample. It is noted that these analytical procedures are time consuming and costly. The results are incomplete and cannot be obtained in a reasonable amount of time to provide a satisfactory feedback mechanism for the control of various unit operations in coal and mineral processing plants. In addition, the sectioning method is unsatisfactory for specific applications, for instance, to measure mineral exposure at the surface of locked particles which is most relevant for flotation separation processes. Even so, such traditional procedures are being used to obtain some limited information at great expense. For example automated instruments for polished section analysis which are currently being used in the mineral industry cost on the order of \$1,000,000.

These multiphase particulate assemblies are heterogeneous and have a wide variation of physical and/or chemical properties. Of course coal and mineral processing separation processes are based on the difference in the physical properties that influence the behavior of a particle inside the separation unit. In this regard, such heterogeneity can have a significant impact on the recovery and on the separation efficiency of concentration processes. In general, the separation efficiency for multiphase particulate systems depends on the statistical characteristics of particle microstructures, such as composition distribution, surface exposure of mineral grains, etc. For continued technological progress in the field of multiphase particulate separation processes, the need for quantitative spatial analysis of multiphase particles in three-dimensions has increased significantly. Such quantitative information must be accurate enough so that the measured values can be used as parameters for simulation

models, process design procedures, and control strategies. Cone-beam x-ray microtomography (XMT) offers a quantitative imaging capability that can produce high-resolution three-dimensional images of the internal structure of multiphase particulate samples at a resolution of 5 to 10 microns<sup>(4,5)</sup>. We propose to adapt this new technology to the mining industry to provide for the advanced analysis of exploration samples, for on-line analysis of plant samples, and eventually for the control of separation processes.

As mention previously, cone-beam x-ray microtomography (XMT) offers a quantitative imaging capability that can produce high-resolution three-dimensional images of the internal structure of particulate samples. We propose to adapt this new technology to the mining industry to provide for the advanced analysis of ore samples and for the on-line analysis of plant samples in order to provide a liberation basis for control of separation processes. In this regard, the goal of the proposed research is to provide the necessary technical information to use XMT for the measurement of mineral composition, and grain exposure. This new method will combine the 3D high-resolution XMT technique and a classification algorithm for determining the sample composition and particle characteristics of plant samples. The XMT technique permits a fast, direct, and detailed 3D-liberation analysis without sample preparation. Reconstruction of 3D particle populations from XMT images will not only provide sufficient information to construct the true liberation spectrum for the particle samples in question, but also provide information on the particle size, grain size distribution, and exposed surface area of the mineral phases which constitute the particle population.

XMT technology will lead to improvements in the efficiency of particle separation by direct measurement of liberation and other particle characteristics in order to establish the necessary conditions for the desired separation efficiency. The XMT technique will be of great utility for the liberation analysis of a wide variety of mineral resources, including coal, industrial minerals, and metallic ores. In this regard, the XMT technique can be used to frequently monitor the size distribution of locked grains; this capability will make it possible to make continuous changes to maintain operations at a high level of efficiency. The results from the proposed research can be easily incorporated into existing plant simulation software systems for convenient application in industrial practice. Development of such an analytical technique will provide the basis for more rapid, detailed, and accurate liberation analysis in the 21<sup>st</sup> century.

The objective of the research is to develop multiphase particle characterization and analysis technology for particle separation processes in the coal and mineral industries using x-ray microtomography. Importantly, the development and evaluation of XTM to establish the relationship between characteristics of multiphase particles and operation parameters will allow for improved design and control of particle separation processes.

### Objective and Approach

The primary objective of the project is the development of x-ray microrotomography technology (XMT) for detailed 3D liberation/exposure analysis of coal and mineral samples, including software for mineral identification. The secondary objective will be to evaluate the feasibility of the XMT technology for the control of separation processes.

## PROJECT TASKS

During the period ending March 31, 2006, Progress of the study is summarized as follows:

The main thrust of this research is the comparison of XMT liberation results in 3D with current assessment techniques for dissimilar mineral components of ore and coal samples. In this regard, copper ore and coal samples from Kennecott and Illinois No. 5 seams were selected for study. A high-resolution cone-beam microtomography system, installed at the University of Utah, is being used for detailed 3D analysis of these samples.

To effectively analyze a packed bed of multiphase particles for the determination of grain and particle size distributions, detection of particle/grain surface boundaries and classification of the particle population is critical. In this regard, implementation of the appropriate XMT software for size/composition classification of particles in ore and coal samples has been accomplished. Subsequent determination of the grain size distribution (including the exposed surface area) and liberation spectrum (coal washability analysis). The 3D-watershed segmentation algorithm for particle separation was developed. Results were discussed in the previous report. In addition, algorithms for the compositional classification of each separated particle in ore were discussed in the previous report. Results for the coal washability analysis from coal samples from Illinois No. 5 seams are discussed as follows:

### X-Ray Linear Attenuation Coefficient

It has been explained in previous report that the reconstruction algorithm applied to the data coming from a x-ray microtomography leads to the determination of attenuation coefficients in each voxel of the space domain. The space domain of measurements is divided in a given number of voxels based on the characteristic resolution of the test which could go up to 10  $\mu\text{m}$ . Each one of these voxels will store a given attenuation coefficient which represents all the material inside of it.

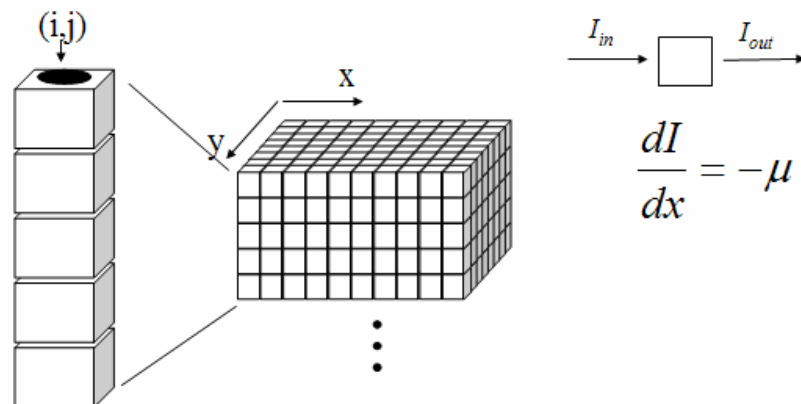


Figure 1. A matrix representation of the x-ray microtomography data.

## Linear Correlation of Density and Attenuation Coefficient

The attenuation coefficient assigned in a voxel is linearly related to the density of the material inside the voxel. A larger attenuation coefficient means that the material has a larger density which attenuates the pass of photons through the sample. This one-to-one relation allows us to match the attenuation coefficient of an unknown material sample with the density of a known material.

Figure 2 shows the result for four coal samples of known density scanned with the x-ray micro CT (XMT). It is clear that the mean of the attenuation coefficient is directly related to the density of the material; for a 1.3-1.5 g/cm<sup>3</sup> density range the attenuation coefficient distribution has a mean value of 0.02477 whereas for a 1.8-2.1 g/cm<sup>3</sup> density range the attenuation coefficient distribution has a mean value of 0.1128.

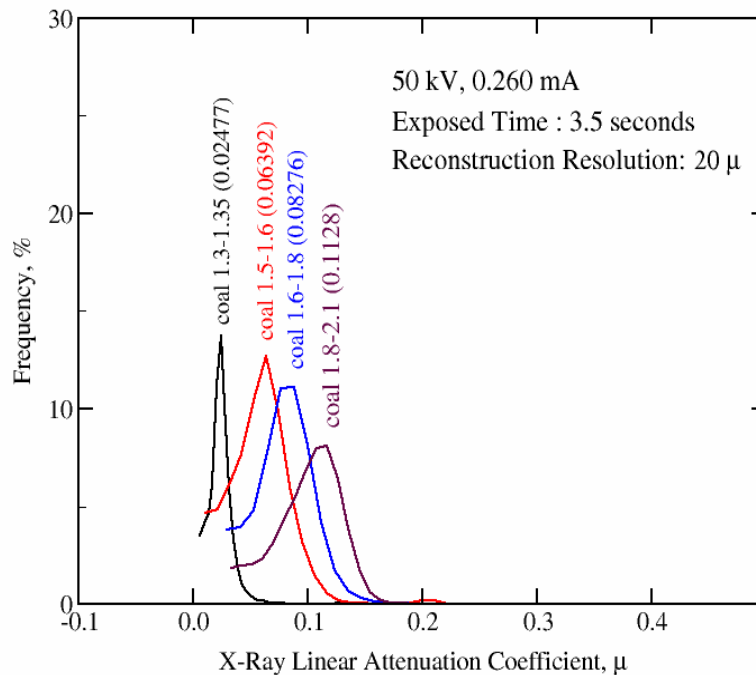


Figure 2. Histogram of four coal samples of known densities. Mean attenuation coefficients are given in parentheses.

From this analysis we may see that a linear relation can be constructed between density and attenuation coefficient mean value. This relation is the starting point to classify elemental voxels in unknown samples. Figure 3 shows the relation between density and mean values for the four coal samples.

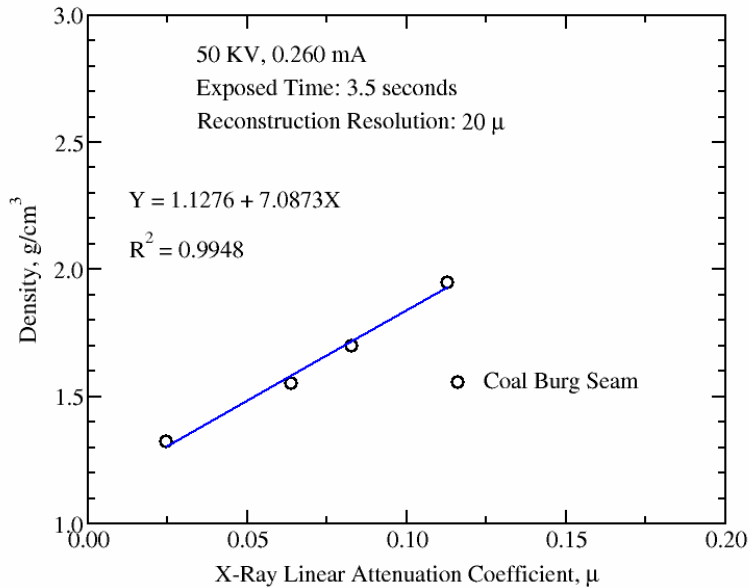


Figure 3. Relation between density and attenuation coefficient for four coal samples of known densities.

As shown in previous reports, for one side the watershed segmentation process allow us to identify individual particles in packed particle beds. For the other side, the density and attenuation coefficient relation associated to the use of Finite Mixture Distributions allow us to discriminate between different materials. These two components are used to show practical applications in mineral processing studies. In this progress report, the determination of the coal washability curves from Illinois No. 5 samples are discussed.

### Washability Curves

Heavy liquids are widely used in coal preparation in order to determine the required density of separation and the expected yield of coal of the required ash content.

The common method to determine the washability curve is through the use of a sequence of containers with heavy liquids of incremental density. This tedious laboratory test is known as sink-float analysis. For example in the case of an ore, the sample is introduced into the liquid of highest density. Then the floats product is removed, washed and placed in the liquid of the next container, whose product is transferred to the next container and so on. Finally the sink material is washed, dried and weighed, together with the final floats product, to give the density distribution of the sample by weight.

### X-ray CT Analysis

As was explained above, the principle behind the sink-float analysis is density fractionation. Therefore, the washability curve is then a result of the density composition of the material forming each particle. Each particle will float or sink according to its apparent density with respect to the fluid.

As discussion previously, the attenuation coefficient has a direct relation with the density of the phases, the atomic number and the x-ray energy of the XMT source. Based on

this principle and assuming appropriate experimental conditions, it would be possible to construct a calibration curve to find the explicit relation between these variables as was shown in Figure 3. With the relation between density and attenuation coefficient established, it is possible to reconstruct a mass distribution function of the sample based in the average density of each particle calculated from the attenuation coefficients acquired from the sample in a 3D cone beam X-ray analysis.

The complete characterization of the sink-float analysis requires the identification of the density of each particle and the assignation of that particle to the respective fraction based on the average density of the voxels belonging to it. The completion of this analysis requires therefore the segmentation of the 3D image to identify each individual particle and then the averaging of the attenuation coefficient assigned to each voxel inside each particle.

### Coal Samples

Two samples with known washability characteristics were used in this experiment. The data were provided by the South Illinois University (SIU). Those are samples are divided in test 1 and test 5 products. The data are shown in the Table 1.

Table 1. Clean Coal Product Samples Test 1 and Test 5 (1 mm and 150  $\mu\text{m}$ ).

Relative Density	Mean R.D.	Product	
		Test1 Wt. (%)	Test5 Wt. (%)
1.15-1.3	1.225	73.91	61.78
1.3-1.4	1.35	20.30	27.77
1.4-1.5	1.45	3.85	7.46
1.5-1.625	1.5625	1.27	2.14
1.625-2.0	1.8125	0.63	0.79
2.0-2.8	2.4	0.04	0.06
Total		100.00	100.00

### Results

Figure 4 shows the results of the CT analysis for the clean coal product sample from test1. The analysis reveals a good correlation between the results from sink and float and the results from XMT scan. The differences in the low density range may be due to by insufficient sample and partial volume effects. The sample used for the CT scan was just a few grams of the sample.

For densities greater than 1.4  $\text{g}/\text{cm}^3$  the difference between measurements is smaller than 3% of the total weight. However, for densities less than 1.3  $\text{g}/\text{cm}^3$  the difference between the measurements increases rapidly up to a value of 13%.

The SIU experimental data was compared with a sink-float analysis carried out in the University of Utah (U of U) from the same sample used in the XMT analysis. The values are shown as unfilled triangles in the Figure 4. The points are very close to the SIU washability curve and in the range of the XMT data. It is a confirmation that the product material was homogenous and a good sample was used for analysis.

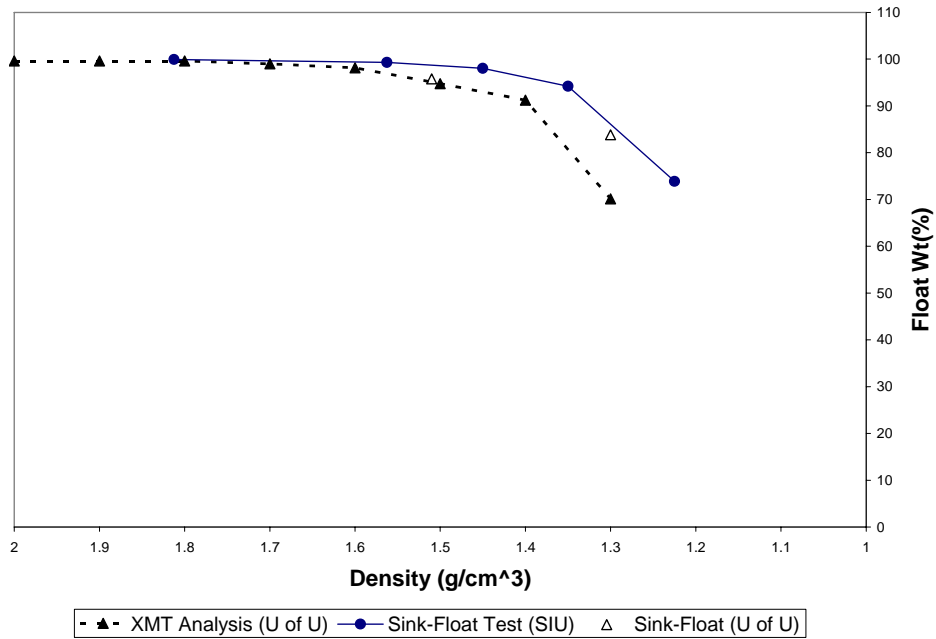


Figure 4. The washability curve for clean coal product from test 1.

The Figure 5 shows the results for the test 5 product stream. Also we see an excellent correlation between XMT analysis and experimental data. In this case, the maximum difference in percentage float in weight is of 2% and it is also generated at a low level density of 1.3 g/cm<sup>3</sup>.

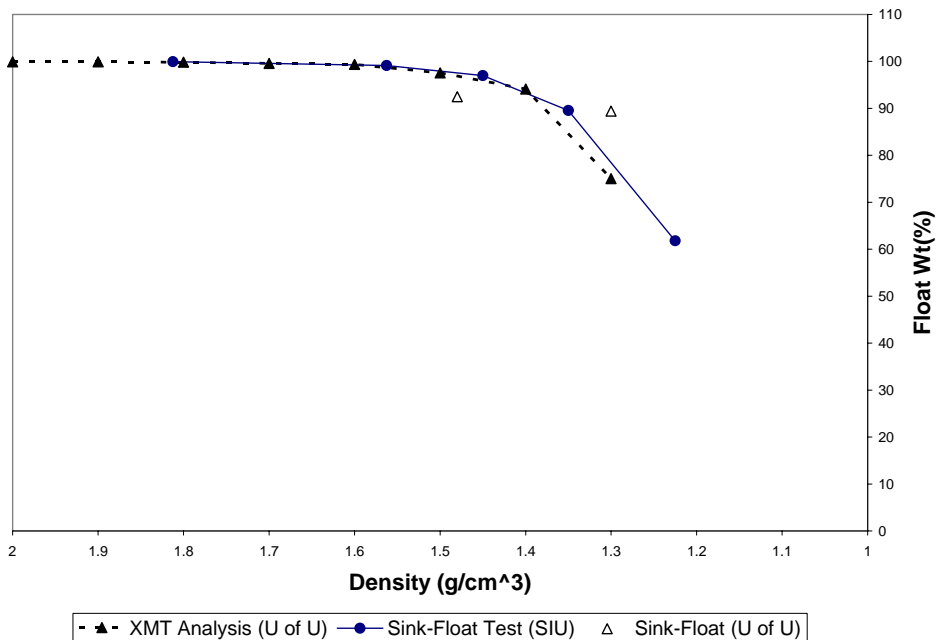


Figure 5. The washability curve for clean coal product from test 5.

As well as in the test 1, the washability curve calculated with the XMT data follows very well the experimental sink-float data test. However, in this case, the comparison

between the SIU data with the experimental test carried out at the University of Utah with the same sample used in the XMT analysis shows important differences. This is due to experimental problems because of the natural difficulties in running a sink-float test with a small sample of just few grams.

## **SUMMARY**

Two major components, namely, the segmentation of individual particles from packed particle bed and compositional classification of each particle, are need to be developed for detailed 3D liberation/exposure analysis of coal and mineral samples using XMT. In this regard, 3D watershed segmentation process was developed which allow us to identify individual particles in packed particle beds. Further, the density and attenuation coefficient relation associated to the use of Finite Mixture Distributions allow us to discriminate between different materials. These two components are used to show practical applications in mineral processing studies. The washability curve of coal samples from Illinois No. 5 seam calculated with the XMT data follows very well the experimental sink-float data.

## **FUTURE WORK**

During the period of 2006, evaluate the performance of the XMT under plant conditions will be evaluated based on plant samples and the data will be used to assess the accuracy for monitoring effectiveness of particle separation processes.

## **PUBLICATIONS/PRESENTATIONS**

1. J. D. Miller and C. L. Lin, "Three-dimensional Analysis of Particulates in Mineral Processing Systems by Cone-Beam X-Ray Microtomography", *Minerals and Metallurgical Processing*, 21, vol. 3 (2004) 113-124.
2. A.R. Videla, C.L. Lin, and J.D.Miller, "Reconstruction and watershed functions applied to a 3D image analysis segmentation problem for a packed bed of multiphase particles", 4th World Congress on Industrial Process Tomography, Aizu, Japan, 5-8 September, 2005, vol. 2, pp. 1000-1005.
3. C.L. Lin, "Quantitative Analysis of Multiphase Particles for Improved Design and Operations of Mineral Processing by X-ray Microtomography", Presentation at Moly-Cop 2005, Chillan, Chile, 14-18, November, 2005.
4. A.R. Videla, C.L. Lin, and J.D.Miller, "3D Characterization and Analysis of Heap Leaching Systems Using X-Ray Microtomography (XMT)", Hydro Copper 2005, Santiago, Chile, 23-25 November, 2005, vol. 2, pp. 363-372.

**Appendix 27: A Comprehensive Study of Froth Behavior (VA011)**

## TECHNICAL PROGRESS REPORT

Contract Title and Number:

Crosscutting Technology Development at the Center  
for Advanced Separation Technologies  
(DE-FC26-02NT41607)

Period of Performance:

Starting Date: 6/1/2004  
Ending Date: 10/31/2006

Sub-Recipient Project Title:

A comprehensive Study of Froth Behavior

Report Information:

Type: Semi-Annual  
Number: 3  
Period: 10/1/05-3/31/06  
Date: 5/15/06  
Code: VA011-R03

Principal Investigators:

Yoon

Contact Information:

Phone:  
Fax:  
E-Mail: ryoon@vt.edu

Contact Address:

Subcontractor Address:

No subcontracts issued.

Subcontractor Information:

Phone:  
Fax:  
E-Mail:

## PROGRESS REPORT ON: FOAM DRAINAGE AND WETTING - A NUMERICAL INVESTIGATION

In the flotation of minerals, bubbles are generated in a stirring tank and mixed with ground product. Particles are then attached to the bubbles and float to the top, where they form froth. Understanding and prediction of foam processes is necessary in order to design efficient machines. And so far, most efforts have been analytical. There is great value in analytical results, because they help us understand the basic parameters that affect the problem. However, analytical methods are very limited in their capacity to produce engineering results for practical situations.

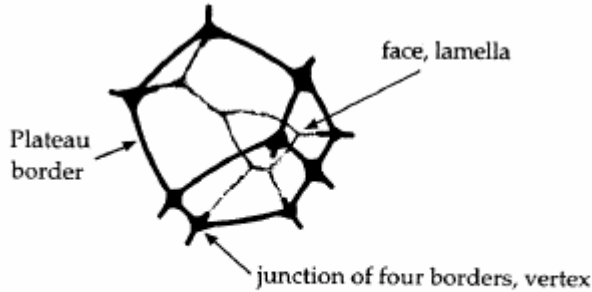


Fig. 1 A single foam cell with its associated Plateau borders

Rising bubbles quickly form a geometrical structure made up of polyhedra. The sides of these polyhedra are flat films called the lamellae, and the edges are tubes with tricuspoid cross-sections called Plateau borders (PB). A typical polyhedron cell is shown in Fig. 1. Small amounts of surfactants are enough to arrest the fluid velocity on the walls of the lamellae and the PBs. A good

approximation is to assume that the lamellae contain very little fluid. This is the state of dry foam. As a result, a dry foam structure is equivalent to a complex network of pipes. Except that these pipes can expand and contract depending on the wetness of the foam. Some authors<sup>1,2</sup> neglect the viscous losses along the junction and arrive at simple equations that govern foam drainage. More advanced modeling has also been achieved<sup>3,4</sup>. But most of these solutions have been limited to ideal situations that neglect the rising of the foam and its coarsening.

Conservation of mass of the fluid yields a simple relationship between the cross-section of the PB,  $A$ , and the mean velocity in a PB,  $u$ :

$$\frac{\partial A}{\partial t} + \frac{\partial}{\partial x}(Au) = 0 \quad (1)$$

This is based on the assumption of uniform distribution of bubble sizes in the vertical direction,  $x$ . If the velocity is related to hydrostatic pressure gradients and laminar viscous pressure drop through the PB, one can arrive at the following nonlinear equation:

$$\frac{\partial A}{\partial t} + \frac{1}{\eta} \frac{\partial}{\partial x} (\rho g A^2 - \frac{C\gamma}{2} \sqrt{A} \frac{\partial A}{\partial x}) = 0 \quad (2)$$

Where  $\eta$  is the viscosity and  $\rho$  is the density of the fluid. Using the following nondimensional quantities

$$x = \xi x_0, \quad A = \alpha x_0^2, \quad t = \tau t_0, \quad x_0 = \sqrt{C\gamma / \rho g}, \quad \eta = \eta^* / \sqrt{C\gamma \rho g} \quad (3)$$

we arrive at the equation<sup>2</sup>

$$\frac{\partial \alpha}{\partial \tau} + \frac{\partial}{\partial \xi} \left( \alpha^2 - \frac{\sqrt{\alpha}}{2} \frac{\partial \alpha}{\partial \xi} \right) = 0 \quad (4)$$

This is essentially the Berger's equation. It is parabolic in nature, but if the last term is small, it accepts wave-like solutions. Its character is similar to boundary-layer equations and can be solved numerically by methods established many years ago<sup>5</sup>.

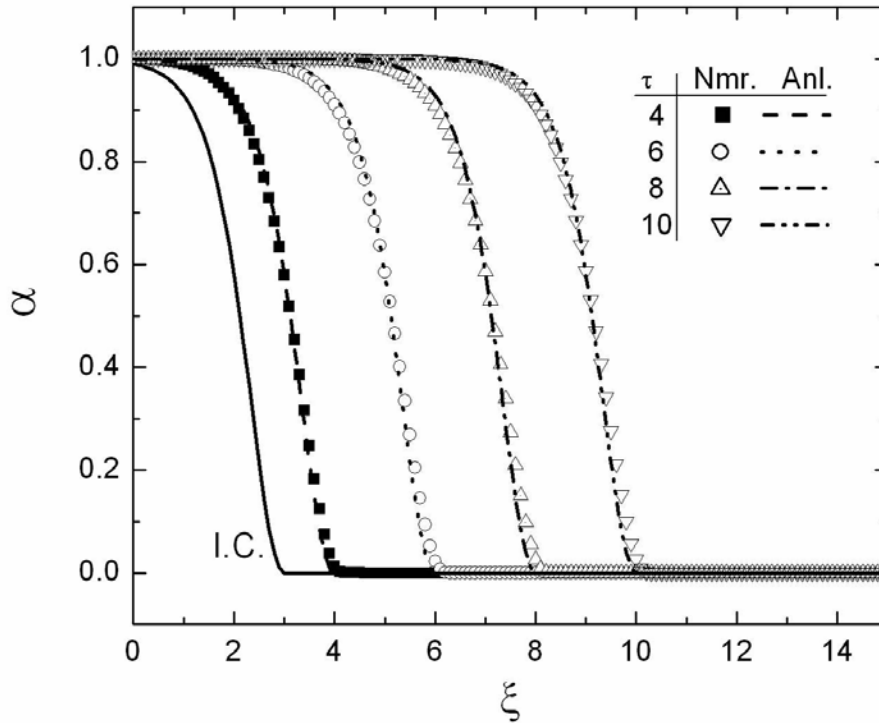


Fig.2. Numerical and Analytical solutions of forced drainage. The initial conditions is given by the analytical solutions when  $\tau=3$ .

We developed a finite-difference numerical approach to solve this equation. This code is now available to solve problems of foam formation. To test the validity of the code we decided to compare with an exact solution of Eq. (4). Such a solution is presented in Ref. 2 for the case of wetting of dry foam from the top:

$$\alpha(\xi, \tau) = \begin{cases} v \tanh^2(\sqrt{v}[\xi - v\tau]) & \xi \leq v\tau \\ 0 & \xi \geq v\tau \end{cases} \quad (5)$$

, where  $v$  is the velocity of the moving wave. This solution has the character of a solitary wave, and satisfies the condition of  $\alpha=1$  at the free surface,  $\xi=0$  and  $\alpha=0$ , at the lower

limit of foam. Wash water is supplied on the top of the foam, at  $\xi=0$ , and  $\xi$  is pointing downwards. The dimensionless PB area,  $\alpha$ , is proportional to the liquid fraction of the foam. This solution is academic in character, since it fails to predict the early part of the wetting process. The slope of the curve is independent of time.

To compare our numerical results with this analytical solution, we chose as initial profile one wave profile at a time  $\tau=3$ . We then carried out the numerical solution for larger times. Our numerical results are presented together with the analytical solution in Fig. 2. It appears that our numerical data match well with the analytical solutions. This confirms the validity of our numerical code and provides confidence to use this method in the development of more advanced models<sup>3</sup>.

The model of Verbist *et al.*<sup>2</sup> does not take into account the losses across foam junctions, and thus it is independent of the cell size and effects like foam coarsening. A more advanced model was developed by Neethling *et al.*<sup>3</sup> We employed a similar approach to our earlier analysis in rendering dependent and independent variables dimensionless. Now the continuity equation, Eq.(1) is expressed in terms of the liquid fraction,  $\varepsilon$ , as follows.

$$\frac{\partial \varepsilon}{\partial t} + \nabla \left( \frac{\varepsilon \rho g}{k \mu} \right) + \nabla \left( \frac{\varepsilon \nabla(-\gamma/r)}{k \mu} \right) = 0 \quad (6)$$

Where,  $k$  is the coefficient representing the pressure drop to the average liquid velocity in the PB and the PB junctions, defined as

$$k = \left( \frac{3C_{PB}}{r^2} + \frac{4.178(C_V - 0.418C_{PB})}{rr_b} (1 - \varepsilon)^{1/3} + \frac{6.806(C_V - 1.588C_{PB})}{rr_b} (1 - \varepsilon)^{2/3} \right) \quad (7)$$

The coefficient  $k$  comprises all effects from the PB network having the pressure loss constants in the PB ( $C_{PB}$ ), in the PB junctions (vertices  $C_V$ ). Here,  $r$  is the radius of curvature along the juncture, and  $r_b$  is the radius of the bubble which was assumed to be constant in the original derivation of Neethling *et al.*<sup>3</sup>.

Noting that  $\varepsilon = NA/S = N\alpha x_0^2/S$ , where  $N$  is the total number of PBs in the channel cross-section, and  $S$  is the cross-section area of the tank, and letting  $x_0 = \sqrt{\gamma/\rho g}$ , we obtain

$$\therefore \varepsilon = \frac{C_1}{Bo} \alpha \quad (8)$$

Here,  $C_1$  is the total number of PBs across the tank, and  $Bo$  is the Bond number, which is a non-dimensional number defined as  $Bo \equiv \rho g d^2 / \gamma$ .

Substituting these expressions into (6) and also letting,  $x = \xi x_0$ ,  $r = r^* x_0$ ,  $t = \tau t_0$ ,  $t_0 = \mu / \sqrt{\gamma \rho g}$ , and  $k = \kappa / x_0^2$ , we finally get :

$$\frac{\partial \alpha}{\partial \tau} + \frac{\partial}{\partial \xi} \left( \frac{\alpha}{\kappa} \right) - \frac{\partial}{\partial \xi} \left( \frac{\alpha}{\kappa} \frac{\partial}{\partial \xi} \left( \frac{1}{r^*} \right) \right) = 0 \quad (9)$$

Note that in this equation the Bond number is included in the definition of  $\kappa$ .

These equations are valid only for a uniform bubble radius  $r_b$ . And in fact the bubble radius remains as an unknown. Moreover, the radius of curvature  $r$  is a function of  $\varepsilon$  according to the following expression from the Reference 3.

$$\varepsilon \approx 0.3316 \left( \frac{r}{r_b} \right)^2 (1 - \varepsilon)^{2/3} + 0.5402 \left( \frac{r}{r_b} \right)^3 (1 - \varepsilon) \quad (10)$$

This can be expressed in terms of  $\alpha$  via the relation in Eq.(8) and can be solved numerically simultaneously with Eq. (9).

Solutions can be obtained only if a cell radius is given. Again therefore, coarsening cannot be modeled. We are in the process of employing models developed by the present group to model film thinning<sup>6,7</sup>, and thus add analytical models to account for the variation of the bubble radius. We will then be able to obtain numerical solutions for problems of greater significance to industry, namely modeling coarsening of foam and rising of bubbles within foam while draining..

## References

1. Leonard, R.A. and Lemlich, R. "A study of interstitial liquid flow in Foam", *AICHE Journal*, 11, (1965), 18-29
2. Verbist, G., Weaire, D. and Kraynik, A.M. "The foam drainage equation", *J.Phys.:Condens.Matter* 8(1996), 3715-3731
3. Neethling, S.J., Lee, H.T. and Cilliers, J.J., "A foam drainage generalized for all liquid contents", *Phys.:Condens.Matter* 14(2002), 331-342
4. Koehler, S.A., Hilgenfeldt, S. and Stone, H.A. "A generalized view of foam drainage: experiment and theory", *Langmuir* 16(2000), 6327-6341
5. Telionis, D.P., *Unsteady Viscous Flow*, Springer, 1981
6. Hartland, S. and Barber, A.S. "A model for a cellular foam", *Trans.Inst.Chem.Engrs.* 52(1974), 43-52
7. Wang, L. and Yoon, R.H. "Hydrophobic forces in thin aqueous films and their role in film thinning", *Colloids and Surfaces A* 263(2005) 267-274

**Appendix 28: Portable Sensor for Detecting Mercury and Other Heavy  
Metals Encountered In Coal Processing and Utilization (WV013)**

## TECHNICAL PROGRESS REPORT

Contract Title and Number:

Crosscutting Technology Development at the Center for  
Advanced Separation Technologies  
(DE-FC26-02NT41607)

Period of Performance:

Starting Date: 6/01/2004  
Ending Date: 10/31/2006

Sub-Recipient Project Title:

Portable sensor for Detecting mercury and other Heavy  
Metals Encountered in Coal Processing and Utilization

Principal Investigator:

M. S. Seehra

Contact Address:

Physics Department  
210 Hodges Hall  
West Virginia University  
Morgantown, WV 26506-6315

Subcontractor Address:

No subcontracts issued.

Report Information:

Type: Semi-Annual  
Number: 03  
Period: 10/01/05 to 03/31/06  
Date: 03/30/06  
Code: WV013-R03

Contact Information:

Phone: 304-293-3422 x1473  
Fax: 304-293-5732  
E-Mail: mseehra@wvu.edu

Subcontractor Information: N/A

Phone:  
Fax:  
E-Mail:

### ABSTRACT

With the resignation and departure of Dr.Manivannan in October 2005, the theoretical and experimental status of the project were carried out by Prof.Seehra. It was decided to abandon the use of GaN as an electrode for the detection of  $Hg^{2+}$  (described in the previous report) since its sensitivity for detecting  $Hg^{2+}$  was found to be inferior to that obtained previously with boron-doped diamond (BDD) electrodes. A new set of BDD electrodes was acquired from England. Experiments are now underway using a new “internal standard method” for quantifying  $Hg^{2+}$  in order to overcome the problem of reproducibility encountered in previous studies using the “standard addition method”. The shifts of the peak with  $Hg^{2+}$  concentration has been successfully explained with the use of the Nernst equation.

### INTRODUCTION

Background

With the resignation and departure of Dr.Manivannan in October 2005 who previously directed this project in consultation with Prof.Seehra, a careful review of the status of the project was carried out by the PI (Seehra). This included a thorough review of

the theoretical basis of electrochemical detection of Hg and other heavy metals and to determine the best procedures for achieving the goal of a truly portable detector which can provide reproducible results. In the last semi-annual report, we had investigated the use of GaN electrode for the detection of mercury.

After further consideration it was decided to abandon the use of GaN since its sensitivity and reproducibility for the detection of Hg was found to be inferior to that obtained previously with the use of boron-doped diamond (BDD) electrodes ( Manivannan, Seehra et al, 2005). Instead, decision was made to refocus on the use of BDD electrodes and develop procedures to solve the problem of reproducibility encountered in previous studies (Manivannan, Seehra et al, 2005). In our recent study we found excellent agreement for the determination of Hg between our electrochemical method and the CVAAS (Cold Vapor Atomic Absorption Spectroscopy) in 10 samples of KCl impinger samples obtained from the NETL pilot-scale combustion facility (Fig.1).

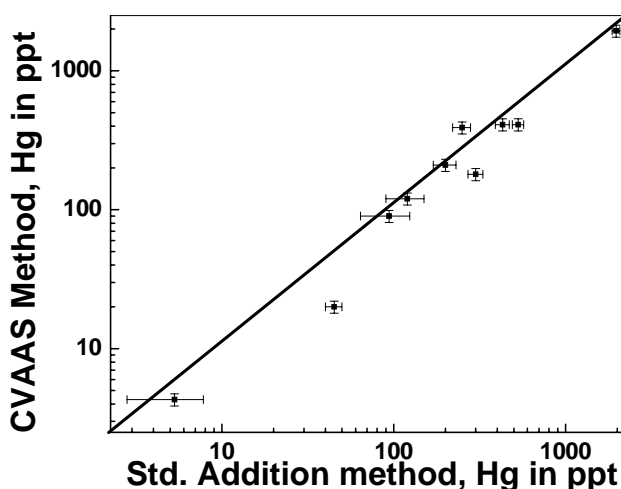


**Fig.1** Comparison plot of concentrations determined by the standard addition and CVAA methods. The solid line represents a one-to-one correlation between the two methods.

We used the “standard addition method” to determine Hg concentration which essentially requires a new calibration plot for each sample. This is a time- consuming and hence costly procedure. The second issue with this technique is that successive calibration curves using the same BDD electrode, even after electrochemical cleaning after each run, give different slopes (Fig.2) leading to the reproducibility issue mentioned earlier. How to overcome these issues of reproducibility and repeated calibrations is the primary focus of our current and future research.

### Objective and Approach

Following the above discussion under ‘background’, our objective is now to address the issues of reproducibility and necessity for repeated calibrations encountered in our recently published work (Manivannan, Seehra et al 2005). The questions of accuracy and sensitivity for the detection of Hg in the ppb to ppt range have been successfully addressed using BDD electrochemistry (Fig.1). After a careful review of the theoretical concepts, decision has been made to use “internal standard method” instead of the previously used

“standard addition method” for determining Hg. In this method we will attempt the use of standard solution of either  $\text{Cu}^{2+}$  or  $\text{Pb}^{2+}$  ions as the internal standards for determining Hg

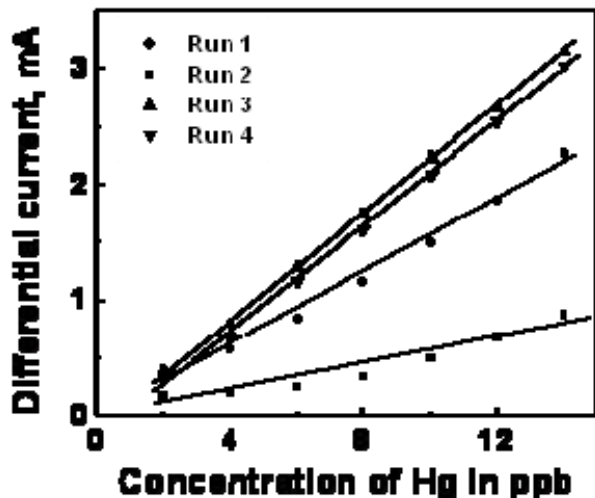


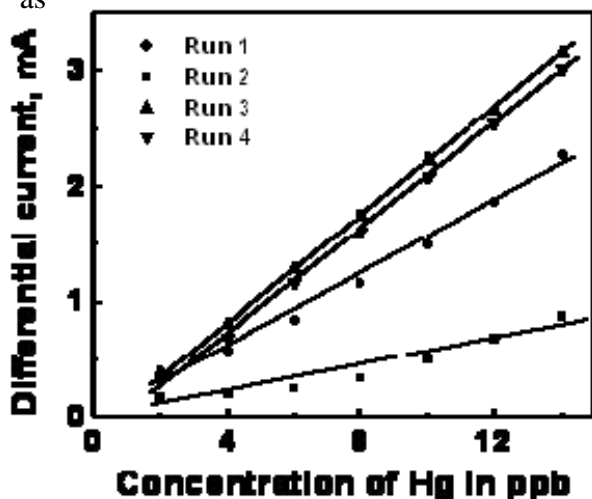
**Fig.2** Four consecutive DPV calibration plots for 2-14 ppb of mercury concentrations in 1M KCl (pH 4). A 3 ppm of Gold standard solution was added; deposition time = 60s; deposition potential = -0.1 V vs. SCE; rotation speed=2000 rpm. Runs 3 & 4 were performed consecutively on the same day.

since the positions of the peaks for these ions are significantly separated from those of  $\text{Hg}^+$  and  $\text{Hg}^{2+}$ . Since any change in the surface morphology of BDD electrodes after repeated runs should affect the standard and unknown Hg equally, the problem of reproducibility might thus be overcome.

## PROJECT TASKS

For this reporting period, our Task 1 was to acquire a new set of BDD electrodes since previously used electrodes were deemed inappropriate for the new studies. An order was placed with Harris International in early fall 2005 for six 2 mm electrodes for the portable detector and two 6 mm electrodes for the table-top apparatus. These electrodes are custom-made in England and it took over three months to finally acquire these electrodes. During this waiting period we focused our attention on the theoretical issues under Task 2 which eventually led to our decision to try the “internal standard method” for overcoming the problem of reproducibility shown in Fig.2. Graduate assistant Sukanya Ranganathan is now setting up the experiments with the new electrodes and during the next several months, we hope to verify the usefulness of this approach. Under Task 3 we are addressing the issue of why the peaks for  $\text{Hg}^{2+}$  in the DPV (Differential Pulse Voltammetry) scans shift to higher voltage as concentration of Hg increases (Fig.3).

**Fig3.**  
 $\text{Hg}^{2+}$   
1.5ppm



DPV scans for 10ppt to 50ppt concentrations in 1M KCl (pH 1). gold standard solution was added; deposition time = 60 sec; deposition potential = -0.1V vs.

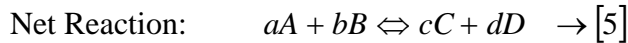
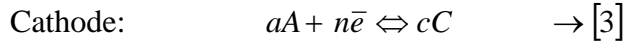
SCE (Saturated Calomel Electrode); rotating disc electrode with rotation speed = 2000rpm.

We suggest that these results can be interpreted through the use of Nernst equation:

$$E = E^0 - \frac{0.05916}{n} \log Q \rightarrow [1]$$

$$Q = \frac{A_C^c A_D^d}{A_A^a A_B^b} \rightarrow [2]$$

Here the general half reactions are:



where A stands for concentration (moles/liters) for each reactant and n is the number of electrons involved in the reaction. For pure liquids, solids and gases A=1 leading to log A= 0. For  $\text{Hg}^{2+}$ , the half reaction is:  $\text{Hg}^{2+} + 2\bar{e} \Leftrightarrow \text{Hg}(l) \rightarrow [6]$

with  $E^0=0.854\text{V}$ . The equation [1] for this reaction reduces to (with n=2)

$$E(\text{cathode}) = 0.854 - 0.02858 \log \frac{1}{A(\text{Hg}^{2+})} \rightarrow [7]$$

The molar concentration for 1ppt of  $\text{Hg}^{2+}$  is  $4.9875 \times 10^{-12} \text{M}$ . Hence for A=10 ppt ( $4.9875 \times 10^{-11} \text{M}$ ), eqn. [7] yields  $E=0.56 \text{ V}$  vs. SHE (Standard Hydrogen Electrode). Correcting for SCE (0.24V) yields  $E = 0.32\text{V}$ . Results for other concentrations are calculated similarly. A comparison of the calculated and observed peak shifts is shown in Fig.4, providing a good semi-quantitative agreement. Further analysis is in progress and the results are expected to be submitted for publication soon.

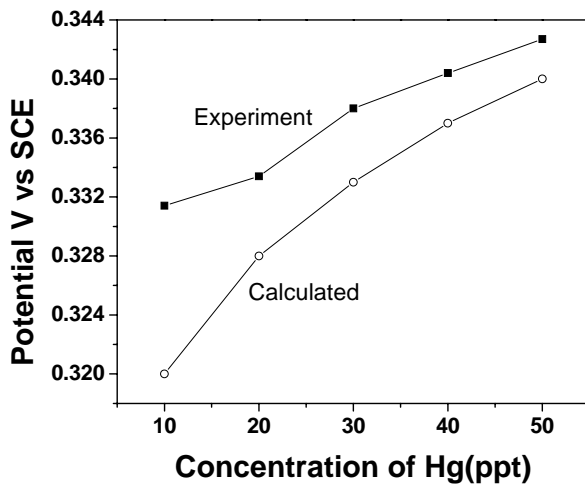


**Fig.4.** Shift in peak voltage position with increase in concentration for 10 to 50 ppt  $\text{Hg}^{2+}$  concentrations in 1M KCl (pH 1) (from Fig.1) and comparison between calculated and observed values.

## **SUMMARY**

During this reporting period, we focused theoretically on the remaining issue of reproducibility of calibration curves and interpretation of the shift of the peaks with concentration. A decision to use “internal standard method” for the quantification of Hg was made in order to overcome the problem of reproducibility of the calibration curves. A new set of BDD electrodes has been acquired and experiments to solve the reproducibility issue are now in progress.

## **FUTURE WORK**

As noted above, our focus in the coming months will be to use the “internal standard method” in experiments to quantify mercury. The goal is to develop a method so that a single reading (or step) may be sufficient for mercury quantification, preferably with the use of the same electrode for several analyses. Experiments to test this concept will be carried out.

## **REFERENCES**

1. A.Manivannan, L.Ramakrishnan, M.S.Seehra, E.Granite, J.E.Butler, D.A.Tryk and A.Fujishima, “Mercury detection at boron doped diamond electrodes using a rotating disk technique”, *J.Electroanalytical Chem.*577, 287-293(2005).

## **PUBLICATIONS/PRESENTATIONS**

1. A.Manivannan, L.Ramakrishnan, M.S.Seehra, E.Granite, J.E.Butler, D.A.Tryk and A.Fujishima, “Mercury detection at boron doped diamond electrodes using a rotating disk technique”, *J.Electroanalytical Chem.*577, 287-293(2005).
2. D.Drago, N.Spataru, R.Kawasaki, A.Manivannan, T.Spataru, D.A.Tryk and A.Fujishima, “Detection of trace levels of Pb<sup>2+</sup> in tap water at boron doped diamond electrodes with anodic stripping voltammetry”, *Electrochimica Acta*,51,2347-2441 (2006)
3. L.Ramakrishnan “Electrochemical detection of mercury using boron doped diamond electrodes”, MS Thesis, West Virginia University (2005).

**Appendix 29: Determining the Effectiveness of Gold Filters for Removing  
Mercury from Coal Fired Power Plants (MT003)**

The PI has notified CAST that work is complete and a Final Report will be issued.

**Appendix 30: Development of Metallic Filters to Control Mercury from  
Coal Fired Power Plant Flue Gas (MT004)**

## TECHNICAL PROGRESS REPORT

<u>Contract Title and Number:</u> Establishment of the Center for Advanced Separation Technologies (DE-FC26-02NT41607)	<u>Period of Performance:</u> Starting Date: 06/01/04 Ending Date: 10/31/06
--	---

<u>Sub-Recipient Project Title:</u> Development of Metallic Filters to Control Mercury from Coal Fired Power Plant Flue Gas	<u>Report Information:</u> Type: Semi Annual Number: 2 Period: 10/01/05-03/31/06 Date: 3/31/06 Code: MT004-R02
<u>Principal Investigators:</u> Dr. Kumar Ganesan	
<u>Contact Address:</u> Department of Environmental Engineering Montana Tech of The University of Montana 1300 West Park Street Butte, Montana 59701	<u>Contact Information:</u> Phone: 406-496-4239 Fax: 406-496-4650 E-Mail: kganesan@mtech.edu
<u>Subcontractor Address:</u> "No subcontracts issued."	<u>Subcontractor Information:</u> Phone: Fax: E-Mail:

### **DETERMINING THE EFFECTIVENESS OF METALLIC FILTERS FOR THE REMOVAL OF MERCURY FROM COAL FIRED POWER PLANTS**

#### **ABSTRACT**

During this reporting period an in-house plating technique and a new thermal de-sorption systems were built. In addition, a new synthetic sponge coated with copper has been explored as a filter media instead of the metal based sponge. This new sponge will be plated with selected metals to use in the removal of mercury from flue gas. The in-house plating system will allow flexibility in the plating of the metals and new thermal de-sorption system provides much more uniform heating for effective regeneration of the spent filters. The new sponge is expected to provide much higher surface area per volume of filter to further improve the mercury removal system and the pressure drop is low due its high porosity.

#### **INTRODUCTION**

Two different metallic filters developed by Montana Tech showed great potential in removing mercury from flue gas of coal-fired power plants. Several tests have been completed previously with different metallic filters for mercury removal efficiency. Combining different metallic filters were tested successfully at the laboratory as well as in the field. Spent filters were desorbed and retested for efficiency.

The filters were tested in a coal fired power plant three times at different flow rates and all three times the mercury removal efficiency was higher than 90 %. The spent filters were thermally regenerated by releasing the mercury captured on the filters. The regenerated filter was tested again for its removal efficiency. The results indicated above 90% removal efficiency even with regenerated filters. The filters again went through a second round of thermal de-sorption and efficiency testing. The current filter has limited surface area per unit volume of filter and therefore a new sponge with high surface area per volume is tried instead of the old metal sponge. This report highlights the progress made from October 2005 to March 2006.

## Background

Mercury is one of the important air toxic metals that are addressed in the 1990 Clean Air Act Amendments<sup>1</sup>. Mercury is a high-priority regulatory concern because of its persistence and bioaccumulation in the environment and due to its neurological health impacts. The largest anthropogenic source of mercury in the United States is the coal-fired power plants, which release 48 tons of mercury annually or about one-third of the total anthropogenic emissions<sup>2</sup>. As a result, coal-fired power plants are the focus of the new EPA mercury regulations. Currently, there is no control technology that removes mercury from coal-fired power plants. The species of mercury present in the flue gas is determined by the chemical composition of the coal burned. Coal chlorine content is one of the main factors that affect the speciation of mercury upon combustion, mainly due to its ability to oxidize  $\text{Hg}^0$  to  $\text{HgCl}_2$ <sup>4</sup>. Other elements in the coal including sulfur, calcium, and iron impact the speciation of mercury, but to a lesser degree than chlorine. Eastern bituminous coals have high mercury and chlorine contents and produce a flue gas predominately composed of  $\text{Hg}^{2+}$ . On the other hand, western sub-bituminous and lignite coals have low mercury and low chlorine contents and produce a flue gas with  $\text{Hg}^0$  as the dominant specie. There is a great deal of research being conducted on the mechanisms of mercury-chlorine chemistry and other mercury speciation reactions that occur upon the combustion of coal at power plants<sup>4</sup>.

## Objective and Approach

The objective was to evaluate the ability of different metallic filters to remove mercury from contaminated air. Because of the high price associated with the metallic filter we have investigated combination of different metallic filters. The goal of the laboratory testing as well as the field testing was to achieve mercury removal efficiencies above 90%, and all testing results are evaluated based on how well this 90% efficiency goal was met.

The goal for this period was (a) to develop a better laboratory scale de-sorption system; (b) develop in-house plating set up and (c) to use a newer sponge which has higher surface area than the previous ones. This will improve the cost effectiveness of the metallic filter for mercury control.

## PROJECT TASKS

### Experimental Procedures

Different filters were tested individually. The removal efficiency was above 90%. The spent filters were subjected to thermal desorption to release the mercury from the filter with an idea to regenerate the filter and to recover mercury.

Figure 1 shows the experimental setup. The filter's inlet and outlet mercury concentrations were measured with a portable mercury analyzer, Mercury Tracker. A mercury generator system (Figure 2) produced the mercury source.

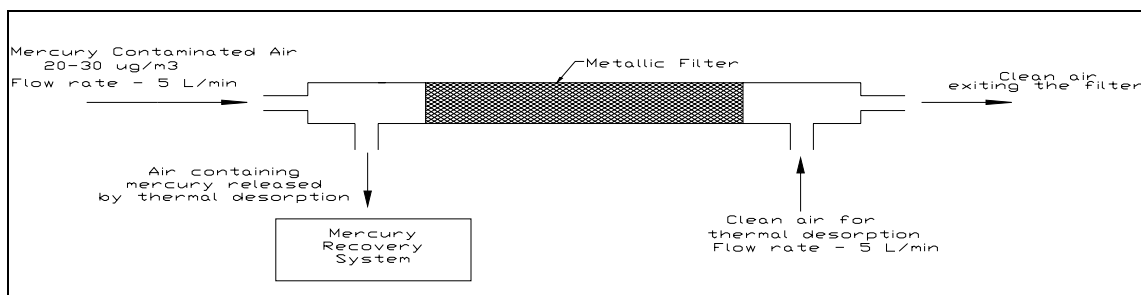


Figure 1 Experimental setup

The tests were terminated once the mercury removal efficiency of the metallic filter dropped to 50%, the test was stopped and the filter went through thermal desorption. The thermal desorption process was continued until the mercury concentration in the air leaving the metallic filter was below  $0.5\mu\text{g}/\text{m}^3$ .

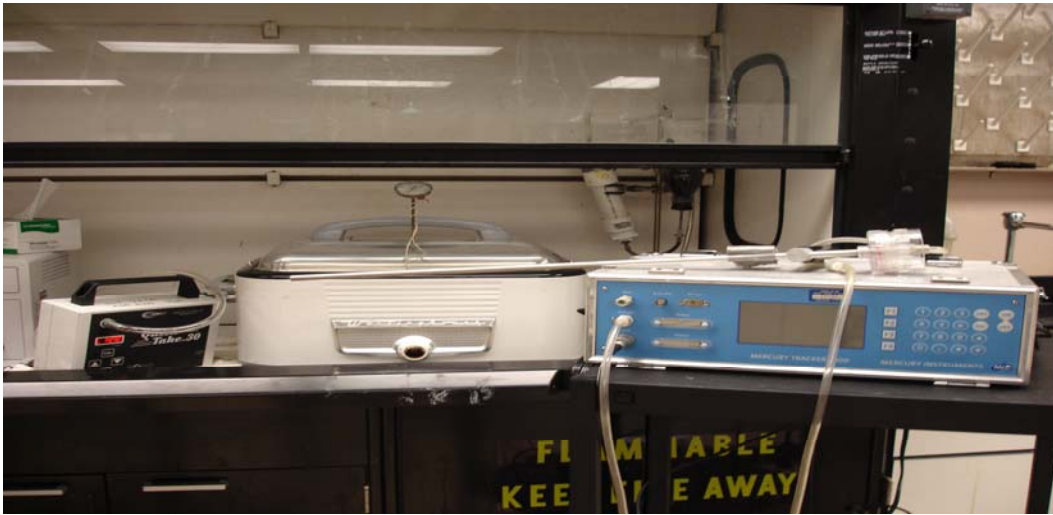


Figure 2 Mercury Generator

### Task 1: Bench Scale Laboratory Desorption System

The thermal de-sorption process consisted of heating the spent metallic filters to release the captured mercury, which was then collected in a mercury recovery system. Thermal de-sorption is an efficient method to remove the captured mercury from the used filters due to mercury's high volatility and the fact that mercury boils at 674°F whereas the tested metallic filters' melting points are much higher than mercury. The earlier results show that the thermal de-sorption process effectively releases mercury from spent filters at temperatures between 150 and 400 °F.

In the past the thermal de-sorption was carried out using heat tapes wrapped around a stainless steel tube holding the filters. Clean filtered air was passed through the tube in the opposite direction. This system was adequate for up to two filters and the heating was not as uniform as we wanted. Therefore in order to accommodate more number of filters and to have more uniform heating a new de-sorption system was developed during this period. Thus a new de-sorption system (Figure 3) was built where the temperature could be controlled more closely and the regeneration of the filters could be done effectively. Also this system will allow larger filters to be desorbed efficiently. This system is fabricated locally and ready for the testing.



**Figure 3.** Thermal De-sorption System

### Task 2: Developing In-house Plating set up

In the past the base metallic filters were sent out for plating to outside commercial vendors. This is proved to be expensive and takes time to get the plated sponges back on time for testing. In addition, we were unable to control the quality and thickness of plating. Therefore, we have setup a small laboratory scale plating system where we can obtain consistent quality with desirable thickness of plating with selected metals. We have completed initial plating of one metal on the new metallic sponge with this new set up and waiting to complete the second metal to be plated. Once these sponges are plated they will be tested for their

performance in removing mercury using a mercury generator and using the mercury tracker to measure the inlet and outlet concentrations of the filter. This efficiency of the filters plated by in-house system will be compared with the ones from commercial vendors. If there is no difference then it shows that the in-house plating system is as effective as the ones plated by the vendors. We plan to use this plating system for plating the base filters in the future.

### Task 3: Substituting Higher Surface Area Filters

The third task we have explored is the new sponge. The new sponge selected as opposed to the one currently used has much higher surface area per volume and therefore will provide a much higher surface area for removing mercury. This synthetic sponge is commercially available with metal coating on it. It has high porosity for low pressure drop. Therefore this new sponge will be plated with the metals of choice and tested for its mercury removal efficiency.

### **SUMMARY**

In summary during this reporting period a laboratory scale thermal de-sorption system was fabricated. And an in-house plating setup has been built to plate the base filters. Further a newer sponge with higher surface area was successfully plated.

### **FUTURE WORK**

Future work includes thermal desorption of used filters using the new de-sorption system and to test the efficiency of the new sponge. The plating will be done in-house instead of a vendor if it proves to be equally effective.

### **REFERENCES**

1. U.S. Environmental Protection Agency. *The Clean Air Act of 1990, a Primer on Consensus Building*; U.S. Government Printing Office: Washington, DC, 1990.
2. U.S. Environmental Protection Agency. *Mercury Report to Congress*; EPA-425/R-97-003; U.S. Government Printing Office: Washington, DC, 1997.
3. *EPA Proposed Options for Significantly Reducing Mercury Emissions from Electric Utilities*; U.S. Environmental Protection Agency: Washington, DC, January 2004; available at <http://www.epa.gov/mercury> (accessed 9/25/04).
4. Li, L.C.; Deng, P.; Tian, A.M.; Xu, M.H.; Zheng, C.G.; Wong, N.B. A study on the reaction mechanism and kinetic of mercury oxidation by chlorine species; *J. Molecular Structure* **2003**, 625, 277-281.
5. Pavlish, J.H.; Everett, E.A.; Sondreal, A; Mann, M.D.; Olson, E.S.; Galbreath, K.C.; Laudal, D.L.; Benson, S.A. Status review of mercury control options for coal-fired power plants; *Fuel Processing Technology* **2003**, 82, 89-165.
6. PPL Corporation homepage, <http://www.pplweb.com> (accessed 4/15/05).
7. Morris, T.; Sun, J.; Szulczewski, G. Measurement of the chemical and morphological changes that occur on gold surfaces following thermal desorption and acid dissolution of adsorbed mercury; *Analytica Chimica Acta* **2003**, 496, 279-287.

## **PUBLICATIONS/PRESENTATIONS**

The research paper was presented at the 45<sup>th</sup> 2005 PNWIS/A&WMA annual conference. Also it was submitted for the A&WMA Journal. The data has been submitted for a technical presentation in an International Conference to be held in January 2006.

**Appendix 31: Recovery of Chromium and Arsenic From Toxic  
Waste Stream by Reactive Polymer-Coated Absorbents (WV013)**

# TECHNICAL PROGRESS REPORT

## Contract Title and Number:

Crosscutting Technology Development at the Center for Advanced Separation Technologies (DE-FC26-02NT41607)

## Period of Performance:

Starting Date: 06/01/2004  
Ending Date: 10/31/06

## Sub-Recipient Project Title:

Recovery of Chromium and Arsenic from Toxic Waste Stream by Reactive Polymer-Coated Absorbents

## Principal Investigators:

Gang, Deng

## Report Information:

Type: Semi-Annual  
Number: 3  
Period: 10/01/2005 – 03/31/2006  
Date: 03/30/2006  
Code: WV014-R03

## Contact Address:

Department of Civil Engineering  
West Virginia University Institute of Technology  
405 Fayette Pike, Montgomery, WV 25316

## Contact Information:

Phone: 304-442-3372  
Fax: 304-442-3391  
E-Mail: [dianchen.gang@mail.wvu.edu](mailto:dianchen.gang@mail.wvu.edu)

## Subcontractor Address:

Baolin Deng  
Department of Civil & Environmental Engineering  
University of Missouri-Columbia  
Columbia, MO 65211

## Subcontractor Information:

Phone: 573-882-0075  
Fax: 573-882-4874  
E-Mail: [DengB@missouri.edu](mailto:DengB@missouri.edu)

## ABSTRACT

Chromium desorption and regeneration studies were conducted and the results demonstrated that the maximum desorption efficiency by NaOH was 80%, and by NH<sub>4</sub>OH was 55% and the desorption rate was fast. The regenerated adsorbent showed adsorption capacities approximately 35%-45% lower than the original adsorbent. Column studies showed that the breakthrough point was at 600 empty bed volumes (EBV) when the flow rate was 4 ml/hr and 760 empty bed volumes when flow rate was 0.85 ml/hr. In addition, iron-chitosan beads were prepared for arsenic removal. SEM micrograph of the iron-chitosan illustrated that the beads are porous in structure. The prepared iron-chitosan could effectively remove arsenic from water and pH had no obvious effect on As (V) removal from DI water at pH 5.8-7.3. The removal efficiency was always higher than 88% under the experimental conditions.

## INTRODUCTION

### Background

Acid mine drainage (AMD) contains high concentrations of sulfate, iron, and many other toxic elements existing in the original mineral assembly, including divalent heavy metals and oxyanions and frequently serves as a large-scale and persistent source of pollution

to surface and ground waters. This study focuses on contaminants in their anionic forms (i.e.,  $\text{AsO}_4^{3-}$  and  $\text{CrO}_4^-$ ) in AMD, because these anions are highly soluble and are normally not removed by treatment processes such as lime neutralization and precipitation designed for divalent heavy metals (e.g.,  $\text{Cu}^{2+}$ ,  $\text{Pb}^{2+}$ , and  $\text{Zn}^{2+}$ ).

### Objective and Approach

Within the first two six-month reporting periods, the investigators finished Task 1 and Task 2 on Cr(VI) removal. In the third reporting period, Task 3 was finished. The efforts focused on: (1) Investigation of Cr desorption and recovery conditions; and (2) Regeneration and reuse of the adsorbents. In addition, arsenic removal from aqueous solution in Task 1 to Task 2 was initiated. The efforts included: (1) Preparing and characterizing the structure of the adsorbents for arsenic removal; and (2) Evaluating arsenic removal efficiency at different pH.

### **PROJECT TASKS**

This research involves 3 tasks. Task 1 involves the development and characterization of the new adsorbents. In Task 2, the sorption under different environmental conditions will be optimized. Task 3 involves the investigation of desorption condition, recovery of Cr(VI) and As, and regeneration and reuse of the adsorbent.

#### Task 3. Investigation of Desorption Condition, Recovery of Cr(VI), and Regeneration and Resue of the Adsorbent.

##### *Desorption Study*

Experiments on the regeneration of adsorbent (GAC-QPVP) were performed. Desorption of Cr(VI) was studied with NaOH and  $\text{NH}_4\text{OH}$  at various concentrations and for different time periods. Results in Figure 1 showed that increasing concentration of the base increased the desorption efficiency. But when the concentration of NaOH was greater than 0.1 M, there was only a small change in the chromium(VI) desorption. It can be seen that maximum desorption by NaOH was 80%, and by  $\text{NH}_4\text{OH}$  (Figure 2) was 55%. Even though desorption efficiency was not 100%; this was fairly good when comparing with other studies. Ward (1990) used kaolinite and illite to remove Cr(VI) from the aqueous solution. Though chromium(VI) removal was 100% at low pH, Cr(VI) was desorbed only about 25%. Desorption studies were also conducted for different time periods, 5 and 30 minutes. There was no significant difference in the desorption efficiency between the two periods, which indicated that desorption rate was fast, due to the larger surface area of the adsorbent.

##### *Regeneration and Reuse of the GAC-QPVP*

The reuse of the adsorbent, following adsorption-desorption process was investigated. The consumed GAC-QPVP was treated with 0.2 M NaOH for 30 minutes to desorb Cr(VI), then adsorbent was washed with 100ml 0.1 M HCL, and 100ml distilled water to regenerate the adsorbent. The regenerated adsorbent was dried in an oven at 100 °C for 6hr, and then it was cooled and stored in desiccators prior to use. Batch adsorption isotherm experiments

were conducted using regenerated GAC-QPVP. Adsorption capacities of regenerated and original GAC-QPVP were compared in Figure 3. It can be observed that adsorption capacities were decreased by 35%-45%. Gang et al (2001) observed that regenerated modified PVP coated silica gel adsorption capacity was decreased about 10-20%.

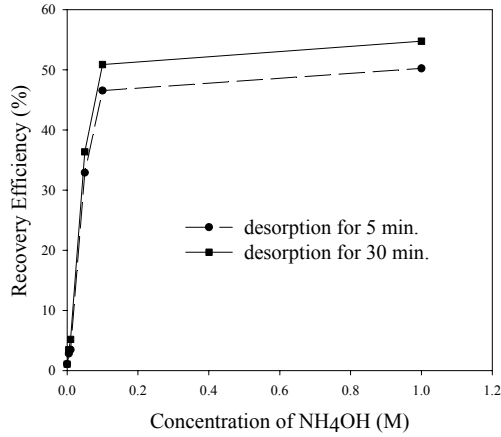
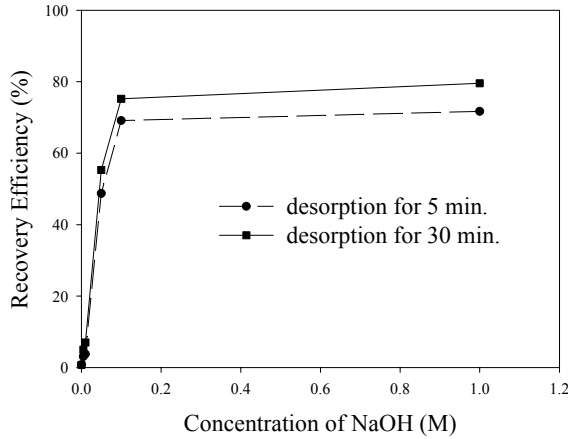


**Fig. 1. Desorption of Cr(VI) with NaOH Fig. 2. Desorption of Cr(VI) with  $\text{NH}_4\text{OH}$  for different time periods.  $T = 25^\circ\text{C}$ .**

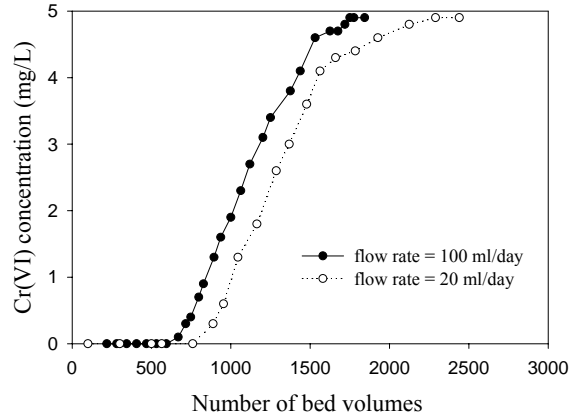
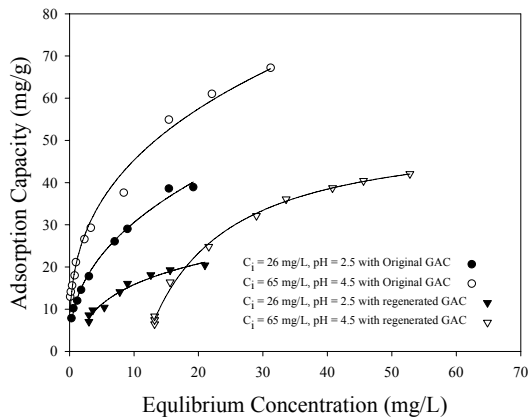


**Fig. 3. Adsorption isotherms of fresh adsorbent and regenerated GAC-QPVP**

**Fig. 4. Column study**

### Column Study

The column study of Cr(VI) on QPVP-GAC was conducted using 5 ppm Cr(VI) solution. Three hundred (300) mg and 1000 mg of the adsorbent were packed in the column with ID of 0.6 cm and 1.2 cm respectively. Figure 4 shows the breakthrough curves for different flow rates. It is found that the breakthrough point was at 600 empty bed volumes (EBV) when the flow rate was 4 ml/hr and 760 bed volumes when flow rate was 0.85 ml/hr.

### Task 1. Development of New Adsorbents for Arsenic Removal and Structural Characterization of the Absorbent.

### *Preparation and Structure Characterization of Iron-Chitosan Beads*

About 10 g of chitosan was added to 0.5 L of 0.01 N  $\text{Fe}(\text{NO}_3)_3 \cdot 9\text{H}_2\text{O}$  solution under continuous stirring for 2 hrs at  $60^\circ\text{C}$  temperature to form a viscous gel. Figure 5 shows the schematic diagram of apparatus for preparing iron-chitosan beads. The bead was formed by drop wise addition of chitosan gel with required viscosity into a 0.5 M concentrated NaOH precipitation bath. The beads were then separated from NaOH solution, and washed several times with de-ionized water to a neutral pH. The wet beads were dried in an oven under vacuum, and in air. Oven dried beads of iron-chitosan are shown in Fig 6. Dried beads were characterized by SEM. SEM micrograph of pure iron-chitosan is shown in Figure 7. From Figure 7 it is evident that the beads are porous in structure.

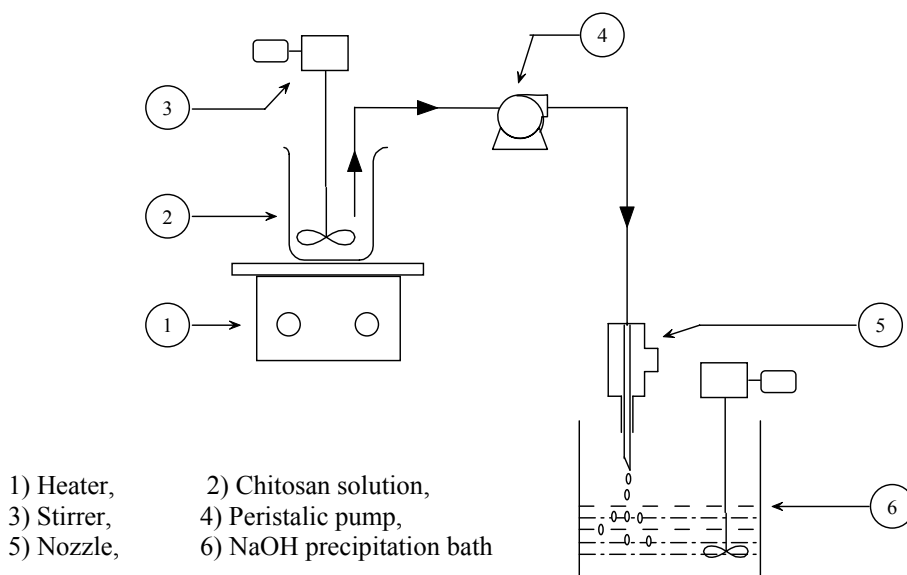


***Fig. 5 Schematic diagram: apparatus for preparing iron-chitosan beads***

### Task 2. Optimization of the Sorption under Different Environmental Conditions.

#### *Effect of pH on Arsenic Removal*

About 0.1g of the adsorbent was weighed into a series of 40 ml glass vials, followed by the addition of 1 ppm arsenic (As (V)/As (III)), to make the final volume 30 ml in each vial, resulting in a solid loading of 3.33 g/L. Ionic strength was controlled by adding 0.05 M NaCl to the solution. The initial pH values of solutions were adjusted to 5.00, 5.50, 6.00, 6.50, 7.00, 7.50, 8.00, 8.50, 9.00, 9.50, 10.00, 10.50, 11.00, and 11.50 with 0.01 M NaOH or 0.1 M HCl. The solutions were then kept on the shaker (160 rpm) for 24 hrs at  $25 \pm 1^\circ\text{C}$ . After 24 hrs, the final pH was recorded for each solution and the solutions were centrifuged for 30 minutes. The supernatant was then filtered through a  $0.45\text{-}\mu\text{m}$  membrane and the filtrate was analyzed for arsenic removal by High Performance Liquid Chromatograph (HPLC)-Atomic Fluorescence Spectroscopy (AFS). Removal efficiency of arsenic was calculated by the difference between the initial and final concentrations of arsenic in solution divided by the initial concentration, i.e.:

$$\text{Arsenic (As) removal (\%)} = \frac{[\text{As}]_{\text{initial}} - [\text{As}]_{\text{final}, \mu\text{g/g}} * 100}{[\text{As}]_{\text{initial}}}$$



**Fig. 6** Oven dried CFeN beads

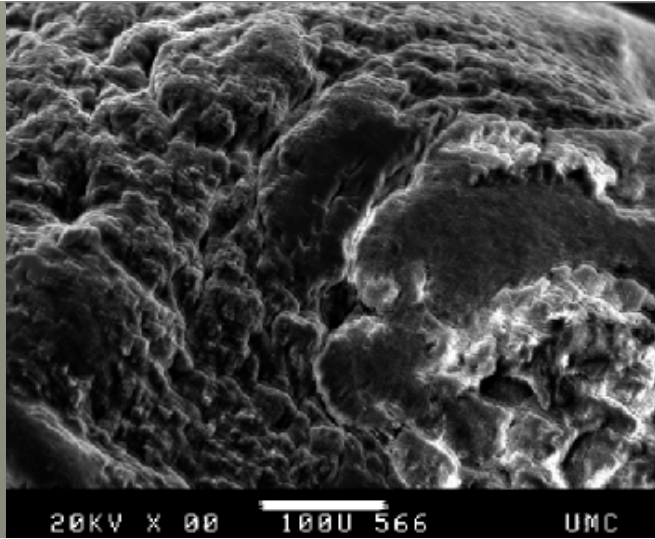


**Fig. 7.** Scanning electron micrograph (SEM) of pure iron-chitosan bead

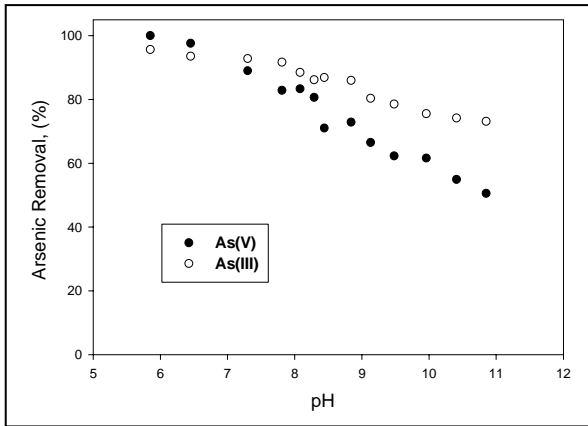


**Fig 8** Effect of pH on the arsenic removal from DI water (original As (III) and As (V) are both 1.00 mg/L.)

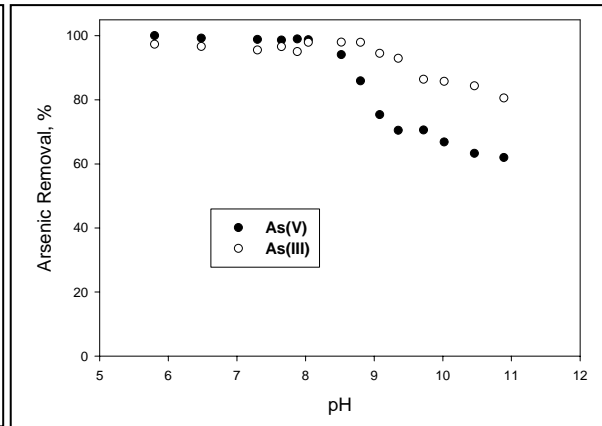


**Fig 9** Effect of pH on the arsenic removal from tap water (original As (III) and As (V) are both 1.00 mg/L.)

The adsorbed amounts of arsenate measured after 24 h of reaction indicated that pH had no obvious effect on As (V) removal from DI water at pH 5.8-7.3, with removal efficiency always higher than 88% under the experimental conditions (see Fig.8). A slight decrease in As (V) removal was observed at pH 7.8-8.8. When pH was higher than 9.00, the As (V) removal decreased with increasing pH. For tap water the adsorbed amounts of arsenate indicated that pH had no much effect on As (V) removal from pH 5.8-8.0 (shown in Fig.9), with removal efficiency always higher than 94% under the experimental conditions. A slight decrease in As (V) removal was observed at pH > 9.0.

## SUMMARY

In the past six months, Task 3 was finished. Chromium desorption and regeneration were conducted. The maximum desorption efficiency by NaOH was 80%, and by NH<sub>4</sub>OH was 55%. The desorption study confirmed that the desorption rate was fast, due to the larger surface area of the adsorbent. The regenerated adsorbent was used in the isotherm experiments. Adsorption capacities were decreased by 35%-45%. The column study results showed that the breakthrough point was at 600 empty bed volumes (EBV) when the flow rate was 4 ml/hr and 760 bed volumes when flow rate is 0.85 ml/hr. Comparing the column operation with the batch adsorption process, column operation has higher removal capacity. In addition, iron-chitosan beads were prepared for arsenic removal. SEM micrograph of the iron-chitosan demonstrated that the beads are porous in structure. Iron-chitosan could effectively remove arsenic from water and pH had no obvious effect on As (V) removal from DI water at pH 5.8-7.3. The removal efficiency was always higher than 88% under the experimental conditions

## FUTURE WORK

In the next reporting period, tasks 2 and 3 for arsenic removal will be finished. The efforts will include: (1) Further characterization of iron-chitosan using X-ray photoelectron spectroscopy (XPS); (2) Determination the adsorption capacity of the adsorbent by studying the equilibrium isotherm; (3) Effects of competing anions on As absorption, and (4) Evaluation the As adsorption kinetics using a pseudo-second-order reaction model.

## REFERENCES

Gang, D.; Benaerji, S.K.; Clevenger, T.E. *Practice periodical of Hazardous, Toxic, and Radioactive Waste Management*, 2001, 5, 58-65.

Ward, N. "Adsorption of hexavalent chromium on kaolinite and illite". MS thesis, The University of Arizona, Tucson, Ariz., 1990.

## PUBLICATIONS/PRESENTATIONS

1. Dhanarekha Vasireddyua, "Arsenic Adsorption onto Iron-Chitosan Composite." MS Thesis, University of Missouri-Columbia, December, **2005**
2. Ravi Kumar Kadari1, Baolin Deng, Gang, D. (**2006**) "Kinetics Modeling of Hexavalent Chromium Adsorption Onto Quaternized Poly(4-Vinylpyridine) Coated Activated Carbon", *Extended abstract of the 231st American Chemical Society (ACS) National Meeting*, March 26-30, Atlanta, GA

**Appendix 32: Alternative Materials for Dense Medium Separations**

**(KY004)**

## TECHNICAL PROGRESS REPORT

Contract Title and Number:

Crosscutting Technology Development at the Center for  
Advanced Separation Technologies  
(DE-FC26-02NT41607)

Period of Performance:

Starting Date: 6/1/2005  
Ending Date: 10/31/2006

Sub-Recipient Project Title:

Alternative Materials for Dense Medium Separation

Report Information:

Type: Semi-Annual  
Number: 1  
Period: 10/1/05-3/31/06  
Date: 4/6/06  
Code: KY004-R01

Principal Investigators:

Rick Honaker

Contact Address:

University of Kentucky  
234-B Mining and Mineral Resources Bldg  
Lexington KY 40506

Contact Information:

Phone: (859) 257-1108  
Fax: (858) 323-1962  
E-Mail: rhonaker@engr.uky.edu

Subcontractor Address:

No subcontracts issued

Subcontractor Information:

Phone:  
Fax:  
E-Mail:

### ABSTRACT

Several alternatives to ultrafine magnetite are being investigated for their application in the dense medium separators used to clean coal. During the initial reporting period of the project, coarse magnetite and steel slag material were collected and characterized. The coarse magnetite is less expensive and more readily available than conventional magnetite. The stability of the medium formed from the coarse magnetite has been evaluated in a dense medium cyclone circuit over a range of medium densities and feed pressures. Acceptable stability values were achieved under low feed pressures and medium densities above 1.6 RD. Approximately 15% of the steel slag material was found to have a particle size less than 100 mesh. Evaluation of the magnetic properties using a Davis tube found that about 35% of the -100 mesh steel slag was magnetic. When the magnetic material was reprocessed through the Davis tube, 96% of the feed material was recovered. The ¼-in x 28 mesh coal that will be used in this study was collected from an Arch coal preparation plant which treats coal from the Coalberg seam in West Virginia, which is known to be a more difficult-to-clean coal due to its middling content. The ash and total sulfur contents of the coal are 36.12% and 0.86%, respectively.

## **INTRODUCTION**

### Background

Dense medium processes are used to clean over 50% of the washed coal worldwide. Ultrafine magnetite is added to water to form the dense medium. Due to inefficiencies in the recovery process, typical magnetite losses equate to 1 to 2 lbs/raw ton. In the U.S., a major impact on the magnetite source occurred recently as a result of the closure of an iron ore mine in Missouri. As a result, the current magnetite supply is imported from South America, which has significantly elevated the cost. A new source of magnetite that can be used in dense medium processes for coal cleaning is commercially available from Minelco. The magnetite is reportedly coarser than the typical sources used in the U.S. coal industries and contains a larger amount of magnetic material. Both characteristics would typically result in expectations for improved magnetite recovery compared to current practices and thus lower costs. Also, the lower surface area would reduce viscosity effects at elevated medium densities. However, coarser magnetite may also result in medium stability problems that tend to negatively affect separation performance.

### Project Objectives

The goal of the project was to evaluate the potential of using an alternative source of magnetite for the cleaning of U.S. coal.

The objectives of the proposal are i) to evaluate alternative materials that could be economically used as a substitute for the traditional magnetite in dense medium processes, ii) to develop and evaluate a process in which fine waste material may be used as whole or part of the material needed for adjusting medium density and iii) to provide an excellent educational experience for a graduate student that can be easily translated to industrial application.

## **PROJECT TASKS**

### Test Program

The dense medium cyclone tests were conducted using a 6-inch diameter Krebs unit that was installed in a closed-loop circuit as shown in Figure 1 in the UK coal preparation laboratory. The test program during this reorting period involved an evaluation of medium stability over a range of medium densities (1.3 – 1.7 R.D.) and feed inlet pressures (2.5 – 10 psi). The stability of a dense medium produced using typical magnetite grade used in the U.S. coal preparation industry was compared to a coarse Minelco source. The assessment was achieved by collecting representative samples of the overflow and underflow streams under the various conditions in the absence of coal. The relative difference in the underflow and overflow medium densities was used as an indicator of magnetite stability.

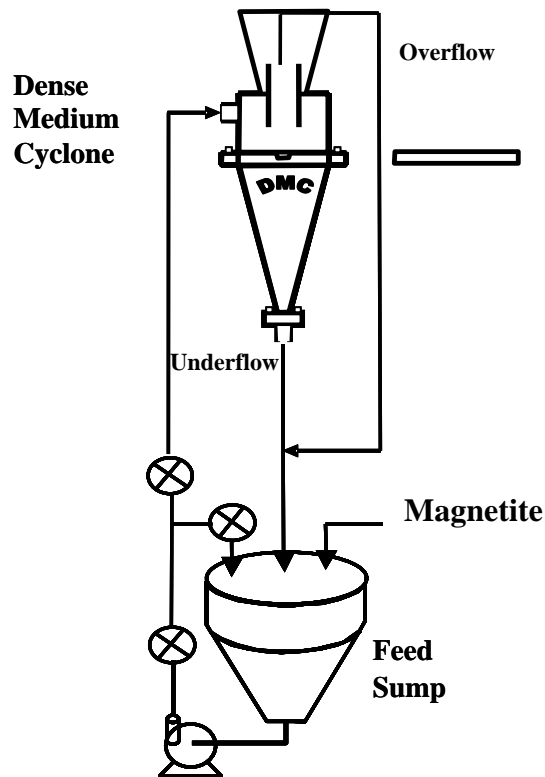


Figure 1. Closed-loop DMC circuit used in the evaluation of the Minelco magnetite.

### Task 1: Sample Collection and Characterization

The raw coal sample was collected from a West Virginia coal preparation plant operated by Arch Coal. The plant processes coal from the Coalberg seam, which contains a significant amount of material having a density between 1.6 and 2.0. As a result, the coal is more difficult to clean than most coal sources. Upon arriving at the UK coal preparation laboratory, the samples were dry screened using  $\frac{1}{4}$ -in and 28 mesh screens. The  $\frac{1}{4}$ -in x 28 mesh fraction was retained while the  $+1/4$ -in material was crushed using a laboratory hammer mill. The mill product was re-screened and the  $\frac{1}{4}$ -in x 28 mesh fraction combined with the previously obtained material. The  $-28$  mesh coal from each screening step was discarded.

A representative sample of  $\frac{1}{4}$  x 28 mesh material was subjected to proximate and particle size analysis. The heating value of the coal is 9120 Btu/lb, which is reflective of the relatively high ash content of 36.12%. The particle size-by-size analysis data is provided in Table 1, which shows that the ash-forming material is equally distributed throughout the sample.

Table 1. Particle size-by-size characterization for the ¼-in x 28 M Coalberg coal.

Particle Size (mesh)	Weight (%)	Ash (%)	Sulfur (%)
+4	16.42	36.74	0.84
4 x 6	18.76	34.70	0.64
6 x 8	22.59	34.45	0.62
8 x 12	18.26	30.97	0.69
12 x 16	15.46	27.98	0.73
16 x 20	4.54	34.73	0.63
20 x 28	1.71	36.72	0.67
-28	2.26	57.84	0.65
Total	100.00	36.12	0.68

Task 2: Magnetic Fly Ash Evaluation

The investigation into the potential use of the magnetic components in fly ash has not started at this time. However, matching funds from the Kentucky Division of Energy have been secured in support of this effort. A pilot-scale processing facility will be installed at a utility operation to recover the magnetic fraction. Work is expected to begin within the next reporting period of this project.

Task 3: Coarse Magnetite Evaluation

Medium stability was evaluated by measuring the difference in the density of the overflow and underflow streams of the DMC under a range of inlet pressures in the absence of coal. As shown in Figures 2 through 5, the medium suspensions developed using the coarse Minelco magnetite was relatively stable under low inlet pressures and high medium densities. The accepted industrial standard for the underflow-overflow medium density difference is 0.4 or less. This condition was satisfied at inlet pressures of 5 psi or less and medium densities greater than 1.55 RD.

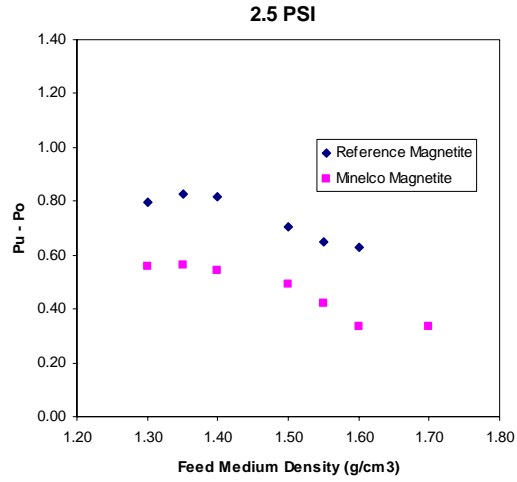


Figure 2. Medium stability at a 2.5 psi inlet pressure.

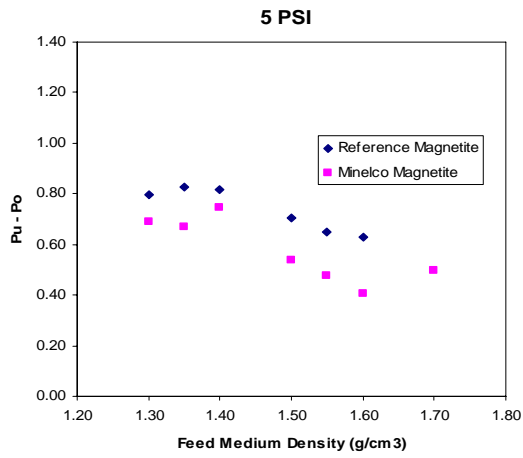


Figure 3. Medium stability at a 5.0 psi inlet pressure

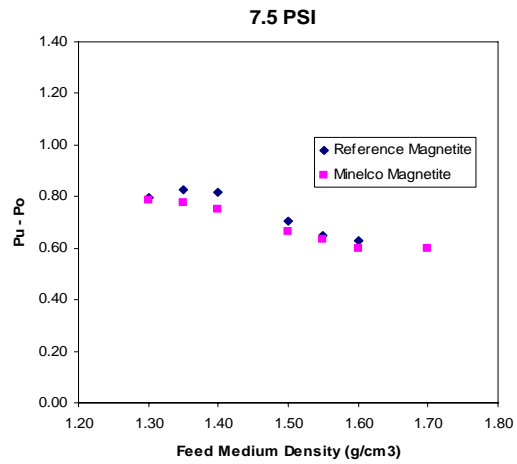


Figure 4. Medium stability at a 7.5 psi inlet pressure.

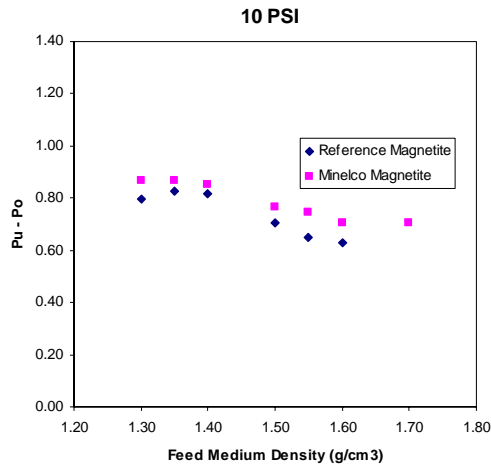


Figure 5. Medium stability at a 10 psi inlet pressure.

Task 4: Autogenous Medium Evaluation

The effort involving the use of fine reject material present in run-of-mine coal has not been initiated. It is expected that the samples will be collected during the next reporting period.

Task 5: Steel Slag Evaluation

Steel slag sample obtained from Stein Inc, Ashland-Kentucky was evaluated and its magnetic fraction compared to the coarse Minelco magnetite. The sample was screened using a 100 mesh screen and the underflow material retained for characterization while the +100 mesh material was discarded. The particle size distributions of the -100 mesh fraction and the coarse magnetite are compared in Figure 6. The -100 mesh material was dried and subjected to Davis tube tests to determine its magnetic content. The magnetic fraction of the coarse magnetite was also evaluated under the same conditions and the results compared in Table 2.

Table 2. Magnetic contents of Minelco magnetite and Steel slag magnetite

Component	Minelco Magnetite (g)	Steel Slag Magnetite (g)
Magnetic	59.24	14.68
Non Magnetic	0.76	27.13
Total	60.00	41.81
% Magnetics	98.73	35.11

The magnetic fraction of the steel slag obtained from the Davis tube was re-evaluated 96.07% magnetics was realized. The particle size distributions of both samples were measured using a Microtrac analyzer.

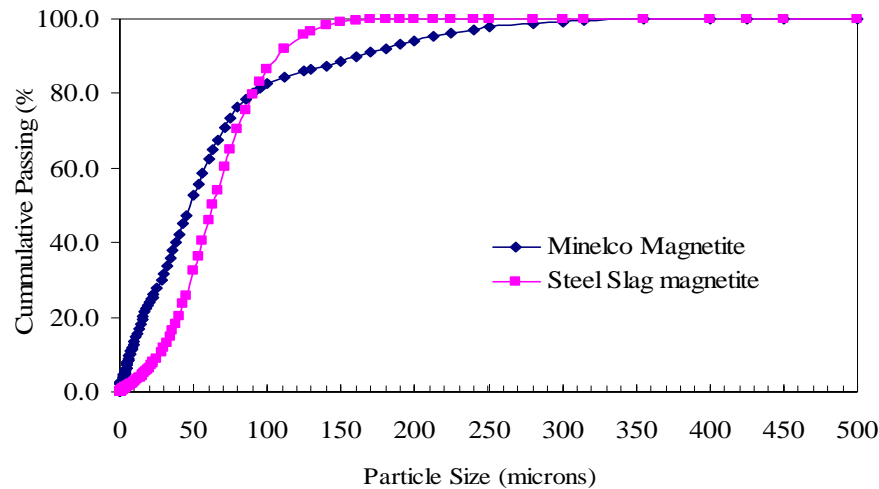


Figure 6. Particle size distributions of the Minelco and Steel slag samples evaluated in the study.

## SUMMARY

Relative coarse magnetite containing 18% +100 mesh material provided medium with acceptable stability characteristics under specific operation conditions when used in a dense medium cyclone. Medium density differentials between the underflow and overflow of around 0.4 density units were measured when inlet pressures of 5 psi or less were applied with medium densities greater than 1.55. Typical industrial feed pressures are around 10 psi. However, the 6-in. diameter cyclone used in this study creates significantly greater centrifugal forces than the large diameter cyclones used in industry. The use of the low pressures in the 6-in unit provides centrifugal forces within the same magnitude as those used in industry.

The steel slag material collected in this study from a production facility in Ashland, Kentucky contained about 15% -100 mesh of which 35% was magnetic. As such, about 5% of the total steel slag could be used in dense medium applications.

The coal sample to be used in the dense medium studies was obtained from a southern West Virginia coal preparation plant. The plant treats coal from the Coalberg seam which contains a significant amount of material having a density between 1.6 and 2.0 thereby

providing relatively difficult cleaning characteristics. The ash content of the coal was 36.12%.

## **FUTURE WORK**

The work in the next reporting period will include continuation of current studies as well as the initiation of efforts to explore other alternative mediums. The work plan includes the following:

1. Quantify and compare the cut point shift achieved from the use of the coarse magnetite and steel slag.
2. Evaluate the separation performance efficiency data generated from the use of the coarse magnetite and steel slag including the recovery-grade relationship, organic efficiency, and probable error.
3. Collect the fine reject sample that will be used to evaluate the potential of using the material to form an acceptable dense medium.
4. Develop and test a pilot-scale process circuit to recover the magnetic particles from fly ash.

## **REFERENCES**

Baird, G. A., Hornsby, D. T. and Lief, H., 1998, "Development of Fly Ash Derived Magnetite for Coal Cleaning," Proceedings, International Coal Preparation Congress, Brisbane, Australia, pp. 315 – 325.

Drugge, Mats, 2004 "A New Magnetite Source," Proceedings, International Coal Preparation Conference, Lexington, Kentucky, pp. 147 – 156.

Honaker, Rick 2006 "Coal Processing Plant Design", Lecture notes, University of Kentucky, Lexington, pp H13 – H15

Kempnich, R. J., 2003, "Coal Preparation – A World View," Proceedings, International Coal Preparation Conference, Lexington, Kentucky, pp. 17 – 39.

## **PUBLICATIONS/PRESENTATIONS**

At this time, no publications or presentations have been generated based on the findings of this study.

Matching funds have been secured from the Kentucky Division of Energy in support of the task associated with recovering and using magnetic fly ash material. The Kentucky funding is being used to install and evaluate a pilot-scale process circuit for recovering the magnetic portions of fly ash.

**Appendix 33: Determination of Factors Affecting the Separation of  
Potentially Hazardous Trace Elements and their Behavior in Coal Tailings  
Impoundments (KY005)**

## TECHNICAL PROGRESS REPORT

Contract Title and Number:

Crosscutting Technology Development at the Center for  
Advanced Separation Technologies  
(DE-FC26-02NT41607)

Period of Performance:

Starting Date: 6/1/2005  
Ending Date: 10/31/2006

Sub-Recipient Project Title:

Determination of Factors Affecting the Separation of  
Potentially Hazardous Trace Elements and their  
Behavior in Coal Tailings Impoundments

Principal Investigators:

Huggins, Shah, Huffman

Report Information:

Type: Semi-Annual  
Number: 1  
Period: 10/1/05-3/31/06  
Date: 03/31/06  
Code: KY005-R01

Contact Address:

University of Kentucky  
533 S. Limestone Street  
Lexington KY 40506

Contact Information:

Phone: (859) 257-4045  
Fax: (859) 257-7215  
E-Mail: fhuggins@engr.uky.edu

Subcontractor Address:

No subcontracts issued.

Subcontractor Information:

Phone:  
Fax:  
E-Mail:

### ABSTRACT

The project has been successfully initiated thanks in part to advice and direction from Prof. R. Honaker and hard work from Mr. Laal Seidu (U.K. Department of Mining Engineering), who will be the Graduate student supported by this project over the next two years. Run-of-mine coal and various cleaned and reject streams from the Peabody Gateway Coal preparation plant in Coulterville, Illinois, have been sampled and collected in >800 lb quantities. These samplings of coal and streams have been crushed to 100 mesh top-size and riffle-split into various fractions for the detailed mineralogical and trace element analyses to be performed in the project. Such information is intended to provide data for a detailed understanding of hazardous trace element partitioning in coal cleaning processes and their solubilization in pond impoundment situations. The samples from the Coulterville Plant will provide such information for gravity separation processes. Samples of the coal and different streams have been distributed for analysis and preliminary results are summarized for iron and arsenic from Mossbauer and XAFS techniques, respectively. Both elements are found to be strongly associated with pyrite in this coal. The forms-of-occurrence of these elements are known to be sensitive indicators to oxidation and weathering of the coal; however, the observed strong associations of these two elements with pyrite in all fractions indicate that weathering of the coal is negligible and that little oxidation has occurred since mining.

## **INTRODUCTION**

### Background

The major goal of separation technology is to increase the yield of valuable product by separating it from undesirable waste components. In the coal separation industry that serves the electrical power generation industry, the specific goal is to separate the incombustible mineral matter from the combustible macerals in order to develop a clean-coal product that has a higher calorific value and generates less combustion wastes and emissions. Such coal cleaning is especially valuable for coals from the bituminous coal regions of the eastern United States, since the mineralogy of the coals from these regions is generally dominated by quartz, clays and pyrite, which are minerals in coal that can be separated efficiently by conventional and/or advanced coal-cleaning methods. Such cleaning also removes certain trace elements designated as hazardous air pollutants (HAPs) by the 1990 Clean Air Act Amendments (CAAA). However, such HAP elements are then often concentrated in coal tailings and may become of concern to the 1976 Resource Conservation and Recovery Act (RCRA) during disposal of the mineral-rich tailings. The partitioning of a trace element between clean product and tailings is determined by the mineral phase in which the element occurs, its valence and magnetic states, and association with major inorganic or carbonaceous components of the coal. These mode-of-occurrence factors have only rarely been determined with respect to trace elements in coal cleaning operations and, as far as we can tell, never with respect to their behavior in coal tailings disposal options.

### Objective and Approach

The principal objective of this investigation is to determine why some hazardous air pollutant (HAP) elements separate well and others poorly during various coal cleaning processes. To address this issue, basic information regarding the occurrence of trace elements and minerals in coal and their behavior in coal cleaning processes will be obtained using a variety of techniques that enable us to determine the mineralogy of the coal and mode of occurrence of specific elements. Such techniques include computer-controlled scanning electron microscopy (CCSEM) to determine the mineralogy and mineral size distributions in both clean and tailings fractions and X-ray absorption fine structure (XAFS) spectroscopy to obtain direct data on the speciation of trace elements of interest. The secondary objective is to investigate and interpret the behavior of the HAP elements in laboratory simulations of the disposal of tailings in ponds using similar methods.

## **PROJECT TASKS**

Thanks in part to a number of discussions with Prof. R. Honaker (University of Kentucky, Department of Mining Engineering), the proposed research plan was defined and successfully implemented. A new Mining Engineering graduate student, Mr. Laal Seidu, has been employed on the project and he has been able to contribute immediately to the research by assisting in the collection of the first set of samples and in preparing the various splits needed for the different analysis methods.

**Task 1 – Sample Preparation:** Approximately 800 lbs each of raw coal, cleaned coal, and two tailings fractions were collected from the Peabody Gateway Coal preparation plant in Coulterville, Illinois. Samples were collected incrementally over 30-minute intervals. The preparation plant treats feed from a single mine on the Illinois #6 seam at a capacity of 1000 tph. The overall separation scheme is shown in Figure 1, below. Reject from the plant is normally sent to a tailings impoundment.

The raw coal to the plant was screened after initial crushing in a rotary breaker. The coarse fraction of the raw coal screen,  $2\frac{1}{2}'' \times 1\text{mm}$ , was fed to heavy media (HM) cyclones. The clean coal overflow from the HM cyclone separates from mineral-rich tailings due to the differences in density between coal, the mineral matter, and the magnetite heavy media. The minus 1 mm fine fraction of the raw coal screen was sent to classifying cyclones which in turn fed a spiral circuit. The spiral circuit also separates clean coal and mineral matter based on density differences. The combined clean product of the coarse and fine cleaning circuits has a size range of  $2\frac{1}{2}'' \times 0$ .

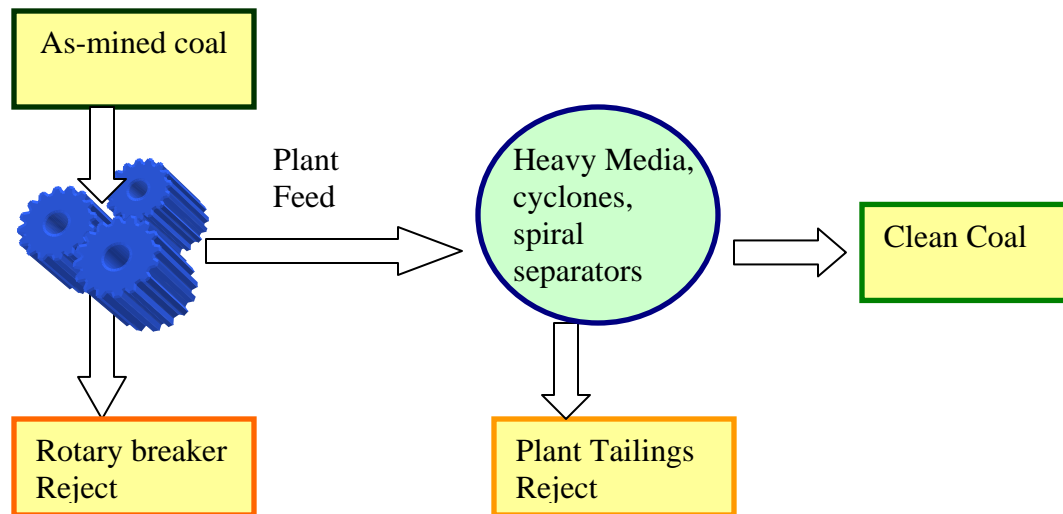


Figure 1: Diagram showing coal fractions generated at the Coulterville prep. plant.

Samples of the raw feed, rotary breaker (RB) reject, the plant reject, and the clean coal were dried, crushed to 100% passing  $\frac{1}{4}''$  mesh, and riffle split to obtain a representative samples. Final samples for the analyses were further crushed to 100 mesh top size and split into various fractions, according to the mass needed for each type of analysis.

**Task 2 – Analysis Methods:** The following analyses are in the process of being carried out on each of the fractions:

- A. Ultimate, proximate, forms of sulfur, heating value
- B. XRF for major elements on 500°C ash prepared from each fraction
- C. Trace element analyses by INAA, ICP-MS, and individual analyses for As, Se, Hg
- D. Mineral matter and mineral size distributions by CCSEM

- E. Fe speciation and oxidation state by Mossbauer spectroscopy
- F. Speciation of key elements by XAFS spectroscopy.

Items A and B are currently being performed at one of two laboratories on the University of Kentucky campus (Kentucky Geological Survey, KGS; Center for Applied Energy Research, CAER). For Item C, arrangements have been made with the University of Missouri Reactor to perform instrumental neutron activation analyses (INAA) and ICP-MS analyses. Mineral matter analyses (Item D) and Fe speciation and oxidation (Item E) will be performed in-house by project personnel using CCSEM and Mossbauer techniques. A start has been made on Item F: data for As and Zn have been collected using the facilities at the National Synchrotron Light Source at Brookhaven National Laboratory. Synchrotron sessions are also scheduled for April and May during which additional XAFS data on elements will be obtained.

**Task 3 – Results:** To date, only a few preliminary results have been obtained on the Illinois #6 set of samples. These include iron Mossbauer spectroscopy of the raw coal and two fractions (clean coal, plant reject), X-ray absorption fine structure (XAFS) spectroscopy of arsenic and zinc in all four streams, proximate analysis, and heating value for the four fractions, as determined at KGS (q.v. Tables 1 and 2 for the latter analyses). Also shown in Table 1 are the approximate wt% fractions of each stream derived from the raw coal based on typical plant performance.

**Table 1: Wt% ash and heating value for four fractions of Illinois #6 coal**

Stream	Wt% Stream*	Ash %	Btu/lb
Rotary breaker feed	100	28.1	10,278
Rotary breaker reject	1.5	83.5	1,869
Clean coal	65	9.7	13,132
Plant reject	33.5	77.8	2,644

\* from plant historical data

**Table 2: Proximate Analyses for four fractions of Illinois #6 coal**

Stream	Moisture wt%	Volatile Matter	Ash %	Fixed Carbon*	VM daf basis
Rotary breaker feed	4.91	29.71	27.11	38.27	43.7
Rotary breaker reject	5.70	10.83	76.83	6.65	--
Clean coal	4.53	36.80	9.14	49.54	42.6
Plant reject	3.01	13.90	73.55	9.54	--

\* by difference

The Mossbauer spectrum of the feed coal is shown in Figure 2; the spectra for the RB reject and clean coal exhibit quite similar spectra. These data provide quantitative information regarding the mineralogy of iron in the different streams. However, the mineralogy of iron is clearly dominated by pyrite, FeS<sub>2</sub>, since 90% or more of the iron is associated with this sulfide mineral. Only small amounts (~ few percent) of the iron are

present in other mineral phases, such as clays and sulfate minerals. The Mossbauer spectrum of the clean coal suggests a slight contamination of the stream by magnetite; this sample will be re-run at a suitable scale so as to allow quantification of magnetite.

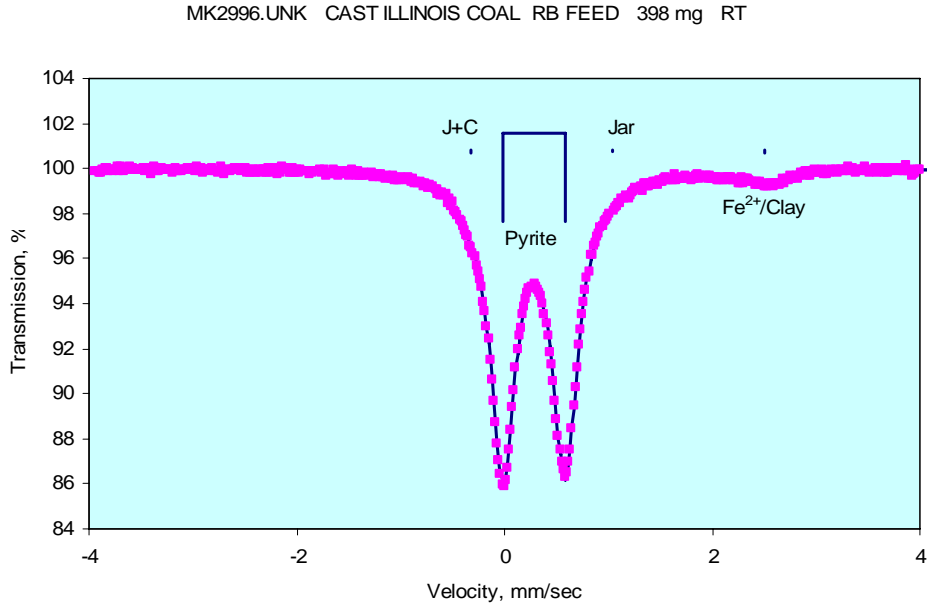


Figure 2: Mossbauer spectrum of the as-mined Illinois #6 coal. Peaks due to pyrite, jarosite (Jar, J) and Fe<sup>2+</sup>-bearing clay (C) are indicated.

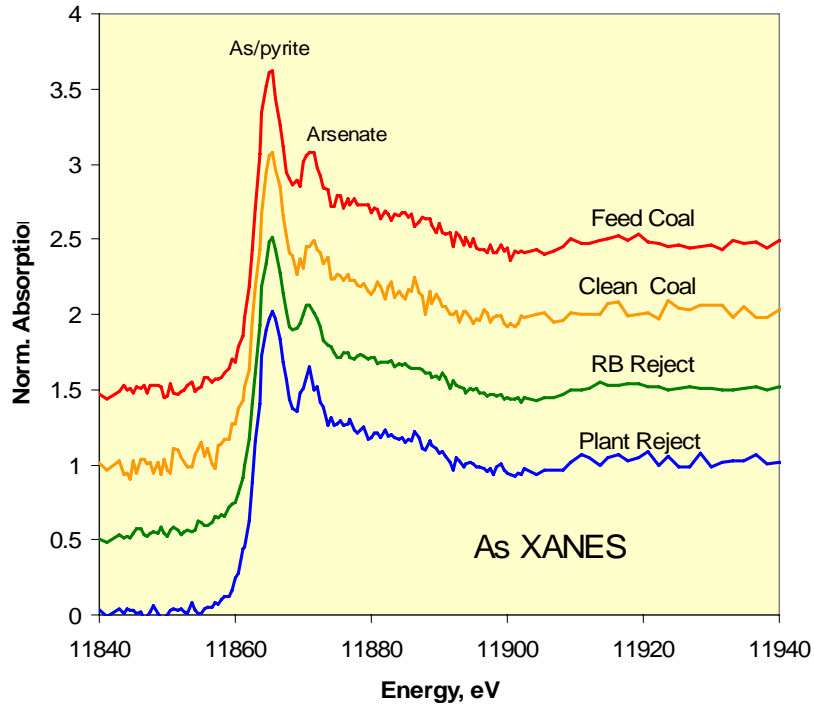


Figure 3: As XANES spectrum of four fractions from Illinois #6 coal. Note the peaks identified as arising from arsenic in pyrite and from arsenic in arsenate forms.

The arsenic mineralogy is also dominated by its association with pyrite. The XAFS spectra (Figure 3) of the different streams exhibit little difference and indicate that only a small fraction of the arsenic is associated with arsenate. Almost all of the arsenic is present as arsenic substituting for sulfur in the pyrite structure. These spectra will be quantified as to the distribution of As between pyrite and arsenate by means of a least-squares procedure.

Both the iron Mossbauer and arsenic XAFS data indicate that weathering and oxidation of the as-mined Illinois #6 coal and the derived fractions are negligible to very minor.

## **SUMMARY**

Work on the project has been initiated by the sampling, preparation, and division of four streams of the Illinois #6 coal from the Peabody Preparation plant, Coulterville, IL, into various fractions for the many coal, mineralogical, and forms-of-occurrence analyses that will constitute the basic data needed for detailed understanding of trace element partitioning in coal cleaning processes and their behavior in coal impoundment simulations. Preliminary analyses relating to iron and arsenic indicate a strong association of these elements with pyrite and virtually no oxidation or weathering of the coal.

## **FUTURE WORK**

Over the next six months, we should be able to gather most, if not all, of the data needed for the evaluation of trace element partitioning in gravity separation procedures employed at the Peabody Preparation Plant, Coulterville, IL. In addition, we will immediately begin the leaching testing of the tailings fractions.

## **REFERENCES**

None.

## **PUBLICATIONS/PRESENTATIONS**

None.

**Appendix 34: Enhanced Flotation Performance Through Column Froth  
Enrichment (KY006)**

## TECHNICAL PROGRESS REPORT

Contract Title and Number:

Crosscutting Technology Development at the Center for  
Advanced Separation Technologies  
(DE-FC26-02NT41607)

Period of Performance:

Starting Date: 6/1/2005  
Ending Date: 10/31/2006

Sub-Recipient Project Title:

Enhanced Flotation Performance Through Column  
Froth Enrichment

Report Information:

Type: Semi-Annual  
Number: 1  
Period: 10/1/05-3/31/06  
Date: 4/6/06  
Code: KY006-R01

Principal Investigators:

Honaker, Tao

Contact Address:

University of Kentucky  
234B Mining and Mineral Resources  
Lexington KY 40506

Contact Information:

Phone: (859) 257-1108  
Fax: (858) 323-1962  
E-Mail: rhonaker@engr.uky.edu

Subcontractor Address:

No subcontracts issued.

Subcontractor Information:

Phone:  
Fax:  
E-Mail:

### ABSTRACT

Flotation column is a complex process where many variables are involved to obtain an optimum performance. The research personnel needed to conduct the investigation were hired and began the performance of column flotation tests. Identifying the optimum flotation column conditions and performances has been the focus of the efforts in the first reporting period. The coal that will be used throughout the investigation was collected and characterized. The coal contained 42.54% ash and 1.64% total sulfur. Flotation tests are continuing into the next reporting period to identify the optimum conditions.

## INTRODUCTION

### Background

The froth flotation process is comprised of two separate and distinctly different zones, i.e., the collection zone and the froth zone. In the collection zone, the separation of the valuable minerals from the non-valuables is achieved based on the bubble-particle attachment process. Due to hydraulic entrainment, a portion of the non-valuable minerals is carried from the collection zone into the froth zone with the mineral-bubble aggregates. Selectivity of the process can be enhanced in the froth zone by providing drainage of the feed pulp and utilizing the selective detachment of the more weak hydrophobic particles as a result of bubble coalescence and the resulting bubble surface area reduction. The importance of the latter sub-process is the subject of recent investigations (van Deventer et al., 2004; Honaker and Ozsever, 2003; Ata et al., 2002; Ralston et al., 1999; Falutsu, 1994; Hewitt et al., 1994; Yianatos et al., 1988). On the other hand, decades of research focused on the froth flotation process have resulted in a clear understanding of the processes and sub-processes involved in the selectivity achieved in the collection zone (Yoon and Mao, 1996; Mao and Yoon, 1997).

Moys (1978) and later Yianatos et al. (1988) confirmed by experimental evidence that the detachment process is selective. From Yianatos et al. (1988), the detachment rate for chalcopyrite under a given set of conditions was  $0.30 \text{ min}^{-1}$  whereas pyrite obtained a higher rate at  $0.41 \text{ min}^{-1}$ . As such, differential detachment rates can be exploited to improve the selectivity between hydrophobic species. Schultz et al. (1991) obtained an improved concentrate grade and recovery in a column by introducing the feed (Alabama shale,  $d_{90}=23$  microns) into the froth zone.

Detailed investigations utilizing modified column apparatus designs have provided promising quantifiable evidence of the selective detachment and drop-back processes (Rubio, 1996; Ata et al., 2002; Honaker and Ozsever, 2003). For example, Ata et al. (2002) used a unique cell design to show that highly hydrophobic particles added directly into the froth zone can selectively replace particles of lower hydrophobicity. Specifically, the addition of hydrophobic silica particles in the froth reduced the recovery of hematite particles that were added in the collection zone by 10 percentage points. Based on this finding, it is plausible that the addition of highly hydrophobic particles in the froth zone could assist in the selective rejection of the more weakly hydrophobic material (e.g., low grade particles) reporting from the collection zone, thereby enhancing the overall selectivity between particles of varying hydrophobicity.

The project will exploit the selective detachment process to enhance the selectivity between particles having varying degrees of floatability. External refluxing and the addition of hydrophobic material directly into the froth zone will be investigated as described in the following sections.

## Objectives

The goals of the proposed project are 1) to fundamentally evaluate the selectivity improvement achieved by external refluxing or adding highly hydrophobic particles in the froth zone, 2) to develop and demonstrate the use of magnetic hydrophobic material to improve the selectivity achieved on a variety of minerals, and 3) to investigate the potential selectivity benefits associated with recycling a portion of the froth product back to the froth phase.

## **PROJECT TASKS**

### Task 1. Fundamental Evaluation of Selective Detachment

This research is being conducted by using a flotation column made of cylindrical Plexiglas tubing with 5 cm inner diameter and 246 cm height. Feed slurry is injected at 45 cm below overflow lip, using a variable speed pump. Pulp level is maintained by utilizing a control valve, which is connected to the tailing stream of the column. Air bubbles and recirculation flow were mixed by using a static mixer of 1.9 cm inner diameter. MIBC reagent is used as frother while fuel oil No. 2 is employed as collector. A fixed mixer was attached to a sump where feed slurry is prepared to run experiments at different feed rates. Collector is directly added to the sump while frother is injected to the recirculation stream by using variable pulp.

### Task 2. Practical Applications of Magnetic, Hydrophobic Particles

Pittsburgh No. 8 raw coal was obtained from a preparation plant in West Virginia. Raw coal sample was collected and crushed below 21  $\mu\text{m}$  in a hammer mill. The sample was screened using a 65 mesh and 200 mesh sieves in a Sweco unit. Representative samples were taken between -65 mesh and 65 x 200 mesh and a complete characterization of these samples was made. Results are showed in Table 1.

Table 1. Characterization raw coal Pittsburgh No. 8

Coal Sample	Ash (%)	Moisture (%)	Sulfur (%)	BTU/lb
-65 mesh	42.54	0.56	1.64	8,203
65 x 200 mesh	16.44	0.67	3.04	12,562

Some tests have been run with oil shale and raw coal. The purpose of these test is obtain enough operation experience and to improve column flotation performance. Release analysis test are compared with column flotation results to evaluate progress.

## **SUMMARY**

A graduate research assistant joined the research team with the responsibility of performing the tests required in this investigation under the direction of the principal

investigator. A significant portion of the reporting period was devoted to flotation operation training and optimization. At the present time, research findings regarding selective detachment as a means of enhancing flotation performance have not developed from the current investigation. However, tests are being performed to optimize the conditions in the collection and froth zones of a flotation column.

The coal sample that will be used in this investigation was obtained from a Consol preparation plant located in Pennsylvania. The plant treats coal from the Pittsburgh No. 8 seam. The sample was obtained from the run-of-mine feed stream to the preparation plant. Upon arriving at the UK laboratory, the sample was crushed and ground to a particle size needed for the flotation experiments.

## **FUTURE WORK**

First priority will be finish with the optimum setting of flotation column by doing some test that guarantee correct performance, comparing their results with release analysis results obtain for the same sample used in flotation column. The step will be to prepare enough samples (crushing and screening process) to first program test and finally run some program schedule test.

## **REFERENCES**

Ata, S, Ahmed, N and Jameson, G J, 2002. Collection of hydrophobic particles in the froth phase, *International Journal of Mineral Processing*, 64:101-122.

Finch, J A and Dobby, G S, 1990. *Column Flotation*, (Pergamon Press: Oxford).

Flinn, D H, Guzonas, D A and Yoon, R.-H, 1994. Characterization of silica surfaces hydrophobized by octadecyltrichlorosilane, *Colloids and Surfaces, A: Physicochemical and Engineering Aspects*, 87(3):163-76.

Falutsu, M, 1994. Column flotation froth characteristics-stability of the bubble-particle system, *International Journal of Mineral Processing*, 40: 25-243.

Hewitt D, Fornasiero, D and Ralston, J, 1994. Bubble particle attachment efficiency. *Minerals Engineering*, 7: 657-665.

Honaker, R Q and Ozsever, A V, 2003. Evaluation of the selective detachment process in flotation froth, *Minerals Engineering*, 16(10): 975-982.

Mao, L and Yoon, R H, 1997. Predicting flotation rates using a rate equation derived from first principles, *International Journal of Mineral Processing*, 51(1-4):171-181.

Moys, M H, 1978. A study of a plug-flow model for flotation froth behavior, *International Journal of Mineral Processing*, 5: 21-28.

Ralston, J, Fornasiero, D and Hayes, R, 1999. Bubble-particle attachment and detachment in flotation, *International Journal of Mineral Processing*, 56(1-4):133-164.

Rubio, J, 1996. Modified column flotation of mineral particles, *International Journal of Mineral Processing*, 48:183-196.

Schultz, C W, Mehta, R K and Bates J B, 1991. The flotation column as a froth separator. SME Annual Meeting, Denver, CO.

Van Deventer, J S J, Feng, D and Burger, A J, 2004. Transport phenomena at the pulp-froth interface in a flotation column: II Detachment, *International Journal of Mineral Processing*, 74(1-4): 217-231.

Yianatos, J B, Finch, J A and Laplante, A R, 1988. Selectivity in column flotation froths, *International Journal of Mineral Processing*, 23: 279-292.

Yoon, R H and Mao, L, 1996. Application of extended DLVO theory, IV - Derivation of flotation rate equation from first principles, *Journal of Colloid and Interface Science*, 181(2): 613-626.

## **PUBLICATIONS/PRESENTATIONS**

No publications or presentations of the research findings from this project have been performed to date.

**Appendix 35: Recovery Of Gold From Thiosulfate Leach Liquor Using  
Activated Carbon (MT005)**

**Appendix 36: The Effect of Alkyl Diphenyl Oxide and Sulfonated Oleic  
Acid Surfactants on Nucleation and Growth of Potassium Sulfate Crystals:  
Optimization of Surfactants for the Potash Industry (NM005)**

## TECHNICAL PROGRESS REPORT

Contract Title and Number:

Crosscutting Technology Development at the Center for  
Advanced Separation Technologies  
(DE-FC26-02NT41607)

Period of Performance:

Starting Date: 6/1/2005  
Ending Date: 10/31/2006

Sub-Recipient Project Title:

The Effect of Alkyl Diphenyl Oxide and Sulfonated  
Oleic Acid Surfactants on Nucleation and Growth of  
Potassium Sulfate Crystals: Optimization of Surfactants  
for the Potash Industry

Principal Investigators:

Bond, Hockensmith

Report Information:

Type: Semi-Annual  
Number: 1  
Period: 10/1/05-3/31/06

Date: 3/29/2006

Code: NM005-R01

Contact Address:

Department: Mat. & Met. Engineering  
New Mexico Tech  
Socorro NM 87801

Contact Information:

Phone: (505) 835-5653  
Fax: (505) 835-6333  
E-Mail: gbond@nmt.edu

Subcontractor Address:

No subcontracts issued

Subcontractor Information:

Phone:  
Fax:  
E-Mail:

### ABSTRACT

Studies on the use of alkyl diphenyl oxide (ADO) surfactants to enhance the crystal size distribution (CSD) of potassium sulfate ( $K_2SO_4$ ) crystals is progressing very well. The effects of cooling rate, and nucleation and growth temperatures have been investigated, and an improved protocol for  $K_2SO_4$  crystallization has been developed. Calfax 16L-35 ADO surfactant has a linear 16-carbon chain. The greatest crystal yield in the desired granular size range of at least 1.4 mm is obtained with the addition of 28% of the critical micelle concentration (CMC) of this surfactant. This corresponds to an increase of more than two orders of magnitude in the yield of granular crystals, compared to crystallization without surfactant. Work is in progress with Calfax DB-45, a branched  $C_{12}$  ADO surfactant that promises to give a still higher yield of granular crystals. The effects of oleic acid surfactants on the CSD of  $K_2SO_4$  are also being studied. So far the crystals produced with these surfactants are small, but this work is still in a relatively early phase.

## INTRODUCTION

### Background

Potassium sulfate ( $K_2SO_4$ ) crystals smaller than 1.4 mm (ASTM mesh size 14) are outside the range for granular fertilizer applications. Smaller crystals, down to  $\sim 250 \mu\text{m}$  (mesh size 60) may be used, but constitute a lower-grade, less desirable product. Smaller fines than this would need to be re-dissolved for subsequent crystallization. Additions of both linear and branched alkyl diphenyl oxide (ADO) surfactants have been found to enhance the crystal size distribution (CSD). Although a greater total crystal yield can be obtained without surfactant additions, more than half of that crystal weight is in the form of small fines that are not marketable.

### Objective and Approach

The present objectives are:

- To optimize the yield obtainable with ADO disulfonate surfactants, while maintaining a desirable CSD of  $K_2SO_4$  crystals applicable for the fertilizer industry.
- To investigate the performance of oleic acid surfactants for comparison with a view to improving performance. The ADO surfactant Calfax 16L-35 (sodium hexadecyl diphenyl oxide disulfonate), with which encouraging results were first obtained, contains a closely similar number of carbon atoms to oleic acid [ $\text{CH}_3(\text{CH}_2)_7\text{CH}=\text{CH}(\text{CH}_2)_7\text{COOH}$ ]. It does not, of course contain the phenyl groups, but it is unsaturated, sulfonated, and has the kinked shape that results from the *cis* double bond.

The approach in this period of the research is:

- To perform further studies with both a linear (Calfax 16L-35) and a branched (Calfax DB-45) ADO surfactant, in which the cooling rate, nucleation and growth temperatures, and surfactant concentration are optimized for the production of granular crystals.
- To study the effects of additions of oleic acid alone, and of oleic acid/potassium hydroxide and oleic acid/kerosene surfactants on crystallization of potassium sulfate.

## PROJECT TASKS

The saturated mother liquor in these experiments is prepared at  $80^\circ\text{C}$ . In earlier tests, the temperature was lowered to  $40^\circ\text{C}$  and held while crystallization occurred. Studies of the influence of both cooling rate and nucleation temperature, prior to crystal growth at  $40^\circ\text{C}$ , have now been conducted. Closer control of these parameters has resulted in much less scatter in the data.

Granular crystals are consistently obtained after cooling at a rate of  $0.0108^\circ\text{C}/\text{s}$  ( $0.65^\circ\text{C}/\text{min}$ ). Optimum results were obtained when the solution temperature was first

lowered to approximately 37°C, and then increased to 40°C so that the largest amount of crystal growth would occur with a minimum amount of nucleation. The solution is at temperatures below 40°C for approximately twenty-two minutes prior to crystal growth at 40°C, which allows for a desirable amount of nucleation to occur.

Once this improved cooling/heating regime had been developed, the goal was then to optimize the ADO surfactant concentration in order to produce as large a crystal yield as possible within the desired size range of 1.4 mm (14 mesh) to 3.35 mm (6 mesh). The concentration is expressed both as g/L, and as percentage of the critical micelle concentration (CMC) based on a gram-molecular weight of 608 g.

The crystal yields obtained in the desired size range with the improved cooling/heating regime and the addition of different percentages of the CMC of Calfax 16L-35 are shown in Figure 1. The addition of 0.241 g/L (28% CMC) of Calfax 16L-35 produced the highest total yield of crystals in the 1.4-3.35 mm size range, and also produced the smallest proportion of fines (crystals of size < 1.4 mm), as illustrated in Figures 2 and 3.

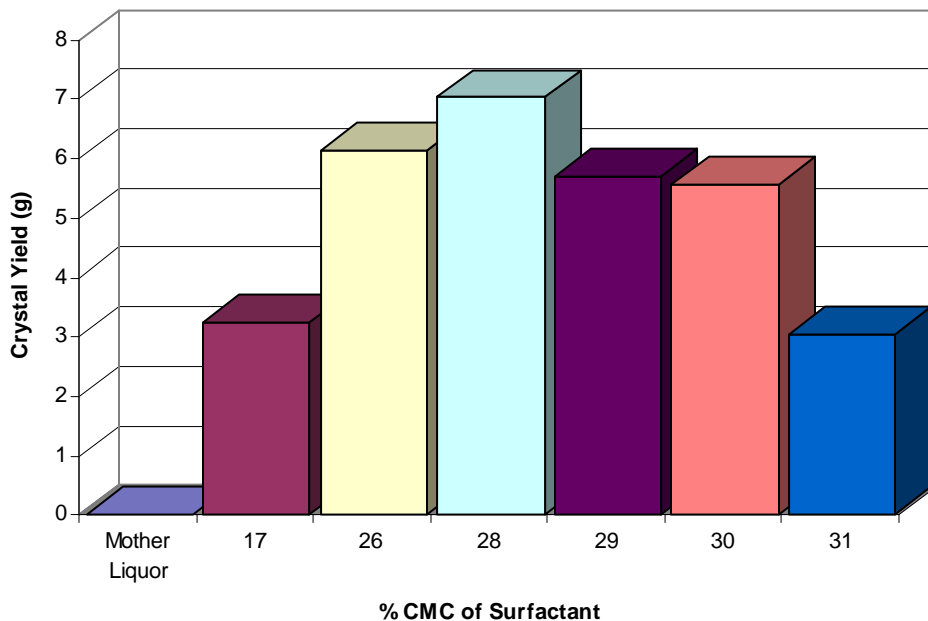


**Figure 1:** Total  $K_2SO_4$  crystal yields in size range 1.4-3.35 mm, obtained with the improved cooling/heating regime and the addition of Calfax 16L-35 surfactant.

In addition to the vastly improved crystal yields, a pronounced change in crystal morphology occurs (as shown in Figure 4), corresponding to the continual adsorption of surfactant on growing crystal faces. The crystal shown in Figure 4b is smaller than many grown with the surfactant (for ease of visualization), but its morphology is representative.

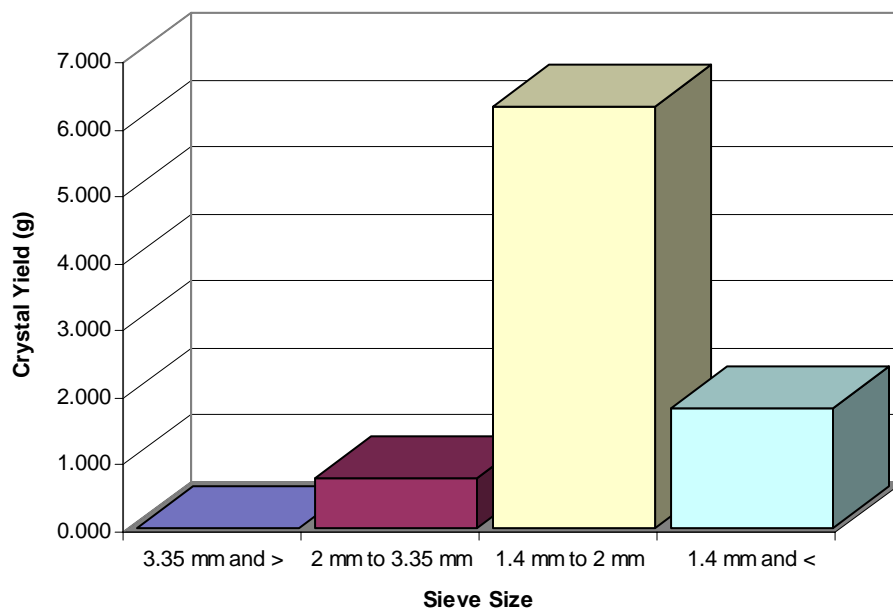


**Figure 2:**  $K_2SO_4$  crystal yields by size range [ $>3.35$  mm (6 mesh and larger), 2-3.35 mm (10 mesh), 1.4-2 mm (14 mesh), and  $< 1.4$  mm (smaller than 14 mesh)], obtained with the addition of 28% CMC of Calfax 16L-35 surfactant.

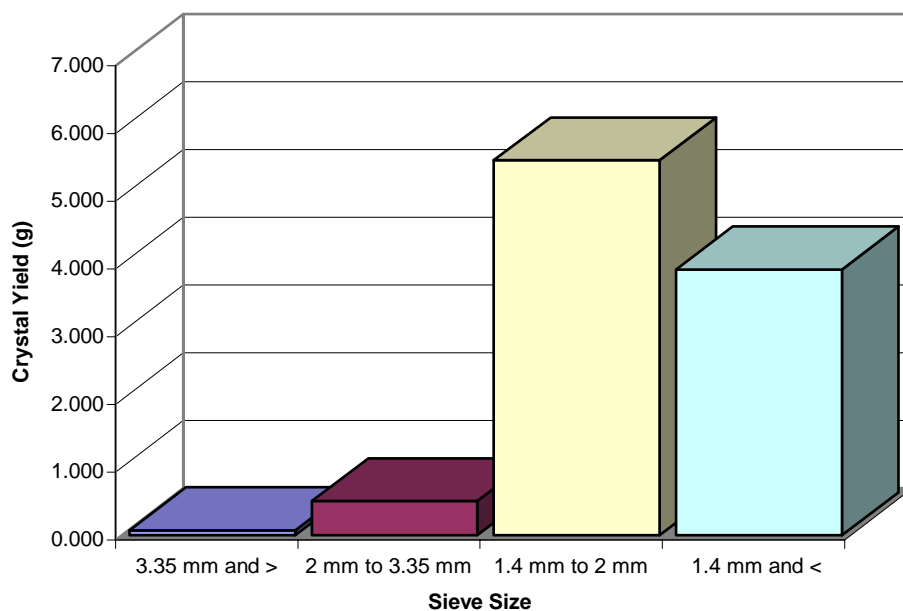


**Figure 3:**  $K_2SO_4$  crystal yields by size range [ $>3.35$  mm (6 mesh and larger), 2-3.35 mm (10 mesh), 1.4-2 mm (14 mesh), and  $< 1.4$  mm (smaller than 14 mesh)], obtained with the addition of 26% CMC of Calfax 16L-35 surfactant.

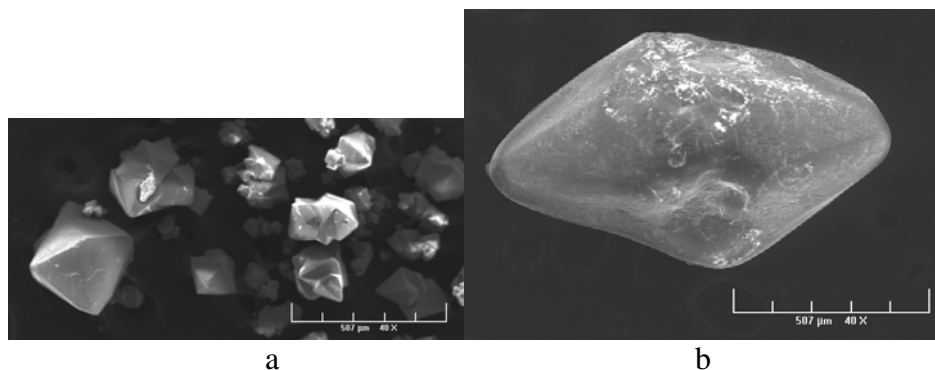


**Figure 4:**  $K_2SO_4$  crystals grown: a) from the mother liquor (no surfactant), b) with 34% CMC of Calfax 16L-35 surfactant. [Scale bar: 507  $\mu\text{m}$ .]

Early results indicate that Calfax DB-45 surfactant produces even greater CSD enhancement with the present cooling/heating regime.

Studies have commenced on the use of oleic acid to enhance the CSD of potassium sulfate. A modified experimental setup, 20% of the size of that used for the ADO surfactants, is being used so that multiple runs can be performed more easily. Priolene 6939 oleic acid has been obtained from Uniqema (Chicago, IL). A value of  $10^{-2}$  M was found for the CMC of oleic acid by Kabil and Ghazy (1994). (A specific value of the CMC for Priolene 6939 is not available at present.)

Initial work has focused on the oleic acid, oleic acid/1M potassium hydroxide (1.25-250% CMC), and oleic acid/kerosene oil (10-600% CMC), as well as small amounts (1-5% CMC) of oleic acid alone. (The use of a  $6.36 \times 10^{-2}$  M oleic acid/kerosene oil solution follows the work of Ghazy, Kabil, Shallaby and Ammar, 2001.) While early data have not shown CSD enhancement, the effects of cooling rate, nucleation and growth temperatures, and chemical modification of the oleic acid are also important factors.

## SUMMARY

An improved cooling/heating regime has been developed for  $K_2SO_4$  crystallization in the presence of Calfax (ADO) surfactants 16L-35 and DB-45. This involves cooling at a rate of  $0.0108^\circ\text{C}/\text{s}$  ( $0.65^\circ\text{C}/\text{min}$ ) from  $80^\circ\text{C}$  to  $37^\circ\text{C}$  for initial nucleation, and then an increase of the temperature back to  $40^\circ\text{C}$  for crystal growth. With this regime, 28% CMC of 16L-35 surfactant produces more than two orders of magnitude improvement in the crystal yield in the desired granular size range of  $>1.4$  mm (14 mesh). Early results for DB-45 with the improved cooling/heating regime indicate that its performance will surpass that of the 16L-35.

Studies on the effect of oleic acid surfactants have commenced. Although initial experiments resulted in the growth of small crystals, several parameters have yet to be optimized, and this work is under way.

## **FUTURE WORK**

Future work will be focused in the following areas:

- Completion of experiments on Calfax DB-45 with the improved cooling/heating regime, which promises to offer even greater enhancement of CSD than that obtained with Calfax 16L-35.
- Further consideration of the influence of Calfax (ADO) surfactants on crystal growth and morphology.
- Development of improved cooling/heating regime for use with oleic acid surfactants.
- Influence of chemical modification of oleic acid.

## **REFERENCES**

Ghazy, S.E., M.A. Kabil, A.M. Shallaby, and N.S. Ammar (2001). *Indian J. Chem. Technol.* **8**, 211-218.

Kabil, M. A. and S.E. Ghazy (1994). *Sep. Sci. Technol.* **29**, 2533-2539.

## **PUBLICATIONS/PRESENTATIONS**

M. Wimberly, G.M. Bond and C. Hockensmith (2005). Development of enhanced surfactants for the potash industry. Poster presented at Rio Grande Symposium on Advanced Materials, (Albuquerque, NM, October 11, 2005).

**Appendix 37: Thiosulfate As A Replacement For Cyanide In The Presence  
Of Activators (NV003)**

## TECHNICAL PROGRESS REPORT

Contract Title and Number:

Crosscutting Technology Development at the Center for  
Advanced Separation Technologies  
(DE-FC26-02NT41607)

Period of Performance:

Starting Date: 6/1/2005  
Ending Date: 10/31/2006

Sub-Recipient Project Title:

Thiosulfate As A Replacement For Cyanide In The  
Presence Of Activators

Report Information:

Type: Semi-Annual  
Number: 1  
Period: 10/1/05-3/31/06  
Date: 3/27/06  
Code: NV003-R01

Principal Investigators:

Fuerstenau

Contact Address:

168 Macay School of Mines  
University of Nevada Reno  
Reno NV 89557

Contact Information:

Phone: (775) 784-4310  
Fax: (775) 784-4764  
E-Mail: mcf@unr.edu

Subcontractor Address:

University of Nevada, Reno  
Reno, NV 89557

Subcontractor Information:

Phone: (775) 784-4312  
Fax: (775) 784-6680  
E-Mail: jerry\_best@vpaf.unr.edu

### ABSTRACT

An experimental setup for this research is described. Gold dissolution rates have been established as a function of electrode rotational velocity, thiosulfate, cupric ion and ammonia concentrations, and pH. The influence of these parameters is discussed.

### INTRODUCTION

#### Background

Since its commercial implementation in 1889, cyanide has been used almost exclusively in the extraction of precious metals from ores. There are a number of reasons for this. Cyanide is very effective as a lixiviant for precious metals, and its cost is not excessive. As is well known, however, this reagent is extremely toxic, and considerable care must be exercised to prevent injury to personnel and damage to the environment during and after processing.

Another drawback to cyanide is the fact that many other toxic metals in the ores including mercury, arsenic, selenium and antimony, are also dissolved with the gold. These dissolved secondary metals not only interfere with the extraction of gold but also pose an additional burden

on the treatment of the liquid streams after extraction. Further, refractory carbonaceous ores 'rob' the pregnant leaching solution of gold values when cyanide is used as lixiviant.

For these reasons, considerable effort has been directed to developing other effective lixiviants to obviate the use of cyanide in precious metals processing. Alternative noncyanide lixiviants have been examined previously. These include: ammonia, thiourea, thiosulfate, iodine, polysulfides and malonitriles. Ammonia requires high temperature (Han and Meng 1992). The drawbacks of using thiourea as lixiviant include high reagent consumption, the formation of passive surface coatings and low leaching efficiencies. Schulze (1984, 1986) has studied SO<sub>2</sub>/redox couple control, while Little (1987) has studied ferric sulfate and lignin sulfonate additions to counter these drawbacks. Iodide is both expensive and corrosive. Malonitriles are expensive and generate free cyanide ions (Scheiner and Lindstrom 1972).

Jiang et al. (1992) and Wan et al. (1994) reported the enhancement in leaching of gold in the presence of cupric tetrammine in ammoniacal thiosulfate solutions. In general, researchers have found that ammonium thiosulfate is a good lixiviant for gold dissolution. The problem of using this reagent, however, is the instability of thiosulfate in solution and excessive reagent loss during processing. Oxidative conditions are essential for the dissolution of gold, and under these conditions, thiosulfate is oxidized to tetrathionate. Therefore, the development of reaction conditions is needed which can increase oxidation of gold while keeping thiosulfate losses minimal.

### Objective and Approach

The objective of this work is to improve and optimize thiosulfate leaching of gold so that a new viable technology can be used to replace cyanide leaching in precious metals extraction. To realize this objective, the following studies will be made:

- A study and development of chemical conditions under which the degradation of thiosulfate is minimized.
- A study and development of chemical conditions under which the oxidation kinetics of gold dissolution are increased.
- Use of developed process to leach oxide and low-grade carbonaceous gold ores.

## **PROJECT TASKS**

### Task 1: Experimental Setup

*Leaching Reactor:* A 125-ml five-neck flask with a PTFE stirring bearing employed as sealed reactor.

*Electrode:* A gold plate on the tip of the electrode with a surface area of 0.31 cm<sup>2</sup> and purity of 99.9985%.

*Driving Motor:* Cafframo BDC 2002 digital motor with an accuracy of ± 1%.

*Chemicals:* Cupric sulfate, 98.5-100.5%. sodium thiosulfate, 99.6%, ammonium thiosulfate, 99.0%, ammonium hydroxide, 5.0 N.

### Task 2: Gold Leaching

The effect of rotation velocity of the electrode was determined first. The experiments were conducted for two hours, and dissolved gold concentrations were measured with Atomic Absorption Spectrometry. These results are shown in Figure 1 and show that dissolution is increased up to 600 rpm indicating that the reaction is mass transfer controlled.

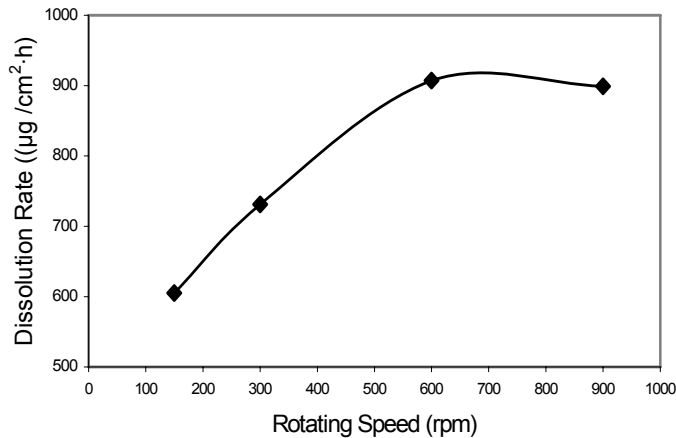


Figure 1. Dissolution rate of gold as a function of rotating speed of electrode. Conditions:  $\text{NH}_4\text{OH}$ , 0.1 M;  $\text{Na}_2\text{S}_2\text{O}_3$ , 0.5 M;  $\text{Cu}^{2+}$ , 0.008 M; pH 11.3-11.4;  $T = 22^\circ\text{C}$ , leaching time, 2 hr.

Cupric ion functions as a catalyst and as an oxidant in this system. The higher the  $\text{Cu}^{2+}$  concentration, then, the faster is the gold dissolution reaction. On the other hand, the higher the cupric concentration, the higher is the thiosulfate decomposition. The effect of cupric concentration of gold dissolution is shown in Figure 2.

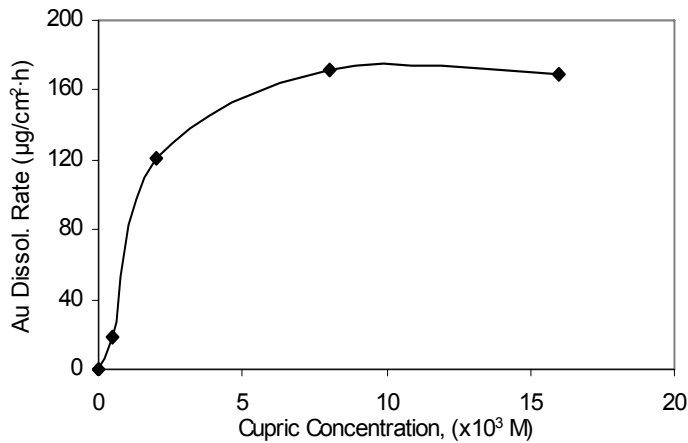


Figure 2. Gold dissolution rate as a function of cupric ion concentration. Conditions:  $\text{NH}_4\text{OH}$ , 0.1 M;  $(\text{NH}_4)_2\text{S}_2\text{O}_3$ , 0.1 M; pH 9.6-9.8; 300 rpm,  $T = 22^\circ\text{C}$ ; leaching time, 2hr.

Ammonia plays a key role in thiosulfate leaching of gold. An alkaline medium is provided, and stable ammonia complexes of cuprous and cupric copper are achieved.  $\text{Cu}(\text{NH}_3)_4^{2+}$  is assumed to be the oxidant in this system which is reduced to  $\text{Cu}(\text{NH}_3)_2^+$  after surface reaction (Aylmore and Muir, 2001). Gold dissolution as a function of ammonia concentration is given in Figure 3. It can be noted that dissolution increases dramatically with ammonia concentration up to 0.5 M, the upper limit of ammonia added. In the absence of ammonia, cupric oxidation of thiosulfate would be rapid and complete.

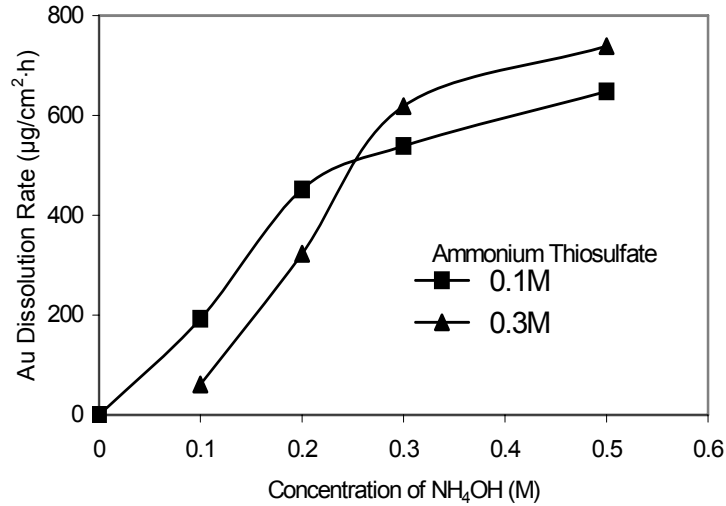


Figure 3. Gold dissolution rate as a function of ammonia concentration. Conditions:  $\text{Cu}^{2+}$ , 0.008 M; pH 9.6-9.8; 300 rpm,  $T = 22^\circ\text{C}$ , leaching time, 2 hr.

Ammonia and ammonium ion constitute a buffer, the pH being 9.6-9.8. The effect of system pH was studied with sodium thiosulfate in place of ammonium thiosulfate. When 0.5 M  $\text{NH}_4\text{OH}$  was used, the natural pH of the system was pH 11.3. Reduction in pH was accomplished by adding sulfuric acid. Gold dissolution rate as a function of pH is shown in Figure 4. It can be seen that the rate was doubled at pH 11.3 as compared to that at pH 10.5.

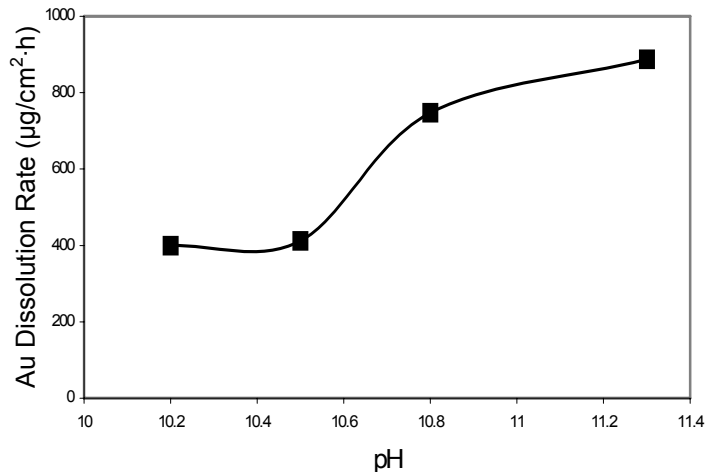


Figure 4. Gold dissolution rate as a function of pH. Conditions:  $\text{NH}_4\text{OH}$ , 0.5 M;  $\text{Na}_2\text{S}_2\text{O}_3$ , 0.5 M;  $\text{Cu}^{2+}$ , 0.002 M; 300 rpm,  $T = 22^\circ\text{C}$ ; leaching time, 2 hr.

## **SUMMARY**

The concentrations of cupric ion, ammonia and thiosulfate are all important in gold leaching. Cupric being the oxidant in this system oxidizes both gold and thiosulfate. Higher cupric concentrations increase the rate of gold dissolution; the extent of thiosulfate oxidation will have to be established. Ammonia is necessary because it maintains the cupric and cuprous ions as ammonia complexes. Dissolution as a function of rotational velocity of the stirrer shows that the reaction is mass transfer controlled through the boundary layer.

## **FUTURE WORK**

Future work will involve establishing the optimum levels of cupric ion, ammonia and ammonium thiosulfate addition for maximal gold dissolution and minimal thiosulfate oxidation.

## **REFERENCES**

Aylmore, M. G. and D. M. Muir. 2001. Minerals Engineering. 14:135.

Han, K.N. and X. Meng. 1992. U.S. Patents 5,114,687; 5,308,381.

Jian, T., S.Chen and S. Xu. 1993. Proceedings of XVIII International Mineral Processing Congress. p. 37.

Little, R. H. 1987. U.S. Patent 4,645,535.

Schulze, R. G. 1983. German Patent –DE 3,347,165.

Schulze, R. G. 1986. J. Metals. 36:62.

Wan, R. Y., K. M. LeVier and J. D. Miller. 1993. Hydrometallurgy:Fundamentals, Technology and Innovation. SME&TMS. p. 425.

**Appendix 38: Development of a 3D Lattice-Boltzmann Model for Fluid  
Flow Simulation under Partially-Saturated Conditions in Packed Particle  
Beds (UT007)**

## TECHNICAL PROGRESS REPORT

Contract Title and Number:

Crosscutting Technology Development at the Center for  
Advanced Separation Technologies  
(DE-FC26-02NT41607)

Period of Performance:

Starting Date: 6/1/2005  
Ending Date: 10/31/2006

Sub-Recipient Project Title:

Development of a 3D Lattice-Boltzmann Model for  
Fluid Flow Simulation under Partially-Saturated  
Conditions in Packed Particle Beds

Principal Investigators:

Miller, Sukop

Report Information:

Type: Semi-Annual  
Number: 1  
Period: 10/1/05-3/31/06  
Date: 3/31/06  
Code: UT007-R01

Contact Address:

University of Utah  
135 South 1460 E. Room 412  
Salt Lake City UT 84112

Contact Information:

Phone: (801) 581-5160  
Fax: (801) 581-8119  
E-Mail: [jdmiller@mines.utah.edu](mailto:jdmiller@mines.utah.edu)

Subcontractor Address:

Subcontractor Information:

## **ABSTRACT**

The proposed research has been designed to develop software capable of simulating the fluid flow of a leaching solution through a packed bed of particles under partially-saturated conditions. The software will use the Lattice Boltzmann Method (LBM), which has numerous advantages over other approaches. The proposed research involves consideration of the mechanics of the heap leaching system as influenced by particle size distribution, pore-network structures, solution flow rate, oxygen flow rate, and moisture content. In a broader sense, this research is part of a long range program using X-Ray Microtomography (XMT) to determine to what extent the rate and practical recovery from heap leaching is limited by: (1) mineral exposure, (2) fluid flow/transport phenomena and (3) chemistry. It is expected that the results from the proposed research will help to design heap leaching operations for more effective utilization of our mineral resources.

Up to this moment, a three dimensional (3D) Lattice-Boltzmann Model (LBM) has been developed for one component fluid flow simulations through packed particle beds under totally saturated conditions. The code has been tested for a simple fluid flow forced by a pressure gradient. Results agree well with the analytical solution of the Stokes equation for moderate/low Reynolds number. Independency of the lattice size, numerical stability, and predictability of the Reynolds number were also tested. Preliminary work has been done in order to use this technique to predict saturated permeability using real X-ray computer tomography (XMT) images of particle samples. We expect to have an extended study in the feasibility to predict saturated permeability based on the LBM simulation and comparison with the well-known Carmen-Kozeny equation.

## **INTRODUCTION**

The fluid flow condition through the packed bed is an important consideration in the design and operation of the heap. In fact, for a given particle size distribution the moisture content, the geometry of the porous structure in the particle bed and the local fluid velocity conditions will determine the extent of leaching and transport of solution from which the metal is recovered by electrolysis after solution purification and concentration.

Until recently it has not been possible to accomplish fluid flow analysis in such packed particle beds under partially-saturated conditions due to the lack of models to simulate multiphase (gas-liquid) flow behavior with very complex boundary conditions (pore network structure/geometry). Now such analysis may be possible by using X-Ray micro CT (XMT) to capture the complex geometry involved in a particle bed structure and using lattice Boltzmann methods (LBM) to simulate fluid dynamics behavior of unsaturated flow.

The relationship between pore structure of a packed particle bed and air/solution transport phenomena are of special interest in heap leaching operations. The pore structure and the connectivity of the pore space are important features which determine fluid flow in a packed particle bed during heap leaching. In this regard, the X-ray micro tomography technique is the best technology available today to characterize complex pore structures.

XMT allows the capture of the shape and connectivity of the void space in three dimensions of a randomly organized particle bed.

LBM has computational aspects that make it a particularly strong method for multiphase fluid dynamics simulations in complex pore spaces. This type of simulation is able to handle the very complex boundary conditions given by the geometry of the packed bed of particles. Also, it has recently been shown that LBM can simulate multi-phase (gas-solid-liquid) multi-component interactions with excellent results (Chen, 2003; Martys & Chen, 1996; Shan & Chen, 1993; Zhang & Chen, 2003). However, so far applications have been largely limited to 2D problems or 3D fluid flow models under saturated conditions. This research will focus on the development and implementation of software able to handle 3D multiphase fluid flow under partially saturated conditions for use in the analysis and control of optimum conditions for recovery of copper and/or gold from heap leaching operations.

## Background

### *History.*

Over the last few years, the Lattice Boltzmann Model (LBM) has become a promising numerical technique for the simulation of fluid flows with complex boundaries geometries as in real porous media. It is also becoming popular for its capabilities to incorporate additional physical complexities such as multiphase flow, (Chen & Doolen, 1998). Unlike the conventional Computer Fluid Dynamics (CFD), 'top-down' approach based on discretization of macroscopic continuum equations, the LBM method is based on a 'bottom-up' approach where constructed kinetic models incorporate microscopic model interactions and mesoscopic kinetic equations so that the macroscopic averaged properties obey the desired macroscopic equations.

In the original lattice gas automata model from which the LBM evolved, the mass and momentum are conserved locally in a discrete space-time model. The space is discretized in a lattice arrangement and particles are defined at each node of the lattice by a Boolean variable. Particles are only allowed to move one lattice unit along the lattice directions during each time step. When two particles arrive at the same node they collide and a collision rule is followed by the particles involved. There are several models developed under this technique, but it was Frish (Frish et. al, 1986) who found the fact that sufficient symmetry of the lattice was necessary for the recovery of the Navier-Stokes equation. For example, in two dimensions a square lattice does not provide enough symmetry whereas hexagonal symmetry is sufficient to recover the Navier-Stokes equation.

The LBM evolved from the lattice gas cellular automata (LGCA) to overcome its difficulties but keeping many of the intrinsic advantages like the locality equilibrium, and the streaming and collision structure. In spite of the remarkable progress achieved in the LGCA, the difficulties related to lack of Galilean invariance, anomalous velocity dependency of the fluid pressure, statistical noise, exponential complexity and spurious invariants plus the interest to develop 3D models and High Reynolds numbers simulations led to the development of the LBM (Succi, 2001).

The first LBM was first by (Macnamara & Zanetti, 1988). The fundamental difference between LGA and LBM is that the later replaced the Boolean variable by a particle distribution function  $f_\alpha$  which eliminates the statistical noise problem present at that moment in its ancestor. Later, Higuera and Jimenez made a great simplification when they linearized the collision term around the local equilibrium state by using a single relaxation term. A model using this type of relaxation term is known as LBGK model for the Bhatnagar-Gross-Krook operator (Bhatnagar et. al., 1954). The Bhatnagar-Gross-Krook (BGK) approximation and discretization of the Boltzmann Equation leads to the following lattice Boltzmann equation:

$$f_\alpha(x + \vec{e}_\alpha, t + \Delta t) - f_\alpha(x, t) = -\frac{1}{\tau} [f_\alpha(x, t) - f_\alpha^e(x, t)] \quad (\text{equation 1})$$

which is equivalent to:

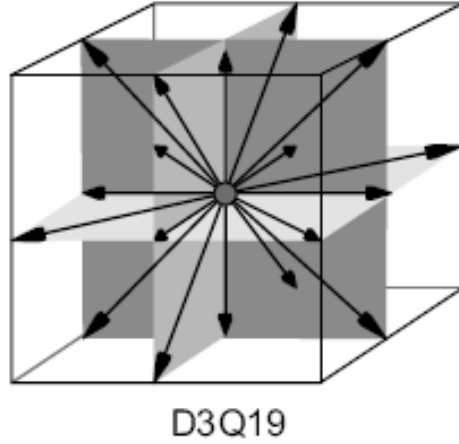
$$f_\alpha(x + \vec{e}_\alpha, t + \Delta t) = (1 - \frac{1}{\tau})f_\alpha(x, t) + \frac{1}{\tau}f_\alpha^e(x, t) \quad (\text{equation 2})$$

where  $f_\alpha(x, t)$  at lattice site  $x$  denotes the particle population moving in the direction  $\vec{e}_\alpha$ . Further,  $f_\alpha^e(x, t)$  is an equilibrium distribution function, and  $\tau$  is the relaxation time. Currently, there are two different ways of showing that this discretization approximates the Navier-Stokes equations – either by the method of Chapman-Enskog expansion from statistical physics (Frisch et. al, 1987), or by direct discretization of the Boltzmann equation (He and Luo, 1997).

In the LBGK model the local equilibrium distribution is chosen in order to recover the Navier-Stokes macroscopic equations. Qian (Qian et al., 1992) provided a whole family of solutions for this matter.

### *Overview of a simple one component LBM.*

Depending in the dimensions and the number of velocity directions different models can be used. We apply the D3Q19 model with 19 velocity directions in three dimensions because this model shows a better numerical stability than other lattice elements. The following figure shows the sketch of a D3Q19 model.



Velocity vectors:

$$e_1 = (0,0,0)$$

$$e_{2,3} = (+/-1,0,0)$$

$$e_{4,5} = (0,+/-1,0)$$

$$e_{6,7} = (0,0,+/-1)$$

$$e_{8..11} = (+/-1,+/-1,0)$$

$$e_{12..15} = (+/-1,0,+/-1)$$

$$e_{16..19} = (0,+/-1,+/-1)$$

Figure 1. Sketch of a three dimensional lattice with nineteen velocities ( D3Q19).

The D3Q19 model consists of nineteen velocity vectors where one is in the center, six along the axis and twelve for all combinations of two axes. For each velocity vector a particle distribution function (DF)  $f_\alpha$  is stored. The DF represents the amount of fluid molecules moving in the direction  $e_\alpha$ . Therefore, in the D3Q19 model there are particles not moving at all ( $f_0$ ), moving with speed 1 ( $f_2, f_3, f_4, \dots, f_7$ ) and moving with speed  $\sqrt{2}$  ( $f_8, f_9, f_{10}, \dots, f_{19}$ ).

The LBM consist of two basic steps, streaming and collision. The streaming step represents the advection of the particles in the fluid and if the size of a cell  $\Delta x$  and the length of the time step  $\Delta t$  are normalized to 1, the streaming DF ( $f_\alpha^{lS}$ ) can be easily represented by copying each DF to its adjacent cell along the corresponding velocity vector.

$$f_\alpha^{lS}(x, t + \Delta t) = f_\alpha(x + e_\alpha, t) \quad (\text{equation 3})$$

For the other component, the collision step describes the evolution of a system towards equilibrium by relaxing the streamed DFs of a cell towards the equilibrium distribution function. It has been shown that LBGK approximation with a Maxwell-Boltzmann equilibrium distribution recovers the Navier-Stokes equations at low Mach number (He & Luo, 1997). For a D3Q19 lattice, a second order expansion of the equilibrium distribution function is commonly used:

$$f_\alpha^{eq}(x) = w_\alpha \rho(x) \left[ 1 + 3 \frac{\bar{e}_\alpha \cdot \mathbf{u}}{c^2} + \frac{9}{2} \frac{(\bar{e}_\alpha \cdot \mathbf{u})^2}{c^4} - \frac{3 \mathbf{u}^2}{2 c^2} \right], \text{ for } \alpha = 1, 2, 3 \dots 19. \quad (\text{equation 4})$$

Where,

$w_\alpha$  : Weights values depending on the velocity direction. For the D3Q19 model they are defined as

$$\begin{aligned}
w_1 &= 1/3 \\
w_\alpha &= 1/18 \quad \text{for } \alpha = 2, \dots, 7 \\
w_\alpha &= 1/36 \quad \text{for } \alpha = 8, \dots, 19
\end{aligned}$$

- $c$  : The lattice speed given by  $\Delta x_{lattice} / \Delta t_{lattice}$ . For simplicity it is defined as 1.  
 $\rho(x)$  : The macroscopic fluid density at the cell  $x$ .  
 $\mathbf{u}$  : The macroscopic fluid velocity at the cell  $x$ .

During iteration the macroscopic density and velocity fluid variables are computed as the first and second momentum of the distribution functions for each cell. Then,

$$\rho(x) = \sum_{\alpha=1}^{19} f_\alpha \quad \text{and} \quad u = \sum_{\alpha=1}^{19} e_\alpha f_\alpha \quad (\text{equation 5})$$

The LBGK model defined as shown above assured mass and momentum conservations laws. Furthermore, the following relations are associated with the pressure ( $P$ ) and kinematic shear viscosity ( $\nu$ ):

$$P = \frac{\rho}{3} \quad (\text{equation 6})$$

$$\nu = \frac{1}{3} \left( \tau - \frac{1}{2} \right) \quad (\text{equation 7})$$

More details about the LBM, treatment of boundary conditions, applications and techniques can be found at (Succi, 2001).

## Objective and Approach

A two-year research program has been designed to develop a 3D lattice Boltzmann model for fluid flow simulation under partially-saturated conditions in packed particle beds in order to help identify optimum flow conditions for copper and/or gold recovery in heaps. This is the continuation of a research developed by Dr. J.D. Miller and Dr. C.L. Lin using LBM in 3D problems in order to improve the understanding of the phenomena associated to fluid flow in packed particle beds (Lin & Miller, 2004; Miller et al., 2003; Miller et. al., 2003).

Develop of multiphase 3D LBM is a difficult and complex task. References and literature in this regard is limited. It is not expected to develop optimized and final-end-user software in the first approach. Instead, it is expected to develop as fast as it is possible a first software to evaluate the capabilities and applicability of this technique for unsaturated flow assessment and characterization.

In order to accomplish the final goal this project has been divided in the following sequential steps: single component flow, surface interactions, two-phase fluid flow. Each step consists of software development and experimental verification in order to get confidence and assure reliability in the technique.

The first stage of the project involves the software development of a single component 3D flow model. This software will be the corner-stone for the development of the next stages and it will give us important insights about implementation issues. In this stage, the 3D simulation results will be compared to analytical solutions of Stokes-Flow in a pipe. Also, the 3D LBM simulation results through porous solids will be verified with the Darcy's Law for flow in porous media. Real XMT images samples obtained from packed particle beds will be used in this regard.

The second stage will incorporate the wettability property of the fluid into the Model. For this effect a fluid-solid interaction potential (Schan & Chen, 1993) will be used. Verification with experimental data will be carried out.

The third stage of the rsearch will involve the incorporation of an additional fluid to the model and the description of the interface interactions. We need to simulate the interface between two fluids of a high difference in viscosity as is the case of water and air. Up to this moment we are evaluating two different approaches: The multicomponent model as proposed by Shan and Chen (1993) and the Free Energy Method as explained by (Swift et al. 1995, 1996). The final version of this software will be applied to complex 3-D pore spaces in packed beds of irregularly shaped particles imaged from real samples using a unique high-resolution cone-beam X-Ray Microtomography system (XMT) installed at the University of Utah. New insights regarding the relation between pore geometry, air ventilation and water saturation are expected to be found. Further tests of the model will include verification of the ability to reproduce Darcy's Law in appropriate laminar flow regimes, saturated and unsaturated permeability measurements, and water potential/particle size/moisture content relationships.

## PROJECT TASKS

### Task 1. Software development

The objective of Task 1 is the development of 3D software to be used in the analysis of fluid flow through porous media. The software is based on lattice Boltzmann Model as explained previously. The software is composed of two major structures: the 3D LBM software and a SILO translator. The former is the main core of the program and it performs the three dimensional Lattice-Boltzmann simulation. The later use the outputs files of the 3D LBM to make a SILO format file which can be finally imported from the open source VISIT platform for Scientific Visualizing.

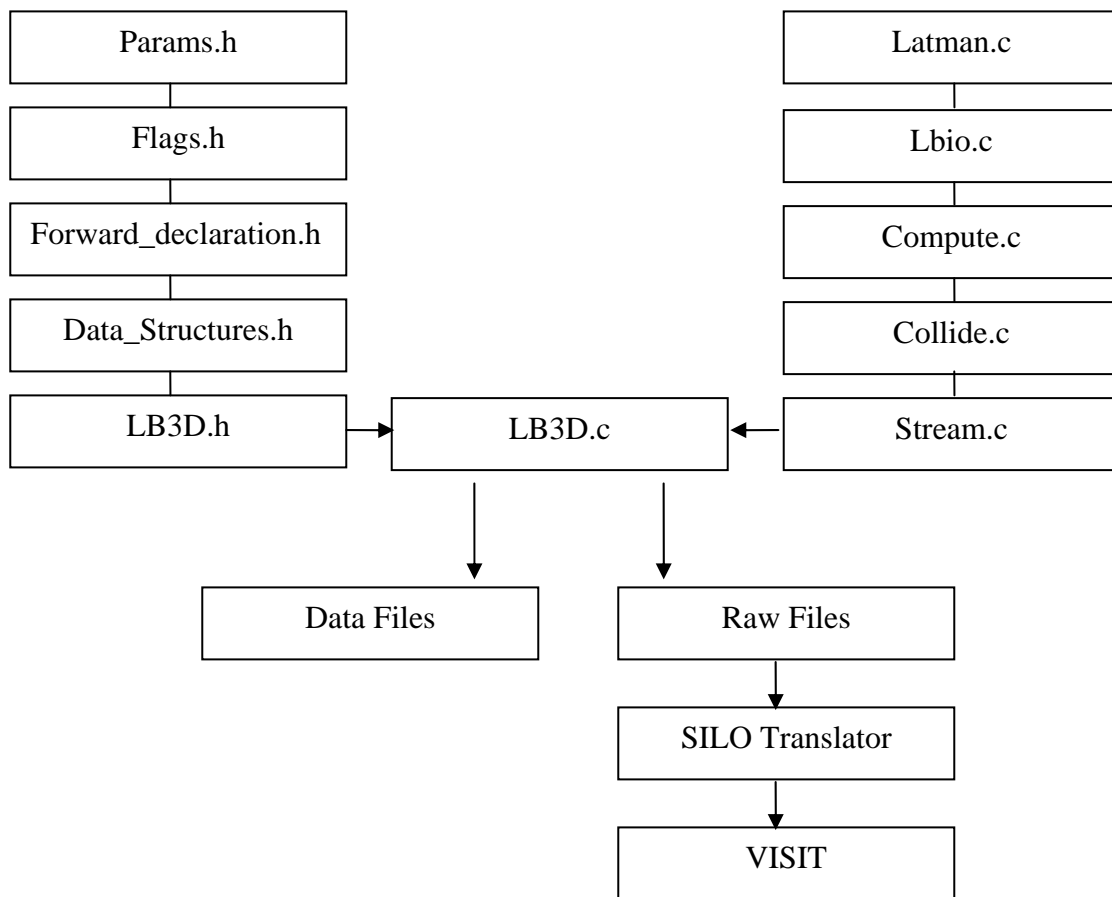


Fig 2. Software Structure for Flow Simulation.

The structure of the code is shown in figure 2. A brief explanation of each file is as follows:

Params.h : This header file contains the functions in charge of reading and writing the parameters used to define the problem being modeled such as the size of the lattice, the relaxation time, the maximum number of iterations, the initial density and the volume force.

Flags.h : This header file contains global parameter definitions common to all the other files.

Forward\_declarations.h : This header file contains the forward declaration of the functions to be used during the execution of the program.

Data\_Structures.h : Definition of all the structure objects common to all the files such as the particle distribution function and the lattice structure.

LB3D.h : Definition of the unitary vector of the D3Q9 model and includes all the files necessary to run the main function.

Latman.c : This file contains the functions to allocate memory for the lattice, initialize the density and velocity values, and destruct the lattice when the program execution is finished.

Lbio.c : This file stores all the routines related to outputs of the simulation such as console text messages and raw output data files.

Stream.c : This file contains the function in charge of the streaming step. Periodic boundary conditions are implemented in this step.

Collide.c : This file contains the collision function which executes the collision step of the LBM. Inside the declaration of this function the bounce-back boundary condition is applied.

Compute.c : This file contains all the functions in charge of calculating the macro variables results of the simulation such as average velocity, maximum velocity, average density, etc.

LB3D.c : This file contains the main function which iterates through the streaming and collision steps until the maximum iteration step or the convergence rule is reached.

The sequential process for the iteration of the 3D LBM is shown in the following pseudo-code below. First the memory necessary to run the software is allocated and the problem is initialized. Then the iterative process of streaming and collision is executed until convergence or the maximum iteration is reached.

```

=====LB3D.c=====
#include "LB3D.h"

int main( int argc, char **argv)
{

    Locate memory and initialize variables.

    Iteration: If maximum iteration or convergence has not been reached thus continue
    {

        Execute Streaming Step.

        Compute macro variables such as density and velocity.

        Execute Collision Step

        Add the volume –force to mimic pressure gradient

        Save outputs files
    }

    free memory;

    return 0;

}

```

Macro variables are computed based on the new values of the velocity distribution function after streaming during the iteration. The software at this step implemented a periodic boundary condition at the inlet and outlet such as the same amount of mass enters and exit the lattice.

After the collision step the collide distribution are modified with the volume force component such as to mimic the equivalent gradient pressure used to force the flow in a particular direction.

## Task 2. Analytical Verification - Stokes Flow in a Pipe

The Stokes Flow through a pipe has a well-known analytical solution. For this reason it was selected to verify the function of the software. The fluid enters the channel from left side and flows steadily down the channel under the effect of a constant pressure drop ( $\Delta P$ ) between the inlet and outlet section as it is shown in figure 3.

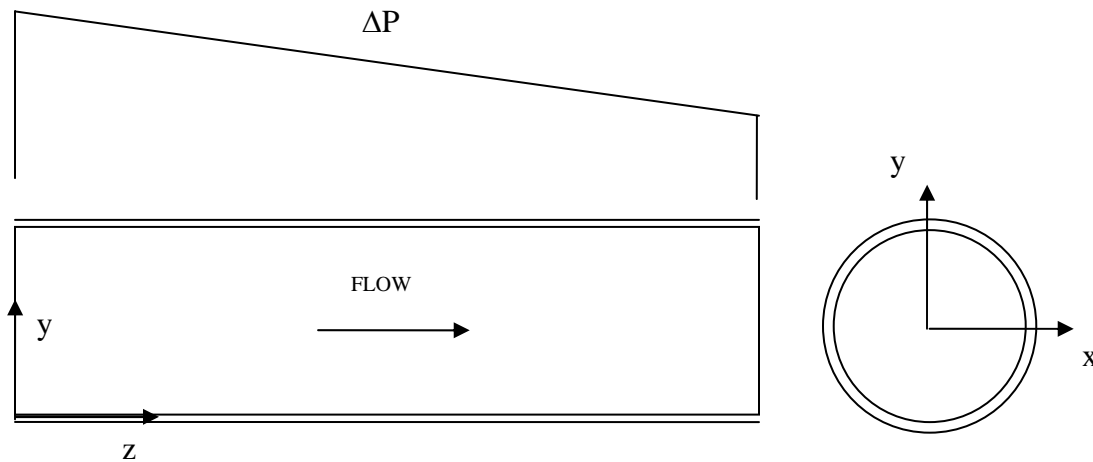


Fig 3. Channel Flow in a Pipe.

At the walls the fluid velocity is assumed to be zero because the drag force of the wall exerted on the fluid. The later is equivalent to setting a non-slip boundary condition. Under moderate-to-low Reynolds Number flow conditions the solution is easily determined and it is given by (Bird et. al, 2002):

$$V_x(y) = V_{\max} \left[ 1 - \left( \frac{y}{R} \right)^2 \right] \quad (\text{equation 8})$$

With,

$$V_{\max} = \frac{R^2 \Delta P}{4 \mu L} \quad (\text{equation 9})$$

Where,

- $V_x(y)$  : Velocity in the x direction at y position.
- $V_{\max}$  : Maximum velocity in the x direction.
- $R$  : Radius of the pipe.
- $L$  : Length of the pipe
- $\mu$  : Dynamic viscosity.

Since in the LBM presented above the pressure depends on the density (see equation 6) then the model can not be considered an exact incompressible method because a change in pressure requires a change in density. Therefore this LBM is known as a weakly compressible model. In this type of model, we can generate the gradient pressure with the application of an equivalent volume force added to the DFs designed in such a way to produce the same momentum input to the flow as the true gradient. This volume-force model does not allow us to recover an exact Reynolds number and/or the internal structure of the pressure field point-wise, however it is extremely efficient to recover the universal behavior of the fluid system in the range of the Reynolds numbers to be studied.

Figure 4 shows a comparison between the analytical solution of the problem described before and the result for a simulation in a 64x64x64 lattice. Because of the symmetry of the problem figure 4 only shows the profile of the velocity along a line perpendicular to the flow for a low Mach number and Low Reynolds Number condition. As is evident there is a very good agreement between the analytical solution and the results from the 3D LBM simulation. As we will see in the next paragraphs this good behavior tends to be lost as the Mach Number and Reynolds Number increase.

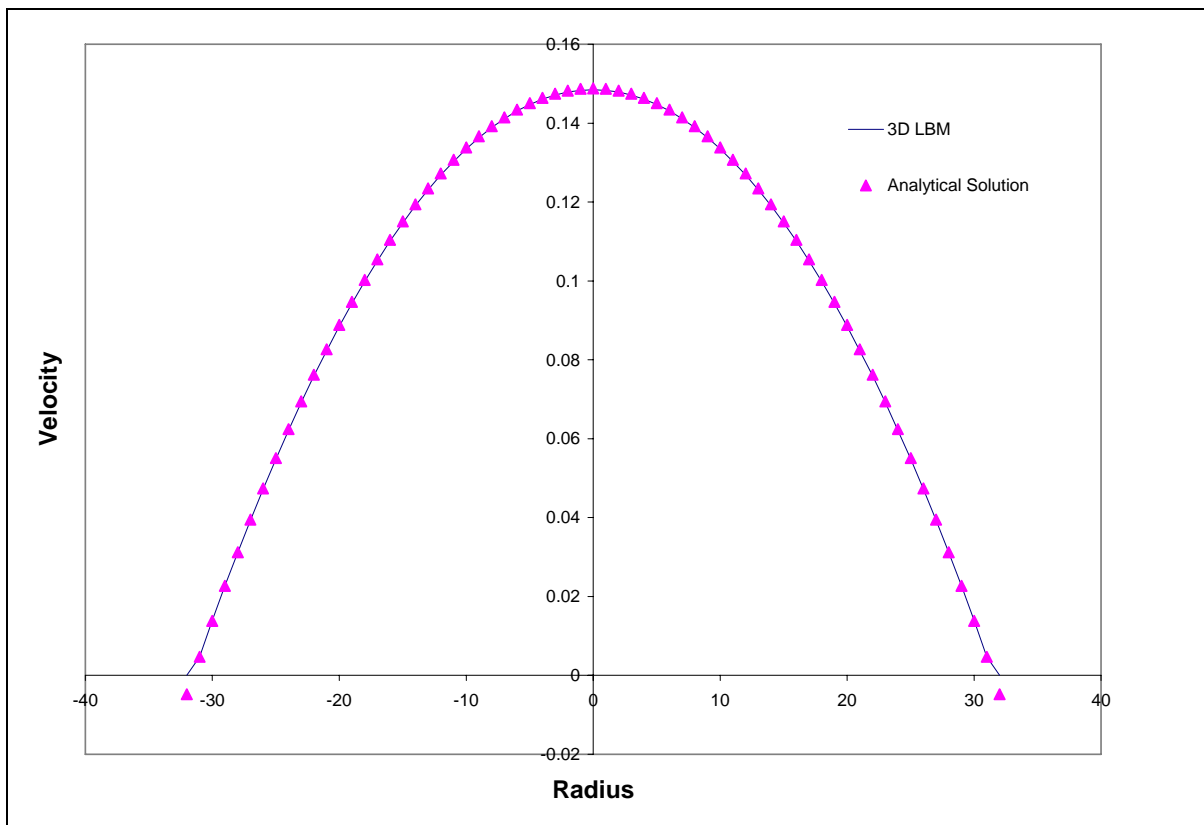


Fig 4. Comparison between Analytical Solution and a 3D LBM simulation for a 64x64x64 lattice.

In a first experiment, a discrete space of 16x16x16 cells was used for the channel flow simulation. The effective diameter (mid-grid bounce-back boundary condition) of the pipe ( $D$ ) was 14 cells. The simulation starts from a homogenous unitary density and a null initial velocity along all the cells. The volume-force and the relaxation time  $\tau$  are set in order to get the desired Reynolds number. The volume-force is set at 0.001 and is added to the DFs after the collision step.

To check the availability of the system to control the fluid flow conditions the system variables were first set around a given Reynolds Number and the results after simulation were compared with analytical solution predicted. The estimated maximum velocity and Reynolds number are calculated using the following equations.

$$V_{\max} = \frac{R^2 \Delta P}{4\mu L} = \frac{R^2 G_{Force}}{4\nu} \quad (\text{equation 10})$$

$$Re = \frac{DV_{\max}}{\nu} \quad (\text{equation 11})$$

The LBM simulations run until the convergence parameter reaches a determined threshold value. We are using in this case the following rule:

$$\frac{\sqrt{\sum_x [u(x,t) - u(x,t - \Delta t)]^2}}{\sqrt{\sum_x u(x,t)}} < 10e - 7 \quad (\text{equation 12})$$

The results of the simulations for Reynolds numbers going from 5 to 1000 were tested and the results are shown in the Table 1.

Density	Effective Pipe Diameter	Relaxation Time $\tau$	Kinematic Viscosity	G Force	Predicted Maximum Velocity	Predicted Re	Predicted Maximum Velocity	Measured Re	Mach Number
1	14	1.00	0.167	0.001	0.07350	6.17	0.06510	5.47	0.13
1	14	0.80	0.100	0.001	0.12250	17.15	0.10881	15.23	0.21
1	14	0.70	0.067	0.001	0.18375	38.59	0.16382	34.40	0.32
1	14	0.60	0.033	0.001	0.36750	154.35	0.33141	139.19	0.64
1	14	0.58	0.027	0.001	0.45938	241.17	0.41673	218.78	0.8
1	14	0.56	0.020	0.001	0.61250	428.75	0.56092	392.64	1.06
1	14	0.55	0.017	0.001	0.73500	617.40	BLOW	BLOW	1.27

Table 1. Channel Flow Simulation for a 16x16x16 lattice size. Values are expressed in Lattice Units.

The simulations show numerical stability for Reynolds number up to 500 and it blows out for higher values. Even though the later, this simple model is still useful for our research since the percolation flow in which we are interested is fairly slow and develop low Reynolds number ( $\ll 100$ ). As figure 5 shows, when the Mach number increases there is a clear departure of the predicted Reynolds Number from the measured ones. This is due to the fact that LBM approximates the Navier-Stokes for low Mach Numbers ( $Ma$ ) and the error increases in proportion to  $(Ma)^2$ . This model is a simple and highly idealized model and the results are close enough for low Mach numbers. The system may be tuned to approximate Reynolds conditions based on this approach but it is not possible to get exact Reynolds numbers without a scanning of the parameters. Since we are interested in develop a model which can give us some insights and not an exact solution about the flow under unsaturated conditions this does not seems to be an important matter. We can also realize that low Mach numbers ( $\ll 1$ ) assure numerical stability conditions as expected.

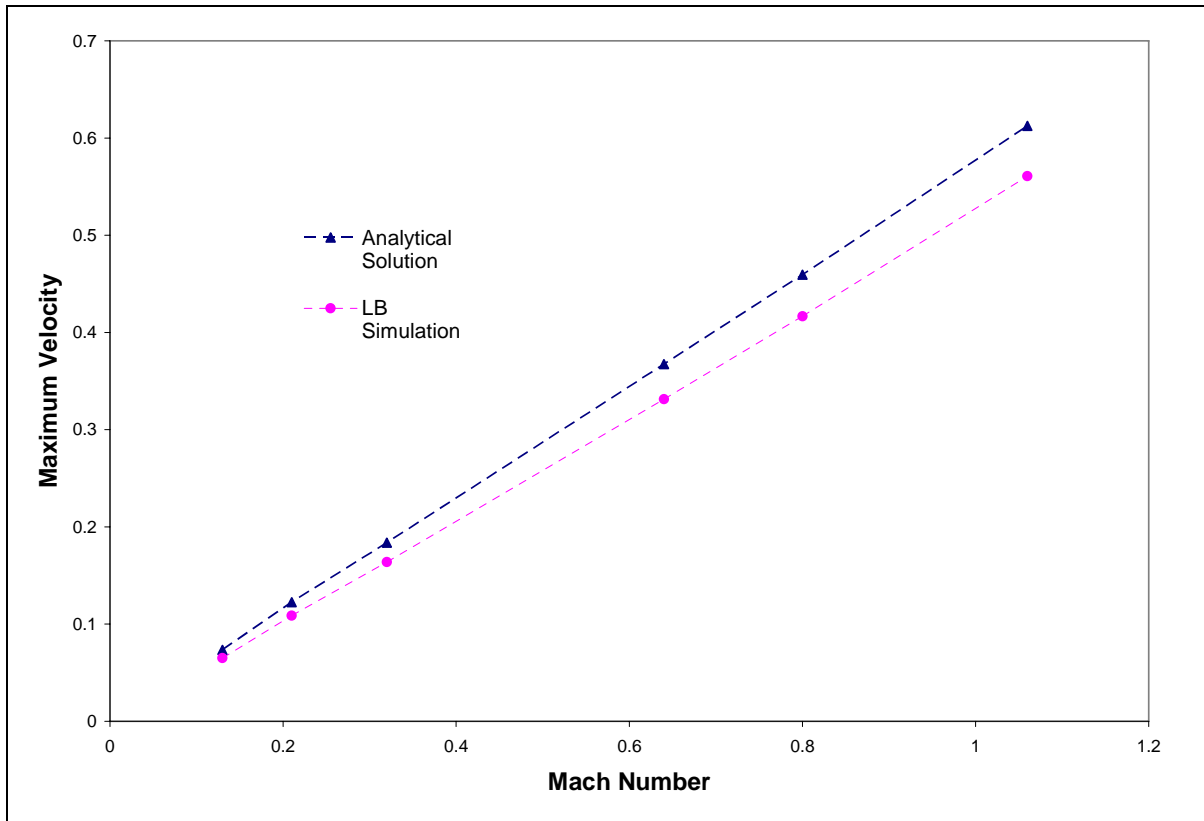


Fig 5. Comparison between the predicted maximum velocity based on Stokes problem solution and the measured value based on the LBM simulation in a 16x16x16 lattice size.

The figures 6 and 7 show the resulting velocity vectors and velocity magnitude in the channel flow for the first simulation in the table 1. The others simulations have been omitted since the results are similar. In figure 6 is possible to see clearly how volume-force mimics the pressure gradient driving the flow motion in the outlet direction since the vector components are completely horizontal. In figure 7 is shown clearly how the maximum

velocities are recovered at the center of the pipe and zero velocity is found at the walls (non-slip boundary condition) as expected.

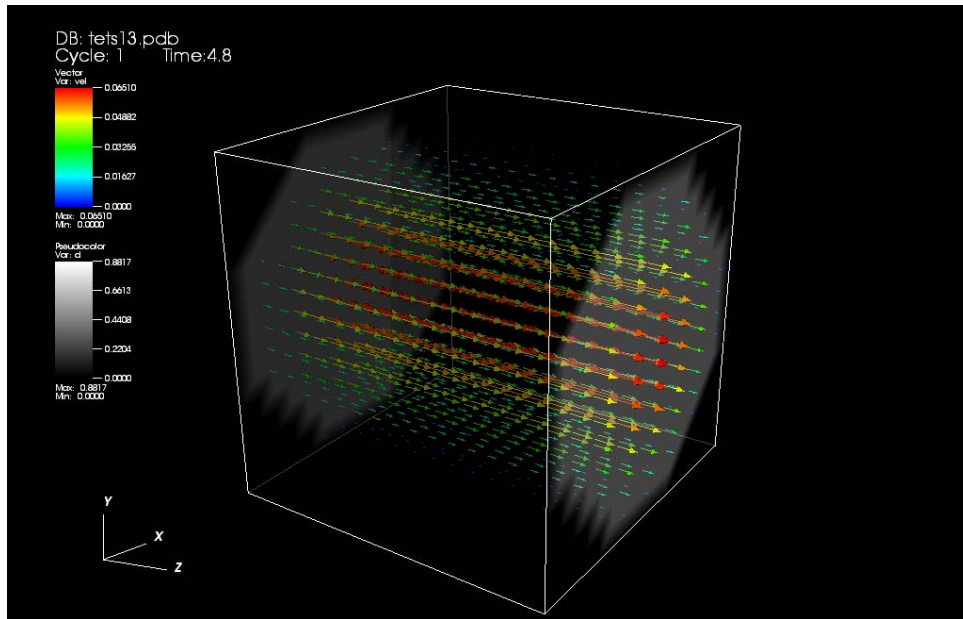


Fig 6. Channel Flow in a 16x16x16 lattice. The image shows the velocity vector of the flow.

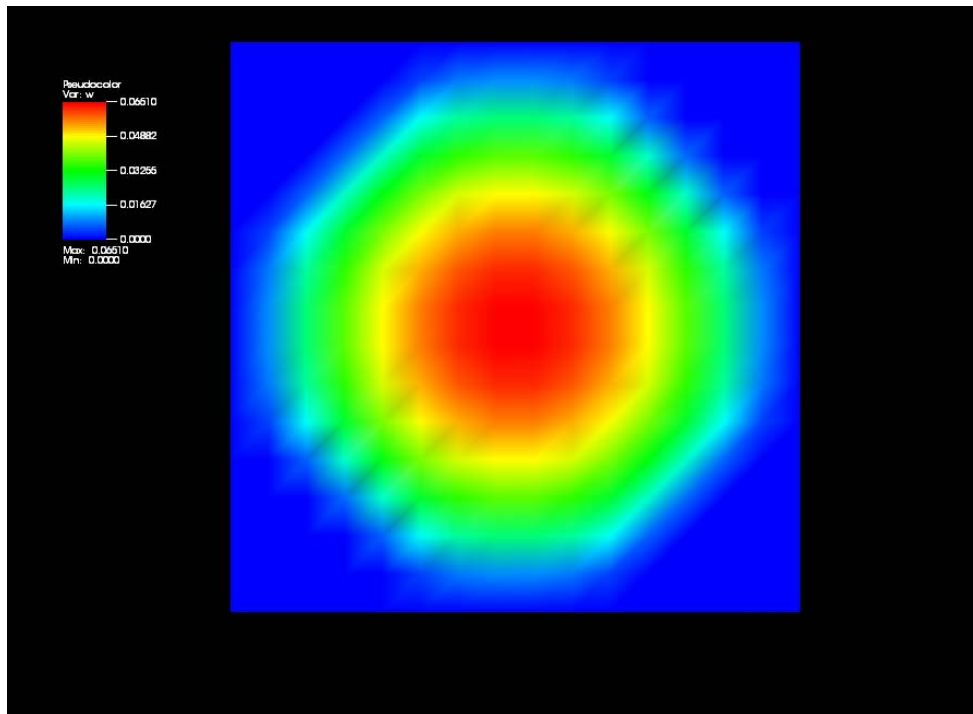


Fig 7. Velocity profile inside the pipe in a 16x16x16 lattice. Image is a slide plane perpendicular to the flow direction.

Figure 8 shows the profile of the velocity magnitude along a line passing from side to side at the middle of the figure 7. The results for different relaxation times ( $\tau$ ) are in agreement with the increasing viscosity experimented for the fluid.

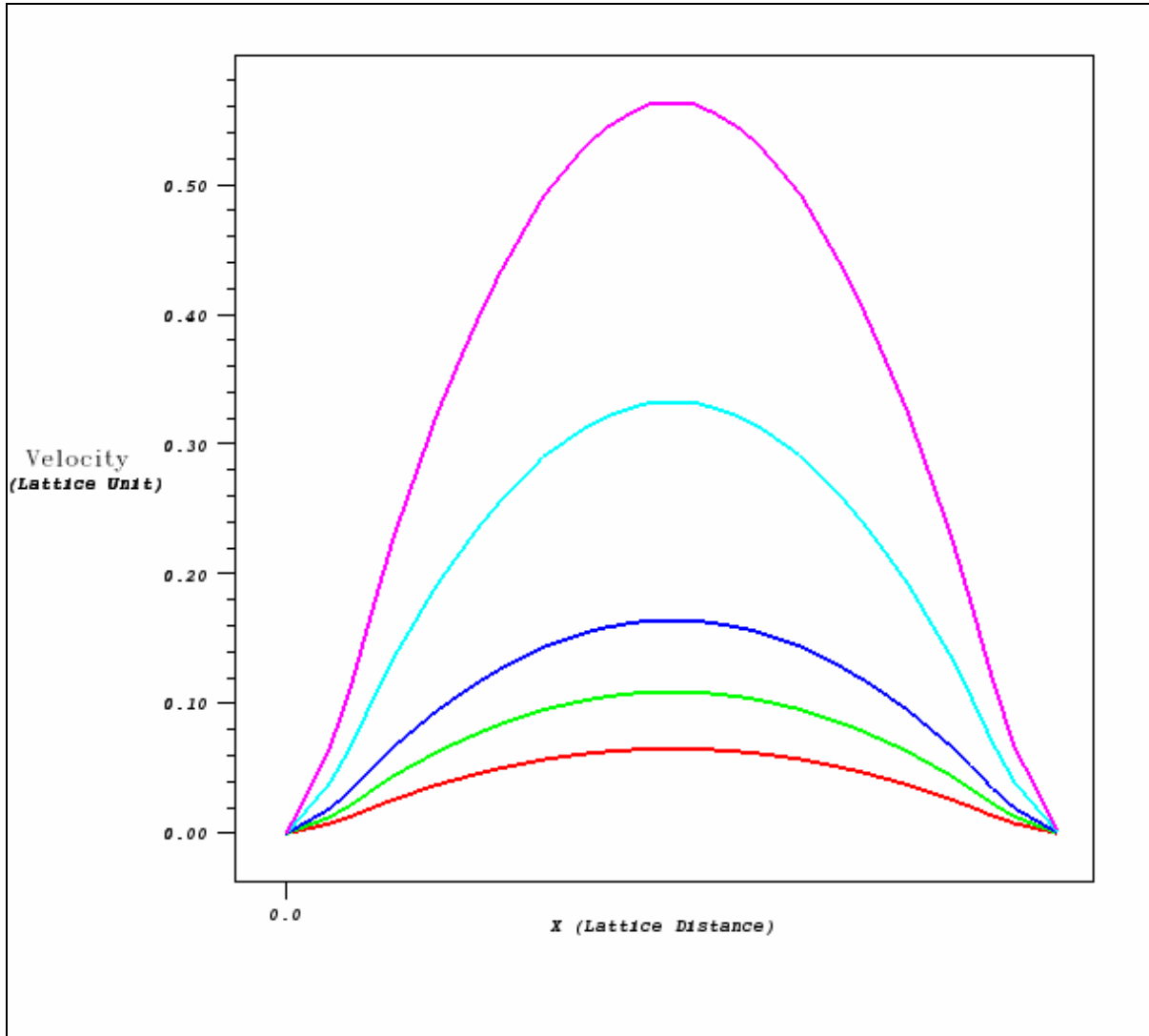


Fig 8. Velocity profiles along the flow direction in a 16x16x16 lattice. The curves show the results for fluids with different kinematic viscosity as defined by  $\tau$  taking the values of 1.0, 0.8, 0.6, 0.58 and 0.56.

In order to prove independency of the simulations to the size of the lattice the same analysis was done for a 64x64x64 lattice. The following table shows the results for this case. In this case, the simulation stops when the convergence value achieves 10e-6 or when the numbers of iteration reach 30 thousands. The volume force has been modified to 0.0001 in order to obtain the desired Reynolds and Mach number.

Density	Effective Pipe Diameter	Relaxation Time $\tau$	Kinematic Viscosity	G Force	Predicted Maximum Velocity	Predicted Re	Measured Maximum Velocity	Measured Re	Mach Number
1	62	4.0	1.17	0.0001	0.020593	1.09	0.01857	0.99	0.04
1	62	1.0	0.17	0.0001	0.144150	53.62	0.14376	53.48	0.25
1	62	0.80	0.1	0.0001	0.240250	148.96	0.21866	137.76	0.42
1	62	0.70	0.07	0.0001	0.360375	335.15	0.32447	306.63	0.62
1	62	0.65	0.05	0.0001	0.480500	595.82	0.4196	560.28	0.83
1	62	0.60	0.03	0.0001	0.720750	1340.60	0.5708	1256.87	1.25
1	62	0.58	0.03	0.0001	0.900938	2094.68	BLOW	BLOW	1.56

Table 2. Channel Flow Simulation for a 64x64x64 lattice size. Values are expressed in Lattice Units.

As in the case of the 16x16x16 lattice, the LBM simulation for the 64x64x64 lattice also shows numerical stability and good agreement with the predicted Reynolds Number for low Mach Numbers. The relation can be clearly seen in the figure 6. Furthermore, in this simulation the model can reach up to a Reynolds number of around 1000 before losing convergence.

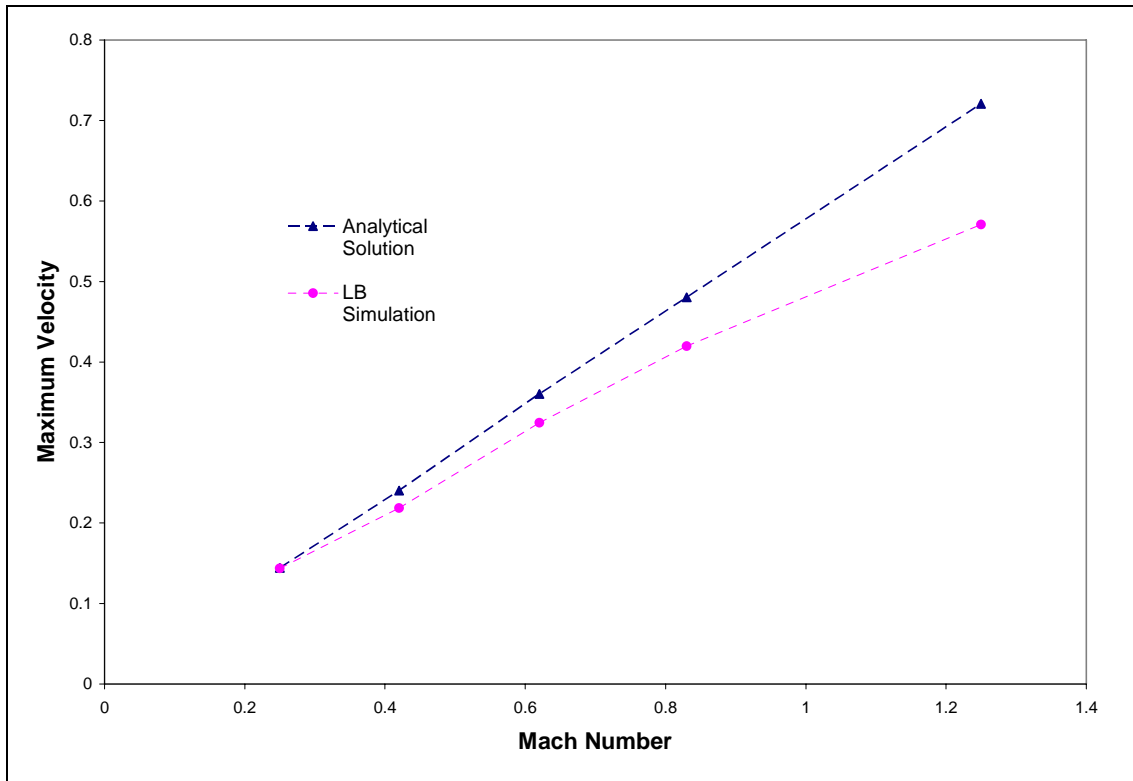


Fig 9. Comparison between the predicted maximum velocity based on Stokes problem solution and the measured value on the LBM simulation in a 64x64x64 lattice size.

As in the case of the 16x16x16 lattice the model shows clearly the difference in velocity profile for different viscosity values as defined by the relaxation time. Figure 10 shows the velocity profile for the different viscosities.

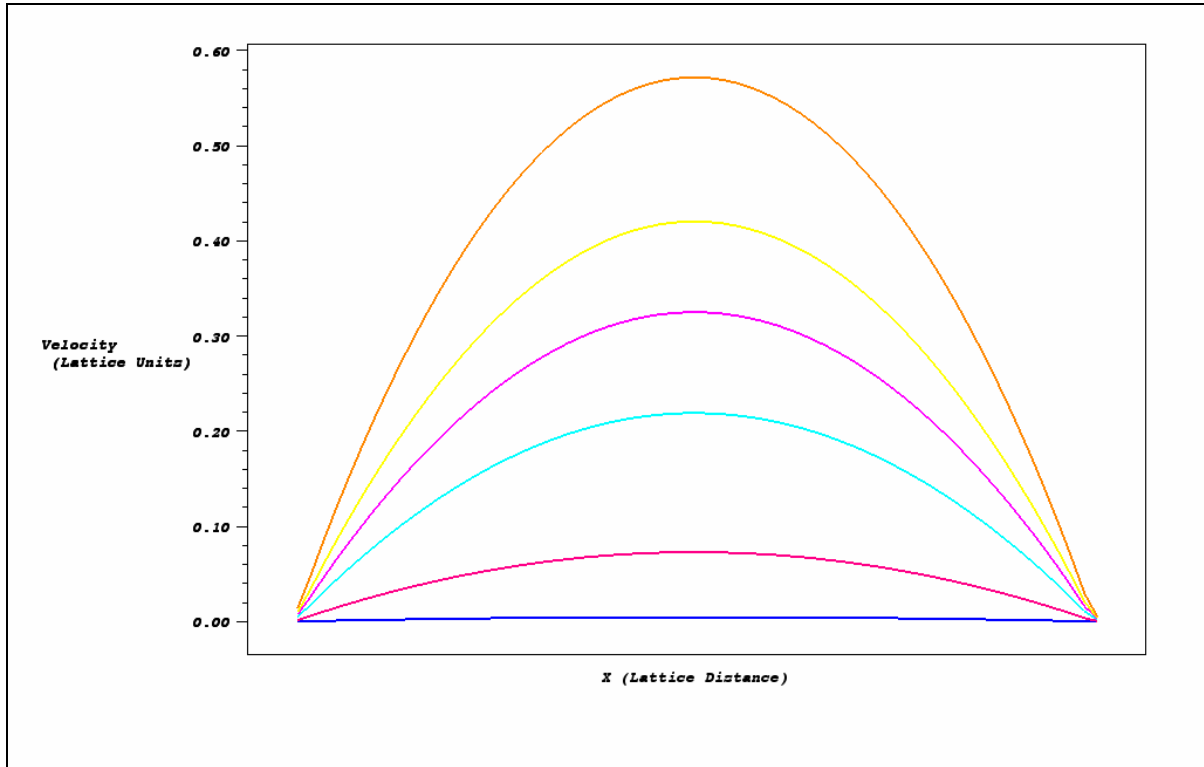


Fig 10. Velocity profiles along the flow direction in a 64x64x64 lattice. The curves show the results for fluids with different kinematic viscosity as defined by  $\tau$  taking the values of 4.0, 1.0, 0.8, 0.7, 0.65 and 0.6.

### Task 3. Determination of saturated permeability for XMT images

Up to this moment only preliminary work had been done to verify the approach for determination of real saturated permeability data. Before further development we have to verify the utility that the 3D LBM developed has to predict saturated permeability of real 3D particles distributions. In this regard, we have been working with a real glass bead sample of well known permeability for initial testing. The experience of running LBM with real 3D porous samples give us some insights about the difficulties that this approach involves. For example, simulations of real images of size bigger than 100x100x100 are extremely demanding requiring long times of simulations, up to 5 days to reach convergence.

Some others issues have come up as part of this preliminary work. The boundary bounce-back condition (non-slip) at the walls of the sample may be needed to be changed to a slip-boundary condition to avoid wall effects in the permeability determination. Also, there is an urgent necessity of code parallelization in order to scale the system to a more complex problem. However, the system has been probed and showed to be able to capture the underlying physics of the system. The following figure shows the results of a 128x128x128 glass bead sample used to calculate the permeability for saturated flow. The first four layers at the bottom and top of the z direction are empty and they are initialized with fluid at the beginning of the simulation. A volume force has been used to mimic the pressure gradient in the z direction. The vectors show in red color display clearly the path followed by the liquid around the solid particles. Even though the underlying physics of the system has been captures the permeability values obtained does not much very well with the expected results and it has been attributed to the boundary conditions at the walls. However, we are still working at this moment to discover and find a solution to the problem.

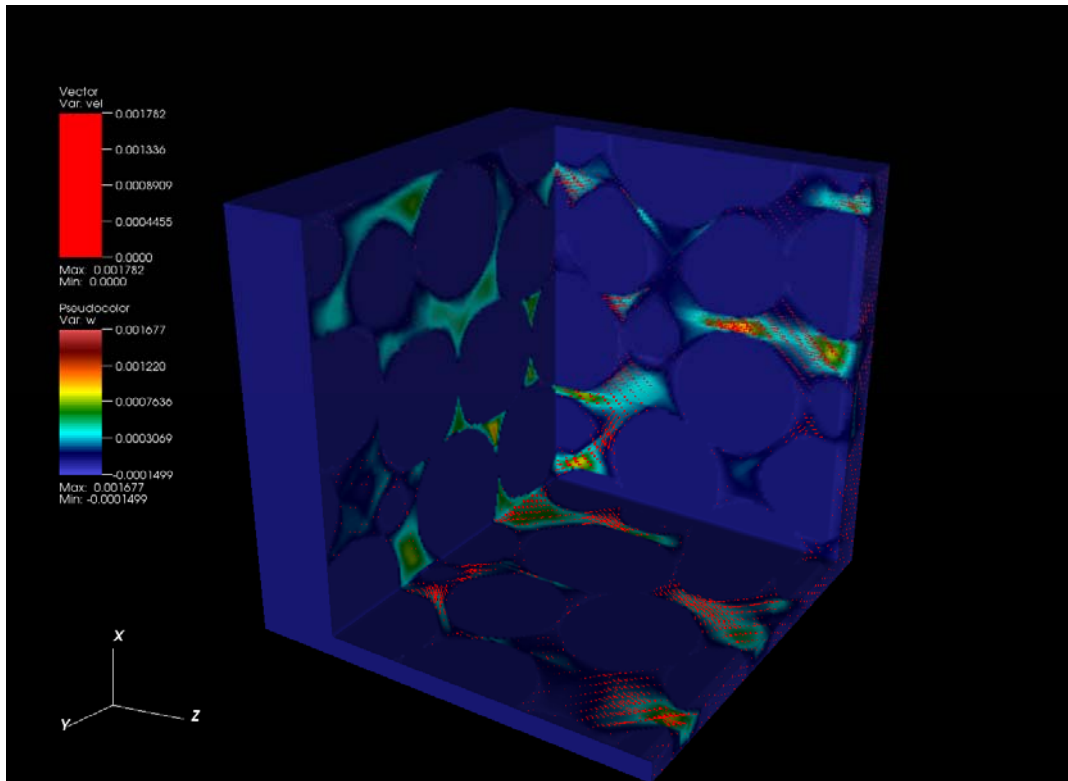
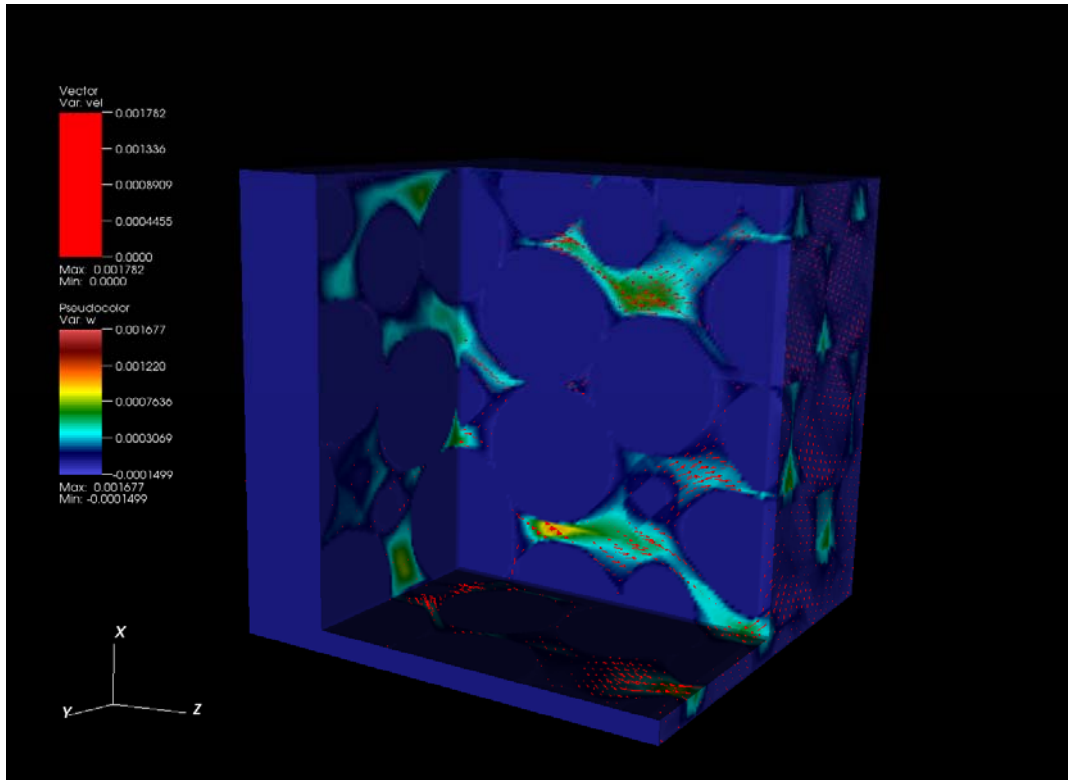


Fig 11. Velocity profiles along the flow direction (left to right) in a 3D XMT image. The vectors (in red) show the flow of the fluid through the pore network structure of glass beads.

## **SUMMARY**

Up to this moment the corner-stone of a 3D LBM has been developed. Comparison of the results with analytical solutions for a Poiseuille flow under Stokes fluid flow conditions shows good agreement. In fact, we are able to predict the range of the Reynolds numbers resulting from the simulation and we have shown independency of the results to the size of the image. Verification of the results with real 3D porous samples acquired with a XMT is in initial stage but the software platform for analysis and display of results has been successfully developed.

## **FUTURE WORK**

In general we will follow the approach explained before in the Objective and Approach section. In days to come we have to finish the verification of the simple one component fluid flow with real samples to increase our confidence and the reliability of the model. Issues such as the computer requirements, procedure and boundary effects will be evaluated in order to come up with a standard methodology to measured saturated permeability.

For the next report we expect to have the second stage of the model development. The incorporation of solid-liquid interaction and verification of the model with real problems will be addressed. Also, a preliminary evaluation of two liquid phases interaction is expected to be done.

## REFERENCES

- Bhatnagar P., E. Gross, M. Krook. A model for collision processes in gases. I: small amplitude processes in charged and neutral one-component system. *Phys. Rev.* 94:511-525, 1954.
- Chen H., *Discrete Boltzmann systems and Fluid Flows*, *Journal of Computer in Physics*, Nov/Dec 1993, page 632 – 637.
- Chen S., G. Doolen. Lattice Boltzmann Method for Fluid Flows. *Annu. Rev. Fluid. Mech.*, 1998, 30:329-64.
- Frish U., B. Hasslacher, and Y. Pomeau. Lattice-gas automata for the Navier-Stokes equation. *Physical Review Letters* 56:1505-1508, 1986.
- Frish U., D. d’Humières, B. Hasslacher, P. Lallemand, Y. Pomeau and J. Rivert. Lattice Gas Hydrodynamics in Two and Three Dimensions. *Complex Systems*, 1:649-707, 1987.
- He X., L. Luo, 1997. A priori derivation of the lattice Boltzmann equation, *Phys. Rev. E* 55(60) R6333-R6336.
- Higuera F., J. Jimenez. Boltzmann approach to lattice gas simulations. *Europhys Lett.*, 9:663-668, 1989.
- Lin, C.L., and Miller, J.D., *Pore Structure Analysis of particle beds for fluid transport simulation during filtration*, *International Journal of Mineral Processing*, Elsevier, Vol. 73, 2004, page 281-294.
- Macnamara G., G. Zannetti. Use of Boltzmann Equation to simulate lattice-gas automata. *Phys. Rev. Lett.*, 61:2332-2335, 1988.
- Martys N., H. Chen, Simulation of Multicomponent Fluids in Complex Three-Dimensional Geometries by the Lattice Boltzmann Model , *Physical Review E*, Vol. E 53, pp. 743-750, 1996.
- Miller, J.D., C.L. Lin, C. Roldan and C. Garcia, *Characterization and Analysis of Copper Heap Leaching by X-ray Computed Tomographic Techniques*, Proc. 3<sup>rd</sup> World Congress on Industrial Process Tomography, Banff, Canada, 2<sup>nd</sup> – 5<sup>th</sup> September 2003, pp. 707-712.
- Miller, J.D., C.L. Lin, C. Roldan and C. Garcia, *Particle Size Distribution for Copper Heap Leaching Operations as Established from 3D Mineral Exposure Analysis by X-ray MicroCT*, Copper 2003, Santiago, Chile, 2003, Vol. VI – Hydrometallurgy of Copper, pp. 83-97.

Qian Y., D d'Humieres, P. Lallemand. Lattice BGK models for Navier-Stokes equation. Europhys. Lett. 17:479-484, 1992.

Shan X., H. Chen, *Lattice Boltzmann model for simulating flows with multiple phases and components*, Physical Review E, Vol. 47, March 1993.

Succi S. *The Lattice Boltzmann Equation for Fluid Dynamics and Beyond*. Oxford University Press, New York, 2001.

Zhang, R., and H. Chen, 2003. Lattice Boltzmann method for simulations of liquid-vapor thermal flows, Phys. Rev. E 67, 066711.

**Appendix 39: Engineering Development of a Fine Particle Heavy  
Medium Separator (VA012)**

## TECHNICAL PROGRESS REPORT

Contract Title and Number:

Crosscutting Technology Development at the Center  
for Advanced Separation Technologies  
(DE-FC26-02NT41607)

Period of Performance:

Starting Date: 6/1/05  
Ending Date: 10/31/06

Sub-Recipient Project Title:

Engineering Development of a Fine Particle Heavy  
Medium Separator

Principal Investigators:

Gerald H. Luttrell and Roe-Hoan Yoon

Contact Address:

146 Holden Hall  
Virginia Tech  
Blacksburg, VA 24061

Subcontractor Address:

No subcontracts issued.

Report Information:

Type: Semi-Annual  
Number: 1  
Period: 10/1/05-3/31/06  
Date: 4/30/06  
Code: VA012

Contact Information:

Phone: (540) 231-4508  
Fax: (540) 231-3948  
E-Mail: luttrell@vt.edu

Subcontractor Information:

Phone:  
Fax:  
E-Mail:

### ABSTRACT

The objective of this project is to develop an innovative heavy medium separator that can reduce the cost and improve the efficiency of fine coal cleaning. The technology is designed to replace inefficient water-based separators such as spirals and water-only cyclones that are currently used by industry to upgrade 1 x 0.15 mm run-of-mine coal. The new heavy medium separator incorporates novel design features that allow it make sharp separations without the need for costly micronized magnetite. As a result, the new technology can share circulating medium from other circuits, thereby avoiding the expense of installing and maintaining an additional medium circuit. These advantages, together with the low headroom design of the module, make it possible to integrate this technology into an existing plant with minimal retrofit costs. The project tasks will include (i) design and construction, (ii) pilot-scale testing, (iii) field testing, and (iv) flowsheet development.

## **INTRODUCTION**

### Background

Heavy medium cyclones (HMCs) have been used for more than 50 years by the mining industry to upgrade a wide variety of raw materials including coal, magnesite, dolomite, diamonds, potash and lead-zinc ores. These inexpensive, high-capacity units utilize centrifugal forces to enhance the separation of smaller particles that cannot be efficiently treated using static density-based separators (e.g., heavy medium vessels and jigs). In the U.S. coal industry, heavy medium cyclones are used in nearly 80% of all coal preparation plants and represent a total installed capacity of nearly 80,000 ton/hr of feed coal. Most of these units treat feed coals in the 50 x 0.5 mm size range (Wood, 1997). More recently, there is renewed interest in using heavy medium cyclones to treat finer coal feeds (i.e., down to 100 mesh) to take advantage of yield gains that may be realized by replacing inefficient water-based separators. Data reported in the literature indicate that a properly configured heavy medium cyclone circuit can provide  $E_p$  values that are 3-4 times better than can be achieved using water-based separators such as spirals or water-only cyclones (Moorhead, 1999). Unfortunately, the use of heavy medium cyclones to upgrade fine coal has not been widely accepted by industry since existing designs of heavy medium cyclones require the use of ultrafine (micronized) magnetite in order to efficiently separate fine coal. The ultrafine magnetite is needed to prevent coal losses associated with an internal buildup of middlings that occur due to excessive medium segregation (Wood, 1990). The milling infrastructure required to generate sufficient tonnages of ultrafine magnetite at an acceptable cost is also not currently available. Production reports also indicate that the consumption of ultrafine magnetite is unacceptably high due to the limited effectiveness of conventional magnetic separators in recovering micronized particles. These difficulties have combined to make the use of heavy medium cyclones impractical for treating coal feeds finer than 0.5 mm (Robertson et al., 1997).

Cyclone designers at Krebs Engineers have been working to develop a new heavy medium separator that can be used to effectively treat fine coal. The proprietary technology incorporates novel design features that allow it make sharp separations without the need for costly micronized magnetite. As a result, the new technology can share circulating medium from other circuits, thereby avoiding the expense of installing and maintaining an additional medium circuit. These advantages, together with the low headroom design of the module, make it possible to integrate this technology into an existing plant with minimal retrofit costs.

### Objective and Approach

The primary objective of this project is to complete the engineering development of an innovative heavy medium separator that can reduce the cost and improve the efficiency of fine coal cleaning. The technology is designed to replace inefficient water-based separators such as spirals and water-only cyclones that are currently used by industry to upgrade 1 x 0.15 mm run-of-mine coal. The proposed work will include (i) design and construction, (ii) pilot-scale testing, (iii) field testing, and (iv) flowsheet development.

## **PROJECT TASKS**

### Task 1 – Design and Construction

Most of the project work performed during the current reporting period focused on the design and construction of a 6-inch diameter prototype separator. To date, technical personnel from Krebs Engineers have provided most of the essential fabricated components necessary to assemble the prototype unit. Additional fabrication work to complete the assembly is currently ongoing in the machine shop at the Virginia Tech. Steps are also underway to set up a pilot-scale test rig at the Virginia Tech off-campus coal testing facility. The test circuit includes a 200 gallon feed medium sump, a variable-flow centrifugal feed pump, associated control/regulation valves, and proportional sample cutters. The construction work and other activities associated with the design, procurement, fabrication, and assembly of the prototype separator and test rig are expected to be completed by the end of the next reporting period.

### Task 2 – Pilot-Scale Testing

This task will require the completion of a variety of experimental test runs to evaluate the performance of the prototype separator. This work is expected to begin shortly after the completion of construction and fabrication activities conducted under Task 1. In anticipation of this activity, a simple two-level parametric study has been developed to investigate the effects of the key operating variables. A statistical software package will be used to assist in the formulation of an appropriate test matrix. At present, a total of 30 individual test runs are expected to be conducted (10 runs/seam x 3 seams = 30 runs) using the prototype unit.

### Task 3 – Field Testing

No experimental test work or analyses were performed under this task during the current reporting period. This effort will not begin until after the successful completion of all previous tasks.

### Task 4 – Flowsheet Development

No engineering work or analyses were performed under this task during the current reporting period. This effort will not begin until after the successful completion of all previous tasks.

## **SUMMARY**

Initial work has begun to design, fabricate and construct a prototype heavy medium cyclone specifically designed for treating fine coal. The work completed to date includes shipping of the necessary components from Krebs Engineers to the Virginia Tech test facility, assembly of these parts with components fabricated at Virginia Tech, and the initial

setup of the associated pilot-scale circuitry necessary to evaluate the new technology. A preliminary test plan has also been developed for future testing of the prototype separator.

## **FUTURE WORK**

Future work will focus on the completion of construction activities and initiation of preliminary shakedown tests for the prototype heavy medium cyclone.

## **REFERENCES**

1. Wood, C.J., 1997. "Coal Preparation Expertise in Australia: In-Plant Issues and the Potential Impact of Broader Applications," Proceedings, Coal Prep '97, Lexington, Kentucky, pp. 179-198.
2. Moorhead, R., 1999. "Heavy Media Cyclones & Classifying Cyclones in the Coal Industry," Unpublished Workshop Report, Workshop sponsored by Powell Construction Company at the Mountaineer Conference Center, Beckley, West Virginia, June 10-11, 1999.
3. Robertson, R., Placha, D., Terry, R., and Watters, L., 1997. "Recent Developments in Dense Medium Cyclone Circuit Design," Proceedings, SME Annual Meeting, Denver, Colorado, February 24-27, 1997, Preprint No. 97-153, 6 pp.

## **PUBLICATIONS/PRESENTATIONS**

None for the current reporting period.

**Appendix 40: Improved Destruction and Control of Residual Flotation**

**Froths (VA014)**

## TECHNICAL PROGRESS REPORT

Contract Title and Number:

Crosscutting Technology Development at the Center for  
Advanced Separation Technologies  
(DE-FC26-02NT41607)

Period of Performance:

Starting Date: 6/1/2005  
Ending Date: 10/31/2006

Sub-Recipient Project Title:

Improved Destruction and Control of Residual Flotation  
Froths

Report Information:

Type: Semi-Annual  
Number: 1  
Period: 10/1/05-3/31/06  
Date: 4/30/06  
Code: VA014

Principal Investigators:

Gerald H. Luttrell and Roe-Hoan Yoon

Contact Address:

146 Holden Hall  
Virginia Tech, Blacksburg, VA 24061

Contact Information:

Phone: (540) 231-4508  
Fax: (540) 231-3948  
E-Mail: luttrell@vt.edu

Subcontractor Address:

No subcontracts issued.

Subcontractor Information:

Phone:  
Fax:  
E-Mail:

### ABSTRACT

Flotation froths containing large amounts of ultra-fine particles can become excessively stable and create serious handling problems for coal preparation plants. Steps taken by operators to combat these problems, such as lowering the frother dosage, have resulted in large reductions in fine coal recovery and plant profitability. The objective of this project is to develop and evaluate several improved methods for the control and destruction of residual flotation froths. The first phase of the proposed work will focus on a detailed laboratory study of the physical and chemical parameters that impact froth stability. These studies will be followed by in-plant sampling campaigns at several coal plants to establish how frothing agents partition within different circuits and to determine whether modifications to the layout or dilution practices can minimize handling problems. The data obtained from these investigations will be used to develop improved mechanical and chemical methods for froth control/destruction at an industrial plant site. During this reporting period, frother partitioning tests were conducted at an industrial plant site. Pilot-scale testing of a froth evacuation system was also carried out. In addition, several series of lab-scale tests were also conducted to gain a better understanding of the froth stability problem.

## **INTRODUCTION**

### Background

Column flotation cells have become widely used in the coal industry as a result of their ability to maintain superior levels of ash removal compared to conventional mechanical cells. Unfortunately, problems associated with the handling of column froths can be a major problem for plant operators. Column cells typically require a relatively high dosage of strong frother to create a froth depth that can properly distribute the wash water and maintain the desired cleaning action. As a result, column froths containing large amounts of ultra-fine (minus 325 mesh) coal generally become excessively stable, creating backup problems in launders and serious handling difficulties throughout the plant in sumps, pumps, thickeners, sprays, etc. Attempts to overcome these problems by selecting weaker frothers or by reducing frother dosages have resulted in unacceptably low recoveries of clean coal.

Several circuit modifications have been adopted by the coal industry to help deal with the froth stability problem. Oversized launders with steep slopes are typically used to minimize the potential for froth backup. Most columns circuits are configured to keep horizontal froth travel distances as short as possible and to provide sufficient vertical head between the column launder and downstream units. Steps are also taken to avoid the need to pump slurries containing large amounts of entrained air. Nearly all new column installations incorporate a de-aeration tank to provide time for the froth to collapse and for air to escape. Downstream dewatering units also have to be modified so that large froth volumes can be accepted. For example, screen-bowl centrifuges are commonly retrofitted with very large feed inlets to minimize flow restrictions for column froths. In addition, most installations find it necessary to add large dosages of expensive defoaming agents to help deal with the froth stability problem. Yet, despite all of these efforts, column froths continue to be a constant source of difficulty for plant operators and a leading cause of poor performance in plants equipped with column cells. One recent study indicated that coal losses attributed to froth handling problems in column circuits cost one eastern U.S. coal producer more than \$8 million annually.

### Objective and Approach

The objective of this project is to develop and evaluate several improved methods for the control and destruction of residual flotation froths generated by industrial coal flotation plants. Specific tasks to be completed as part of this effort include (i) laboratory studies of physical/chemical parameters influencing froth stability, (ii) quantitative assessments of frother partitioning in industrial coal preparation plants, (iii) evaluation of mechanical methods for froth control/destruction, and (iv) evaluation of chemical methods for froth control/destruction. The work associated with the proposed R&D activities will be carried out by a multidisciplinary team consisting of university personnel from Virginia Tech as well as key industrial personnel from a major eastern U.S. coal company.

## PROJECT TASKS

### Task 1 – Parametric Study of Froth Stability

The objective of this task is to conduct a variety of fundamental laboratory studies that are needed to identify the key factors that influence froth stability. To date, most of the work performed under this task focused on the construction and setup of an experimental apparatus that can be used to monitor froth height profiles as a function of various test parameters (e.g., particle size, shape, concentration, surface wettability, frother dosage, defoamer dosage, gas rate, etc.). The results obtained from these fundamental tests will be reported in the next technical progress report.

### Task 2 – Investigation of Residual Frother Partitioning

The objective of this task is to conduct measurements that provide an indication of (i) the effective frother concentrations in different plant circuits, (ii) how these concentrations are impacted by circulation and dilution streams, (iii) which unit operations are adversely impacted by excessively stable froths, and (iv) the level of severity of the froth stability. In this work, the effective frother concentration was determined by measuring the liquid surface tension of the sampled solutions (after solids removal using a microfilter or centrifuge) and comparing the measured value to a laboratory calibration curve of concentration versus surface tension. Surface tension measurements were initially performed using the du Nüoy ring method and were later compared to those obtained using the Wilhemy plate method. It was found out that due to technical limitations, the du Nüoy Ring Method gave inconsistent results. Thus, it was decided to use Wilhemy plate method for future testing.

Two sets of samples were subjected to surface tension measurements to establish residual frother concentrations. The first series were carried out on samples collected from a laboratory-scale flotation cell. These lab tests were performed in order to check whether the surface tension method can provide the required data. The results obtained from the laboratory experiments are summarized in Figure 1. As expected, the surface tension of the pulp within the flotation cell increased as the frother was depleted during the flotation test run. However, the surface tension values for the froth concentrates were inconsistent and did not follow any expected trend. The relatively high surface tension values for the

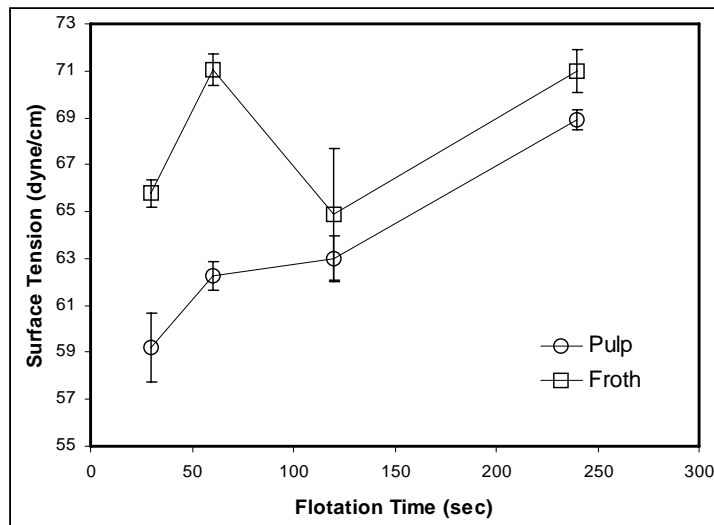


Figure 1. Surface tension measurements for samples from a laboratory flotation machine.

froth products suggest that this method of monitoring the concentrations of frother may not be reliable due to the presence of ultrafine coal particles in the samples.

The second group of samples was obtained from an operating plant (see Figure 2). In the preliminary evaluation, samples that were taken included (i) clarified water from the plant thickener, (ii) feed, concentrate and tailings samples from the two plant columns, and (iii) feed, concentrate and tailings samples from the first and last cells in the bank of plant conventional cells. The results of these measurements are plotted in Figure 3. As can be seen, some of the surface tension values are not as expected. The froth concentrate samples tended to give higher surface tension values which are indicative of lower frother concentrations. This unexpected result is believed to be due to sampling issues in which slurry is collected from the plant and transported back to the lab before the measurements of surface tension can be done. Recent tests show the frother concentration changes during this time due to decomposition and/or by deposition on coal particles in the system. Thus, to counter these negative effects, filtering during sampling via syringe microfilters is going to be performed at the plant site for the next round of in-plant tests.

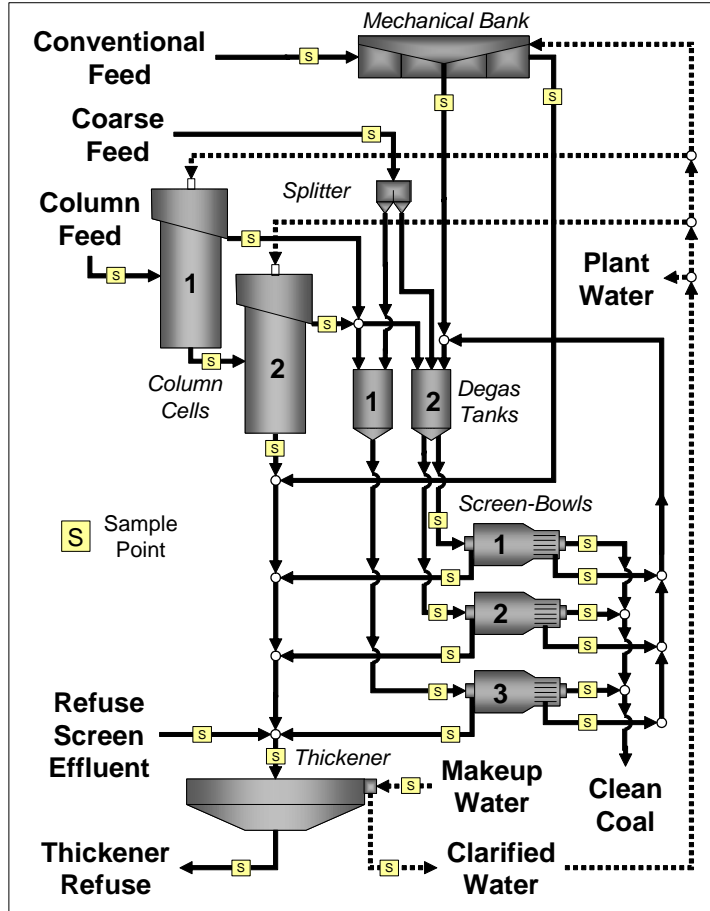


Figure 2. Flowsheet showing sampling points.

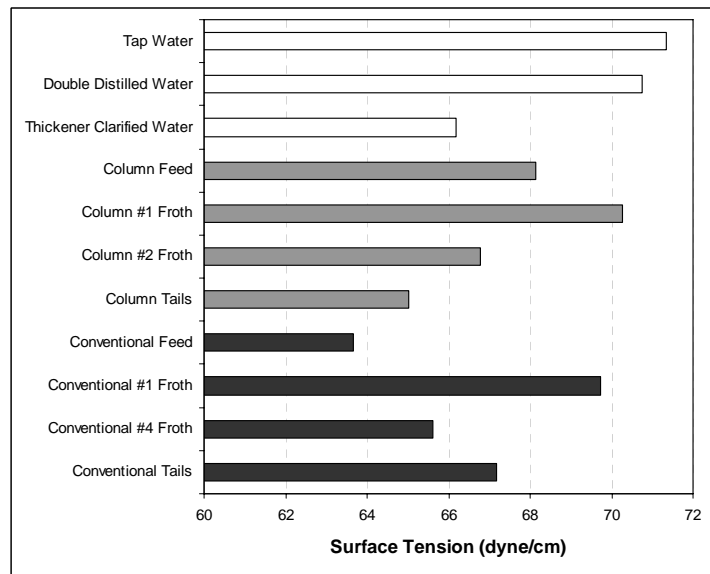


Figure 3. Comparison of plant surface tension values.

### Task 3 – Evaluation of Mechanical Control Methods

This task focuses on the evaluation of several mechanical methods for froth destruction and/or prevention. This approach is less costly than chemical control methods and avoids recycled defoamer in the clarified return water that may inhibit flotation performance. The first mechanical method evaluated as part of this task was a froth evacuation system (FES). This method uses a vacuum system to draw froth into a vacuum chamber where entrained air bubbles are expanded or collapsed (see Figure 4). A barometric leg is then used to carry the deaerated slurry to a refuse thickener for disposal. During this reporting period, tests were carried out using a pilot-scale FES at an industrial plant site. Preliminary tests conducted with this unit showed that a larger volume vacuum receiver tank as well as a more powerful vacuum pump is needed to increase throughput. Problems of heavy frothing were also observed in both the effluent and receiver sumps. These problems were solved using paddle mixers to keep the frothing to an acceptable level by agitating the contents. Although several tests were run to date, satisfactory results could not be obtained. Deaerated samples from the receiver tank did not settle after the application of flocculants. To correct this issue, modifications have recently been made to the vacuum receiver tank so that the material is fed to it tangentially to create a cyclonic action to achieve separation of froth and foamy material from rest of the slurry. Testing to evaluate this modification is currently underway.

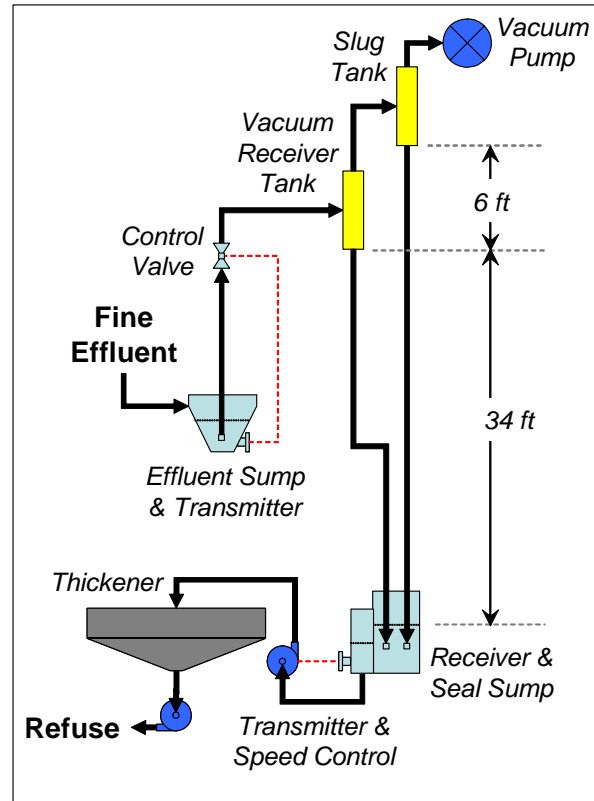


Figure 4. Froth evacuation system (FES).

### **SUMMARY**

During this reporting period, frother partitioning studies and froth evaluation tests were conducted at an industrial plant site. The frother partitioning studies indicate that the samples must be taken in the field to avoid frother decomposition and/or adsorption on coal particles that interfere with the measurements. Preliminary results from the froth evacuation tests indicate that direct evacuation is not by itself capable of deaerating coal flotation froths. Modifications have been made to the test apparatus in an attempt to improve this technique.

## **FUTURE WORK**

During the next reporting period, plant water will be analyzed with the new approach described above for its frother content (surface tension measurements), size distribution, combustibles and ash content and, chemical composition. Froth stability tests will also be carried out to develop a better understanding of the effects of particles size and frother content on froth stability. A modified froth evacuation system will also be examined in more detail.

## **REFERENCES**

1. Höfer et al., 2001. Foams and Foam Control, Ullmann's Encyclopedia of Industrial Chemistry, 6th Edition, John Wiley & Sons, Inc., June 2001.
2. Kulkarni, R.D., Goddard, E.D., Kanner, B., 1977. Ind. Eng. Chem. Fundamentals, Vol. 16, pp. 472-474.
3. Schnurmann, R., 1939. Ind. Eng. Chem. Anal. Ed., Vol. 11, pp. 287-297.
4. Zlokarnik, M., 1984. Chem. Ing. Technology, Vol. 56, pp. 839-844.

## **PUBLICATIONS/PRESENTATIONS**

None are available for the current reporting period.

**Appendix 41: Development of a Turbulent Flotation Model and a  
Computer Simulator (VA015)**

## TECHNICAL PROGRESS REPORT

Contract Title and Number:

Crosscutting Technology Development at the Center for  
Advanced Separation Technologies  
(DE-FC26-02NT41607)

Period of Performance:

Starting Date: 6/1/2005  
Ending Date: 10/31/2006

Sub-Recipient Project Title:

Development of a Turbulent Flotation Model and a  
Computer Simulator

Report Information:

Type: Semi-Annual  
Number: 1  
Period: 10/1/05-3/31/06  
Date: 05/12/06  
Code: VA015-R01

Principal Investigators:

Yoon, Luttrell

Contact Address:

Contact Information:

Phone:  
Fax:  
E-Mail: ryoon@vt.edu

Subcontractor Address:

No subcontracts issued.

Subcontractor Information:

Phone:  
Fax:  
E-Mail:

### ABSTRACT

Flotation is a technology separating valuable minerals from the raw materials that is designed to selectively attach hydrophobic particles on the surfaces of air bubbles and collect the concentrate. This process has been modeled by many researchers but those models are not sufficient in describing the practical flotation process by missing the critical chemistry parameters such as the hydrophobicity of particles. In addition, the limitations on the analysis of turbulence in the flotation cell, and the froth phase make the task even more difficult. Overcoming those defects, CAST has developed a new flotation model using energy barriers and kinetic energies for bubble-particle interactions in turbulent flow. This model could predict flotation from both surface chemistry and hydrodynamic parameters. In addition, the model simulations showed good agreement with experimental data from the literature. From this point of view, completing this flotation model will make significant contributions to enhancing the productivity of mineral processing and other industries of similar applications.

## INTRODUCTION

### Background

Froth flotation is an important separation process that is widely used in the minerals, coal, oil, recycling, and environmental industries. It is designed to separate hydrophobic particles from hydrophilic ones by selectively attaching the former to the surface of rising stream of air bubbles in aqueous media (pulp), leaving the latter behind. The air bubbles carrying the hydrophobic particles form a froth (three-phase foam) phase, in which some of the particles drop back to the pulp phase due to bubble coarsening and drainage. The parameters affecting the process may be divided into hydrodynamic (*e.g.*, bubble size, particle size, turbulence, energy dissipation) and chemistry parameters (*e.g.*, hydrophobicity, surface tension,  $\zeta$ -potentials). Most of the models derived until recently incorporated only the hydrodynamic parameters, which made it impossible to predict the efficiency of separation. In general, hydrodynamic parameters affect recovery, while chemistry parameters control both recovery and separation efficiency. Yoon and Mao (1996) derived a first-order flotation rate equation using both the hydrodynamic and chemistry parameters. In an attempt to derive the equation from first principles, the model was limited to describing frothless flotation under laminar flow conditions. On the other hand, most of the industrial flotation machines operate under turbulent flow conditions, and the froth phase plays a critical role in determining the efficiency of hydrophobic and hydrophilic separation and also the recovery, particularly that of coarse particles.

The turbulence is important because it is used to disperse air in water, induce bubble-particle collision, keep solid particles in suspension, and to transport the suspension from one cell to another. Therefore, it involves in the efficiencies of bubble-particle attachment, detachment, and collision. In relating the kinetic energy of bubble-particle collision to the energy barrier, it is important to consider the hydrodynamic resistance to film thinning, which causes deceleration of the particles approaching the bubble's vicinity (Mao and Yoon, 1997; Schimmoller *et al.*, 1993; Yoon and Mao, 1996). During the process of bubble-particle collision, a particle can approach the surface of an air bubble within the distance where its behavior is also affected by the 'non-hydrodynamic' forces acting between the two macroscopic particles. These forces are, namely, electrostatic, Van der Waals dispersion, and hydrophobic forces. (Dejarguin and Dhukin, 1961; Dejarguin and Dhukin, 1969; Israelachvili and Parshley, 1982; Mika and Fuerstenau, 1968). The role of the hydrophobic force in flotation may be to reduce the energy barrier for bubble-particle interaction so that flotation can become a fast process. It was shown previously that coagulation of hydrophobic particles requires much less kinetic energies than required to overcome the energy barriers calculated using the DLVO theory (Chia and Somasundaran, 1983; Xu and Yoon, 1989; Xu and Yoon, 1990)

Based on the concept presented above, a flotation model has been developed under quiescent flow conditions (Mao and Yoon, 1997; Yoon and Mao, 1996). The model is difficult to use, however, for flotation as industrial flotation machines are operating under

turbulent flow conditions. It is, therefore, the purpose of the present work to develop a turbulent flotation model.

### Objective and Approach

The objective of this project is to derive a turbulent flotation model using both hydrodynamic and chemistry parameters based on the concept presented above. The model describes the events occurring in both the pulp and froth phases. The model predictions are compared with the general trends reported in the literature with regards to the effects of particle size, bubble size, energy dissipation, particle hydrophobicity, and the  $\zeta$ -potentials of particles and bubbles, all of which are recognized as important parameters affecting flotation.

### **PROJECT TASKS**

The proposed model was developed based on the energy relations between bubble and particle interacting in turbulent flow. Due to the characteristics of the turbulent flow and its applications, the current model depends much on the probability models. The calculations (simulations) were implemented by the computer programming on the final model. The details and results of the model development are discussed in the following sections.

#### Task 1- Development of a Model

##### *Flotation Model*

Abrahamson (1975) had a probabilistic approach to calculate the number of collision between two species of particles. Considering the bubble and the hydrophobic particle as two different species, denoted as 1 (particle) and 2 (bubble), the number of collisions ( $Z_{12}$ ) can be incorporated in describing the rate of decrease of the particle number density (*i.e.* the rate constant,  $k$ ). It is essentially a product of the number of collisions ( $Z_{12}$ ), and probabilities of collision ( $P_c$ ), attachment ( $P_a$ ) and detachment ( $P_d$ ). Therefore, one obtains  $k$  as

$$k = 2^{3/2} \pi^{1/2} N_2 d_{12}^2 \sqrt{(\bar{U}_1^2 + \bar{U}_2^2)} P_c P_a (1 - P_d) \quad . \quad (1)$$

where  $N_2$  is the number density of bubble,  $d_{12}$  the sum of radii of particle and bubble,  $\sqrt{\bar{U}_1^2}$  and  $\sqrt{\bar{U}_2^2}$  are the RMS velocities of bubbles and particles respectively. Velocities are functions of energy dissipations ( $\varepsilon$ ) and calculated by the relationships suggested by Liepe and Moeckel (1976) and Lee *et al.* (1987) respectively.

##### *Probabilities of Attachment ( $P_a$ ) and Detachment ( $P_d$ )*

$P_a$  and  $P_d$  were considered to be functions of the energy barrier ( $E_1$ ) and the kinetic energies of the corresponding bubble-particle interaction as suggested by Yoon and Mao (1996). Original derivation was for the quiescent flow conditions but it can be extended to the turbulent conditions too.

### *Energy Barrier ( $E_1$ )*

In the present work, the energy barrier,  $E_1$ , has been determined using the DLVO theory extended. The total free energy of interaction ( $V_T$ ) between a bubble and a particle comprises the contribution from the hydrophobic force ( $V_H$ ), in addition to those from the electrostatic ( $V_E$ ) and van der Waals-dispersion ( $V_D$ ) forces.  $V_E$  can be calculated using the relation by Hogg *et al.* (1966) which incorporates the chemical properties called  $\zeta$ -potentials.  $V_D$  was suggested by Rabinovich and Churaev (1979) where the value is determined by the characteristics of the materials of interacting particles and the medium. Finally,  $V_H$  is obtained from the hydrophobic interactions due to contact angle and surfactant molar concentration Yoon and Mao (1996)

### *Kinetic Energies of Attachment ( $E_k$ ) and Detachment ( $E'_k$ )*

It was stated that a particle experiences the hydrodynamic resistance to film thinning, hence decelerates in the bubble's vicinity. Luttrell and Yoon (1992) considered this for  $E_k$  introducing a factor referencing the literature (Goren and O'Neil, 1971; Luttrell and Yoon, 1992). Same approach for  $E'_k$ , but the shear is now assumed to mainly cause detachment, hence the expression follows Camp and Stein's (1943) mean shear rate in the tank.

### *Energy Dissipation*

Energy dissipation plays a critical role in determining the particle and bubble velocities. One could use the mean energy dissipation ( $\bar{\varepsilon}$ ) but the local values are preferred because physical properties show big difference depending on its locality. The current model assumed two different energy dissipations following the literature (Lu *et al.*, 1998; Okamoto *et al.*, 1981; Pyke *et al.*, 2003), one at the impeller region ( $\bar{\varepsilon}_i = 15 \bar{\varepsilon}$ ) and another at the remaining (bulk,  $\bar{\varepsilon}_b = 0.2 \bar{\varepsilon}$ ).

### *Collision Efficiency*

The Abrahamson's collision model ( $Z_{12}$ ) was originally derived with an assumption of  $P_c=1$ , which is not true in real flotation. Therefore, it would be reasonable to use a collision efficiency model suggested by Luttrell and Yoon (1992).

### *Froth Recovery*

The fractional recovery,  $R_F$ , of the particles in a froth phase includes both the mechanism by bubble-particle attachment ( $R_{F-a}$ ), and by the entrainment ( $R_{F-e}$ ). They are two independent mechanisms and expressions were suggested by Do *et al.* (2006). Thus,  $R_F$  can be obtained as the sum of  $R_{F-a}$  and  $R_{F-e}$ . This value can be incorporated into Eq. (1):

$$k = 2^{3/2} \pi^{1/2} N_2 (r_1 + r_2)^2 \sqrt{(\bar{U}_1^2 + \bar{U}_2^2)} P_c P_a (1 - P_d) R_F \quad (2)$$

so that  $k$  can represent the overall flotation rate constant encompassing the events occurring in both the pulp and froth phases of a flotation machine.

### Task 2- Simulation and Analysis

Simulations were run on the proposed model to show the effect of different variables on the flotation rate constant,  $k$ . The values of  $k$  were obtained under various chemistry and hydrodynamic parameters that are typically employed in mineral flotation. The variables studied were: the particle diameter ( $d_1$ ), bubble diameter ( $d_2$ ), surface tension ( $\gamma_v$ ), contact angle ( $\theta$ ), zeta potentials of particles ( $\zeta_1$ ) and of bubbles ( $\zeta_2$ ), and specific energy input ( $\varepsilon_{sp}$ ).

As shown in Fig.1-A,  $k$  reaches a maximum at  $d_1$  of approximately 100  $\mu\text{m}$  due, and the plot shows the difficulty in floating ultra-fine and coarse particles. It should be noted here that the values of  $k$  obtained from the simulation are close to those reported in the literature. Trahar and Warren(1976) reported, for example,  $k$  values in the range of 0.2 to 5  $\text{min}^{-1}$  for copper flotation. Ahmed and Jameson (1985) for another reported the value in the range of 0.01 to 3  $\text{min}^{-1}$  for the flotation of quartz. To compare with data, the values of  $k$  were converted to the flotation recovery ( $R$ ) with the relation  $R = 1 - (1 + kt)^{-N}$ , where  $t$  is the flotation time per cell, and  $N$  is the number of cells in a bank. Figure 1-B shows a good agreement of the model with experimental data available.

From other simulation results with the changes of the variables of interests, CAST could make many conclusions that are useful in understanding flotation. A higher energy input ( $\varepsilon_{sp}$ ) increased  $k$ , especially for fine particles, and this seems to be the effect from the increase of  $E_k$ . The higher values of contact angle ( $\theta$ ) and the surface tension ( $\gamma_v$ ) also enhanced flotation. The increase of  $k$  by higher contact angle seems because  $\theta$  causes  $E_1$  to

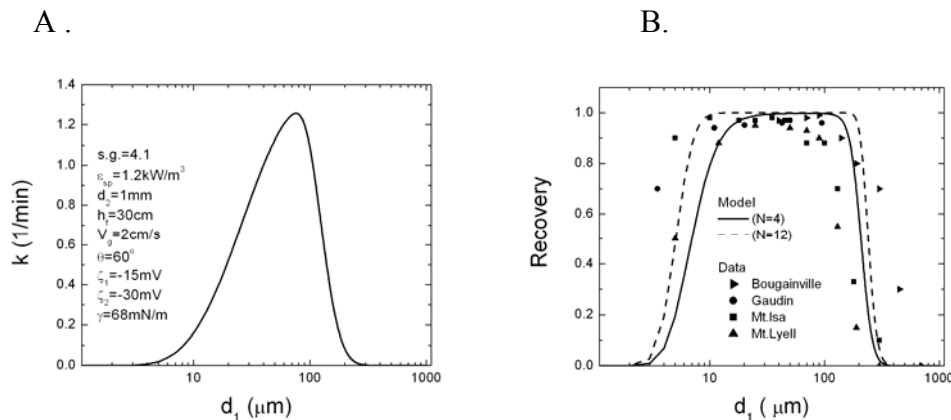


Figure 1. A) Predicted flotation rate constant ( $k$ ) vs. particle size ( $d_1$ ) for the flotation of chalcopyrite. It was assumed that the bubble gets the maximum 20 times larger at the froth top. B) Predicted recovery using the flotation rate constant values given (lines) and the copper recovery data from several plants (dots). Processing time in the calculation is 3 minutes per cell and the number of cell in a bank is 4 and 12. Data are from Lynch *et al.* (1981) and Gaudin *et al.* (1931).

decrease while  $W_a$  to increase, both contributing to higher  $k$ . The surface tension,  $\gamma_{lv}$ , was especially good for coarse particle flotation. This is presumed to result from the increase in  $W_a$ , which in turn makes  $P_d$  smaller. Effect of the particle zeta potential ( $\zeta_1$ ), however, showed the opposite trend. A decrease in the negative zeta-potential of the particles made  $k$  increase due to a decrease in  $E_1$ . The effect by zeta potential attenuated when higher energy input is applied. This indicates that chemical properties are relatively less important when the energy dissipation is high. Finally, the effect of bubble size ( $d_2$ ) was employed. The overall  $k$  increased as  $d_2$  got smaller, and the optimum particle size shifted to smaller sizes. This indicates why it has been considered empirically that smaller bubbles are beneficial for fine particle flotation.

## SUMMARY

CAST has developed a new flotation model using energy barriers and kinetic energies for bubble-particle interactions in turbulent flow. This model could predict flotation from both surface chemistry and hydrodynamic parameters. The model developed in the present work is by no means complete, as flotation is a complex three-phase phenomenon and much is still unknown. The most difficult part of modeling flotation under turbulent flow conditions is to accurately determine the kinetic energies involved in the subprocesses of bubble-particle attachment and detachment, which in turn are related to the energy dissipation. In the present work, a flotation cell was subdivided into two compartments, *i.e.*, high and low energy dissipation zones. The model simulations showed good agreement with experimental data from the literature.

## FUTURE WORK

Better understandings and modeling may be made from the studies of local energy dissipations via CFD (Computational Fluid Dynamics). The model can also be implemented by taking into account the bubble size changes due to energy input. In addition, a more analytical, not the empirical, model of froth recovery is another key factor for advanced model.

## REFERENCES

- Abrahamson, J., 1975. Collision rates of small particles in a vigorously turbulent fluid. *Chem. Eng. Sci.*, 30(11): 1371-1379.
- Ahmed, N. and Jameson, G.J., 1985. The effect of bubble size on the rate of flotation of fine particles *Int. J. Miner. Process.*, 14, 195-215.
- Camp, T.R. and Stein, P.C., 1943. Velocity gradients and integral work in fluid motion. *J. Boston Society Civil Engineers*, 30(4), 219-237.
- Chia, Y.H. and Somasundaran, P., 1983. A theoretical approach to flocculation in carrier flotation for beneficiation of clay. *Colloids and surfaces*, 8, 187-202.
- Dejarguin, B.V. and Dhukin, S.S., 1961. Theory of flotation of small and medium size particles. *Trans. Inst. Min. Metall.*, 70, 221-246.

- Dejarguin, B.V. and Dhukin, S.S., 1969. Kinetic theory of the flotation of fine particles, 13th international Mineral Processing Congress, pp. 21-62.
- Do, H., Sherrel, I.M. and Yoon, R.H., 2006. Development of a froth recovery model in mineral process. *Minerals Engineering*, to be submitted.
- Gaudin, A.M., Groh, J.O. and Henderson, H.B., 1931. AIME Eng., Tech. Pub. No. 414 (1931).
- Goren, S.L. and O'Neil, M.E., 1971. On the hydrodynamic resistance to a particle of a dilute suspension when in the neighbourhood of a large obstacle, *Chem. Eng. Sci.* 26, 325-338.
- Hogg, R., Healy, T.W. and Fuerstenau, D.W., 1966. Mutual coagulation of colloidal dispersions. *Trans. Faraday. Soc.* 62, 1638-1651.
- Israelachvili, J.N. and Parshley, R.M., 1982. The hydrophobic interaction is long range, decaying exponentially with distance, *Nature*, pp. 341-342.
- Lee, C.H., Erickson, L.E. and Glasgow, L.A., 1987. Bubble breakup and coalescence in turbulent gas-liquid dispersions. *Chem. Eng. Comm.* 59(1-6), 65-84.
- Liepe, F. and Moeckel, H.O., 1976. Studies of the combination of substances in liquid phase. Part 6, The influence of the turbulence on the mass transfer of suspended particles. *Chemische Technik* (Leipzig, Germany), 28(4), 205-209.
- Lu, S., Ding, Y. and Guo, J., 1998. Kinetics of fine particle aggregation in turbulence. *Adv. Colloid and Interface Sci.* 78, 197-235.
- Luttrell, G.H. and Yoon, R.H., 1992. A hydrodynamic model for bubble--particle attachment. *J. Colloid and Interface Sci.* 154(1), 129-137.
- Lynch, A.J., Johnson, N.W., Manlapig, E.V. and Thorne, C.G. (Editors), 1981. Mineral and coal flotation circuits their simulation and control. Developments in minerals processing, 3. elsevier.
- Mao, L. and Yoon, R.-H., 1997. Predicting flotation rates using a rate equation derived from first principles. *Int. J. Miner. Process.*, 51(1-4), 171-181.
- Mika, T.S. and Fuerstenau, D.W., 1968. A microscopic model of the flotation process, 8th International Mineral Processing Congress, Leningrad, U.S.S.R, pp. 246-269.
- Okamoto, Y., Nishikawa, M. and Hashimoto, K., 1981. Energy dissipation rate in mixing vessels and its effects on liquid-liquid dispersion and solid-liquid mass transfer. *Int. Chem. Eng.* 21(1), 88-94.
- Pyke, B., Fornasiero, D. and Ralston, J., 2003. Bubble particle heterocoagulation under turbulent conditions. *J. Colloid and Interface Sci.* 265, 141-145.
- Rabinovich, Y.I. and Churaev, N.V., 1979. Effect of electromagnetic delay on the forces of molecular attraction. *Kolloidnyi Zhurnal* 41(3), 468-74.
- Schimmoller, B.K., Luttrell, G.H. and Yoon, R.-H., 1993. Hydrodynamic surface force model for bubble particle collection, 18th International Mineral Processing Congress, Sydney, Australia, pp. 751-756.
- Trahar, W.J. and Warren, L.J., 1976. The flotability of very fine particles -- A review. *Int. J. Miner. Process*, 3(2), 103-131.
- Xu, Z. and Yoon, R.-H., 1989. The role of hydrophobic interactions in coagulation. *J. Colloid and Interface Sci.* 132(2), 532-541.
- Xu, Z. and Yoon, R.-H., 1990. A study of hydrophobic coagulation. *J. Colloid and Interface Sci.* 134(2), 427-434.

Yoon, R.-H. and Mao, L., 1996. Application of extended DLVO theory, IV. Derivation of flotation rate equation from first principles. *J. Colloid and Interface Sci.* 181(2), 613-626.

## **PUBLICATIONS/PRESENTATIONS**

This section of the report should include a listing of any scholarly works that resulted from the project activities. These items include, but are not limited to, journal articles, books or book chapters, conference proceedings, magazine articles, patent awards, theses or dissertations, major published reports, technical manuals, workshop or short course booklets, and presentations at professional meetings.

## **APPENDICES (IF ABSOLUTELY NECESSARY)**

**Appendix 42: Measurement of Surface Forces Between Hydrophobic  
Surfaces (VA016)**

## TECHNICAL PROGRESS REPORT

Contract Title and Number:

Crosscutting Technology Development at the Center for  
Advanced Separation Technologies  
(DE-FC26-02NT41607)

Period of Performance:

Starting Date: 6/1/2005  
Ending Date: 10/31/2006

Sub-Recipient Project Title:

Measurement of Surface Forces Between Hydrophobic  
Surfaces

Principal Investigators:

Yoon

Contact Address:

Subcontractor Address:

No subcontracts issued.

Report Information:

Type: Semi-Annual  
Number: 1  
Period: 10/1/05-3/31/06  
Date: 05/10/2006  
Code: VA016-R01

Contact Information:

Phone:  
Fax:  
E-Mail: ryoon@vt.edu

Subcontractor Information:

Phone:  
Fax:  
E-Mail:

### ABSTRACT

An atomic force microscope (AFM) was used to measure the surface forces between macroscopic gold surfaces. Spheres of gold and gold-coated glass plates were immersed in thiol-in-ethanol ( $10^{-2}$  mM) solutions to hydrophobize the surfaces. The degree of hydrophobization was controlled by varying immersion time and using thiols of different chain lengths. In the present work, alkane thiols of C-4 (1-butanethiol), C-12 (1-dodecanethiol) and C-16 (1-hexadecanethiol) were used. The maximum equilibrium water contact angles obtained with these surfactants were  $94^\circ$ ,  $105^\circ$  and  $105^\circ$ , respectively. At higher contact angles, the measured forces were substantially larger than the van der Waals force. Unlike the work reported by Ederth and his coworkers (1998, 2001), the force curves were smooth with no steps. Only when the thiol-coated surfaces were exposed for prolonged time in air or contaminated, discontinuities were observed. The maximum hydrophobic forces measured using the C-4 thiol was weaker than those measured with the C-12 and C-16 thiols. The two longer chain thiols were indistinguishable with respect to the measured hydrophobic forces. The hydrophobic forces measured with the C-16 thiol exhibited decay lengths in the range of 1.2-20.9 nm. The current work provided experimental evidence for the existence of hydrophobic force on hydrophobic gold surfaces which is not due to air cavities or nanobubbles.

## **INTRODUCTION**

### Background

Froth flotation is the most widely used solid-solid separation technique used in the mining industry. It is based on separating particles on the basis of hydrophobicity difference. Thus, rendering a selected mineral more hydrophobic than others is the key to the success of a flotation process. For this reason, the early days of flotation research was focused on hydrophobizing minerals and monitoring the changes in hydrophobicity by measuring contact angles. However, contact angle is a thermodynamic property and does not provide kinetic information. On the other hand, flotation is a kinetic process and the industry strives for improving flotation kinetics and, hence, increasing recovery and throughput.

In colloid chemistry, the kinetics of coagulation can be predicted by the DLVO theory, which considers two surface forces, namely, repulsive double-layer force and attractive van der Waals force. The theory is useful for describing interactions between particles. However, it is inadequate for studying bubble-particle interactions, as both of these forces are repulsive under typical flotation conditions. It was not until recently that one could actually measure the surface forces acting between two hydrophobic surfaces, and observed additional attractive force, which is naturally referred to as “hydrophobic force”. It has been shown that the use of the hydrophobic force allows one to model coagulation of hydrophobic particles (Xu and Yoon, 1989, 1990) and bubble-particle adhesion (Yoon, 1991; Yoon and Mao, 1996; Mao and Yoon, 1997). However, there has been a great deal of controversy regarding the existence of the hydrophobic force and its possible origins. Furthermore, most of the hydrophobic force measurements conducted in the past was made with mica and silica surfaces using surfactants that are not commonly used for flotation. It is therefore, proposed to conduct direct force measurements using sulfide minerals, gold, and rutile ( $\text{TiO}_2$ ) in the presence of thiols, cationic surfactants, and anionic surfactants. The results of the proposed work should help alleviate the controversy and collect information that can help further the flotation technology.

### Objective and Approach

Our objective in the reporting period is to discover whether or not this hydrophobic force on thiol treated gold surfaces is of cavitation origin, and to discover its range, magnitude and its relation with water contact angle. An atomic force microscopy will be used to measure the surface force between microscopic gold surfaces, which are hydrophobized with thiols of different carbon chain length.

## **PROJECT TASKS**

### Task 1: Fabrication of Micromanipulator

To conduct surface force measurement using the colloidal probe technique developed by Ducker et al (1991, 1992), gold microspheres must be attached to the AFM cantilever. In the reporting period, a micromanipulator has been fabricated for gluing small spherical

particles to cantilever. This micromanipulation apparatus was assembled using a translation stage (Parker automation, daedal division), an optical view system (Digital Instrument) and a hot plate.

## Task 2: Preparation of Gold Surfaces

The gold coated glass slides were purchased from evaporated metal films (EMF, NY) corporation, and the gold coatings were especially made upon customer's requirement. A 50 Å chromium layer was initially deposited on the glass slide before a 1000 Å of gold in an evaporator. The chromium adhesive layer was used to ensure the strong bonding between the gold layer and glass slide. We also tried to deposit gold directly on glass and mica surfaces with a sputter machine, but the gold coatings were easily removed when cleaned in the acid solutions. An atomic force microscope image of a typical clean gold surface is shown in Figure 1. The surface consisted of island like grains. AFM image showed the maximum peak to valley distance was 3.3 nm on gold surface, and the root mean square (RMS) roughness was 0.8 nm over an area of  $1 \times 1 \mu\text{m}^2$ .

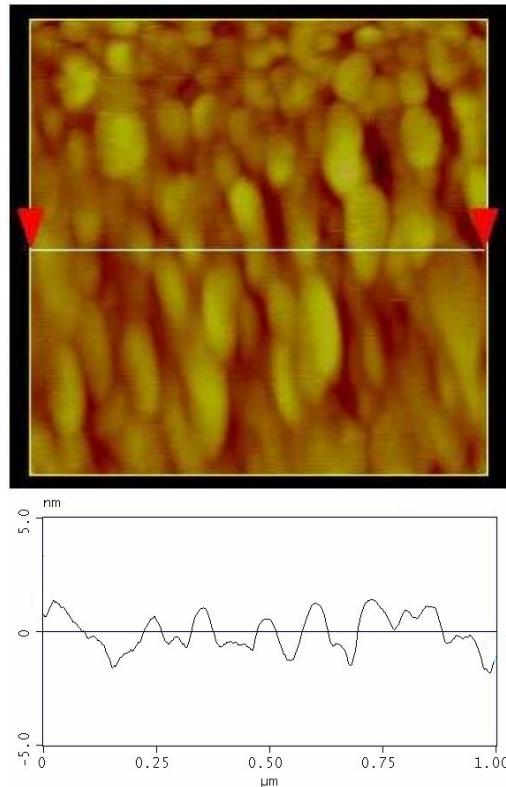


Figure 1. AFM image and cross section of evaporated gold film on Cr-coated glass after treatment with piranha solution.

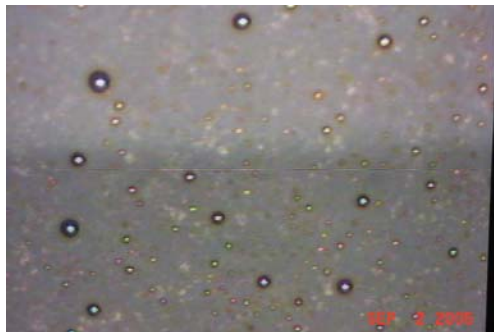


Figure 2. The optical microscopy image of gold spheres.

Gold spheres with appropriate diameters were produced by melting the gold micro powder (1.5-3.0 micron, 99.96+%, Alfa Aesar) in a high temperature furnace. The gold powder was placed in an  $\text{Al}_2\text{O}_3$  crucible and heated until above its melting point (1064.18 °C), the temperature was kept at 1100 °C for 15 min, and then the furnace cooled down slowly. During the process, the furnace was flushed with nitrogen to maintain oxygen free atmosphere. By this way, gold spheres with a wide size distribution in the micrometer range were produced (Figure 2). The spheres with diameter of 20-40 micrometer were chosen for

experiments.

### Task 3: Surface Forces Measurement

A great deal of effort has been focused on the long-range attractive interactions between hydrophobic surfaces. Ederth and his coworkers (1998, 2000, 2001) conducted force measurements with a bimorph surface force apparatus on gold which has been hydrophobized with alkanethiol, mixtures of hydrophilically (-OH) and hydrophobically (-CH<sub>3</sub>) terminated thiols, and semifluorinated thiols. They found step-like onsets of the attraction when the surface contact angle is larger than 90°, and they concluded that excess attraction force is caused by the coalescence of microscopic bubbles on the surfaces. In the current reporting period, AFM was used to measure the surface force on gold. The gold surface were hydrophobized by immersion in the thiol-in-ethanol solution (10<sup>-5</sup> M), and the degree of hydrophobicity was controlled by varying immersion time and using thiols of different chain length (C-4, C-12 and C-16). The investigation of the Hamaker constant and surface charge of gold in water was also included in the current work.

#### *Subtask 1: Bare Gold*

Measurement of surface force between sphere of gold and gold-coated glass plate in water was conducted. Due to the high surface energy, gold easily adsorbs organic contaminants, even when exposed to air for short periods (Gaines, 1981). The gold substrates must be cleaned prior to force measurement. There are several cleaning procedures for gold have been reported, such as “piranha solution” (Kane and Mulvaney, 1998), chromic acid (Biggs and Mulvaney, 1994), UV/ozone treatment (Woodward, et al, 2000), and “electrochemical cleaning” (Schoenfisch, et al, 2000). In the present work, the flat gold plate was cleaned by immersion into a boiling “piranha solution” (1: 3 H<sub>2</sub>O<sub>2</sub>/H<sub>2</sub>SO<sub>4</sub>) for 20 min. (WARNING: Piranha solution reacts violently with organic matter, especially when hot, and is extremely corrosive). And then the surface was flushed with nanopure water for 1 min, rinsed in pure ethanol for 2 min and was immediately followed by thiol absorption. The hot mixture of H<sub>2</sub>O<sub>2</sub> and H<sub>2</sub>SO<sub>4</sub> is a very strong oxidizing agent, it is not only efficient in removing organic contaminants, but also it tends to oxidize the gold surface itself (Ron and Rubinstein, 1994). The cleaning procedure results in a surface with zero contact angle with water, which is due to the formation of gold oxide (Au<sub>2</sub>O<sub>3</sub>). The gold oxide is thermodynamically unstable in the ambient and it tends to decompose. The ethanol was reported to reduce the gold oxide to gold [9]. After rinsed with ethanol for 2 min, the gold oxide was reduced and gets a water contact angle of 65°. Gold sphere was glued to cantilever probe before cleaning. To avoid been destroyed in the “piranha solution”, the gold sphere probe was cleaned with UV light instead. Before the force measurement, the gold sphere probe was flushed with pure ethanol, illuminated in the UV light (254 nm) for 2 hours and rinsed with ethanol.

Figure 3 shows the force profiles (F/R vs H) between bare gold surfaces in pure water, 1 mM and 10<sup>2</sup> mM NaCl aqueous electrolyte solution. Repulsive force was observed when the force measurements were conducted in pure water and 1 mM NaCl solution. And in

$10^2$  mM NaCl, a pure attractive force at separation of 0~20 nm was obtained. In pure water, there is a short range attractive force at separation of 0~10 nm and a long range electrostatic repulsive force beyond 10 nm. The repulsive force decreased in pure water when NaCl solution was introduced, because the thickness of electronic double layer was decreased by adding electrolyte.

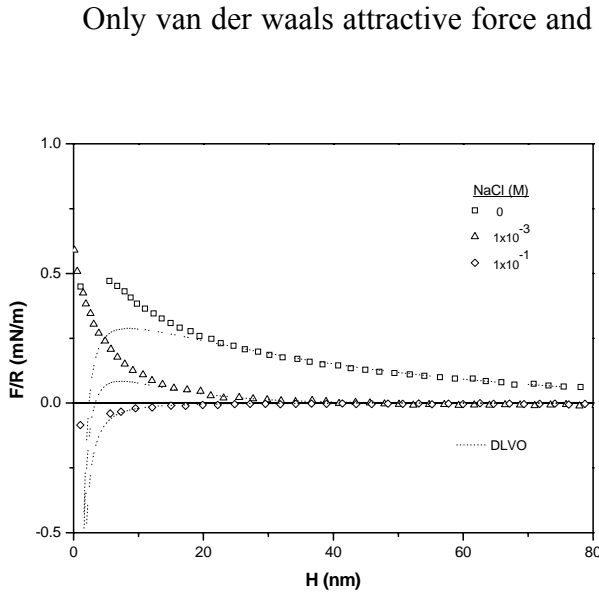


Figure 3. Surface forces between bare gold sphere and gold coated glass plate in water, 1 mM and  $10^2$  mM NaCl.

Only van der waals attractive force and electrostatic repulsive force operates between bare gold surfaces. The force curves obtained in water and NaCl solution were fitted with classic DLVO theory under constant potential condition, and the dotted lines represent the fitting curve. A Hamaker constant of  $1.2 \times 10^{-20}$  J was obtained using an approximate equation (1) for non retarded van der waals force:

$$\frac{F}{R} = \frac{A}{6H^2} \quad (1)$$

Constant potential model (Oshima et al., 1982) was used to calculate double layer repulsive force, and the thickness of double layer and surface potential on the gold surfaces were obtained, with  $\psi_0 = -$

53 mV and  $\kappa^{-1}$  (the Debye length) of 359 Å in water. The value of  $\psi_0 = -53$  mV in nanopure water agrees well with the value of zeta potential measurement ( $-53 \pm 3$  mV). The surface potential on gold increases with increased NaCl concentration. In 1 mM NaCl, fitted value is -20 mV, which increases to -6 mV in  $10^2$  mM NaCl.

Hamaker constant of  $1.2 \times 10^{-20}$  J obtained in the current experiment is comparable to the value of  $4 \times 10^{-20}$  J which was reported by Ederth, et al (2000), though it is much less than the value of  $2.5 \times 10^{-19}$  J predicted by Lifschitz theory. In fact, there is a disagreement with the value of Hamaker constant in accordance with observations of other researchers. Raiter, et al (1998) and Biggs, et al (J. Am. Chem. Soc 1994) didn't find attractive Van der Waals interaction force for gold-coated surfaces, or the attraction is much smaller than expected from Lifschitz theory was observed by Ducker and Senden (1992), Kane and Mulvaney (1998). Results of coagulation experiments on gold sols (Enüstün and Turkevich, 1963) also point to much lower values for the Hamaker constant of  $2.3 \times 10^{-20}$  J. The only case to our knowledge is that the high Hamaker constant for gold ( $2.5 \times 10^{-19}$  J) was confirmed by Biggs, et al (J. Chem. Phys, 1994) with AFM force measurement.

The above experimental value of Hamaker constant may be compared with that obtained using the methylene-iodide contact angle method. In the present work, the contact angle ( $\theta_m$ ) of methylene iodide on cleaned gold surface was measured to be  $6^\circ$ . By substituting this experimental value into the following equation [Z. Xu, R. H. Yoon, 1989, and F. M. Fowkes, 1964]:

$$\gamma_1^d = [(1 + \cos \theta_m) \gamma_m / 2\sqrt{\gamma_m^d}]^2 \quad (2)$$

where  $\gamma_m$  (=50.8 mN/m) is the surface tension of methylene iodide and  $\gamma_m^d$  (=48.5 mN/m) is its dispersion component, one obtains the value  $\gamma_1^d$  (dispersion component of the surface tension of gold) to be 52.9 mN/m. one can substitute this value into the following equation [Van Oss 1994]:

$$A_{131} = 1.86 \times 10^{-21} (\sqrt{\gamma_1^d} - \sqrt{\gamma_3^d}) \quad (3)$$

where  $\gamma_3^d$  (=21.8 mN/m) is the dispersion component of the surface tension of water, to obtain the value of  $A_{131} = 1.26 \times 10^{-20}$  J, which is very close to the value of  $A_{131} = 1.2 \times 10^{-20}$  J obtained from the direct force measurement.

### Subtask 2: Hydrophobic Gold Surfaces

Surfaces of gold sphere and gold coated glass plate were hydrophobized prior to surface force measurement. Hydrophobization with C4SH, C12SH and C16SH was achieved by immersing the gold sphere probe and gold flat substrate in a  $10^{-2}$  mM thiol-in-ethanol at room temperature. The strong specific interaction between the sulfur atom and the gold surface induces the spontaneous assembly of an adsorbed monolayer at the gold-solution

interface (Bain, et al, 1989). The gold plate and gold sphere probe were immersed in the solution for different periods of time to vary the surface hydrophobicity, and then the gold substrates were washed with ethanol and dried under a nitrogen gas stream at room temperature. In a given force measurement, we used the same immersion times for gold flat plate and gold sphere probe, so that their hydrophobicities were approximately the same. Special attention should be paid that the gold sphere should be glued to cantilever probe before hydrophobization. Otherwise, the glue can not adhere to the hydrophobic surface of gold sphere.

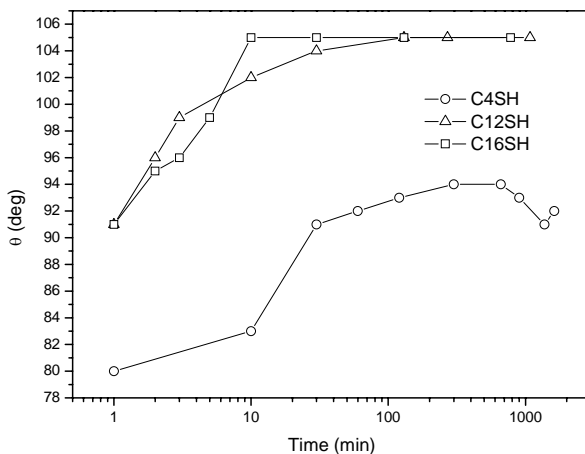


Figure 4. Kinetics of adsorption of n-alkanethiols from ethanol to gold coated glass slides as a function of chain length

Contact angle was used to assess the degree of hydrophobicity of gold surfaces. The contact angle measurements (Fig 4) show that the water contact angle increases with immersion time for gold surfaces in C-4, C-12 and C-16 thiol ethanol solution ( $10^{-2}$  mM), and the maximum equilibrium contact angles of longer chain thiols (C-12 and C-16) are larger than that of the short chain thiol (C-4). Less time was taken to get maximum equilibrium contact angle for longer carbon chain thiol. Maximum equilibrium contact angles of gold surfaces were obtained in C-16 ( $105^\circ$ ), C-12 ( $105^\circ$ ) and C-4 ( $94^\circ$ ) after a immersion time of 10, 130 and 300 min respectively.

The force measurement experiments show that the most attractive forces are much greater in magnitude than the van der Waals force. Unlike the work reported by Ederth and his coworkers (1998, 2001), the force curves obtained in current work were smooth with no steps.

Only when the thiol-coated surfaces were exposed for prolonged time in air or contaminated, discontinuities were observed, which is shown in Fig 5. The step-like force curves was obtained under the condition that C4SH hydrophobized gold coated glass slide was exposed in air for elongated time prior to commencement of force measurement. The inset represents the force obtained with the same C4SH surfaces after flush with fresh water. The contamination of substrate could be an explanation for the step or discontinuity.

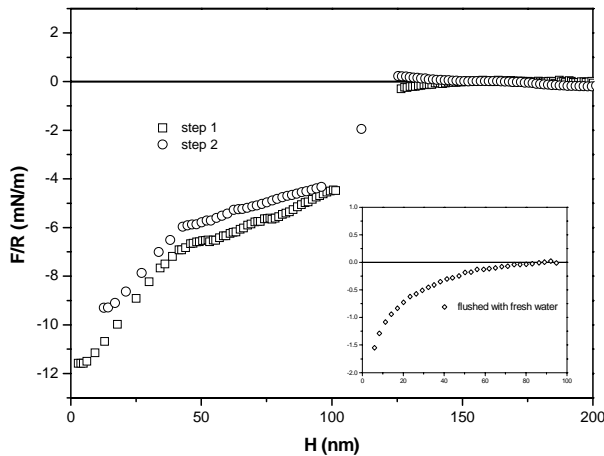


Figure 5. Normalized forces between C4SH surfaces in water.

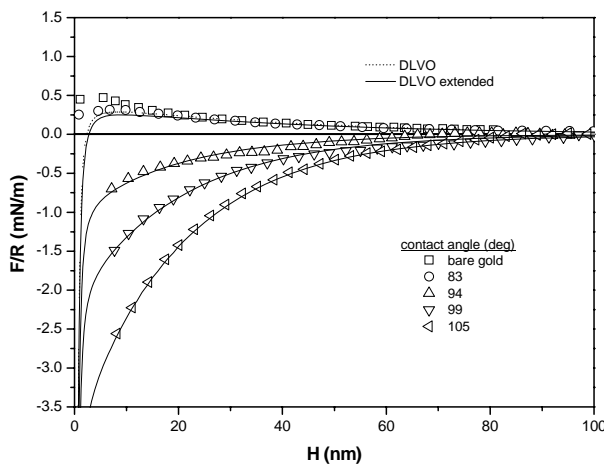


Figure 6. Surface forces obtained with C16SH coated gold sphere-plate in water.

Figure 6 shows interaction force between C-16 thiol coated gold surfaces with different water contact angle. An extra attractive hydrophobic force that was not included in classic DLVO theory was observed, and it increased with contact angle. At  $\theta > 90^\circ$ , no electrical double layer repulsive force was found; attractive forces dominated at all separations. An extended DLVO theory that includes hydrophobic force ( $F_h$ ) was used to fit the all the force data obtained between hydrophobized gold surfaces:

$$F_t = F_d + F_e + F_h \quad (4)$$

in which  $F_t$  is the total force between surfaces in close proximity,  $F_d$  is the London-van der Waals dispersion force, and  $F_e$  is the electrical double layer repulsive force. Measured hydrophobic forces are most commonly described by the empirical relationship:

$$\frac{F_h}{R} = C_0 \exp\left(-\frac{H}{D_0}\right) \quad (5)$$

in which  $C_0$  and  $D_0$  are fitting parameters.  $C_0$  is sensitive to contact angle, which decreased from -0.5 mN/m to -3.8 mN/m when the contact angle increased from  $83^\circ$  to  $105^\circ$ . At  $\theta=83^\circ$ ,

$D_0$  is 1.2 nm; at  $\theta>90^\circ$ ,  $D_0$  is around 20 nm

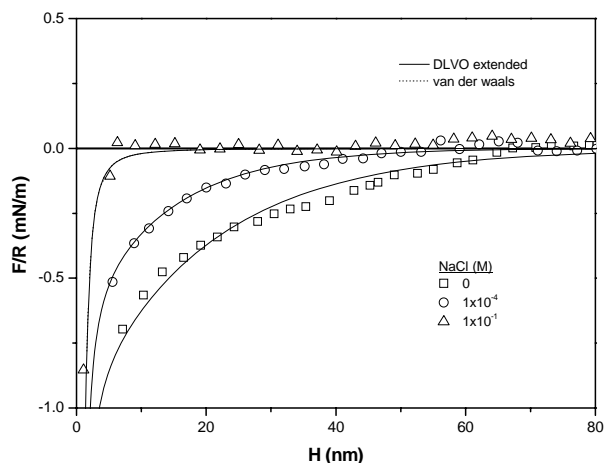


Figure 7. Effect of NaCl on the forces measured with C16SH coated gold sphere-plate.

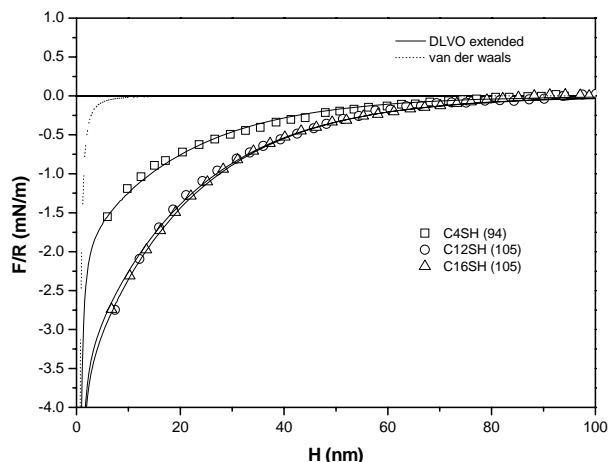


Figure 8. Normalized forces recorded between SAMs of C4SH, C12SH and C16SH with maximum equilibrium contact angle in water.

Fig 7 showed the change of hydrophobic forces between C-16 thiol treated gold surfaces when different concentration of NaCl electrolyte was added. The solid lines represent the extended DLVO theory with a single-exponential force law (equation 5). The contact angle of gold surfaces was controlled to be  $94^\circ$  by immersion time. The hydrophobic force is diminished by introducing NaCl, probably because that the electrolyte ions destroy the water structure between the hydrophobic surfaces. At high concentration of NaCl (0.1 M), no hydrophobic force was found, and only van der Waals attractive force dominated at separation of 0~10 nm.

Figure 8 shows the hydrophobic force between gold surfaces treated with C-4, C-12 and C-16 thiol. The dotted line represents the van der Waals force, and the dashed lines represent the fits by extending the DLVO theory. At the present work, the gold surfaces were immersed in the thiol solutions for a long time to get the maximum equilibrium contact angle. The C-12 and C-16

got the same value on contact angle (105°). Likewise, the hydrophobic force is of the same magnitude for C-12 and C-16, and the hydrophobic force is weaker for C-4 which has smaller contact angle. There is no much difference for C-4, C-12 and C-16 on  $D_0$  value, and the  $C_0$  value is larger with smaller contact angle.

## SUMMARY

1. Accomplished fabrication of micromanipulator which is used to glue small spherical particles to cantilever.
2. Gold spheres were produced by melting the gold micro powder in a high temperature furnace.
3. A Hamaker constant of  $1.2 \times 10^{-20}$  J was derived from surface force measurement on bare gold surface.
4. Attractive hydrophobic force was observed on the thiol treated gold surface, while no step was found in the force measurement.

## FUTURE WORK

1. Conduct force measurement on gold which will be treated with a thiol solution at different electrochemical potentials.
2. Conduct force measurement using spheres and plates of zinc sulfide.
3. Conduct force measurement using spheres and plates of silver.

## REFERENCES

- Bain et al., *J. Am. Chem. Soc* **1989**, 111 (1), 321.  
Biggs, S.; Mulvaney, P., *J. Chem. Phys* **1994**, 100(11).  
Biggs, S., Mulvaney, P., Zukoski, C. F., and Grieser, F., *J. Am. Chem. Soc* **1994**, 116, 9150-9157.  
Biggs, S., Mulvaney, P., *J. Chem. Phys* **1994**, 100 (11), 8501-8505.  
Ducker, W. A., Senden, T. J. and Pashley, R. M., *Nature* **1991**, 353: 239-241.  
Ducker, W. A., Senden, T. J., *Langmuir* **1992**, 8, 1831-1836.  
Ederth, T., Claesson, P. M. and Liedberg, B., *Langmuir* **1998**, 14, 4782-4789.  
Ederth, T., *J. Phys. Chem. B* **2000**, 104, 9704-9712.  
Ederth, T., Liedberg, B., *Langmuir* **2000**, 16, 2177-2184.  
Ederth, T., et al, *Journal of Colloid and Interface Science* **2001**, 235, 391-397.  
Enüstün, B. V., Turkevich, J., *J. Am. Chem. Soc* **1963**, 85, 3317.  
Fowkes, F. M., *Ind. Engng Chem* **1964**, 56, 40.  
Gaines, G. L., *J. Colloid Interface Sci*, **1981**, 79, 295.  
Kane, V.; Mulvaney, P., *Langmuir* **1998**, 12, 3303.  
Kane, V., Mulvaney, P., *Langmuir* **1998**, 14, 3303-3311.  
Mao, L. and Yoon, R.-H., *Int. J. Mineral Process*, **1997**, 50, 171-181.  
Oshima, H., Healy, T. W., White, L. R., *J. Colloid Interface Sci* **1982**, 89, 484.  
Ron, H., Rubinstein, I., *Langmuir*, **1994**, 10, 4566-4573.

Schoenfish, M. H.; Ross, A. M.; Pemberton, J. E., *Langmuir* **2000**, 16, 2907-2914.  
Van Oss, C. J., *Interfacial Forces in Aqueous Media* **1994**, Marcel Dekker, Inc.  
Woodward et al., *Langmuir* **2000**, 16, 5347-5353.  
Xu, Z., and Yoon, R.-H., *J. Colloid Interface Sci* **1989**, 132(2), 532-541.  
Xu, Z., and Yoon, R.-H., *J. Colloid and Interface Sci* **1990**, 134(2), 427-434.  
Yoon, R.-H., "Hydrodynamic and Surface Forces in Bubble-Particle Interactions," a plenary lecture at the XVII International Mineal Processing Congress, Dresden, Germany, September 23-28, **1991**, Proceedings, pp. 17-31; *Aufbereitungs-Technik*, **1991**, 32(9), 474-485.  
Yoon, R.-H. and Mao, Laiqun, *J. Colloid and Interface Sci* **1996**, 181, 613-626.

## **PUBLICATIONS/PRESENTATIONS**

Conference abstract "Surface Forces Measured with Thiol-Coated Gold Surfaces" for XIIIth International Conference on Surface Forces

**Appendix 43: Novel Surfactants as Collectors for Froth Flotation (VA017)**

# TECHNICAL PROGRESS REPORT

Contract Title and Number:

Crosscutting Technology Development at the Center for  
Advanced Separation Technologies  
(DE-FC26-02NT41607)

Period of Performance:

Starting Date: 6/1/2005  
Ending Date: 10/31/2006

Sub-Recipient Project Title:

Novel Surfactants as Collectors for Froth Flotation

Report Information:

Type: Semi-Annual  
Number: 1  
Period: 10/1/05-3/31/06  
Date: 3/31/06  
Code: VA017-R01

Principal Investigators:

Gandour

Contact Address:

Virginia Tech  
302 Davidson Hall  
Blacksburg VA 24060

Contact Information:

Phone: (540) 231-3731  
Fax: (540) 231-3255  
E-Mail: gandour@vt.edu

Subcontractor Address:

No subcontracts issued.

Subcontractor Information:

Phone:  
Fax:  
E-Mail:

## ABSTRACT

The synthesis of two homologous series of two-tailed, tricarboxylate amphiphiles has been achieved. All compounds have been fully characterized by the standards of organic chemistry. The compounds are soluble in water as tristriethanolammonium salts at a concentration of  $1 \times 10^{-5}$  M or greater.

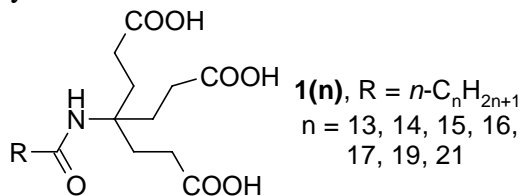
## INTRODUCTION

### Background

Froth-flotation separation is the most widely used unit process in the minerals processing industry with nearly 100,000 tons of mined ores and coal being floated daily.(Fuerstenau, 1999) Selective hydrophobization of mineral particles by collectors (surfactants) enables separation from the gangue; the hydrophobized particles “attach” to microbubbles(Yoon, 2000) and float to the top of the slurry. One key parameter is the surface charge of the mineral. The adsorption of collectors occurs at specific sites on the mineral surface; knowledge of the surface properties (zeta potential, point of zero charge)(Fuerstenau and Pradip, 2005) are crucial for designing a useful collector. The strength of the hydrophobic

force (Pazhianur and Yoon, 2003) that creates the attachment of the particle to the bubble is another key parameter in designing useful collectors. Collectors that are designed to optimize both absorption at specific sites on the surface and hydrophobicity can improve both efficiency and selectivity in froth flotation. From the point of view of the design of an optimal collector, the head group of an amphiphile provides the functional groups that interact with the surface and the tail group provides the hydrophobicity.

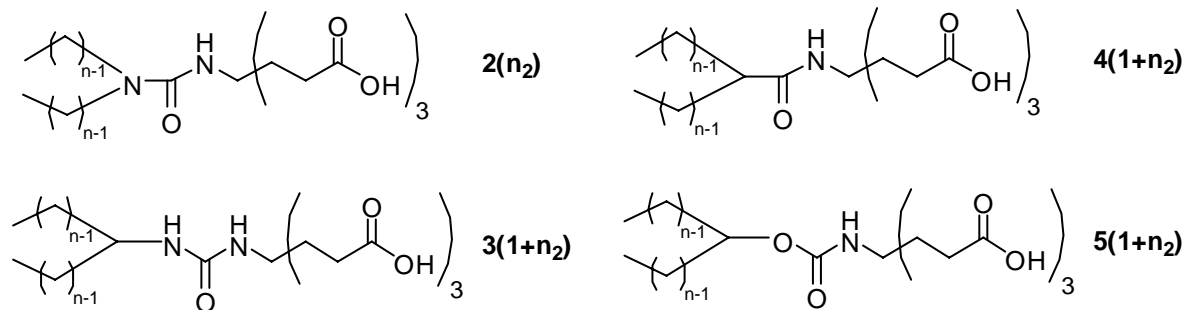
A novel approach to the design of collectors involves supramolecular preorganization in the head group (polar part) and in the tail group (hydrophobic part) to improve the packing density of the adsorption layer on the mineral particles. (Müller et al., 2005) Improving the packing density should increase the hydrophobicity of the modified surface. A recent report (Müller et al., 2005) from Weber's laboratory describes flotation studies with three types of oligofunctional surfactants—two feature geometrically constrained, preorganized structures and the third has a dendritic structure. We have also been examining the interactions of dendritic amphiphiles with surfaces. (Williams et al., 2005) Homologous, single-tailed, long-chain alkyl dendrons **1(n)** with three carboxyl groups form homologous thin films on silver oxide surfaces. Our observations demonstrate that assemblies of these molecules should make hydrophobic coatings. The uniqueness of this homologous series is that it contains very long alkyl chains of 19 and 21 carbons, derived from icosanoic (arachidic) and docosanoic (behenic) acid, respectively.



The head group, when neutralized with triethanolamine, is sufficiently hydrophilic to enable good aqueous solubility of the longest chain. The three carboxylates offer a strong binding to a surface because of multiple attachments. Preliminary results show the several members of the homologous series **1(n)** produce, at concentrations  $<1 \times 10^{-6}$  M, strongly hydrophobic coatings (contact angles  $> 90^\circ$ ) on an apatite and calcite surfaces.

### Objective and Approach

We propose to synthesize four homologous series of three-headed, two-tail amphiphiles—**2(n<sub>2</sub>)**, **3(1+n<sub>2</sub>)**, **4(1+n<sub>2</sub>)**, and **5(1+n<sub>2</sub>)**. The design idea for these series is to produce the amphiphiles with the same number of carbons as the respective single-tailed amphiphiles.



Our hypothesis is that the two-tail amphiphiles will make a more hydrophobic surface because the packing density of the chains has increased compared to single tail amphiphiles. The validation of the hypothesis will occur if the contact angle of a hydrophobized surface is

greater for a two-tail amphiphile than a single-tail amphiphile when the concentrations of both amphiphiles are equal. The ultimate goal of the project is to find the amphiphile that gives a contact angle  $>90^\circ$  with the smallest concentration.

## PROJECT TASKS

Syntheses (Figure 1) began with Weisocyanate<sup>TM</sup>. (Newkome et al., 1998) Condensation of two-tail amines with the isocyanate occurred at room temperature to afford good-to-high yields (step i) of triesters (not shown). Formolysis of the trimesters (step ii) produced the triacids—**2(n<sub>2</sub>)**, where  $n=6-10$  and **3(1+n<sub>2</sub>)**, where  $n=6-11$ —in good yields of recrystallized products. All compounds were fully characterized by the standards of organic chemistry. The compounds were soluble in water as triethanolammonium salts at a concentration of  $1 \times 10^{-3} \text{M}$  or greater.

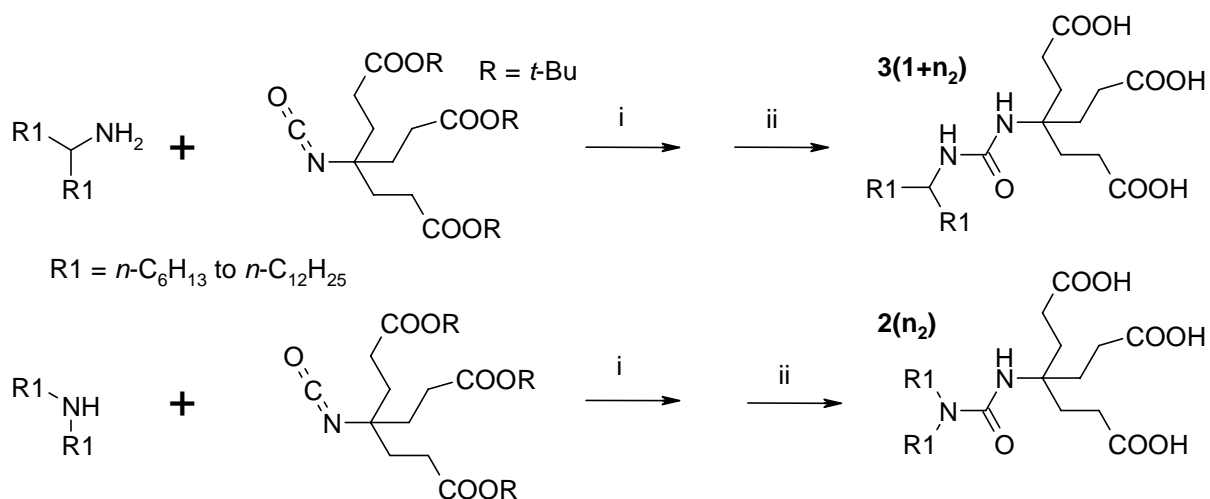


**Figure 1.** Reagents and conditions: i.  $\text{NEt}_3$ ,  $\text{CH}_2\text{Cl}_2$ , rt, 18 h; ii.  $\text{HCOOH}$ , rt, 48 h

## SUMMARY

Two homologous series of two-tail, tricarboxylate amphiphiles were synthesized in good yields.

## FUTURE WORK

In the next 6-month period, we shall work on two projects. One is the synthesis of **4(1+n<sub>2</sub>)** and **5(1+n<sub>2</sub>)** and the other is the measurement of contact angles on apatite and calcite for **2(n<sub>2</sub>)**, where  $n=6-10$ , and **3(1+n<sub>2</sub>)**, where  $n=6-11$  as a function of concentration. The synthesis is described in Figure 2.

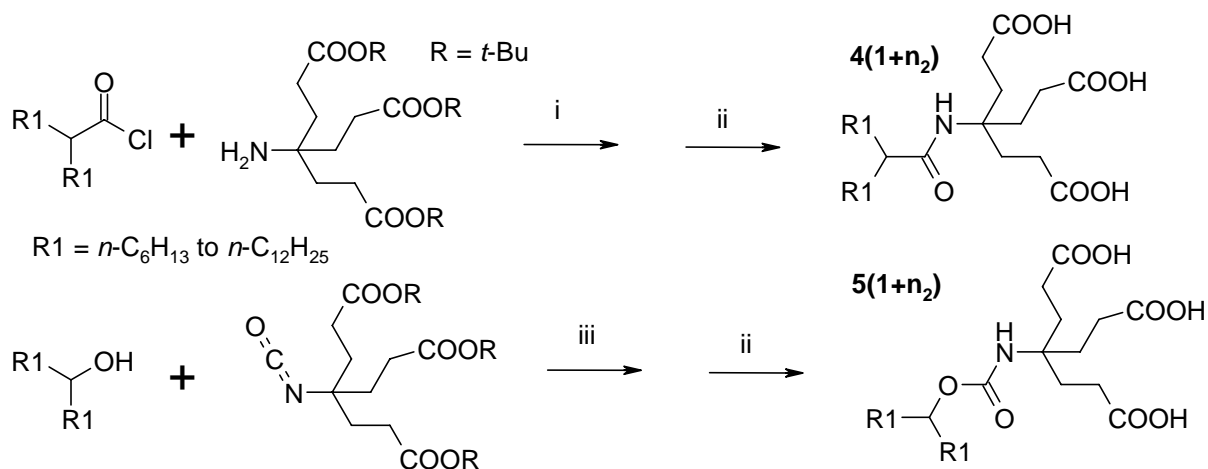


**Figure 2.** Reagents and conditions: i.  $\text{NEt}_3$ ,  $\text{CH}_2\text{Cl}_2$ , rt, 18 h; ii.  $\text{HCOOH}$ , rt, 48 h; i.  $\text{NEt}_3$ ,  $\text{CH}_2\text{Cl}_2$ ,  $95^\circ\text{C}$ , 18 h;

## REFERENCES

- Fuerstenau, D.W., 1999. The froth flotation century. In: B.K. Parekh and J.D. Miller (Editors), *Advances in Flotation Technology*. Society for Mining, Metallurgy, and Exploration, Littleton, CO, pp. 3–21.
- Fuerstenau, D.W. and Pradip, 2005. Zeta potentials in the flotation of oxide and silicate minerals. *Advances in Colloid and Interface Science*, 114–115: 9-26.
- Müller, P.U., Akpo, C.C., Stöckelhuber, K.W. and Weber, E., 2005. Novel amphiphiles with preorganized functionalities - formation of Langmuir-films and efficiency in mineral flotation. *Advances in Colloid and Interface Science*, 114–115: 291-302.
- Newkome, G.R. et al., 1998. Isocyanate-based dendritic building blocks: combinatorial tier construction and macromolecular-property modification. *Angew. Chem., Int. Ed.*, 37(3): 307-310.
- Pazhianur, R. and Yoon, R.H., 2003. Model for the origin of hydrophobic force. *Minerals & Metallurgical Processing*, 20(4): 178–184.
- Williams, A.A. et al., 2005. Homologous, long-chain alkyl dendrons form homologous thin films on silver oxide surfaces. *Chemical Communications*(40): 5053–5055.
- Yoon, R.H., 2000. The role of hydrodynamic and surface forces in bubble-particle interaction. *International Journal of Mineral Processing*, 58(1-4): 129–143.

## PUBLICATIONS/PRESENTATIONS

None to report this period.

**Appendix 44: Mercury Reduction From Coal Power Plant Emission Using  
Functionalized Ordered Mesoporous Carbons (FOMCs) (WV015)**

# TECHNICAL PROGRESS REPORT

Contract Title and Number:

Crosscutting Technology Development at the Center for  
Advanced Separation Technologies  
(DE-FC26-02NT41607)

Period of Performance:

Starting Date: 06/01/2005  
Ending Date: 10/31/2006

Sub-Recipient Project Title:

Mercury Reduction From Coal Power Plant  
Emission Using Functionalized Ordered  
Mesoporous Carbons (FOMCs)

Principal Investigators:

Dianchen Gang, Baolin Deng

Report Information:

Type: Semi-Annual  
Number: 1  
Period: 10/1/05-3/31/06  
Date: 03/31/06  
Code: WV015-R01

Contact Address:

Dept. of Civil Engineering  
West Virginia University  
Montgomery WV 25316

Contact Information:

Phone: (304) 442-3372  
Fax: (304) 442-3391  
E-Mail: dianchen.gang@mail.wvu.edu

Subcontractor Address:

Baolin Deng  
Department of Civil & Environmental Engineering  
University of Missouri-Columbia  
Columbia, MO 65211

Subcontractor Information:

Phone: 573-882-0075  
Fax: 573-882-4874  
E-Mail: DengB@missouri.edu

## ABSTRACT

Coal-fired power plants are the largest source of anthropogenic mercury emissions in the U.S. The objective of this project is to develop functionalized ordered mesoporous carbons (FOMCs) for the removal of elemental mercury from the coal-fired power plants. In this first project time period, we have focused on acquisition of experimental instrumentation and setting up of testing systems. An ordered mesoporous carbon has also been synthesized in multiple-gram quantity. This sample will be functionalized and evaluated for its mercury removal capacity in the second and third project time period.

## INTRODUCTION

### Background

Risk assessment under the 1990 Clean Air Act Amendments (CAAAAs) demonstrated that mercury exposure had been associated with both neurological and developmental damage in humans. To reduce the health risks caused by mercury emissions, the United States Environmental Protection Agency (USEPA) has recently issued the Clean Air Mercury Rule (CAMR) to permanently cap and reduce mercury emissions from coal-fired power plants. Based on the new regulation, a first phase cap of 38 tons per year (tpy) will

become effective in 2010 and a second phase cap of 15 tpy will become effective in 2018. This new regulation has significant financial implications for the CFPPs, because of the high costs associated with mercury removal. Therefore, developing innovative technologies for cost effective mercury emission control is critical to sustain and promote coal usage as an integrated component of the Nation's energy policy and to ensure the Nation's energy security.

Technologies for mercury control from coal-fired power plants (CFPPs) have been well explored. The main processes include pre-combustion and post combustion. Pre-combustion involves coal-cleaning technologies to reduce mercury burden at the source. Post combustion involves adsorption by carbon-based materials by wet system or particulate filters. Mercury emissions from CFPPs exist in various valence states: elemental  $\text{Hg}^0$  and oxidized  $\text{Hg}^{2+}$  forms. However, elemental mercury gas is the dominant form of mercury in the plume of a CFPP, ranging from 92% to 99% of the total mercury concentration in the flue gas (Lindberg, 1980). The chemical forms in the mercury emissions determine the effectiveness of controls to remove mercury because of the significant differences of their chemical and physical properties. For example, elemental mercury ( $\text{Hg}^0$ ) should not be absorbed significantly by water-based scrubbing processes, because it has very low water solubility. Other existing measures, such as electrostatic precipitators, have been demonstrated ineffective in removing volatile elements such as elemental mercury, allowing at least 90% of the mercury to be discharged into the atmosphere (Kaakinen, et al 1975).

Activated carbon adsorption has been demonstrated to be capable of controlling mercury emissions. These adsorption processes can be accomplished in two different ways: powdered activated carbon (PAC) injection and fixed-bed granular activated carbon (GAC) adsorption. PAC injection involves the injection of PAC directly into the plant's flue gas stream where it adsorbs gas-phase mercury and is collected in downstream particulate control devices, such as fabric filters. In the fixed-bed GAC adsorption situations, GAC is placed downstream of the flue gas desulfurization (FGD) units and particulate collectors, serving as the final treatment process before the flue gas is discharged into the atmosphere. The regular activated carbons with large fraction of micropores ( $< 2$  nm) are not suitable for large-sized contaminants and their applications can be limited by slow diffusion kinetics, especially in the high particulate environment. Another study demonstrated that regular activated carbon showed little adsorptive capacity for elemental mercury when temperature is over  $90^\circ$  because of the physical adsorption mechanism between the Hg and virgin GAC (Vidic, et al 1996).

In recent couple years, ordered mesoporous carbons (OMCs) have attracted much attention because OMCs could be widely utilized in industries as catalyst supports and gas separation media, etc. There is also a great potential to use OMCs for environmental improvement, including the removal of inorganic and organic contaminants from liquid and gas phases. Although functionalized regular thermal activated carbons have been prepared using sulfur, salt, and other chemicals, to remove mercury from flue gas of CFPPs, no research work has been started in functionalized OMCs. The investigators believe that functionalized OMCs would have great potential in the elemental mercury removal from flue

gas because of their desirable properties, such as high surface area, controlled pore size, and elemental mercury reactive function groups.

### Objective and Approach

The objective of this project is to develop and evaluate a novel method for removing elemental mercury by using functionalized ordered mesoporous carbons (FOMCs). Ordered mesoporous carbons (OMCs) will be synthesized under defined conditions and their structure will be optimized according to their capability toward mercury removal in the high particulate environment. Then, OMCs will be functionalized by sulfur and other chemicals to enhance the Hg uptake at high temperature. Advantages of using FOMCs for mercury removal include: (1) fast kinetics, (2) large capacity per unit weight, (3) tolerant for particulate environment and high temperature. Three research tasks are proposed: (i) Synthesize high surface area ordered mesoporous carbons (OMCs); (ii) Functionalize the OMCs with different chemicals to enhance Hg uptake; and (iii) Optimize conditions for mercury removal. Within the first six months reporting time period, we have focused on acquisition of experimental instrumentation and task 1, i.e., synthesis of OMCs. An ordered mesoporous carbon has also been synthesized in multiple-gram quantity. This sample will be functionalized and evaluated for its mercury removal capacity in the second and third project time period.

### **PROJECT TASKS**

#### Task 1. Synthesis high surface area ordered mesoporous carbons (OMCs)

##### *Synthesis of Silica Template*

One important type of silica hosts, hexagonal SBA-15, was synthesized. In a typical synthesis, 100 ml of concentrated hydrochloric acid (HCl, 37%) was added into 525 ml of distilled water with stirring, and then 20 g of triblock copolymer Pluronic P123 (EO<sub>20</sub>PO<sub>70</sub>EO<sub>20</sub>, BASF) was added. After Pluronic P123 was completely dissolved with stirring for 1 hrs, 46.5 ml of tetraethylorthosilicate (TEOS, 98%, Aldrich) was added to the homogenous solution with vigorous stirring for 10min. The resulting mixture was left for 4 hrs at 40°C (Fig. 1. and 2.) and subsequently for 24 hrs at 90°C (Fig. 3.). The solid product obtained was washed with 80~90°C hot distilled water (Fig. 4.), and dried in an oven at 105°C overnight (Fig. 5.). After drying, product was calcined at 550°C for 8 hrs. The white silica template SBA-15 was stored for the next preparation of OMC (Fig. 6.).



**Fig. 1. Initial stage at 40 °C**



**Fig. 2. After 4 hrs at 40 °C**



**Fig. 3. After 24 hrs at 90 °C**



**Fig. 4. Washing with distilled water**



**Fig. 5. Drying at 105 °C overnight**



**Fig. 6. SBA-15 template**

### *Preparation of OMC*

The synthesis of ordered mesoporous carbon (OMC) was accomplished by *in situ* polymerization of monomeric acrylic acid in the porous structure of silica template SBA-15 (hexagonal structure) in a basic aqueous solution. Ninety (90) ml of monomer acrylic acid (>99%, Aldrich) was added into 180 ml of distilled water with stirring, and then 9 g of SBA-15 host was added and suspended in acrylic acid solution (Fig. 7.). After the mixture was stirred for 30 min, 0.02 g of 2,2-azobisisobutyronitrile (AIBN) was added as a free radical initiator. The mixture was then heated to 60°C for the *in situ* polymerization (Fig. 8.). The polyacrylic acid (PAA) with the silica template was dried by oven at 200°C overnight (Fig. 9.). Afterwards, the sample composite was heated under N<sub>2</sub> flow at a temperature ramp rate of 5°C min<sup>-1</sup> to 700°C and held for 8 hrs for carbonization (Fig. 10.). OMC was recovered by the dissolution of silica template using aqueous hydrofluoric acid (HF, 48%, Aldrich) for 15hrs (Fig. 11.). After etching, the product was washed and dried in oven at 90~100°C overnight (Fig. 12.). SBA-15 silicate templates and ordered mesoporous carbon prepared following the above procedure have highly ordered porous structure, as shown in Figure 13.



**Fig. 7. Mixing solution**



**Fig. 8. Polimerization**



**Fig. 9. After drying at 200 °C**



**Fig. 10. Carbonization product using N<sub>2</sub> chamber**



**Fig. 11. Etching**



**Fig. 12. Final product**

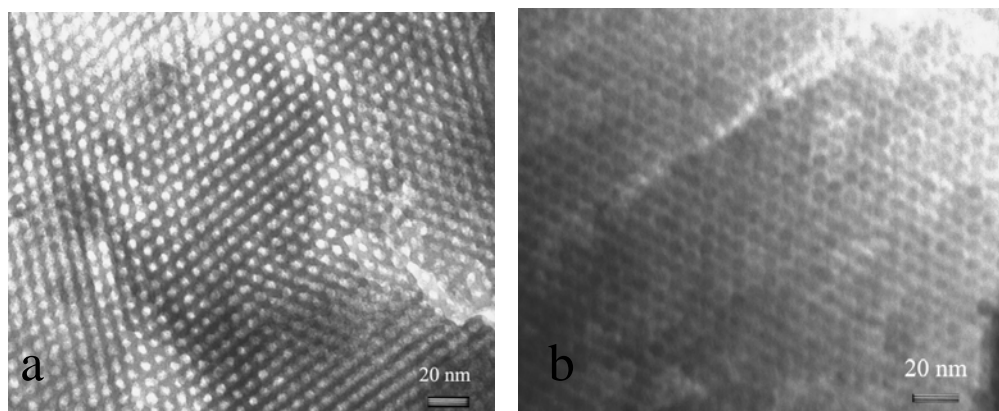


**Fig. 13. TEM micrographs of silica templates SBA-15 (a) and ordered mesoporous carbon b).**

## **SUMMARY**

In the first project time period, we have set up main experimental apparatus and instrumentation for the project, refined the procedure for OMC preparation, and prepared significant amount of OMC for further testing. Sample characterization and assessment for mercury removal is underway.

## **FUTURE WORK**

Because significant amount of ordered mesoporous carbons have already been synthesized, the next step of the research will focus on functionalizing the OMCs with sulfur, iodine, and chlorine to enhance Hg uptake; and optimizing conditions for mercury removal. Task 1 will be finished, and tasks 2 and 3 will be initiated in the second project time period

## **REFERENCES**

Gu, Z., Fang, J. and Deng, B. (2005) "Preparation and evaluation of GAC-based iron-containing adsorbents for arsenic removal", *Environ. Sci. Technol.*, 39, 3833-3843.

Kaakinen, J. W.; Jorden, R. M.; Lawasani, M. H.; West, R. E. *Environ. Sci. Technol.* 1975, 9, 862.

Lindberg, S. E. *Atmos. Environ.* 1980, 14, 227.

Vidic, Radisav D.; McLaughlin, J. Brendan. *Journal of the Air & Waste Management Association* (1996), 46(3), 241-50.

## **PUBLICATIONS/PRESENTATIONS**

(None)

**Appendix 45: Phytomining for Nickel and Silver Nanoparticles (WV016)**

## TECHNICAL PROGRESS REPORT

Contract Title and Number:

Crosscutting Technology Development at the Center for  
Advanced Separation Technologies  
(DE-FC26-02NT41607)

Period of Performance:

Starting Date: 6/1/2005  
Ending Date: 10/31/2006

Sub-Recipient Project Title:

Phytomining for Nickel and Silver Nanoparticles

Report Information:

Type: Semi-Annual  
Number: 1  
Period: 10/1/05-3/31/06  
Date: 3/31/06  
Code: WV016-R01

Principal Investigators:

Ray Y. K. Yang, Eung Ha Cho

Contact Information:

Phone: (304) 293 2111x2419  
Fax:  
E-Mail: ryang@mail.wvu.edu

Contact Address:

Ray Y. K. Yang  
Chemical Engineering Department  
West Virginia University  
Morgantown WV 26506-6102

Subcontractor Address:

No subcontracts issued

Subcontractor Information:

Phone:  
Fax:  
E-Mail:

### ABSTRACT

Phytomining is the production of a metal by growing high-biomass plants that hyperaccumulate high concentrations of a target metal. A conventional phytomining operation would consist of planting a hyperaccumulator crop over a low-grade ore body or mineralized soil, followed by harvesting and incineration of the biomass to ash to produce "bio-ore". In this project, we have expanded conventional phytomining to include other forms of plants, notably sprouts and plant cells.

Preliminary results during this period indicate that the two cultivars of geranium chosen and tested, "Rober's Lemon Rose" and "Rose", may be used for biosynthesis of silver nanoparticles. Callus culture of periwinkle (*Catharanthus roseus*) on solid agar Murashige & Skoog (MS) medium has been established and maintained by sub-culturing. Callus culture of red beet (*Beta vulgaris*) on solid agar Gamborg's B5 medium has also been established and will be maintained by sub-culturing approximately every four weeks.

## INTRODUCTION

### Background

Phytomining is the production of a metal by growing high-biomass plants that hyper-accumulate high concentrations of a target metal. A conventional phytomining operation would consist of planting a hyperaccumulator crop over a low-grade ore body or mineralized soil, followed by harvesting and incineration of the biomass to ash to produce “bio-ore”. In this project, we have expanded conventional phytomining to include other forms of plants, notably sprouts and plant cells.

There are over 300 species of known natural nickel hyperaccumulator, with *Alyssum murale* and *Alyssum corsicum* being considered as the two top performers. From these two species, two cultivars, *Alyssum murale* Waldst & Kit and *Alyssum corsicum* Duby, were developed by Inco and collaborators [1]; their bio-ores were found to contain up to 30 % nickel by dry matter, as compared to the nickel ores, which usually contain only 2-5% nickel. Since revegetation of mined area has to be done anyway, it is believed that in the near future phytomining for nickel will become competitive to open pit mining and deep mining [1].

Leaf extract of geranium (*Pelargonium graveolens*) treated with silver nitrate solution were used recently for rapid biosynthesis of stable silver nanoparticles [2]. The nanoparticles were found to be predominantly spherical ranging from 16 to 40 nm with average size of approximately 27 nm. It was speculated that proteins and/or terpenoids in the geranium leaves caused the biosynthesis of silver nanoparticles as well as their stabilization.

Gardea-Torresdey and co-workers [3, 4] were the first to use X-ray absorption spectroscopy (XAS) and transmission electron microscopy (TEM) to show the existence of gold and silver nanoparticles in live alfalfa sprouts grown on agar-agar treated respectively with potassium tetrachloroaurate and silver nitrate. They found that the nanoparticles produced by the bean sprouts are in random shapes, but may be made more uniform by changing the acidity of the solid growing medium. However, to the best of our knowledge, no scanning probe microscopy studies of surface characteristics of silver nanoparticles formed in bean sprouts have so far been reported in the literature, nor are the existences of silver nanoparticles in plant cells grown in suspension cultures.

### Objective

The objective of this project is to show the existence of nickel and silver nanoparticles in a few carefully selected species of plants in various forms including their ashes, and to study the sizes, shapes, surface characteristics, and other pertinent features of the nickel and silver nanoparticles formed therein.

## **PROJECT TASKS**

### Task 1 – Investigation of silver nanoparticles by geranium

Literature search was conducted to determine the cultivars of geranium (*Pelargonium graveolens*) available in the U. S., which have excellent potential for rapid biosynthesis of stable silver nanoparticle. Three cultivars of scented geranium, “Rober’s Lemon Rose”, “Rose”, and “Lady Plymouth”, were chosen and purchased. They are now growing well in the high-bay area of the PI’s Bioreaction Engineering Laboratory.

A series of exploratory experiments were conducted with the leaves of Rober’s Rose (RR) and Rose (R) geraniums. Effective and practical means of rupturing leaf cells was developed and applied to RR and R. Yellowish-brown color, well known to be the color of silver nanoparticles in water, was observed when the leaf broth and aqueous silver nitrate solution were combined in suitable ratios of concentrations. As expected, the intensity of the color increases with time; it eventually reaches a steady value after about 24 hours, indicating the completion of the reaction involved. Other factors that affect the formation of silver nanoparticles are currently being studied.

### Task 2 – Investigation of silver nanoparticles in bean sprouts

Mung bean (*Vigna radiate*) and alfalfa (Mesa variety), and two different sprouters were purchased. Green-Shield, a disinfectant considered to be most suitable for disinfecting the sprouters to prevent fungal contamination during sprouting, was accrued. Standard solution (ULTRAgrade) for silver for use in atomic absorption analysis, and amber glass bottles for storing them in different standard concentrations were purchased.

### Task 3 – Investigation of silver nanoparticles in plant cells

Callus culture of periwinkle (*Catharanthus roseus*) on solid agar Murashige & Skoog (MS) medium has been established; it is being maintained by sub-culturing approximately every four weeks. Callus culture of red beet (*Beta vulgaris*) on solid agar Gamborg’s B5 medium has also been established (from beet seedlings grown in agar from seeds) now; it will be maintained by sub-culturing approximately every four weeks. In addition, callus culture of stevia (*stevia rebaudiana*) on MS solid medium has also been established; it is being maintained by sub-culturing approximately every four to six weeks.

## **SUMMARY**

Preliminary results indicate that two cultivars of geranium, “Rober’s Lemon Rose” and “Rose”, may be used for biosynthesis of silver nanoparticles.

## **FUTURE WORK**

We expect all tasks of the project will move in full speed during the summer months of 2006 starting May; a research assistant will join the project at that time, and the PIs, with no teaching during the summer, will be able to focus their academic efforts fully on the project. No qualified research assistant, who can devote fully to the project, was available for the Spring semester 2006, causing a slow start on this project

Future experimental work to be conducted include: (1) To continue our investigation on the formation of silver nanoparticles by geranium and the factors affecting their formation; (2) To grow nickel-hyperaccumulator plants, *Alyssum murale* Waldst & Kit (or *Alyssum murale*), *Alyssum corsicum* Duby (or *Alyssum corsicum*), and *Alyssum bertolonii*, and study the nickel nanoparticles formed in those plants; (3) To initiate and develop suspension cultures from the callus cultures developed so far, and to study the silver nanoparticles produced from these suspension cultures; and (4) To investigate silver nanoparticles produced in the sprouts of mung bean and alfalfa.

## **REFERENCES**

1. Hill, S., *Materials World*, 11, 20-22 (2003).
2. Shankar, S. S., et al., *Biotechnology Progress*, 19, 1627-1631 (2003).
3. Gardea-Torresdey, J. L. et al., *Langmuir*, 19, 1357-1361 (2003).
4. Gardea-Torresdey, J. L. et al., *Nano Letters*, 2, 397-401 (2002).

**Appendix 46: Removal of Metal Ions from Acid Mine Drainage using a  
Novel Low-Cost, Low Technology (WV017)**

## TECHNICAL PROGRESS REPORT

<u>Contract Title and Number:</u> Crosscutting Technology Development at the Center for Advanced Separation Technologies (DE-FC26-02NT41607)	<u>Period of Performance:</u> Starting Date: 6/1/2005 Ending Date: 10/31/2006
---	---

<u>Sub-Recipient Project Title:</u> Removal of Metal Ions from Acid Mine Drainage using a Novel Low-Cost, Low Technology	<u>Report Information:</u> Type: Semi-Annual Number: 1 Period: 10/1/05-3/31/06 Date: Code: WV017-R01
<u>Principal Investigators:</u> Benjamin Dawson-Andoh	
<u>Contact Address:</u> Division of Forestry West Virginia University Morgantown WV 26506	<u>Contact Information:</u> Phone: (304) 293-3825 x2487  Fax: E-Mail: bdawsona@mail.wvu.edu
<u>Subcontractor Address:</u> Insert address of subcontractor. If none awarded, insert "No subcontracts issued." 304-293-2441 bdawsona@wvu.edu	<u>Subcontractor Information:</u> Phone:  Fax: E-Mail:

## **ABSTRACT**

Preliminary studies to test the proof of concept that wood residues can absorb and remove metal ions from Acid Mine Drainage water is in progress.

## **INTRODUCTION**

Acid Mine Drainage (AMD) produced by active and dormant coal mines continues to pose a major threat to the environment. One of the goals of the National Energy Policy developed by President Bush in 2001 is “to ensure the steady supply of affordable energy in **environmentally responsible and sustaining manner.**” Current technologies employed to remove toxic environmental polluting metals from AMD are expensive and economically challenging to the Coal Mining Industry. The work proposed here seeks to evaluate a low-cost, low technology that employs renewable biomaterials: wood and fungal biomass, to remove toxic metals that occur in AMD from solutions. Additionally, the proposed work also seeks to determine the recovery potential of toxic metals from the biomaterials and the regeneration and re-use of the biomaterials. West Virginia is one of the premier hardwood States in the US and tremendous amount of wood biomass is available as residue. The proposed study if successful will provide an avenue for the use of the tremendous wood biomass generated by both the primary and secondary forestry operations in West Virginia.

## **OBJECTIVES AND APPROACH**

The objective of the work proposed here is to compare the relative efficacy of four types of biomaterials: (1) wood residues, (2) chemically modified wood residues, (3) fungal (non-living) biomass, and (4) biologically modified wood biomass containing non-living fungal biomass. Fungal biomass will be immobilized in polyurethane foam. Wood biomass will be evaluated in two forms: particulates (5 mesh size) and mats (low density fiberboards). Since West Virginia is a hardwood (angiosperms) State, this study will focus on two hardwood species: red oak and yellow-poplar. Both wood species commonly occur in West Virginia. Also, two fungal species, *Aspergillus niger* and *Penicillium chrysogenum* will be investigated.

The efficacy of the biosorptive uptake of each biomaterial will be evaluated by measuring the kinetics of sorption and biosorptive equilibrium isotherm. This study will be carried out at bench scale level. The experimental design will be a factorial:

1. Biomaterials: 2 levels – wood biomass and fungal (non-living) biomass.
2. Modification of biomaterials: 2 levels - chemical and biological.
3. pH: 2 levels – 3 and 5.

## **PROJECT TASKS**

### **Task 1: Equipment Setup:**

We are in the process of purchasing a LIBS system from Ocean Optics, FL. In the meantime, analytical work will be done using inductively coupled plasma emission spectrometry.

### **Task 2: Experimental**

Twenty five gallons of Acid Mine Drainage material was collected from Lick Run, Preston County, WV, on 04/05/2006 and is stored at 3 °C. Four types of wood residues, oak residue, oak bark, miscellaneous wood mulch and miscellaneous wood residues have been received from Burke-Parsons-Bowlby Corp. 25 g of each wood type, in triplicate, were weighed into 250 ml Erlenmeyer flasks. 200 ml of AMD was added to each flask (wood-AMD ratio, 1:4) and shaken on a rotary shaker (50 rpm) for 48 hours. Control flasks contained 200 ml AMD and no wood residue. At the end of this period, 10 ml aliquots were taken from each flask and filtered through 0.22 µm filter. And is currently being analyzed by inductively coupled plasma emission spectrometry

### **Task 3: Data Analysis**

None available now

## **SUMMARY**

Initial studies have commenced and some results will be ready be next report period.

## **FUTURE WORK**

Future studies will focus on:

- 1.0. The effect of fungal hyphae of removal of metal ions
- 2.0. The kinetics of metal adsorption by wood.